GENOMIC CHARACTERIZATION OF EMERGING HUMAN FUNGAL PATHOGENS

EDITED BY: Christina A. Cuomo, Bridget Marie Barker and Nelesh P. Govender
PUBLISHED IN: Frontiers in Genetics

frontiers Research Topics

frontiers

ISSN 1664-8714
ISBN 978-2-88966-807-6
DOI 10.3389/978-2-88966-807-6

About Frontiers

Frontiers is more than just an open-access publisher of scholarly articles: it is a pioneering approach to the world of academia, radically improving the way scholarly research is managed. The grand vision of Frontiers is a world where all people have an equal opportunity to seek, share and generate knowledge. Frontiers provides immediate and permanent online open access to all its publications, but this alone is not enough to realize our grand goals.

Frontiers Journal Series

The Frontiers Journal Series is a multi-tier and interdisciplinary set of open-access, online journals, promising a paradigm shift from the current review, selection and dissemination processes in academic publishing. All Frontiers journals are driven by researchers for researchers; therefore, they constitute a service to the scholarly community. At the same time, the Frontiers Journal Series operates on a revolutionary invention, the tiered publishing system, initially addressing specific communities of scholars, and gradually climbing up to broader public understanding, thus serving the interests of the lay society, too.

Dedication to Quality

Each Frontiers article is a landmark of the highest quality, thanks to genuinely collaborative interactions between authors and review editors, who include some of the world's best academicians. Research must be certified by peers before entering a stream of knowledge that may eventually reach the public - and shape society; therefore, Frontiers only applies the most rigorous and unbiased reviews.
Frontiers revolutionizes research publishing by freely delivering the most outstanding research, evaluated with no bias from both the academic and social point of view. By applying the most advanced information technologies, Frontiers is catapulting scholarly publishing into a new generation.

What are Frontiers Research Topics?

Frontiers Research Topics are very popular trademarks of the Frontiers Journals Series: they are collections of at least ten articles, all centered on a particular subject. With their unique mix of varied contributions from Original Research to Review Articles, Frontiers Research Topics unify the most influential researchers, the latest key findings and historical advances in a hot research area! Find out more on how to host your own Frontiers Research Topic or contribute to one as an author by contacting the Frontiers Editorial Office: frontiersin.org/about/contact

GENOMIC CHARACTERIZATION OF EMERGING HUMAN FUNGAL PATHOGENS

Topic Editors:
Christina A. Cuomo, Broad Institute, United States
Bridget Marie Barker, Northern Arizona University, United States
Nelesh P. Govender, National Institute of Communicable Diseases (NICD), South Africa

Citation: Cuomo, C. A., Barker, B. M., Govender, N. P., eds. (2021). Genomic Characterization of Emerging Human Fungal Pathogens.
Lausanne: Frontiers Media SA. doi: 10.3389/978-2-88966-807-6

Table of Contents

frontiers in Genetics

EDITORIAL
published: 25 March 2021
doi: 10.3389/fgene.2021.674765

Editorial: Genomic Characterization of Emerging Human Fungal Pathogens

Bridget M. Barker[1]*, *Christina A. Cuomo*[2]* and *Nelesh P. Govender*[3,4,5]*

[1] Pathogen and Microbiome Institute, Northern Arizona University, Flagstaff, AZ, United States, [2] Broad Institute of MIT and Harvard, Cambridge, MA, United States, [3] National Institute for Communicable Diseases, National Health Laboratory Service, Johannesburg, South Africa, [4] School of Pathology, University of the Witwatersrand, Johannesburg, South Africa, [5] Division of Medical Microbiology, University of Cape Town, Cape Town, South Africa

Keywords: Candida, black fungi, *Aspergillus*, Mucoralesi, *Coccidioides*, *Paracoccidioides*, RNA-seq

Editorial on the Research Topic

Genomic Characterization of Emerging Human Fungal Pathogens

Human fungal pathogens pose a major clinical challenge with the emergence of new species, expanded geographic ranges impacting new populations, and the increasing frequency of antifungal drug resistance. Rapidly addressing these new threats can leverage genomic approaches to characterize new species or lineages and trace the origin and spread of outbreaks. Genomic data can also guide the improvement or development of diagnostic approaches to detect new species and genetic elements conferring drug resistance. This issue features reports of species from across the fungal kingdom, and highlights the range of genomic approaches being used to study these important pathogens.

Bombassaro et al. compared the enzyme-coding gene profile of *F. pugnacius* to other neutropic black fungi such as *Cladophialaphora bantiana*, *Exophiala dermatitidis*, and *Rhinocladiella mackenziei* and examined the virulence of this pathogen in invertebrate and mouse models of infection. *F. pugnacius* is a very rare human pathogen with a single strain described to date in a case of chromoblastomycosis with secondary neurotropic dissemination (phaeohyphomycosis) from a presumed subcutaneous source. Its sibling species, *F. pedrosoi* and *F. nubica*, cause chromoblastomycosis which is characterized by muriform cells in subcutaneous tissue usually of the extremities, while another related species, *F. monophora* causes primary brain infection. In this paper, the authors describe a 34.8 Mb genome and 12,217 protein-coding genes associated with extremotolerance, virulence and neurotropism. *F. pugnacius* survived in an invertebrate model with lower mortality than *F. monophora* and *F. pedrosoi* but with high colony-forming units, melanisation of larval hemolymph, and melanised hyphae in tissue. In a murine intradermal model, muriform cells were found in the footpads but with no dissemination; whereas with intraperitoneal inoculation, the pathogen was recovered from multiple tissues. The authors conclude that this is probably an opportunistic fungus with enhanced ability to tolerate stress and with adaptability to new niches.

Dos Santos et al. characterized and compared six clinical strains of *Aspergillus fumigatus*, a known major pathogen and cryptic species, *A. lentulus* ($n = 5$) and *A. fumigatiaffinis* ($n = 4$). Based on a *Galleria mellonella* model, they describe high heterogeneity in virulence across strains in each of the three species; in general, the cryptic species were as virulent as *A. fumigatus*. They performed susceptibility testing using the EUCAST method for polyenes, azoles, echinocandins, and allylamines. While *A. fumigatus* had lower amphotericin

Edited and reviewed by:
Ludmila Chistoserdova, University of Washington, United States

***Correspondence:**
Bridget M. Barker
bridget.barker@nau.edu
Christina A. Cuomo
cuomo@broadinstitute.org
Nelesh P. Govender
Neleshg@nicd.ac.za

Specialty section:
This article was submitted to Evolutionary and Genomic Microbiology, a section of the journal Frontiers in Genetics

Received: *01 March 2021*
Accepted: *08 March 2021*
Published: *25 March 2021*

Citation:
Barker BM, Cuomo CA and Govender NP (2021) Editorial: Genomic Characterization of Emerging Human Fungal Pathogens. Front. Genet. 12:674765. doi: 10.3389/fgene.2021.674765

B minimum inhibitory concentrations, susceptibility in general could not be predicted by cryptic species-level identification. They found a paralog of the *CYP51A* gene in *A. fumigatiaffinis* similar to *CYP51C*. They found no *FKS* mutations but some changes in *FKS* hotspot region 2 specific to the cryptic species. Based on genomic sequencing, they identified single nucleotide polymorphisms, virulence genes, and performed a phylogenomic analysis. Most genes were shared among all three species, including most virulence genes.

Soare et al. reviewed biological and virulence determinants of fungi in the Order Mucorales. They describe that the Order Mucorales diverged from common ancestor with Ascomycetes and Basidiomycetes 800 million years ago. Next-generation sequencing has facilitated an understanding of the genomic architecture of fungi in this Order (including an ancestral whole genome duplication event in some genera), virulence (nearly 800 candidate genes are truncated, discontiguous, or absent in avirulent strains), host response and important host-pathogen interactions, resistance, diagnostics (no specific biomarkers are available; molecular tests are few and not validated though a pan-Mucorales COTH gene family not present in *Aspergillus* can be amplified using a single primer set) and novel therapies (mycoviruses).

Misas et al. discuss new mitochondrial sequence data of *Paracoccidioides brasiliensis* strain Pb18 and *P. americanum* strain Pb03. They confirm the observation of a previous incomplete assembly that the *NAD5* gene contains a large insertion between exons 2 and 3 by using long read sequencing and additional sequencing data for bioinformatic assembly and annotation approaches. The authors point to a lack of well-assembled mitochondrial genomes and a need to functionally understand the mitochondria in Onygenalean fungi in general.

Mead et al. present new RNA-seq data for *Coccidioides posadasii*. The comparison of a chitinase 2/3 deletion mutant that is unable to complete the parasitic life cycle to the wild type parent strain reveals new insight into genes that might be responsible for the survival and growth of the fungus in the host. The volatilome was assessed for the mutant, and revealed numerous changes compared to the wildtype. Scanning electron microscopy suggests incomplete nuclear division in the mutant in response to loss of internal cell wall structure during spherule maturation. Several putative virulence factors are identified in this pathogen that causes coccidioidomycosis (valley fever) across the Americas.

Genomic approaches have played a key role in studies of the emergence and drug resistance of *Candida auris*. Chybowska et al. review nine areas where genomic data has been used to draw insights into this emerging species. Gade et al. characterize isolates from the *Candida haemulonii* species complex, the closest relatives of *C. auris*, which also are commonly resistant to antifungal drugs and are increasing in incidence. This study of global isolates included primarily *C. haemnulonii* and *C. duobushaemulonii*, with smaller numbers of *C. pseudohaemulonii* and *C. vulturna*. Genetic relationships and candidate mutations associated with azole resistance are described using whole genome sequence data. This use of genomic epidemiology reveals the need for further monitoring of outbreaks in healthcare settings as well as surveillance sequencing to follow the frequency of mutations associated with drug resistance.

Rodriguez-Leguizamon et al. examine a set of 10 *Candida albicans* isolates collected in Colombia for which initial studies indicated some shared properties with *Candida africana*. Multi-locus sequence analysis of seven standard genes showed that the *C. albicans* isolates belong to three clusters and do not appear closely related to *C. africana* isolates. Isolates showed varying levels of virulence in a *Galleria* model, and only one displayed resistance to fluconazole.

Thomas et al. carry out a co-expression network analysis using data from a prior RNA-Seq timecourse of *C. albicans* interactions with epithelial and endothelial cells. Analysis of the resulting network-extracted ontology (NeXO) identified clusters of genes enriched for roles in pathogenesis. In phenotypic tests of genes in clusters of interest revealed an unusual colony morphology for *PEP8*, which the authors go on to show is involved in hyphal development. This and other examples illustrate how the NeXO may be used to predict gene functional classes.

Usher et al. transformed a *C. glabrata* ORF library into *S. cerevisiae* and screened for transformants that were resistant to oxidative stress. This identified 16 candidates including genes known to have a role in stress protection, endosomal soring, transcription or translation, and epigenetic modification. One novel candidate gene named *ORI1* is shown to be required for oxidative stress resistance in *C. glabrata* using deletion and overexpression studies, and this role is further supported by a synthetic lethality screen.

In summary, this collection of manuscripts highlights important contributions to the field of human fungal pathogen genomics, and suggests future directions for research to advance progress in these important but often understudied human pathogens.

AUTHOR CONTRIBUTIONS

All authors listed have made a substantial, direct and intellectual contribution to the work, and approved it for publication.

Conflict of Interest: The authors declare that the research was conducted in the absence of any commercial or financial relationships that could be construed as a potential conflict of interest.

frontiers in Genetics

REVIEW
published: 15 April 2020
doi: 10.3389/fgene.2020.00351

Nine Things Genomics Can Tell Us About *Candida auris*

*Aleksandra D. Chybowska[1], Delma S. Childers[2] and Rhys A. Farrer[3]**

[1] School of Medicine, Medical Sciences, and Nutrition, Institute of Medical Sciences, University of Aberdeen, Aberdeen, United Kingdom, [2] Aberdeen Fungal Group, Institute of Medical Sciences, University of Aberdeen, Aberdeen, United Kingdom, [3] Medical Research Council Centre for Medical Mycology at The University of Exeter, Exeter, United Kingdom

Candida auris is a recently emerged multidrug-resistant fungal pathogen causing severe illness in hospitalized patients. *C. auris* is most closely related to a few environmental or rarely observed but cosmopolitan *Candida* species. However, *C. auris* is unique in the concern it is generating among public health agencies for its rapid emergence, difficulty to treat, and the likelihood for further and more extensive outbreaks and spread. To date, five geographically distributed and genetically divergent lineages have been identified, none of which includes isolates that were collected prior to 1996. Indeed, *C. auris*' ecological niche(s) and emergence remain enigmatic, although a number of hypotheses have been proposed. Recent genomic and transcriptomic work has also identified a variety of gene and chromosomal features that may have conferred *C. auris* with several important clinical phenotypes including its drug-resistance and growth at high temperatures. In this review we discuss nine major lines of enquiry into *C. auris* that big-data technologies and analytical approaches are beginning to answer.

Keywords: *Candida auris*, genomics, emergence, antifungal resistance mechanisms, virulence factors, epigenetics

OPEN ACCESS

Edited by:
Bridget Marie Barker, Northern Arizona University, United States

Reviewed by:
Anastasia Litvintseva, Centers for Disease Control and Prevention (CDC), United States
Jolene Bowers, Translational Genomics Research Institute, United States

****Correspondence:***
Rhys A. Farrer
rfarrer@broadinstitute.org;
r.farrer@exeter.ac.uk

Specialty section:
This article was submitted to Evolutionary and Genomic Microbiology, a section of the journal Frontiers in Genetics

Received: *14 January 2020*
Accepted: *23 March 2020*
Published: *15 April 2020*

Citation:
Chybowska AD, Childers DS and Farrer RA (2020) Nine Things Genomics Can Tell Us About Candida auris. Front. Genet. 11:351. doi: 10.3389/fgene.2020.00351

THE EVOLUTION OF *C. auris* AND CLOSEST RELATIVES

Candida auris was first isolated from the external ear canal (*auris* is Latin for "ear") of an 70 years old Japanese woman, who was a patient at Tokyo Metropolitan Geriatric Hospital (Tokyo, Japan) in 2009 (Satoh et al., 2009). This first isolate (type strain JCM15448; CBS10913; DSM21092) had several attributes that distinguished it from its closest known relatives, warranting its demarcation as a new species. Unique features of *C. auris* included the ability to grow (albeit slow and with weak growth) at 42°C, while isolates from its three closest relatives (*C. haemulonii*, *C. pseudohaemulonii,* or *C. heveicola*) were unable to grow at this temperature (Satoh et al., 2009). JCM15448 showed a reduced ability to assimilate different carbon sources (galactose, l−sorbose, cellobiose, l−arabinose, ethanol, glycerol, salicin, or citrate), whilst *C. ruelliae* was able to assimilate all of those as carbon sources (although *C. ruelliae* is able to grow at 42°C). JCM15448 produced no pseudohypae while all closest relatives (*C. haemulonii* species complex. *C. heveicola*, and *C. ruelliea*) were able to. The authors concluded that isolate JCM15448 belonged to a new species, and "may have pathogenicity, but this will be elucidated in future studies" (Satoh et al., 2009).

C. auris falls within the Clavispora clade of the Metschnikowiaceae family of the order Saccharomycetales, which are ascomycetous (hemiascomycetes) yeasts that reproduce by budding.

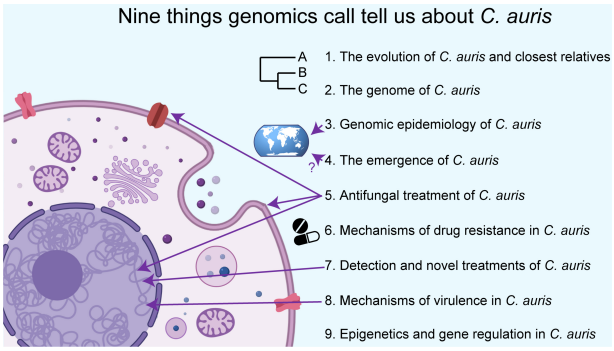

GRAPHICAL ABSTRACT | An overview of the nine chapters of this review.

Saccharomycetales includes approximately 1000 described species including human commensals and pathogens (e.g., *C. albicans*), plant pathogens (e.g., *Eremothecium gossypii*), species important for baking and brewing (e.g., *Saccharomyces cerevisiae*), species that have associations and interactions with plants and/or arthropods, as well as numerous free living saprobes. The most widely studied *Candida* species are *C. albicans*, *C. tropicalis,* and *C. parapsilosis* from the CTG clade – defined by predominantly translating the codon CTG to serine instead of leucine (Santos et al., 2011). Genetically distinct is *C. glabrata,* which falls in the Nakaseomyces clade (Angoulvant et al., 2016) and is also of growing interest primarily due to its increasing prevalence in nosocomial infections (Toda et al., 2019). These four species together accounted for approximately 90% of species responsible for invasive candidiasis during 2003 (Pfaller and Diekema, 2007). Although *C. auris* is genetically divergent from the other commonly studied CTG clade species, it also translates the codon CTG to serine and is within the CTG clade (Muñoz et al., 2018). *C. auris*' genetic distance from other more commonly studied species and its recent emergence raises many questions regarding its evolution, epidemiology, and the genetic basis for its pathogenicity and drug resistance.

The phylogenetic relationship of *C. auris* to other known species is still not fully resolved, mainly owing to the rarity of some of its closest relatives. Maximum likelihood phylogenetic reconstruction has revealed that four of the five clades of *C. auris* (with genomic analyses of Clade V not reported yet) are highly genetically related (98.7% average pairwise nucleotide identity), all of which are more distantly related to other *Candida* species that have their genome sequenced including *C. haemulonii*, *C. duobushaemulonii,* and *C. psuedohaemulonii* (88% average pairwise nucleotide identity) (Muñoz et al., 2018). Given the recency of emergence and discovery of already five clades within the *C. auris* species, it seems likely that further clades await discovery. Muñoz et al. found the most closely related species to be *C. haemulonii*, followed by *C. pseudohaemulonii* – both of which are occasionally found in animal or clinical settings (Cendejas-Bueno et al., 2012).

Early non-whole-genome sequencing (specifically 26S rDNA D1/D2 domain) suggested *C. auris* may be more closely related to *C. ruelliae* than *C. haemulonii* (Satoh et al., 2009), a species identified from the flowers of the *Ruellia* species of the Acanthaceae family (Saluja and Prasad, 2008). *C. ruelliae* has not been reported since to the best of our knowledge, and has not had its genome sequenced, thereby hampering efforts to phylogenetically place it, and verify its relationship to *C. auris*. ITS and rDNA sequencing meanwhile suggest that *C. auris* groups phylogenetically with *C. heveicola* (Satoh et al., 2009), a species described by a single isolate YJ2E(T) identified from tree sap from tropical forests in Yunnan and Hainan Provinces in southern China (Wang et al., 2008). Similarly, *C. heveicola* has also not been re-identified or had its full genome sequenced. Evidently, much remains to be known about true genome diversity of both *C. auris* and its closest relatives.

One of the closest known relatives of *C. auris* is *C. haemulonii,* which was first discovered in 1962 (formerly named *Torulopsis haemulonii*) from the gut of a blue-striped grunt fish (*Haemulon scirus*) (van Uden and Kolipinski, 1962), which is found in the Western Atlantic, Gulf of Mexico and the Caribbean. It was also isolated from the skin of dolphins and seawater off the coast of Portugal (van Uden and Kolipinski, 1962; Khan et al., 2007). *C. haemulonii* has also been found from terrestrial sources including the roots of Cassava (*Manihot esculenta*) in Brazil in 2010, and in a laboratory tick colony (*Ornithodoros moubata*) in the Czech Republic in 2001 (Jackson et al., 2019). *C. haemulonii* has also been the cause of candidemia and other bloodstream infections, catheter-related fungemia, osteitis, and even outbreaks in intensive care units (Cendejas-Bueno et al., 2012) including in Kuwait in 2005 (Khan et al., 2007).

In 1993, Lehmann et al. (1993) found *C. haemulonii* to comprise two separate groups (group I and II). In 2012, Cendejas-Bueno et al. (2012) redefined group I as the *C. haemulonii* species, and re-categorized group II as the new species *C. duobushaemulonii* based on genetic differences, ability to grow at different temperatures and on different carbon sources, and drug susceptibilities. *C. duobushaemulonii* has been isolated from patients' blood and foot ulcers in Asia, Europe, and North America, and has been the cause of recurrent vulvovaginal candidiasis (VVC) in Brazil (Jackson et al., 2019). *C. duobushaemulonii* has also been isolated from a firebug (*Pyrrhocoris apterus*) in Germany (Jackson et al., 2019). In 2006, Sugita et al. (2006) described a closely related but distinct species to *C. haemulonii*, *C. pseudohaemulonii*, which was isolated from the blood of a Thai patient. Recent genome sequencing showed 92% nucleotide genome identity between *C. pseudohaemulonii* and *C. duobushaemulonii* and several chromosomal rearrangements confirming their genetic divergence (Muñoz et al., 2018).

The evolution and phylogenetics of *C. auris* remain enigmatic, due to the disparate ecological sources of its closest relatives, their genetic distance, and that most have not yet had their genomes sequenced and compared, thus precluding detailed population genetic analysis within these species. The discovery of more closely related species by concerted sampling efforts, along with genome sequencing of others already identified but without

reference genomes such as *C. ruelliae* or *C. heveicola* may provide additional clues about their and *C. auris*' evolution.

THE GENOME OF *C. auris*

To date, five genetically diverse clades have been discovered. The first genome assemblies came from isolates belonging to Clade I, such as the Illumina-based genome of isolate Ci6684 (Chatterjee et al., 2015), and Illumina and Nanopore based genomes of five isolates from an outbreak in London, United Kingdom (Rhodes et al., 2018b). Shortly after, Muñoz et al. (2018) assembled and compared genomes across four (Clade I- > IV) of the then known lineages. Muñoz mapped the genomes into seven chromosomes using optical maps, and recent work using long-reads and telomere-to-telomere assemblies confirm the chromosome count. Genome assembly sizes ranged from 12.1 and 12.7 Mb, and the number of predicted protein coding genes ranged from 5,288 and 5,601, similar to other *Candida* species. The correlation between the genome assembly size and the number of predicted genes was surprisingly negative (n = 7, r^2 = 0.0725) (Muñoz et al., 2018). To date, the genome of clade V has not been reported.

The seven chromosomes of *C. auris* have undergone chromosomal rearrangements between clades. For example, inversions and translocations of hundreds of kilobase genomic regions have been reported between Clade I (isolate B8441) and Clade III (isolate B11221) (Muñoz et al., 2018). More recent work using long-read telomere-to-telomere sequencing has shown the Clade II genome appears highly rearranged compared with the other 3 clades, with 2 inversions and 9 translocations resulting in a substantially different karyotype (Muñoz et al., 2019). It was hypothesized that these rearrangements could potentially prevent genetic exchange between those lineages (Muñoz et al., 2018). However, a phylogenetically conserved (at least between *C. auris*, *C. haemulonii* species complex, and *C. lusitaniae*) mating type locus (MTL) is present in the *C. auris* genome, consisting of a1 and a2 genes in MTLa isolates and a single α1 gene in the MTLα isolates (Muñoz et al., 2018). Interestingly, Clade I and Clade IV of *C. auris* isolates have so far all been MTLa, while Clade II and Clade III have all been MTLα. The mating type of Clade V has not yet been reported. The presence of a conserved mating type suggests that *C. auris* can mate, despite a lack of clear recombinants between or within clades.

Genomic variation between and within clades of *C. auris* may have an impact on gene function. The four clades of *C. auris* share an average pairwise nucleotide identity of 98.7% (Muñoz et al., 2018). In terms of nucleotide diversity (π), the four clades of *C. auris* had a value of 0.0039 which is less than *C. neoformans var. grubii* and more than the exclusively clonal *Trichophyton rubrum* (Muñoz et al., 2018). In terms of microevolution, Chow et al. (2018) found between 0 and 12 SNPs among clinical and screening cases in the United States within a patient, and also similar numbers within the facility during an outbreak. Comparisons between *C. auris* and its closest relatives showed changes to genes linked to drug resistance and virulence, including expanded families of transporters and lipases (Muñoz et al., 2018). However, much work remains to study positive selection between clades, and various features of population genetics within clades – including the identification of crossovers, effective population sizes, fixation indices, or evidence for bottlenecking.

Given the rapid clinical emergence of *C. auris*, including the newly identified Clade V in 2018 (Chow et al., 2019), the allelic variation within the species remains unclear. Further sampling of *C. auris* is clearly necessary, both in terms of screening historic samples that may have been mischaracterized, as well as new sampling efforts in both clinical and environmental settings. The discovery of additional clades, and the identification of clades with multiple mating types would assist in understanding the evolution of *C. auris*. A greater understanding of *C. auris*' phylogenetics and population genetics would also be achieved by additional bioinformatic analysis – including a comprehensive characterization of gene gain/loss events and selection of alleles between or within those species or clades.

GENOMIC EPIDEMIOLOGY OF *C. auris*

Since 2009, five genetically diverse clades have been discovered from India and Pakistan (South Asian; Clade I), Japan (East Asian; Clade II), South Africa (African; Clade III), Venezuela (South American; Clade IV) (Lockhart et al., 2017b) and most recently in 2019, Iran (Clade V) (Chow et al., 2019). Over the past decade, isolates of *C. auris* have also been detected across all major continents, including elsewhere in Asia, Europe, the Middle East, Africa, Australia, and North and South America (**Table 1**). This nearly simultaneous and recent independent emergence is both unprecedented and raises questions regarding its origins and transmission events.

Genome sequencing of isolates from clinical environments is revealing detailed insights into how *C. auris* is spreading between continents, within countries, and even within wards of hospitals and over time in patients. For example, between 2013 and 2017, 133 isolates (73 clinical cases and 60 screening cases) from ten US states were collected and evaluated by whole genome sequencing (Chow et al., 2018) and compared to standardized case report forms and contact investigations, including travel history and epidemiological links. Chow et al. found that isolates were related to South Asian, South American, African and East Asian isolates, indicating multiple clades of *C. auris* were introduced into the United States, some of which perhaps several times. Surprisingly however, only 7% of the clinical cases had clear evidence of being acquired through health-care exposures abroad, suggesting travel data were lacking, the index patient with exposure were not identified, or that the infection many may have been acquired from other sources, perhaps including environmental sources. Chow et al. found a similarly small number of SNPs (between 0 and 12) among clinical and screening cases within a patient compared with those within a facility during an outbreak. The low numbers of genomic variants indicate that there is local and ongoing transmission of *C. auris* in the United States, with most (82%) of the clinical isolates reported from hospitals

TABLE 1 | *C. auris* has caused outbreaks across all major continents over the last decade.

Region	Country	Details	Clade(s)	Date	Citation
Asia	China	15 patients, 35 isolates (26 from urine, 4 catheter, 3 sputum, 1 blood, 1 fluid)	III	2011–2017	Tian et al., 2018
	India	3 hospitals, 19 isolates	I	2012–2015	Lockhart et al., 2017b
	Japan	1 patient (external ear canal)	II	2009	Satoh et al., 2009
	Malaysia	1 hospital, 1 patient	Unknown	2017	Mohd Tap et al., 2018
	Pakistan	2 hospitals, 18 isolates	I	2010–2015	Lockhart et al., 2017b
	Singapore	1 hospital, 3 patients (all with recent hospitalizations in India or Bangladesh)	Unknown	2012–2017	Tan and Tan, 2018
	South Korea	61 patients (4 blood, 57 ear) from 13 hospitals	II	1996–2018	Kwon et al., 2019
Europe	Austria	1 case	Unknown	2018	Kohlenberg et al., 2018
	Belgium	1 case	Unknown	2013–2017	Kohlenberg et al., 2018
	France	2 cases	Unknown	2013–2017	Kohlenberg et al., 2018
	Germany	7 cases (6 from patients previously hospitalized abroad)	I, III	2015–2017	Hamprecht et al., 2019
	Norway	1 case	Unknown	2013–2017	Kohlenberg et al., 2018
	Russia	1 hospital (49 cases in an ICU)	I	2016–2017	Barantsevich et al., 2019
	Spain	79 isolates, 738 environmental samples	Unknown	2017–2019	Ruiz-Gaitán et al., 2019
	Switzerland	1 patient who was on holiday in Spain, transferred to Switzerland hospital	Unknown	2017	Riat et al., 2018
	The Netherlands	2 cases (both from patients previously hospitalized in India)	I	2019	Vogelzang et al., 2019
	United Kingdom	72 patients (colonization, candidaemia, vascular lines)	I	2015–2016	Rhodes et al., 2018b
Middle East	Iran	1 patient	V	2018	Chow et al., 2019
	Israel	2 hospitals, 5 patients	Unknown	2014–2015	Ben-Ami et al., 2017
	Kuwait	56 patients, 158 isolates	Unknown	2014–2017	Khan et al., 2018
	Oman	2 patients	Unknown	2016–2017	Mohsin et al., 2017
	Saudi Arabia	1 hospital, 2 patients	I	2017–2018	Abdalhamid et al., 2018
	United Arab Emirates	1 hospital, 1 patient	Unknown	2017	Alatoom et al., 2018
Africa	Kenya	1 patient	III	2012	Heath et al., 2019
	South Africa	1,576 cases	III	2012–2016	Govender et al., 2018
Australia	Australia	1 patient (a 65-year old with recent hospitalization in Kenya)	III	2015	Heath et al., 2019
Americas	Canada	1 patient (a 64-year old with a recent hospitalization in India)	Unknown	2017	Schwartz and Hammond, 2017
	Columbia	4 hospitals, 7 people colonized, 37 environmental samples	IV	2015–2016	Escandón et al., 2019
	Panama	1 hospital, 9 patients, 14 isolates	Unknown	2016	Araúz et al., 2018
	United States	10 US states (133 isolates; 73 clinical cases and 60 screening cases)	I, II, III, IV	2013–2017	Chow et al., 2018
	Venezuela	1 hospital, 5 isolates	IV	2012–2013	Lockhart et al., 2017b

located in New York and New Jersey (Chow et al., 2018; Tracking Candida auris | CDC, 2020).

Outbreaks in Europe and Australia have also been attributed to recent spread from other continents. For example, of the 7 cases of *C. auris* identified in Germany during 2015–2017, 6 were from patients previously hospitalized abroad (Hamprecht et al., 2019). Whole-genome sequencing and epidemiologic analyses revealed that all patients in Germany were infected with different strains: five related to isolates from South Asia (Clade I), and one related to isolates from South Africa (Clade III) (Hamprecht et al., 2019). More recently (2019), the first two cases of *C. auris* were reported in The Netherlands, with both cases arising in patients that were treated in a healthcare facility in India prior to admission. Indeed, genetic analysis showed that these isolates also belonged to the South Asian *C. auris* Clade I (Vogelzang et al., 2019). In Australia in 2015, a 65-year-old man with a history of intensive care treatment in Kenya in 2012, was diagnosed with the South African Clade III of *C. auris* causing sternal osteomyelitis (Heath et al., 2019).

The largest outbreak in the United Kingdom to date of *C. auris* occurred between April 2015 and November 2016 in the Royal Brompton hospital in London, which involved 72 separate patients (Schelenz et al., 2016). Using Oxford Nanopore and Illumina sequencing technologies to gather genomic data on those clinical isolates, Rhodes et al. placed the United Kingdom outbreak in the India/Pakistan clade (Clade I), demonstrating an Asian origin for the outbreak. Rhodes et al. (2018a) were also able to estimate the timing for the most recent common ancestor (MRCA) of those outbreak strains to late March 2015, which was just weeks prior to the first patient identified with a *C. auris* infection. Additionally, by using root-to-tip regression, Rhodes et al. (2018a) estimated the evolutionary rate of the *C. auris* nuclear genome to 5.7×10^{-5} substitutions per site per year, a slower rate to the nuclear DNA of other related fungal species in the Saccharomycetales such as *Saccharomyces cerevisiae*

(5.7×10^{-3}), as well as more distantly related species such as the *Schizosaccharomyces pombe* traditional beer strains (3.0×10^{-3}).

Multiple outbreaks of *C. auris* in Colombia between 2015 and 2016 led to a concerted effort to understand its epidemiology within Colombian health-care clinics (Escandón et al., 2019). By sampling infected patients, patient contacts, healthcare workers, and the environment across 4 hospitals, they identified likely sources of transmission events, including health-care workers, and in the hospital environment. For all studied groups, the swabbed body sites included: axillae, groins, nostrils and ears. Samples were also taken from the mouth and rectum of patients. Among patients, the axilla, groin, and rectum had the highest positivity rate (2/7; 28% each). *C. auris* was isolated from the hands of two healthcare workers and the groin of another healthcare worker (Escandón et al., 2019). None of the 4 patient contacts swabbed were positive for *C. auris*, although the low sample size does not preclude this as a mechanism of spread. *C. auris* was isolated from 37 of 322 (11%) environmental samples, including a diverse range of hospital equipment including on a stethoscope, hospital floor, body cables, bed railing, mattresses, stretchers, bedpans, a closet, towel, cell phone, mops, TV control, meal table, sink, toilet, wheelchair, and a nurse's shoe. The results demonstrate that contamination can occur, and also that *C. auris* can survive on a variety of substances, at least in the short term (Escandón et al., 2019). Unlike the aforementioned European outbreaks, whole-genome sequencing and phylogenomics showed that the genetic background of isolates throughout the four hospitals were all similar (suspected Clade IV), despite the four hospitals spanning 700 km across Colombia. Isolates from the two northern Colombian hospitals grouped into a sub-clade, while those from the two southern hospitals grouped into a separate sub-clade, suggesting some geographically defined population structure in the country, and possibly endemism.

Since it was first discovered in Tokyo Metropolitan Geriatric Hospital (Tokyo, Japan) in 2009 (Satoh et al., 2009), *C. auris* has caused hospital acquired infections and outbreaks across all main continents including Asia, Europe, Africa, Australia, North America and South America. Given the recency of these outbreaks, further outbreaks across the world in the upcoming decade appear likely, unless concerted mitigation efforts are made (Escandón et al., 2019; Ong et al., 2019). It is also likely that cases are being misidentified (Chatterjee et al., 2015; Govender et al., 2018) or undetected, especially across Sub-Saharan Africa, South America and Eastern Europe where there are currently few reports (Ong et al., 2019). Exemplifying this is how common *C. auris* has become in some hospitals from regions with few additional reports of cases (van Schalkwyk et al., 2019). For example, in the Aga Khan University Hospital in Nairobi, Kenya between 2010 and 2016, *C. auris* was the most common cause of candidemia (38% of 201 patients) (Adam et al., 2019), suggesting that other hospitals in Kenya and in neighboring countries are likely to also harbor *C. auris*. Necessary steps to better understanding the epidemiology of *C. auris* will therefore include greater sampling and reporting from regions that underreported *C. auris* cases, a transition away from unreliable diagnostic methods, and further genomic analysis describing the population genetics of the various lineages, all of which may reveal its geospatial origin and subsequent spread.

THE EMERGENCE OF *C. auris*

To date, the earliest reports of *C. auris* have been from a Clade II isolate in 1996, retrospectively from a case of misidentified nosocomial fungemia in South Korea (Lee et al., 2011). The species was first described over 10 years later from a case in Japan (Satoh et al., 2009), and simultaneously arising in South Africa with a Clade III isolate also from 2009 (Govender et al., 2018). *C. auris* has not been detected earlier than 2009 by The SENTRY Antifungal Surveillance Program, which has been collecting consecutive invasive *Candida* isolates from 135 participating medical centers in North America, Europe, Latin America and the Asia-Pacific regions since 1997 (Pfaller et al., 2019). However, molecular clock estimates from 304 worldwide genomes date the most recent common ancestor of each of the four clades within the last 339 years, and outbreak isolates from Clades I, III, and IV to 34–35 years ago (∼10 years prior to first being detected) (Chow et al., 2020). While the details of its origin remain unclear, *C. auris* is not the only fungal pathogen to have recently clinically emerged. Indeed, a variety of phylogenetically diverse emerging fungal pathogens are rapidly increasing in their incidence, geographic or host range and virulence (Morse, 1995; Farrer and Fisher, 2017). Recently highlighted examples include the emergence and increasing incidence of a separate ascomycete responsible for human infections: *Emergomyces africanus* (Dukik et al., 2017), the newly-described chytrid fungus *Batrachochytrium salamandrivorans* causing rapid declines of fire salamanders across an expanding region of northern Europe (Farrer, 2019), and the basidiomycete fungus *Cryptococcus gattii* expanding its range into non-endemic environments with a consequential increase of fatal disease in humans (Fraser et al., 2005; Byrnes et al., 2010).

One suggestion for the absence of *C. auris* isolates prior to 1996 is that it has only recently become part of the human microbiome, and has either recently acquired sufficient virulence to cause invasive infections or been newly introduced into human populations in which invasive *Candida* infections can be identified (Jackson et al., 2019). For example, recent genetic recombination, hybridization, or other biological changes could potentially increase the organism's transmissibility or virulence (Jackson et al., 2019). However, for this hypothesis to hold, such genetic changes would need to have occurred across all clades of *C. auris* recently.

One line of inquiry to understand the recency of the emergence has been to re-screen isolates taken prior to 2009 that may have been misdiagnosed as other *Candida* species. Indeed, *C. auris* has been misdiagnosed as its closest relatives *C. haemulonii* or *C. pseudohaemulonii* (Chatterjee et al., 2015), species which have even been identified alongside *C. auris* in the same month in the same hospital (Ben-Ami et al., 2017). Lee et al. (2011) identified the oldest known case of *C. auris* from South Korea, which dates to 1996, belongs to Clade II, and had

been misidentified as *C. haemulonii* by Vitek 2. Another clinical isolate originally characterized as *C. haemulonii* from a hospital in South Africa, was later shown to be a Clade III isolate of *C. auris* (Govender et al., 2018). This isolate was taken from a patient in 2009 demonstrating independent emergences in 2009 of at least two of the *C. auris* lineages (Clade II and Clade III). A recent study comparing 204 genomes of *C. auris* using Bayesian molecular clock phylogenetics estimated the origin of each of the four clades within the last 339 years, and outbreak clusters (Clade I, III, and IV) originating 34–35 years ago (Chow et al., 2020), suggesting more historic samples were not identified.

The spread of *C. auris* within and between hospital settings has been clearly demonstrated by at least clades I, III and IV (e.g., Chow et al., 2018; Rhodes et al., 2018b; Escandón et al., 2019), so it is possible that abiotic factors could explain the emergence. For example, human activities such as deforestation, expansion of farmland, and coastal ecosystem disruption could have allowed an ecological jump (Jackson et al., 2019). Indeed, *C. auris*' closest relatives include *C. ruelliae* from flowers of the *Ruellia* species (Saluja and Prasad, 2008), and *C. haemulonii* that can also cause clinical infections but also found in the GI tract and skin of marine animals (van Uden and Kolipinski, 1962; Khan et al., 2007). Furthermore, *C. auris* has been shown to persist on a wide variety of hospital equipment (Escandón et al., 2019). It therefore seems likely that *C. auris* may also have an environmental niche (plants or aquatic). The widespread use of fungicides, especially triazoles in agriculture could have been responsible for *C. auris* to become more prominent in the environment, as it shows high levels of antifungal resistance. At the same time, increased human travel, trade or other anthropogenic factors may have simply led to the globalization and emergence of *C. auris* (Jackson et al., 2019).

C. auris is able to grow (albeit slowly) at 42°C, while isolates from close relatives (*C. haemulonii*, *C. pseudohaemulonii* or *C. heveicola*) were unable to grow at this temperature (Satoh et al., 2009). *C. auris*' thermotolerance enables it to cause invasive candidemia, including tolerating the fever response (Jackson et al., 2019), but may also enable it to sustain body temperatures of other animals including birds (Casadevall et al., 2019). For example, pigeons body temperature can be up to 44°C during flight (Aulie, 1971), compared with only a few degrees above 37°C during exercise for humans (Gleeson, 1998). Similarly, sea birds may serve as reservoirs for indirect transmission of drug-resistant *Candida* species, such as *C. glabrata*, to humans (Al-Yasiri et al., 2016; Casadevall et al., 2019). *C. auris* is also able to survive high salt concentrations (broth containing 10% NaCl), which might allow it survive environmentally including hypersaline desert lakes, salt-evaporating ponds, or tidal pools (Jackson et al., 2019). Thus, *C. auris* is thought likely to survive both in the environment, as well as colonizing human skin. On skin it is likely to compete with other commensals such as *Malassezia*, although studies on *C. auris* interactions with bacteria or other fungi are lacking.

The thermotolerance of *C. auris* has led to the hypothesis that its emergence may be linked to climate change and global temperature changes, and may even be the first example of a new pathogenic fungus emerging from human-induced global warming (Casadevall et al., 2019). Indeed, it has been proposed that as the gap between the environmental temperature and human body temperature narrows, new fungal diseases of mammals will increase (Garcia-Solache and Casadevall, 2010). Casadevall et al. (2019) suggest a number of factors that supports the hypothesis of a climate change emergence, including that *C. auris* can grow on skin but not anaerobically in the gut (suggesting a recent environmental source), the constitutive overexpression of heat shock protein HSP90, and the inability of many relatives to grow at high temperatures. *C. auris* clades I, II, III, and IV differ by an average of 1.3% average pairwise nucleotide identity (Muñoz et al., 2018). Although a time to most recent common ancestor of multiple clades has not yet been predicted, the ancestor to all clades almost certainly predates industrial era warming, which begun in 1800 AD (Abram et al., 2016). Given that all known clades of *C. auris* are able to colonize skin and cause infections, its ability to colonize these niches are more likely to be an evolutionary conserved trait, rather than five independent recent trait acquisitions. It nevertheless remains to be shown if climate change had a role to play in exposing each clade into an alternative niche they already had the ability to colonize (Casadevall et al., 2019).

Further environmental sampling, genome sequencing and metagenomics studies focusing on fungi are necessary to identify and confirm environmental sources of *C. auris*. Further genomic epidemiology studies, including on the genetic diversity within each clade will help to find older natural populations that could indicate the progenitor of *C. auris*. Clade II (East Asian clade) exhibits higher genetic diversity than the other clades (Jackson et al., 2019), although it also exhibits large karyotypic variation and loss of sub-telomeric regions, suggesting it is not ancestral to Clade I, III and IV. The discovery of further ecological niches and the geographical origin will be important to prevent similar emergences in future as well as identify and mitigate emergence of new clades of *C. auris* that have the potential to cause outbreaks.

ANTIFUNGAL TREATMENT OF *C. auris*

Treating invasive fungal infections is a considerable challenge due to the limited number of available antifungal agents. The five major antifungal drug classes that are used in hospital settings are azoles, allylamines, polyenes, echinocandins and nucleoside analogs (Bidaud et al., 2018). To date, there are only a few alternative antifungal agents (de Oliveira Santos et al., 2018). While the efficacy of some antifungal classes is highly dependent on the site of infection due to their tissue penetration properties (Felton et al., 2014), other classes of antifungals (i.e., polyenes) often lead to serious side effects such as renal injury or cardiomyopathy (Bandeira et al., 2016), primarily due to conserved or structural similarities in drug targets such as cholesterol and ergosterol (Kamiński, 2014). Given the lack of treatment options, the emergence of fungal resistance to even one of the major drug classes is very alarming, as it makes the infection considerably more challenging to treat.

TABLE 2 | *Candida auris* resistance patterns.

Drug category	Drug	Method	Resistant	Samples no	Resistance threshold used (μg/mL)	References
Azoles	Fluconazole	CLSI	93%	54	32	Lockhart et al., 2017b
		CLSI	86%	123	32	Arendrup et al., 2017
		EUCAST	96%	123	32	Arendrup et al., 2017
		CLSI	90%	320	32	Chowdhary et al., 2018
	Voriconazole	CLSI	54%	54	2	Lockhart et al., 2017b
		CLSI	33%	123	2	Arendrup et al., 2017
		EUCAST	15%	123	2	Arendrup et al., 2017
		CLSI	39%	90	2	Kathuria et al., 2015
		Vitek 2	29%	90	2	Kathuria et al., 2015
		Etest	28%	90	2	Kathuria et al., 2015
		CLSI	15%	320	2	Chowdhary et al., 2018
	Isavuconazole	CLSI	4%	123	2	Arendrup et al., 2017
		EUCAST	4%	123	2	Arendrup et al., 2017
	Itraconazole	CLSI	0%	54	2	Lockhart et al., 2017b
		CLSI	1%	123	2	Arendrup et al., 2017
		EUCAST	0%	123	2	Arendrup et al., 2017
		CLSI	6%	320	1	Chowdhary et al., 2018
	Posaconazole	CLSI	0%	54	2	Lockhart et al., 2017b
		CLSI	2%	123	2	Arendrup et al., 2017
		EUCAST	0%	123	2	Arendrup et al., 2017
Polyenes	Amphotericin B	CLSI	35%	54	2	Lockhart et al., 2017b
		CLSI	16%	90	2	Kathuria et al., 2015
		Vitek 2	100%	90	2	Kathuria et al., 2015
		Etest	1%	90	2	Kathuria et al., 2015
		CLSI	8%	320	2	Chowdhary et al., 2018
		CLSI	10%	123	2	Arendrup et al., 2017
		EUCAST	0%	123	2	Arendrup et al., 2017
	Nystatin	CLSI	100%	320	2	Chowdhary et al., 2018
Echinocandins	Anidulafungin	CLSI	2%	320	8	Chowdhary et al., 2018
		CLSI	6%	123	8	Arendrup et al., 2017
		EUCAST	0%	123	8	Arendrup et al., 2017
		CLSI	7%	54	8	Lockhart et al., 2017b
	Caspofungin	CLSI	2%	320	8	Chowdhary et al., 2018
		CLSI	3%	90	8	Kathuria et al., 2015
		Vitek 2	0%	90	8	Kathuria et al., 2015
		Etest	0%	90	8	Kathuria et al., 2015
		CLSI	7%	54	8	Lockhart et al., 2017b
	Micafungin	CLSI	2%	320	8	Chowdhary et al., 2018
		CLSI	7%	54	8	Lockhart et al., 2017b
		CLSI	6%	123	8	Arendrup et al., 2017
		EUCAST	6%	123	8	Arendrup et al., 2017
Nucleoside analogs	5-Flucytosine	CLSI	6%	54	128	Lockhart et al., 2017b
Allylamines	Terbinafine	CLSI	100%	320	2	Chowdhary et al., 2018

Prior to publishing C. auris tentative resistance thresholds, various research groups used different concentrations to determine the resistance of their isolates. Their choices were based on a comparison of the treatment outcomes associated with drug exposure observed in C. auris and in other Candida spp. *infections.*

It is of considerable concern to health authorities that the emergent *C. auris* includes isolates that are resistant to all antifungals (Warris, 2018). *C. auris* isolates are resistant to fluconazole, the major drug in treating candidemia, with MIC values > 64 μg/mL (Chowdhary et al., 2018; Warris, 2018). Other azoles such as voriconazole show variable antifungal activity (**Table 2**). While more than 95% of isolates from India were resistant to a topical allylamine, terbinafine (Chowdhary et al., 2018), currently UK strains remain susceptible to terbinafine and polyene nystatin (Sarma and Upadhyay, 2017). Almost one-third of isolates observed so far were resistant to amphotericin B (a polyene used as a last resort drug) (Warris, 2018). Although

TABLE 3 | Tentative MIC breakpoints of *C. auris* defined by CDC (Antifungal Susceptibility Testing and Interpretation, 2019).

Drug class	Drug	Tentative MIC breakpoint (μg/mL)
Azoles	Fluconazole	≥32
Azoles	Other azoles	N/A
Polyenes	Amphotericin B	≥2
Echinocandins	Anidulafungin	≥4
Echinocandins	Caspofungin	≥2
Echinocandins	Micafungin	≥4

the nucleoside analog 5-flucytosine successfully treated more than 95% of *C. auris* infection cases *in vitro* (Lockhart et al., 2017a; Osei Sekyere, 2018), it is not used extensively as therapy because resistance arises rapidly, potentially during treatment (Rhodes et al., 2018a), and it elicits toxic effects on bone marrow that may lead to death in immunosuppressed patients (Vermes et al., 2000). Between 2 and 7% of *C. auris* isolates have developed resistance to echinocandins (Lockhart et al., 2017b; Chowdhary et al., 2018), one the newest classes of antifungal drug to be developed (Sucher et al., 2009). Reported adverse effects of echinocandin therapy are generally mild and include nausea and dose-related elevation of liver aminotransferases levels (Aguilar-Zapata et al., 2015) and therefore, this group of drugs is still the most effective for treating the majority of *C. auris* infections. Resistance to all three common antifungal classes used as therapy (azoles, polyenes and echinocandins) was observed in 4% of *C. auris* outbreak samples in North America from 2012–2015 (Lockhart et al., 2017b).

Although *C. auris* is typically multidrug-resistant, levels of susceptibility to various drugs differ greatly between isolates and clades (Kean and Ramage, 2019). To find the most suitable drug candidate, susceptibility is typically measured over the period of 24 h, when the fungus grows in the presence of a drug concentration gradient. If the observed minimal inhibitory concentration (MIC) is greater than the resistance MIC breakpoint, the examined isolate is considered resistant to the drug. Tentative susceptibility MIC breakpoints for *C. auris* established by CDC are shown in **Table 3**. Currently, these *C. auris* susceptibility breakpoints should be treated as a general guide as the connection between them and clinical outcome is not known yet.

Importantly, some *Candida* such as *C. albicans* exhibit drug tolerance defined as the ability of a fraction of a population to grow above the population resistance level (Rosenberg et al., 2018). The presence of highly tolerant sub-populations may lead to persistent candidemia that is associated with a mortality rate higher than 50% (Hammoud et al., 2013) despite appropriate treatment (Alatoom et al., 2018). *In vivo* data suggest that reducing drug susceptibility without affecting the resistance of the population may be possible using adjuvant drugs (Rosenberg et al., 2018). Adjuvants such as the antidepressant fluoxetine that impairs biofilm development (Oliveira et al., 2018) or Hsp90 inhibitor called radicicol that blocks stress responses (Rosenberg et al., 2018) have been shown to clear tolerance without altering the susceptibility level when given in combination with fluconazole in *C. albicans* (Rosenberg et al., 2018). Future clinical control trials are required to confirm the effectiveness of adjuvants before being considered for inclusion as a possible treatment protocol.

MECHANISMS OF DRUG RESISTANCE IN *C. auris*

C. auris has evolved a range of molecular drug-resistance mechanisms which are shown in **Figure 1**. They include (1) Drug target mutation (Bidaud et al., 2018), (2) drug target overexpression (Bhattacharya et al., 2019), (3) changes in drug uptake and efflux (Muñoz et al., 2018), (4) activation of stress response pathways (Kim et al., 2019), and (5) biofilm formation (Kean et al., 2018). By aggregating into a colony and forming a biofilm, *Candida* spp. increase their resistance to all currently available antifungals by up to 1000-fold (Taff et al., 2013). Some of the key regulators of fungal biofilm dispersion, antibiotic tolerance, and cell wall remodeling are molecular chaperones belonging to Hsp90 family (Robbins et al., 2011; Leach et al., 2016). In *C. auris*, these proteins were found to promote cell-wall integrity signaling and stress responses related to azoles administration thereby contributing to the evolution of drug resistance (Kim et al., 2019).

Azoles are an important group of antifungal agents that were first developed in the late 1960s, and function by inhibiting the synthesis of ergosterol, a key component of the fungal membrane, thereby preventing growth and proliferation (Ghannoum and Rice, 1999). Since the action of azoles is largely dependent on the affinity of the drug to the active site of Erg11p, any mutations that affect the active site of the enzyme may lead to the development of drug resistance (Berkow and Lockhart, 2017). Such resistance mechanisms have been observed in *C. albicans*, in which more than 140 ERG11 mutations have been identified to date (Debnath and Addya, 2014). These mutations accumulated in three regions of the ERG11 gene (Marichal et al., 1999). Bioinformatic analysis of these substitutions combined with 3D modeling showed that most of them are located near the predicted catalytic center or on elements of the fungus-specific external loop (Whaley et al., 2017). Many of the described mutations can also be found in *C. auris*, but not all have the same effects (Muñoz et al., 2018). In both species, amino acid substitutions at F126L, Y132F, K143R result in azole resistance (Morio et al., 2010; Chowdhary et al., 2018; Healey et al., 2018), with Y132F the most widespread mutation associated with azole resistance (Chow et al., 2020). Another mechanism of azole resistance is the overexpression of Erg11p, which can be caused either by increasing the number of ERG11 transcription factors such as Upc2p or by duplicating ERG11 (Bhattacharya et al., 2019). In both cases, the high concentration of azole target dilutes the effects of drug activity (Muñoz et al., 2018).

The activity of azoles can be also reduced by decreasing the concentration of antifungals in the cell by means of efflux pumps. Recently, 20 ABC transporters that are putative efflux pumps have been identified in the *C. auris* genome, strain-type CBS 10913T (Wasi et al., 2019). Two drug transporters (CDR1 and

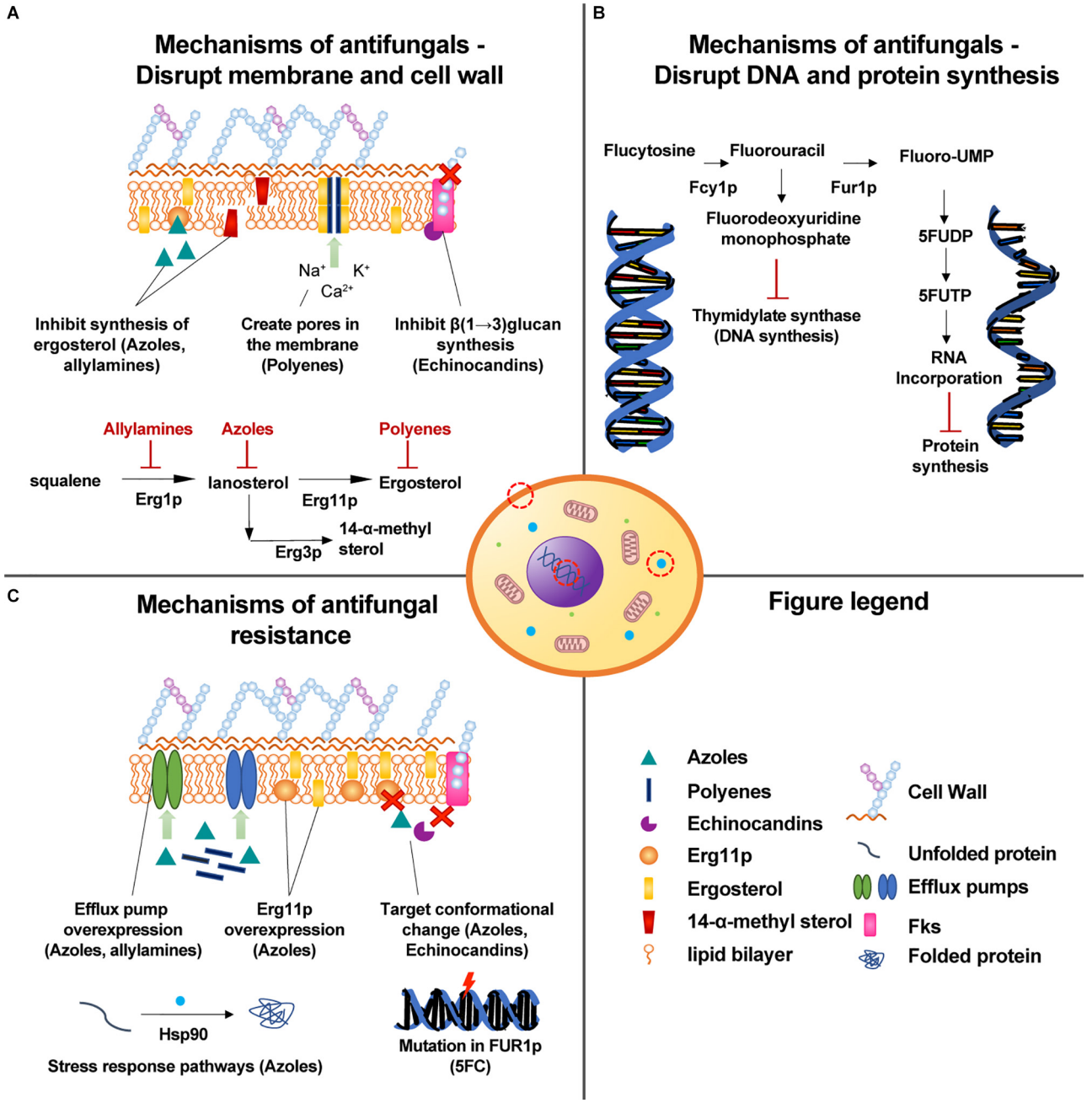

FIGURE 1 | Mechanisms of drug action and resistance observed in *C. auris*. **(A)** The main mechanisms of antifungals that disrupt the cell membrane or cell wall. **(B)** In the nucleus, 5-flucytosine inhibits the synthesis of fungal DNA and RNA. **(C)** Mechanisms of antifungal resistance to drugs that damage the cell membrane or cell wall.

MDR1) that have primarily been studied in *C. albicans* have orthologs in *C. auris*, and these orthologs are overexpressed in azole-resistant *C. auris* (Rybak et al., 2019). CDR1 is an ABC transporter that confers azole-derived compounds resistance, while MDR1 is a Major Facilitator Superfamily (MFS) pump and a member of the multidrug resistance family which is responsible for fluconazole resistance (de Oliveira Santos et al., 2018). Rybak et al. demonstrated that deletion of CDR1 restored susceptibility of highly resistant *C. auris* isolates to fluconazole. Furthermore, domains associated with transporters such as OPT and glutathione were found to be significantly enriched in *C. auris*, *C. haemulonii*, *C. duobushaemulonii*, and *C. pseudohaemulonii* when compared to related species (Muñoz et al., 2018). Oligopeptide transporters (OPT) are small peptide transporters expression of which is upregulated in *C. albicans* upon administration of azoles (Muñoz et al., 2018). Similarly,

glutathione transporters may contribute to azole resistance by exporting oxidized glutathione derivatives out of the cell and thereby protecting the cell against oxidative damage elicited by the drugs (Maras et al., 2014).

Polyenes are a commonly used group of drugs used to treat *C. auris* infections. The most known polyene, amphotericin B, binds membrane-bound ergosterol, causing pores to form in the fungal membrane through which small molecules leak to the outside of the cell (de Oliveira Santos et al., 2018). The release of intracellular constituents such as sugars, potassium or calcium strongly contributes to cell death (de Oliveira Santos et al., 2018). We are not aware of any mechanism of polyenes resistance reported for *C. auris* so far, which would presumably be analogous to ERG3 dependent alternations in sterol synthesis observed in *C. albicans* or alternations in cell membrane sterol composition (Taff et al., 2013). However, in 2018, Muñoz et al. (2018) showed that intrinsic transcription of multidrug transporters in *C. auris* was higher when compared to susceptible and resistant isolates and that upon administering Amphotericin-B, eight genes including OPT1-like transporter (high-affinity glutathione, tetra- and pentapeptides transporter), CSA1 (conserved cell wall protein 1 involved in biofilm formation), MET15 (sulfhydrylase) and ARG1 (argininosuccinate synthase) were upregulated. In 2019, another study identified five novel mutations that associate strongly with amphotericin B resistance in Colombian *C. auris* ($p \leq 0.001$). Four of the identified mutations fall within protein-coding regions (Escandón et al., 2019). One of the mutations occurs within FLO8, a transcription factor that is required for virulence and biofilm formation in *C. albicans* (Escandón et al., 2019). Another one is located within a predicted transmembrane protein that could contribute to drug resistance (Escandón et al., 2019). Drug transporters overexpression upon administering amphotericin B was also observed by Wasi et al. In their study, they found 8.7-fold increase in expression of a homolog of CDR6 ABC transporter (Wasi et al., 2019). In the search for more robust drugs and drug targets, we urgently need to better understand the structure and function of drug pumps in pathogenic fungi, as well as how allelic diversity and mutations can affect drug efficacy.

Echinocandins act through the non-competitive inhibition of FKS1 gene product called β(1→3) glucan synthase, which results in stopping production of glucan. Because of depleted glucan, the fungal cell becomes weak and prone to osmotic stress (de Oliveira Santos et al., 2018). *C. auris*' resistance to echinocandins has been linked to mutations S639F, S639P and S639Y that occur in the highly conserved hot-spot 1 of FKS1 and decrease the sensitivity of the enzyme to the drug (Bidaud et al., 2018; Hou et al., 2019). S639P in FKS1 was recently shown to be the most widespread mutation associated with echinocandin resistance (Chow et al., 2020). A recent multi-omics analysis revealed that although the cell wall remodeling enzymes concentration was lower in *C. auris* when compared to *C. albicans*, in a drug-resistant *C. auris* isolate (MIC fluconazole: > 256 μg/mL, MIC caspofungin: 2 μg/mL) cell wall integrity proteins were upregulated, suggesting that the cell wall metabolism can be adjusted in response to drug treatment (Zamith-Miranda et al., 2019).

Little is known about *C. auris* resistance mechanisms to other drug classes such as nucleoside analogs or allylamines (Jeffery-Smith et al., 2018). The nucleoside analogs class contains only 5-flucytosine (5FC) – a drug inhibiting RNA and DNA synthesis in pathogenic fungi (Rapp, 2004). One amino acid substitution (F211I) that is associated with 5FC resistance has been identified in the conserved FUR1 sequence encoding uracil phosphoribosyltransferase (Rhodes et al., 2018b). However, further work is required to understand how such polymorphisms may affect the functioning of the enzyme, which is responsible for the conversion of 5-fluorouracil into 5-fluoro-UMP acid monophosphate. For allylamines, a homolog of ABC transporter CDR6 was found to be significantly upregulated in drug-resistant *C. auris* following terbinafine treatment (Wasi et al., 2019).

DETECTION AND NOVEL TREATMENTS OF *C. auris*

Successful treatment of *C. auris* infection depends heavily on its accurate identification. In the early stages of infection, symptoms are non-specific and blood cultures typically remain negative (Pfaller and Castanheira, 2016). The resulting delay in diagnosis directly translates to decreased chances of survival; in the study of *C. auris* outbreak in a European hospital between 2016 and 2017, 41% of patients died within 1 month from infection (Ruiz-Gaitán et al., 2018).

C. auris does not possess phenotypic features that could easily distinguish it from other *Candida* spp. (Osei Sekyere, 2018). Depending on the strain it appears purple, red, pink or white on CHROMagar (Kordalewska and Perlin, 2019b) but unlike most types of yeast, it is able to withstand high temperatures (42°C) (Osei Sekyere, 2018). Many misidentifications related to automated tools such as VITEK 2, BD Phoenix, RapID Yeast Plus, API 20C have been reported to date. Ambaraghassi et al. (2019) demonstrated that VITEK 2 was unable to consistently identify *C. auris* and that the identification depended on the clade. While the tool identified correctly the South American clade ($n = 8$), its accuracy was variable for isolates from the African (7%, $n = 10$) and East Asian clades (0%, $n = 4$) (Ambaraghassi et al., 2019). Genomics analysis showed that the low identification rate was likely due to the deletion of the L-rhamnose 7-gene cluster in all clades except for the South African clade (Ambaraghassi et al., 2019). As one of 20 tests performed by the VITEK 2 platform is based on the ability of the tested organism to assimilate L-rhamnose (Graf et al., 2000, 2), the deletion of L-rhamnose gene cluster can have an impact on identification results. The most reliable way to identify *C. auris* without genomic sequencing is MALDI-TOF MS (Vatanshenassan et al., 2019). Although not all reference databases contain its protein profile, a free supplemental update is available from MicrobeNet (Lockhart et al., 2017a). A variety of groups have also had success with sub-genomic methods such as sequencing D1-D2 region of 28s ribosomal DNA (rDNA) or internal transcribed spacer region of rDNA (Jeffery-Smith et al., 2018). Unfortunately, access to such tools is limited in many community hospitals.

TABLE 4 | New antifungals in trials.

Company	Drug	Trial (Phase)	Activity	References
Amplyx	Fosmanogepix (APX001)*	*C. auris* (Ib), Candidemia (II)	Gwt1 inhibitor (novel)	Hager et al., 2018
Synexis	Ibrexafungerp*	*C. auris* (III)	Glucan synthase inhibitor (novel, orally available)	Berkow and Lockhart, 2017; Larkin et al., 2019
NQP 1598	VT-1598	*C. auris* (I)	CYP51 (Erg11p) inhibitor	Wiederhold et al., 2019
Mycovia	VT-1161	Candidiasis (III)	CYP51 (Erg11p) inhibitor	Brand et al., 2018, p. 2
Cidara	Rezafungin	Candidemia (III)	Long half-life echinocandin	Lepak et al., 2018

**Fosmanogepix (Hodges et al., 2017) and Ibrexafungerp (Juneja et al., 2019) are available in an emergency in fungi research centers such as University Hospital Graz (Graz), University Hospital Innsbruck (Innsbruck), Radboud University (Nijmegen) and University Hospital of Manchester (Manchester).*

The necessity for expeditious identification of *C. auris* in order to effectively treat patients and prevent outbreaks combined with slow current standard laboratory techniques creates a pressing need for new diagnostic tools that could rapidly recognize *C. auris* and its drug resistance patterns. Most of biochemical automated systems and MALDI-TOF MS require cultures, which can take up to 2 weeks to obtain (Kordalewska and Perlin, 2019a). To identify *C. auris* directly from skin swabs, molecular-based assays such as loop-mediated isothermal amplification (LAMP), T2 magnetic resonance and PCR/qPCR have been applied (Kordalewska and Perlin, 2019b). Since DNA can be isolated directly from the clinical sample, these tests can deliver diagnostic results within several hours (Kordalewska and Perlin, 2019a), which dramatically increases the probability of survival, given that the time window appropriate for initiating appropriate antifungal therapy in *Candida* bloodstream infection was estimated to 12 h (Morrell et al., 2005).

The choice of optimal *C. auris* treatment method depends on both the patient (age, previous use of antifungal medications, infection site, immune status) and the attacking pathogen (strain, possible biofilm formation, drug resistance patterns) (Dodgson et al., 2004; Felton et al., 2014; Bidaud et al., 2018; Moser et al., 2019). The mainstay of therapy is antibiotics. In adults, it is encouraged to begin the therapy with echinocandins even before receiving susceptibility test results (Bidaud et al., 2018). Amphotericin B should be considered for neonates, infants below 2 months of age and as a single or in combination with micafungin when monotherapy with echinocandins fails (Alfouzan et al., 2019; Park et al., 2019). Among azoles, the highest antifungal activity has been observed for itraconazole, isavuconazole and posaconazole (Bidaud et al., 2018), which are sometimes used as a secondary therapy. When voriconazole and micafungin are taken together they show greater effects when compared to the sum of the effects of these drugs taken separately (Cortegiani et al., 2018). While systemic antibiotic treatment is not advised for people colonized with *C. auris*, control measures should be followed in all cases (Bidaud et al., 2018). Invasive devices such as catheters and ventricular shunts should be removed as soon as they are no longer needed as they may be infected with a biofilm (Bidaud et al., 2018).

C. auris develops resistance rapidly while the patient is being treated and therefore it is crucial to use the available antifungals for the right amount of time and in the right dose (Jeffery-Smith et al., 2018). Close monitoring of drug susceptibility is necessary in both infection and colonization cases in order to identify changes in antifungal resistance (Bidaud et al., 2018). Furthermore, special care is required when administering fungistatic drugs as they may provide the opportunity for resistance to emerge (Berkow and Lockhart, 2017). A small number of new anti-fungal agents are showing successes in clinical trials that may become available for wider use in hospital settings in the upcoming years (**Table 4**).

MECHANISMS OF VIRULENCE IN *C. auris*

Stress resistance, thermotolerance, adherence to host cells, and immune evasion are important virulence traits across *Candida* species. Investigations of *C. auris* virulence traits often draw comparisons to the extensively-studied pathogen, *C. albicans*. The *C. auris* genome encodes several orthologs of known virulence factors in *C. albicans* including genes associated with biofilm formation, antifungal drug resistance, and phenotypic switching (Muñoz et al., 2018). Recent virulence, transcriptome, and other studies are highlighting how these conserved fungal virulence mechanisms may contribute to *C. auris*' emergence as a nosocomial pathogen (**Figure 2**).

Virulence

Conflicting reports abound regarding *C. auris*' virulence *in vivo* compared to other pathogenic *Candida* species. Depending on the isolate and infection model used, *C. auris* may be regarded as more virulent (Sherry et al., 2017), as virulent (Borman et al., 2016; Fakhim et al., 2018), or less virulent (Ben-Ami et al., 2017; Wang et al., 2018) than *C. albicans* in murine and invertebrate infection models. In studies utilizing the *Galleria mellonella* invertebrate infection model, *C. auris* isolates exhibit similar virulence phenotypes, or even slightly more virulent phenotypes, than *C. albicans* (Borman et al., 2016; Sherry et al., 2017).

Investigators have used immunocompetent and immunocompromised murine models of invasive candidiasis to evaluate *C. auris* virulence. In immunocompromised animals infected with Israeli *C. auris* clinical isolates, infection lead to rapid death within 5 days, but overall *C. auris* exhibited decreased virulence and lower kidney fungal burdens compared to *C. albicans* strain CBS 8837 (Ben-Ami et al., 2017). One study with immunocompetent animals established that two clade II *C. auris* isolates had similar virulence outcomes compared to

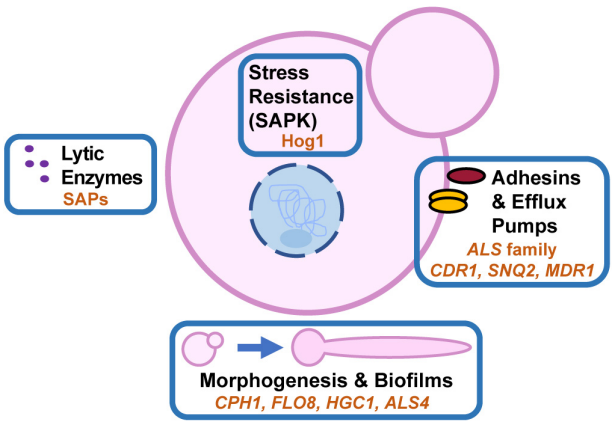

FIGURE 2 | Putative *C. auris* virulence factors. Key orthologs of *C. albicans* virulence factors that are transcriptionally induced during *C. auris* growth at 37°C are indicated by orange text within each box. *C. auris* Hog1 is the only conserved ortholog with *C. albicans* that has been experimentally confirmed to play a role in virulence.

one *C. albicans* clinical isolate (IFRC 1442) (Fakhim et al., 2018), while a study in China determined that the first *C. auris* isolate identified in China was significantly less virulent than the standard *C. albicans* laboratory strain SC5314 (Wang et al., 2018). To date, data from murine infection models are difficult to interpret due to inconsistencies in the *C. auris* and comparator *C. albicans* strains employed between studies. Consequently, it is not currently possible to speculate whether *C. auris* or individual clades of *C. auris* are generally more, less, or similarly virulent during mammalian infection compared to the prototypic pathogen *C. albicans*.

Phenotypic and genotypic variability between different *C. auris* isolates are plausible explanations for the discrepancies described in virulence studies. This variability is somewhat unsurprising given the broad geographical distribution and genetic diversity among clades of *C. auris* outbreaks, but also highlights our poor understanding of *C. auris* pathogenesis. Further characterization of virulence determinants, some of which will be discussed in this section, are important for understanding the virulence potential of this organism. The field would significantly benefit from standardizing virulence investigations by adopting one major *C. albicans* comparison strain and utilizing high-throughput *in vitro* methodologies to rapidly identify type strains for each *C. auris* clade that are suitable for comparative *in vivo* studies.

Lytic Enzymes

Lytic enzymes, such as secreted aspartyl proteases (SAPs), lipases, phospholipases, and hemolysins, are important virulence factors in human pathogenic fungi (Chaffin, 2008). These enzymes facilitate host cell invasion and tissue destruction by *C. albicans* (Polke et al., 2015). *C. auris* encodes orthologs of many known *C. albicans* lytic enzymes, including secreted aspartyl proteases, secreted lipases, and phospholipases (Chatterjee et al., 2015). Several studies have demonstrated lytic activity for *C. auris* SAPs (Yue et al., 2018), phospholipases (Larkin et al., 2017), and hemolysin (Kumar et al., 2015), but little is known about how the expression profiles of these enzymes compare to their *C. albicans* orthologs *in vitro* or *in vivo*. Two SAP orthologs were transcriptionally induced in *C. auris* filamentous cells compared to yeast cells (Yue et al., 2018), but their relative roles in virulence remain unknown. Further molecular and virulence studies are necessary to determine the importance of lytic enzymes to *C. auris*' infection strategy.

Filamentous Growth

While filamentation is integral to *C. albicans* virulence (Zheng et al., 2004), its contribution to *C. auris* virulence is less certain given that *in vivo* evidence to date has identified only yeast cells in animal tissues (Ben-Ami et al., 2017). Interestingly, *in vivo* passage can confer a filamentation-competent (FC) phenotype, but FC and yeast cells have comparable virulence in mice suggesting that filamentation is dispensable for *C. auris* virulence (Yue et al., 2018).

In vitro C. auris filamentation occurs under a restricted and/or atypical set of growth conditions compared to *C. albicans* (Wang et al., 2018; Yue et al., 2018). Like *C. albicans*, Hsp90 depletion or pharmacological inhibition induces filamentous growth and the expression of adhesins and cell wall genes orthologous to *C. albicans* filament-associated genes (Kim et al., 2019). During FC-triggered filamentous growth, orthologs of *C. albicans CPH1* and *FLO8*, which encode transcriptional regulators of filamentous growth, were induced in *C. auris* filamentous cells compared to yeast (Yue et al., 2018). In addition, orthologs of *C. albicans* filament-associated genes were upregulated during *C. auris* filamentation, including the G1 cyclin-related gene *HGC1* and glycosylphosphatidylinositol (GPI) anchored gene *ALS4*. However, there were key differences in the filamentation transcriptomes for *C. auris* relative to *C. albicans*. *EFG1*, an important transcriptional regulator of filamentation in *C. albicans*, was down-regulated in *C. auris* filamentous cells. Other *C. albicans* filament-associated cell wall orthologs were preferentially expressed during *C. auris* yeast growth (*PGA34, PGA38,* and *PGA58*) (Yue et al., 2018). Thus, while *C. auris* shares some transcriptomic aspects of the *C. albicans* filamentous growth program, the role of *C. auris* filamentation and filament-associated genes in its pathogenicity requires further study.

Adherence and Biofilm Formation

Adherence to host cells is essential to microbial colonization, persistence, and virulence (Mayer et al., 2013; Tsui et al., 2016). In addition, microbe-microbe adherence mediates the formation of microbial communities, or biofilms, which are an important virulence trait in *Candida* species that confer enhanced antimicrobial resistance. The *C. auris* genome encodes several orthologs of *C. albicans* adhesins implicated in biofilm formation and virulence. Clade II strains of *C. auris*, which predominantly cause ear infections, have lost significant sections of subtelomeric regions that are enriched in putative adhesins, but are conserved in strains from Clades I, III, and IV (Muñoz et al., 2019).

Perhaps future studies will unravel what role these subtelomeric-encoded adhesins have in human colonization and virulence. Recent studies have identified differentially regulated adhesin expression under physiologically-relevant conditions, including growth at 37°C in RPMI medium (Kean et al., 2018; Yue et al., 2018).

Several GPI-anchored cell wall proteins contribute to microbe-microbe and microbe-host adherence. *ALS4* is a member of the well-characterized *ALS* adhesin gene family in *C. albicans* (Zhao et al., 2005) and its ortholog is also differentially expressed during *C. auris* filamentous growth (Yue et al., 2018). Other GPI-anchored cell wall genes and potential adhesins were upregulated during *C. auris in vitro* biofilm formation compared to planktonic cells (*IFF4, CSA1, PGA26, PGA52,* and *HYR3*) (Kean et al., 2018). Furthermore, putative orthologs of *ALS3*, the *C. albicans* adhesin and invasin that induces host cell endocytosis of *C. albicans* hyphae (Liu and Filler, 2011), were detected on the *C. auris* cell surface by an anti-Als3p antibody (Singh et al., 2019). In addition, two *ALS* family orthologs, *ALS1* and *ALS5*, were expressed in biofilms (Kean et al., 2018). Each adhesin may play an important role in *C. auris* biofilm formation, persistence in hospital environments, and virulence, but further molecular studies are required to tease apart their independent contributions.

Several efflux pumps were induced in *C. auris* biofilms versus planktonic cells (Kean et al., 2018). ATP-binding cassette (ABC) transporters *SNQ2* and *CDR1* and major facilitator superfamily (MFS) genes *YHD3, RDC3*, and *MDR1* were upregulated between 2- and 4-fold in mature 24 h biofilms compared to planktonic cells. In line with these observations, efflux pump activity was elevated in mature biofilms relative to planktonic cells (Kean et al., 2018). Altogether, these findings suggest that biofilm formation may promote *C. auris* multi-drug resistance and virulence. Therefore, as with *C. albicans*, clinical measures to tackle *C. auris* drug resistance should consider the possibility that biofilms may harbor more drug-resistant cells and reduce the bioavailability of therapeutics.

Stress Resistance and Persistence

One of the fascinating traits linked to *C. auris*' emergence as a nosocomial pathogen is its ability to persist on abiotic hospital surfaces under stringent cleaning protocols (Schelenz et al., 2016; Welsh et al., 2017). Viable *C. auris* can be recovered from plastic surfaces or be detected via esterase activity for up to 2 and 4 weeks post-contamination, respectively (Welsh et al., 2017). These findings pose an interesting question: can *C. auris* form viable but non-culturable cells that persist in hospital environments? Although no studies to date have directly addressed this question, current metabolomic, transcriptomic, and molecular studies hold clues to *C. auris*' stress tolerance and persistence.

C. auris metabolism favors respiration as evidenced by enrichment in glycolytic and sugar transporter gene expression during yeast growth (Yue et al., 2018) and TCA cycle protein enrichment compared to *C. albicans* (Zamith-Miranda et al., 2019). Respiratory metabolism enhances ATP production and can reduce oxidative stress in *C. albicans*, thus promoting *in vivo* fitness and fluconazole resistance (Guo et al., 2017). Furthermore, *C. auris* lipid profiles show elevated levels of ergosterol and structural lipids compared to *C. albicans*, which may influence stress and antifungal resistance (Zamith-Miranda et al., 2019).

In addition, iron transport (Kean et al., 2018) and iron metabolism-associated genes (Yue et al., 2018) were upregulated in *C. auris* biofilm and filamentous cells, respectively. The *C. auris* genome provides evidence for expansion of siderophore-based iron transporters compared to *C. albicans*, further highlighting the importance of iron acquisition in this pathogen (Muñoz et al., 2018). Iron is an essential micronutrient that is depleted *via* nutritional immunity mechanisms *in vivo*, thus upregulation of iron uptake and metabolism-associated genes may improve *C. auris* fitness during infection. However, the contribution of *C. auris* iron transport gene families to virulence and drug resistance are currently unknown. Still, the expansion of the iron transport gene family suggests that iron deprivation may play an influential role in *C. auris*' environmental reservoir.

Recent evidence has demonstrated that the stress-activated protein kinase Hog1 plays an evolutionarily conserved role in *C. auris* stress resistance, cell wall homeostasis, and virulence (Day et al., 2018). *C. auris* Hog1 shares 87% identity with the *C. albicans* Hog1 sequence. Consistent with findings from other *Candida* species, *C. auris HOG1* was required for osmotic stress resistance and SDS protection. However, *C. auris HOG1* was not required for weak acid or nitrosative stress tolerance, which contrasts its role in *C. glabrata* and *C. albicans*, respectively (Day et al., 2018). However, we do not know which *C. auris* genes are regulated in a Hog1-dependent manner or which Hog1 targets are responsible for these stress-adaptive phenotypes. Future transcriptomics and molecular studies will hopefully reveal which *C. auris* stress response genes are regulated via Hog1, which will highlight the evolutionary diversification of stress response circuitry across *Candida* species.

EPIGENETICS AND GENE REGULATION IN *C. auris*

Phenotypic plasticity is the interaction between a given genotype and the environment to produce multiple phenotypes. This plasticity is often the result of alterations in gene expression, which can be influenced by genetic or epigenetic mechanisms. In pathogens, phenotypic plasticity is often viewed as system for evolutionary bet-hedging to ensure microbial survival under shifting and/or hostile environmental conditions (Carja and Plotkin, 2017).

In the case of *C. auris*, very little is known about epigenetics and gene regulation or how these contribute to pathogenesis. As with other biological and virulence traits, early insights into *C. auris* epigenetics have been informed by previous work in *C. albicans*. Chromatin modification, including histone acetylation and deacetylation, plays an important role in *C. albicans* virulence (Garnaud et al., 2016; Kuchler et al., 2016). *C. auris* histone proteins and modifying enzymes were

differentially expressed during filamentous growth relative to yeast, suggesting that epigenetic mechanisms may influence gene expression patterns in yeast and FC cells (Yue et al., 2018). In fact, the observation that *in vivo* passage can trigger a heritable, filamentation-competent phenotype is suggestive of epigenetic regulation, but more investigation is required to understand the mechanisms underlying this trait and its role in virulence.

Currently, available data demonstrates that *C. auris* has significant similarities in gene expression for important established virulence mechanisms in *C. albicans*, but there are also significant differences (Kean et al., 2018; Yue et al., 2018). Phenotypic heterogeneity between different *C. auris* clades provides an opportunity to understand how genetic mechanisms contribute to pathogenesis (*via* for example gene knock out or mutagenesis studies). Indeed, the adaptation of *C. albicans* gene deletion technologies for use in *C. auris* will enable future molecular investigations to understand gene regulatory networks and virulence in this emerging pathogen. Consequently, the *C. albicans NAT1*-Clox system has been successfully employed to disrupt *C. auris HOG1* and demonstrate its conserved role in stress responses (Shahana et al., 2014; Day et al., 2018). Future pathfinding molecular studies should reveal the conservation and divergence of gene regulatory networks in *C. albicans* and *C. auris* and highlight new avenues for antifungal development.

SUMMARY

Genomics and other omics studies have provided significant insight into the biology and pathogenesis of *C. auris* since its emergence as a modern human fungal pathogen. However, several questions remain about the evolution and fitness of this multi-drug resistant yeast which require further study.

AUTHOR CONTRIBUTIONS

All authors wrote and reviewed the manuscript and contributed and worked on figures.

FUNDING

RF was supported by MRC grant MR/N006364/2 and a Wellcome Trust Seed Award (215239/Z/19/Z).

ACKNOWLEDGMENTS

We would like to give thanks to Carolina Coelho for helpful discussions and assistance with **Figure 1** and Jose Muñoz for valuable feedback on the manuscript.

REFERENCES

Abdalhamid, B., Almaghrabi, R., Althawadi, S., and Omrani, A. (2018). First report of *Candida auris* infections from Saudi Arabia. *J. Infect. Public Health* 11, 598–599. doi: 10.1016/j.jiph.2018.05.010

Abram, N. J., McGregor, H. V., Tierney, J. E., Evans, M. N., McKay, N. P., Kaufman, D. S., et al. (2016). Early onset of industrial-era warming across the oceans and continents. *Nature* 536, 411–418. doi: 10.1038/nature19082

Adam, R. D., Revathi, G., Okinda, N., Fontaine, M., Shah, J., Kagotho, E., et al. (2019). Analysis of *Candida auris* fungemia at a single facility in Kenya. *Int. J. Infect. Dis. IJID Off. Publ. Int. Soc. Infect. Dis.* 85, 182–187. doi: 10.1016/j.ijid.2019.06.001

Aguilar-Zapata, D., Petraitiene, R., and Petraitis, V. (2015). Echinocandins: the expanding antifungal armamentarium. *Clin. Infect. Dis. Off. Publ. Infect. Dis. Soc. Am.* 61(Suppl. 6), S604–S611. doi: 10.1093/cid/civ814

Alatoom, A., Sartawi, M., Lawlor, K., AbdelWareth, L., Thomsen, J., Nusair, A., et al. (2018). Persistent candidemia despite appropriate fungal therapy: first case of *Candida auris* from the United Arab Emirates. *Int. J. Infect. Dis. IJID Off. Publ. Int. Soc. Infect. Dis.* 70, 36–37. doi: 10.1016/j.ijid.2018.02.005

Alfouzan, W., Dhar, R., Albarrag, A., and Al-Abdely, H. (2019). The emerging pathogen *Candida auris*: a focus on the middle-Eastern countries. *J. Infect. Public Health* 12, 451–459. doi: 10.1016/j.jiph.2019.03.009

Al-Yasiri, M. H., Normand, A.-C., L'Ollivier, C., Lachaud, L., Bourgeois, N., Rebaudet, S., et al. (2016). Opportunistic fungal pathogen *Candida glabrata* circulates between humans and yellow-legged gulls. *Sci. Rep.* 6:36157. doi: 10.1038/srep36157

Ambaraghassi, G., Dufresne, P. J., Dufresne, S. F., Vallières, É, Muñoz, J. F., Cuomo, C. A., et al. (2019). Identification of *Candida auris* by use of the updated Vitek 2 yeast identification system, version 8.01: a multilaboratory evaluation study. *J. Clin. Microbiol.* 57:e00884-19. doi: 10.1128/JCM.00884-19

Angoulvant, A., Guitard, J., and Hennequin, C. (2016). Old and new pathogenic Nakaseomyces species: epidemiology, biology, identification, pathogenicity and antifungal resistance. *FEMS Yeast Res.* 16:fov114. doi: 10.1093/femsyr/fov114

Antifungal Susceptibility Testing and Interpretation (2019). Available online at: https://www.cdc.gov/fungal/candida-auris/c-auris-antifungal.html (accessed November 26, 2019). doi: 10.1093/femsyr/fov114

Araúz, A. B., Caceres, D. H., Santiago, E., Armstrong, P., Arosemena, S., Ramos, C., et al. (2018). Isolation of *Candida auris* from 9 patients in Central America: importance of accurate diagnosis and susceptibility testing. *Mycoses* 61, 44–47. doi: 10.1111/myc.12709

Arendrup, M. C., Prakash, A., Meletiadis, J., Sharma, C., and Chowdhary, A. (2017). Comparison of EUCAST and CLSI reference microdilution MICs of eight antifungal compounds for *Candida auris* and associated tentative epidemiological cutoff values. *Antimicrob. Agents Chemother.* 61:e00485-17. doi: 10.1128/AAC.00485-17

Aulie, A. (1971). Body temperatures in pigeons and budgerigars during sustained flight. *Comp. Biochem. Physiol. A Physiol.* 39, 173–176. doi: 10.1016/0300-9629(71)90074-0

Bandeira, A. C., Filho, J. M., and de Almeida Ramos, K. (2016). Reversible cardiomyopathy secondary to Amphotericin-B. *Med. Mycol. Case Rep.* 13, 19–21. doi: 10.1016/j.mmcr.2016.10.001

Barantsevich, N. E., Orlova, O. E., Shlyakhto, E. V., Johnson, E. M., Woodford, N., Lass-Floerl, C., et al. (2019). Emergence of *Candida auris* in Russia. *J. Hosp. Infect.* 102, 445–448. doi: 10.1016/j.jhin.2019.02.021

Ben-Ami, R., Berman, J., Novikov, A., Bash, E., Shachor-Meyouhas, Y., Zakin, S., et al. (2017). Multidrug-resistant *Candida haemulonii* and *C. auris*, Tel Aviv, Israel. *Emerg. Infect. Dis.* 23, 195–203. doi: 10.3201/eid2302.161486

Berkow, E. L., and Lockhart, S. R. (2017). Fluconazole resistance in *Candida* species: a current perspective. *Infect. Drug Resist.* 10, 237–245. doi: 10.2147/IDR.S118892

Bhattacharya, S., Holowka, T., Orner, E. P., and Fries, B. C. (2019). Gene duplication associated with increased Fluconazole tolerance in *Candida auris* cells of advanced generational age. *Sci. Rep.* 9:5052. doi: 10.1038/s41598-019-41513-6

Bidaud, A. L., Chowdhary, A., and Dannaoui, E. (2018). *Candida auris*: an emerging drug resistant yeast – a mini-review. *J. Mycol. Medicale* 28, 568–573. doi: 10.1016/j.mycmed.2018.06.007

Borman, A. M., Szekely, A., and Johnson, E. M. (2016). Comparative pathogenicity of United Kingdom isolates of the emerging pathogen *Candida auris* and other key pathogenic *Candida* species. *mSphere* 1:e00189-16. doi: 10.1128/mSphere.00189-16

Brand, S. R., Degenhardt, T. P., Person, K., Sobel, J. D., Nyirjesy, P., Schotzinger, R. J., et al. (2018). A phase 2, randomized, double-blind, placebo-controlled, dose-ranging study to evaluate the efficacy and safety of orally administered VT-1161 in the treatment of recurrent vulvovaginal candidiasis. *Am. J. Obstet. Gynecol.* 218, 624.e1–624.e9. doi: 10.1016/j.ajog.2018.03.001

Byrnes, E. J. III, Li, W., Lewit, Y., Ma, H., Voelz, K., Ren, P., et al. (2010). Emergence and pathogenicity of highly virulent *Cryptococcus gattii* genotypes in the Northwest United States. *PLoS Pathog.* 6:e1000850. doi: 10.1371/journal.ppat.1000850

Carja, O., and Plotkin, J. B. (2017). The evolutionary advantage of heritable phenotypic heterogeneity. *Sci. Rep.* 7:5090. doi: 10.1038/s41598-017-05214-2

Casadevall, A., Kontoyiannis, D. P., and Robert, V. (2019). On the emergence of *Candida auris*: climate change, azoles, swamps, and birds. *mBio* 10:e001397-19. doi: 10.1128/mBio.01397-19

Cendejas-Bueno, E., Kolecka, A., Alastruey-Izquierdo, A., Theelen, B., Groenewald, M., Kostrzewa, M., et al. (2012). Reclassification of the *Candida haemulonii* complex as *Candida haemulonii* (*C. haemulonii* Group I), *C. duobushaemulonii sp. nov.* (*C. haemulonii* Group II), and *C. haemulonii var. vulnera var. nov.*: three multiresistant human pathogenic yeasts. *J. Clin. Microbiol.* 50, 3641–3651. doi: 10.1128/JCM.02248-12

Chaffin, W. L. (2008). *Candida albicans* cell wall proteins. *Microbiol. Mol. Biol. Rev. MMBR* 72, 495–544. doi: 10.1128/MMBR.00032-07

Chatterjee, S., Alampalli, S. V., Nageshan, R. K., Chettiar, S. T., Joshi, S., and Tatu, U. S. (2015). Draft genome of a commonly misdiagnosed multidrug resistant pathogen *Candida auris*. *BMC Genomics* 16:686. doi: 10.1186/s12864-015-1863-z

Chow, N. A., de Groot, T., Badali, H., Abastabar, M., Chiller, T. M., and Meis, J. F. (2019). Potential fifth clade of *Candida auris*. *Emerg. Infect. Dis.* 25, 1780–1781. doi: 10.3201/eid2509.190686

Chow, N. A., Gade, L., Tsay, S. V., Forsberg, K., Greenko, J. A., Southwick, K. L., et al. (2018). Multiple introductions and subsequent transmission of multidrug-resistant *Candida auris* in the USA: a molecular epidemiological survey. *Lancet Infect. Dis.* 18, 1377–1384. doi: 10.1016/S1473-3099(18)30597-8

Chow, N. A., Muñoz, J. F., Gade, L., Berkow, E., Li, X., Welsh, R. M., et al. (2020). Tracing the evolutionary history and global expansion of *Candida auris* using population genomic analyses. *bioRxiv* [Preprint]. doi: 10.1101/2020.01.06.896548

Chowdhary, A., Prakash, A., Sharma, C., Kordalewska, M., Kumar, A., Sarma, S., et al. (2018). A multicentre study of antifungal susceptibility patterns among 350 *Candida auris* isolates (2009-17) in India: role of the ERG11 and FKS1 genes in azole and echinocandin resistance. *J. Antimicrob. Chemother.* 73, 891–899. doi: 10.1093/jac/dkx480

Cortegiani, A., Misseri, G., Fasciana, T., Giammanco, A., Giarratano, A., and Chowdhary, A. (2018). Epidemiology, clinical characteristics, resistance, and treatment of infections by *Candida auris*. *J. Intensive Care* 6:69. doi: 10.1186/s40560-018-0342-4

Day, A. M., McNiff, M. M., da Silva Dantas, A., Gow, N. A. R., and Quinn, J. (2018). Hog1 regulates stress tolerance and virulence in the emerging fungal pathogen *Candida auris*. *mSphere* 3:e00506-18. doi: 10.1128/mSphere.00506-18

de Oliveira Santos, G. C., Vasconcelos, C. C., Lopes, A. J. O., de Sousa Cartágenes, M., do, S., Filho, A. K. D. B., et al. (2018). *Candida* infections and therapeutic strategies: mechanisms of action for traditional and alternative agents. *Front. Microbiol.* 9:1351. doi: 10.3389/fmicb.2018.01351

Debnath, S., and Addya, S. (2014). Structural basis for heterogeneous phenotype of ERG11 dependent Azole resistance in *C. albicans* clinical isolates. *SpringerPlus* 3:660. doi: 10.1186/2193-1801-3-660

Dodgson, A. R., Dodgson, K. J., Pujol, C., Pfaller, M. A., and Soll, D. R. (2004). Clade-specific flucytosine resistance is due to a single nucleotide change in the FUR1 gene of *Candida albicans*. *Antimicrob. Agents Chemother.* 48, 2223–2227. doi: 10.1128/AAC.48.6.2223-2227.2004

Dukik, K., Muñoz, J. F., Jiang, Y., Feng, P., Sigler, L., Stielow, J. B., et al. (2017). Novel taxa of thermally dimorphic systemic pathogens in the Ajellomycetaceae (Onygenales). *Mycoses* 60, 296–309. doi: 10.1111/myc.12601

Escandón, P., Chow, N. A., Caceres, D. H., Gade, L., Berkow, E. L., Armstrong, P., et al. (2019). Molecular epidemiology of *Candida auris* in Colombia reveals a highly related, countrywide colonization with regional patterns in Amphotericin B resistance. *Clin. Infect. Dis. Off. Publ. Infect. Dis. Soc. Am.* 68, 15–21. doi: 10.1093/cid/ciy411

Fakhim, H., Vaezi, A., Dannaoui, E., Chowdhary, A., Nasiry, D., Faeli, L., et al. (2018). Comparative virulence of *Candida auris* with *Candida haemulonii*, *Candida glabrata* and *Candida albicans* in a murine model. *Mycoses* 61, 377–382. doi: 10.1111/myc.12754

Farrer, R. A. (2019). Batrachochytrium salamandrivorans. *Trends Microbiol.* 27, 892–893. doi: 10.1016/j.tim.2019.04.009

Farrer, R. A., and Fisher, M. C. (2017). Describing genomic and epigenomic traits underpinning emerging fungal pathogens. *Adv. Genet.* 100, 73–140. doi: 10.1016/bs.adgen.2017.09.009

Felton, T., Troke, P. F., and Hope, W. W. (2014). Tissue penetration of antifungal agents. *Clin. Microbiol. Rev.* 27, 68–88. doi: 10.1128/CMR.00046-13

Fraser, J. A., Giles, S. S., Wenink, E. C., Geunes-Boyer, S. G., Wright, J. R., Diezmann, S., et al. (2005). Same-sex mating and the origin of the Vancouver Island *Cryptococcus gattii* outbreak. *Nature* 437, 1360–1364. doi: 10.1038/nature04220

Garcia-Solache, M. A., and Casadevall, A. (2010). Global warming will bring new fungal diseases for mammals. *mBio* 1:e00061-10. doi: 10.1128/mBio.00061-10

Garnaud, C., Champleboux, M., Maubon, D., Cornet, M., and Govin, J. (2016). Histone deacetylases and their inhibition in *Candida* species. *Front. Microbiol.* 7:1238. doi: 10.3389/fmicb.2016.01238

Ghannoum, M. A., and Rice, L. B. (1999). Antifungal agents: mode of action, mechanisms of resistance, and correlation of these mechanisms with bacterial resistance. *Clin. Microbiol. Rev.* 12, 501–517. doi: 10.1128/cmr.12.4.501

Gleeson, M. (1998). Temperature regulation during exercise. *Int. J. Sports Med.* 19(Suppl. 2), S96–S99. doi: 10.1055/s-2007-971967

Govender, N. P., Magobo, R. E., Mpembe, R., Mhlanga, M., Matlapeng, P., Corcoran, C., et al. (2018). *Candida auris* in South Africa, 2012–2016. *Emerg. Infect. Dis.* 24, 2036–2040. doi: 10.3201/eid2411.180368

Graf, B., Adam, T., Zill, E., and Göbel, U. B. (2000). Evaluation of the VITEK 2 system for rapid identification of yeasts and yeast-like organisms. *J. Clin. Microbiol.* 38, 1782–1785. doi: 10.1128/jcm.38.5.1782-1785.2000

Guo, H., Xie, S., Li, S., Song, Y., Zhong, X., and Zhang, H. (2017). Involvement of mitochondrial aerobic respiratory activity in efflux-mediated resistance of *C. albicans* to fluconazole. *J. Mycol. Med.* 27, 339–344. doi: 10.1016/j.mycmed.2017.04.004

Hager, C. L., Larkin, E. L., Long, L., Zohra Abidi, F., Shaw, K. J., and Ghannoum, M. A. (2018). In Vitro and *In Vivo* evaluation of the antifungal activity of APX001A/APX001 against *Candida auris*. *Antimicrob. Agents Chemother.* 62:e02319-17. doi: 10.1128/AAC.02319-17

Hammoud, M. S., Al-Taiar, A., Fouad, M., Raina, A., and Khan, Z. (2013). Persistent candidemia in neonatal care units: risk factors and clinical significance. *Int. J. Infect. Dis. IJID Off. Publ. Int. Soc. Infect. Dis.* 17, e624–e628. doi: 10.1016/j.ijid.2012.11.020

Hamprecht, A., Barber, A. E., Mellinghoff, S. C., Thelen, P., Walther, G., Yu, Y., et al. (2019). *Candida auris* in Germany and previous exposure to foreign healthcare. *Emerg. Infect. Dis.* 25, 1763–1765. doi: 10.3201/eid2509.190262

Healey, K. R., Kordalewska, M., Jiménez Ortigosa, C., Singh, A., Berrío, I., Chowdhary, A., et al. (2018). Limited ERG11 mutations identified in isolates of *Candida auris* directly contribute to reduced azole susceptibility. *Antimicrob. Agents Chemother.* 62:e01427-18. doi: 10.1128/AAC.01427-18

Heath, C. H., Dyer, J. R., Pang, S., Coombs, G. W., and Gardam, D. J. (2019). *Candida auris* sternal osteomyelitis in a man from Kenya visiting Australia, 2015. *Emerg. Infect. Dis.* 25, 192–194. doi: 10.3201/eid2501.181321

Hodges, M. R., Ople, E., Shaw, K. J., Mansbach, R., Van Marle, S. J., Van Hoogdalem, E.-J., et al. (2017). First-in-human study to assess safety, tolerability and pharmacokinetics of APX001 administered by intravenous infusion to healthy subjects. *Open Forum Infect. Dis.* 4, S526–S526. doi: 10.1093/ofid/ofx163.1370

Hou, X., Lee, A., Jiménez-Ortigosa, C., Kordalewska, M., Perlin, D. S., and Zhao, Y. (2019). Rapid detection of ERG11-associated azole resistance and FKS-associated echinocandin resistance in *Candida auris*. *Antimicrob. Agents Chemother.* 63:e01811-18. doi: 10.1128/AAC.01811-18

Jackson, B. R., Chow, N., Forsberg, K., Litvintseva, A. P., Lockhart, S. R., Welsh, R., et al. (2019). On the origins of a species: what might explain the rise of *Candida auris*? *J. Fungi Basel Switz* 5:58. doi: 10.3390/jof5030058

Jeffery-Smith, A., Taori, S. K., Schelenz, S., Jeffery, K., Johnson, E. M., Borman, A., et al. (2018). *Candida auris*: a review of the Literature. *Clin. Microbiol. Rev.* 31:e00029-17. doi: 10.1128/CMR.00029-17

Juneja, D., Singh, O., Tarai, B., and Angulo, D. A. (2019). "Successful treatment of two patients with Candida auris candidemia with the investigational agent, oral Ibrexafungerp (formerly SCY-078), from the CARES Study," in *Poster at the 29th European Congress of Clinical Microbiology and Infectious Diseases with Amsterdam*, The Netherlands.

Kamiński, D. M. (2014). Recent progress in the study of the interactions of amphotericin B with cholesterol and ergosterol in lipid environments. *Eur. Biophys. J. EBJ* 43, 453–467. doi: 10.1007/s00249-014-0983-8

Kathuria, S., Singh, P. K., Sharma, C., Prakash, A., Masih, A., Kumar, A., et al. (2015). Multidrug-resistant *Candida auris* misidentified as *Candida haemulonii*: characterization by matrix-assisted laser desorption ionization–time of flight mass spectrometry and DNA sequencing and Its antifungal susceptibility profile variability by Vitek 2, CLSI broth microdilution, and etest method. *J. Clin. Microbiol.* 53, 1823–1830. doi: 10.1128/JCM.00367-15

Kean, R., Delaney, C., Sherry, L., Borman, A., Johnson, E. M., Richardson, M. D., et al. (2018). Transcriptome assembly and profiling of *Candida auris* reveals novel insights into biofilm-mediated resistance. *mSphere* 3:e00334-18. doi: 10.1128/mSphere.00334-18

Kean, R., and Ramage, G. (2019). Combined antifungal resistance and biofilm tolerance: the global threat of *Candida auris*. *mSphere* 4:e00458-19. doi: 10.1128/mSphere.00458-19

Khan, Z., Ahmad, S., Benwan, K., Purohit, P., Al-Obaid, I., Bafna, R., et al. (2018). Invasive *Candida auris* infections in Kuwait hospitals: epidemiology, antifungal treatment and outcome. *Infection* 46, 641–650. doi: 10.1007/s15010-018-1164-y

Khan, Z. U., Al-Sweih, N. A., Ahmad, S., Al-Kazemi, N., Khan, S., Joseph, L., et al. (2007). Outbreak of fungemia among neonates caused by *Candida haemulonii* resistant to amphotericin B, itraconazole, and fluconazole. *J. Clin. Microbiol.* 45, 2025–2027. doi: 10.1128/JCM.00222-07

Kim, S. H., Iyer, K. R., Pardeshi, L., Muñoz, J. F., Robbins, N., Cuomo, C. A., et al. (2019). Genetic analysis of *Candida auris* implicates Hsp90 in morphogenesis and azole tolerance and Cdr1 in azole resistance. *mBio* 10:e02529-18. doi: 10.1128/mBio.02529-18

Kohlenberg, A., Struelens, M. J., Monnet, D. L., and Plachouras, D. (2018). *Candida auris*: epidemiological situation, laboratory capacity and preparedness in European Union and European Economic Area countries, 2013 to 2017. *Eurosurveillance* 23:18-00136. doi: 10.2807/1560-7917.ES.2018.23.13.18-00136

Kordalewska, M., and Perlin, D. S. (2019a). Identification of drug resistant *Candida auris*. *Front. Microbiol.* 10:1918. doi: 10.3389/fmicb.2019.01918

Kordalewska, M., and Perlin, D. S. (2019b). Molecular diagnostics in the times of surveillance for *Candida auris*. *J. Fungi* 5:77. doi: 10.3390/jof5030077

Kuchler, K., Jenull, S., Shivarathri, R., and Chauhan, N. (2016). Fungal KATs/KDACs: a new highway to better antifungal drugs? *PLoS Pathog.* 12:e1005938. doi: 10.1371/journal.ppat.1005938

Kumar, D., Banerjee, T., Pratap, C. B., and Tilak, R. (2015). Itraconazole-resistant *Candida auris* with phospholipase, proteinase and hemolysin activity from a case of vulvovaginitis. *J. Infect. Dev. Ctries.* 9, 435–437. doi: 10.3855/jidc.4582

Kwon, Y. J., Shin, J. H., Byun, S. A., Choi, M. J., Won, E. J., Lee, D., et al. (2019). *Candida auris* clinical isolates from South Korea: identification, antifungal susceptibility, and genotyping. *J. Clin. Microbiol.* 57:e01624-18. doi: 10.1128/JCM.01624-18

Larkin, E., Hager, C., Chandra, J., Mukherjee, P. K., Retuerto, M., Salem, I., et al. (2017). The emerging pathogen *Candida auris*: growth phenotype, virulence factors, activity of antifungals, and effect of SCY-078, a novel glucan synthesis inhibitor, on growth morphology and biofilm formation. *Antimicrob. Agents Chemother.* 61:e02396-16. doi: 10.1128/AAC.02396-16

Larkin, E. L., Long, L., Isham, N., Borroto-Esoda, K., Barat, S., Angulo, D., et al. (2019). A novel 1,3-Beta-d-Glucan Inhibitor, Ibrexafungerp (Formerly SCY-078), shows potent activity in the lower pH environment of vulvovaginitis. *Antimicrob. Agents Chemother.* 63:e02611-18. doi: 10.1128/AAC.02611-18

Leach, M. D., Farrer, R. A., Tan, K., Miao, Z., Walker, L. A., Cuomo, C. A., et al. (2016). Hsf1 and Hsp90 orchestrate temperature-dependent global transcriptional remodelling and chromatin architecture in *Candida albicans*. *Nat. Commun.* 7:11704. doi: 10.1038/ncomms11704

Lee, W. G., Shin, J. H., Uh, Y., Kang, M. G., Kim, S. H., Park, K. H., et al. (2011). First three reported cases of nosocomial fungemia caused by *Candida auris*. *J. Clin. Microbiol.* 49, 3139–3142. doi: 10.1128/JCM.00319-11

Lehmann, P. F., Wu, L. C., Pruitt, W. R., Meyer, S. A., and Ahearn, D. G. (1993). Unrelatedness of groups of yeasts within the *Candida haemulonii* complex. *J. Clin. Microbiol.* 31, 1683–1687. doi: 10.1128/jcm.31.7.1683-1687.1993

Lepak, A. J., Zhao, M., and Andes, D. R. (2018). Pharmacodynamic evaluation of Rezafungin (CD101) against *Candida auris* in the neutropenic mouse invasive candidiasis model. *Antimicrob. Agents Chemother.* 62:e01572-18. doi: 10.1128/AAC.01572-18

Liu, Y., and Filler, S. G. (2011). *Candida albicans* Als3, a multifunctional adhesin and invasin. *Eukaryot. Cell* 10, 168–173. doi: 10.1128/EC.00279-10

Lockhart, S. R., Berkow, E. L., Chow, N., and Welsh, R. M. (2017a). *Candida auris* for the clinical microbiology laboratory: not your grandfather's *Candida* species. *Clin. Microbiol. Newsl.* 39, 99–103. doi: 10.1016/j.clinmicnews.2017.06.003

Lockhart, S. R., Etienne, K. A., Vallabhaneni, S., Farooqi, J., Chowdhary, A., Govender, N. P., et al. (2017b). Simultaneous emergence of multidrug-resistant *Candida auris* on 3 continents Cconfirmed by whole-genome sequencing and epidemiological analyses. *Clin. Infect. Dis. Off. Publ. Infect. Dis. Soc. Am.* 64, 134–140. doi: 10.1093/cid/ciw691

Maras, B., Angiolella, L., Mignogna, G., Vavala, E., Macone, A., Colone, M., et al. (2014). Glutathione metabolism in *Candida albicans* resistant strains to fluconazole and micafungin. *PLoS One* 9:e98387. doi: 10.1371/journal.pone.0098387

Marichal, P., Koymans, L., Willemsens, S., Bellens, D., Verhasselt, P., Luyten, W., et al. (1999). Contribution of mutations in the cytochrome P450 14alpha-demethylase (Erg11p, Cyp51p) to azole resistance in *Candida albicans*. *Microbiol. Read. Engl.* 145(Pt 10), 2701–2713. doi: 10.1099/00221287-145-10-2701

Mayer, F. L., Wilson, D., and Hube, B. (2013). *Candida albicans* pathogenicity mechanisms. *Virulence* 4, 119–128. doi: 10.4161/viru.22913

Mohd Tap, R., Lim, T. C., Kamarudin, N. A., Ginsapu, S. J., Abd Razak, M. F., Ahmad, N., et al. (2018). A fatal case of *Candida auris* and *Candida tropicalis* candidemia in neutropenic patient. *Mycopathologia* 183, 559–564. doi: 10.1007/s11046-018-0244-y

Mohsin, J., Hagen, F., Al-Balushi, Z. A. M., de Hoog, G. S., Chowdhary, A., Meis, J. F., et al. (2017). The first cases of *Candida auris* candidaemia in Oman. *Mycoses* 60, 569–575. doi: 10.1111/myc.12647

Morio, F., Loge, C., Besse, B., Hennequin, C., and Le Pape, P. (2010). Screening for amino acid substitutions in the *Candida albicans* Erg11 protein of azole-susceptible and azole-resistant clinical isolates: new substitutions and a review of the literature. *Diagn. Microbiol. Infect. Dis.* 66, 373–384. doi: 10.1016/j.diagmicrobio.2009.11.006

Morrell, M., Fraser, V. J., and Kollef, M. H. (2005). Delaying the empiric treatment of *Candida* bloodstream infection until positive blood culture results are obtained: a potential risk factor for hospital mortality. *Antimicrob. Agents Chemother.* 49, 3640–3645. doi: 10.1128/AAC.49.9.3640-3645.2005

Morse, S. S. (1995). Factors in the emergence of infectious diseases. *Emerg. Infect. Dis.* 1, 7–15. doi: 10.3201/eid0101.950102

Moser, C., Lerche, C. J., Thomsen, K., Hartvig, T., Schierbeck, J., Jensen, P. Ø, et al. (2019). Antibiotic therapy as personalized medicine – general considerations and complicating factors. *APMIS* 127, 361–371. doi: 10.1111/apm.12951

Muñoz, J. F., Gade, L., Chow, N. A., Loparev, V. N., Juieng, P., Berkow, E. L., et al. (2018). Genomic insights into multidrug-resistance, mating and virulence in *Candida auris* and related emerging species. *Nat. Commun.* 9:5346. doi: 10.1038/s41467-018-07779-6

Muñoz, J. F., Welsh, R. M., Shea, T., Batra, D., Gade, L., Litvintseva, A. P., et al. (2019). Chromosomal rearrangements and loss of subtelomeric adhesins linked to clade-specific phenotypes in *Candida auris*. *bioRxiv* [Preprint]. doi: 10.1101/754143

Oliveira, A. S., Martinez-de-Oliveira, J., Donders, G. G. G., Palmeira-de-Oliveira, R., and Palmeira-de-Oliveira, A. (2018). Anti-*Candida* activity of antidepressants sertraline and fluoxetine: effect upon pre-formed biofilms. *Med. Microbiol. Immunol. (Berl.)* 207, 195–200. doi: 10.1007/s00430-018-0539-0

Ong, C. W., Chen, S. C.-A., Clark, J. E., Halliday, C. L., Kidd, S. E., Marriott, D. J., et al. (2019). Diagnosis, management and prevention of *Candida auris* in hospitals: position statement of the Australasian Society for Infectious Diseases. *Intern. Med. J.* 49, 1229–1243. doi: 10.1111/imj.14612

Osei Sekyere, J. (2018). *Candida auris*: a systematic review and meta-analysis of current updates on an emerging multidrug-resistant pathogen. *MicrobiologyOpen* 7:e00578. doi: 10.1002/mbo3.578

Park, J. Y., Bradley, N., Brooks, S., Burney, S., and Wassner, C. (2019). Management of patients with *Candida auris* fungemia at community hospital, Brooklyn, New York, USA, 2016-2018. *Emerg. Infect. Dis.* 25, 601–602. doi: 10.3201/eid2503.180927

Pfaller, M. A., and Castanheira, M. (2016). Nosocomial candidiasis: antifungal stewardship and the importance of rapid diagnosis. *Med. Mycol.* 54, 1–22. doi: 10.1093/mmy/myv076

Pfaller, M. A., and Diekema, D. J. (2007). Epidemiology of Invasive candidiasis: a persistent public health problem. *Clin. Microbiol. Rev.* 20, 133–163. doi: 10.1128/CMR.00029-06

Pfaller, M. A., Diekema, D. J., Turnidge, J. D., Castanheira, M., and Jones, R. N. (2019). Twenty years of the SENTRY antifungal surveillance program: results for *Candida* species from 1997–2016. *Open Forum Infect. Dis.* 6, S79–S94. doi: 10.1093/ofid/ofy358

Polke, M., Hube, B., and Jacobsen, I. D. (2015). *Candida* survival strategies. *Adv. Appl. Microbiol.* 91, 139–235. doi: 10.1016/bs.aambs.2014.12.002

Rapp, R. P. (2004). Changing strategies for the management of invasive fungal infections. *Pharmacotherapy* 24, 4S–28S. doi: 10.1592/phco.24.3.4s.33151

Rhodes, J., Abdolrasouli, A., Farrer, R. A., Cuomo, C. A., Aanensen, D. M., Armstrong-James, D., et al. (2018a). Author correction: genomic epidemiology of the UK outbreak of the emerging human fungal pathogen *Candida auris*. *Emerg. Microbes Infect.* 7:104. doi: 10.1038/s41426-018-0098-x

Rhodes, J., Abdolrasouli, A., Farrer, R. A., Cuomo, C. A., Aanensen, D. M., Armstrong-James, D., et al. (2018b). Genomic epidemiology of the UK outbreak of the emerging human fungal pathogen *Candida auris*. *Emerg. Microbes Infect* 7:43. doi: 10.1038/s41426-018-0045-x

Riat, A., Neofytos, D., Coste, A., Harbarth, S., Bizzini, A., Grandbastien, B., et al. (2018). First case of *Candida auris* in Switzerland: discussion about preventive strategies. *Swiss Med. Wkly.* 148:w14622. doi: 10.4414/smw.2018.14622

Robbins, N., Uppuluri, P., Nett, J., Rajendran, R., Ramage, G., Lopez-Ribot, J. L., et al. (2011). Hsp90 governs dispersion and drug resistance of fungal biofilms. *PLoS Pathog.* 7:e1002257. doi: 10.1371/journal.ppat.1002257

Rosenberg, A., Ene, I. V., Bibi, M., Zakin, S., Segal, E. S., Ziv, N., et al. (2018). Antifungal tolerance is a subpopulation effect distinct from resistance and is associated with persistent candidemia. *Nat. Commun.* 9:2470. doi: 10.1038/s41467-018-04926-x

Ruiz-Gaitán, A., Moret, A. M., Tasias-Pitarch, M., Aleixandre-López, A. I., Martínez-Morel, H., Calabuig, E., et al. (2018). An outbreak due to *Candida auris* with prolonged colonisation and candidaemia in a tertiary care European hospital. *Mycoses* 61, 498–505. doi: 10.1111/myc.12781

Ruiz-Gaitán, A. C., Cantón, E., Fernández-Rivero, M. E., Ramírez, P., and Pemán, J. (2019). Outbreak of *Candida auris* in Spain: a comparison of antifungal activity by three methods with published data. *Int. J. Antimicrob. Agents* 53, 541–546. doi: 10.1016/j.ijantimicag.2019.02.005

Rybak, J. M., Doorley, L. A., Nishimoto, A. T., Barker, K. S., Palmer, G. E., and Rogers, P. D. (2019). Abrogation of triazole resistance upon deletion of CDR1 in a clinical Isolate of *Candida auris*. *Antimicrob. Agents Chemother.* 63:e00057-19. doi: 10.1128/AAC.00057-19

Saluja, P., and Prasad, G. S. (2008). *Candida ruelliae sp. nov.*, a novel yeast species isolated from flowers of *Ruellia sp.* (Acanthaceae). *FEMS Yeast Res.* 8, 660–666. doi: 10.1111/j.1567-1364.2008.00372.x

Santos, M. A. S., Gomes, A. C., Santos, M. C., Carreto, L. C., and Moura, G. R. (2011). The genetic code of the fungal CTG clade. *C. R. Biol.* 334, 607–611. doi: 10.1016/j.crvi.2011.05.008

Sarma, S., and Upadhyay, S. (2017). Current perspective on emergence, diagnosis and drug resistance in *Candida auris*. *Infect. Drug Resist.* 10, 155–165. doi: 10.2147/IDR.S116229

Satoh, K., Makimura, K., Hasumi, Y., Nishiyama, Y., Uchida, K., and Yamaguchi, H. (2009). *Candida auris sp. nov.*, a novel ascomycetous yeast isolated from the external ear canal of an inpatient in a Japanese hospital. *Microbiol. Immunol.* 53, 41–44. doi: 10.1111/j.1348-0421.2008.00083.x

Schelenz, S., Hagen, F., Rhodes, J. L., Abdolrasouli, A., Chowdhary, A., Hall, A., et al. (2016). First hospital outbreak of the globally emerging *Candida auris* in a European hospital. *Antimicrob. Resist. Infect. Control* 5:35. doi: 10.1186/s13756-016-0132-5

Schwartz, I. S., and Hammond, G. W. (2017). First reported case of multidrug-resistant *Candida auris* in Canada. *Can. Commun. Dis. Rep.* 43, 150–153. doi: 10.14745/ccdr.v43i78a02

Shahana, S., Childers, D. S., Ballou, E. R., Bohovych, I., Odds, F. C., Gow, N. A. R., et al. (2014). New *Clox* systems for rapid and efficient gene disruption in *Candida albicans*. *PLoS One* 9:e100390. doi: 10.1371/journal.pone.0100390

Sherry, L., Ramage, G., Kean, R., Borman, A., Johnson, E. M., Richardson, M. D., et al. (2017). Biofilm-forming capability of highly virulent, multidrug-resistant *Candida auris*. *Emerg. Infect. Dis.* 23, 328–331. doi: 10.3201/eid2302.161320

Singh, S., Uppuluri, P., Mamouei, Z., Alqarihi, A., Elhassan, H., French, S., et al. (2019). The NDV-3A vaccine protects mice from multidrug resistant *Candida auris* infection. *PLoS Pathog.* 15:e1007460. doi: 10.1371/journal.ppat.1007460

Sucher, A. J., Chahine, E. B., and Balcer, H. E. (2009). Echinocandins: the newest class of antifungals. *Ann. Pharmacother.* 43, 1647–1657. doi: 10.1345/aph.1M237

Sugita, T., Takashima, M., Poonwan, N., and Mekha, N. (2006). *Candida pseudohaemulonii sp. nov.*, an amphotericin B-and azole-resistant yeast species, isolated from the blood of a patient from Thailand. *Microbiol. Immunol.* 50, 469–473. doi: 10.1111/j.1348-0421.2006.tb03816.x

Taff, H. T., Mitchell, K. F., Edward, J. A., and Andes, D. R. (2013). Mechanisms of *Candida* biofilm drug resistance. *Future Microbiol.* 8, 1325–1337. doi: 10.2217/fmb.13.101

Tan, Y. E., and Tan, A. L. (2018). Arrival of *Candida auris* fungus in Singapore: report of the first 3 Cases. *Ann. Acad. Med. Singapore* 47, 260–262.

Tian, S., Rong, C., Nian, H., Li, F., Chu, Y., Cheng, S., et al. (2018). First cases and risk factors of super yeast *Candida auris* infection or colonization from Shenyang, China. *Emerg. Microbes Infect.* 7:128. doi: 10.1038/s41426-018-0131-0

Toda, M., Williams, S. R., Berkow, E. L., Farley, M. M., Harrison, L. H., Bonner, L., et al. (2019). Population-based active surveillance for culture-confirmed candidemia — four sites, United States, 2012–2016. *MMWR Surveill. Summ.* 68, 1–15. doi: 10.15585/mmwr.ss6808a1

Tracking Candida auris | CDC (2020). Available online at: https://www.cdc.gov/fungal/candida-auris/tracking-c-auris.html (Accessed March 4, 2020). doi: 10.15585/mmwr.ss6808a1

Tsui, C., Kong, E. F., and Jabra-Rizk, M. A. (2016). Pathogenesis of *Candida albicans* biofilm. *Pathog. Dis.* 74:ftw018. doi: 10.1093/femspd/ftw018

van Schalkwyk, E., Mpembe, R. S., Thomas, J., Shuping, L., Ismail, H., Lowman, W., et al. (2019). Epidemiologic shift in candidemia driven by *Candida auris*, South Africa, 2016-2017. *Emerg. Infect. Dis.* 25, 1698–1707. doi: 10.3201/eid2509.190040

van Uden, and Kolipinski, M. C. (1962). *Torulopsis haemulonii nov*. spec., a yeast from the Atlantic Ocean. *Antonie Van Leeuwenhoek* 28, 78–80. doi: 10.1007/bf02538724

Vatanshenassan, M., Boekhout, T., Meis, J. F., Berman, J., Chowdhary, A., Ben-Ami, R., et al. (2019). *Candida auris* identification and rapid antifungal susceptibility testing against echinocandins by MALDI-TOF MS. *Front. Cell. Infect. Microbiol.* 9:20. doi: 10.3389/fcimb.2019.00020

Vermes, A., Guchelaar, H. J., and Dankert, J. (2000). Flucytosine: a review of its pharmacology, clinical indications, pharmacokinetics, toxicity and drug interactions. *J. Antimicrob. Chemother.* 46, 171–179. doi: 10.1093/jac/46.2.171

Vogelzang, E. H., Weersink, A. J. L., van Mansfeld, R., Chow, N. A., Meis, J. F., and van Dijk, K. (2019). The first two cases of *Candida auris* in The Netherlands. *J. Fungi* 5:91. doi: 10.3390/jof5040091

Wang, S.-A., Jia, J.-H., and Bai, F.-Y. (2008). *Candida alocasiicola sp. nov.*, *Candida hainanensis sp. nov.*, *Candida heveicola sp. nov.* and *Candida musiphila sp. nov.*, novel anamorphic, ascomycetous yeast species isolated from plants. *Antonie Van Leeuwenhoek* 94, 257–265. doi: 10.1007/s10482-008-9238-y

Wang, X., Bing, J., Zheng, Q., Zhang, F., Liu, J., Yue, H., et al. (2018). The first isolate of *Candida auris* in China: clinical and biological aspects. *Emerg. Microbes Infect.* 7:93. doi: 10.1038/s41426-018-0095-0

Warris, A. (2018). *Candida auris*, what do paediatricians need to know? *Arch. Dis. Child.* 103, 891–894. doi: 10.1136/archdischild-2017-313960

Wasi, M., Khandelwal, N. K., Moorhouse, A. J., Nair, R., Vishwakarma, P., Bravo Ruiz, G., et al. (2019). ABC transporter genes show upregulated expression in drug-resistant clinical isolates of *Candida auris*: a genome-wide characterization of ATP-Binding Cassette (ABC) transporter genes. *Front. Microbiol.* 10:1445. doi: 10.3389/fmicb.2019.01445

Welsh, R. M., Bentz, M. L., Shams, A., Houston, H., Lyons, A., Rose, L. J., et al. (2017). survival, persistence, and isolation of the emerging multidrug-resistant pathogenic yeast *Candida auris* on a plastic health care surface. *J. Clin. Microbiol.* 55, 2996–3005. doi: 10.1128/JCM.00921-17

Whaley, S. G., Berkow, E. L., Rybak, J. M., Nishimoto, A. T., Barker, K. S., and Rogers, P. D. (2017). Azole antifungal resistance in *Candida albicans* and emerging non-*albicans Candida* Species. *Front. Microbiol.* 7:2173. doi: 10.3389/fmicb.2016.02173

Wiederhold, N. P., Lockhart, S. R., Najvar, L. K., Berkow, E. L., Jaramillo, R., Olivo, M., et al. (2019). The fungal Cyp51-specific inhibitor VT-1598 demonstrates *in vitro* and *in vivo* activity against *Candida auris*. *Antimicrob. Agents Chemother.* 63:e02233-18. doi: 10.1128/AAC.02233-18

Yue, H., Bing, J., Zheng, Q., Zhang, Y., Hu, T., Du, H., et al. (2018). Filamentation in *Candida auris*, an emerging fungal pathogen of humans: passage through the mammalian body induces a heritable phenotypic switch. *Emerg. Microbes Infect.* 7:188. doi: 10.1038/s41426-018-0187-x

Zamith-Miranda, D., Heyman, H. M., Cleare, L. G., Couvillion, S. P., Clair, G. C., Bredeweg, E. L., et al. (2019). Multi-omics signature of *Candida auris*, an emerging and multidrug-resistant pathogen. *mSystems* 4:e00257-19. doi: 10.1128/mSystems.00257-19

Zhao, X., Oh, S.-H., Yeater, K. M., and Hoyer, L. L. (2005). Analysis of the *Candida albicans* Als2p and Als4p adhesins suggests the potential for compensatory function within the Als family. *Microbiol. Read. Engl.* 151, 1619–1630. doi: 10.1099/mic.0.27763-0

Zheng, X., Wang, Y., and Wang, Y. (2004). Hgc1, a novel hypha-specific G1 cyclin-related protein regulates *Candida albicans* hyphal morphogenesis. *EMBO J.* 23, 1845–1856. doi: 10.1038/sj.emboj.7600195

Conflict of Interest: The authors declare that the research was conducted in the absence of any commercial or financial relationships that could be construed as a potential conflict of interest.

frontiers in Genetics

ORIGINAL RESEARCH
published: 24 April 2020
doi: 10.3389/fgene.2020.00375

Identifying *Candida albicans* Gene Networks Involved in Pathogenicity

Graham Thomas[1], *Judith M. Bain*[2], *Susan Budge*[2], *Alistair J. P. Brown*[2,3] *and Ryan M. Ames*[1]*

[1] Biosciences, University of Exeter, Exeter, United Kingdom, [2] Aberdeen Fungal Group, Institute of Medical Sciences, University of Aberdeen, Aberdeen, United Kingdom, [3] MRC Centre for Medical Mycology at the University of Exeter, Biosciences, University of Exeter, Exeter, United Kingdom

Candida albicans is a normal member of the human microbiome. It is also an opportunistic pathogen, which can cause life-threatening systemic infections in severely immunocompromized individuals. Despite the availability of antifungal drugs, mortality rates of systemic infections are high and new drugs are needed to overcome therapeutic challenges including the emergence of drug resistance. Targeting known disease pathways has been suggested as a promising avenue for the development of new antifungals. However, <30% of *C. albicans* genes are verified with experimental evidence of a gene product, and the full complement of genes involved in important disease processes is currently unknown. Tools to predict the function of partially or uncharacterized genes and generate testable hypotheses will, therefore, help to identify potential targets for new antifungal development. Here, we employ a network-extracted ontology to leverage publicly available transcriptomics data and identify potential candidate genes involved in disease processes. A subset of these genes has been phenotypically screened using available deletion strains and we present preliminary data that one candidate, *PEP8*, is involved in hyphal development and immune evasion. This work demonstrates the utility of network-extracted ontologies in predicting gene function to generate testable hypotheses that can be applied to pathogenic systems. This could represent a novel first step to identifying targets for new antifungal therapies.

Keywords: *Candida albicans*, co-expression network, network-extracted ontology, pathogen, pathogenicity genes, PEP8

OPEN ACCESS

Edited by:
Christina A. Cuomo,
Broad Institute, United States

Reviewed by:
David Kadosh,
The University of Texas Health Science Center at San Antonio, United States
Matt Anderson,
The Ohio State University, United States

***Correspondence:**
Ryan M. Ames
r.ames@exeter.ac.uk

Specialty section:
This article was submitted to Evolutionary and Genomic Microbiology, a section of the journal Frontiers in Genetics

Received: *29 January 2020*
Accepted: *26 March 2020*
Published: *24 April 2020*

Citation:
Thomas G, Bain JM, Budge S, Brown AJP and Ames RM (2020) Identifying Candida albicans Gene Networks Involved in Pathogenicity. Front. Genet. 11:375. doi: 10.3389/fgene.2020.00375

1. INTRODUCTION

Candida albicans is the most common cause of nosocomial fungal infections and is particularly important in vulnerable populations with suppressed immune function (Brown et al., 2012b). Mortality rates for systemic candidiasis have been estimated to be as high as 40% (Kullberg and Arendrup, 2015) and antifungal treatments for these invasive infections have only modest success in reducing these high rates (Brown et al., 2012a), despite the introduction of new antifungals, such as the echinocandins (Denning and Bromley, 2015). The discovery and development of new antifungal drugs to treat these life-threatening infections must overcome several challenges including the evolutionary similar fundamental cellular processes of humans and fungi, and the emergence of drug resistance (Denning and Hope, 2010). With high mortality rates, the emergence of drug resistance and the emergence of other pathogenic fungal species, such as *Candida auris* (Chowdhary et al., 2017), there is a drastic need for methods and targets to aid development of novel antifungal therapies.

The *C. albicans* community have employed elegant molecular and genetic approaches to identify genes involved in disease processes (Mayer et al., 2013). The key processes involved in disease are well-known and include; adhesion of yeast cells to host cell surfaces, morphological transition from yeast cells to hyphal cells, hyphal invasion by thigmotrophism, endocytosis, release of candidalysin, micronutrient scavenging, stress responses, and biofilm formation (Mayer et al., 2013; Brown A. J. et al., 2014; Brown A. J. P. et al., 2014; Moyes et al., 2016; Noble et al., 2016; Lohse et al., 2018). Indeed, targeting of these processes has been proposed as a promising strategy for antifungal development (Gauwerky et al., 2009; Vila et al., 2017). However, to identify promising targets we need a detailed understanding of these processes and, in many cases, the full complement of genes involved in these pathways is unknown. In fact, ∼70% of *C. albicans* genes are uncharacterized (*Candida* Genome Database, Nov 2019) and have no experimental evidence for functional annotation (Skrzypek et al., 2016). The bioinformatic prediction of genes involved in known disease processes provides an alternative, complementary approach to potentially time-consuming experimental screens for such genes.

In the last decade, high-throughput RNA sequencing methods have empowered systems-wide studies of cellular organization and function. Methods to identify differential expression of genes (Robinson et al., 2010; Love et al., 2014) and infer gene co-expression networks (Langfelder and Horvath, 2008; Ames et al., 2013; Kramer et al., 2014) aim to predict the function of uncharacterized genes. One such method, Clique Extracted Ontology (CliXO) infers a network-extracted ontology (NeXO) from gene similarity data, such as correlated gene expression (Kramer et al., 2014). An ontology consists of entities, such as groupings or clusters of genes, that are connected by relationships. The structure is a hierarchy and provides several advantages over static network representations, as NeXOs are capable of representing the organization of biological systems on multiple scales such as pathways, complexes, and individual genes as well as capturing pleiotropy. In addition, NeXOs are data-driven and unbiased, enabling *de novo* modeling of biological processes that can generate predictions about the functions of uncharacterized genes for experimental validation. NeXOs have previously been applied to predict the functions of uncharacterized genes and identify novel functional links in yeast (Dutkowski et al., 2013). More recently, NeXOs have been used to generate hypotheses about autophagy processes implicated in disease (Kramer et al., 2017) and novel, disease-related genes in a prominent fungal phytopathogen (Ames, 2017).

In this study we have assembled publicly available transcriptomics data for *C. albicans* and use CliXO to infer a *C. albicans* NeXO that represents pathogenicity without relying on existing annotation. We demonstrate that this network is robust and can recapitulate known biological functions. By overlaying the *C. albicans* NeXO with data on characterized disease genes, we are able to make predictions about uncharacterized genes involved in various disease processes. These genes have putative roles in adhesion, hyphal development and stress responses. Furthermore, using available deletion strains we are able to phenotypically screen a subset of these candidates. Our data suggest that one such gene, *PEP8*, might play a role in hyphal development and immune evasion, which has also been suggested by other authors. Ultimately, this study demonstrates the utility of NeXOs to identify functional links between genes that can be used to generate testable hypotheses. This has allowed us to identify a potential role for a partially characterized gene in an important disease process. These tools therefore, may represent an attractive and cost effective approach to identifying virulence targets for new antifungal therapies.

2. MATERIALS AND METHODS

2.1. Calculating Gene Co-expression

RNA-Seq data for *C. albicans* grown in a number of conditions, stresses and environments were downloaded from the Gene Expression Omnibus (GEO) database. These data include *C. albicans* grown in YPD and YPS (GSE41749, Grumaz et al., 2013), in planktonic and biofilm states (GSE45141, Desai et al., 2013), with a range of weak organic acids (GSE49310, Cottier et al., 2015), and in contact with host cells (GSE56091, Liu et al., 2015). In all cases all replicates, treatments and control data for strain SC5314 were used. In total, 130 RNA-Seq samples were used, as maximizing the number of samples used allows us to create the most robust NeXO possible. We note that the majority of samples were taken from an infection-related environment composed of *C. albicans* cells exposed to endothelial and epithelial cells with RNA taken at 1.5, 5, and 8 h during infection (Liu et al., 2015). Therefore, the NeXO built in this study will predominantly represent *C. albicans* infection processes related to these cell types and timepoints and is suitable for the application in this study. The addition of more expression data, from varied environments or infection stages, would allow the NeXO to represent a broader range of functions and processes.

Raw data for all publicly available data sets was re-analyzed as experimental setups and conditions may vary between sources. The *C. albicans* (strain SC5314, assembly 22, haplotype A) reference genome was downloaded from the *Candida* Genome Database (CGD, Inglis et al., 2012). RNA-Seq reads were aligned to the reference genome using bowtie (Langmead et al., 2009) and bowtie2 (Langmead and Salzberg, 2012) for single-end and paired-end reads, respectively. Alignment was performed using default parameters on a single processor and alignment files were sorted and converted to binary format using samtools (Li et al., 2009). Reads aligned to known genes were counted using the union model with HT-Seq (Anders et al., 2014) and these counts were used to estimate gene expression as reads per kilobase per million mapped reads (RPKM) with edgeR (Robinson et al., 2010). By generating estimates of expression from raw data we ensure that the data is as comparable as possible. Finally, correlations were calculated for all pairs of genes across all samples using the Pearson's correlation coefficient (PCC).

2.2. Generating a *C. albicans* NeXO

CliXO was used to create a *C. albicans* NeXO from correlations in gene expression (Kramer et al., 2014). CliXO requires a user-defined noise parameter α and a parameter to infer missing edges β. CliXO has been benchmarked on several 'omics data sets for the yeast *Saccharomyces cerevisiae*, including gene expression profile correlations, and it has been shown that $\alpha = 0.01$ and $\beta = 0.5$ produces ontologies that are very similar to that of the Gene Ontology (GO) (Kramer et al., 2014). Therefore, in this study α and β were set to 0.01 and 0.5, respectively. Varying these parameters produces similar NeXO structures. Altering the α parameter to $\alpha = 0.02$ produces a NeXO structure where entities have an average similarity to the reference *C. albicans* NeXO of 0.66 ± 0.28 (max 1.0) using the alignment and similarity metrics of Kramer et al. (2014) with a the strict hierarchy model. Varying the β parameter to $\beta = 0.4$ and $\beta = 0.6$ also produced a similar NeXO structure with average entity similarity of 0.83 ± 0.22 and 0.75 ± 0.23, respectively.

2.3. Aligning the *C. albicans* NeXO to the Gene Ontology

The Gene Ontology (GO) structure (OBO file) and annotations for *C. albicans* were downloaded from geneontology.org. To prepare the GO for alignment to the *C. albicans* NeXO, the structure of the GO was extracted using "is_a" GO relations, terms with no annotations to known *C. albicans* genes were removed, and redundant terms were removed. Redundant terms were defined as terms that share the same gene content as their direct descendants. When redundant terms were identified the more general term, i.e., the parent, was removed. After processing of the GO there were 776, 1,919, and 3,804 terms in the Cellular Component, Molecular Function, and Biological Process ontologies, respectively. The method of Kramer et al. (2014) was used to align the *C. albicans* NeXO to the GO ontologies using the strict hierarchy model and to generate an alignment for all nodes.

2.4. Scoring the Robustness of the *C. albicans* NeXO

The *C. albicans* NeXO is split into a number of entities with hierarchical relationships between them. As these entities will represent biological pathways and processes it was important to estimate the robustness of the entities with regard to the underlying experimental data used to construct the NeXO. To score the robustness of each term a measure of entity quality that considers the network support of a term and its robustness to perturbations of input data was taken from Dutkowski et al. (2013). In this measure, network support $NS(e)$ for an entity e is defined as the enrichment for co-expression between genes within an entity where co-expression is defined as PCC > 0.2. Enrichment [-log(P-value)] is estimated using the hypergeometric distribution where the sample size is equal to all possible co-expressed genes in an entity, sample successes are the observed co-expressed genes in an entity, the population size is all possible co-expressed genes in the NeXO, and population successes are the observed co-expressed genes in the NeXO.

To quantify an entity's robustness to changes in the input data, a bootstrapping approach was employed. Samples were randomly selected with replacement to build an expression set of 130 samples. Correlations for all pairs of genes were calculated and a NeXO was inferred as described above. This process was repeated to produce 100 bootstrapped ontologies. Each bootstrapped NeXO was then aligned to the original NeXO using the method described in Kramer et al. (2014). Alignment was performed using the strict hierarchy model and all nodes were aligned. The bootstrap score $B(e)$ for an entity (e) was then calculated as:

$$B(e) = \frac{1}{n}\sum_{i=1}^{n} S_i(e) \quad (1)$$

where n is the number of bootstrapped NeXOs and S_i is the alignment score for entity e when the original NeXO is aligned to the i-th bootstrapped NeXO. Finally, the robustness score for each entity was calculated as a geometric mean of the entity's network support and bootstrap score:

$$R(e) = \sqrt{NS(e)B(e)} \quad (2)$$

2.5. Identifying Entities Associated With Disease

Entities, clusters of genes identified from their correlated expression profiles, potentially important for disease, were identified as those containing more than two members and that show enrichment for genes implicated in disease. Two sources were used to annotate disease genes; (i) 167 disease genes identified from the pathogen-host interaction database (Winnenburg et al., 2006) and (ii) 255 genes that produce secreted and cell wall proteins thought to be associated with disease were taken from Butler et al. (2009). Fisher's exact test was used to identify enrichment by comparing the proportion of genes within each entity associated with disease to the proportion of genes in the whole NeXO associated with disease. The method of Benjamini and Hochberg (1995) was used to control for a false discovery rate of 0.05.

2.6. Annotating Entities in the *C. albicans* NeXO

Entities within the NeXO were annotated by identifying enriched GO terms (Ashburner et al., 2000). The GO slim ontology and annotations were downloaded from the CGD and Fisher's exact test was used to identify enriched GO terms in each entity. Briefly, for each entity each annotated GO term was tested for enrichment where the population size was the number of genes in the *C. albicans* NeXO and the sample size was the size of the entity. The population successes are the number of genes in the *C. albicans* NeXO (i.e., whole network) annotated with the specific GO term and the sample successes are the number of genes within the entity (i.e., a single cluster) annotated with that term. The method of Benjamini and Hochberg (1995) was used to control for a false discovery rate of 0.05.

2.7. Phenotypic Assays

Homozygous deletion strains for genes identified in entities associated with disease were assembled from Rauceo et al. (2008) and Noble et al. (2010) in VB GKO plate 1 obtained from the Fungal Genetics Stock Center (McCluskey et al., 2010). A full list of strains used in this study can be found in **Supplementary File 1**. Strains were stored at −80°C in 96-well plates, replicated on agar plates and subjected to a variety of phenotypic assays including; (i) thermotolerance on YPD at 25, 30, 37, and 42°C, (ii) osmotic stress with YPD+NaCl and YPD+KCl at 30°C at both 0.5 and 1 M; (iii) YPD+H_2O_2 at 30°C with concentrations of 2.5, 5, 7.5, and 10 mM; (iv) acidic environments from pH 4.0 to pH 7.0 at both 30 and 37°C; and (v) YPD+Fluconazole and YPD+Caspofungin at 30°C with concentrations of 1, 2 μg/ml and 0.064 and 0.128 μg/ml, respectively. Strains were incubated under these conditions for 48 h.

2.8. Characterization of Hyphal Growth

Hyphal growth was assessed by first examining colony morphology on agar plates containing YPD+20% serum and in Spider medium incubated at 30 and 37°C for 48 h (Liu et al., 1994). Second, overnight cultures were diluted to OD_{600}, incubated in a shaking incubator in liquid YPD containing 20% serum at 37°C and cells were fixed in 10% formalin after 90 m so that hyphal growth could be observed by microscopy.

2.9. Macrophage Escape Assay

Bone marrow was harvested from three eight-week old male C57BL/6 mice, from which bone marrow derived macrophages (BMDMs) were differentiated, as described previously (Davies and Gordon, 2005). BMDMs were transferred to a 96-well plate at 2.4×10^4 cells per well. *C. albicans* cells were grown overnight in YPD and then washed three times in phosphate-buffered saline (PBS) and resuspended in 1 ml PBS. Following counting, 7.2×10^4 of *C. albicans* cells were added to each well, ensuring a 3:1 ratio of yeast to macrophage. YOYO-1 dye (150 μl) was then added to each well. Fluorescence arising from lysed macrophages was measured at 30 m intervals for 12 h in a FLUOstar Optima plate reader (BMG Labtech) using excitation 485 nm/emission 520 nm at 37°C (Bain et al., 2014).

2.10. Ethical Statement

BMDMs were prepared from three 8-week old male C57BL/6 mice, which were selected randomly, bred in-house, and housed in stock cages under specific pathogen-free conditions. The mice did not undergo surgical procedures prior to culling by cervical dislocation. All animal experimentation was approved by the UK Home Office and by the University of Aberdeen Animal Welfare and Ethical Review Body.

3. RESULTS

3.1. A *C. albicans* NeXO

Expression of *C. albicans* genes from different growth states, environments, stresses, and infection models representing 130 individual samples were used to characterize the *C. albicans* system. Correlated gene expression profiles for 5,698 *C. albicans* genes were used to infer a network-extracted ontology (NeXO) with the CliXO method (Kramer et al., 2014). The resulting NeXO consists of 1,366 entities connected by 1,801 relationships where larger entities split into smaller subsets representing functions on multiple scales. The *C. albicans* NeXO structure can be found in **Supplementary File 2**.

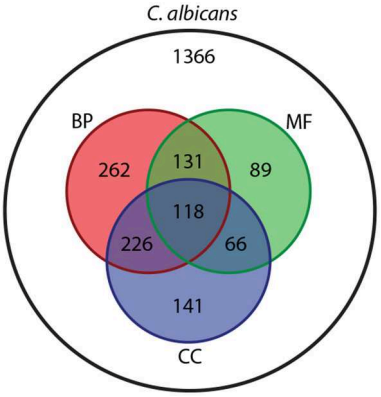

FIGURE 1 | Venn diagram showing the number of entities in the *C. albicans* NeXO (white) that align to Biological Process (BP, red), Molecular Function (MF, green) or Cellular Component (CC, blue) GO ontologies.

Aligning this *C. albicans* NeXO to the GO shows that 1,033/1,366 (75.6%) entities can be aligned to at least one ontology within the GO, with many terms mapping to more than one (**Figure 1**). Of the 496 entities that contain more than 4 genes, 336 can be aligned to GO terms. The *C. albicans* NeXO captures 70.6% of terms in the Cellular Component ontology but only captures 18.1 and 20.9% of terms in the Biological Process and Molecular Function ontologies, respectively (**Supplementary File 3**). This suggests that the *C. albicans* NeXO largely describes subcellular structures and macromolecular complexes.

Aligning the *C. albicans* NeXO to the GO provides useful information about the similarity between the structure of the two ontologies. To gain more information about the function, or multiple functions, of entities within the *C. albicans* NeXO, enriched GO terms for each entity were identified using Fisher's Exact Test (*adjusted P* <0.05) and used as a functional annotation. There are 333/1,366 (24.3%) entities with significant GO term enrichment and 159/496 (32.0%) entities with significant enrichment when examining entities with greater than four genes. GO term enrichment covers terms from all three GO ontologies with 35, 20, and 23 unique GOslim terms enriched from the biological process, molecular function, and cellular component ontologies, respectively (**Supplementary File 4**). This suggests that our *C. albicans* NeXO focusses on a subset of functions across all GO ontologies with many entities showing no functional enrichment. These may represent noise in NeXO generation or the identification of currently unknown or unannotated pathways and functions.

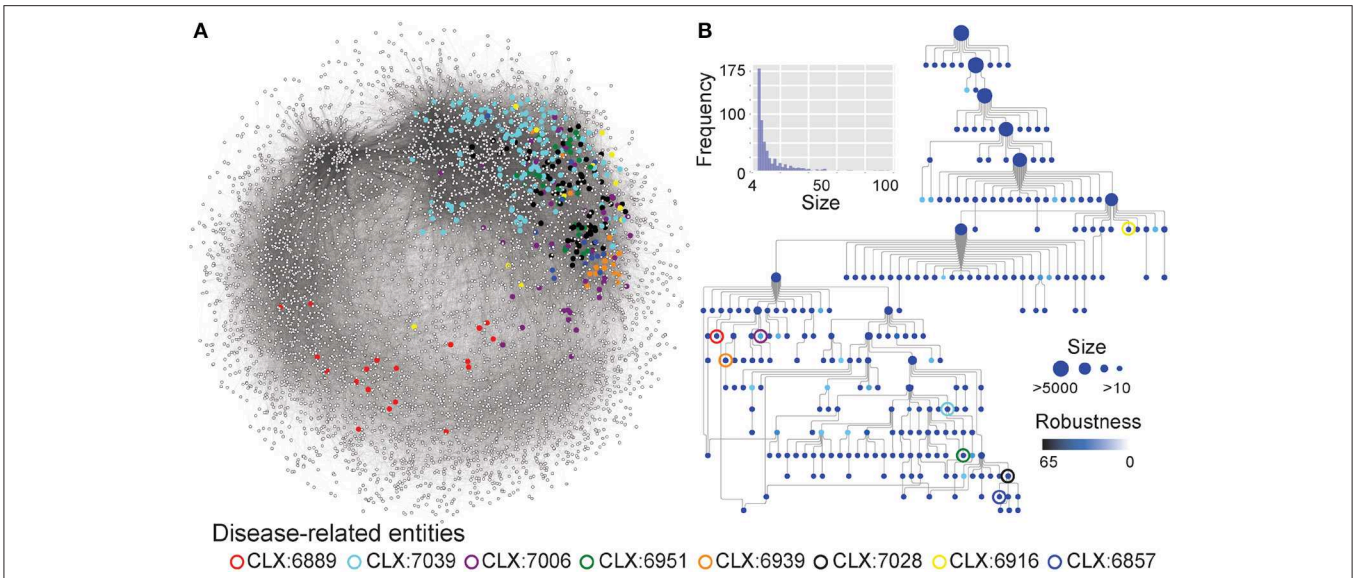

FIGURE 2 | (A) The *C. albicans* co-expression network represented as nodes (genes) connected by edges where genes show correlated expression profiles with Pearson's Correlation Coefficient > 0.4. Entities enriched for disease genes, described in **Table 1**, are highlighted by colored circles and the genes that are part of these entities are also highlighted. **(B)** A network-extracted ontology (NeXO) inferred from the co-expression data, organized into entities (nodes) of genes and connected by relationships (edges). Node sizes represent the number of genes associated with each entity and only entities associated with 10 or more genes are shown. Node colors represent the robustness of the entities calculated by bootstrap analysis, where darker colors indicate a higher robustness score. Entities enriched for disease genes, described in **Table 1**, are highlighted by colored circles.

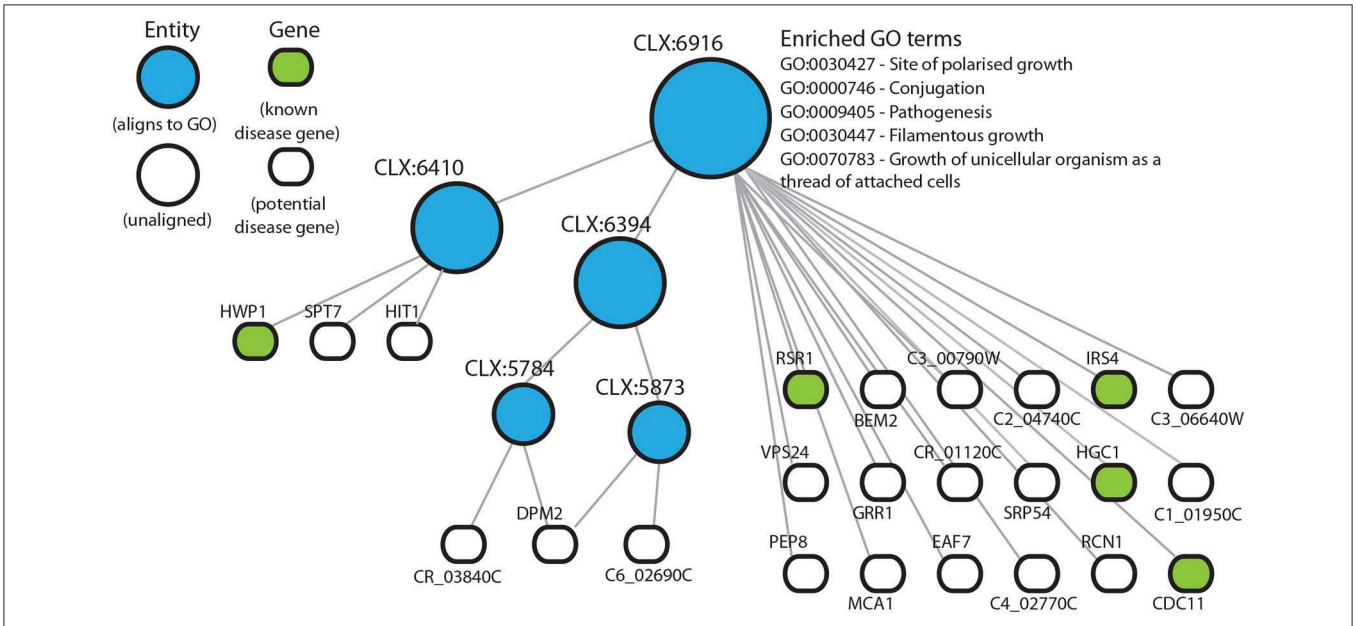

FIGURE 3 | Entity CLX:6916 in the *C. albicans* NeXO is enriched for known disease genes in the pathogen-host interaction database (Winnenburg et al., 2006). The hierarchical structure shows CLX:6916 connected by edges to sub-entities (circles), and the genes (rounded rectangles) contained within the entity. Entities that are aligned to the Gene Ontology are shown in blue. Genes found in the pathogen-host interaction database are highlighted in green. Enriched Gene Ontology terms are also shown.

To validate the *C. albicans* NeXO, robustness scores for each entity were calculated based on network support from co-expression and bootstrapping of the input expression data. We find a strong correlation between term size and robustness with larger terms being more robust (R^2 = 0.87, P = <0.0001 on log transformed data, **Figure S1**).

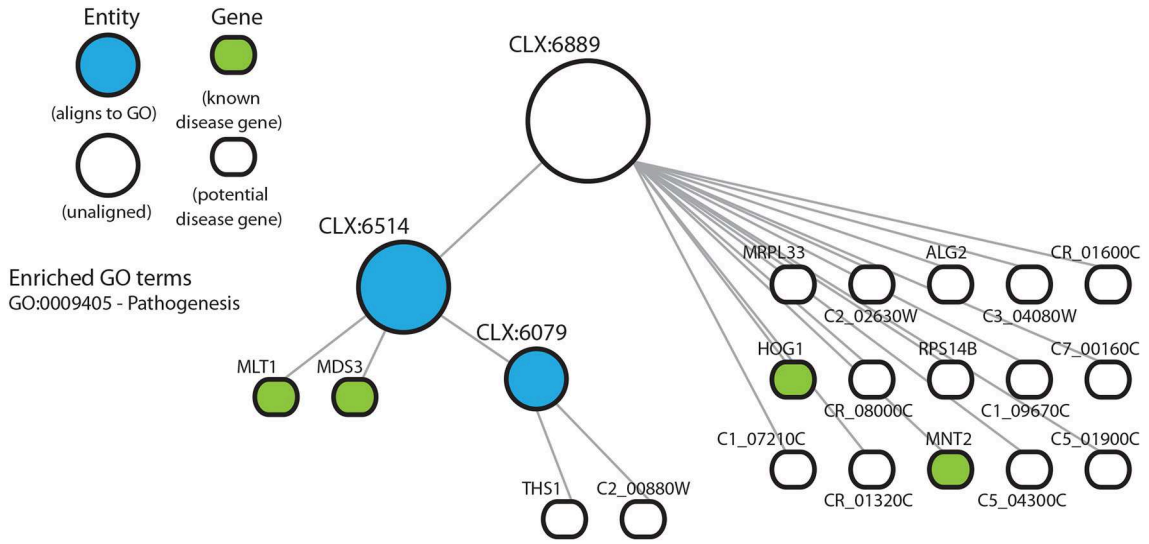

FIGURE 4 | Entity CLX:6889 in the *C. albicans* NeXO is enriched for known disease genes in the pathogen-host interaction database (Winnenburg et al., 2006). The hierarchical structure shows CLX:6889 connected by edges to sub-entities (circles), and the genes (rounded rectangles) contained within the entity. Entities that are aligned to the Gene Ontology are shown in blue. Genes found in the pathogen-host interaction database are highlighted in green. Enriched Gene Ontology terms are also shown.

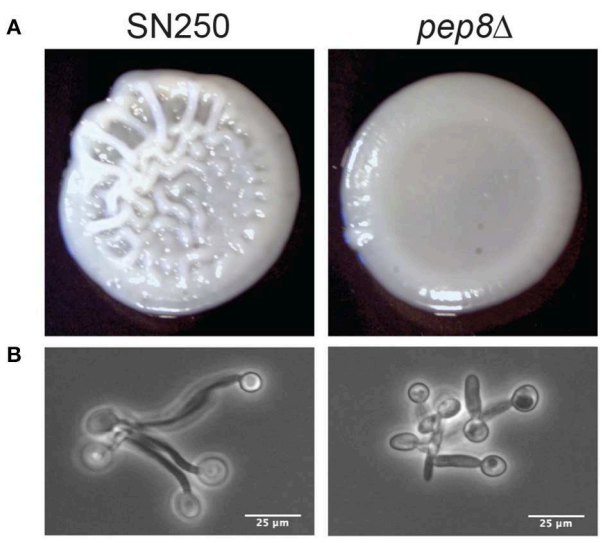

FIGURE 5 | (A) Images of colony formation for wild-type (SN250) and *pep8* mutants grown on Spider media at 37°C for 48 h. **(B)** Evidence of reduced hyphal formation by *pep8*Δ cells compared to wild-type cells fixed in formalin at 90 m hyphal development.

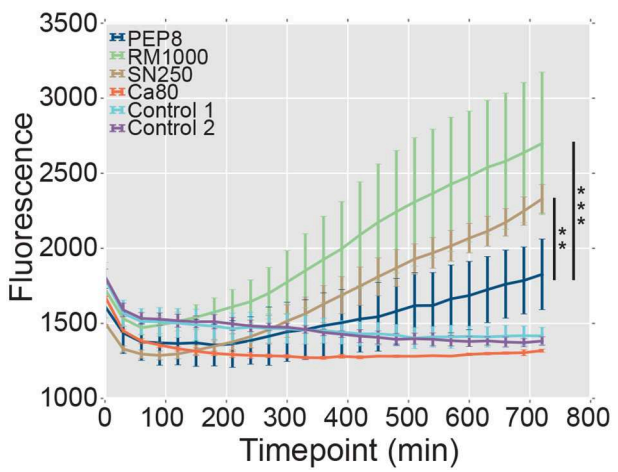

FIGURE 6 | The lysis of macrophages was assayed by measuring release of the fluorescent dye, YOYO-1 (section Materials and Methods). The *pep8*Δ mutant (dark blue) displays a reduced ability to lyse and escape macrophages compared to the control wild-type strains RM1000 (green; Mann–Whitney U, ***P = 5.875e-11) and SN250 (brown; Mann–Whitney U, **P = 0.002). Uninfected macrophages (light blue, Control 1; purple, Control 2), and a hypha-deficient *cph1*Δ *efg1*Δ mutant (Lo et al., 1997) (red, Ca80) were also included as controls.

Therefore, the larger entities in the NeXO are more robust. Excluding entities with fewer than 10 members yields a mean robustness score of 4.47 compared to 0.82 when all entities are analyzed. There were two clear outliers: these were two entities immediately under the root, which both contain >5,400 genes and are far larger than any other entities in the NeXO (**Figure S1**), suggesting that these may be spurious entities. Overall, entities within the *C. albicans* NeXO, particularly larger entities, are robust to the underlying data suggesting that the addition or removal of data wouldn't change their composition and so they are likely to represent biological functions.

TABLE 1 | Co-expression entities enriched for known disease genes in the pathogen-host interaction database.

Co-expression entity	Num genes	Num disease genes	P_{raw}	P_{adj}
CLX:6916	24	5	4.92E-4	0.019
CLX:6951	33	6	2.91E-4	0.014
CLX:7006	75	9	2.55E-4	0.016
CLX:6939	30	6	1.67E-4	0.016
CLX:7039	181	14	6.16E-4	0.019
CLX:7028	139	13	1.51E-4	0.029
CLX:6857	16	4	8.97E-4	0.024
CLX:6889	19	4	0.001	0.043

P_{raw} Fisher's exact test p-value. *P_{adj} Adjusted* p-value *to control for a false discovery rate of 0.05 (Benjamini and Hochberg, 1995).*

3.2. The *C. albicans* NeXO Contains Entities Enriched for Disease Genes

Although many entities in the NeXO were annotated by identifying enriched GO terms, many remain unannotated (**Figure 1**). The unannotated entities may represent understudied, functionally-related genes with roles in pathogenicity that are lacking GO annotation. To identify entities related to pathogenesis irrespective of GO annotation, we identified entities enriched for known disease genes in the pathogen-host interaction database (Winnenburg et al., 2006) (**Figure 2**). This is a major advantage of using a data-driven NeXO that can complement existing GO annotation but can also discover new entities with roles in specific biological processes.

Eight entities within the *C. albicans* NeXO are enriched for known disease genes. Six of these eight entities are also enriched for the GO term "*pathogenesis*" (GO:0009405) indicating that the genes in these entities are related to disease. Additionally, several other terms related to *C. albicans* disease processes are also enriched in these entities. GO terms "*interspecies interaction between organisms*" (GO:0044419), "*filamentous growth*" (GO:0030447), and "*growth of unicellular organism as a thread of attached cells*" (GO:0070783) are all regularly enriched in putative disease-related entities. However, entities CLX:6939 and CLX:6889 show no GO enrichment and may represent areas of unstudied function associated with disease that have only been detected using this approach.

3.3. Entities Enriched for Known Disease Genes Predict New Candidates Associated With Disease

In those entities that are enriched for known disease genes, many other genes are uncharacterized and could potentially be involved in disease processes. In this way we can predict functional annotations for genes not present in literature-curated sources such as the GO. The entity CLX:6916 (**Figure 3**), contains 24 genes with 5 genes annotated as being part of the disease process in the pathogen-host interaction database (Winnenburg et al., 2006). Of the other 19 genes in this entity 6 genes have experimental annotation in the CGD and the remaining 11 genes are uncharacterized. CLX:6916 is a highly connected entity with 189 edges with a Pearson correlation coefficient >0.2, suggesting that the genes in this entity may be functionally related. The entity CLX:6916 contains genes involved in the disease process. These include *RCN1* (C6_01160W), which encodes a calcineurin-dependent signaling protein that has a role in controlling the stress response and virulence (Reedy et al., 2010). The genes VPS24 (C2_00930C) and C6_02690C have been linked to the processes of adherence Marchais et al. (2005) and hyphal growth (Bensen et al., 2004), respectively. Also, the entity CLX:6857 (**Figure S2**) contains the gene *TRY5* (C6_01500C), which acts as a regulator of adhesion genes (Finkel et al., 2012). These entities display tight clustering suggesting that the genes they contain are functionally related. Since these entities are enriched for known disease genes, we reasoned that the uncharacterized genes in these entities may also play roles in disease and *C. albicans* pathogenicity.

3.4. Entities With No Known Functional Annotation May Represent Understudied Cellular Processes

Entity CLX:6889 (**Figure 4**) shows enrichment for known disease genes but no significant enrichment for any GO terms. CLX:6889 may represent an understudied process, detectable directly from transcriptomic data using the NeXO approach, where incorrect or missing GO term annotation means we cannot detect any significant GO term enrichment or existing functional annotation. Interestingly, CLX:6939 (**Figure S3**) shows no GO term enrichment. However, its descendent entities, CLX:6819 and CLX:6036, are enriched for multiple GO terms. Possible interpretations again include the possibility of missing GO term annotation, or that CLX:6939 represents multiple disease-related processes with no coherent GO description while the descendent entities CLX:6819 and CLX:6036 represent singular functions with adequate GO descriptions. In these entities we find that the majority of genes annotated with GO terms have been annotated on the basis of sequence similarity or inferred from electronic annotation, with few terms annotated by mutant phenotypes or from direct assays. This suggests that the GO annotations for these genes may be inaccurate or incomplete. Indeed, ∼70% of *C. albicans* genes are uncharacterized (*Candida* Genome Database, Nov 2019) and have no experimental evidence for functional annotation (Skrzypek et al., 2016). Together, the enrichment of known disease genes in this entity and the lack of experimental annotation of GO terms, may suggest that these entities, and their genes, represent coherent, but under-characterized, functional units related to disease.

The entity CLX:6889 (**Figure 4**) contains characterized genes involved in biofilm production (*MRPL33*—C3_01080W) (Nett et al., 2009) and response to mouse macrophages (*RPS14B*—C1_06450C) (Lorenz et al., 2004). Both of these genes have not been shown to contribute to the disease process, but have functions associated with disease. CLX:6889 also contains uncharacterized genes that are induced in response to stress (C5_04300C), involved in protein secretion (C5_01900C) and involved in the response to macrophages (THS1) (Nobile et al.,

2012). These have inferred functions potentially related to disease. These entities suggest that some genes, that may have been partially characterized or annotated with GO terms, might yet have undiscovered functions involved in the disease process, which might be niche-specific, for example.

3.5. Phenotypic Analysis of Mutant Strains

To test whether some partially characterized genes might have undiscovered functions involved in the disease process, we selected available, homozygous null mutants corresponding to genes associated with disease-related entities in the NeXO (*AHR1, WOR2, CST20, GRR1, HGC1, HOG1, HST7, HWP1, INT1, PBS2, PEP8, RIM101, RSR1, SEF1, TRY5 HIT1, NVL6*) and irrespective of GO annotation. The mutants were subjected to a range of phenotypic assays alongside their respective control strains (CAI4+Clp10, RM1000+Clp20, SN250). These virulence-related assays included yeast-hypha morphogenesis, macrophage phagocytosis, thermotolerance, resistance to osmotic, oxidative and acid stresses, and sensitivity to the antifungal drugs, fluconazole, and caspofungin (**Figure S4**).

There were detectable phenotypes for mutant strains in a range of conditions. Several mutants (*HIT1, NVL6, HOG1, PBS2*) showed differing levels of sensitivity to YPD+H_2O_2, particularly at concentrations of 7.5 and 10 mM. We also observed potential reduced growth of *hit1*Δ when exposed to fluconazole and *rsr1*Δ when treated with caspofungin. Finally, *pep8*Δ, showed an aberrant colony morphology on Spider medium (**Figure 5**). Whilst the control strain, SN250, displayed the distinctive wrinkly appearance associated with hyphal development, *pep8*Δ colonies were smooth, similar to the appearance of *hwp1*Δ colonies with known hyphal abnormalities, suggesting a potential defect in hyphal development (**Figure S4**).

3.6. Pep8 Promotes Hypha Formation

To explore the potential defect of *pep8*Δ cells in hyphal development, we compared their morphology to control cells (SN250) after growth in YPD containing 20% serum at 37°C (**Figure 5B**). The *pep8*Δ cells formed stunted hyphae compared to the control. This confirmed that the loss of Pep8 either delays or stunts hyphal development in *C. albicans*, suggesting that Pep8 plays a role in hyphal development.

The formation of hyphae after phagocytosis is known to promote the escape of *C. albicans* cells from innate immune cells (Lo et al., 1997; McKenzie et al., 2010). Therefore, we reasoned that, given their attenuated hypha formation, *pep8*Δ cells might be less able to lyse and escape macrophages following phagocytosis. We tested this by comparing the ability of *C. albicans* strains to promote the release of the fluorescent dye, YOYO-1, from macrophages (**Figure 6**). Macrophages infected with wild type *C. albicans* control strains (SN250 or RM1000+CIp20) released significant amounts of the dye over the time course, whereas uninfected macrophages did not. Also, macrophages infected with the hypha-defective *C. albicans cph1*Δ *efg1*Δ mutant did not display significant levels of lysis (**Figure 6**), which was consistent with the role that hypha formation plays in fungal escape from macrophages (Lo et al., 1997; McKenzie et al., 2010). Significantly, the *pep8*Δ cells displayed a reduced ability to lyse the macrophages compared to the wild-type controls RM1000 (Mann–Whitney U, $P = 5.875e\text{-}11$) and SN250 (Mann–Whitney U, $P = 0.002$). However, the *pep8*Δ cells were able to escape these innate immune cells to some degree (**Figure 6**). This was entirely consistent with our observation that loss of Pep8 partially attenuates, but does not completely block, hypha formation (**Figure 6**). We conclude that Pep8 plays a role in hyphal development and defects in this gene's function affect the ability of *C. albicans* to evade the host immune system.

4. DISCUSSION

Ontologies extracted from network data have been used to predict novel, disease-related genes in an important phytopathogen (Ames, 2017) and identify the function of uncharacterized genes that can be experimentally validated (Dutkowski et al., 2013). In this study, we compiled RNA-Seq data for the human fungal pathogen *C. albicans*, inferred a NeXO from correlated expression profiles, and overlaid information on known disease genes to make functional predictions for poorly- and un-characterized genes. A subset of these predictions were then tested using phenotypic screens and infection assays to identify potentially novel disease-related genes.

NeXOs have been proposed as useful tools to predict a range of cellular phenotypes and answer important biological questions (Carvunis and Ideker, 2014). These network structures have proven to be robust (Dutkowski et al., 2013), as is the *C. albicans* NeXO (**Figure S1**). NeXOs also recapitulate known functions; a NeXO built from a range of interaction data for *S. cerevisiae* aligns to many GO categories and best represents the Cellular Component ontology (Dutkowski et al., 2013). The same pattern can be seen in this study with many entities aligning to GO terms and best representing the Cellular Component ontology (**Figure 1**). Previous work looking at functional modules identified from a yeast co-expression network shows that many (>80%) Biological Process and Cellular Component terms can be represented by co-expression data (Ames et al., 2013). These results therefore suggest that the structure of NeXOs may be well suited to representing Cellular Component terms. To better represent biological processes and molecular functions, methods of generating NeXOs may have to take into account functional links between genes whose expression could be dispersed over time. Indeed, sequential activation of functionally related genes has been demonstrated during differentiation and development (Queva et al., 1998), cell wall stress in *S. cerevisiae* (Bermejo et al., 2008) and *C. albicans*-host interactions (Wilson et al., 2009).

Based on location in a NeXO and functions of characterized genes in the same entity, it is possible to generate hypotheses about the functions of poorly- or un-characterized genes. Here, we used enrichment of disease-associated genes in entities as evidence that these entities may represent disease related pathways containing as yet unknown disease genes. CLX:6916 (**Figure 3**) is enriched for disease-associated genes with virulence related functions, *RSR1* (CR_02140W) guides hyphal growth

(Hausauer et al., 2005), *IRS4* (C3_03660W) contributes to hyphal formation (Badrane et al., 2005), *HGC1* (C1_00780C) regulates hyphal morphogenesis (Zheng et al., 2004), *CDC11* (C5_00070W) is also involved in hyphal morphology (Warenda et al., 2003) and *HWP1* (C4_03570W) encodes a major protein in the cell wall and functions in cell-surface adhesion (Staab and Sundstrom, 1998; Staab et al., 2004). This entity also contains several characterized genes that have implicated roles in disease but are not present in the pathogen-host interaction database. *GRR1* (C5_04600C) is required for cell cycle progression and involved in the negative control of pseudohyphal growth (Butler et al., 2006) and *RCN1* (C6_01160W) is a calcineurin-dependent signaling protein that controls stress response and virulence (Reedy et al., 2010). The identification of entities containing known disease genes not found in the pathogen-host interaction database highlights the reliability of these methods and also the usefulness of using pre-existing databases without the need to include expert or literature-curated knowledge. There are also several partially or uncharacterized genes, that have been linked to the disease process. For example *PEP8*, a partially characterized gene, has previously been associated with filamentation in a large-scale haploinsufficiency assay (Uhl et al., 2003).

A homozygous *pep8*Δ/*pep8*Δ deletion strain was included in the strains phenotypically assayed in this study. We find that *pep8*Δ cells produce delayed or stunted hyphae and show attenuated macrophage escape (**Figures 5**, **6**), confirming a role for this gene in filamentation as previously reported (Uhl et al., 2003) and suggesting a role in infection. This finding also confirms recent work, which is entirely independent from this study, that has shown that *pep8* mutants demonstrate severe filamentation defects in a range of conditions (Azadmanesh et al., 2017) and these mutants abrogate azole resistance (Mount et al., 2018). Loss of function of Pep8 abrogates azole resistance by overwhelming the functional capacity of calcineurin. Interestingly, *PEP8* is clustered with *RCN1*, which encodes a calcineurin-dependent signaling protein, among other genes involved in filamentation and drug resistance. We note that not all the strains phenotypically tested appear to have roles in virulence-related processes with the recall and precision of these approaches estimated to be 0.43 and 0.31, respectively (Yu et al., 2019). However, given that NeXOs are data-driven and can be generated quickly with little expert knowledge or human intervention, they provide useful approaches for the identification of novel pathways, prediction of functions and generation of testable hypotheses, especially in those organisms that lack comprehensive annotation.

This work also demonstrates the utility of NeXOs to reveal functions at multiple levels. Entities CLX:6916 (**Figure 3**), CLX:6088 (**Figure S2**) and CLX:7006 all contain the hyphal cell wall protein Hwp1. This indicates that the *C. albicans* NeXO is capturing function at different levels and may indicate a role for Hwp1 in several disease related pathways. CLX:6088 and CLX:7006 both seem to be specifically associated with cell adhesion based on alignment to the GO and enrichment for GO terms, respectively (**Supplementary Files 3**, **4**). These entities are children of the much larger entity CLX:7055 (2,764 members), that shows enrichment for multiple disease-related GO terms including "*pathogenesis*," "*cell adhesion*," and "*biofilm formation*," and may represent a higher, or more general, description of pathogenicity. CLX:6916 appears to be associated with yeast-hypha morphogenesis and hypha function. The entity is enriched for terms relating to "*filamentous growth*" (GO:0030447), "*site of polarized growth*" (GO:0030427) and "*pseudohyphal growth*" (GO:0007124). The presence of Hwp1 in entities related to adhesion and hyphal growth tallies perfectly with the known presence of Hwp1 on the surface of hyphal cells and the protein's role in adhesion (Staab and Sundstrom, 1998; Staab et al., 1999). The ontological view allows us to identify the importance of Hwp1 in multiple-related processes that are important for pathogenesis. This is a major advantage of organizing these data into a NeXO to identify relations between entities, highlight genes present in multiple pathways or processes and find entities that represent function on different scales (Dutkowski et al., 2013).

NeXOs may also provide a tool for the functional annotation of poorly characterized genes (Dutkowski et al., 2013). The entity, CLX:6889 (**Figure 4**), shows an enrichment of disease-associated genes, but does not align to any term in the GO and has no enrichment for GO terms despite all genes having GO annotations. Although descendants of CLX:6889 do align to the GO and CLX:6514 is enriched for the GO term for pathogenesis (GO:0009405). The members of CLX:6889 include: *HOG1* (C2_03330C) which encodes the stress activated protein kinase involved in the core stress response (Alonso-Monge et al., 2009), *MLT1* (C1_08210C) a vacuolar membrane transporter that is needed for virulence (Theiss et al., 2002), *MNT2* (C3_01830C) a transferase with a role in adherence and virulence (Munro et al., 2005), and *MDS3* (C3_07320W) encoding a TOR signaling pathway component required for growth and hyphal formation (Davis et al., 2002; Richard et al., 2005). Other genes in this entity, both verified and uncharacterized, have roles that can be linked to disease processes. For example, a putative metallodipeptidase (C5_04300C) is a target gene of a small network of transcription regulators that control biofilm development (Nobile et al., 2012) and is targeted for sumoylation, where sumoylation targets have been shown to have roles in cell cycle progression and stress responses (Leach et al., 2011). The genes in this entity have varied roles and seem loosely to be related to growth and its regulation. Although this entity might be produced by a random clustering of genes, the enrichment for disease-associated genes and functions assigned to the entity's descendents suggests CLX:6889 may represent a true functional module related to disease not described by current GO annotations. Indeed, most of the GO annotations for genes in this entity are inferred from electronic annotation rather than direct experimental evidence and previous work using network extracted ontologies has shown that entities that do not align to the GO can represent true biological modules (Dutkowski et al., 2013). The genes in this entity therefore, may represent new targets for functional characterization related to pathogenesis.

In this study, we use a *C. albicans* NeXO to generate testable hypotheses about this important fungal pathogen. It is important to note that the underlying data used to infer

NeXOs is crucial to the types of questions that can be answered. The *C. albicans* NeXO, leverages publicly available data and is largely constructed from infection-related data (see section Materials and Methods), making it well suited to generating hypotheses about infection-related processes. This may be why the NeXO is useful to identify groups of genes related to hyphal development and similar pathogenic processes. However, we note that other processes are clearly represented by the *C. albicans* NeXO, with 24% of entities enriched for GO terms across all 3 Gene Ontologies and only ∼2% of entities enriched with the "*pathogenesis*" GO term. Previous studies have used NeXOs to describe broad functional categories for the yeast *S. cerevisiae* and generate hypotheses about the function of uncharacterized genes (Dutkowski et al., 2013). This was made possible by utilizing integrated data from protein-protein interactions, gene co-expression and genetic interactions, which represent varied areas of biological function (Ames et al., 2013). Therefore, the addition of further data, both for different infection scenarios and environments, would produce a *C. albicans* NeXO that represents more varied areas of biological function and may well increase alignment to the GO. Likewise, the addition of known disease genes from the literature to supplement the pathogen-host interaction database would increase our set of known disease genes and may well allow the identification of further disease processes in the NeXO. Nevertheless, the data used in this study have been able to recapitulate known functions (**Figure 1**) and generate hypotheses for the role of several uncharacterized genes in disease processes (**Figures 3**, **4**, **Figures S2**, **S3**). Even though only a handful of genes predicted to be involved in disease were available from the FGSC, we were still able to identify *PEP8* as having a potential role in hyphal development and immune system evasion.

5. CONCLUSION

Here, we have built a NeXO for *C. albicans*, leveraging publicly available data, to identify novel gene networks involved in pathogenicity. We have shown that the NeXO is robust and recapitulates known biology by aligning to the GO. By identifying enrichment of known disease genes in entities we make predictions about pathways and partially or uncharacterized genes potentially involved in pathogenicity. One such gene, *PEP8*, is shown to produce stunted or delayed hyphae and attenuated immune system evasion. This work, along with that of others, suggests further characterization of *PEP8* would be important for a more detailed understanding of infection processes. This study, therefore, shows the utility of NeXOs for pathway identification, functional annotation, and hypothesis generation that can be applied to multiple systems and processes.

DATA AVAILABILITY STATEMENT

The publicly-available datasets analyzed for this study can be found in the Gene Expression Omnibus (IDs: GSE41749, GSE45141, GSE49310, GSE56091). The network-extracted ontology generated as part of this study is available in the **Supplementary Information**.

AUTHOR CONTRIBUTIONS

RA and AB contributed conception and design of the study. RA performed the computation analysis and wrote the first draft of the manuscript. RA, JB, and SB performed the experimental analysis. GT, JB, and AB wrote sections of the manuscript. All authors contributed to manuscript revision, read, and approved the submitted version.

FUNDING

RA was generously supported by a Wellcome Trust Institutional Strategic Support Award [WT105618MA], a Microbiology Research Visit Grant [RVG16/18], and a EPSRC/BBSRC Innovation Fellowship [EP/S001352/1]. AB was supported by a programme grant from the UK Medical Research Council [MR/M026663/1] and by the Medical Research Council Centre for Medical Mycology at the University of Aberdeen [MR/N006364/1]. The funders had no role in study design, data collection and analysis, decision to publish, or preparation of the manuscript.

ACKNOWLEDGMENTS

This is a short text to acknowledge the contributions of specific colleagues, institutions, or agencies that aided the efforts of the authors.

SUPPLEMENTARY MATERIAL

The Supplementary Material for this article can be found online at: https://www.frontiersin.org/articles/10.3389/fgene.2020.00375/full#supplementary-material

REFERENCES

Alonso-Monge, R., Carvaihlo, S., Nombela, C., Rial, E., and Pla, J. (2009). The Hog1 MAP kinase controls respiratory metabolism in the fungal pathogen *Candida albicans*. *Microbiology* 155, 413–423. doi: 10.1099/mic.0.023309-0

Ames, R. M. (2017). Using network extracted ontologies to identify novel genes with roles in appressorium development in the rice blast fungus *Magnaporthe oryzae*. *Microorganisms* 5:3. doi: 10.3390/microorganisms5010003

Ames, R. M., MacPherson, J. I., Pinney, J. W., Lovell, S. C., and Robertson, D. L. (2013). Modular biological function is most effectively captured by combining molecular interaction data types. *PLoS ONE* 8:e62670. doi: 10.1371/journal.pone.0062670

Anders, S., Pyl, P. T., and Huber, W. (2014). HTSeq–a python framework to work with high-throughput sequencing data. *Bioinformatics* 31, 166–169. doi: 10.1093/bioinformatics/btu638

Ashburner, M., Ball, C., Blake, J., Botstein, D., Butler, H., Cherry, J., et al. (2000). Gene ontology: tool for the unification of biology. The Gene Ontology Consortium. *Nat. Genet.* 25, 25–29. doi: 10.1038/75556

Azadmanesh, J., Gowen, A. M., Creger, P. E., Schafer, N. D., and Blankenship, J. R. (2017). Filamentation involves two overlapping, but distinct, programs of filamentation in the pathogenic fungus *Candida albicans*. *G3* 7, 3797–3808. doi: 10.1534/g3.117.300224

Badrane, H., Cheng, S., Nguyen, M. H., Jia, H. Y., Zhang, Z., Weisner, N., et al. (2005). *Candida albicans* IRS4 contributes to hyphal formation and virulence after the initial stages of disseminated candidiasis. *Microbiology* 151, 2923–2931. doi: 10.1099/mic.0.27998-0

Bain, J. M., Louw, J., Lewis, L. E., Okai, B., Walls, C. A., Ballou, E. R., et al. (2014). *Candida albicans* hypha formation and mannan masking of beta-glucan inhibit macrophage phagosome maturation. *MBio* 5:e01874. doi: 10.1128/mBio.01874-14

Benjamini, Y., and Hochberg, Y. (1995). Controlling the false discovery rate: a practical and powerful approach to multiple testing. *J. R. Stat. Soc. Ser. B* 57, 289–300. doi: 10.1111/j.2517-6161.1995.tb02031.x

Bensen, E. S., Martin, S. J., Li, M., Berman, J., and Davis, D. A. (2004). Transcriptional profiling in *Candida albicans* reveals new adaptive responses to extracellular pH and functions for Rim101p. *Mol. Microbiol.* 54, 1335–1351. doi: 10.1111/j.1365-2958.2004.04350.x

Bermejo, C., Rodríguez, E., García, R., Rodríguez-Peña, J. M., de la Concepción, M. L. R., Rivas, C., et al. (2008). The sequential activation of the yeast HOG and SLT2 pathways is required for cell survival to cell wall stress. *Mol. Biol. Cell* 19, 1113–1124. doi: 10.1091/mbc.e07-08-0742

Brown, A. J., Brown, G. D., Netea, M. G., and Gow, N. A. (2014). Metabolism impacts upon candida immunogenicity and pathogenicity at multiple levels. *Trends Microbiol.* 22, 614–622. doi: 10.1016/j.tim.2014.07.001

Brown, A. J. P., Budge, S., Kaloriti, D., Tillmann, A., Jacobsen, M. D., Yin, Z., et al. (2014). Stress adaptation in a pathogenic fungus. *J. Exp. Biol.* 217, 144–155. doi: 10.1242/jeb.088930

Brown, G. D., Denning, D. W., Gow, N. A., Levitz, S. M., Netea, M. G., and White, T. C. (2012a). Hidden killers: human fungal infections. *Sci. Transl. Med.* 4:165rv13. doi: 10.1126/scitranslmed.3004404

Brown, G. D., Denning, D. W., and Levitz, S. M. (2012b). Tackling human fungal infections. *Science* 336, 647–647. doi: 10.1126/science.1222236

Butler, D. K., All, O., Goffena, J., Loveless, T., Wilson, T., and Toenjes, K. A. (2006). The GRR1 gene of *Candida albicans* is involved in the negative control of pseudohyphal morphogenesis. *Fungal Genet. Biol.* 43, 573–582. doi: 10.1016/j.fgb.2006.03.004

Butler, G., Rasmussen, M. D., Lin, M. F., Santos, M. A., Sakthikumar, S., Munro, C. A., et al. (2009). Evolution of pathogenicity and sexual reproduction in eight candida genomes. *Nature* 459, 657–662. doi: 10.1038/nature08064

Carvunis, A.-R., and Ideker, T. (2014). Siri of the cell: what biology could learn from the iphone. *Cell* 157, 534–538. doi: 10.1016/j.cell.2014.03.009

Chowdhary, A., Sharma, C., and Meis, J. F. (2017). *Candida auris*: a rapidly emerging cause of hospital-acquired multidrug-resistant fungal infections globally. *PLoS Pathog.* 13:e1006290. doi: 10.1371/journal.ppat.1006290

Cottier, F., Tan, A. S. M., Chen, J., Lum, J., Zolezzi, F., Poidinger, M., et al. (2015). The transcriptional stress response of *Candida albicans* to weak organic acids. *G3* 5, 497–505. doi: 10.1534/g3.114.015941

Davies, J. Q., and Gordon, S. (2005). Isolation and culture of murine macrophages. *Methods Mol. Biol.* 290, 91–103. doi: 10.1385/1-59259-838-2:091

Davis, D. A., Bruno, V. M., Loza, L., Filler, S. G., and Mitchell, A. P. (2002). *Candida albicans* Mds3p, a conserved regulator of pH responses and virulence identified through insertional mutagenesis. *Genetics* 162, 1573–1581. Available online at: https://www.genetics.org/content/162/4/1573.long

Denning, D. W., and Bromley, M. J. (2015). How to bolster the antifungal pipeline. *Science* 347, 1414–1416. doi: 10.1126/science.aaa6097

Denning, D. W., and Hope, W. W. (2010). Therapy for fungal diseases: opportunities and priorities. *Trends Microbiol.* 18, 195–204. doi: 10.1016/j.tim.2010.02.004

Desai, J. V., Bruno, V. M., Ganguly, S., Stamper, R. J., Mitchell, K. F., Solis, N., et al. (2013). Regulatory role of glycerol in *Candida albicans* biofilm formation. *MBio* 4, e00637–12. doi: 10.1128/mBio.00637-12

Dutkowski, J., Kramer, M., Surma, M., Balakrishnan, R., Cherry, J., Krogan, N., et al. (2013). A gene ontology inferred from molecular networks. *Nat. Biotechnol.* 31, 38–45. doi: 10.1038/nbt.2463

Finkel, J. S., Xu, W., Huang, D., Hill, E. M., Desai, J. V., Woolford, C. A., et al. (2012). Portrait of *Candida albicans* adherence regulators. *PLoS Pathog.* 8:e1002525. doi: 10.1371/journal.ppat.1002525

Gauwerky, K., Borelli, C., and Korting, H. C. (2009). Targeting virulence: a new paradigm for antifungals. *Drug Discov. Today* 14, 214–222. doi: 10.1016/j.drudis.2008.11.013

Grumaz, C., Lorenz, S., Stevens, P., Lindemann, E., Schöck, U., Retey, J., et al. (2013). Species and condition specific adaptation of the transcriptional landscapes in *Candida albicans* and *Candida dubliniensis*. *BMC Genomics* 14:212. doi: 10.1186/1471-2164-14-212

Hausauer, D. L., Gerami-Nejad, M., Kistler-Anderson, C., and Gale, C. A. (2005). Hyphal guidance and invasive growth in *Candida albicans* require the Ras-like GTPase Rsr1p and its GTPase-activating protein Bud2p. *Eukaryot. cell* 4, 1273–1286. doi: 10.1128/EC.4.7.1273-1286.2005

Inglis, D. O., Arnaud, M. B., Binkley, J., Shah, P., Skrzypek, M. S., Wymore, F., et al. (2012). The candida genome database incorporates multiple candida species: multispecies search and analysis tools with curated gene and protein information for *Candida albicans* and *Candida glabrata*. *Nucleic Acids Res.* 40, D667–D674. doi: 10.1093/nar/gkr945

Kramer, M., Dutkowski, J., Yu, M., Bafna, V., and Ideker, T. (2014). Inferring gene ontologies from pairwise similarity data. *Bioinformatics* 30, i34–i42. doi: 10.1093/bioinformatics/btu282

Kramer, M. H., Farré, J.-C., Mitra, K., Yu, M. K., Ono, K., Demchak, B., et al. (2017). Active interaction mapping reveals the hierarchical organization of autophagy. *Mol. Cell* 65, 761–774. doi: 10.1016/j.molcel.2016.12.024

Kullberg, B. J., and Arendrup, M. C. (2015). Invasive candidiasis. *N. Engl. J. Med.* 373, 1445–1456. doi: 10.1056/NEJMra1315399

Langfelder, P., and Horvath, S. (2008). WGCNA: an R package for weighted correlation network analysis. *BMC Bioinformatics* 9:559. doi: 10.1186/1471-2105-9-559

Langmead, B., and Salzberg, S. L. (2012). Fast gapped-read alignment with Bowtie 2. *Nat. Methods* 9, 357–359. doi: 10.1038/nmeth.1923

Langmead, B., Trapnell, C., Pop, M., Salzberg, S. L., et al. (2009). Ultrafast and memory-efficient alignment of short DNA sequences to the human genome. *Genome Biol.* 10:R25. doi: 10.1186/gb-2009-10-3-r25

Leach, M. D., Stead, D. A., Argo, E., and Brown, A. J. (2011). Identification of sumoylation targets, combined with inactivation of SMT3, reveals the impact of sumoylation upon growth, morphology, and stress resistance in the pathogen *Candida albicans*. *Mol. Biol. Cell* 22, 687–702. doi: 10.1091/mbc.e10-07-0632

Li, H., Handsaker, B., Wysoker, A., Fennell, T., Ruan, J., Homer, N., et al. (2009). The sequence alignment/map format and samtools. *Bioinformatics* 25, 2078–2079. doi: 10.1093/bioinformatics/btp352

Liu, H., Kohler, J., and Fink, G. R. (1994). Suppression of hyphal formation in *Candida albicans* by mutation of a STE12 homolog. *Science* 266:1723. doi: 10.1126/science.7992058

Liu, Y., Shetty, A. C., Schwartz, J. A., Bradford, L. L., Xu, W., Phan, Q. T., et al. (2015). New signaling pathways govern the host response to *C. albicans* infection in various niches. *Genome Res.* 25, 679–689. doi: 10.1101/gr.187427.114

Lo, H.-J., Köhler, J. R., DiDomenico, B., Loebenberg, D., Cacciapuoti, A., and Fink, G. R. (1997). Nonfilamentous *C. albicans* mutants are avirulent. *Cell* 90, 939–949. doi: 10.1016/S0092-8674(00)80358-X

Lohse, M. B., Gulati, M., Johnson, A. D., and Nobile, C. J. (2018). Development and regulation of single- and multi-species *Candida albicans* biofilms. *Nat. Rev. Microbiol.* 16, 19–31. doi: 10.1038/nrmicro.2017.107

Lorenz, M. C., Bender, J. A., and Fink, G. R. (2004). Transcriptional response of *Candida albicans* upon internalization by macrophages. *Eukaryot. Cell* 3, 1076–1087. doi: 10.1128/EC.3.5.1076-1087.2004

Love, M. I., Huber, W., and Anders, S. (2014). Moderated estimation of fold change and dispersion for RNA-Seq data with DESeq2. *Genome Biol.* 15:550. doi: 10.1186/s13059-014-0550-8

Marchais, V., Kempf, M., Licznar, P., Lefrançois, C., Bouchara, J.-P., Robert, R., et al. (2005). DNA array analysis of *Candida albicans* gene expression

in response to adherence to polystyrene. *FEMS Microbiol. Lett.* 245, 25–32. doi: 10.1016/j.femsle.2005.02.014

Mayer, F. L., Wilson, D., and Hube, B. (2013). *Candida albicans* pathogenicity mechanisms. *Virulence* 4, 119–128. doi: 10.4161/viru.22913

McCluskey, K., Wiest, A., and Plamann, M. (2010). The fungal genetics stock center: a repository for 50 years of fungal genetics research. *J. Biosci.* 35, 119–126. doi: 10.1007/s12038-010-0014-6

McKenzie, C. G. J., Koser, U., Lewis, L. E., Bain, J. M., Mora-Montes, H. M., Barker, R. N., et al. (2010). Contribution of *Candida albicans* cell wall components to recognition by and escape from murine macrophages. *Infect. Immun.* 78, 1650–1658. doi: 10.1128/IAI.00001-10

Mount, H. O., Revie, N. M., Todd, R. T., Anstett, K., Collins, C., Costanzo, M., et al. (2018). Global analysis of genetic circuitry and adaptive mechanisms enabling resistance to the azole antifungal drugs. *PLoS Genet.* 14:e1007319. doi: 10.1371/journal.pgen.1007319

Moyes, D. L., Wilson, D., Richardson, J. P., Mogavero, S., Tang, S. X., Wernecke, J., et al. (2016). Candidalysin is a fungal peptide toxin critical for mucosal infection. *Nature* 532, 64–68. doi: 10.1038/nature17625

Munro, C. A., Bates, S., Buurman, E. T., Hughes, H. B., MacCallum, D. M., Bertram, G., et al. (2005). Mnt1p and mnt2p of *Candida albicans* are partially redundant α-1, 2-mannosyltransferases that participate in o-linked mannosylation and are required for adhesion and virulence. *J. Biol. Chem.* 280, 1051–1060. doi: 10.1074/jbc.M411413200

Nett, J. E., Lepak, A. J., Marchillo, K., and Andes, D. R. (2009). Time course global gene expression analysis of an *in vivo* candida biofilm. *J. Infect. Dis.* 200, 307–313. doi: 10.1086/599838

Nobile, C. J., Fox, E. P., Nett, J. E., Sorrells, T. R., Mitrovich, Q. M., Hernday, A. D., et al. (2012). A recently evolved transcriptional network controls biofilm development in *Candida albicans*. *Cell* 148, 126–138. doi: 10.1016/j.cell.2011.10.048

Noble, S. M., French, S., Kohn, L. A., Chen, V., and Johnson, A. D. (2010). Systematic screens of a *Candida albicans* homozygous deletion library decouple morphogenetic switching and pathogenicity. *Nat. Genet.* 42, 590–598. doi: 10.1038/ng.605

Noble, S. M., Gianetti, B. A., and Witchley, J. N. (2016). *Candida albicans* cell-type switching and functional plasticity in the mammalian host. *Nat. Rev. Microbiol.* 15, 96–108. doi: 10.1038/nrmicro.2016.157

Queva, C., Hurlin, P. J., Foley, K. P., and Eisenman, R. N. (1998). Sequential expression of the mad family of transcriptional repressors during differentiation and development. *Oncogene* 16, 967–977. doi: 10.1038/sj.onc.1201611

Rauceo, J. M., Blankenship, J. R., Fanning, S., Hamaker, J. J., Deneault, J.-S., Smith, F. J., et al. (2008). Regulation of the *Candida albicans* cell wall damage response by transcription factor Sko1 and PAS kinase Psk1. *Mol. Biol. Cell* 19, 2741–2751. doi: 10.1091/mbc.e08-02-0191

Reedy, J. L., Filler, S. G., and Heitman, J. (2010). Elucidating the *Candida albicans* calcineurin signaling cascade controlling stress response and virulence. *Fungal Genet. Biol.* 47, 107–116. doi: 10.1016/j.fgb.2009.09.002

Richard, M. L., Nobile, C. J., Bruno, V. M., and Mitchell, A. P. (2005). *Candida albicans* biofilm-defective mutants. *Eukaryot. Cell* 4, 1493–1502. doi: 10.1128/EC.4.8.1493-1502.2005

Robinson, M. D., McCarthy, D. J., and Smyth, G. K. (2010). edgeR: a bioconductor package for differential expression analysis of digital gene expression data. *Bioinformatics* 26, 139–140. doi: 10.1093/bioinformatics/btp616

Skrzypek, M. S., Binkley, J., Binkley, G., Miyasato, S. R., Simison, M., and Sherlock, G. (2016). The candida genome database (CGD): incorporation of assembly 22, systematic identifiers and visualization of high throughput sequencing data. *Nucleic Acids Res.* 45, D592–D596. doi: 10.1093/nar/gkw924

Staab, J. F., Bahn, Y.-S., Tai, C.-H., Cook, P. F., and Sundstrom, P. (2004). Expression of transglutaminase substrate activity on *Candida albicans* germ tubes through a coiled, disulfide-bonded N-terminal domain of Hwp1 requires C-terminal glycosylphosphatidylinositol modification. *J. Biol. Chem.* 279, 40737–40747. doi: 10.1074/jbc.M406005200

Staab, J. F., Bradway, S. D., Fidel, P. L., and Sundstrom, P. (1999). Adhesive and mammalian transglutaminase substrate properties of *Candida albicans* Hwp1. *Science* 283, 1535–1538. doi: 10.1126/science.283.5407.1535

Staab, J. F., and Sundstrom, P. (1998). Genetic organization and sequence analysis of the hypha-specific cell wall protein gene Hwp1 of *Candida albicans*. *Yeast* 14, 681–686. doi: 10.1002/(SICI)1097-0061(199805)14:7<681::AID-YEA256>3.0.CO;2-8

Theiss, S., Kretschmar, M., Nichterlein, T., Hof, H., Agabian, N., Hacker, J., et al. (2002). Functional analysis of a vacuolar ABC transporter in wild-type *Candida albicans* reveals its involvement in virulence. *Mol. Microbiol.* 43, 571–584. doi: 10.1046/j.1365-2958.2002.02769.x

Uhl, M. A., Biery, M., Craig, N., and Johnson, A. D. (2003). Haploinsufficiency-based large-scale forward genetic analysis of filamentous growth in the diploid human fungal pathogen *C. albicans*. *EMBO J.* 22, 2668–2678. doi: 10.1093/emboj/cdg256

Vila, T., Romo, J. A., Pierce, C. G., McHardy, S. F., Saville, S. P., and Lopez-Ribot, J. L. (2017). Targeting *Candida albicans* filamentation for antifungal drug development. *Virulence* 8, 150–158. doi: 10.1080/21505594.2016.1197444

Warenda, A. J., Kauffman, S., Sherrill, T. P., Becker, J. M., and Konopka, J. B. (2003). *Candida albicans* septin mutants are defective for invasive growth and virulence. *Infect. Immun.* 71, 4045–4051. doi: 10.1128/IAI.71.7.4045-4051.2003

Wilson, D., Thewes, S., Zakikhany, K., Fradin, C., Albrecht, A., Almeida, R., et al. (2009). Identifying infection-associated genes of *Candida albicans* in the postgenomic era. *FEMS Yeast Res.* 9, 688–700. doi: 10.1111/j.1567-1364.2009.00524.x

Winnenburg, R., Baldwin, T. K., Urban, M., Rawlings, C., Köhler, J., and Hammond-Kosack, K. E. (2006). PHI-base: a new database for pathogen host interactions. *Nucleic Acids Res.* 34(Suppl. 1), D459–D464. doi: 10.1093/nar/gkj047

Yu, M. K., Ma, J., Ono, K., Zheng, F., Fong, S. H., Gary, A., et al. (2019). DDOT: A swiss army knife for investigating data-driven biological ontologies. *Cell Syst*. 8, 267–273.e3. doi: 10.1016/j.cels.2019.02.003

Zheng, X., Wang, Y., and Wang, Y. (2004). Hgc1, a novel hypha-specific G1 cyclin-related protein regulates *Candida albicans* hyphal morphogenesis. *EMBO J.* 23, 1845–1856. doi: 10.1038/sj.emboj.7600195

Conflict of Interest: The authors declare that the research was conducted in the absence of any commercial or financial relationships that could be construed as a potential conflict of interest.

frontiers in Genetics

ORIGINAL RESEARCH
published: 12 May 2020
doi: 10.3389/fgene.2020.00459

Genomic and Phenotypic Heterogeneity of Clinical Isolates of the Human Pathogens *Aspergillus fumigatus*, *Aspergillus lentulus*, and *Aspergillus fumigatiaffinis*

Renato A. C. dos Santos[1,2], Jacob L. Steenwyk[2], Olga Rivero-Menendez[3], Matthew E. Mead[2], Lilian P. Silva[1], Rafael W. Bastos[1], Ana Alastruey-Izquierdo[3], Gustavo H. Goldman[1] and Antonis Rokas[2]**

[1] Departamento de Ciências Farmacêuticas, Faculdade de Ciências Farmacêuticas de Ribeirão Preto, Universidade de São Paulo, São Paulo, Brazil, [2] Department of Biological Sciences, Vanderbilt University, Nashville, TN, United States, [3] Medical Mycology Reference Laboratory, National Center for Microbiology, Instituto de Salud Carlos III, Madrid, Spain

OPEN ACCESS

Edited by:
Bridget Marie Barker, Northern Arizona University, United States

Reviewed by:
Megan C. McDonald, Australian National University, Australia
Praveen Rao Juvvadi, Duke University, United States

***Correspondence:**
Gustavo H. Goldman
ggoldman@usp.br
Antonis Rokas
antonis.rokas@vanderbilt.edu

Specialty section:
This article was submitted to Evolutionary and Genomic Microbiology, a section of the journal Frontiers in Genetics

Received: *28 February 2020*
Accepted: *14 April 2020*
Published: *12 May 2020*

Citation:
dos Santos RAC, Steenwyk JL, Rivero-Menendez O, Mead ME, Silva LP, Bastos RW, Alastruey-Izquierdo A, Goldman GH and Rokas A (2020) Genomic and Phenotypic Heterogeneity of Clinical Isolates of the Human Pathogens Aspergillus fumigatus, Aspergillus lentulus, and Aspergillus fumigatiaffinis. Front. Genet. 11:459. doi: 10.3389/fgene.2020.00459

Fungal pathogens are a global threat to human health. For example, fungi from the genus *Aspergillus* cause a spectrum of diseases collectively known as aspergillosis. Most of the >200,000 life-threatening aspergillosis infections per year worldwide are caused by *Aspergillus fumigatus*. Recently, molecular typing techniques have revealed that aspergillosis can also be caused by organisms that are phenotypically similar to *A. fumigatus* but genetically distinct, such as *Aspergillus lentulus* and *Aspergillus fumigatiaffinis*. Importantly, some of these so-called cryptic species are thought to exhibit different virulence and drug susceptibility profiles than *A. fumigatus*, however, our understanding of their biology and pathogenic potential has been stymied by the lack of genome sequences and phenotypic profiling of multiple clinical strains. To fill this gap, we phenotypically characterized the virulence and drug susceptibility of 15 clinical strains of *A. fumigatus*, *A. lentulus*, and *A. fumigatiaffinis* from Spain and sequenced their genomes. We found heterogeneity in drug susceptibility across species and strains. We further found heterogeneity in virulence within each species but no significant differences in the virulence profiles between the three species. Genes known to influence drug susceptibility (*cyp51A* and *fks1*) vary in paralog number and sequence among these species and strains and correlate with differences in drug susceptibility. Similarly, genes known to be important for virulence in *A. fumigatus* showed variability in number of paralogs across strains and across species. Characterization of the genomic similarities and differences of clinical strains of *A. lentulus*, *A. fumigatiaffinis*, *and A. fumigatus* that vary in disease-relevant traits will advance our understanding of the variance in pathogenicity between *Aspergillus* species and strains that are collectively responsible for the vast majority of aspergillosis infections in humans.

Keywords: *Aspergillus*, antifungal drug susceptibility, genomics, strain heterogeneity, drug resistance, cryptic species, virulence, genetic determinants of virulence

INTRODUCTION

Aspergillosis is a major health problem, with rapidly evolving epidemiology and new groups of at-risk patients (Patterson et al., 2016). Aspergillosis infections are usually caused by inhalation of airborne asexual spores (conidia) of *Aspergillus fumigatus* and a few other *Aspergillus* species (Rokas et al., 2020). Aspergillosis covers a spectrum of diseases (Latgé and Chamilos, 2020). For example, non-invasive diseases caused by *Aspergillus*, such as aspergilloma, are currently classified as chronic pulmonary aspergillosis and are commonly associated to pulmonary tuberculosis (Denning et al., 2016). In atopic patients, the most severe form of aspergillosis is allergic bronchopulmonary aspergillosis (ABPA), which develops following sensibilization to *A. fumigatus* allergens in atopic patients with cystic fibrosis or individuals with genetic predisposition to ABPA (Agarwal et al., 2013). However, the most common invasive type of infection is invasive pulmonary aspergillosis (IPA), whose risk is significantly increased in immunocompromised individuals, in patients with acute leukemia and recipients of hematopoietic stem cells transplantation, or in solid-organ transplant recipients (Brown et al., 2012). Importantly, IPA has recently been described in new groups of traditionally low-risk patients, such as patients in intensive care units recovering from bacterial sepsis (Latgé and Chamilos, 2020).

Although *A. fumigatus* is the major etiologic agent of aspergillosis, a few other *Aspergillus* species, such as *Aspergillus flavus*, *Aspergillus terreus*, *Aspergillus niger*, and *Aspergillus nidulans*, can also cause infections (Zakaria et al., 2020). While most of these pathogens can be phenotypically easily distinguished, infections can also be caused by *Aspergillus* species that are morphologically very similar to *A. fumigatus* (Rokas et al., 2020). These close pathogenic relatives of *A. fumigatus* are considered sibling species or cryptic species because they are undistinguishable from each other and from *A. fumigatus* by classical identification methods (Alastruey-Izquierdo et al., 2014); these species vary mostly in their colony growth, robustness of the production of conidia, conidial surface markings, presence and absence of septation in phialides, and maximum growth temperatures (Taylor et al., 2000; Balajee et al., 2005; Katz et al., 2005). As a result of their near identical morphological characteristics, most of these cryptic species have only recently been described. For example, *Aspergillus lentulus* was first described in 2005 in a case of human aspergillosis (Balajee et al., 2005). Similarly, *A. fumigatiaffinis*, another pathogenic species that is closely related to *A. fumigatus,* was first described in 2005 (Hong et al., 2005). Even though cryptic species were only discovered relatively recently, understanding their genetic and phenotypic similarities and differences from the major pathogen *A. fumigatus* is important for two reasons. First, their prevalence in the clinic has been estimated to be between 11 and 19% (Balajee et al., 2009; Alastruey-Izquierdo et al., 2014; Negri et al., 2014). Second, several of these species, including *A. lentulus* and *A. fumigatiaffinis*, have been shown to differ in their drug susceptibility to amphotericin B and azoles compared to *A. fumigatus* (Alastruey-Izquierdo et al., 2014).

Antifungal resistance is of worldwide concern in human pathogenic *Aspergillus* species as well as in many other human, animal, and plant fungal pathogens (Parker et al., 2014; Sharma and Chowdhary, 2017). Several antifungal-resistance mechanisms have been proposed in fungi (Sharma and Chowdhary, 2017; Perez-Cantero et al., 2020). In azole-resistant *Aspergillus* strains, known mechanisms are particularly well-described in genes of the cytochrome P450 sterol 14 α-demethylase family (*cyp51*), and include sequence variants in diverse positions of the Cyp51A protein sequence (e.g., G54, G138, M220, G448, Y121, P216, F219, A284, Y431, G432, and G434; reviewed in Wei et al., 2015; Perez-Cantero et al., 2020), as well as combinations of the aforementioned protein sequence changes with tandem repeat (TR) variants in the promoter region, such as TR34/L98H or TR46/Y121F/T289A (reviewed in Wei et al., 2015). Non-*cyp51* based mechanisms of antifungal resistance, such as in multidrug efflux pumps and pathways such as ergosterol biosynthesis and stress response, have also been proposed (Perez-Cantero et al., 2020). Mechanisms of echinocandin resistance have mostly been attributed to FKS subunits of glucan synthase (Sharma and Chowdhary, 2017). While most of these studies are in *Candida* species (Desnos-Ollivier et al., 2008; Garcia-Effron et al., 2008), a recent study in *A. fumigatus* also observed mutations associated with echinocandin resistance (Jiménez-Ortigosa et al., 2017).

An emerging realization in the study of *Aspergillus* pathogens is the presence of phenotypic heterogeneity among strains of the same species (Keller, 2017). For example, recent studies have shown how variation in hypoxic growth phenotypes is associated with virulence among *A. fumigatus* strains (Kowalski et al., 2016, 2019). Similarly, *A. fumigatus* strains have previously been shown to exhibit great quantitative and qualitative heterogeneity in light response (Fuller et al., 2016); in this case, heterogeneity in light response was not associated with heterogeneity in virulence. Finally, Ries et al. (2019) found a high heterogeneity among *A. fumigatus* strains with regard to nitrogen acquisition and metabolism during infection and correlation between nitrogen catabolite repression-related protease secretion and virulence. These studies highlight the biological and clinical relevance of understanding strain heterogeneity in *Aspergillus* pathogens, especially with respect to virulence and antifungal drug susceptibility. However, comparisons of strain heterogeneity in virulence and drug resistance profiles among clinical strains in *A. fumigatus* and closely related cryptic species, such as *A. lentulus* and *A. fumigatiaffinis*, are lacking.

To address this gap in the field, we phenotypically characterized and sequenced the genomes of 15 clinical strains of *A. fumigatus*, *A. lentulus*, and *A. fumigatiaffinis* from Spain. At the phenotypic level, we found strain heterogeneity in both virulence and drug susceptibility profiles within each species as well as differences in drug susceptibility profiles between the three species. Interestingly, we found that the virulence profiles of the three species were similar. At the genomic level, we found that gene families known to influence drug susceptibility, such as *cyp51*, exhibit variation in their

numbers of paralogs and sequence among these species and strains. Similarly, we found variability in the number of paralogs within and between species in many genes known to be important for virulence in *A. fumigatus*. Characterization of the genomic similarities and differences of clinical strains of *A. lentulus*, *A. fumigatiaffinis*, *and A. fumigatus* that vary in disease-relevant traits will advance our understanding of the variation in pathogenicity between *Aspergillus* species and strains that are collectively responsible for the vast majority of aspergillosis infections in humans.

MATERIALS AND METHODS

Strains and Species Identification

To understand the degree of genomic heterogeneity among strains, we sequenced six clinical strains of *A. fumigatus*, five of *A. lentulus,* and four of *A. fumigatiaffinis* available in the Mycology Reference Laboratory of the National Center for Microbiology (CNM) in Instituto de Salud Carlos III in Spain (**Supplementary Table S1**). For initial species identification, we sequenced the Internal Transcribed Spacer region (ITS) and beta-tubulin (*benA*) gene amplicons (primer pairs in **Supplementary Table S2**). We downloaded reference sequences for the type strains of *A. fumigatiaffinis* IBT12703 and *A. lentulus* IFM54703, and of *Aspergillus clavatus* NRRL1 (section *Clavati*), which we used as the outgroup. We aligned DNA sequences with MAFFT v.7.397 (Katoh and Standley, 2013), followed by model selection and phylogenetic inference in IQ-TREE v.1.6.7 (Nguyen et al., 2015).

Characterization of Virulence and Antifungal Susceptibility Profiles

To understand the pathogenic potential of the 15 clinical strains, we carried out virulence assays using the moth *Galleria mellonella* model of fungal disease (Fuchs et al., 2010; Slater et al., 2011). Briefly, we obtained moth larvae by breeding adult moths that were kept for 24 h prior to infection under starvation, in the dark, and at a temperature of 37°C. We selected only larvae that were in the sixth and final stage of larval development. We harvested fresh asexual spores (conidia) from each strain from yeast extract-agar-glucose (YAG) plates in PBS solution and filtered through a Miracloth (Calbiochem). For each strain, we counted the spores using a hemocytometer and created a 2×10^8 conidia/ml stock suspension. We determined the viability of the administered inoculum by plating a serial dilution of the conidia on YAG medium at 37°C. We inoculated 5 μl (1×10^6 conidia/larvae) to each larva (n = 10). We used as the control a group composed of larvae inoculated with 5 μl of PBS. We performed inoculations via the last left proleg using a Hamilton syringe (7000.5KH). After infection, we maintained the larvae in petri dishes at 37°C in the dark and scored them daily (i.e., recorded the number of dead larvae each day) during a 10-day period. We considered larvae that did not move in response to touch as dead.

We tested the virulence of each clinical strain by infecting 10 larvae, i.e., for each strain tested we have one experimental replicate with an sample size n of 10. We performed two sets of analyses. First, we statistically assessed if the survival curves of different strains in a given species are identical (null hypothesis of strain homogeneity) or different (alternative hypothesis of strain heterogeneity). Second, we used strains within each species as "biological replicates" and statistically assessed if the survival curves between species were similar or different. We performed these statistical assessments using the log-rank test implemented in the survival R package (Therneau, 2014), followed by multiple test correction of p-values (Benjamini and Hochberg). Scripts used to perform these analyses are available on the GitLab repository[1] under 'experimentalData/'.

To measure the antifungal susceptibility of the clinical strains, we applied the EUCAST (European Committee for Antimicrobial Susceptibility Testing) reference microdilution method version 9.3.1 (Arendrup et al., 2017), in which fungi are grown on plates with increasing concentrations of antifungals and the first concentration in which fungal growth is inhibited (MIC) is recorded. For all strains, we tested their susceptibility to four antifungal drug classes: (a) Polyenes: amphotericin B (Sigma-Aldrich Quimica, Madrid, Spain); (b) Azoles: itraconazole (Janssen Pharmaceutica, Madrid, Spain), voriconazole (Pfizer SA, Madrid, Spain), and posaconazole (Schering-Plough Research Institute, Kenilworth, NJ, United States); (c) Echinocandins: caspofungin (Merck & Co. Inc., Rahway, NJ, United States), micafungin (Astellas Pharma Inc., Tokyo, Japan), and anidulafungin (Pfizer SA, Madrid, Spain); and (d) Allylamines: Terbinafine (Novartis, Basel, Switzerland). The final concentrations tested ranged from 0.03 to 16 mg/L for amphotericin B, terbinafine, and caspofungin; from 0.015 to 8 mg/L for itraconazole, voriconazole and posaconazole; from 0.007 to 4 mg/L for anidulafungin; and from 0.004 to 2 mg/L for micafungin. *A. flavus* ATCC 204304 and *A. fumigatus* ATCC 204305 were used as quality control strains in all tests performed. MICs for amphotericin B, itraconazole, voriconazole, posaconazole, and terbinafine, and minimal effective concentrations (MECs) for anidulafungin, caspofungin, and micafungin were visually read after 24 and 48 h of incubation at 35°C in a humid atmosphere. To assess the relationship between antifungal susceptibility and strain/species identification, we carried out principal component analysis (PCA) with scaled MIC/MEC values with the R package FactoMineR (Lê et al., 2008), and data visualization with the factoextra v.1.0.6 package. Scripts used to perform these analyses are available on the GitLab repository (see text footnote 1) under 'experimentalData/'.

Genome Sequencing

To understand the genomic similarities and differences within and between these pathogenic *Aspergillus* species and how they are associated with differences in drug susceptibility and virulence profiles, we sequenced the genomes of all 15 strains. Each strain was grown in glucose-yeast extract-peptone (GYEP) liquid medium (0.3% yeast extract and 1% peptone; Difco, Soria Melguizo) with 2% glucose (Sigma-Aldrich, Spain)

[1]https://gitlab.com/SantosRAC/afum_afma_alen2020

for 24 h to 48 h at 30°C. After mechanical disruption of the mycelium by vortex mixing with glass beads, genomic DNA of isolates was extracted using the phenol–chloroform method (Holden, 1994). The preparation of DNA libraries was performed using the Nextera® TM DNA Library PrepKit (Illumina Inc., San Diego, CA, United States) according to manufacturer's guidelines. DNA quantification was carried out using the QuantiFluor® dsDNA System and the QuantiFluor® ST Fluorometer (Promega, Madison, WI, United States) and its quality was checked with the Agilent 2100 Bioanalyzer (Agilent Technologies Inc., Santa Clara, CA, United States). Sequencing was performed in the Illumina platform NextSeq500, following the manufacturer's protocols (Illumina Inc., San Diego, CA, United States). We performed an initial quality analysis of the sequence reads using FastQC, v.0.11.7[2]. We inspected sequence reads for contaminants using BLAST (Altschul et al., 1990) and MEGAN5 (Huson and Weber, 2013). We trimmed low quality bases (LEADING = 3; TRAILING = 3; SLIDINGWINDOW: windowSize = 4 and requiredQuality = 15), removing both short sequences (<90 bp) and Nextera adaptors, with Trimmomatic v.0.38 (Bolger et al., 2014).

Genome Assembly and Annotation

We assembled the genomes of all strains with SPAdes v3.12.0 (Bankevich et al., 2012). We corrected bases, fixed mis-assemblies, and filled gaps with Pilon, v.1.22 (Walker et al., 2014). We assessed genome assembly quality using QUAST, v.4.6.3 (Gurevich et al., 2013). We assessed genome assembly completeness using Benchmarking Universal Single-Copy Orthologs (BUSCO) (Simão et al., 2015) and the 4,046 Eurotiomycetes BUSCO gene set (genes from OrthoDB that are thought to be universally single copy). We carried out gene prediction with AUGUSTUS v.3.3.1 (Stanke et al., 2004) using the gene models of *A. fumigatus* Af293 strain (Nierman et al., 2005) as reference. We carried out functional annotation with InterProScan 5.34-73.0 (Jones et al., 2014).

Orthogroup Identification

To identify orthologs (and closely related paralogs) across strains, we performed all-vs.-all searches with blastp 2.7.1+ (Altschul et al., 1990) using the strains' predicted proteomes. We used OrthoFinder v.2.3.3 (Emms and Kelly, 2019) to generate orthogroups using pre-computed BLAST results (-og option) and a Markov Clustering (MCL) inflation value of 1.5. We considered an orthogroup "species-specific" if it possessed one or more protein sequences from only one species. Information on performing these analyses is available on the GitLab wiki page 'orthology-calling[3]'.

Identification of Single Nucleotide Polymorphisms and Insertions/Deletions

To characterize genetic variation within and between the three pathogenic *Aspergillus* species, we assessed single nucleotide polymorphisms (SNPs) and insertions/deletions (indels). We used BWA-MEM v.0.7.17 (Li and Durbin, 2009) with default parameters to map reads to the reference genome sequences for *A. fumigatus*, *A. lentulus*, and *A. fumigatiaffinis* (CNM-CM8686, CNM-CM7927, and CNM-CM6805, respectively). We did not use type strains as reference genomes for the species under study, because they are not from Spain. Duplicate reads were identified using PICARD MarkDuplicates, v.2.9.2[4]. We indexed genomes using SAMTOOLS v.1.8 (Li et al., 2009) for subsequent variant detection analyses.

We used GenomeAnalysisTK (GATK) v.3.6 for SNP calling with the recommended hard filtering parameters (McKenna et al., 2010; Depristo et al., 2011). We used SnpEff v.4.3t (Cingolani et al., 2013) to annotate and predict the functional effect of SNPs and indels. Variants assumed to have high (disruptive) impact in the protein, probably causing protein truncation, loss of function or triggering nonsense mediated decay were classified as "high," variants assumed that might change protein effectiveness but were non-disruptive were classified as "moderate," and variants most likely to be harmless or unlikely to change protein behavior were classified as "low." Finally, non-coding variants or variants affecting non-coding genes, where predictions are difficult or there is no evidence of impact, were classified as "modifier." Details can be found on the SnpEff manual[5].

We aligned protein and coding sequences for genes of interest with MAFFT v.7.397 (Katoh and Standley, 2013), using the –auto mode. We used Jalview v.2.10.3 (Waterhouse et al., 2009) to visualize SNPs, and a Python script to recover non-synonymous mutations compared to the reference, *A. fumigatus* A1163. Enrichment analysis of GO terms in genes with high impact SNPs and indels for each species was carried out with GOATOOLS v.0.9.9 (Klopfenstein et al., 2018). Scripts used to perform these analyses are available on the GitLab repository (see text footnote 1) under 'genomePolymorphisms/' and 'goatools/'.

Genetic Determinants Important for Virulence

To examine whether SNPs, indels, and number of paralogs in a given orthogroup were associated with virulence, we recovered 215 genes in *A. fumigatus* Af293 considered genetic determinants of virulence based on their presence in PHI-base (Winnenburg, 2006) and in previously published studies (Abad et al., 2010; Kjærbølling et al., 2018). We obtained functional annotation of these virulence-related genes from FungiDB (Basenko et al., 2018).

Maximum-Likelihood Phylogenomics

To reconstruct the evolutionary history of our 15 strains and closely related *Aspergillus* species, we first downloaded or assembled genomes of other strains of the three pathogenic species or their closely relatives that are publicly available. Specifically, we downloaded the genomes of *Aspergillus*

[2]https://www.bioinformatics.babraham.ac.uk/projects/fastqc/

[3]https://gitlab.com/SantosRAC/afum_afma_alen2020/-/wikis/orthology-calling

[4]http://broadinstitute.github.io/picard

[5]http://snpeff.sourceforge.net/SnpEff_manual.html

novofumigatus IBT16806 (Kjærbølling et al., 2018), *Aspergillus lentulus* IFM 54703^T (Kusuya et al., 2016), *Aspergillus fischeri* NRRL181 (Fedorova et al., 2008), *Aspergillus udagawae* IFM46973 (Kusuya et al., 2015), and *Aspergillus viridinutans* FRR_0576 (GenBank accession: GCA_004368095.1). To ensure our analyses also captured the genetic diversity of *A. fumigatus*, we also included additional *A. fumigatus* genomes that spanned the known diversity of *A. fumigatus* strains (Lind et al., 2017). Specifically, we downloaded the genomes of *A. fumigatus* A1163 (Fedorova et al., 2008) and *A. fumigatus* Af293 (Nierman et al., 2005). Additionally, we obtained the raw reads of *A. fumigatus* strains 12-750544 and F16311 (SRA accessions: SRR617737 and ERR769500, respectively). To assemble these genomes, we first quality-trimmed the sequence reads using Trimmomatic, v0.36 (Bolger et al., 2014) using parameters described elsewhere (leading:10, trailing:10, slidingwindow:4:20, and minlen:50). The resulting quality-trimmed reads were then used for genome assembly using SPAdes, v3.8.1 (Bankevich et al., 2012), using the 'careful' parameter and the 'cov-cutoff' parameter set to 'auto.' Altogether, we analyzed a total of 24 genomes.

To identify single-copy orthologous genes among the 24 genomes, we implemented the BUSCO, v.2.0.1 pipeline (Waterhouse et al., 2013; Simão et al., 2015). Specifically, we used the BUSCO pipeline to identify single-copy orthologous genes from genomes using the Eurotiomycetes database of 4,046 orthologs from OrthoDB, v9 (Waterhouse et al., 2013). Among the 4,096 orthologs, we identified 3,954 orthologs with at least 18 taxa represented and aligned the protein sequence each ortholog individually using Mafft, v7.294b (Katoh and Standley, 2013), with the same parameters as described elsewhere (Steenwyk et al., 2019). We then forced nucleotide sequences onto the protein alignment with a custom Python, v3.5.2 script (indicated on the Gitlab repository README.md file) using BioPython, v1.7 (Cock et al., 2009). The resulting nucleotide alignments were trimmed using trimAl, v1.4 (Capella-Gutierrez et al., 2009), with the 'gappyout' parameter. The trimmed alignments were then concatenated into a single matrix with 7,147,728 sites. We then used the concatenated data matrix as input into IQ-TREE, v1.6.11 (Nguyen et al., 2015), with the 'nbest' parameter set to 10. The best-fitting model of substitutions was automatically determined using the Bayesian information criterion. The best-fitting model was a general time general time-reversible model with empirical base frequencies, a discrete Gamma model with 4 rate categories, and a proportion of invariable sites (GTR+I+F+G4) (Tavaré, 1986; Yang, 1994, 1996; Vinet and Zhedanov, 2011). Lastly, we evaluated bipartition support using 5,000 ultrafast bootstrap approximations (Hoang et al., 2018).

In order to build the phylogeny with Cyp51 paralogs, we recovered protein sequences from two orthogroups that included Cyp51A and Cyp51B from *A. fumigatus* Af293 (Afu4g06890 and Afu7g03740, respectively). We generated a maximum-likelihood phylogeny in IQ-Tree v. 1.6.12 (Nguyen et al., 2015), using 1000 Ultrafast Bootstrap Approximation (UFBoot) replicates. The LG+G4 model was chosen as the best according to Bayesian Information Criterion. The protein sequences and tree files are available on the GitLab repository (see text footnote 1) under 'AntifungalGenes/'.

RESULTS

Clinical Strains Show Varying Antifungal Drug Susceptibility

To study susceptibility to antifungals across all strains of the three *Aspergillus* pathogens, we employed the EUCAST reference microdilution method with the four different known classes of antifungal drugs (**Table 1**). By performing PCA on the antifungal drug susceptibility values of all 15 strains, we found that the strains exhibited high heterogeneity in their drug resistance profiles (**Figure 1A**). In many cases, we found that strains from different species were more similar to each other (e.g., strain CNM-CM8686 from *A. fumigatus* with strain CNM-CM6069 from *A. lentulus*) than to other strains from the same species (e.g., strain CNM-CM8686 with strain CNM-CM8057 from *A. fumigatus*), highlighting the magnitude of heterogeneity in drug susceptibility of these species and strains. Principal component 1 (PC1) explained 37.2% of the variation and separated almost all *A. fumigatus* strains from those of the other two species. Principal component 2 (PC2) explained 21% of the variation, but did not separate species. The individual contributions of each antifungal drug to each PC are shown in **Supplementary Figure S1**. Finally, we found that the susceptibility of amphotericin B (in the polyenes class) was negatively correlated with micafungin (echinocandins) and terbinafine (allylamines), whereas anidulafungin (echinocandins) and voriconazole (azoles) were positively correlated (**Supplementary Figure S2**). Interestingly, the drugs exhibiting these negative or positive correlations are from different classes (e.g., polyenes *versus* allylamines or echinocandins *versus* azoles).

We also looked at the differences in susceptibility between strains for each antifungal drug (**Figure 1B**). Our data show that clinical strains of *A. fumigatus* exhibit lower MICs to amphotericin B compared to *A. lentulus* and *A. fumigatiaffinis*, albeit different levels are observed among different strains (one-way ANOVA; $\alpha < 0.05$; Tukey multiple comparisons of means for amphotericin B) (**Table 1**). With the exception of susceptibility of *A. fumigatus* and *A. lentulus* to amphotericin B, for which a significant difference is observed between these two species, we observed high heterogeneity among strains of different species for the other drugs (**Table 1**). Among azoles, itraconazole and voriconazole displayed higher levels of variability across strains. With respect to terbinafine, the four *A. fumigatiaffinis* strains exhibited low MICs, whereas four *A. fumigatus* strains displayed higher MICs (MIC values >1 mg/L) and the other two *A. fumigatus* strains even higher; finally, one *A. lentulus* strain (CNM-CM8694) displayed the highest MICs across all strains (albeit other strains showed in general lower MICs). Among echinocandin drugs, caspofungin showed high MECs for the three species. In particular, one strain of *A. fumigatiaffinis* and three of *A. lentulus* were notable in exhibiting very high MECs (MECs $\geq$ 1 mg/L). MECs for micafungin and anidulafungin were low ($\leq$0.125 mg/L) for all strains.

TABLE 1 | Susceptibility profile of cryptic *Aspergillus* species isolated in the Mycology Reference Laboratory of Spain.

Species	Strain identifier	MIC (mg/L)				MEC (mg/L)			
		AMB	*ICZ*	*VCZ*	*PCZ*	*TRB*	*CPF*	*MCF*	*AND*
Aspergillus lentulus	CNM-CM6069	8	0.5	2	0.12	0.5	1	0.015	0.015
	CNM-CM6936	16	0.5	4	0.25	2	2	0.03	0.03
	CNM-CM7927	8	0.5	2	0.12	0.5	0.06	0.015	0.007
	CNM-CM8060	0.12	0.25	1	0.12	0.5	2	0.06	0.03
	CNM-CM8694	2	0.12	0.25	0.06	32	0.03	0.03	MD
	CNM-CM8927	16	2	1	0.25	2	0.25	0.015	0.015
Aspergillus fumigatiaffinis	CNM-CM5878	1	0.25	0.5	0.06	0.25	1	0.03	0.015
	CNM-CM6457	16	16	2	0.25	1	0.25	0.03	0.007
	CNM-CM6805	16	0.25	2	0.12	0.25	0.5	0.03	0.03
	CNM-CM8980	16	0.5	2	0.5	0.5	0.12	0.007	0.015
Aspergillus fumigatus	CNM-CM8057	0.25	>8	>8	1	16	0.5	0.06	0.12
	CNM-CM8714	0.25	>8	4	1	4	0.25	0.007	0.03
	CNM-CM8812	0.25	0.25	0.5	0.12	1	0.25	0.03	0.03
	CNM-CM8686	0.5	0.25	0.25	0.12	2	0.25	0.015	0.015
	CNM-CM8689	1	1	8	0.25	16	0.5	0.125	0.03
	Af293	0.5	1	1	0.125	2	0.125	0.007	0.007
One-way ANOVA (between species)	*P*-value	0.025*	0.435	0.209	0.171	0.492	0.364	0.462	0.242
Tukey multiple comparisons of means	*Aspergillus fumigatus* – *Aspergillus fumigatiaffinis*	0.0245507*	–	–	–	–	–	–	
	Aspergillus lentulus - *Aspergillus fumigatiaffinis*	0.5595621	–	–	–	–	–	–	
	Aspergillus lentulus - *Aspergillus fumigatus*	0.0982057	–	–	–	–	–	–	

*AMB, amphotericin B; ICZ, itraconazole; VCZ, voriconazole; PCZ, posaconazole; CPF, caspofungin; MCF, micafungin; AND, anidulafungin; TRB, terbinafine. *P-values < 0.05 were considered significant.*

Clinical Strains Within Each Species Show Varying Levels of Virulence

Given functional similarities of the greater wax moth *Galleria mellonella* innate immune system with that of mammals, and prior work showing that moth larvae and mice exhibit similar survival rates when infected with *A. fumigatus* (Slater et al., 2011; Mead et al., 2019), we infected *G. mellonella* larvae with all 15 strains to assess their virulence profiles (**Figure 2**).

Survival curves revealed high heterogeneity in virulence across clinical strains within each of the three species (**Figure 2**). We observed highly virulent strains for which all ten larvae were dead at day 10, such as *A. fumigatus* Af293 (one of our reference strains), *A. fumigatiaffinis* CNM-CM5878 and *A. lentulus* CNM-CM8927. In contrast, other strains were less virulent and >25% larvae survived to the last day of data collection, such as *A. lentulus* CNM-CM6069 and CNM-CM8060. Moreover, we found significant heterogeneity in the survival curves between strains within each species (Benjamini and Hochberg adjusted *p*-values: 0.00285 in *A. fumigatus*, 0.00054 in *A. fumigatiaffinis*, and 0.014 in *A. lentulus*; log-rank test) (**Figures 2A–C**). We also tested differences between species (considering each strain as a biological replicate), and observed no significant difference between the kill curves of the various species (*p*-value = 0.17; log-rank test) – that is, we found that both *A. lentulus* and *A. fumigatiaffinis* were as virulent as *A. fumigatus* (**Figure 2D**).

Genomic Variation Within and Between Spanish Strains of *A. fumigatus*, *A. lentulus*, and *A. fumigatiaffinis*

To begin exploring the potential genetic underpinnings of species and strain variation in drug susceptibility and virulence, we conducted comparative genomic analyses. The genomes of all 15 strains were of high quality and contained 97–98% of expected complete and single-copy BUSCOs (**Supplementary Table S3**). *A. lentulus* and *A. fumigatiaffinis* genomes had larger gene repertoires (9,717–9,842 and 10,329–10,677, respectively) than *A. fumigatus* (8,837–8,938), consistent with previous genome studies of *A. lentulus* and *A. fumigatus* (Nierman et al., 2005; Fedorova et al., 2008; Kusuya et al., 2016). A genome-scale phylogenetic analysis using the nucleotide sequences of BUSCOs with previously sequenced strains (**Figure 3A**) supports the close relationship between *A. lentulus* and *A. fumigatiaffinis*.

Genome Diversity Among and Within Species Across Clinical Strains

Examination of orthogroups across the 15 strains and three species revealed that most genes (7,938) are shared by all three species (**Figure 3B**). *A. fumigatiaffinis* has a larger set of species-specific genes (1,062) than *A. lentulus* (656) or *A. fumigatus* (645), consistent with its larger genome size and gene number. The numbers of shared genes between *A. lentulus*

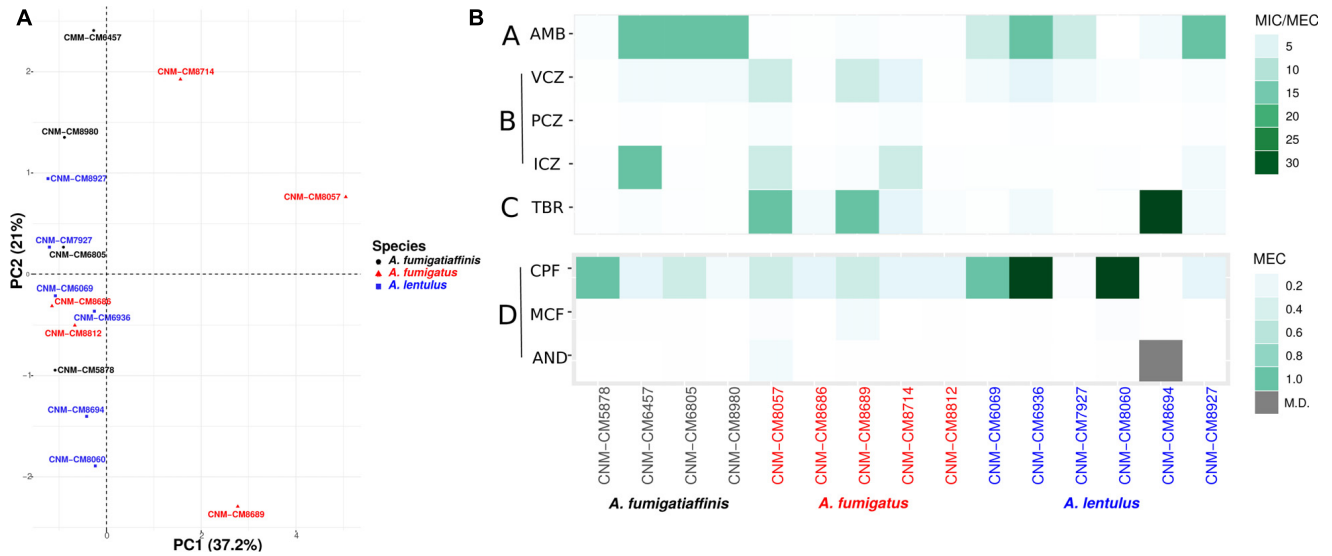

FIGURE 1 | High heterogeneity in drug susceptibility profiles among Spanish strains of three closely related *Aspergillus* pathogens. **(A)** Principal component analysis (PCA) carried out for antifungal susceptibility testing. PC1 (Dim1) explains most of the variation (37.2% of the variation) and is able to separate *A. fumigatus* from other two species, whereas an overlap is observed in cryptic species (*A. lentulus* and *A. fumigatiaffinis*). **(B)** Antifungal susceptibility testing was carried out using the EUCAST reference microdilution method. The minimum inhibitory concentration (MIC) was obtained for AMB, VCZ, PCZ, and ICZ and the minimum effective concentration (MEC) was obtained for TRB, CPF, MCF, and AND. A lower scale is shown for echinocandins (bottom panel). Antifungal classes are A: polyenes; B: azoles; C: allylamines; D: echinocandins. AMB, amphotericin B; ICZ, itraconazole; VCZ, voriconazole; PCZ, posaconazole; CPF, caspofungin; MCF, micafungin; AND, anidulafungin; TRB, terbinafine.

and *A. fumigatiaffinis* are also higher than intersections between each of them with *A. fumigatus*, consistent with their closer evolutionary relationship (**Figure 3A**). Within each species, most orthogroups are found in all strains (9,008, 8,321, and 9,423 in *A. lentulus*, *A. fumigatus*, and *A. fumigatiaffinis*, respectively); approximately 5.4–6.13% of genes in each species appear to vary in their presence between strains (**Supplementary Figure S3**). Among these, we noted that orthogroups that are present all but one strain are usually the most frequent (**Figure 3C**).

We identified a total of 114,378, 160,194, and 313,029 SNPs in *A. fumigatus*, *A. fumigatiaffinis*, and *A. lentulus*, respectively. We identified 406, 493, and 747 SNPs in *A. fumigatus*, *A. fumigatiaffinis*, and *A. lentulus*, respectively, as high-impact polymorphisms; these polymorphisms are those whose mutation is presumed to be highly deleterious to protein function. Similarly, out of a total of 11,698 (*A. fumigatus*), 20,135 (*A. fumigatiaffinis*) and 34,506 (*A. lentulus*) indels segregating within each species, we identified 615, 1,739, and 1,830 high-impact indels in *A. fumigatus*, *A. fumigatiaffinis*, and *A. lentulus*, respectively.

Gene ontology (GO) enrichment analysis was carried out for genes with high impact SNPs and indels ($\alpha = 0.05$). *A. fumigatus* only showed GO terms identified as underrepresented in "cellular process" and several cellular compartments ("protein-containing complex," "intracellular organelle part," "organelle part," "cytoplasmic part," "cell part"). *A. lentulus* had "nucleoside metabolic" and "glycosyl compound metabolic processes" enriched, and *A. fumigatiaffinis* showed enriched terms for "modified amino acid binding," "phosphopantetheine binding," "amide binding," "transition metal ion binding," "zinc ion binding," "chitin binding," and "ADP binding." *A. lentulus* and *A. fumigatiaffinis* genes with high impact SNPs and indels also showed underrepresented GO terms (**Supplementary Table S4**). We also analyzed SNPs and indels separately (**Supplementary Table S4**).

Polymorphisms in Major Antifungal Target Genes Correlate With Antifungal Susceptibility

Given the observed variation within and between species in antifungal drug susceptibility, we examined DNA sequence polymorphisms in genes known to be involved in antifungal susceptibility to azoles and echinocandins. In particular, we examined patterns of sequence variation in the 14α-sterol demethylase gene *cyp51A* (Afu4g06890) and in the 1,3-beta-glucan synthase catalytic subunit gene *fks1* (Afu6g12400). Using *A. fumigatus* A1163 as reference, we identified important species- and strain-specific polymorphisms in both *cyp51A* and *fks1* (**Figure 4A** and **Table 2** shows a detailed breakdown of all SNP and indel polymorphisms per strain).

An alignment of Cyp51A protein sequences in the three species shows possible insertions in different sites (**Figure 4A** – red arrow). We observed substitutions in at least one of the clinical strains in the three species in 42 positions that might be correlated with the strains' varying drug susceptibility levels. For instance, Cyp51A in *A. fumigatus* CNM-CM8714 revealed a well-documented substitution related to azole resistance at position 98

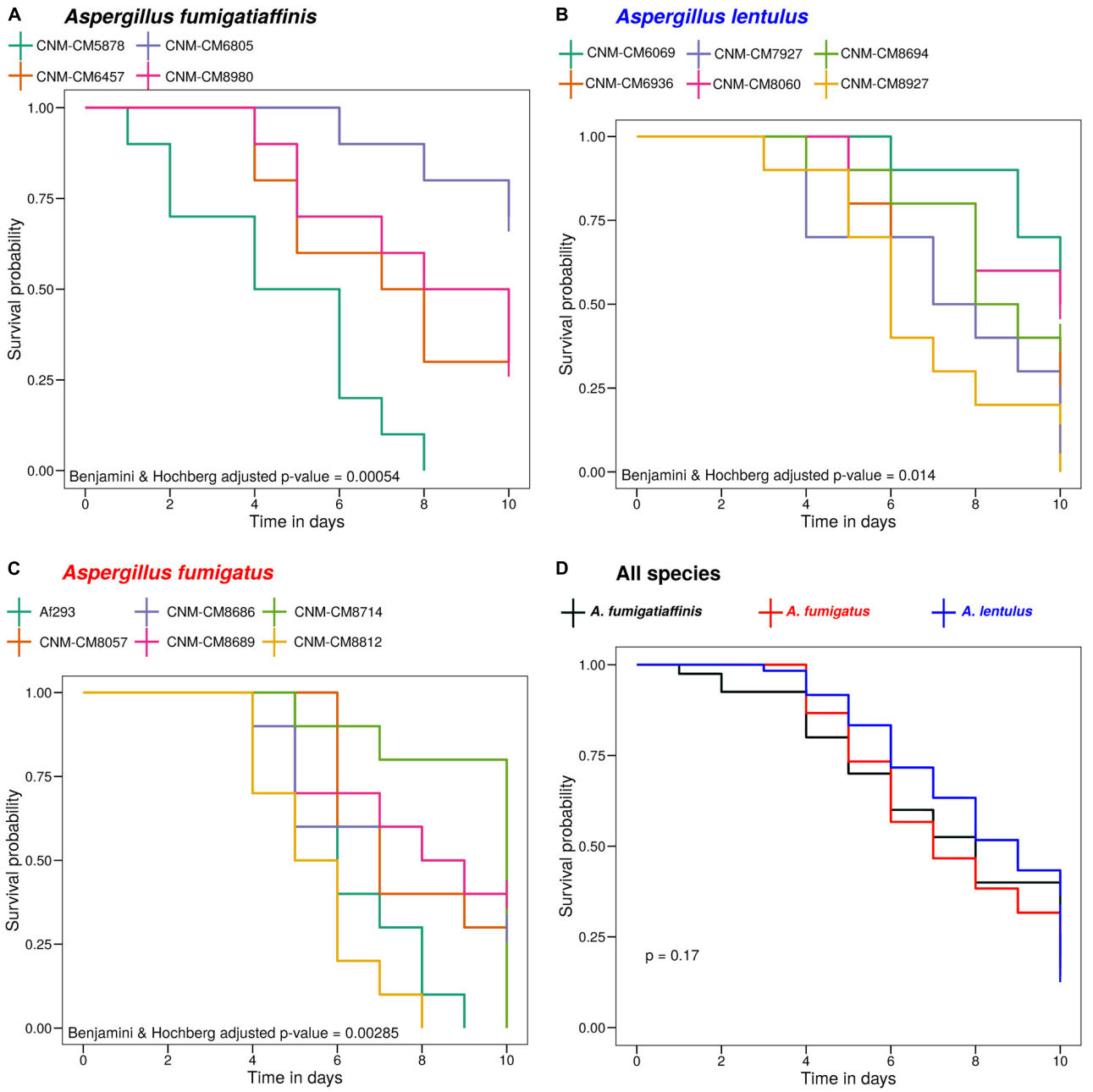

FIGURE 2 | High heterogeneity of virulence levels among Spanish strains of three closely related *Aspergillus* pathogens. We found significant heterogeneity in the survival curves between strains within *A. fumigatiaffinis* **(A)**, *A. lentulus* **(B)**, and *A. fumigatus* **(C)** (Benjamini and Hochberg adjusted *p*-values using the log-rank test are shown). We also tested differences between species (considering each strain as a biological replicate), and found that the virulence profiles of Spanish strains of all three species are not significantly different **(D)** (*p*-value using the log-rank test is shown).

(L98H) (**Figure 4A** – blue arrows), which might be correlated to its lower susceptibility to itraconazole or voriconazole compared to other *A. fumigatus* strains (**Figure 1B**).

We also looked at the promoter region of the *cyp51A* gene (**Figure 4B**) and identified the TR insertions TR34 and TR46 (region highlighted between blue arrows), previously reported in antifungal resistant strains (Dudakova et al., 2017). These changes were specific to certain clinical strains of *A. fumigatus* and were previously reported in combination with specific point mutations leading to amino acid substitutions. For example, *A. fumigatus* CNM-CM8714 carries the TR34 promoter insertions combined with L98H (**Figure 4A** – blue arrow), whereas *A. fumigatus* CNM-CM8057 has a TR46 insertion combined with Y121F/T289A (**Figure 4A** – blue arrow). There are other variants (short indels) that were exclusive to either *A. lentulus* or *A. fumigatiaffinis*, or both.

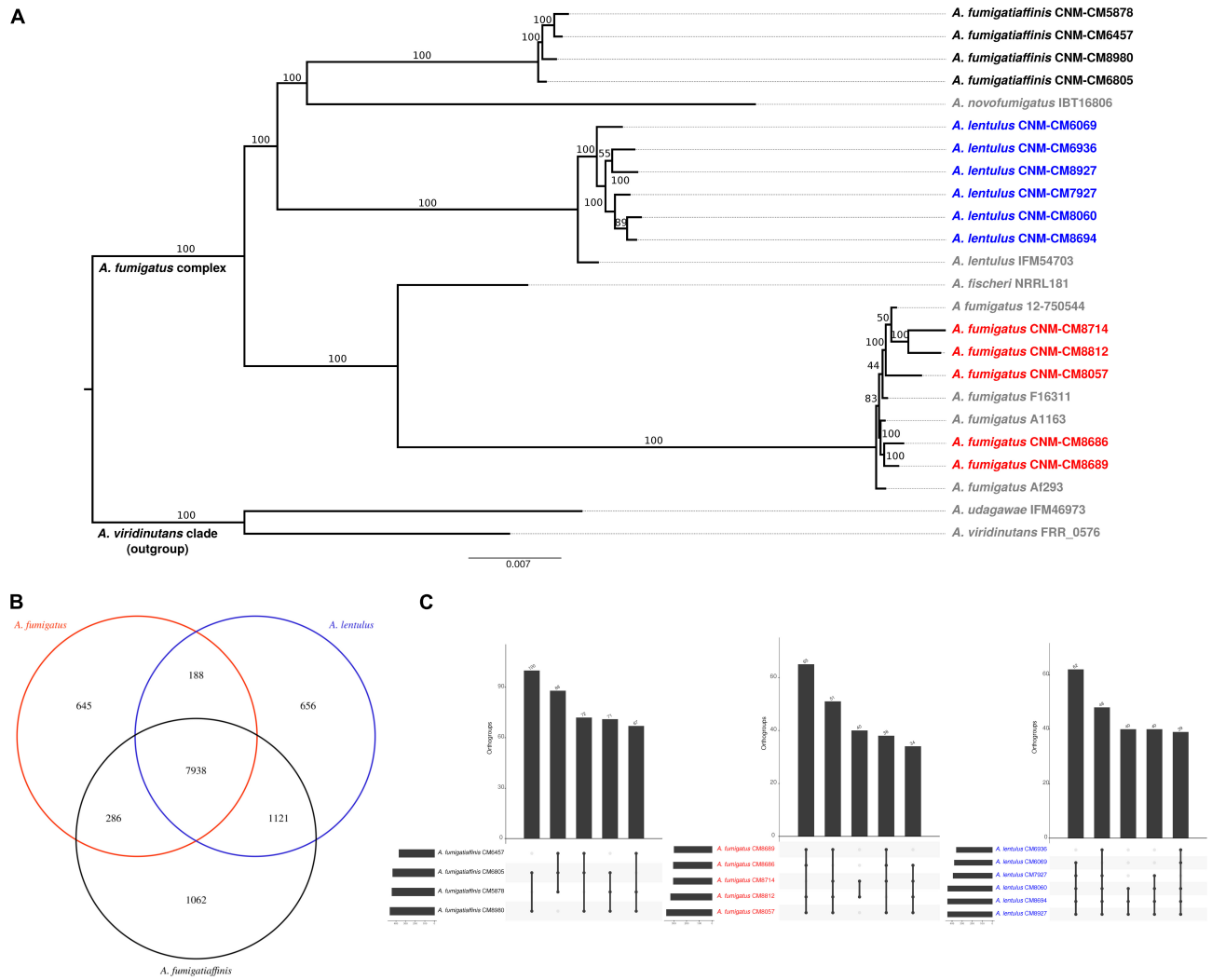

FIGURE 3 | Genomics of the three closely related *Aspergillus* pathogens. **(A)** Genome-scale phylogeny of the section *Fumigati* species used in this study and additional species with sequenced genomes. The *A. viridinutans* clade is presented as a sister clade. Spanish strains sequenced in this work are colored in red (*A. fumigatus*), blue (*A. lentulus*) and black (*A. fumigatiaffinis*). The newly sequenced *A. fumigatiaffinis* strains form a separated group that is closely related to *A. novofumigatus*. All *A. lentulus* strains in this work group together and share an ancestor with *A. lentulus* IFM54703, the only sequenced strain in this species to date. The *A. fumigatus* strains sequenced in this work form different internal groups in the clade with other strains in the species (e.g., strains CNM-CM8714 and CNM-CM8812 group together and strains CNM-CM8686 and CNM-CM8689 form another group). **(B)** *A. fumigatiaffinis* and *A. lentulus* shares the highest number of common orthogroups and *A. fumigatiaffinis* displays the highest number of species-specific orthogroups. We considered species-specific orthologs those that were present in at least one strain of a given species, with no representative from another species. **(C)** Orthogroups shared by all and "all but one" strains are the most frequent in three closely related *Aspergillus* pathogens. *A. lentulus*, *A. fumigatus*, and *A. fumigatiaffinis* have 9,008, 8,321, and 9,423 orthologous genes present in all strains, respectively. The five largest combinations of orthogroups are shown. As expected, the most frequent combination of orthogroups are those in all strains but one.

Examination of the Fks1 protein sequence alignment from strains of the three species also revealed substitutions in 39 sites (**Figure 4A**). We also observed an insertion at position 1,626 of *A. lentulus* CNM-CM8927 (red arrow). Fks1 also showed substitutions at positions comprising an important hot-spot 2 (HS2) (blue arrows): all *A. lentulus* strains have a substitution at position 1,349 (I1349V) and all *A. fumigatiaffinis* have a substitution at position 1,360 (T1360I).

Examination of orthogroups revealed that the orthogroup that includes the *cyp51A* gene (Afu4g06890) contained additional paralogs of the *cyp51* family in *A. fumigatiaffinis*. Thus, we carried out a phylogenetic analysis with the amino acid sequences with the orthogroups containing *cyp51A* and *cyp51B* genes in *A. fumigatus* Af293 (**Figure 4C**) that comprises the three species in this work. We observed three well-defined clades. The *A. fumigatiaffinis* paralog related to *cyp51A* is likely to represent *cyp51C*, which has been previously reported in other *Aspergillus* species, such as *A. flavus* and *A. oryzae* (Hagiwara et al., 2016; Perez-Cantero et al., 2020). Sequence identity between the putative Cyp51C protein in *A. fumigatiaffinis* CNM-CM6805 and

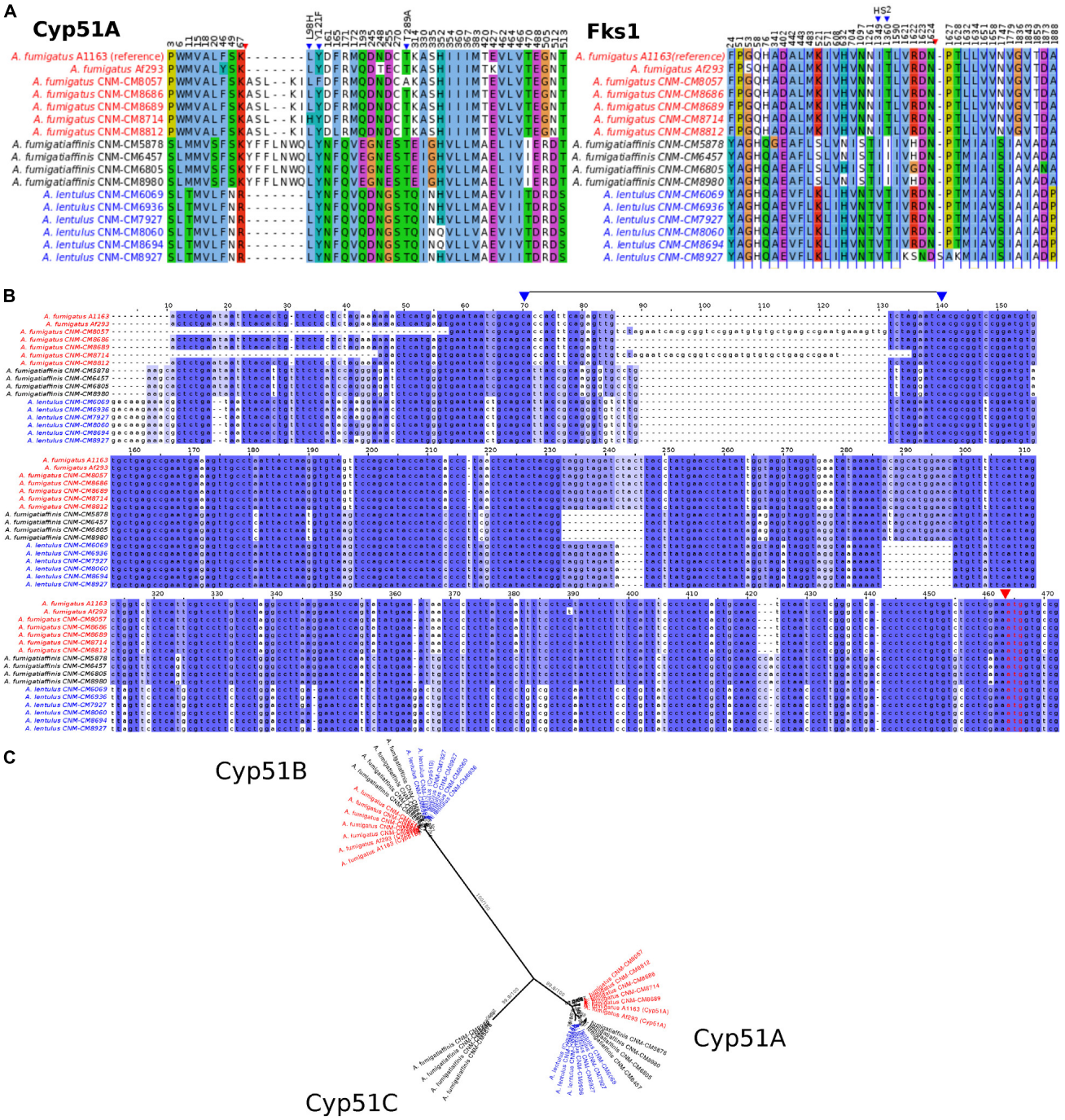

FIGURE 4 | Changes in important genes related to antifungal susceptibility in the three *Aspergillus* pathogens. **(A)** Products of genes related to antifungal resistance, *Cyp51A* (azoles) and *Fks1* (echinocandins), display species- and strain-specific polymorphisms. Only the positions with changes in at least one strain are shown (substitutions or insertions/deletions). Blue triangles highlight important amino acid changes in positions 98, 121, and 289 in Cyp51A and in hot spot 2 (HS2) of *Fks1*. Red triangles indicate insertions/deletions. **(B)** Promoter region of the *cyp51A* gene displays strain-specific mutations among Spanish strains of three closely related *Aspergillus* pathogens. Well-known tandem repeat regions in antifungal-resistant strains of *A. fumigatus* are shown between positions 70–140 in the alignment (i.e., TR34 and TR46, observed in CNM-CM8714 and CNM-CM8057, respectively, delimited by two blue arrows in upper part). Polymorphisms in cryptic species were also identified, for instance, the short deletions exclusively found in the cryptic species (either in *A. fumigatiaffinis* or *A. lentulus*) around positions 230–250. Red arrow and red font indicate the start codon. **(C)** Phylogeny of Cyp51 gene family (protein sequences) reveals three different members (Cyp51A, Cyp51B, and the putative Cyp51C) in *A. fumigatiaffinis*. Ultrafast Boostrap Approximation and SH-aLRT support values are shown.

TABLE 2 | Single-nucleotide polymorphisms and insertions/deletions in *cyp51* family and *fks1* genes in each species individually.

Species	Polymorphism type	Gene	High impact variant	Low impact variant	Moderate impact variant	Modifier impact variant
A. fumigatus	INDELs	*cyp51A*	0	0	0	6
A. fumigatus	SNPs	*cyp51A*	0	0	5	23
A. lentulus	INDELs	*cyp51A*	0	0	0	10
A. lentulus	SNPs	*cyp51A*	0	8	3	92
A. fumigatus	INDELs	*cyp51B*	0	0	0	1
A. fumigatus	SNPs	*cyp51B*	0	1	1	7
A. lentulus	INDELs	*cyp51B*	0	0	0	1
A. lentulus	SNPs	*cyp51B*	0	0	0	2
A. fumigatiaffinis	INDELs	*cyp51C*	0	0	0	28
A. fumigatiaffinis	SNPs	*cyp51C*	0	10	1	157
A. fumigatiaffinis	INDELs	*fks1*	0	0	0	45
A. fumigatiaffinis	SNPs	*fks1*	0	23	5	143
A. fumigatus	INDELs	*fks1*	0	0	0	3
A. fumigatus	SNPs	*fks1*	0	4	0	10
A. lentulus	INDELs	*fks1*	4	0	0	50
A. lentulus	SNPs	*fks1*	0	43	5	218

HIGH = The variant is assumed to have high (disruptive) impact in the protein, probably causing protein truncation, loss of function or triggering nonsense mediated decay. MODERATE = A non-disruptive variant that might change protein effectiveness. LOW = A variant that is most likely to be harmless or unlikely to change protein behavior. MODIFIER = Usually non-coding variants or variants affecting non-coding genes, where predictions are difficult or there is no evidence of impact. Details can be found on the SnpEff manual (http://snpeff.sourceforge.net/SnpEff_manual.html).

Cyp51C (XM_002383890.1) and Cyp51A (XM_002375082.1) of *A. flavus* (Liu et al., 2012) is 471/512 (92%) and 391/508 (77%), respectively.

Genetic Determinants Involved in Virulence: Single-Nucleotide Polymorphisms, Insertions/Deletions Across Strains and Within Species Conservation

To explore the genetic underpinnings of the observed strain heterogeneity in virulence we next examined the SNPs and indels in 215 genes that have previously been characterized as genetic determinants of virulence in *A. fumigatus* (**Supplementary Table S5**).

Most virulence genetic determinants (146 genes) were found in single-copy in all strains (**Supplementary Table S6**), whereas 57 genes varied in their number of paralogs across clinical strains (**Figure 5**). We also identified four virulence determinants that had no orthologs in either *A. lentulus* or *A. fumigatiaffinis*, such as Afu6g07120 (*nudC*), which is an essential protein involved in nuclear movement (Morris et al., 1998), and considered an essential gene in *A. fumigatus* (Hu et al., 2007). Interestingly, we noted 17 virulence determinants that are present in *A. fumigatus* and *A. fumigatiaffinis* but absent in *A. lentulus* (**Figure 5** – top panel), such as Afu8g00200 (*ftmD*), one of the genes in the fumitremorgin biosynthetic gene cluster (Abad et al., 2010).

Several virulence determinants exhibited larger numbers of paralogs in one or more species. For example, the conidial pigment polyketide synthase *alb1* (Afu2g17600), which is involved in conidial morphology and virulence (Tsai et al., 1998), is one of the determinants with highest number of paralogs in *A. lentulus* and *A. fumigatiaffinis* (n = 7) when compared to *A. fumigatus* strains (n = 4). For determinants that contained a gene in at least one strain, we tested correlations between number of paralogs and virulence (lethal time 50: day at which 50% of the larvae were dead, or "ND-end": the number of dead larvae at the end of the experiment) and we observed no significant correlation suggesting paralog number does not associate with virulence.

DISCUSSION

A. fumigatus and the closely related species *A. lentulus* and *A. fumigatiaffinis* are important causal agents of aspergillosis (Zbinden et al., 2012; Lamoth, 2016). Importantly, the emergence of antifungal resistance is of increasing worldwide concern (Fisher et al., 2018) and antifungal resistant strains of *A. lentulus* and *A. fumigatiaffinis* (Alastruey-Izquierdo et al., 2014) have been identified. Heterogeneity in virulence across different strains of *A. fumigatus* has also been known for some time (Mondon et al., 1996). Analyses of strain phenotypic and genetic heterogeneity allow us to identify correlations between phenotype and genotype in strains of *Aspergillus* pathogens.

We found that high heterogeneity exists in drug susceptibility and virulence across different strains of *A. fumigatus*, *A. lentulus*, and *A. fumigatiaffinis* (**Figures 1**, **2**). For one specific antifungal drug, amphotericin B, our results confirmed previous findings that *A. fumigatus* is more susceptible to amphotericin B than strains of cryptic species (Balajee et al., 2004). Studies on the intrinsic resistance to amphotericin B reported for *A. terreus* highlight the importance of stress response pathways, in particular heat shock proteins (such as Hsp90 and Hsp70), as well as enzymes detoxifying reactive oxygen species (Posch et al., 2018). Future work involving genomics on the cryptic species will be able to exploit changes in genetic determinants

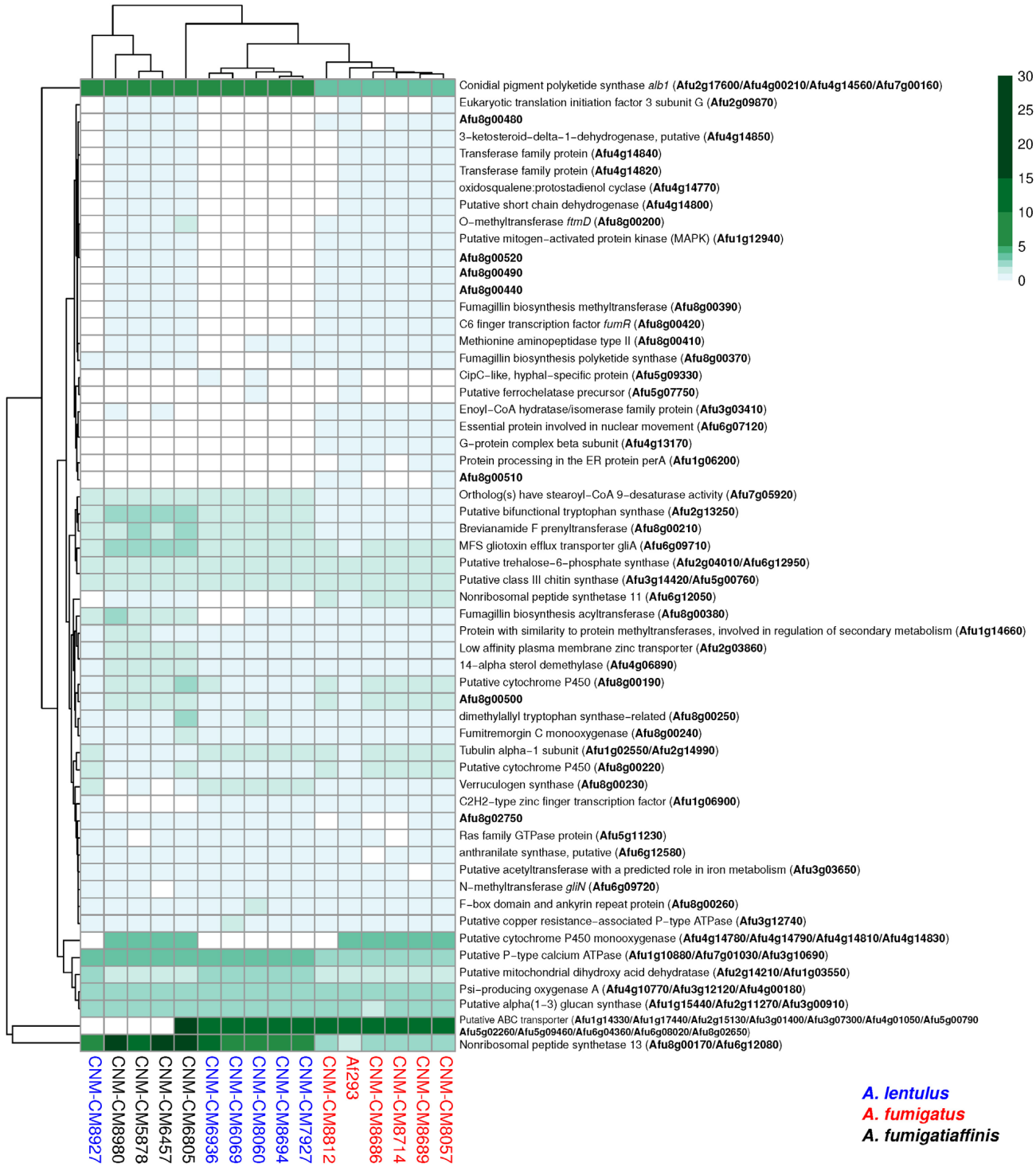

FIGURE 5 | Orthogroups for virulence determinants reveals variable number of paralogs among the three closely related *Aspergillus* pathogens. We searched for 215 known genetic determinants of virulence in *A. fumigatus* Af293 in the species of interest and found they were grouped into 203 orthogroups. 146/203 were found in single copy across all strains and are not shown here. The cladogram above the species reflects similarities between strain presence/absence patterns. *A. fumigatus* Af293 shows a different pattern compared to other strains of *A. fumigatus*, grouping with one of the *A. lentulus* strains (CNM-CM8927). This may reflect the phylogenetic divergence of *A. fumigatus* strain Af293 from other species members. Conidial pigment polyketide synthase *alb1* (Afu2g17600) is one of the genetic determinants of virulence with highest number of copies in cryptic species (n = 7) when compared to *A. fumigatus* strains (n = 4). Gene identifiers in *A. fumigatus* Af293 are highlighted in bold. Color scale indicates the number of genes found within the orthogroup.

involved in amphotericin B susceptibility, although this drug is not commonly used in clinical settings. Interestingly, our PCA identified pairs of positively and negatively correlated antifungal drugs from different classes (**Supplementary Figure S2**), suggestive of potential synergistic effects (resistance to one drug leads to resistance to the other) and trade-offs (resistance to one drug leads to susceptibility to the other), which could be important for clinical applications.

Comparison of the three species showed that the virulence profiles of *A. fumigatiaffinis* and *A. lentulus* strains were not significantly different from the virulence profiles of *A. fumigatus* strains (**Figure 2**). This finding is in contrast to a previous comparison of survival curves of the type strains of *A. lentulus* and *A. fumigatus*, which found that *A. fumigatus* is significantly more virulent than *A. lentulus* (Sugui et al., 2014). The likely explanation for this is our finding that there is significant strain heterogeneity within each species (**Figure 2**), suggesting that comparisons of individual strains between species are not going to be representative of the variation in virulence within species. While additional testing using diverse models of fungal disease will be required to test the validity of these observations, our findings reinforce the emerging view (Kowalski et al., 2016, 2019; Ries et al., 2019; Bastos et al., 2020) that examining within-species variation in *Aspergillus* pathogens is an important, yet poorly studied and understood, dimension of fungal virulence.

The advent of whole genome sequencing boosted our understanding of the biology of the genus *Aspergillus* (de Vries et al., 2017). Several studies have previously analyzed genomic data of *A. fumigatus* strains (Abdolrasouli et al., 2015; Takahashi-Nakaguchi et al., 2015), uncovering *cyp51A* mutations in *A. fumigatus* populations (Abdolrasouli et al., 2015). Some studies have also used population genomic data for strains of *A. fumigatus* to gain insights on antifungal drug susceptibility (Garcia-Rubio et al., 2018) or virulence potential (Puértolas-Balint et al., 2019). Correlations between phenotypic traits, such as antifungal susceptibility or virulence and genetic traits have been also studied in other well-studied pathogens, such as the opportunistic yeast *Candida albicans* (Hirakawa et al., 2015). However, to our knowledge, this is the first study that examines the phenotypic and genetic heterogeneity among strains of species closely related to *A. fumigatus*.

The three main classes of antifungal drugs comprise polyenes, azoles, and echinocandins, involved in ergosterol composition of fungal membrane, ergosterol biosynthesis, and the cell wall biopolymer (1,3)-β-D-glucan, respectively (Robbins et al., 2017). Due to toxicity to host cells, polyenes are only used in exceptional cases, and first-line prophylaxis and treatment of aspergillosis is usually carried out with azoles (Garcia-Rubio et al., 2017; Garcia-Vidal et al., 2019). Mechanisms of azole resistance involving mutations in the *cyp51* genes have been identified in diverse fungi, including in multiple animal and plant pathogens (Parker et al., 2014). In *A. fumigatus*, research has focused on azole susceptibility testing and correlation with point mutations in the *cyp51A* gene and TR insertions in its promoter region (Chen et al., 2020; Zakaria et al., 2020). Major changes in protein *Cyp51A* that correlated with azole resistance include point mutations, such as in positions G54, G138, M220, and G448, or combination of point mutations with TRs in the promoter region, such as the TR34/L98H and the TR46/Y121F/T289A (Wei et al., 2015; Beardsley et al., 2018). In previous studies, alterations such as the insertion of TR34 and TR46 (Dudakova et al., 2017) were only found in the *cyp51A* promoter of *A. fumigatus* strains, but these have also been found in other pathogens, such as the wheat pathogen *Zymoseptoria tritici* (Cools, Hans et al., 2012). Our work explored the promoter region of the *cyp51A* gene in *A. lentulus* and *A. fumigatiaffinis*, two closely related pathogenic species, and identified these promoter region changes only in two strains of *A. fumigatus* and not in either of the two cryptic species. Interestingly, two of the *A. fumigatus* strains in this work presented the combined TR34/L98H and the TR46/Y121F/T289A. We also identified other changes in proteins encoded by *cyp51A* and *fks1* that can be used in the future to generate mutants and test the effect of mutations in well-studied wild-type strains of *A. fumigatus* (Chen et al., 2020).

The evolution of the gene families that contain genes involved in drug resistance might also give us clues on how drug resistance evolves in fungal populations; previous studies (Hawkins et al., 2014; Zheng et al., 2019) report two paralogs of *cyp51* in diverse species, including *A. fumigatus*, *A. nidulans*, *Penicillium digitatum*, and *Magnaporthe oryzae*, while *Fusarium graminearum*, *A. flavus*, and *A. oryzae* have three *cyp51* genes (Dudakova et al., 2017). Recently, a study proposed the existence of *cyp51C* gene arising from a duplication in *cyp51B* in *A. terreus* and *A. carbonarius* (Perez-Cantero et al., 2020). Interestingly, our study found a paralog of the *cyp51A* gene in *A. fumigatiaffinis* that likely corresponds to *cyp51C*. Whole-genome sequence analysis in *A. flavus* reported substitutions in the three paralogous genes (*cyp51A, cyp51B,* and *cyp51C*) in the context of antifungal resistance (Sharma et al., 2018). Novel substitutions identified in *cyp51C* and modeling of protein changes suggested possible effects on drug binding. Next steps in studies of azole susceptibility in *A. fumigatiaffinis* strains could include the analysis of this putative *cyp51C* gene and its role in the organism's observed drug susceptibility profile.

Studies on echinocandins have focused on the (1,3)-β-D-glucan synthase enzyme, encoded by the *fks1* gene (Robbins et al., 2017). Particularly, two hot-spots have been studied (Gonçalves et al., 2016). Although most studies report mutations in *Candida* (Desnos-Ollivier et al., 2008; Garcia-Effron et al., 2008), previous work reported point mutations in *fks1* hot spot 1 associated with echinocandin resistance in *A. fumigatus* (Jiménez-Ortigosa et al., 2017). Our work did not find changes among *A. fumigatus* clinical strains, and didn't find any mutation in the hot spot 1 of sequences of the cryptic species, which is in agreement with previous study that analyzed *fks1* sequences in *A. lentulus* (Staab et al., 2010). However, we did observe changes in hot spot 2 that were specific to the cryptic species; further examination of these changes with respect to echinocandin susceptibility is an interesting future avenue of research.

Although this study focused on polymorphisms in genes *cyp51A* and *fks1*, there is also increasing research on non-*cyp51* (Zakaria et al., 2020) and non-*fks1* (Szalewski et al., 2018) genetic changes. Future exploitation of genomic data on strains

of *A. fumigatus* and closely related species could also exploit these additional genes. These future studies could also exploit new antifungal drugs, such as olorofim, which has also been tested on cryptic species of *Aspergillus* (Rivero-Menendez et al., 2019). Finally, future phenotypic and genomic analyses can help us to better understand more complex topics involving antifungal drugs, such as resistance, persistence, and tolerance (as well as the role of tolerance in resistance) (Berman and Krysan, 2020). Given possible emergence of antifungal resistance in agriculture (Hawkins et al., 2019), future work could also exploit correlations in antifungals and the origin of these isolates.

DATA AVAILABILITY STATEMENT

All genomes sequenced as part of this work can be accessed through BioProject PRJNA592352; the raw sequence reads are also available through the NCBI Sequence Read Archive. BioSample and Assembly identifiers are presented in **Supplementary Table S4**. The data and scripts used in this project are available on the Gitlab repository under https://gitlab.com/SantosRAC/afum_afma_alen2020.

AUTHOR CONTRIBUTIONS

RS, JS, MM, AA-I, GG, and AR designed the experiments. LS, OR-M, and RB performed the experiments. RS and JS ran bioinformatic analyses. RS, MM, JS, and AR wrote the manuscript. All authors revised the manuscript.

FUNDING

RS was supported by the Brazilian São Paulo Research Foundation (FAPESP) grant numbers 17/21983-3 and 19/07526-4. JS and AR are supported by the Howard Hughes Medical Institute through the James H. Gilliam Fellowships for Advanced Study program. MM and AR were supported by a Vanderbilt University Discovery Grant. Research in AR's lab is also supported by the National Science Foundation (DEB-1442113), and GG by the Brazilian São Paulo Research Foundation (FAPESP) (grant number 2016/07870-9) and Conselho Nacional de Desenvolvimento Científico e Tecnológico (CNPq). AA-I is supported by research projects from the Fondo de Investigación Sanitaria (PI13/02145 and PI16CIII/00035).

ACKNOWLEDGMENTS

This work used resources of the "Centro Nacional de Processamento de Alto Desempenho em São Paulo (CENAPAD-SP)." Computational infrastructure was provided by The Advanced Computing Center for Research and Education (ACCRE) at Vanderbilt University.

SUPPLEMENTARY MATERIAL

The Supplementary Material for this article can be found online at: https://www.frontiersin.org/articles/10.3389/fgene.2020.00459/full#supplementary-material

REFERENCES

Abad, A., Fernández-Molina, V. J., Bikandi, J., Ramírez, A., Margareto, J., Sendino, J., et al. (2010). What makes *Aspergillus fumigatus* a successful pathogen? Genes and molecules involved in invasive aspergillosis. *Rev. Iberoam. Micol.* 27, 155–182. doi: 10.1016/j.riam.2010.10.003

Abdolrasouli, A., Rhodes, J., Beale, M. A., Hagen, F., Rogers, T. R., Chowdhary, A., et al. (2015). Genomic context of azole resistance mutations in *Aspergillus fumigatus* determined using whole-genome sequencing. *mBio* 6:e00536. doi: 10.1128/mBio.00536-15

Agarwal, R., Chakrabarti, A., Shah, A., Gupta, D., Meis, J. F., Guleria, R., et al. (2013). Allergic bronchopulmonary aspergillosis: review of literature and proposal of new diagnostic and classification criteria. *Clin. Exp. Allergy* 43, 850–873. doi: 10.1111/cea.12141

Alastruey-Izquierdo, A., Alcazar-Fuoli, L., and Cuenca-Estrella, M. (2014). Antifungal susceptibility profile of cryptic species of *aspergillus*. *Mycopathologia* 178, 427–433. doi: 10.1007/s11046-014-9775-z

Altschul, S. F., Gish, W., Miller, W., Myers, E. W., and Lipman, D. J. (1990). Basic local alignment search tool. *J. Mol. Biol.* 215, 403–410. doi: 10.1016/S0022-2836(05)80360-2

Arendrup, M. C., Meletiadis, J., Mouton, J. W., Lagrou, K., Howard, S. J., and Subcommittee on Antifungal Susceptibility Testing of the Escmid European Committee for Antimicrobial Susceptibility Testing (2017). *EUCAST DEFINITIVE DOCUMENT E.DEF 9.3.1: Method for the Determination of Broth Dilution Minimum Inhibitory Concentrations of Antifungal Agents for Conidia Forming Moulds*. Available online at: http://www.eucast.org/fileadmin/src/media/PDFs/EUCAST_files/AFST/Files/EUCAST_E_Def_9_3_1_Mould_testing__definitive.pdf (accessed February 26, 2020).

Balajee, S. A., Gribskov, J. L., Hanley, E., Nickle, D., and Marr, K. A. (2005). *Aspergillus lentulus* sp. nov., a new sibling species of *A. fumigatus*. *Eukaryot. Cell* 4, 625–632. doi: 10.1128/EC.4.3.625-632.2005

Balajee, S. A., Kano, R., Baddley, J. W., Moser, S. A., Marr, K. A., Alexander, B. D., et al. (2009). Molecular identification of *Aspergillus* species collected for the transplant-associated infection surveillance network. *J. Clin. Microbiol.* 47, 3138–3141. doi: 10.1128/JCM.01070-09

Balajee, S. A., Weaver, M., Imhof, A., Gribskov, J., and Marr, K. A. (2004). *Aspergillus fumigatus* variant with decreased susceptibility to multiple antifungals. *Antimicrob. Agents Chemother.* 48, 1197–1203. doi: 10.1128/AAC.48.4.1197-1203.2004

Bankevich, A., Nurk, S., Antipov, D., Gurevich, A. A., Dvorkin, M., Kulikov, A. S., et al. (2012). SPAdes: a new genome assembly algorithm and its applications to single-cell sequencing. *J. Comput. Biol.* 19, 455–477. doi: 10.1089/cmb.2012.0021

Basenko, E. Y., Pulman, J. A., Shanmugasundram, A., Harb, O. S., Crouch, K., Starns, D., et al. (2018). FungiDB: an integrated bioinformatic resource for fungi and oomycetes. *J. Fungi* 4:39. doi: 10.3390/jof4010039

Bastos, R. W., Valero, C., Silva, L. P., Schoen, T., Drott, M., Brauer, V., et al. (2020). Functional characterization of clinical isolates of the opportunistic fungal pathogen *Aspergillus nidulans*. *mSphere* 5:e00153-20.

Beardsley, J., Halliday, C. L., Chen, S. C. A., and Sorrell, T. C. (2018). Responding to the emergence of antifungal drug resistance: perspectives from the bench and the bedside. *Fut. Microbiol.* 13, 1175–1191. doi: 10.2217/fmb-2018-0059

Berman, J., and Krysan, D. J. (2020). Drug resistance and tolerance in fungi. *Nat. Rev. Microbiol.* 18. doi: 10.1038/s41579-019-0322-2

Bolger, A. M., Lohse, M., and Usadel, B. (2014). Trimmomatic: a flexible trimmer for Illumina sequence data. *Bioinformatics* 30, 2114–2120. doi: 10.1093/bioinformatics/btu170

Brown, G. D., Denning, D. W., Gow, N. A. R., Levitz, S. M., Netea, M. G., and White, T. C. (2012). Hidden killers: human fungal infections. *Sci. Transl. Med.* 4:165rv13. doi: 10.1126/scitranslmed.3004404

Capella-Gutierrez, S., Silla-Martinez, J. M., and Gabaldon, T. (2009). trimAl: a tool for automated alignment trimming in large-scale phylogenetic analyses. *Bioinformatics* 25, 1972–1973. doi: 10.1093/bioinformatics/btp348

Chen, P., Liu, M., Zeng, Q., Zhang, Z., Liu, W., Sang, H., et al. (2020). Uncovering new mutations conferring azole resistance in the *Aspergillus fumigatus* cyp51A Gene. *Front. Microbiol.* 10:3127. doi: 10.3389/fmicb.2019.03127

Cingolani, P., Platts, A., Wang le, L., Coon, M., Nguyen, T., Wang, L., et al. (2013). A program for annotating and predicting the effects of single nucleotide polymorphisms, SnpEff: SNPs in the genome of *Drosophila melanogaster* strain w1118; iso-2; iso-3. *Fly (Austin)* 6, 80–92. doi: 10.1016/S1877-1203(13)70353-7

Cock, P. J. A., Antao, T., Chang, J. T., Chapman, B. A., Cox, C. J., Dalke, A., et al. (2009). Biopython: freely available Python tools for computational molecular biology and bioinformatics. *Bioinformatics* 25, 1422–1423. doi: 10.1093/bioinformatics/btp163

Cools, Hans, J., Bayon, C., Atkins, S., Lucas, J. A., and Fraaije, B. A. (2012). Overexpression of the sterol 14α−demethylase gene (MgCYP51) in *Mycosphaerella graminicola* isolates confers a novel azole fungicide sensitivity phenotype. *Pest. Manag. Sci.* 68, 1034–1040. doi: 10.1002/ps.3263

de Vries, R. P., Riley, R., Wiebenga, A., Aguilar-Osorio, G., Amillis, S., Uchima, C. A., et al. (2017). Comparative genomics reveals high biological diversity and specific adaptations in the industrially and medically important fungal genus *Aspergillus*. *Genome Biol.* 18:28. doi: 10.1186/s13059-017-1151-0

Denning, D. W., Cadranel, J., Beigelman-Aubry, C., Ader, F., Chakrabarti, A., Blot, S., et al. (2016). Chronic pulmonary aspergillosis: rationale and clinical guidelines for diagnosis and management. *Eur. Respir. J.* 47, 45–68. doi: 10.1183/13993003.00583-2015

Depristo, M. A., Banks, E., Poplin, R., Garimella, K. V., Maguire, J. R., Hartl, C., et al. (2011). A framework for variation discovery and genotyping using next-generation DNA sequencing data. *Nat. Genet.* 43, 491–498. doi: 10.1038/ng.806

Desnos-Ollivier, M., Bretagne, S., Raoux, D., Hoinard, D., Dromer, F., Dannaoui, E., et al. (2008). Mutations in the fks1 gene in *Candida albicans*, *C. tropicalis*, and *C. krusei* correlate with elevated caspofungin MICs uncovered in AM3 medium using the method of the European committee on antibiotic susceptibility testing. *Antimicrob. Agents Chemother.* 52, 3092–3098. doi: 10.1128/aac.00088-08

Dudakova, A., Spiess, B., Tangwattanachuleeporn, M., Sasse, C., Buchheidt, D., Weig, M., et al. (2017). Molecular tools for the detection and deduction of azole antifungal drug resistance phenotypes in *Aspergillus* species. *Clin. Microbiol. Rev.* 30, 1065–1091. doi: 10.1128/CMR.00095-16

Emms, D. M., and Kelly, S. (2019). OrthoFinder: phylogenetic orthology inference for comparative genomics. *Genome Biol.* 20:238.

Fedorova, N. D., Khaldi, N., Joardar, V. S., Maiti, R., Amedeo, P., Anderson, M. J., et al. (2008). Genomic islands in the pathogenic filamentous fungus *Aspergillus fumigatus*. *PLoS Genet.* 4:e1000046. doi: 10.1371/journal.pgen.1000046

Fisher, M. C., Hawkins, N. J., Sanglard, D., and Gurr, S. J. (2018). Worldwide emergence of resistance to antifungal drugs challenges human health and food security. *Science* 360, 739–742. doi: 10.1126/science.aap7999

Fuchs, B. B., O'Brien, E., Khoury, J. B. E., and Mylonakis, E. (2010). Methods for using *Galleria mellonella* as a model host to study fungal pathogenesis. *Virulence* 1, 475–482. doi: 10.4161/viru.1.6.12985

Fuller, K. K., Cramer, R. A., Zegans, M. E., Dunlap, J. C., and Loros, J. J. (2016). *Aspergillus fumigatus* photobiology illuminates the marked heterogeneity between isolates. *mBio* 7:e01517-16. doi: 10.1128/mBio.01517-16

Garcia-Effron, G., Katiyar, S. K., Park, S., Edlind, T. D., and Perlin, D. S. (2008). A naturally occurring proline-to-alanine amino acid change in Fks1p in *Candida parapsilosis*, *Candida orthopsilosis*, and *Candida metapsilosis* accounts for reduced echinocandin susceptibility. *Antimicrob. Agents Chemother.* 52, 2305–2312. doi: 10.1128/aac.00262-08

Garcia-Rubio, R., Alcazar-Fuoli, L., Monteiro, M. C., Monzon, S., Cuesta, I., Pelaez, T., et al. (2018). Insight into the significance of *Aspergillus fumigatus* cyp51A polymorphisms. *Antimicrob. Agents Chemother.* 62:e00241-18. doi: 10.1128/AAC.00241-18

Garcia-Rubio, R., Cuenca-Estrella, M., and Mellado, E. (2017). Triazole resistance in *Aspergillus* species: an emerging problem. *Drugs* 77, 599–613. doi: 10.1007/s40265-017-0714-4

Garcia-Vidal, C., Alastruey-Izquierdo, A., Aguilar-Guisado, M., Carratalà, J., Castro, C., Fernández-Ruiz, M., et al. (2019). Executive summary of clinical practice guideline for the management of invasive diseases caused by *Aspergillus*: 2018 update by the GEMICOMED-SEIMC/REIPI. *Enferm. Infecc. Microbiol. Clin.* 37, 535–541. doi: 10.1016/j.eimc.2018.03.018

Gonçalves, S. S., Souza, A. C. R., Chowdhary, A., Meis, J. F., and Colombo, A. L. (2016). Epidemiology and molecular mechanisms of antifungal resistance in *Candida* and *Aspergillus*. *Mycoses* 59, 198–219. doi: 10.1111/myc.12469

Gurevich, A., Saveliev, V., Vyahhi, N., and Tesler, G. (2013). QUAST: quality assessment tool for genome assemblies. *Bioinformatics* 29, 1072–1075. doi: 10.1093/bioinformatics/btt086

Hagiwara, D., Watanabe, A., Kamei, K., and Goldman, G. H. (2016). Epidemiological and genomic landscape of azole resistance mechanisms in *Aspergillus fungi*. *Front. Microbiol.* 7:1382. doi: 10.3389/fmicb.2016.01382

Hawkins, N. J., Bass, C., Dixon, A., and Neve, P. (2019). The evolutionary origins of pesticide resistance. *Biol. Rev.* 94, 135–155. doi: 10.1111/brv.12440

Hawkins, N. J., Cools, H. J., Sierotzki, H., Shaw, M. W., Knogge, W., Kelly, S. L., et al. (2014). Paralog re-emergence: a novel, historically contingent mechanism in the evolution of antimicrobial resistance. *Mol. Biol. Evol.* 31, 1793–1802. doi: 10.1093/molbev/msu134

Hirakawa, M. P., Martinez, D. A., Sakthikumar, S., Anderson, M. Z., Berlin, A., Gujja, S., et al. (2015). Genetic and phenotypic intra-species variation in *Candida albicans*. *Genome Res.* 25, 413–425. doi: 10.1101/gr.174623.114

Hoang, D. T., Chernomor, O., von Haeseler, A., Minh, B. Q., and Vinh, L. S. (2018). UFBoot2: improving the ultrafast bootstrap approximation. *Mol. Biol. Evol.* 35, 518–522. doi: 10.1093/molbev/msx281

Holden, D. W. (1994). "DNA mini prep method for *Aspergillus fumigatus* (and other filamentous fungi)," in *Molecular Biology of Pathogenic Fungi, a Laboratory Manual*, eds B. Maresca and G. S. Kobayashi (New York, NY: Telos Press), 3–4.

Hong, S. B., Go, S. J., Shin, H. D., Frisvad, J. C., and Samson, R. A. (2005). Polyphasic taxonomy of *Aspergillus fumigatus* and related species. *Mycologia* 97, 1316–1329. doi: 10.3852/mycologia.97.6.1316

Hu, W., Sillaots, S., Lemieux, S., Davison, J., Kauffman, S., Breton, A., et al. (2007). Essential gene identification and drug target prioritization in *Aspergillus fumigatus*. *PLoS Pathog.* 3:e24. doi: 10.1371/journal.ppat.0030024

Huson, D. H., and Weber, N. (2013). Microbial community analysis using MEGAN. *Methods Enzymol.* 531, 465–485. doi: 10.1016/b978-0-12-407863-5.00021-6

Jiménez-Ortigosa, C., Moore, C., Denning, D. W., and Perlin, D. S. (2017). Emergence of echinocandin resistance due to a point mutation in the fks1 gene of *Aspergillus fumigatus* in a patient with chronic pulmonary aspergillosis. *Antimicrob. Agents Chemother.* 61:e01277-17. doi: 10.1128/AAC.01277-17

Jones, P., Binns, D., Chang, H. Y., Fraser, M., Li, W., McAnulla, C., et al. (2014). InterProScan 5: genome-scale protein function classification. *Bioinformatics* 30, 1236–1240. doi: 10.1093/bioinformatics/btu031

Katoh, K., and Standley, D. M. (2013). MAFFT multiple sequence alignment software version 7: improvements in performance and usability. *Mol. Biol. Evol.* 30, 772–780. doi: 10.1093/molbev/mst010

Katz, M. E., Dougall, A. M., Weeks, K., and Cheetham, B. F. (2005). Multiple genetically distinct groups revealed among clinical isolates identified as atypical *Aspergillus fumigatus*. *J. Clin. Microbiol.* 43, 551–555. doi: 10.1128/JCM.43.2.551-555.2005

Keller, N. P. (2017). Heterogeneity confounds establishment of "a" model microbial strain. *mBio* 8:e00135-17. doi: 10.1128/mBio.00135-17

Kjærbølling, I., Vesth, T. C., Frisvad, J. C., Nybo, J. L., Theobald, S., Kuo, A., et al. (2018). Linking secondary metabolites to gene clusters through genome sequencing of six diverse *Aspergillus* species. *Proc. Natl. Acad. Sci. U.S.A.* 115, E753–E761. doi: 10.1073/pnas.1715954115

Klopfenstein, D. V., Zhang, L., Pedersen, B. S., Ramírez, F., Vesztrocy, A. W., Naldi, A., et al. (2018). GOATOOLS: a python library for gene ontology analyses. *Sci. Rep.* 8:10872. doi: 10.1038/s41598-018-28948-z

Kowalski, C. H., Beattie, S. R., Fuller, K. K., McGurk, E. A., Tang, Y. W., Hohl, T. M., et al. (2016). Heterogeneity among isolates reveals that fitness in low

oxygen correlates with *Aspergillus fumigatus* virulence. *mBio* 7:e01515-16. doi: 10.1128/mBio.01515-16

Kowalski, C. H., Kerkaert, J. D., Liu, K.-W., Bond, M. C., Hartmann, R., Nadell, C. D., et al. (2019). Fungal biofilm morphology impacts hypoxia fitness and disease progression. *Nat. Microbiol.* 4, 2430–2441. doi: 10.1038/s41564-019-0558-7

Kusuya, Y., Sakai, K., Kamei, K., Takahashi, H., and Yaguchi, T. (2016). Draft genome sequence of the pathogenic filamentous fungus *Aspergillus lentulus* IFM 54703T. *Genome Announc.* 4:e01568-15. doi: 10.1128/genomeA.01568-15

Kusuya, Y., Takahashi-Nakaguchi, A., Takahashi, H., and Yaguchi, T. (2015). Draft genome sequence of the pathogenic filamentous fungus *Aspergillus udagawae* strain IFM 46973T. *Genome Announc.* 3:e00834-15. doi: 10.1128/genomeA.00834-15

Lamoth, F. (2016). *Aspergillus fumigatus*-related species in clinical practice. *Front. Microbiol.* 7:683. doi: 10.3389/fmicb.2016.00683

Latgé, J. P., and Chamilos, G. (2020). *Aspergillus fumigatus* and aspergillosis in 2019. *Clin. Microbiol. Rev.* 33:e00140-18. doi: 10.1128/CMR.00140-18

Lê, S., Josse, J., and Husson, F. (2008). FactoMineR: an R package for multivariate analysis. *J. Stat. Softw.* 25, 1–18. doi: 10.18637/jss.v025.i01

Li, H., and Durbin, R. (2009). Fast and accurate short read alignment with Burrows-Wheeler transform. *Bioinformatics* 25, 1754–1760. doi: 10.1093/bioinformatics/btp324

Li, H., Handsaker, B., Wysoker, A., Fennell, T., Ruan, J., Homer, N., et al. (2009). The sequence alignment/map format and SAMtools. *Bioinformatics* 25, 2078–2079. doi: 10.1093/bioinformatics/btp352

Lind, A. L., Wisecaver, J. H., Lameiras, C., Wiemann, P., Palmer, J. M., Keller, N. P., et al. (2017). Drivers of genetic diversity in secondary metabolic gene clusters within a fungal species. *PLoS Biol.* 15:e2003583. doi: 10.1371/journal.pbio.2003583

Liu, W., Sun, Y., Chen, W., Liu, W., Wan, Z., Bu, D., et al. (2012). The T788G mutation in the cyp51C gene confers voriconazole resistance in *Aspergillus flavus* causing aspergillosis. *Antimicrob. Agents Chemother.* 56, 2598–2603. doi: 10.1128/AAC.05477-11

McKenna, A., Hanna, M., Banks, E., Sivachenko, A., Cibulskis, K., Kernytsky, A., et al. (2010). The genome analysis toolkit: a MapReduce framework for analyzing next-generation DNA sequencing data. *Genome Res.* 20, 1297–1303. doi: 10.1101/gr.107524.110

Mead, M. E., Knowles, S. L., Raja, H. F., Beattie, S. R., Kowalski, C. H., Steenwyk, J. L., et al. (2019). Characterizing the pathogenic, genomic, and chemical traits of *Aspergillus fischeri*, a close relative of the major human fungal pathogen *Aspergillus fumigatus*. *mSphere* 4:e00018-19.

Mondon, P., De Champs, C., Donadille, A., Ambroise-Thomas, P., and Grillot, R. (1996). Variation in virulence of *Aspergillus fumigatus* strains in a murine model of invasive pulmonary aspergillosis. *J. Med. Microbiol.* 45, 186–191. doi: 10.1099/00222615-45-3-186

Morris, S. M., Albrecht, U., Reiner, O., Eichele, G., and Yu-Lee, L. Y. (1998). The lissencephaly gene product Lis1, a protein involved in neuronal migration, interacts with a nuclear movement protein, NudC. *Curr. Biol.* 8, 603–606. doi: 10.1016/S0960-9822(98)70232-5

Negri, C. E., Gonçalves, S. S., Xafranski, H., Bergamasco, M. D., Aquino, V. R., Castro, P. T. O., et al. (2014). Cryptic and rare *Aspergillus* species in Brazil: prevalence in clinical samples and in Vitro susceptibility to Triazoles. *J. Clin. Microbiol.* 52, 3633–3640. doi: 10.1128/JCM.01582-14

Nguyen, L. T., Schmidt, H. A., Von Haeseler, A., and Minh, B. Q. (2015). IQ-TREE: a fast and effective stochastic algorithm for estimating maximum-likelihood phylogenies. *Mol. Biol. Evol.* 32, 268–274. doi: 10.1093/molbev/msu300

Nierman, W. C., Pain, A., Anderson, M. J., Wortman, J. R., Kim, H. S., Arroyo, J., et al. (2005). Genomic sequence of the pathogenic and allergenic filamentous fungus *Aspergillus fumigatus*. *Nature* 438, 1151–1156. doi: 10.1038/nature04332

Parker, J. E., Warrilow, A. G. S., Price, C. L., Mullins, J. G. L., Kelly, D. E., and Kelly, S. L. (2014). Resistance to antifungals that target CYP51. *J. Chem. Biol.* 7, 143–161. doi: 10.1007/s12154-014-0121-1

Patterson, T. F., Thompson, G. R., Denning, D. W., Fishman, J. A., Hadley, S., Herbrecht, R., et al. (2016). Practice guidelines for the diagnosis and management of aspergillosis: 2016 update by the infectious diseases society of America. *Clin. Infect. Dis.* 63, e1–e60. doi: 10.1093/cid/ciw326

Perez-Cantero, A., López-Fernández, L., Guarro, J., and Capilla, J. (2020). Azole resistance mechanisms in *Aspergillus*: update and recent advances. *Int. J. Antimicrob. Agents* 55:105807. doi: 10.1016/j.ijantimicag.2019.09.011

Posch, W., Blatzer, M., Wilflingseder, D., and Lass-Flörl, C. (2018). *Aspergillus terreus*: novel lessons learned on amphotericin B resistance. *Med. Mycol.* 56(Suppl. 1), 73–82. doi: 10.1093/mmy/myx119

Puértolas-Balint, F., Rossen, J. W. A., Oliveira dos Santos, C., Chlebowicz, M. M. A., Raangs, E. C., van Putten, M. L., et al. (2019). Revealing the virulence potential of clinical and environmental *Aspergillus fumigatus* isolates using whole-genome sequencing. *Front. Microbiol.* 10:1970. doi: 10.3389/fmicb.2019.01970

Ries, L. N. A., Steenwyk, J. L., De Castro, P. A., De Lima, P. B. A., Almeida, F., De Assis, L. J., et al. (2019). Nutritional heterogeneity among *Aspergillus fumigatus* strains has consequences for virulence in a strain- and host-dependent manner. *Front. Microbiol.* 10:854. doi: 10.3389/fmicb.2019.00854

Rivero-Menendez, O., Cuenca-Estrella, M., and Alastruey-Izquierdo, A. (2019). In vitro activity of olorofim (F901318) against clinical isolates of cryptic species of *Aspergillus* by EUCAST and CLSI methodologies. *J. Antimicrob. Chemother.* 74, 1586–1590. doi: 10.1093/jac/dkz078

Robbins, N., Caplan, T., and Cowen, L. E. (2017). Molecular evolution of antifungal drug resistance. *Annu. Rev. Microbiol.* 71, 753–775. doi: 10.1146/annurev-micro-030117-020345

Rokas, A., Mead, M. E., Steenwyk, J. L., Oberlies, N. H., and Goldman, G. H. (2020). Evolving moldy murderers: *Aspergillus* section Fumigati as a model for studying the repeated evolution of fungal pathogenicity. *PLoS Pathog.* 16:e1008315. doi: 10.1371/journal.ppat.1008315

Sharma, C., and Chowdhary, A. (2017). Molecular bases of antifungal resistance in filamentous fungi. *Int. J. Antimicrob. Agents* 50, 607–616. doi: 10.1016/j.ijantimicag.2017.06.018

Sharma, C., Kumar, R., Kumar, N., Masih, A., Gupta, D., and Chowdhary, A. (2018). Investigation of multiple resistance mechanisms in voriconazole-resistant *Aspergillus flavus* clinical isolates from a chest hospital surveillance in Delhi, India. *Antimicrob. Agents Chemother.* 62:e01928-17. doi: 10.1128/AAC.01928-17

Simão, F. A., Waterhouse, R. M., Ioannidis, P., Kriventseva, E. V., and Zdobnov, E. M. (2015). BUSCO: assessing genome assembly and annotation completeness with single-copy orthologs. *Bioinformatics* 31, 3210–3212. doi: 10.1093/bioinformatics/btv351

Slater, J. L., Gregson, L., Denning, D. W., and Warn, P. A. (2011). Pathogenicity of *Aspergillus fumigatus* mutants assessed in *Galleria mellonella* matches that in mice. *Med. Mycol.* 49(Suppl. 1), S107–S113.

Staab, J. F., Jennifer, N. K., and Kieren, A. M. (2010). Differential *Aspergillus lentulus* echinocandin susceptibilities are Fksp independent. *Antimicrob. Agents Chemother.* 54, 4992–4998. doi: 10.1128/aac.00774-10

Stanke, M., Steinkamp, R., Waack, S., and Morgenstern, B. (2004). AUGUSTUS: a web server for gene finding in eukaryotes. *Nucleic Acids Res.* 32, W309–W312.

Steenwyk, J. L., Shen, X.-X., Lind, A. L., Goldman, G. H., and Rokas, A. A. (2019). Robust phylogenomic time tree for biotechnologically and medically important fungi in the genera *Aspergillus* and *Penicillium*. *mBio* 10:e00925-19.

Sugui, J. A., Peterson, S. W., Figat, A., Hansen, B., Samson, R. A., Mellado, E., et al. (2014). Genetic relatedness versus biological compatibility between *Aspergillus fumigatus* and related species. *J. Clin. Microbiol.* 52, 3707–3721. doi: 10.1128/JCM.01704-14

Szalewski, D. A., Hinrichs, V. S., Zinniel, D. K., and Barletta, R. G. (2018). The pathogenicity of *Aspergillus fumigatus*, drug resistance, and nanoparticle delivery. *Can. J. Microbiol.* 64, 439–453. doi: 10.1139/cjm-2017-0749

Takahashi-Nakaguchi, A., Muraosa, Y., Hagiwara, D., Sakai, K., Toyotome, T., Watanabe, A., et al. (2015). Genome sequence comparison of *Aspergillus fumigatus* strains isolated from patients with pulmonary aspergilloma and chronic necrotizing pulmonary aspergillosis. *Med. Mycol.* 53, 353–360. doi: 10.1093/mmy/myv003

Tavaré, S. (1986). Some probabilistic and statistical problems in the analysis of DNA sequences. *Lect. Math. Life Sci.* 17, 57–86.

Taylor, J. W., Jacobson, D. J., Kroken, S., Kasuga, T., Geiser, D. M., Hibbett, D. S., et al. (2000). Phylogenetic species recognition and species concepts in fungi. *Fungal Genet. Biol.* 31, 21–32. doi: 10.1006/fgbi.2000.1228

Therneau, T. M. (2014). *A Package for Survival Analysis in S. R Package Version 2.37-7*. Available online at: https://cran.r-project.org/web/packages/survival/index.html (accessed April 10, 2020).

Tsai, H. F., Chang, Y. C., Washburn, R. G., Wheeler, M. H., and Kwon-Chung, K. J. (1998). The developmentally regulated alb1 gene of *Aspergillus fumigatus*: its role in modulation of conidial morphology and virulence. *J. Bacteriol.* 180, 3031–3038. doi: 10.1128/jb.180.12.3031-3038.1998

Vinet, L., and Zhedanov, A. (2011). A 'missing' family of classical orthogonal polynomials. *J. Phys. A Math. Theor.* 44:085201. doi: 10.1088/1751-8113/44/8/085201

Walker, B. J., Abeel, T., Shea, T., Priest, M., Abouelliel, A., Sakthikumar, S., et al. (2014). Pilon: an integrated tool for comprehensive microbial variant detection and genome assembly improvement. *PLoS One* 9:e112963. doi: 10.1371/journal.pone.0112963

Waterhouse, A. M., Procter, J. B., Martin, D. M. A., Clamp, M., and Barton, G. J. (2009). Jalview version 2-A multiple sequence alignment editor and analysis workbench. *Bioinformatics* 25, 1189–1191. doi: 10.1093/bioinformatics/btp033

Waterhouse, R. M., Tegenfeldt, F., Li, J., Zdobnov, E. M., and Kriventseva, E. V. (2013). OrthoDB: a hierarchical catalog of animal, fungal and bacterial orthologs. *Nucleic Acids Res.* 41, D358–D365.

Wei, X., Yuanwei, Z., and Ling, L. (2015). The molecular mechanism of azole resistance in *Aspergillus fumigatus*: from bedside to bench and back. *J. Microbiol.* 53, 91–99. doi: 10.1007/s12275-015-5014-7

Winnenburg, R. (2006). PHI-base: a new database for pathogen host interactions. *Nucleic Acids Res.* 34, D459–D464. doi: 10.1093/nar/gkj047

Yang, Z. (1994). Maximum likelihood phylogenetic estimation from DNA sequences with variable rates over sites: approximate methods. *J. Mol. Evol.* 39, 306–314. doi: 10.1007/bf00160154

Yang, Z. (1996). Among-site rate variation and its impact on phylogenetic analyses. *Trends Ecol. Evol.* 11, 367–372. doi: 10.1016/0169-5347(96)10041-0

Zakaria, A., Osman, M., Dabboussi, F., Rafei, R., Mallat, H., Papon, N., et al. (2020). Recent trends in the epidemiology, diagnosis, treatment, and mechanisms of resistance in clinical *Aspergillus* species: a general review with a special focus on the Middle Eastern and North African region. *J. Infect. Public Health* 13, 1–10. doi: 10.1016/j.jiph.2019.08.007

Zbinden, A., Imhof, A., Wilhelm, M. J., Ruschitzka, F., Wild, P., Bloemberg, G. V., et al. (2012). Fatal outcome after heart transplantation caused by *Aspergillus lentulus*. *Transpl. Infect. Dis.* 14, E60–E63. doi: 10.1111/j.1399-3062.2012.00779.x

Zheng, B., Yan, L., Liang, W., and Yang, Q. (2019). Paralogous Cyp51s mediate the differential sensitivity of *Fusarium oxysporum* to sterol demethylation inhibitors. *Pest Manag. Sci.* 75, 396–404. doi: 10.1002/ps.5127

Conflict of Interest: The authors declare that the research was conducted in the absence of any commercial or financial relationships that could be construed as a potential conflict of interest.

frontiers in Genetics

ORIGINAL RESEARCH
published: 15 May 2020
doi: 10.3389/fgene.2020.00483

Defining Critical Genes During Spherule Remodeling and Endospore Development in the Fungal Pathogen, *Coccidioides posadasii*

*H. L. Mead[1], C. C. Roe[1], E. A. Higgins Keppler[2,3], M. C. Caballero Van Dyke[1], K. L. Laux[1], A.L. Funke[1,4], K. J. Miller[1], H. D. Bean[2,3], J. W. Sahl[1] and B. M. Barker[1]**

[1] Pathogen and Microbiome Institute, Northern Arizona University, Flagstaff AZ, United States, [2] School of Life Sciences, Arizona State University, Tempe, AZ, United States, [3] Center for Fundamental and Applied Microbiomics, The Biodesign Institute, Arizona State University, Tempe, AZ, United States, [4] Imaging Histology Core Facility, Northern Arizona University, Flagstaff AZ, United States

OPEN ACCESS

Edited by:
Daniel Yero, Autonomous University of Barcelona, Spain

Reviewed by:
Don Natvig, The University of New Mexico, United States
Oliver Keatinge Clay, Del Rosario University, Colombia

***Correspondence:**
B. M. Barker
bridget.barker@nau.edu

Specialty section:
This article was submitted to Evolutionary and Genomic Microbiology, a section of the journal Frontiers in Genetics

Received: *27 February 2020*
Accepted: *17 April 2020*
Published: *15 May 2020*

Citation:
Mead HL, Roe CC, Higgins Keppler EA, Van Dyke MCC, Laux KL, Funke AL, Miller KJ, Bean HD, Sahl JW and Barker BM (2020) Defining Critical Genes During Spherule Remodeling and Endospore Development in the Fungal Pathogen, Coccidioides posadasii. Front. Genet. 11:483. doi: 10.3389/fgene.2020.00483

Coccidioides immitis and *C. posadasii* are soil dwelling dimorphic fungi found in North and South America. Inhalation of aerosolized asexual conidia can result in asymptomatic, acute, or chronic respiratory infection. In the United States there are approximately 350,000 new infections per year. The *Coccidioides* genus is the only known fungal pathogen to make specialized parasitic spherules, which contain endospores that are released into the host upon spherule rupture. The molecular determinants involved in this key step of infection remain largely elusive as 49% of genes are hypothetical with unknown function. An attenuated mutant strain *C. posadasii* Δ*cts2*/Δ*ard1*/Δ*cts3* in which chitinase genes 2 and 3 were deleted was previously created for vaccine development. This strain does not complete endospore development, which prevents completion of the parasitic lifecycle. We sought to identify pathways active in the wild-type strain during spherule remodeling and endospore formation that have been affected by gene deletion in the mutant. We compared the transcriptome and volatile metabolome of the mutant Δ*cts2*/Δ*ard1*/Δ*cts3* to the wild-type C735. First, the global transcriptome was compared for both isolates using RNA sequencing. The raw reads were aligned to the reference genome using TOPHAT2 and analyzed using the Cufflinks package. Genes of interest were screened in an *in vivo* model using NanoString technology. Using solid phase microextraction (SPME) and comprehensive two-dimensional gas chromatography – time-of-flight mass spectrometry (GC × GC-TOFMS) volatile organic compounds (VOCs) were collected and analyzed. Our RNA-Seq analyses reveal approximately 280 significantly differentially regulated transcripts that are either absent or show opposite expression patterns in the mutant compared to the parent strain. This suggests that these genes are tied to networks impacted by deletion and may be critical for endospore development and/or spherule rupture in the wild-type strain. Of these genes, 14 were specific to the *Coccidioides* genus. We also found that the wild-type and mutant strains differed

significantly in their production versus consumption of metabolites, with the mutant displaying increased nutrient scavenging. Overall, our results provide the first targeted list of key genes that are active during endospore formation and demonstrate that this approach can define targets for functional assays in future studies.

Keywords: *Coccidioides*, Valley fever, dimorphic fungi, thermotolerance, spherules

INTRODUCTION

Fungal infections have become an increasing threat to human health, claiming the lives of ∼1.5 million people worldwide each year (Brown et al., 2012). Dimorphic fungi, which have evolved the ability to switch between specialized environmental or host-specific lifecycles, are a major cause of the increase in cases (Van Dyke et al., 2019). These fungi can cause disease in both immune-compromised and competent individuals, and this is attributed to their ability to shift to a host specific lifecycle at 37°C. *Coccidioides immitis* and *C. posadasii* are two of these dimorphic fungi associated with animals/animal burrows in arid desert soil (Kollath et al., 2019; Taylor and Barker, 2019). The genus has a broad distribution in both North and South America (Barker et al., 2012). In the United States alone, these fungi are estimated to cause disease in 350,000 individuals each year (Chiller, 2019). Disease burden in other regions is poorly documented; however, case rates are increasing across the new world (Alvarado et al., 2018; Freedman et al., 2018; Laniado-Laborin et al., 2019). Coccidioidomycosis (Valley fever) can result in a broad range of clinical symptoms. Respiratory infection is the most common, resulting in asymptomatic, acute, or chronic pneumonia. Dissemination occurs in rare cases (1–5%), infecting organs, bones, and the central nervous system (Galgiani et al., 2000, 2016; Ampel, 2015). As with other fungal infections, there is no vaccine and treatment options are limited to triazoles or polyenes (Thompson et al., 2019).

Disease prevention is difficult because natural or human caused disruption of the soil can cause the fungal propagules to become airborne, which can be inhaled by a susceptible mammal. In the environment, these arthroconidia germinate as polarized filamentous mycelia. Exposure to the host respiratory system triggers fungal morphogenesis to the host-specific lifecycle. Unknown factors cause isotropic swelling into large parasitic structures called spherules. These spherules swell over the course of about 5 days at which point they rupture releasing ∼100 endospores; and each of these endospores can develop into another rupturing spherule. Endosporulation is a fundamental step in host colonization as it allows for exponential increase in fungal burden approximately every 5 days (Drutz and Huppert, 1983; Cole and Hung, 2001).

Endosporulation is a key step in coccidioidomycosis; however, this stage is not well understood. *Coccidioides* is the only dimorphic fungal pathogen known to undergo this cyclical release of spores within a host (Sil and Andrianopoulos, 2014; Van Dyke et al., 2019). Understandably, research has focused on the genes utilized to develop from arthroconidia into the spherule structure. Thus far, only one published study compared the global transcriptome between the environmental and parasitic lifecycle between the two species (Whiston et al., 2012). They found 1,880 genes up-regulated in the spherules structure, which were shared by both species. While insightful, of the top 15 differentially expressed genes, 10 were hypothetical proteins without predicted function. This challenge is common in *Coccidioides* research as ∼49% of the genome is not annotated, and function is often inferred by orthologs to other well studied fungi. However, this strategy is only helpful with shared characteristics. Because endosporulation is unique to *Coccidioides*, we sought to develop an alternative approach to identify genes required to complete this unique lifecycle.

To accomplish this, we utilized a mutant strain of *C. posadasii* Δ*cts2*/Δ*ard1*/Δ*cts3* which develops into sterile spherules that are unable to endosporulate (**Figure 1**; Xue et al., 2009). Chitinase 2 (*cts2*) and chitinase 3 (*cts3*) were selected by the authors based on real time PCR analysis of all chitinase gene activity during spherule remodeling and endospore formation. During cts3 disruption the open reading frame of a contiguous gene, D-arabinotol-2-dehydrogenase (*ARD1*) was impacted. In the study, the authors show that individual mutants Δ*cts2* or Δ*ard1*/Δ*cts3* retained the ability to endosporulate and cause disease. However, the combination of Δ*cts2*/Δ*ard1*/Δ*cts3* deletion prevented endosporulation and subsequently attenuation. The molecular determinants involved in the lack of endospore formation or release remains elusive. We compared growth of this mutant to the wild-type parent strain as a method of filtering through the previously identified differentially regulated transcripts based on the non-endosporulating phenotype. Consequently, this study focused on the 96 h time point which is when endospores are forming, and the cell wall is remodeling in preparation for spherule rupture (Cole and Hung, 2001). Additionally, this was the time point investigated in the study mentioned above comparing the transcriptome of environmental and parasitic stages of the wild-type parent, *C. posadasii* C735 (Whiston et al., 2012). Therefore, we compared the global transcriptome of the mutant strain, Δ*cts2*/Δ*ard1*/Δ*cts3*, to its wild-type parent strain C735 to define gene regulation during this crucial stage in disease establishment during a *Coccidioides* infection.

RESULTS

The pathways that regulate spherule development and survival of *Coccidioides* within a host are complex. The attenuated mutant strain Δ*cts2*/Δ*ard1*/Δ*cts3* provides an appropriate strategy for the reverse genetic studies used here. This strain is capable of creating the parasitic structure yet lacks necessary signaling pathways that allow for endospore formation and release

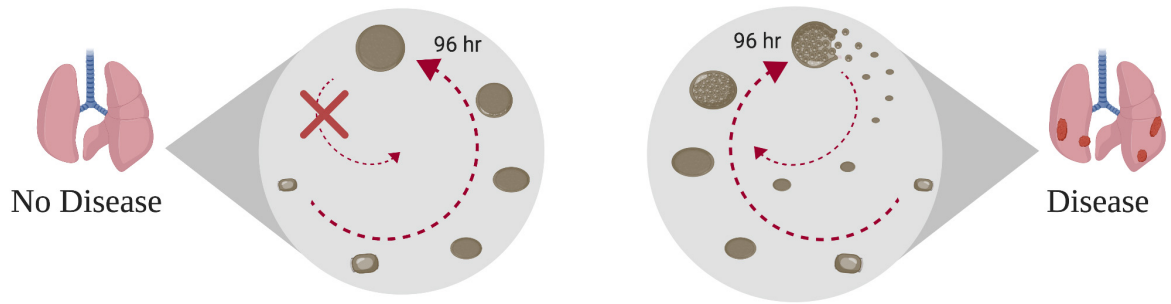

FIGURE 1 | Comparison of mutant and parent lifecycles. The attenuated mutant **(A)** develops from arthroconidia into non-rupturing spherules that do not contain endospores. **(B)** In contrast, the wild-type strain begins to develop endospores around 96 h. These structures rupture near 120 h, releasing endospores which individually develop into mature, rupturing spherules every 120 h. Illustration created with BioRender.

(**Figure 1**). Therefore, the transcriptional profile of wild-type *C. posadasii* strain C735 and the attenuated mutant strain was compared to identify genes that are active in a key stage of disease establishment. Read data was generated by collecting 96 h spherules and mycelia from the attenuated strain of *Coccidioides,* Δ*cts2*/Δ*ard1*/Δ*cts3*, using growth conditions from the previously published experiment with the wild-type strain (Whiston et al., 2012). The raw reads for the wild-type parent strain were retrieved and subject to *de novo* analysis using the TopHat2/Cufflinks package alongside the newly generated mutant reads. This package uses two normalization parameters. Read counts are normalized based on the total reads obtained per sequencing run, which account for differences in sequencing runs. Additionally, within sample read counts are normalized based on total transcript length to avoid long transcripts accumulating more counts than short ones. The individual replicates for each condition had a high degree of similarity for each sample in terms of total transcript density and expression (**Supplementary Figure 1**). The transcripts clustered by lifecycle rather than strain (**Supplementary Figure 2**). Together these results indicate a high degree of similarity between individual replicates and data sets. For the full data set see **Supplementary Table 1**.

Comparison of Wild-Type and Mutant Lifecycles; Mycelia Versus Spherules

Using transcript data, we searched for deviations from the wild-type transcriptional profile using two approaches. First, the differential expression between lifecycle stages: the environmental (mycelia) versus parasitic (spherule) was quantified, for each strain respectively. The Δ*cts2*/Δ*ard1*/Δ*cts3* is derived from *C. posadasii* C735; therefore, the transcriptional pattern between lifecycles for each isolate was similar (**Figures 2A,C**). In the mutant strain, there were a total of 4,646 significantly differentially expressed genes, 2,423 were up-regulated and 2,223 down-regulated in 96 h spherules [False Discovery Rate (FDR), $p < 0.05$] (**Figure 2B**). In comparison, the parent strain had a total of 4,020 significantly expressed genes, 2,118 of which are up-regulated and 1,902 down-regulated in 96 h spherules (FDR, $p < 0.05$) (**Figure 2D**). Investigations were restricted to transcripts that are up or down-regulated twofold or greater between lifecycle stages for each strain respectively (FDR, $p < 0.05$). A Venn diagram was used to visualize similarity and differences between wild-type and mutant gene expression patterns (**Figure 3**; Oliveros, 2007). Genes from the Venn diagram are listed in **Supplementary Table 2**.

Acquisition of Iron and Other Metal Co-factors Is Key to Preparation of Wild-Type Spherule Remodeling or Endosporulation

When searching for shared or disparate expression patterns between strains, 19 transcripts were identified that are up-regulated in the *C. posadasii* C735 parasitic lifecycle and down-regulated in *C. posadasii* Δ*cts2*/Δ*ard1*/Δ*cts3* (**Figure 4**). The transcriptional pattern of C735 can give insight into wild-type gene regulation during infection. In contrast, mutant deviations from the wild-type transcriptional pattern may represent genes necessary during endospore formation that are receiving improper signals or responding inappropriately during spherule remodeling. Of these genes, five are annotated as hypothetical proteins; however, function was inferred for these genes using annotated orthologs (**Figure 4**). Overrepresented biological categories were iron acquisition, metal ion homeostasis, and response to oxidative stress (**Supplementary Table 3**). In the wild-type expression profile, a GATA transcription factor was significantly up-regulated in spherules but down-regulated in the mutant. This gene is conserved across fungi and implicated in iron homeostasis, siderophore biosynthesis, and morphogenesis (Oberegger et al., 2001; Hwang et al., 2008; Gauthier et al., 2010; Attarian et al., 2018). These data suggest that the acquisition of

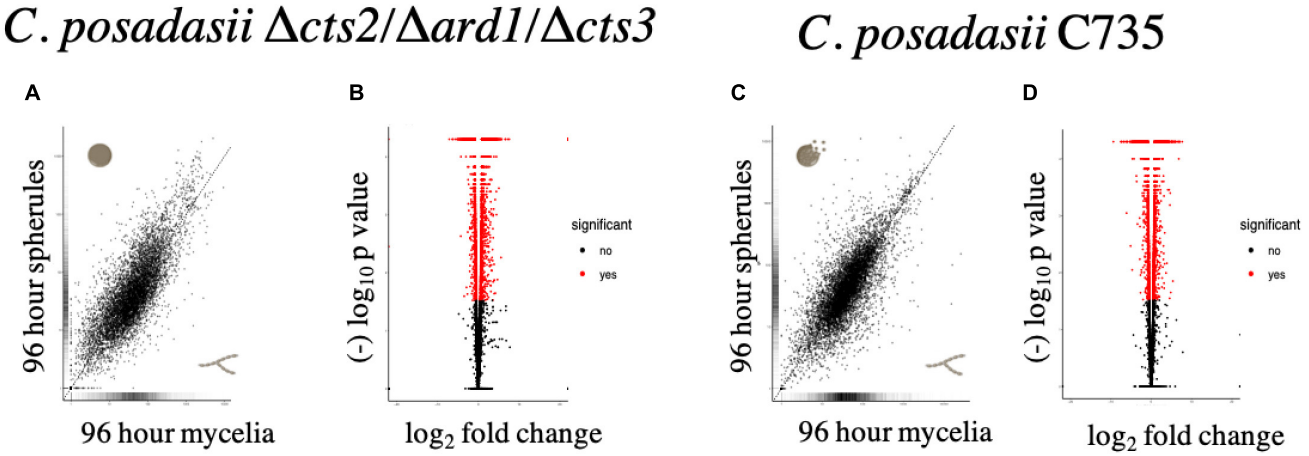

FIGURE 2 | Comparison of global transcriptome and differentially expressed genes measured between 96-h spherules and mycelia for each strain. **(A,C)** The global expression pattern between spherules and mycelia are similar between strains. Transcripts that fall on the line are equally expressed in both cell types. Distance from the line indicates increased transcript abundance for spherules (y-axis) or mycelia (x-axis). **(B,D)** Using an FDR $p < 0.05$ there were 4,646 differentially expressed genes (2,409 up-regulated) in the mutant strain and 4,020 differentially expressed genes (2,118 up-regulated) in the parent strain.

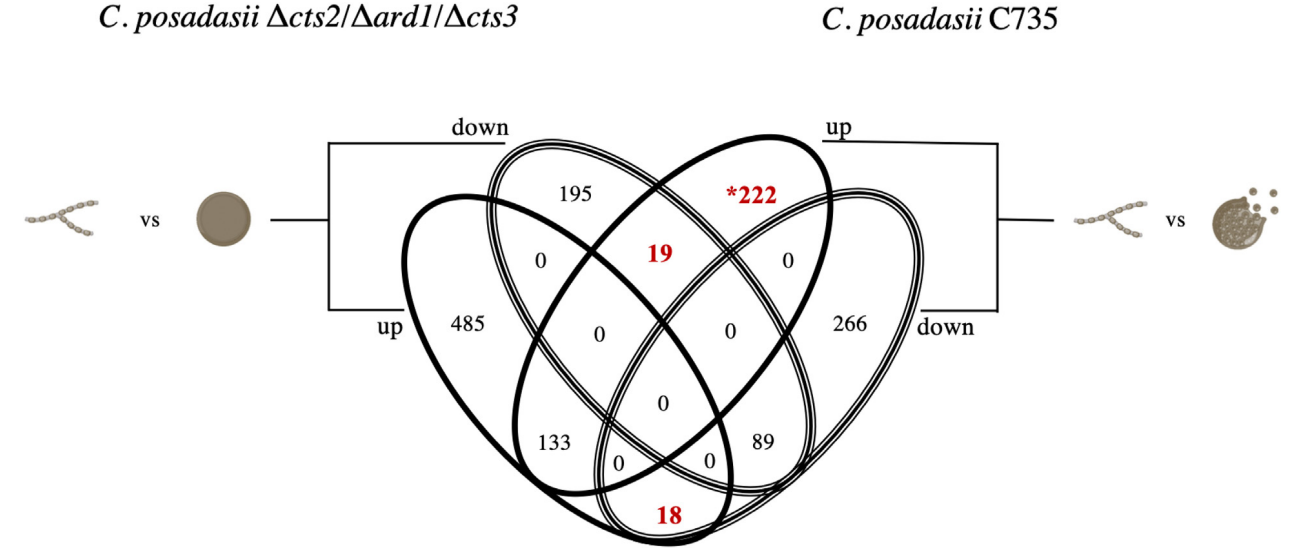

FIGURE 3 | Venn diagram of differentially expressed genes between mycelia and spherules for each strain, respectively. Diagram shows genes that change expression in spherules compared to mycelia for the wild-type and mutant strain. Genes were included if expression was significantly (FDR $p < 0.05$) up-regulated (solid oval) or down-regulated (striped oval) twofold or more. Of interest are 259 gene transcripts that in the mutant deviate from the pattern of the wild-type parent: 19 genes up-regulated in the wild-type parasitic lifecycle and down in the mutant, 18 down-regulated in the wild-type parasitic lifecycle and up in the mutant, and 222 up regulated only in the wild-type lifecycle. Of these 259 genes, the asterisk (*) indicates that seven are unique to *Coccidioides*.

iron and other metals in *Coccidioides* is a key cellular process in preparation for spherule remodeling or endosporulation. Interestingly, these processes are impacted by the dysregulation of chitinases, as observed in the mutant strain expression profile. Similarly, there were 18 transcripts that are down-regulated in the wild-type parasitic lifecycle (mycelia versus spherule) while up-regulated in the mutant (**Figure 5**). These transcripts are specific to chitin remodeling, secreted proteins, and pheromone sensing. GO terms are enriched for catabolism, membrane transport, and programmed cell death (**Supplementary Table 4**).

Nitrogen Recycling, Mitochondrial Respiration and Heat Shock Proteins Are Key Transcripts Up-Regulated in Wild-Type Spherules Compared to Mycelia

Next, the 222 genes that are up-regulated in the wild-type parasitic lifecycle, but not in the mutant lifecycle (**Figure 3**) were investigated. We predict that genes up-regulated in both strains are required for spherule growth and maintenance. In

A

Gene Name	Product Description
CPC735_068190	hypothetical protein/SET domain-containing*
CPC735_029090	major facilitator superfamily protein
CPC735_026240	alcohol dehydrogenase I, putative
CPC735_022250	peroxidase, putative
CPC735_045240	trehalose-phosphatase, putative
CPC735_044150	trehalose-phosphatase, putative
CPC735_039850	succinate dehydrogenase flavoprotein subunit, putative
CPC735_024240	succinate dehydrogenase iron-sulfur protein
CPC735_009410	hypothetical protein/cell wall organization, hypoxia, Rim 101 regulated, required for virulence *
CPC735_040950	cytochrome b2, mitochondrial precursor, putative
CPC735_062440	hypothetical protein/copper/iron homeostasis, cell all localization, copper chelation*
CPC735_056160	GATA family transcription factor
CPC735_051000	hypothetical protein/hypothetical in all orthologs *
CPC735_037240	aspartic protease, putative
CPC735_047430	Hsp9/Hsp12 family heat shock protein
CPC735_045450	isocitrate lyase, putative
CPC735_033850	integral membrane family protein
CPC735_073920	catalase, putative
CPC735_009570	hypothetical protein/possible role in melanin biosynthesis, tyrosine catabolism *

B

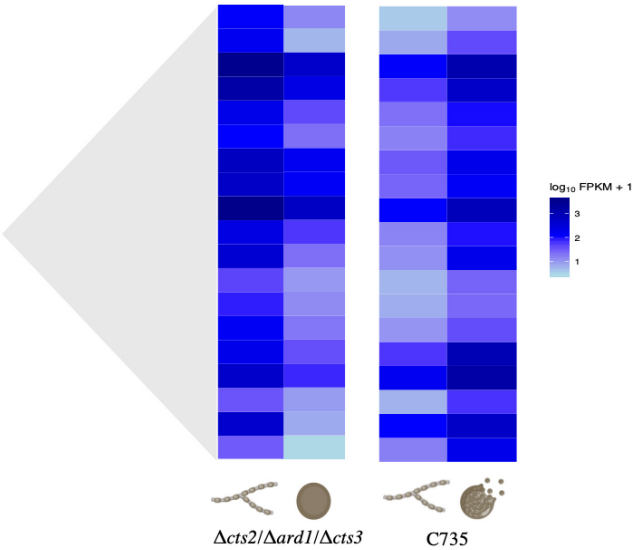

FIGURE 4 | Gene description and heatmap of 19 improperly down-regulated genes. When comparing wild-type mycelia to spherules, these genes are significantly up-regulated. However, they are down-regulated in the mutant spherules compared to mycelia. **(A)** Table of the 19 genes and product descriptions, some of which have been shown to be important in stress response, pH, and metal ion acquisition in other fungi. When genes were annotated as hypothetical the asterisk (*) indicates ortholog function in other fungi. **(B)** Heatmap visualization in $\log_{10}$FPKM of the opposing expression patterns for wild-type and mutant lifecycle. A darker color indicates increased expression while lighter indicates decreased expression measured in $\log_{10}$ FPKM.

A

Gene ID	Product Description
CPC735_036390	complement fixation-chitinase
CPC735_024440	hypothetical protein/ hypothetical in all orthologs *
CPC735_023010	Chitosanase CSN1, putative
CPC735_034070	hypothetical protein/ hypothetical in all orthologs *
CPC735_023730	hypothetical /DUF3112 domain-containing protein *
CPC735_018710	uracil phosphoribosyltransferase, putative
CPC735_033630	GNAT family acetyltransferase, putative
CPC735_043750	apoptosis-inducing factor, putative
CPC735_035780	subtilisin-like protease, putative
CPC735_055830	Major Facilitator Superfamily protein
CPC735_015490	Microsomal dipeptidase precursor, putative
CPC735_030640	O-methyltransferase family protein
CPC735_050000	Major Facilitator Superfamily protein
CPC735_045990	hypothetical protein/ hypothetical in all orthologs *
CPC735_050050	ABC transporter, putative
CPC735_043570	hypothetical protein/SAM-dependent methyltransferase *
CPC735_060100	Fungal pheromone mating factor STE2 GPCR family protein
CPC735_043760	GNAT family acetyltransferase, putative

B

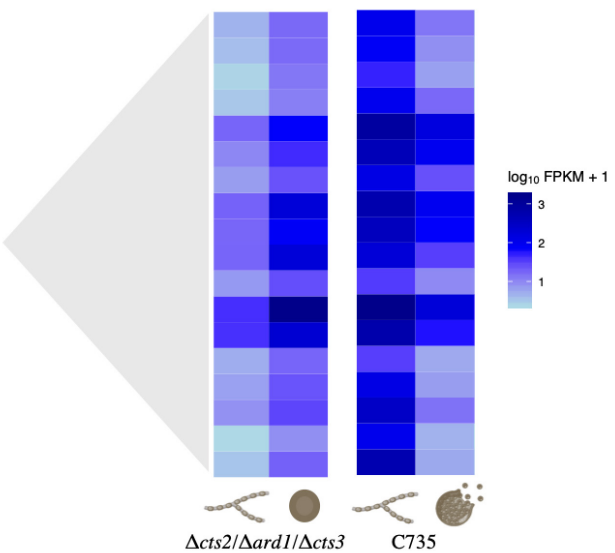

FIGURE 5 | Gene description and heatmap of 18 improperly up-regulated genes. When comparing wild-type mycelia to spherules, these genes are significantly down-regulated. **(A)** Table showing gene descriptions, some of which are involved with chitin remodeling, mating pheromones/quorum sensing, and programmed cell death. When genes were annotated as hypothetical the asterisk (*) indicates ortholog function in other fungi. **(B)** Heatmap visualization in $\log_{10}$FPKM of the opposing expression patterns for wild-type and mutant lifecycles. A darker color indicates increased expression while lighter indicates decreased expression measured in $\log_{10}$ FPKM.

contrast, genes that are only up-regulated in the wild type at 96 h may be involved in the cellular signals that lead to endospore formation, or spherule rupture. GO terms suggest that the wild-type strain exhibits transcripts specific to nitrogen assimilation or metabolism (**Table 1**). Out of the 222 genes mentioned, 102 are annotated as hypothetical proteins, with orthologs in many other fungi (**Supplementary Table 5**). This indicates that *Coccidioides* uses conserved genes to complete

TABLE 1 | Significantly enriched biological processes up-regulated in wild-type spherule compared to mycelia.

GO ID	GO term	Percent of bkgd genes in your result	Fold enrichment	Odds ratio	Benjamini	Bonferroni	Organism
GO:0120029	Proton export across plasma membrane	100	36.51	Infinity	5.64E-03	2.26E-02	A. f f293
GO:0120029	Proton export across plasma membrane	100	27.97	Infinity	4.80E-05	3.36E-04	A. n 1015
GO:0140115	Export across plasma membrane	100	27.97	Infinity	4.80E-05	3.36E-04	A. n 1015
GO:0008272	Sulfate transport	75	20.98	81.99	2.65E-03	3.71E-02	A. n 1015
GO:0072348	Sulfur compound transport	75	20.98	81.99	2.65E-03	3.71E-02	A. n 1015
GO:0042126	Nitrate metabolic process	57.1	15.98	36.59	1.08E-03	1.08E-02	A. n 1015
GO:0042128	Nitrate assimilation	57.1	15.98	36.59	1.08E-03	1.08E-02	A. n 1015
GO:0071941	Nitrogen cycle metabolic process	50	13.99	27.44	1.75E-03	2.10E-02	A. n 1015
GO:2001057	Reactive nitrogen species metabolic process	50	13.99	27.44	1.75E-03	2.10E-02	A. n 1015
GO:0006979	Response to oxidative stress	47.4	13.25	25.23	2.91E-07	1.16E-06	A. n 1015
GO:0006995	Cellular response to nitrogen starvation	31.3	11.41	16.43	9.37E-03	5.62E-02	A. f f293
GO:0043562	Cellular response to nitrogen levels	31.3	11.41	16.43	9.37E-03	5.62E-02	A. f f293
GO:0016999	Antibiotic metabolic process	13	4.75	5.52	1.15E-03	3.44E-03	A. f f293
GO:0055085	Transmembrane transport	8.3	2.32	2.98	8.72E-09	8.72E-09	A. n 1015
GO:0055114	Oxidation-reduction process	6.5	2.38	2.76	5.96E-05	5.96E-05	A. f f293
GO:0055085	Transmembrane transport	6.5	2.37	2.73	9.96E-05	1.99E-04	A. f f293
GO:0006810	Transport	7.2	2.02	2.54	2.91E-07	1.04E-06	A. n 1015
GO:0051234	Establishment of localization	7.2	2.02	2.54	2.91E-07	1.09E-06	A. n 1015
GO:0051179	Localization	7.1	1.99	2.51	3.43E-07	1.71E-06	A. n 1015
GO:0055114	Oxidation-reduction process	6.1	1.7	1.99	6.50E-04	5.20E-03	A. n 1015

Terms are based on A. niger (A.n 1015) and A. fumigatus (A.f f293). Over represented biological processes suggest nitrogen utilization, toxin production, and mitochondrial related genes demonstrate increased activity during cellular preparation for endospore release.

the parasitic lifecycle, at least in part. In contrast, eight genes are currently identified as exclusive to the *Coccidioides* genus. Although other pathogenic fungi undergo host-specific morphogenesis, endospore formation and release is a unique characteristic of *Coccidioides*. With this in mind, the amino acid sequences for each gene were used to search for conserved protein domains using several prediction algorithms; NCBI conserved domains search, EggNOG Mapper and InterProScan (**Supplementary Table 6**). Several of the hypothetical proteins are suggested to have protein kinase-like or phosphotransferase-like domains. Thus, these unknown genes could potentially participate in signal cascades modifying other proteins by the addition of a phosphate group. We determined that one gene, CPC735_012730, is similar to pyoverdine/dityrosine biosynthesis protein which is a precursor to the ascospore cell wall of *Saccharomyces cerevisiae* (Briza et al., 1994). This conserved architecture was identified by all three of the prediction algorithms utilized. For two of these *Coccidioides*-specific genes, the prediction methods used in this study were unable to derive any putative function. Nevertheless, the transcriptional activity of these genes in the wild-type lifecycle makes them interesting candidates for future investigations. We further interrogated this list of 222 genes for transcripts exhibiting the highest fold change in wild-type mycelia to spherules. Of interest is Hsp20, a heat shock protein which is likely involved in chaperoning proteins in response to heat stress. Curiously, this gene is expressed sixfold higher in the wild-type parasitic lifecycle while there is little expression change in the mutant from mycelia to spherules (**Table 2**). We predict that this chaperone protein is related to spherule structural remodeling, which is impaired in the mutant. Not surprisingly, other genes with known function in this highly up-regulated group are implicated in stress response, or in mitochondrial function. These genes do not display the same transcriptional activity in the mutant suggesting that they are important in wild-type spherules during the time point when spherules remodel, form endospores and subsequently prepare for rupture and dissemination.

Comparison of Transcript Abundance Between Wild-Type and Mutant Spherules Identifies Several *Coccidioides* Specific Hypothetical Proteins

As a second approach, we compared transcript expression specifically between wild-type and mutant spherules (**Figure 6A**). Because different sequencing platforms were used to obtain reads (GAII, MiSeq), significance comparisons were further restricted to FDR corrected $p < 0.001$ to reduce the possibility of false positives. There were 2,018 significantly differentially expressed genes 151 of which were up-regulated twofold or more in the wild-type spherules as compared to the mutant spherules (**Figure 6B**). GO terms indicate enrichment of biological processes specific to transport across the membrane and response to oxidative stress (**Supplementary Table 7**). Of specific interest, cell division control (CPC735_003020) and circadian rhythm (CPC735_054180) proteins were significantly up-regulated in

TABLE 2 | Transcripts that are up-regulated fivefold or more in wild-type spherules compared to mycelia and not in the mutant.

Gene ID	Product description	Ortholog group	*C. posadasii* C735 log2 fold change*	*C. posadasii* Δ*cts2*/Δ*ard1*/Δ*cts3* log2 fold change*
CPC735_010730	Hypothetical protein/Fungal dehydrin-like protein that plays a role in oxidative, osmotic and pH stress responses**	OG5_155947	7.68551	0.885797
CPC735_018870	Hypothetical protein/conserved hypothetical**	OG5_144599	6.50284	−0.574354
CPC735_037080	Hypothetical protein/conserved hypothetical**	OG5_180711	5.71183	1.98425
CPC735_047390	Hsp20/alpha crystallin family protein	OG5_126935	6.96036	0.716718
CPC735_053080	Oxidoreductase, short chain dehydrogenase/reductase family protein	OG5_128170	5.03474	0.539224
CPC735_070700	Hypothetical protein/mitochondrial integral membrane protein**	OG5_139306	5.32416	0.860862
CPC735_070990	Hemerythrin family protein	OG5_139259	5.84751	−1.3612

Gene ID, product description, ortholog group and fold change are listed for both wild-type and mutant comparisons. These transcripts are associated with heat or stress tolerance and mitochondrial respiration. Asterisk (*) indicates fold change between mycelia and spherules, (**) indicates ortholog function.

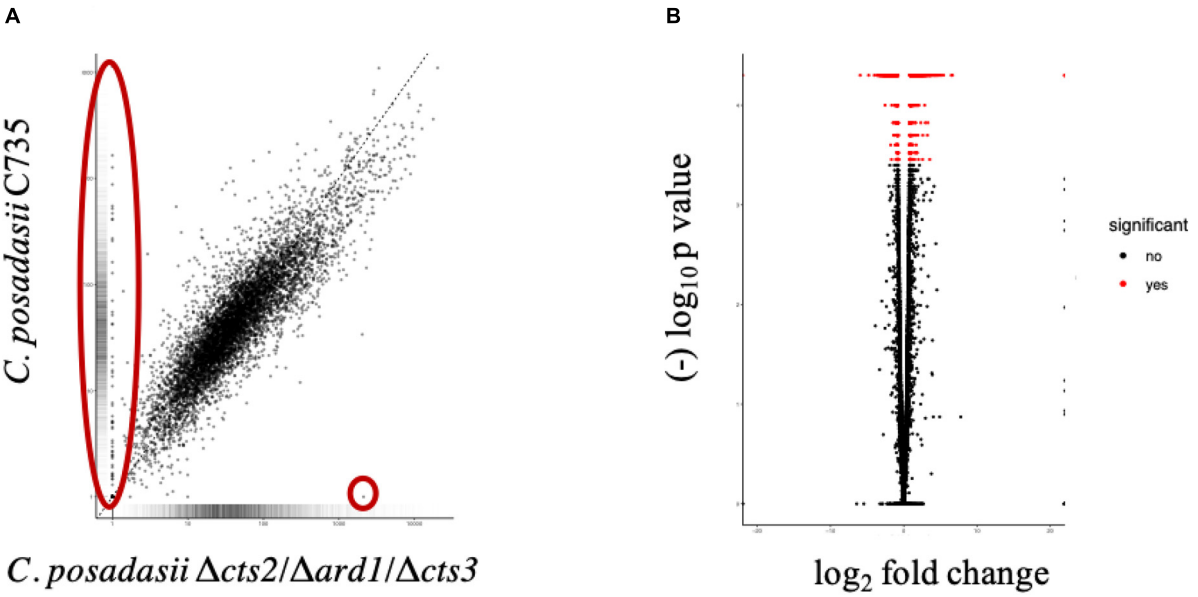

FIGURE 6 | Comparisons of global transcriptome and differentially expressed genes measured between 96 h spherules for parent (C735) and mutant (Δ*cts2*/Δ*ard1*/Δ*cts3*). We observed a subset of genes that are expressed (FDR, $p < 0.001$) in wild-type spherules and inactive in the mutant (**A**, large oval) compared to the attenuated mutant. These genes may be related to endospore formation or release. Hygromycin resistance cassette is expressed in the mutant only (**A**, small circle). **(B)** There are 2,018 genes differentially expressed (FDR, $p < 0.001$) between spherules, 151 are upregulated twofold or more.

wild-type spherules compared to mutant spherules. These genes could be part of the signaling pathways responsible for endospore formation in wild-type *Coccidioides*. From the list of 151 genes, 77 are annotated as hypothetical proteins with orthologs to other fungi. However, six are specific to *Coccidioides*. For each gene, three prediction methods (NCBI conserved domains search, EggNOG Mapper and InterProScan) were used to query the protein sequence to search for a conserved architecture. These strategies were unable to detect conserved domains, or similar sequences for any of these genes (**Table 3**). Without conserved domain structure it is difficult to speculate function of these unknown gene transcripts. However, the observed expression patterns would suggest these genes are important during spherule remodeling and endospore formation. Within this list of unknown proteins, there were a subset that are active in wild-type spherules and not active in the mutant spherules (**Table 3**). Two of these genes, CPC735_037660 and CPC735_037670, are adjacent to each other, and are unique to *Coccidioides* (**Figure 7A**). The wild-type expression pattern of the gene set reveals that 037660 demonstrates increased transcript abundance in spherules and its genomic neighbor 037670 is active during hyphal growth. Intriguingly, both transcripts are absent in mutant spherules, further suggesting a specific association with morphogenesis in spherules (**Figure 7B**). To ensure that these genes are operational during infection, a custom set of RNA probes was employed. These transcripts

TABLE 3 | Six *Coccidioides* specific hypothetical proteins that are significantly up regulated in the wild-type spherules compared to mutant spherules.

Gene description			Conserved domains			Transcript abundance		
Gene ID	**Product description**	**Ortholog group**	**NCBI**	**InterproScan**	**EggNOG mapper**	**Δ*cts2*/Δ*ard1*/Δ*cts3* Spherules FPKM**	**C735 wild-type spherules FPKM**	**FDR *p*-value**
CPC735_025360	Hypothetical protein	OG5_cpos CPAG_03276	No hits	No hits	No hits	16.4916	94.7691	0.000150527
CPC735_030120	Hypothetical protein	OG5_cpos CPC735_030120	No hits	No hits	No hits	0	256.854	0.000150527
CPC735_037660	Predicted protein	OG5_223849	No hits	No hits	No hits	0	12.6279	0.000150527
CPC735_037670	Predicted protein	OG5_cpos CPC735_037670	No hits	No hits	No hits	0	4.74221	0.000150527
CPC735_040990	Hypothetical protein	OG5_cpos CPAG_00370	No hits	No hits	No hits	8.62265	87.1783	0.000150527
CPC735_073570	Hypothetical protein	OG5_223158	No hits	No hits	No hits	14.7823	59.9105	0.000150527

Results of in silico predictions based on amino acid sequence are listed. The lack of expression in the mutant strain might indicate improperly signaling due to gene deletion. These Coccidioides specific genes are likely important to spherule remodeling.

were detected *in vivo* in a murine model at the same time point, suggesting that these genes are active in a host environment (**Figure 8**).

Differential Volatile Metabolome of Δ*cts2*/Δ*ard1*/Δ*cts3* Compared to Parent Strain Reveals Unique Compounds Produced by Wild-Type *C. posadasii*

Several of the genes that are differentially regulated in *C. posadasii* C735 versus Δ*cts2*/Δ*ard1*/Δ*cts3* are predicted to be involved in key metabolic processes, such as nitrate and sulfate transport and metabolism and detoxification of alcohols and reactive oxygen species, and therefore we compared the metabolomes of the wild-type and mutant strain. Our group is focused on developing breath-based biomarkers of *Coccidioides* infections, and therefore analyses were restricted to metabolites that are detected in the gas phase. Solid phase microextraction (SPME) and comprehensive two-dimensional gas chromatography – time-of-flight mass spectrometry (GC × GC-TOFMS) were used to collect and analyze the volatile organic compounds (VOCs) produced by 96 h spherules of C735 and attenuated strain. After data alignment and removal of chromatographic artifacts, 522 VOCs were detected across the nine samples, which included three biological replicates of each strain and three media blanks.

A comparison of the *C. posadasii* C735 and Δ*cts2*/Δ*ard1*/Δ*cts3* VOCs shows these two strains are quite different, with an almost fivefold increase in the number of metabolites detected in wild-type *C. posadasii* C735 cultures (**Figure 9**). Of the total metabolome, about a third (n = 158) of the VOCs were highly reproducible across biological replicates and either uniquely produced (present in one strain but absent in the other strain and media blanks) or uniquely consumed (absent in one strain but present in the other strain and media blanks) by one strain or the other, these were the focus for further characterization (**Supplementary Table 8**). The unique production of VOCs was dominated by *C. posadasii* C735, with 40 VOCs compared to 16 by Δ*cts2*/Δ*ard1*/Δ*cts3*, and the converse was true for metabolite consumption, with 90 compounds uniquely consumed by Δ*cts2*/Δ*ard1*/Δ*cts3* versus 12 by C735. A Wilcoxon Rank Sum test with Benjamini and Hochberg FDR correction was performed on these 158 VOCs, and all 40 volatiles uniquely produced by *C. posadasii* C735 and all 90 volatiles uniquely consumed by *C. posadasii* Δ*cts2*/Δ*ard1*/Δ*cts3* were found to be significant ($p < 0.05$) (**Figure 9**). Based upon mass spectral and chromatographic data, putative identities were assigned to 13 VOCs, the majority of which were aromatic, heteroaromatic, or aldehyde compounds (**Supplementary Table 8**). For the unnamed VOCs, chemical classifications were assigned to 58 of them based on a combination of mass spectral and chromatographic characteristics. The remaining 87 VOCs are classified as unknowns, due to a lack of mass spectral or chromatographic data of sufficient quality for identification.

The metabolomics data broadly reflect the same trends as the transcriptomics data, with higher proportions of metabolites being found specifically in the C735 cultures (**Figure 9** and

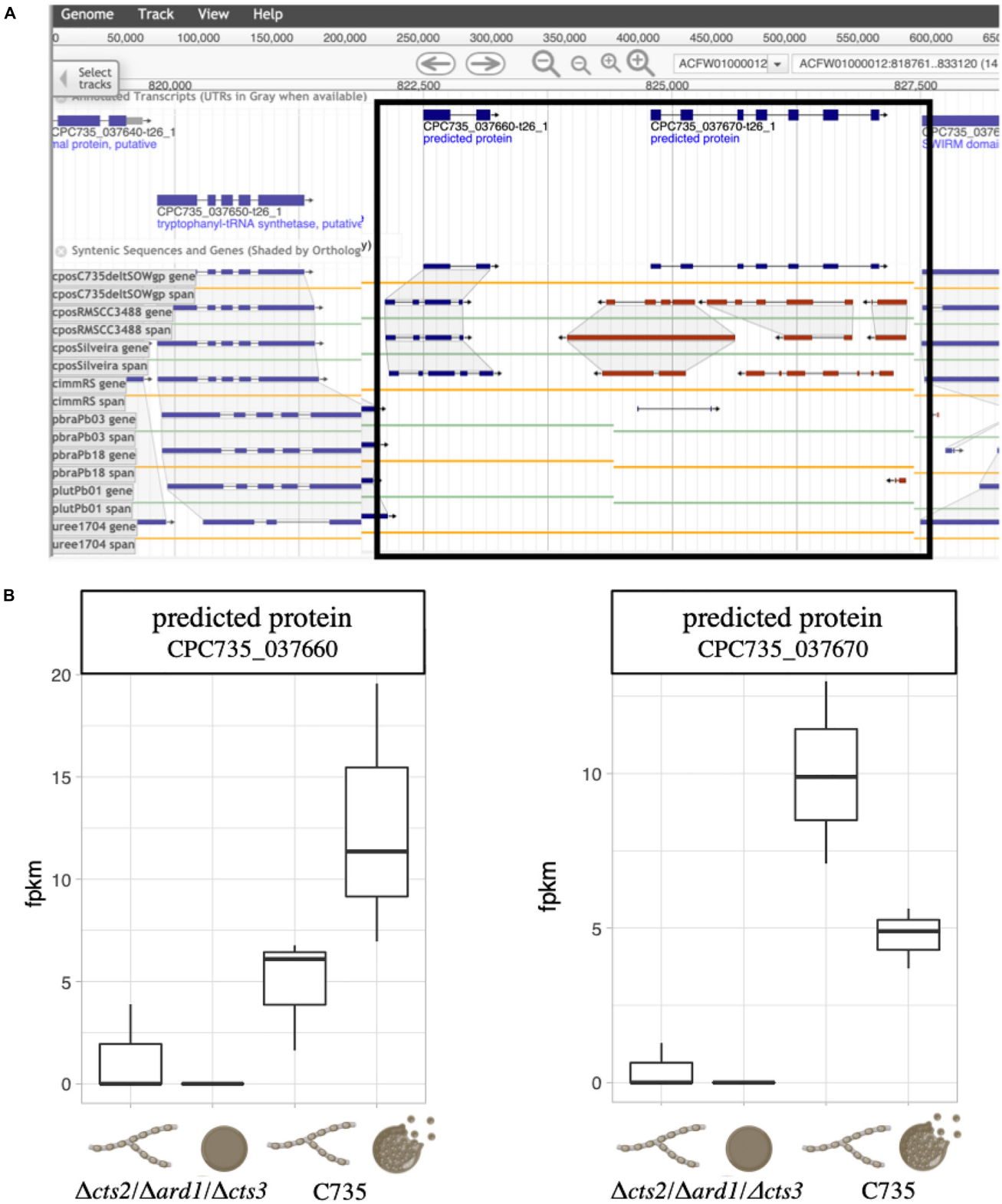

FIGURE 7 | Location and expression of putative morphogenesis related genes. **(A)** The predicted proteins are located adjacent to one another and are unique to *Coccidioides*. **(B)** In the *C. posadasii* C735 strain, the gene CPC735_037660 is up-regulated in wild-type spherules and CPC735_037670 is down-regulated. In the non-endosporulating mutant spherules, no transcripts were detected and low levels were detected in the mycelia phase.

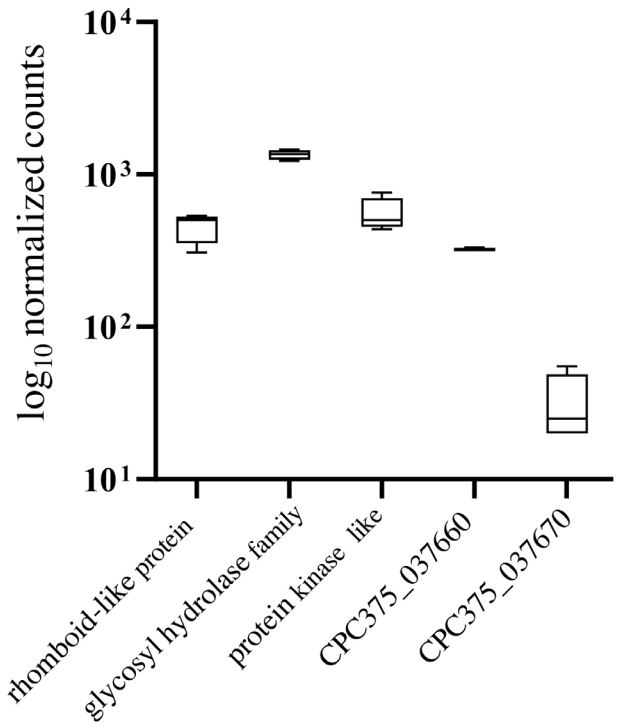

FIGURE 8 | *In vivo* expression in a murine model. Normalized counts of housekeeping genes and candidate genes at 96 h using NanoString technology. The genes CPC735_037660 and CPC735_037670 are active at 96 h in the host tissue in both *C. posadasii* strain C735 and *C. posadasii* Silveira. CPC735_037660 shows higher activity than CPC735_037670 similar to the *in vitro* observations.

Supplementary Table 8). The metabolomics data also provide a second window into the physiology of these two strains by quantifying the balance of metabolic production versus consumption by comparing VOC abundances in the fungal cultures versus the media blanks. Of the 158 uniquely produced or consumed VOCs, C735 has a threefold net production, while Δ*cts2*/Δ*ard1*/Δ*cts3* has a fivefold net consumption. These data would suggest that the mutant is able to consume the nutrient resources it would require for spherule remodeling or endospore formation, but the downstream metabolic pathways for this physiological transformation are not activated.

The comparative transcriptomics of C735 and Δ*cts2*/Δ*ard1*/Δ*cts3* predicted lower peroxidase, catalase, and alcohol dehydrogenase activity in the mutant, which we hypothesized would yield higher relative abundances of peroxides and lower aldehydes in the mutant versus wild type. Further, with higher levels of sulfur and nitrate transport and metabolism genes in the wild type, we would predict differences in heteroaromatic, nitrogen-containing, and sulfur-containing VOCs between wild type and mutant. Some of the metabolomics data support these hypotheses, while other data refute them. For instance, fewer aldehydes were produced by Δ*cts2*/Δ*ard1*/Δ*cts3*, but also fewer peroxides. However, the very large imbalance in the numbers of VOCs produced by C735 and Δ*cts2*/Δ*ard1*/Δ*cts3*, or consumed by these two strains inhibit our ability to robustly test these pathway-specific hypotheses.

Transmission Electron Microscopy Demonstrates Impaired Cell Wall and Internal Remodeling Activity in Δ*cts2*/Δ*ard1*/Δ*cts3* Spherules Compared to C735 Spherules

Finally, we used transmission electron microscopy (TEM) to view the internal landscape of 96 h Δ*cts2*/Δ*ard1*/Δ*cts3* and C735 spherules to look for evidence of phenotypic differences at this time point (**Figure 10**). The exterior of the wild-type spherules possesses loose layers of material, likely glycoproteins which have previously been reported to consistently shed from the cell wall (**Figures 10A,B**)(Hung et al., 2002). In *C. posadasii* C735 spherules, there were thick cell walls, and irregular shaped spherules which would indicate active cell wall remodeling (**Figures 10A–C**). This phenotype is consistent with previous reports and precedes internal segmentation (Huppert et al., 1982). Additionally, there were a variety of internal structural patterns, indicating active spherule remodeling and evidence of initiation of cross wall formation (**Figure 10C**). In contrast, the Δ*cts2*/Δ*ard1*/Δ*cts3* spherule development appeared partially arrested, with little cell wall or internal structure variation through-out all images (**Figures 10D–F**). We did not observe evidence of glycoprotein sloughing, rather the cell walls were consistently even in thickness and overall shape. The cell wall of the mutant strain appears moderately thicker than the wild type. Interestingly, the mutant strain exhibited abnormally large nuclei compared to the wild type (**Figures 10D–F** and **Supplementary Table 9**). These images suggest that the mutant strain may undergo DNA replication, but not nuclear division. In wild-type strains, free nuclear division occurs prior to internal segmentation and endospore formation (Huppert et al., 1982). This phenotypic evidence implies that gene deletion impairs both cell wall and internal remodeling at this time point.

DISCUSSION

For this study, the transcriptional and volatile profile of a non-endosporulating attenuated strain, Δ*cts2*/Δ*ard1*/Δ*cts3*, of *Coccidioides posadasii* was compared to its pathogenic parent strain, C735. The mutant strain develops into non-rupturing spherules and is incapable of causing disease in a murine model (Xue et al., 2009). This phenotype was obtained by deletion of two chitinase genes (*cts2*, *cts3*), which were targeted due to their increased expression in spherules. Interestingly, the investigation revealed that independent mutants Δ*cts2*/Δ*ard1* and Δ*cts3* demonstrated delayed endosporulation and could still cause disease. Attenuation was achieved only during the removal of both chitinase genes (Xue et al., 2009). Chitinases are responsible for remodeling the cell wall; however, why the combination results in attenuated spherules is not understood. Consequently, the gene regulation related to endospore formation, spherule

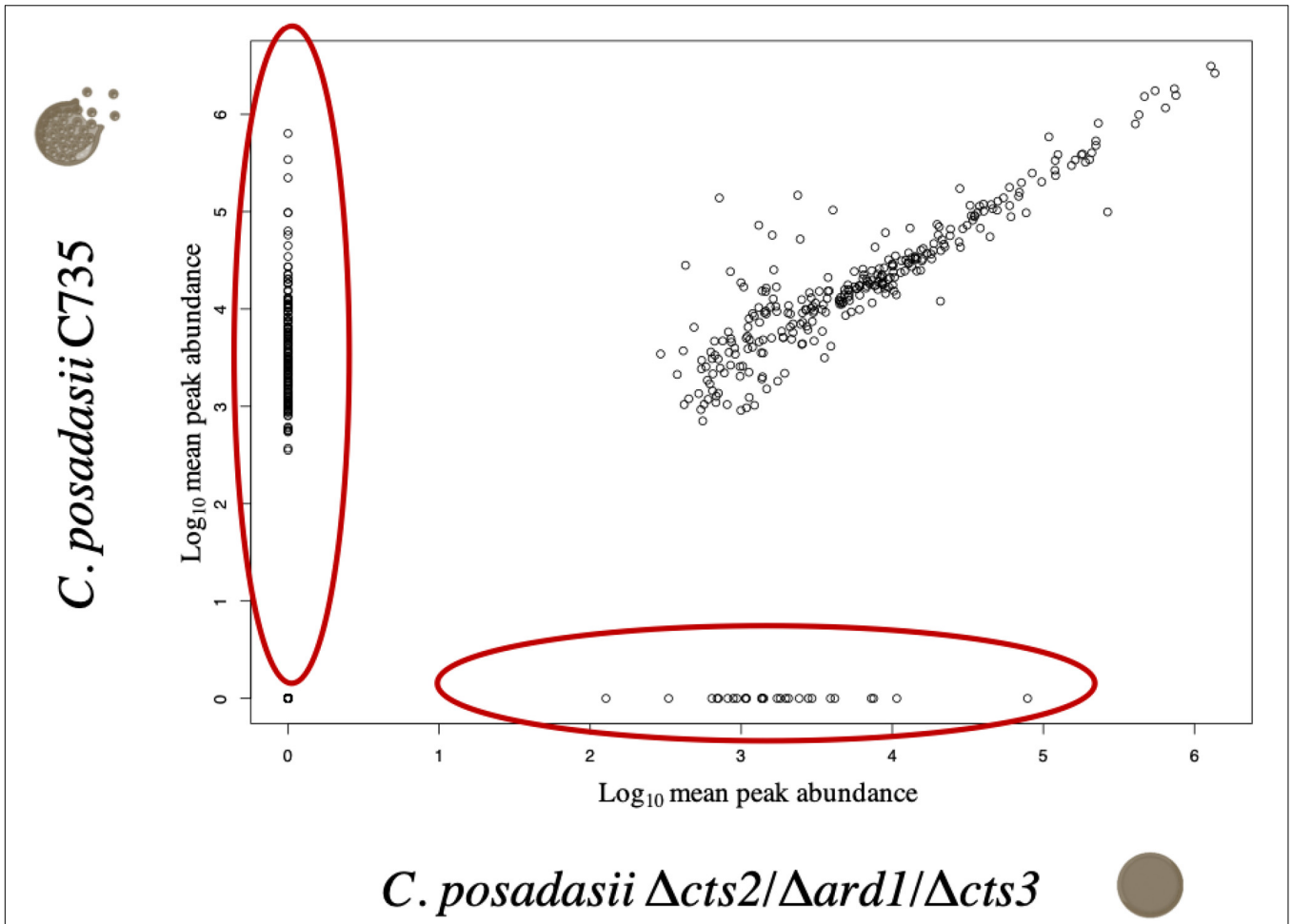

FIGURE 9 | Comparisons of the volatile metabolomes of 96-h spherules for *C. posadasii* strain C735 and attenuated mutant (Δ*cts2/*Δ*ard1/*Δ*cts3*). Individual circles represent log-transformed mean peak abundance across three biological replicates. Compounds in large red oval on the y-axis are the 130 significant VOCs uniquely produced by C735 (n = 40; FDR $p < 0.05$) or uniquely consumed by Δ*cts2/*Δ*ard1/*Δ*cts3* (n = 90; FDR $p < 0.05$). Compounds in large red oval on the x-axis are the 28 VOCs uniquely consumed by C735 (n = 12; $p < 0.05$) or uniquely produced by Δ*cts2/*Δ*ard1/*Δ*cts3* (n = 16; $p < 0.05$).

remodeling and subsequently disease establishment might be elucidated through comparing the wild-type and mutant.

We observed 252 gene transcripts that are evolutionarily conserved and improperly expressed by the mutant strain. Of these, 18 are improperly down-regulated and 19 improperly up-regulated when comparing the mutant lifecycle (96-h spherules to mycelia) to the wild-type lifecycle (96-h spherules to mycelia). Additionally, 215 conserved transcripts (out of 222) are only up-regulated twofold or more in wild-type spherules (**Figure 3**). We can take advantage of these universal fungal adaptations to predict how these genes function in *Coccidioides*. For instance, upon exposure to the host environment, dimorphic fungi must initiate niche specific morphogenesis (Sil and Andrianopoulos, 2014; Boyce and Andrianopoulos, 2015; Van Dyke et al., 2019). While all fungal pathogens face the challenge of acquiring nutrients and avoiding immune system detection, the cell wall serves as an interface between the fungal cell and host milieu. The interaction between the cell wall, cell membrane, and mitochondrial function is key to this intricate response, which we also observed at a transcriptional level in our study (Verma et al., 2018; Koch and Traven, 2019).

One gene showing improper response in the mutant strain is a predicted Hsp9/Hsp12 family heat shock protein. This highly conserved gene is expressed during stress response, changes in pH, and may increase cell membrane stability (Sheth et al., 2008; Welker et al., 2010; Fu et al., 2012). Importantly, heat shock proteins have been shown to be up-regulated in other fungal pathogens such as *Cryptococcus neoformans* at low temperatures and *Candida albicans* at high temperatures (Steen et al., 2003; Fu et al., 2012). The function of this gene is unknown in *Coccidioides;* however, the abnormal down-regulation in the mutant strain could indicate that Hsp9/Hsp12 are chaperones for endospore related proteins, or increase the cell membrane stability prior to rupture.

Upon exposure to the mammalian environment (often the respiratory system), fungal pathogens must utilize potentially different carbon or nitrogen sources while competing with host cells for limited co-factors such as iron and copper

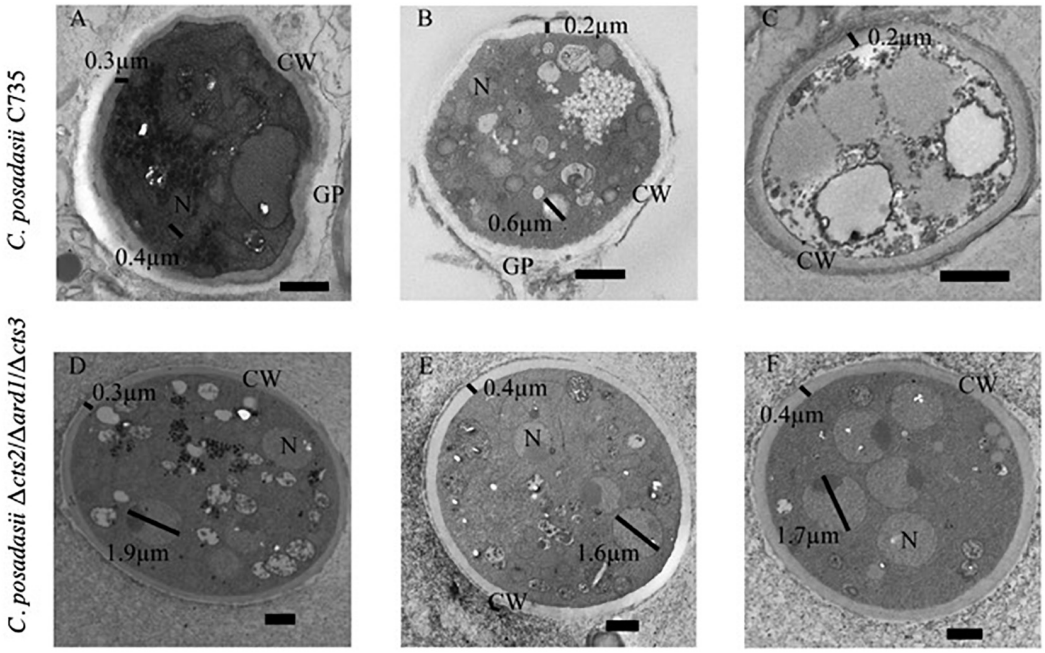

FIGURE 10 | Transmission Electron Microscopy Images of *C. posadasii* strain C735 and ∆cts2/∆ard1/∆cts3 spherules. Wild-type spherule with thick, irregular cell wall (CW) and sloughing glycoprotein (GP) shell that are visible after 96-h development *in vitro* **(A)**. Small nuclei (N), irregular cell wall, sloughing glycoprotein were consistently visible in wild-type spherules **(B)**. Cross-walls indicating the possible commencement of endospore formation were visible in wild-type spherules after 96-h development **(C)** but not in the mutant. In general, the Δ*cts2/*Δ*ard1/*Δ*cts3* cell wall is rounder and more consistent **(D)** than the wild type. Glycoprotein coating is less visible in mutant spherules **(E)** than in wild type. Nuclei are larger, more distinct and visible in spherules of the mutant **(F)** than of the wild type. Black bars in the bottom right corner of images represent 1 μm.

(Marzluf, 1997; Chung et al., 2012; Braunsdorf et al., 2016; Bairwa et al., 2017). In many pathogenic fungi, genes related to trehalose biosynthesis have been implicated as critical in metabolism and stress response (Thammahong et al., 2017). In *Aspergillus,* deletion of tspA/B delayed germination and decreased virulence (Al-Bader et al., 2010). Interestingly, the authors observed thinner cell walls in tspA/B mutants, in contrast to our TEM observations. The Δ*cts2/*Δ*ard1/*Δ*cts3* strain down regulated trehalose-phosphotase transcripts where as they are up-regulated in the wild-type expression profile (**Figure 4**). This suggests that the trehalose-related pathways may affect the cell wall in both *Aspergillus* and *Coccidioides* but through different mechanisms. Another key nutrient, nitrogen, may be readily available in the environment and can become scarce inside the host. *A. fumigatus* senses nitrogen availability via a mitogen-activated protein (MAP) kinase pathway (Xue et al., 2004). Additionally, transcription factors (TFs) such as the highly conserved class of GATA TF's activate alternative nitrogen processing pathways in the absence of preferred sources. These regulators are often highly expressed in both *in vitro* and *in vivo* infection conditions and are linked to fungal virulence (Oberegger et al., 2001; Gauthier et al., 2010; Lee et al., 2011; Chung et al., 2012; Hwang et al., 2012). In *C. neoformans*, the Gat1 TF regulates capsule formation (Lee et al., 2011). This same class of transcription factors has been shown to be essential for virulence in *C. albicans* (Limjindaporn et al., 2003). The GATA class of TFs are also associated with stimulating iron acquisition and host phase transition in *Blastomyces dermatitidis* (Gauthier et al., 2010). In our study, this GATA ortholog is improperly down-regulated compared to the pattern observed in the wild type (**Figure 4**).

In this study, metabolic dissimilarities were also detected in the uniquely produced and consumed volatile compounds between the parent and mutant strain. The Δ*cts2/*Δ*ard1/*Δ*cts3* demonstrated a fivefold consumption versus production of compounds that was not observed in the parent strain, indicating improper scavenging of resources; whereas, in the wild-type strain we observe the unique consumption of compound classes such as nitrogen containing, hydrocarbons, ethers, and alcohols. In addition, our RNAseq data demonstrate that transcripts for nutrient assimilation strategies specific to nitrogen and iron are up-regulated in 96-h wild-type spherules, but not in the mutant strain. Together these data implicate nitrogen and metal co-factors as necessary components during spherule structural remodeling to create or release endospores. Nitrogen containing functional groups were also among the uniquely produced VOCs in wild-type spherules. Previous studies have shown that rupturing spherules release ammonia (Wise et al., 2013) and urease (Mirbod-Donovan et al., 2006), which contribute to host damage and virulence. Further, it has been demonstrated that extracellular concentrations of ammonia begin to accumulate at 96 h peaking at 120 h, the time point just before spherule rupture (Wise et al., 2013). The lack of transcript abundance in the non-rupturing mutant highlights the importance of

nitrogen recycling at this time point and subsequently disease establishment upon rupture.

Another crucial step in disease establishment is the ability of fungal organisms to avoid immune system detection and clearing (Erwig and Gow, 2016). Host cells respond to pathogen associated recognition patterns (PAMPs) located on the fungal cell wall (Latge, 2010). Consequently, the fungal cell wall is remodeled, a process controlled by the protein kinase c pathway (Munro et al., 2007; Gow et al., 2017; Koch and Traven, 2019). The masking of exposed ß-glucan, a key PAMP, is associated with cAMP-protein kinase A pathway (cAMP/PKA). This pathway is triggered by hypoxic conditions due to influx of immune cells or inflamed tissue (Pradhan et al., 2018; Duvenage et al., 2019). In *C. albicans,* chemical inhibition of respiration decreased ß-glucan masking and cell wall integrity (Pradhan et al., 2018; Duvenage et al., 2019) thus increasing immune system recognition and phagocytosis. In our data, mitochondria-associated genes, oxidation-reduction, cytochrome P450, and FAD binding proteins were all significantly up-regulated in the wild-type spherules compared to mycelia, but not in the same comparison for the mutant (**Table 1** and **Supplementary Table 6**). We also observed more peroxide compounds in the VOCs produced by wild-type spherules versus the mutant. We suggest this is related to the deletion of *cts2*/*cts3* which impairs chitin remodeling and alters cell wall composition. This subsequently alters normal cell membrane communication and associated mitochondrial response.

We have previously shown that the exterior surface of these attenuated spherules is strikingly different to wild type at high resolution (Mead et al., 2019). In this study, we observed reduction in glycoprotein sloughing and a slight decrease in cell wall thickness in the mutant. The Δ*cts2*/Δ*ard1*/Δ*cts3* mutant was originally developed as a vaccine candidate and provides full protection to wild-type challenge in a murine model (Xue et al., 2009). Host protection is accomplished by a mixed Th1, Th2, and Th17 immune response (Xue et al., 2009; Hung et al., 2011). This is interesting given that previous studies have shown that the cell wall associated ß-glucan receptor dectin-1 is required for resistance to coccidioidomycosis. This receptor stimulates proinflammatory infiltrates through a Th1 and Th17 immune response in mice (Viriyakosol et al., 2005, 2013). To our knowledge, the ß-glucan composition of the attenuated strain has not been characterized. Our results suggest that deletion of the Δ*cts2*/Δ*ard1*/Δ*cts3* changes the cell wall structure which might alter ß-glucan masking. Our TEM images from this study further support this idea.

Lastly, in this study, we identified 14 *Coccidioides*-specific genes that are either inactive or improperly expressed by the mutant strain at this crucial time point. Seven were up-regulated twofold or higher in the wild-type 96-h spherules compared to mycelia, and but not in mutant spherules compared to mutant mycelia (**Figure 3**, **Table 3** and **Supplementary Table 6**). We identified conserved architecture for some of these proteins. Based on this, these unknown proteins might be involved in kinase cascade activation or endonuclease activity. Furthermore, two genes were found to be inactive in the mutant spherules but active in wild-type spherules and expressed in host tissue. The close genomic proximity of these two genes suggests that they may be co-regulated in a *Coccidioides*-specific manner (**Figure 7**). We hypothesize that these two genes are crucial for spherule morphogenesis and endospore formation, which is necessary for proliferation within the host. In future studies, we hope to elucidate the role of these two *Coccidioides*-specific genes.

In summary, we compare the transcriptional and metabolic profiles of *C. posadasii* C735 and the attenuated mutant, Δ*cts2*/Δ*ard1*/Δ*cts3*. We reveal significant changes in both *Coccidioides*-specific transcripts involved in endospore formation, and those that are conserved among many fungal pathogens. We identified approximately 280 transcripts that are inappropriately regulated in the mutant strain with 14 specific to the *Coccidioides* genus. With the increase of fungal infections and emerging novel species, we suggest that comparing gene expression between a pathogenic parent and an attenuated mutant could be used to link phenotypic traits of interest to transcript specific pathways in many fungal systems. While each species may employ unique strategies, the challenges of survival within the mammalian host are shared. Attenuation of virulence can be achieved via several mechanisms; however, a shared pattern of transcriptional regulation may elucidate crucial conserved pathways for virulence, and suggest novel targets for drug development and vaccines.

MATERIALS AND METHODS

Fungal Isolates and Growth Conditions

Isolates: The wild-type strain utilized was *C. posadasii* isolate C735 (ATCC 96335). The attenuated strain was derived from the clinical isolate C735 and was obtained through Biodefense and Emerging Infections (BEI Resources) repository, (NIAID, NIH: *Coccidioides posadasii*, Δ*cts2*/Δ*ard1*/Δ*cts3*, NR-166). *C. posadasii* isolates C735 and Silveira were also used in the pulmonary infections. All wild-type *Coccidioides* spp. strains are grown under biosafety level 3 containment.

Saprobic growth conditions: Arthroconidia were pipetted into a 250 ml vented baffle flask containing 50 ml of 2 × glucose yeast extract (2 × GYE; 2% glucose (VWR), 1% yeast extract (Difco) on a shaking incubator (Gene-Mate Orbital Shaker Mini) at 30°C for 96 h. Samples were grown in triplicate. Sterile media controls were treated in the same manner.

Parasitic growth conditions: Arthroconidia were pipetted into vented baffled flasks (VWR) on a shaking incubator (GeneMate Orbital Shaker Mini) at 90 rpm, incubated at 10% CO_2, 39°C, at ambient oxygen (ThermoForma Series II water jacketed CO_2/O_2 incubator) in chemically defined modified Converse media (ammonium acetate 0.016 M (Sigma-Aldrich), KH_2PO_4 0.0037 M (Amresco), K_2HPO_4 0.003 M (Amresco), $MgSO_4$ 0.0016 M (Amresco), $ZnSO_4$ 1.25×10^{-5} M (Fisher Scientific), NaCl 2.4×10^{-4} M (Fisher Scientific), $CaCl_2$ 2.04×10^{-5} M (Amresco), $NaHCO_3$ $0.1.43 \times 10^{-4}$ M (Sigma-Aldrich),0.05% Tamol® (Dupont, purchased from Northeastern Laboratories), 4% glucose (Amresco), 0.5% N-Z amine (Sigma-Aldrich) was made as previously reported and stored at room temperature

(Converse, 1955; Mead et al., 2019). Samples were grown in triplicate. Sterile media controls were treated in the same manner.

Mice: Female ICR (CD-1®) outbred mice (Envigo) 6–8 weeks of age were used for these studies. Mice were housed according to NIH guidelines for housing and care in a biosafety level 3 animal laboratory. All procedures were approved by the Institutional Animal Care and Use Committee (protocol number 16-009) of Northern Arizona University.

Pulmonary coccidioidal infection: ICR mice were anesthetized with ketamine-xylene (80/8 mg/kg) and intranasally inoculated with 1×10^6 of arthroconidia of *C. posadasii* strains C735 or Silveira suspended in 30 µl phosphate-buffered saline (PBS) as described previously (Shubitz et al., 2008). Two mice from each infection group (C735 and Silveira) were sacrificed on day four. The right lobe of the lung was harvested and flash frozen in liquid nitrogen.

In vitro Expression

Total RNA: Spherule cell pellets were collected by filtering cultures through 70 µm filters followed by centrifugation at 12,000 × *g* for 15 min at 4°C. Mycelia cultures were centrifuged at 12,000 × *g* for 15 min at 4°C. These pellets were suspended in 1 mL of Trisure (Bioline) and homogenized (Beadbug) with 1.4 mm glass beads for four 30 s cycles at max speed. The tubes were stored on ice between cycles for 5 min. Next, the tubes were inverted at room temperature for 5 min followed by the addition of 1/5 the volume of chloroform. After inverting the mixture for 2 min, the cell debris was pelleted by centrifugation at max speed for 15 min at 4°C. The aqueous phase was collected and placed in 500 µl isopropanol and gently mix at room temperature for 10 min. Nucleic acid was pelleted at max speed for 10 min at 4°C. This pellet was washed with 75% ethanol twice and resuspended in RNAase free water. Total RNA quality was checked using the RNA 6000 nanochip (Agilent).

RNA sequencing: mRNA was isolated using the Magnetic mRNA Isolation Kit (New England BioLabs) according to the manufacturers guidelines and prepared for sequencing using NEbNext Ultra Directional Library Prep Kit (New England Biolabs) according to the manufacturer's guidelines. Stranded, paired-end sequencing was performed using a MiSeq 600-cycle V3 kit (Illumina) with six libraries on a single flow cell.

In vitro Differential Expression Analysis

Raw reads for *C. posadasii* C735 from the previously published Winston data set were obtained from NCBI short read archive using accession number SRA054882. These raw reads and the newly generated mutant reads were aligned to the reference genome, *C. posadasii* C735 SOWgp (GCA_000151335.1) using TopHat2 (Trapnell et al., 2012; Kim et al., 2013). Gene expression quantification and statistical comparison was completed with the Cufflinks package (Trapnell et al., 2012; Kim et al., 2013). These data were visualized using the Cummerbund Package for R (Trapnell et al., 2012; Goff et al., 2019). Analysis was focused on genes that passed the Cufflinks quality filter for sufficient reads that were differentially expressed up or down by twofold change, and after Benjamini-Hochberg False Discovery Rate (FDR) correction were statistically significant ($p < 0.05$) (Benjamini and Hochberg, 1995). Gene product descriptions were obtained from FungiDB (Stajich et al., 2012; Basenko et al., 2018). When *Coccidioides* genes were classified as hypothetical or predicted proteins, ortholog functions were queried using the FungiDB, OrthoMC, and Interpro databases (Li et al., 2003). We used orthologs from *Aspergillus niger* (plant pathogen) and *A. fumigatus* (human pathogen) to investigate significantly enriched gene ontology (GO) terms (Ashburner et al., 2000; Carbon et al., 2009). For the full data set see **Supplementary Table 1**.

In silico predictions: When gene orthologs were *Coccidioides*-specific three prediction programs; NCBI Classifier, EggNOG Mapper, and InterProScan were utilized to predict conserved protein domains. The amino acid sequences were obtained through the FungiDB website. These sequences were submitted to the NCBI, Interproscan and EggNOG Mapper online servers using default parameters. EggNOG Mapper was restricted to the Fungal Kingdom (Jones et al., 2014; Huerta-Cepas et al., 2016, 2017, 2019; Marchler-Bauer et al., 2017; Mitchell et al., 2019). All three predictions are reported in **Supplementary Table 6** and **Table 3**.

In vivo Expression

Total RNA: Briefly, for mouse lungs, 30 mg frozen tissue was mixed with 0.5 mm glass beads (Sigma-Aldrich) suspended in 1 ml of Trizol reagent (ThermoFisher Scientific) and homogenized (Beadbug) six times, 30 s per round. Tubes were cooled on ice for 30 s between rounds. Next, 1/5 the volume chloroform was added and mixed well, incubated for 2 min, and homogenized for 15 s. Samples were centrifuged 12,000 × *g* for 15 min at 4°C. The aqueous layer was collected and mixed with 500 µl isopropanol for 10 min and pipetted onto RNeasy spin columns (Qiagen). Columns were centrifuged 10,000 rpm for 1 min, flow through discarded, and washed twice with RPE buffer. Columns were moved to a fresh RNase free 1.5 ml tube and 100 µl RNase free water was added and centrifuged for 1 min and centrifuged to collect nucleic acid. Ten units of RNasin™ Plus RNase Inhibitor (Promega) (1 µ/µl) was added. Extraction method based on (Chung et al., 2014).

RNA purification: Purified total RNA quantities of all samples, including *in vitro,* were initially measured using the NanoDrop 1000 Spectrophotometer and verified with the Qubit 2.0 Fluorometric RNA HS assay (Thermo Fisher Scientific). RNA quality was assessed using the Agilent Standard Sensitivity RNA assay with the Fragment Analyzer Automated CE system (Advanced Analytical Technologies). Total RNA extracted from *in vitro Coccidioides* spherules was purified following manufacturer protocol using the RNA Clean & Concentrator-5 kit (Zymo Research) and run through the same quality checks (QC). Purification, additional QC and nCounter gene expression services were performed by the University of Arizona Genetics Core (UAGC, Tucson, AZ, United States).

NanoString Gene Expression

Total RNA from *in vivo* samples (100–200 ng) and *in vitro* samples (1–200 ng, depending on assay protocol) was used to analyze gene expression changes using nCounter FLEX Analysis

System and nSolver 4.0 software (NanoString Technologies Inc.). *Coccidioides* target counts were obtained using a custom panel targeting endogenous *Coccidioides* genes and five internal reference controls, was designed using NanoString Technologies services (NanoString Technologies) and performed by UAGC.

Based on RNA integrity, 200 ng purified total RNA was initially hybridized to reporter and capture barcoded probe sets using the NanoString assay XT protocol at 65°C for 19 h. Samples were processed on an nCounter FLEX Analysis system (NanoString Technologies Inc.). Purification and binding of the hybridized probes to the optical cartridge was performed on the nCounter Prep Station using high sensitivity settings, and the cartridge was scanned on the nCounter Digital Analyzer using Field of View setting (FOV) of 555. Raw counts from each gene were imported into the nSolver Analysis Software and normalized against background and housekeeping genes. Data were normalized using internal positive and negative controls and selected housekeeping genes (CIMG_01599, CIMG_10083, and CIMG_12902) and overall assay performance was assessed through evaluation of built-in positive controls.

After initial results from the *Coccidioides* panel, the *Coccidioides* panel sample set was repeated using the NanoString Low RNA Input protocol (NanoString Technologies Inc.) for cDNA synthesis and multiplexed targeted enrichment (MTE) of *Coccidioides* targets. Depending on strain and previous results, 10–100 ng total inoculated mouse RNA or 1 ng *in vitro Coccidioides* RNA was cDNA-converted and amplified. This was done using custom-designed cocci-specific MTE oligonucleotide pool [Integrated DNA Technologies (IDT)] for 8 cycles in an MJ Research PTC-225 Peltier Thermal Cycler (Bio-Rad) following NanoString Low RNA Input protocol cycling conditions.

In vitro Volatile Metabolome

Sample Collection: Spherules of C735 and the attenuated mutant strain and sterile media controls were pelleted at 12,000 × *g* at 4°C for 10 min, the supernatant was placed in a 0.22 μm spin filter and centrifuged at 4,000 rpm for 4 min. The filtrate was stored at −80°C until volatile metabolomics analysis. The samples were allowed to thaw at 4°C overnight, and then 2 ml were transferred and sealed into sterilized 10 ml GC headspace vials with PTFE/silicone septum screw caps. Three biological replicates each of wild type, mutant, and Converse media blanks were prepared. All samples were stored for up to 10 days at 4°C until analyzed.

Volatile metabolite sampling: Measurements were performed using a Gerstel Multipurpose Sampler directed by Maestro software. Two-dimensional gas chromatography-time-of-flight mass spectrometry (GC × GC–TOFMS) was performed using a LECO Pegasus 4D and Agilent 7890 GC with chromatographic, mass spectrometric, and peak detection parameters provided in **Supplementary Table 10**. An external alkane standards mixture (C_8 – C_{20}; Sigma-Aldrich), was sampled multiple times for use in determining retention indices (RI). The injection, chromatographic, and mass spectrometric methods for analyzing the alkane standards were the same as for the samples. All conditions and parameters are listed in **Supplementary Table 10**.

Volatile Compound Analysis

Compound Processing: Data collection, processing, and alignment were performed using ChromaTOF software version 4.71 with the Statistical Compare package (Leco Corp.), using parameters listed in **Supplementary Table 10**. Peaks were identified by forward and reverse searches of the NIST 2011 mass spectral library. Peaks were assigned a putative identification based on mass spectral similarity and retention index (RI) data, and the confidence of those identifications are indicated by assigning levels 1–4 (with 2 being the highest in this study) (Sumner et al., 2007). Peaks with a level 2 identification were named, and were identified based on ≥800 mass spectral match by a forward and reverse search of the NIST 2011 mass spectral library and RI that are consistent with the midpolar Rxi-624Sil stationary phase, as previously described (Bean et al., 2016), but using an RI range of 0–43%, which was empirically determined by comparing the Rxi-624Sil RIs for Grob mix standards to published polar and non-polar values. Level 2 and 3 compounds were assigned to chemical functional groups based upon characteristic mass spectral fragmentation patterns and second dimension retention times. Level 4 compounds have mass spectral matches <600 and are reported as unknowns.

Volatile Statistical Analysis

Before statistical analyses, compounds eluting prior to 358 s (acetone retention time) and siloxanes (i.e., chromatographic artifacts) were removed from the peak table. Peaks that were present in only one of the three biological replicates were imputed to zero for all three replicates. Peaks that were present in two out of three biological replicates were imputed to half of the minimum value of the two other biological replicates. The relative abundance of compounds across chromatograms was normalized using probabilistic quotient normalization (PQN) (Dieterle et al., 2006) and $\log_{10}$ transformed in R version 3.4.3. Intraclass correlation coefficients (ICCs) were calculated, using R ICC package version 2.3.0, and peaks with an ICC < 0.9 were not further processed. Analytes were retained for further analysis if they were present in one strain but absent in media and the other strain (uniquely produced) or if they were present in media and one strain but absent in the other strain (uniquely consumed). Wilcoxon Rank Sum test with Benjamini and Hotchberg FDR correction was performed with $\alpha = 0.05$, using R stats package version 3.5.3.

Transmission Electron Microscopy

After 96 h of growth *C. posadasii* strain C735 and Δ*cts2*/Δ*ard1*/Δ*cts3* spherules were collected by filtering cultures through 70 μm filters (Corning) and centrifuged at 12,000 × *g* for 15 min at 4°C. Pellets were re-suspended in 1% formalin for 72 h. Following fixation, the cells were centrifuged at 10,000 × *g* for 5 min and washed in PBS [Electron Microscopy Sciences, (EMS)] for 10 min, three times. The pellet was then fixed in 2.5% glutaraldehyde (EMS) in PBS overnight at 4°C. Cells were pelleted and washed in PBS for 10 min, three times. Next, cells were suspended in 2% sodium alginate, dropped into cold calcium chloride, and then chilled at 4°C for 1 h to

form concentrated beads. The chilled cells were washed in PBS for 10 min, twice. Osmium tetroxide, 1% in H_2O (EMS) was added to the sodium alginate beads and left for 30 min at room temperature. The beads were washed in water for 10 min, three times. These beads were subjected to a dehydration series; 50% ethanol for 10 min, 70% ethanol overnight at 4°C, in 95% ethanol for 10 min and 100% ethanol for 10 min, three times. The beads were then infiltrated with a 50:50 mixture of 100% ethanol and Spurrs' resin (EMS) for 3 h on a rotator followed by a 3:1 ratio of Spurrs' resin to 100% ethanol overnight. The beads were subjected to several changes of 100% Spurrs' resin over a 2 day period on a rotatator before being embedded in BEEM capsules and cured at 70°C for 3 days in an oven. The resulting resin blocks of both wild-type and the attenuated mutant spherules were then trimmed using a microtome and razor blade. Thick sections were cut and stained with toluidine blue to confirm spherule location before 50 nm thin sections were cut and placed on 200 mesh copper grids. Grids were left to dry and then post-stained with Uranyless (EMS) for 30 min and lead citrate (EMS) for 12 min and left to dry. Sections on grids were then analyzed with a JEOL 1200 EX-II TEM at 60 kV. Images were taken from all five blocks and from deep within the beads as verified with thick sections in order to ensure accurate representation of both wild type and the attenuated mutant.

DATA AVAILABILITY STATEMENT

The datasets generated for this study have been deposited at NCBI using project accession number PRJNA608815, https://www.ncbi.nlm.nih.gov/sra/PRJNA608815.

ETHICS STATEMENT

The animal study was reviewed and approved by Northern Arizona University Institutional Animal Care and Use Committee.

AUTHOR CONTRIBUTIONS

HM analyzed data and wrote manuscript, performed differential expression data analysis. HM performed the *in vitro* experiments with assistance from KM. CR assisted HM with raw read analysis. MV and HM performed *in vivo* RNA extractions and MV performed NanoString Analysis. EH performed volatile collection and analysis with supervision and support from HB. KL and AF processed samples and captured TEM images. MV, CR, HB, BB, and JS provided manuscript edits. BB funded, supervised and advised throughout the study. All authors read and approved of the manuscript.

FUNDING

Funding to this support this work was provided to HM by the Northern Arizona University Hooper Undergraduate Research Grant (HURA), to BB by NIH/NIAID award R21 AI28536 and the Arizona Biomedical Research Commission (ABRC) award ADHS14-082975, and to HB by the ABRC award ADHS18-198861.

ACKNOWLEDGMENTS

The authors would like to thank Mark Voorhies, Ph.D. for his insight and expertise. The authors also would like to thank Chiung-Yu Hung, Ph.D. and Garry Cole, Ph.D. for creation of the Δ*cts2*/Δ*ard1*/Δ*cts3* and depositing at BEI Resources. The strain was obtained through BEI resources, NIAID/NIH: *Coccidioides posadasii*, Δcts2/Δard1/Δcts3, NR-166.

SUPPLEMENTARY MATERIAL

The Supplementary Material for this article can be found online at: https://www.frontiersin.org/articles/10.3389/fgene.2020.00483/full#supplementary-material

REFERENCES

Al-Bader, N., Vanier, G., Liu, H., Gravelat, F. N., Urb, M., Hoareau, C. M., et al. (2010). Role of trehalose biosynthesis in *Aspergillus fumigatus* development, stress response, and virulence. *Infect. Immun.* 78, 3007–3018. doi: 10.1128/IAI.00813-09

Alvarado, P., Teixeira, M. M., Andrews, L., Fernandez, A., Santander, G., Doyle, A., et al. (2018). Detection of *Coccidioides posadasii* from xerophytic environments in Venezuela reveals risk of naturally acquired coccidioidomycosis infections. *Emerg. Microbes Infect.* 7:46. doi: 10.1038/s41426-018-0049-6

Ampel, N. M. (2015). The treatment of coccidioidomycosis. *Rev. Inst. Med. Trop. Sao Paulo* 57(Suppl. 19), 51–56. doi: 10.1590/S0036-46652015000700010

Ashburner, M., Ball, C. A., Blake, J. A., Botstein, D., Butler, H., Cherry, J. M., et al. (2000). Gene ontology: tool for the unification of biology. The gene ontology consortium. *Nat. Genet.* 25, 25–29. doi: 10.1038/75556

Attarian, R., Hu, G., Sanchez-Leon, E., Caza, M., Croll, D., Do, E., et al. (2018). The monothiol glutaredoxin Grx4 regulates iron homeostasis and virulence in *Cryptococcus neoformans*. *mBio* 9:e02377-18. doi: 10.1128/mBio.02377-18

Bairwa, G., Hee Jung, W., and Kronstad, J. W. (2017). Iron acquisition in fungal pathogens of humans. *Metallomics* 9, 215–227. doi: 10.1039/c6mt00301j

Barker, B. M., Tabor, J. A., Shubitz, L. F., Perrill, R., and Orbach, M. J. (2012). Detection and phylogenetic analysis of *Coccidioides posadasii* in arizona soil samples. *Fungal Ecol.* 5, 163–176. doi: 10.1016/j.funeco.2011.07.010

Basenko, E. Y., Pulman, J. A., Shanmugasundram, A., Harb, O. S., Crouch, K., Starns, D., et al. (2018). FungiDB: an integrated bioinformatic resource for fungi and oomycetes. *J. Fungi (Basel)* 4:39. doi: 10.3390/jof4010039

Bean, H. D., Rees, C. A., and Hill, J. E. (2016). Comparative analysis of the volatile metabolomes of *Pseudomonas aeruginosa* clinical isolates. *J. Breath Res.* 10:047102. doi: 10.1088/1752-7155/10/4/047102

Benjamini, Y., and Hochberg, Y. (1995). Controlling the false discovery rate – a practical and powerful approach to multiple testing. *J. R. Stat. Soc. B* 57, 289–300.

Boyce, K. J., and Andrianopoulos, A. (2015). Fungal dimorphism: the switch from hyphae to yeast is a specialized morphogenetic adaptation allowing colonization of a host. *FEMS Microbiol. Rev.* 39, 797–811. doi: 10.1093/femsre/fuv035

Braunsdorf, C., Mailander-Sanchez, D., and Schaller, M. (2016). Fungal sensing of host environment. *Cell Microbiol.* 18, 1188–1200. doi: 10.1111/cmi.12610

Briza, P., Eckerstorfer, M., and Breitenbach, M. (1994). The sporulation-specific enzymes encoded by the DIT1 and DIT2 genes catalyze a two-step reaction leading to a soluble LL-dityrosine-containing precursor of the yeast spore wall. *Proc. Natl. Acad. Sci. U.S.A.* 91, 4524–4528. doi: 10.1073/pnas.91.10.4524

Brown, G. D., Denning, D. W., Gow, N. A., Levitz, S. M., Netea, M. G., and White, T. C. (2012). Hidden killers: human fungal infections. *Sci. Transl. Med.* 4:165rv113. doi: 10.1126/scitranslmed.3004404

Carbon, S., Ireland, A., Mungall, C. J., Shu, S., Marshall, B., Lewis, S., et al. (2009). AmiGO: online access to ontology and annotation data. *Bioinformatics* 25, 288–289. doi: 10.1093/bioinformatics/btn615

Chiller, T. (2019). "Overview of endemic mycoses," in *Vaccine Strategies for Endemic Fungal Pathogens* (Rockville, MD: NIAID).

Chung, D., Barker, B. M., Carey, C. C., Merriman, B., Werner, E. R., Lechner, B. E., et al. (2014). ChIP-seq and in vivo transcriptome analyses of the *Aspergillus fumigatus* SREBP SrbA reveals a new regulator of the fungal hypoxia response and virulence. *PLoS Pathog.* 10:e1004487. doi: 10.1371/journal.ppat.1004487

Chung, D., Haas, H., and Cramer, R. A. (2012). Coordination of hypoxia adaptation and iron homeostasis in human pathogenic fungi. *Front. Microbiol.* 3:381. doi: 10.3389/fmicb.2012.00381

Cole, G. T., and Hung, C. Y. (2001). The parasitic cell wall of *Coccidioides immitis*. *Med. Mycol.* 39(Suppl. 1), 31–40.

Converse, J. L. (1955). Growth of spherules of *Coccidioides immitis* in a chemically defined liquid medium. *Proc. Soc. Exp. Biol. Med.* 90, 709–711. doi: 10.3181/00379727-90-22144

Dieterle, F., Ross, A., Schlotterbeck, G., and Senn, H. (2006). Probabilistic quotient normalization as robust method to account for dilution of complex biological mixtures. Application in 1H NMR metabonomics. *Anal. Chem.* 78, 4281–4290. doi: 10.1021/ac051632c

Drutz, D. J., and Huppert, M. (1983). Coccidioidomycosis: factors affecting the host-parasite interaction. *J. Infect. Dis.* 147, 372–390. doi: 10.1093/infdis/147.3.372

Duvenage, L., Walker, L. A., Bojarczuk, A., Johnston, S. A., MacCallum, D. M., Munro, C. A., et al. (2019). Inhibition of classical and alternative modes of respiration in *Candida albicans* leads to cell wall remodeling and increased macrophage recognition. *mBio* 10:e02535-18. doi: 10.1128/mBio.02535-18

Erwig, L. P., and Gow, N. A. (2016). Interactions of fungal pathogens with phagocytes. *Nat. Rev. Microbiol.* 14, 163–176. doi: 10.1038/nrmicro.2015.21

Freedman, M., Jackson, B. R., McCotter, O., and Benedict, K. (2018). Coccidioidomycosis outbreaks, United States and worldwide, 1940-2015. *Emerg. Infect. Dis.* 24, 417–423. doi: 10.3201/eid2403.170623

Fu, M. S., De Sordi, L., and Muhlschlegel, F. A. (2012). Functional characterization of the small heat shock protein Hsp12p from *Candida albicans*. *PLoS One* 7:e42894. doi: 10.1371/journal.pone.0042894

Galgiani, J. N., Ampel, N. M., Blair, J. E., Catanzaro, A., Geertsma, F., Hoover, S. E., et al. (2016). 2016 infectious diseases society of America (IDSA) clinical practice guideline for the treatment of coccidioidomycosis. *Clin. Infect. Dis.* 63, 717–722. doi: 10.1093/cid/ciw538

Galgiani, J. N., Ampel, N. M., Catanzaro, A., Johnson, R. H., Stevens, D. A., and Williams, P. L. (2000). Practice guidelines for the treatment of coccidioidomycosis. *Clin. Infect. Dis.* 30, 658–661. doi: 10.1086/313747

Gauthier, G. M., Sullivan, T. D., Gallardo, S. S., Brandhorst, T. T., Vanden Wymelenberg, A. J., Cuomo, C. A., et al. (2010). SREB, a GATA transcription factor that directs disparate fates in *Blastomyces dermatitidis* including morphogenesis and siderophore biosynthesis. *PLoS Pathog.* 6:e1000846. doi: 10.1371/journal.ppat.1000846

Goff, L., Trapnell, C., and Kelley, D. (2019). *Cummerbund: Analysis, Exploration, Manipulation, and Visualization of Cufflinks High-Throughput Sequencing Data*. Burlington, MA: ScienceOpen, Inc.

Gow, N. A. R., Latge, J. P., and Munro, C. A. (2017). The fungal cell wall: structure, biosynthesis, and function. *Microbiol. Spectr.* 5, 1–25. doi: 10.1128/microbiolspec.FUNK-0035-2016

Huerta-Cepas, J., Forslund, K., Coelho, L. P., Szklarczyk, D., Jensen, L. J., von Mering, C., et al. (2017). Fast genome-wide functional annotation through orthology assignment by eggNOG-mapper. *Mol. Biol. Evol.* 34, 2115–2122. doi: 10.1093/molbev/msx148

Huerta-Cepas, J., Szklarczyk, D., Forslund, K., Cook, H., Heller, D., Walter, M. C., et al. (2016). eggNOG 4.5: a hierarchical orthology framework with improved functional annotations for eukaryotic, prokaryotic and viral sequences. *Nucleic Acids Res.* 44, D286–D293. doi: 10.1093/nar/gkv1248

Huerta-Cepas, J., Szklarczyk, D., Heller, D., Hernandez-Plaza, A., Forslund, S. K., Cook, H., et al. (2019). eggNOG 5.0: a hierarchical, functionally and phylogenetically annotated orthology resource based on 5090 organisms and 2502 viruses. *Nucleic Acids Res.* 47, D309–D314. doi: 10.1093/nar/gky1085

Hung, C. Y., Gonzalez, A., Wuthrich, M., Klein, B. S., and Cole, G. T. (2011). Vaccine immunity to coccidioidomycosis occurs by early activation of three signal pathways of T helper cell response (Th1, Th2, and Th17). *Infect. Immun.* 79, 4511–4522. doi: 10.1128/IAI.05726-11

Hung, C. Y., Yu, J. J., Seshan, K. R., Reichard, U., and Cole, G. T. (2002). A parasitic phase-specific adhesin of *Coccidioides immitis* contributes to the virulence of this respiratory fungal pathogen. *Infect. Immun.* 70, 3443–3456. doi: 10.1128/iai.70.7.3443-3456.2002

Huppert, M., Sun, S. H., and Harrison, J. L. (1982). Morphogenesis throughout saprobic and parasitic cycles of *Coccidioides immitis*. *Mycopathologia* 78, 107–122. doi: 10.1007/bf00442634

Hwang, L. H., Mayfield, J. A., Rine, J., and Sil, A. (2008). *Histoplasma* requires SID1, a member of an iron-regulated siderophore gene cluster, for host colonization. *PLoS Pathog.* 4:e1000044. doi: 10.1371/journal.ppat.1000044

Hwang, L. H., Seth, E., Gilmore, S. A., and Sil, A. (2012). SRE1 regulates iron-dependent and -independent pathways in the fungal pathogen *Histoplasma capsulatum*. *Eukaryot. Cell* 11, 16–25. doi: 10.1128/EC.05274-11

Jones, P., Binns, D., Chang, H. Y., Fraser, M., Li, W., McAnulla, C., et al. (2014). InterProScan 5: genome-scale protein function classification. *Bioinformatics* 30, 1236–1240. doi: 10.1093/bioinformatics/btu031

Kim, D., Pertea, G., Trapnell, C., Pimentel, H., Kelley, R., and Salzberg, S. L. (2013). TopHat2: accurate alignment of transcriptomes in the presence of insertions, deletions and gene fusions. *Genome Biol.* 14:R36. doi: 10.1186/gb-2013-14-4-r36

Koch, B., and Traven, A. (2019). Mitochondrial control of fungal cell walls: models and relevance in fungal pathogens. *Curr. Top. Microbiol. Immunol.* 1–20. doi: 10.1007/82_2019_183

Kollath, D. R., Teixeira, M. M., Funke, A., Miller, K. J., and Barker, B. M. (2019). Investigating the role of animal burrows on the ecology and distribution of *Coccidioides spp*. in arizona soils. *Mycopathologia* 185, 145–159. doi: 10.1007/s11046-019-00391-2

Laniado-Laborin, R., Arathoon, E. G., Canteros, C., Muniz-Salazar, R., and Rendon, A. (2019). Coccidioidomycosis in latin America. *Med. Mycol.* 57(Suppl. 1), S46–S55. doi: 10.1093/mmy/myy037

Latge, J. P. (2010). Tasting the fungal cell wall. *Cell Microbiol.* 12, 863–872. doi: 10.1111/j.1462-5822.2010.01474.x

Lee, I. R., Chow, E. W., Morrow, C. A., Djordjevic, J. T., and Fraser, J. A. (2011). Nitrogen metabolite repression of metabolism and virulence in the human fungal pathogen *Cryptococcus neoformans*. *Genetics* 188, 309–323. doi: 10.1534/genetics.111.128538

Li, L., Stoeckert, C. J. Jr., and Roos, D. S. (2003). OrthoMCL: identification of ortholog groups for eukaryotic genomes. *Genome Res.* 13, 2178–2189. doi: 10.1101/gr.1224503

Limjindaporn, T., Khalaf, R. A., and Fonzi, W. A. (2003). Nitrogen metabolism and virulence of *Candida albicans* require the GATA-type transcriptional activator encoded by GAT1. *Mol. Microbiol.* 50, 993–1004. doi: 10.1046/j.1365-2958.2003.03747.x

Marchler-Bauer, A., Bo, Y., Han, L., He, J., Lanczycki, C. J., Lu, S., et al. (2017). CDD/SPARCLE: functional classification of proteins via subfamily domain architectures. *Nucleic Acids Res.* 45, D200–D203. doi: 10.1093/nar/gkw1129

Marzluf, G. A. (1997). Genetic regulation of nitrogen metabolism in the fungi. *Microbiol. Mol. Biol. Rev.* 61, 17–32.

Mead, H. L., Teixeira, M. M., Galgiani, J. N., and Barker, B. M. (2019). Characterizing in vitro spherule morphogenesis of multiple strains of both species of *Coccidioides*. *Med. Mycol.* 57, 478–488. doi: 10.1093/mmy/myy049

Mirbod-Donovan, F., Schaller, R., Hung, C. Y., Xue, J., Reichard, U., and Cole, G. T. (2006). Urease produced by *Coccidioides posadasii* contributes to the virulence of this respiratory pathogen. *Infect. Immun.* 74, 504–515. doi: 10.1128/IAI.74.1.504-515.2006

Mitchell, A. L., Attwood, T. K., Babbitt, P. C., Blum, M., Bork, P., Bridge, A., et al. (2019). InterPro in 2019: improving coverage, classification and access to

protein sequence annotations. *Nucleic Acids Res.* 47, D351–D360. doi: 10.1093/nar/gky1100

Munro, C. A., Selvaggini, S., de Bruijn, I., Walker, L., Lenardon, M. D., Gerssen, B., et al. (2007). The PKC, HOG and Ca2+ signalling pathways co-ordinately regulate chitin synthesis in *Candida albicans*. *Mol. Microbiol.* 63, 1399–1413. doi: 10.1111/j.1365-2958.2007.05588.x

Oberegger, H., Schoeser, M., Zadra, I., Abt, B., and Haas, H. (2001). SREA is involved in regulation of siderophore biosynthesis, utilization and uptake in *Aspergillus nidulans*. *Mol. Microbiol.* 41, 1077–1089. doi: 10.1046/j.1365-2958.2001.02586.x

Oliveros, J. C. (2007). *Venny. An Interactive Tool for Comparing Lists With Venn Diagrams*. Available online at: http://bioinfogp.cnb.csic.es/tools/venny/index.html (accessed December 1, 2019).

Pradhan, A., Avelar, G. M., Bain, J. M., Childers, D. S., Larcombe, D. E., Netea, M. G., et al. (2018). Hypoxia promotes immune evasion by triggering beta-glucan masking on the *Candida albicans* cell surface via mitochondrial and cAMP-protein kinase A signaling. *mBio* 9:e01318-18. doi: 10.1128/mBio.01318-18

Sheth, C. C., Mogensen, E. G., Fu, M. S., Blomfield, I. C., and Muhlschlegel, F. A. (2008). *Candida albicans* HSP12 is co-regulated by physiological CO2 and pH. *Fungal Genet. Biol.* 45, 1075–1080. doi: 10.1016/j.fgb.2008.04.004

Shubitz, L. F., Dial, S. M., Perrill, R., Casement, R., and Galgiani, J. N. (2008). Vaccine-induced cellular immune responses differ from innate responses in susceptible and resistant strains of mice infected with *Coccidioides posadasii*. *Infect. Immun.* 76, 5553–5564. doi: 10.1128/IAI.00885-08

Sil, A., and Andrianopoulos, A. (2014). Thermally dimorphic human fungal pathogens–polyphyletic pathogens with a convergent pathogenicity trait. *Cold Spring Harb. Perspect. Med.* 5:a019794. doi: 10.1101/cshperspect.a019794

Stajich, J. E., Harris, T., Brunk, B. P., Brestelli, J., Fischer, S., Harb, O. S., et al. (2012). FungiDB: an integrated functional genomics database for fungi. *Nucleic Acids Res.* 40, D675–D681. doi: 10.1093/nar/gkr918

Steen, B. R., Zuyderduyn, S., Toffaletti, D. L., Marra, M., Jones, S. J., Perfect, J. R., et al. (2003). *Cryptococcus neoformans* gene expression during experimental cryptococcal meningitis. *Eukaryot. Cell* 2, 1336–1349. doi: 10.1128/ec.2.6.1336-1349.2003

Sumner, L. W., Amberg, A., Barrett, D., Beale, M. H., Beger, R., Daykin, C. A., et al. (2007). Proposed minimum reporting standards for chemical analysis chemical analysis working group (CAWG) metabolomics standards initiative (MSI). *Metabolomics* 3, 211–221. doi: 10.1007/s11306-007-0082-2

Taylor, J. W., and Barker, B. M. (2019). The endozoan, small-mammal reservoir hypothesis and the life cycle of *Coccidioides* species. *Med. Mycol.* 57(Suppl. 1), S16–S20. doi: 10.1093/mmy/myy039

Thammahong, A., Puttikamonkul, S., Perfect, J. R., Brennan, R. G., and Cramer, R. A. (2017). Central role of the trehalose biosynthesis pathway in the pathogenesis of human fungal infections: opportunities and challenges for therapeutic development. *Microbiol. Mol. Biol. Rev.* 81:e00053-16. doi: 10.1128/MMBR.00053-16

Thompson, G. R., Lewis, J. S., Nix, D. E., and Patterson, T. F. (2019). Current concepts and future directions in the pharmacology and treatment of coccidioidomycosis. *Med. Mycol.* 57, S76–S84. doi: 10.1093/mmy/myy029

Trapnell, C., Roberts, A., Goff, L., Pertea, G., Kim, D., Kelley, D. R., et al. (2012). Differential gene and transcript expression analysis of RNA-seq experiments with TopHat and Cufflinks. *Nat. Protoc.* 7, 562–578. doi: 10.1038/nprot.2012.016

Van Dyke, M. C. C., Teixeira, M. M., and Barker, B. M. (2019). Fantastic yeasts and where to find them: the hidden diversity of dimorphic fungal pathogens. *Curr. Opin. Microbiol.* 52, 55–63. doi: 10.1016/j.mib.2019.05.002

Verma, S., Shakya, V. P. S., and Idnurm, A. (2018). Exploring and exploiting the connection between mitochondria and the virulence of human pathogenic fungi. *Virulence* 9, 426–446. doi: 10.1080/21505594.2017.1414133

Viriyakosol, S., Fierer, J., Brown, G. D., and Kirkland, T. N. (2005). Innate immunity to the pathogenic fungus *Coccidioides posadasii* is dependent on toll-like receptor 2 and dectin-1. *Infect. Immun.* 73, 1553–1560. doi: 10.1128/iai.73.3.1553-1560.2005

Viriyakosol, S., Jimenez Mdel, P., Gurney, M. A., Ashbaugh, M. E., and Fierer, J. (2013). Dectin-1 is required for resistance to coccidioidomycosis in mice. *mBio* 4:e00597-12. doi: 10.1128/mBio.00597-12

Welker, S., Rudolph, B., Frenzel, E., Hagn, F., Liebisch, G., Schmitz, G., et al. (2010). Hsp12 is an intrinsically unstructured stress protein that folds upon membrane association and modulates membrane function. *Mol. Cell* 39, 507–520. doi: 10.1016/j.molcel.2010.08.001

Whiston, E., Zhang Wise, H., Sharpton, T. J., Jui, G., Cole, G. T., and Taylor, J. W. (2012). Comparative transcriptomics of the saprobic and parasitic growth phases in *Coccidioides spp*. *PLoS One* 7:e41034. doi: 10.1371/journal.pone.0041034

Wise, H. Z., Hung, C. Y., Whiston, E., Taylor, J. W., and Cole, G. T. (2013). Extracellular ammonia at sites of pulmonary infection with *Coccidioides posadasii* contributes to severity of the respiratory disease. *Microb. Pathog.* 5, 19–28. doi: 10.1016/j.micpath.2013.04.003

Xue, J., Chen, X., Selby, D., Hung, C. Y., Yu, J. J., and Cole, G. T. (2009). A genetically engineered live attenuated vaccine of *Coccidioides posadasii* protects BALB/c mice against coccidioidomycosis. *Infect. Immun.* 77, 3196–3208. doi: 10.1128/IAI.00459-09

Xue, T., Nguyen, C. K., Romans, A., and May, G. S. (2004). A mitogen-activated protein kinase that senses nitrogen regulates conidial germination and growth in *Aspergillus fumigatus*. *Eukaryot. Cell* 3, 557–560. doi: 10.1128/ec.3.2.557-560.2004

Conflict of Interest: The authors declare that the research was conducted in the absence of any commercial or financial relationships that could be construed as a potential conflict of interest.

frontiers in Genetics

ORIGINAL RESEARCH
published: 10 June 2020
doi: 10.3389/fgene.2020.00554

Understanding the Emergence of Multidrug-Resistant *Candida*: Using Whole-Genome Sequencing to Describe the Population Structure of *Candida haemulonii* Species Complex

Lalitha Gade[1], Jose F. Muñoz[2], Mili Sheth[3], Darlene Wagner[1,4], Elizabeth L. Berkow[1], Kaitlin Forsberg[1], Brendan R. Jackson[1], Ruben Ramos-Castro[5], Patricia Escandón[6], Maribel Dolande[7], Ronen Ben-Ami[8], Andrés Espinosa-Bode[9], Diego H. Caceres[1,10†], Shawn R. Lockhart[1], Christina A. Cuomo[2] and Anastasia P. Litvintseva[1]*

[1] *Mycotic Diseases Branch, Centers for Disease Control and Prevention, Atlanta, GA, United States,* [2] *Infectious Disease and Microbiome Program, Broad Institute, Cambridge, MA, United States,* [3] *Biotechnology Core Facility Branch, DSR/NCEZID - Centers for Disease Control and Prevention, Atlanta, GA, United States,* [4] *IHRC, Inc., Atlanta, GA, United States,* [5] *Department of Clinical and Molecular Microbiology, Instituto Conmemorativo Gorgas de Estudios de La Salud, Panama City, Panama,* [6] *Grupo de Microbiologia, Instituto Nacional de Salud, Bogotá, Colombia,* [7] *Departamento de Micología, Instituto Nacional de Higiene Rafael Rangel, Caracas, Venezuela,* [8] *Tel Aviv Sourasky Medical Center, Sackler School of Medicine, Tel Aviv University, Tel Aviv, Israel,* [9] *DGHP (Division of Global Health Protection), Central America Region Office, Centers for Disease Control and Prevention, Atlanta, GA, United States,* [10] *Center of Expertise in Mycology Radboudumc/CWZ, Nijmegen, Netherlands*

The recent emergence of a multidrug-resistant yeast, *Candida auris,* has drawn attention to the closely related species from the *Candida haemulonii* complex that include *C. haemulonii*, *Candida duobushaemulonii, Candida pseudohaemulonii*, and the recently identified *Candida vulturna.* Here, we used antifungal susceptibility testing and whole-genome sequencing (WGS) to investigate drug resistance and genetic diversity among isolates of *C. haemulonii* complex from different geographic areas in order to assess population structure and the extent of clonality among strains. Although most isolates of all four species were genetically distinct, we detected evidence of the in-hospital transmission of *C. haemulonii* and *C. duobushaemulonii* in one hospital in Panama, indicating that these species are also capable of causing outbreaks in healthcare settings. We also detected evidence of the rising azole resistance among isolates of *C. haemulonii* and *C. duobushaemulonii* in Colombia, Panama, and Venezuela linked to substitutions in *ERG11* gene as well as amplification of this gene in *C. haemulonii* in isolates in Colombia suggesting the presence of evolutionary pressure for developing azole resistance in this region. Our results demonstrate that these species need to be monitored as possible causes of outbreaks of invasive infection.

Keywords: Candida, haemulonii, duobushaemulonii, pseudohaemulonii, vulturna

OPEN ACCESS

Edited by:
Feng Gao,
Tianjin University, China

Reviewed by:
Johanna Rhodes,
Imperial College London,
United Kingdom
Cheshta Sharma,
The University of Texas Health Science Center at San Antonio, United States

****Correspondence:***
Anastasia P. Litvintseva
frq8@cdc.gov

†ORCID:
Diego H. Caceres
orcid.org/0000-0001-8749-9809

Specialty section:
This article was submitted to Evolutionary and Genomic Microbiology, a section of the journal Frontiers in Genetics

Received: *28 February 2020*
Accepted: *07 May 2020*
Published: *10 June 2020*

Citation:
Gade L, Muñoz JF, Sheth M, Wagner D, Berkow EL, Forsberg K, Jackson BR, Ramos-Castro R, Escandón P, Dolande M, Ben-Ami R, Espinosa-Bode A, Caceres DH, Lockhart SR, Cuomo CA and Litvintseva AP (2020) Understanding the Emergence of Multidrug-Resistant Candida: Using Whole-Genome Sequencing to Describe the Population Structure of Candida haemulonii Species Complex. Front. Genet. 11:554. doi: 10.3389/fgene.2020.00554

INTRODUCTION

Yeasts from *Candida haemulonii* complex that include *C. haemulonii, Candida duobushaemulonii, Candida pseudohaemulonii,* and the recently identified *Candida vulturna* (Sipiczki and Tap, 2016) are often misidentified as *Candida auris,* especially in laboratories that do not have access to DNA sequencing and matrix-assisted laser desorption/ionization time of flight mass spectroscopy (MALDI-TOF MS) (Hou et al., 2016; Araúz et al., 2018). Together with *C. lusitaniae*, another infrequent cause of candidemia, these four species belong to the Metschnikowiaceae family, which includes species that are often resistant to antifungal drugs (Jackson et al., 2019). Recent comparative genomic analysis identified the substantial amount of conservation and synteny among genomes of *C. auris, C. haemulonii, C. duobushaemulonii,* and *C. pseudohaemulonii* as well as similar expansions of the oligopeptide transporters and lipase gene families (Muñoz et al., 2018). These shared genomic features suggest similarities in ecology and physiology of these species and raise a possibility that they may also start emerging as drug-resistant pathogens in human populations.

In contrast to *C. auris*, which was described in 2009 from an external ear canal from a Japanese patient (Satoh et al., 2009; Chowdhary et al., 2013), *C. haemulonii* was first isolated from a fish off the coast of the Bahamas in 1962 and later isolated from a dolphin and seawater off the coast of Portugal (Van Uden and Kolipinski, 1962). The first clinical isolate was described in 1984 from blood of a patient with renal failure, and since then, isolates of *C. haemulonii* have been infrequently but regularly reported in patients causing wound and other types of infections (Gargeya et al., 1991; Cendejas-Bueno et al., 2012; Hou et al., 2016). *C. pseudohaemulonii* and *C. duobushaemulonii* were identified in 2006 and 2012, respectively, as the distinct lineages within *C. haemulonii* species complex based on the phylogenetic analysis of rDNA intragenic spacer region (ITS) (Cendejas-Bueno et al., 2012). Finally, in 2016, *C. vulturna* was identified as a distinct species most closely related to *C. duobushaemulonii* based on the phylogenetic analysis of rDNA locus (Sipiczki and Tap, 2016). The first isolate of this species was isolated from flowers in the Philippines, and later it was isolated as a cause of human candidemia (Sipiczki and Tap, 2016).

Subsequent studies identified phenotypical and clinical features associated with different species. Specifically, most strains of *C. haemulonii* cannot grow at 37°C, whereas most *C. duobushaemulonii* and *C. pseudohaemulonii* grow well at body temperature, and most strains of *C. auris* can grow up to 42°C (Ben-Ami et al., 2017). Compared with *C. auris* and *C. albicans*, *C. haemulonii* is less virulent in a murine model of infection (Ben-Ami et al., 2017). In humans, yeasts from *C. haemulonii* complex are primarily known to cause wound infections or colonization although a few cases of invasive blood infections have also been described (Ramos et al., 2015; Hou et al., 2016; Ben-Ami et al., 2017). Conversely, *C. auris* frequently causes invasive infections although the first isolates of *C. auris* were isolated from ear infections, and the East Asian clade of *C. auris* (Clade II) are commonly isolated from the external ear canal (Jackson et al., 2019). *C. auris* and the four species from the *C. haemulonii* complex are known for their resistance to antifungal drugs, especially to amphotericin B and azoles; however, resistance to echinocandins is rare (Ramos et al., 2015; Hou et al., 2016).

Unlike *C. auris*, which is known to colonize human skin and cause rampant healthcare-associated outbreaks in numerous countries, other species from *C. haemulonii* species complex have been associated with relatively few suspected outbreaks and clusters. In 2007, an outbreak of fungemia caused by *C. haemulonii* resistant to amphotericin B, fluconazole, and itraconazole was described among four patients in a neonatal unit in Kuwait (Khan et al., 2007). Although this outbreak occurred before *C. auris* and *C. duobushaemulonii* species were described, ITS sequences from the isolates deposited into NCBI identify the isolates from this outbreak as *C. haemulonii sensu stricto* (Isla et al., 2017). In 2016, a cluster of three *C. haemulonii* wound infections was identified in an Israeli hospital overlapping in time with a *C. auris* outbreak (Ben-Ami et al., 2017). In 2017, an unusual number of *C. duobushaemulonii* and *C. auris* infections were identified in Panama City, Panama, and a subsequent epidemiological investigation confirmed outbreaks of both species (Araúz et al., 2018). The goal of this study was to investigate the genetic relationships and drug-resistance profiles among isolates of the *C. haemulonii* complex from different countries and healthcare facilities to determine genetic diversities in different populations and to examine possible evidence of transmission if it existed.

METHODS

Isolates

Isolates were received in the Mycotic Diseases Branch Reference Laboratory at the CDC for routine fungal identification or as part of ongoing fungal disease surveillance. Upon arrival, isolates were identified by sequencing of the ITS2 region of the rDNA and MALDI-TOF MS (Bruker, Bremen, Germany) using a CDC-developed database MicrobeNet (https://www.cdc.gov/microbenet/index.html). Isolates were stored in 20% glycerol at −70°C. When available, limited metadata, such as geographic region or site of the infection, were collected.

Whole-Genome Sequencing (WGS)

DNA was extracted using the ZR Fungal/Bacterial DNA MiniPrep kit (Zymo Research, Irvine, CA, USA) according to the manufacturer's instructions. Genomic libraries were constructed and barcoded using the NEBNext Ultra DNA Library Prep kit for Illumina (New England Biolabs, Ipswich, MA, USA) following the manufacturer's instructions. Libraries were sequenced on either the Illumina HiSeq 2500 platform (Illumina, San Diego, CA, USA) using the HiSeq Rapid SBS Kit v2 500 cycles or the MiSeq platform using the MiSeq Reagent Kit v2 500 cycles or Illumina MiSeq Reagent Kit v3 (600 cycles). HiSeq and MiSeq v2 500-cycle kits generated 251 bp paired reads, whereas MiSeq v3 600-cycle kits generated 301 bp paired reads.

Single Nucleotide Polymorphism (SNP) Analysis

Paired-end sequences that had at least 50X coverage were used for downstream analyses. Read quality was assessed using FastQC v0.11.5 (http://www.bioinformatics.babraham.ac.uk/projects/fastqc/), and for filtering low-quality sequences, PRINSEQ v0.20.3 (http://prinseq.sourceforge.net/manual.html) was performed using the following command: "-trim_left 15 -trim_qual_left 20 -trim_qual_right 20 -min_len 100 -min_qual_mean 25 -derep 14." For identifying SNPs, paired-end reads of each species were aligned using BWA mem v0.7.12 ((Li and Durbin, 2009)) to their respective previously published assemblies [*C. haemulonii* strain B11899, GenBank accession PKFO00000000 (Chow et al., 2018a); *C. duobushaemulonii* strain B09383, GenBank accession PKFP00000000 (Chow et al., 2018b); *C. pseudohaemulonii* strain B12108, GenBank accession PYFQ00000000 (Muñoz et al., 2018); and *C. vulturna* strain CBS14366 BioProject PRJNA560499 (Navarro-Muñoz et al., 2019)]. SNPs were identified and filtered using the publicly available pipeline NASP (http://tgennorth.github.io/NASP/) to remove positions that had <10x coverage, <90% variant allele calls, or that were identified by Nucmer (Kurtz et al., 2004) as being within duplicated regions in the reference (**Supplementary Table 1**).

In addition, we performed variant identification to each of the four mapped species using GATK v3.7 (https://gatk.broadinstitute.org/hc/en-us) with the haploid mode and GATK tools. Sites were filtered with variant filtration using "QD < 2.0 || FS > 60.0 || MQ < 40.0." Genotypes were filtered if the minimum genotype quality <50, percentage alternate allele <0.8, or depth <10 (https://github.com/broadinstitute/broad-fungalgroup/blob/master/scripts/SNPs/filterGatkGenotypes.py). For the *C. haemulonii* species complex phylogeny, SNPs from the representative isolates were identified by aligning reads to B8441 *C. auris* reference genome assembly, GenBank accession PEKT00000000.2 (Muñoz et al., 2018). To investigate genetic relationships within each species, phylogenetic trees were constructed by identifying SNPs by aligning reads to the reference genome assemblies of each corresponding species.

Phylogenetic and Population Genetic Analyses

For phylogenetic analysis, maximum parsimony phylogenies were constructed using the subtree-pruning-regrafting (SPR) algorithm and bootstrapped using 500 reiterations in MEGA7.0 (Kumar et al., 2018) and visualized in Interactive Tree of Life (iTOL) v4 (Letunic and Bork, 2019). All positions containing gaps and missing data were eliminated. The average genome-wide nucleotide diversity (π) and Tajima's D were calculated from the GATK SNPs set using PopGenome v2.6.1 R package (https://www.rdocumentation.org/packages/PopGenome/versions/2.7.2) using 5 kb sliding windows. Mating type locus (MTLa and MTLα) was determined using the normalized average read depth at the locus from aligned BAM files for each isolate mapped to the corresponding reference genomes. Genomic regions that exhibit copy number variation (CNV) were identified using normalized read depth.

Antifungal Susceptibility Testing

Antifungal susceptibility testing was performed as outlined by Clinical and Laboratory Standards Institute (CLSI) standard M27 (CLSI, 2008). However, for several slow-growing isolates of *C. haemulonii,* the plates were read at 48 h as suggested in CLSI standard M27. Etests (BioMérieux, Marcy l'Etoile, France) were used for amphotericin B. Custom-prepared frozen panels (Trek Diagnostics, Thermo Fisher Scientific, Oakwood Village, OH) were used for the echinocandins (anidulafungin, caspofungin, and micafungin) and the azoles (fluconazole, voriconazole, itraconazole, posaconazole, and isavuconazole).

Identification of Mutations Associated With Elevated MICs

The annotated GATK VCF files were used to determine the genotype of known mutation sites in *ERG11*, *FKS1,* and other genes of interest (**Supplementary Table 2**) (Arendrup and Patterson, 2017; Berkow and Lockhart, 2017) using SnpEff v4.3T (http://snpeff.sourceforge.net/).

RESULTS

Isolates Description

Between 2011 and 2018, 38 isolates of *C. haemulonii* from Colombia ($N = 11$), Israel ($N = 3$), Panama ($N = 4$), Venezuela ($N = 7$), and the United States ($N = 13$); 55 isolates of *C. duobushaemulonii* from Colombia ($N = 6$), Guatemala ($N = 2$), Panama ($N = 14$), Venezuela ($N = 1$), and the United States ($N = 32$); and six isolates of *C. pseudohaemulonii* from Colombia ($N = 2$), Panama ($N = 2$), Venezuela ($N = 1$), and the United States ($N = 1$) were received (**Table 1**). In addition, five isolates from Colombia ($N = 2$), Panama ($N = 2$), and the United States ($N = 1$) that were identified by MALDI-TOF as closely resembling *C. duobushaemulonii*, which the subsequent analysis confirmed as *C. vulturna,* were also included (**Table 1**). We included two historic isolates from the Mycotic Diseases Branch culture collection: B10441 (CBS5149) strain of *C. haemulonii* isolated from a fish in 1962 and B10440 strain of *C. duobushaemulonii* isolated from a foot ulcer of a patient in 1990.

In the United States, 91% of *C. haemulonii* and 87% of *C. duobushaemulonii* were isolated from wounds, bones, and other non-invasive sites, and the remaining isolates were from blood (**Table 2**). A different distribution of cases was observed in Latin America: 77% of *C. haemulonii* and 67% of *C. duobushaemulonii* from Latin American countries (Colombia, Panama, and Venezuela combined) were from blood, and the remaining isolates were from wounds and non-invasive sites. All isolates of *C. haemulonii* from Israel were from wounds. All six *C. pseudohaemulonii* isolates were from blood (**Table 2**). One isolate of *C. vulturna* was from blood, and the other four were wounds and other non-invasive sites (**Table 2**).

TABLE 1 | List of isolates included in the study.

Isolate	Species	Origin	Year collected	Location	Mating type
B10441	*C. haemulonii*	Fish (CBS 5149)	1962	Florida, USA	α
B11786	*C. haemulonii*	Blood	2016	Colombia	α
B11792	*C. haemulonii*	Blood	2016	Colombia	α
B11798	*C. haemulonii*	Blood	2016	Colombia	α
B11803	*C. haemulonii*	Blood	2016	Colombia	α
B11898	*C. haemulonii*	Wound	2014	Israel	α
B11899	*C. haemulonii*	Wound	2015	Israel	α
B11900	*C. haemulonii*	Wound	2015	Israel	α
B12068	*C. haemulonii*	Bronchial Wash	2018	Alabama, USA	α
B12109	*C. haemulonii*	Blood	2011	Venezuela	α
B12112	*C. haemulonii*	Blood	2012	Venezuela	α
B12126	*C. haemulonii*	Blood	2013	Venezuela	α
B12127	*C. haemulonii*	Blood	2014	Venezuela	α
B12128	*C. haemulonii*	Blood	2014	Venezuela	α
B12129	*C. haemulonii*	Blood	2014	Venezuela	α
B12185	*C. haemulonii*	Blood	2016	Venezuela	α
B12201	*C. haemulonii*	Foot	2016	Michigan, USA	α
B12343	*C. haemulonii*	Wound	2016	Georgia, USA	α
B12615	*C. haemulonii*	Wound (big toe)	2017	Indiana, USA	α
B12643	*C. haemulonii*	Wound	2017	Washington, USA	α
B12989	*C. haemulonii*	Foot	2017	Wisconsin, USA	α
B13065	*C. haemulonii*	Vaginal secretion	2016	Panama	α
B13067	*C. haemulonii*	Toenail	2017	Panama	α
B13068	*C. haemulonii*	Blood	2017	Panama	α
B13081	*C. haemulonii*	Catheter	2017	Panama	α
B13273	*C. haemulonii*	Bone	2017	Wisconsin, USA	α
B13444	*C. haemulonii*	Wound	2017	Tennessee, USA	α
B13704	*C. haemulonii*	Bone	2017	Florida, USA	α
B13909	*C. haemulonii*	Blood	2017	Virginia, USA	α
B15318	*C. haemulonii*	Unknown	2018	Hawaii, USA	α
B15393	*C. haemulonii*	Blood	2016	Colombia	α
B15394	*C. haemulonii*	Blood	2016	Colombia	α
B15400	*C. haemulonii*	Urine	2017	Colombia	α
B15401	*C. haemulonii*	Nail	2017	Colombia	α
B15406	*C. haemulonii*	Blood	2017	Colombia	α
B15408	*C. haemulonii*	Peritoneal fluid	2017	Colombia	α
B15409	*C. haemulonii*	Blood	2018	Colombia	α
B16299	*C. haemulonii*	Foot (tissue)	2018	Florida, USA	α
B09383	*C. duobushaemulonii*	Blood	2011	Tennessee, USA	α
B10440	*C. duobushaemulonii*	Foot ulcer	1990	Alabama, USA	α
B11839	*C. duobushaemulonii*	Blood	2016	Mississippi, USA	α
B12075	*C. duobushaemulonii*	Scalp Tissue	2016	Kentucky, USA	α
B12111	*C. duobushaemulonii*	Blood	2011	Venezuela	α
B12240	*C. duobushaemulonii*	Foot	2016	Florida, USA	α
B12437	*C. duobushaemulonii*	Unknown	Missing	Guatemala	α
B12484	*C. duobushaemulonii*	Skin	2017	Florida, USA	α
B12492	*C. duobushaemulonii*	Ear fluid	2017	Florida, USA	α
B12539	*C. duobushaemulonii*	Skin	2017	Florida, USA	α
B12593	*C. duobushaemulonii*	Wound (foot)	2017	Florida, USA	α
B12594	*C. duobushaemulonii*	Wound (toe)	2017	Mississippi, USA	α
B12613	*C. duobushaemulonii*	Wound (toe)	2017	Florida, USA	α

(Continued)

TABLE 1 | Continued

Isolate	Species	Origin	Year collected	Location	Mating type
B12614	*C. duobushaemulonii*	Wound (big toe)	2017	Indiana, USA	α
B12709	*C. duobushaemulonii*	Blood	2017	Alabama, USA	α
B12845	*C. duobushaemulonii*	Wound (leg)	2017	Washington, USA	α
B12848	*C. duobushaemulonii*	Wound (toe)	2017	Washington, USA	α
B12972	*C. duobushaemulonii*	Wound (foot)	2017	Florida, USA	α
B12985	*C. duobushaemulonii*	Wound (leg)	2017	Washington, USA	α
B12987	*C. duobushaemulonii*	Wound (toe)	2017	Nebraska, USA	α
B12988	*C. duobushaemulonii*	Nail	2017	Wisconsin, USA	α
B13055	*C. duobushaemulonii*	Blood-tip CVC	2016	Panama	α
B13056	*C. duobushaemulonii*	Blood-tip CVC	2016	Panama	α
B13057	*C. duobushaemulonii*	Blood-tip CVC	2016	Panama	α
B13058	*C. duobushaemulonii*	Toenail scraping	2016	Panama	α
B13059	*C. duobushaemulonii*	Blood	2016	Panama	α
B13063	*C. duobushaemulonii*	Blood	2016	Panama	α
B13066	*C. duobushaemulonii*	Blood	2016	Panama	α
B13071	*C. duobushaemulonii*	Urine	2017	Panama	α
B13072	*C. duobushaemulonii*	Toenail	2017	Panama	α
B13073	*C. duobushaemulonii*	Blood	2017	Panama	α
B13076	*C. duobushaemulonii*	Skin	2017	Panama	α
B13088	*C. duobushaemulonii*	Blood	2017	Panama	α
B13089	*C. duobushaemulonii*	Open fracture	2017	Panama	α
B13091	*C. duobushaemulonii*	Blood	2017	Panama	α
B13267	*C. duobushaemulonii*	Wound (toe)	2017	Oklahoma, USA	α
B13331	*C. duobushaemulonii*	Tissue (foot)	2017	Florida, USA	α
B13465	*C. duobushaemulonii*	Wound	2017	Washington, USA	α
B13467	*C. duobushaemulonii*	Unknown	Missing	Guatemala	α
B13908	*C. duobushaemulonii*	Wound	2017	Virginia, USA	α
B14153	*C. duobushaemulonii*	Bone	2018	Pennsylvania, USA	α
B14185	*C. duobushaemulonii*	Urine	2018	Florida, USA	α
B14283	*C. duobushaemulonii*	Tissue	2018	Virginia, USA	α
B15056	*C. duobushaemulonii*	Wound	2018	Indiana, USA	α
B15179	*C. duobushaemulonii*	Bone	2018	Ohio, USA	α
B15319	*C. duobushaemulonii*	Bone	2018	Tennessee, USA	α
B15360	*C. duobushaemulonii*	Blood	2018	Texas, USA	α
B15396	*C. duobushaemulonii*	Eye secretion	2017	Colombia	α
B15397	*C. duobushaemulonii*	Blood	2017	Colombia	α
B15399	*C. duobushaemulonii*	Blood	2017	Colombia	α
B15403	*C. duobushaemulonii*	Blood	2017	Colombia	α
B15407	*C. duobushaemulonii*	Blood	2017	Colombia	α
B15410	*C. duobushaemulonii*	Tissue	2018	Colombia	α
B16327	*C. duobushaemulonii*	Unknown	2018	New York, USA	α
B16366	*C. duobushaemulonii*	Tissue	2018	Virginia, USA	α
B12108	*C. pseudohaemulonii*	Blood	2011	Venezuela	a
B12384	*C. pseudohaemulonii*	Blood	2016	Georgia, USA	a
B13062	*C. pseudohaemulonii*	Blood	2016	Panama	a
B13064	*C. pseudohaemulonii*	Blood	2017	Panama	a
B15395	*C. pseudohaemulonii*	Blood	2017	Colombia	a
B15405	*C. pseudohaemulonii*	Blood	2017	Colombia	a
B13074	*C. vulturna*	Endothelial secretion	2017	Panama	a
B13075	*C. vulturna*	Mesh Wound	2017	Panama	a
B14309	*C. vulturna*	Wound	2018	Indiana, USA	α
B15411	*C. vulturna*	Gastric acid	2018	Colombia	a
B15412	*C. vulturna*	Blood	2018	Colombia	a

TABLE 2 | Country and specimen sources of *Candida haemulonii* species complex isolates.

Organism (*n*)	Country (*n*)	Blood	Wound and other non-invasive sites
C. haemulonii (38^)	USA (11)	1 (9%)	10 (91%)
	Latin America (22)	17 (77%)	5 (23%)
C. duobushaemulonii (55^)	USA (31)	4 (13%)	27 (87%)
	Latin America (21)	14 (67%)	7 (33%)
C. pseudohaemulonii (6)	USA (1)	1 (100%)	0 (0%)
	Latin America (5)	5 (100%)	0 (0%)
C. vulturna (5)	USA (1)	0 (0%)	1 (100%)
	Latin America (4)	1 (25%)	3 (75%)

^*Five C. haemulonii and 3 C. duobushaemulonii isolates were excluded, because for 4 isolates, the infection site information was unavailable, one isolate was from fish and only 3 isolates were available from Israel.*

Phylogenetic Relationships Within the Species Complex

Phylogenetic analysis using SNPs called against the *C. auris* reference strain B8441 (Muñoz et al., 2018) confirmed previous observations that *C. duobushaemulonii* is closely related to *C. pseudohaemulonii*. This analysis also identified a subgroup of isolates from Colombia, Panama, and the Unites States, which was identified by MALDI-TOF as closely resembling *C. duobushaemulonii*, which formed a distinct monophyletic branch on the phylogenetic tree (**Figure 1**). Comparison with a recently assembled genome identified these strains as *C. vulturna* (Navarro-Muñoz et al., 2019) (**Figure 4B**). Conversely, isolates identified by MALDI-TOF as *C. haemulonii* var. *vulnera*, a previously recognized variety within the *C. haemulonii* complex (Cendejas-Bueno et al., 2012), were intermixed with other *C. haemulonii* strains and did not form a phylogenetically distinct cluster (**Figures 1**, **2**).

Genetic Diversity Among *C. haemulonii*

Genetic relationships among *C. haemulonii* isolates are shown in **Figure 2** and at https://microreact.org/project/Candida_haemulonii. The average pairwise difference between the isolates was 214 SNPs (range 0–399), and there was no distinct phylogeographic population structure. Most isolates were genetically distinct; however, three isolates, B13067, B13068, and B13081, were different from each other by fewer than 27 SNPs and formed a small, well-supported cluster in the phylogenetic tree based on bootstrap analysis (**Figure 2**). These three isolates were recovered from different patients treated at the same hospital in Panama City, Panama, which reported contemporaneous outbreaks of *C. duobushaemulonii* and *C. auris* (Araúz et al., 2018). B13067 was isolated from a toenail of a patient in November 2016, and B13068 was from the blood of another patient isolated in December 2016; the two isolates were genetically identical (0 SNPs). The other isolate from this cluster, B13081, was recovered from a central venous catheter in March 2017. In addition, two isolates from Venezuela, B12112 and B12127, differed by only 32 SNPs although they were isolated from patients treated in different healthcare facilities in the city of Valencia (**Figure 2**). The rest of the isolates from these and other countries were different from each other by >69 SNPs. All isolates from the United States were genetically distinct. Interestingly, B10441, recovered in 1962 from a seawater fish, was only 176 SNP different from B13909, isolated in 2017 from a patient's blood. All *C. haemulonii* isolates were mating type alpha. The average genome-wide nucleotide diversity (π) was 2.59e-05, and the average Tajima's D estimate was −0.97, which is consistent with recent population expansion.

Genetic Diversity Among *C. duobushaemulonii*

The average pairwise distance between *C. duobushaemulonii* isolates was 458 SNPs (range 0–1,243). The isolates can be separated into two genetically distinct clades separated by more than 600 SNPs. One of these clades included isolates from Panama, Colombia, Guatemala, Venezuela, and the United States, and the other included primarily isolates from the United States, one isolate from Venezuela, and one from Panama (**Figure 3** and https://microreact.org/project/Candida_duobushaemulonii).

Nine of the 14 isolates from Panama were from a previously reported outbreak in a large hospital in Panama City (Araúz et al., 2018); five of those were genetically distinct and intermixed with isolates from other regions, and four others, each isolated from a different patient, formed a tight cluster on the phylogenetic tree (**Figure 3**). B13058 from a toenail and B13059 from blood were isolated in November 2016 and were identical (0 SNPs), and the other two, B13056 from the catheter isolated in November 2016 and B13088 from blood isolated in April 2017, were separated by <42 SNPs. Clusters of *C. duobushaemulonii* and *C. haemulonii* overlapped in time. All *C. duobushaemulonii* isolates were mating type alpha. The genome-wide nucleotide diversity (π) was 4.86e-05, which was almost twice that observed in *C. haemulonii*; however, the average Tajima's D estimate was −1.17, which was similar to that of *C. haemulonii* and consistent with recent population expansion.

Genetic Relationships Among Isolates of *C. pseudohaemulonii* and *C. vulturna*

Five of the six tested isolates of *C. pseudohaemulonii* clustered together (441-845 SNPs), and the sixth isolate, B12108 from blood of a Venezuelan patient, was >200,000 SNPs different from the other group (**Figure 4A** and https://microreact.org/project/Candida_pseudohaemulonii). Similarly, four isolates of *C. vulturna* from Colombia, Panama, and Venezuela were different from each other and the type isolate, CBS14366, isolated from a flower in the Philippines (Sipiczki and Tap, 2016) by 104–209 SNPs. However, the fifth isolate from a U.S. patient was more than 81,000 SNPs different from the other four, suggesting multiple clades of *C. vulturna* (**Figure 4B** and https://microreact.org/project/Candida_vulturna) although more isolates are needed to test this hypothesis. All *C. pseudohaemulonii* isolates were mating type a. In *C. vulturna*, four isolates where mating type a, and the fifth isolate from the United States (B14309) was mating type alpha.

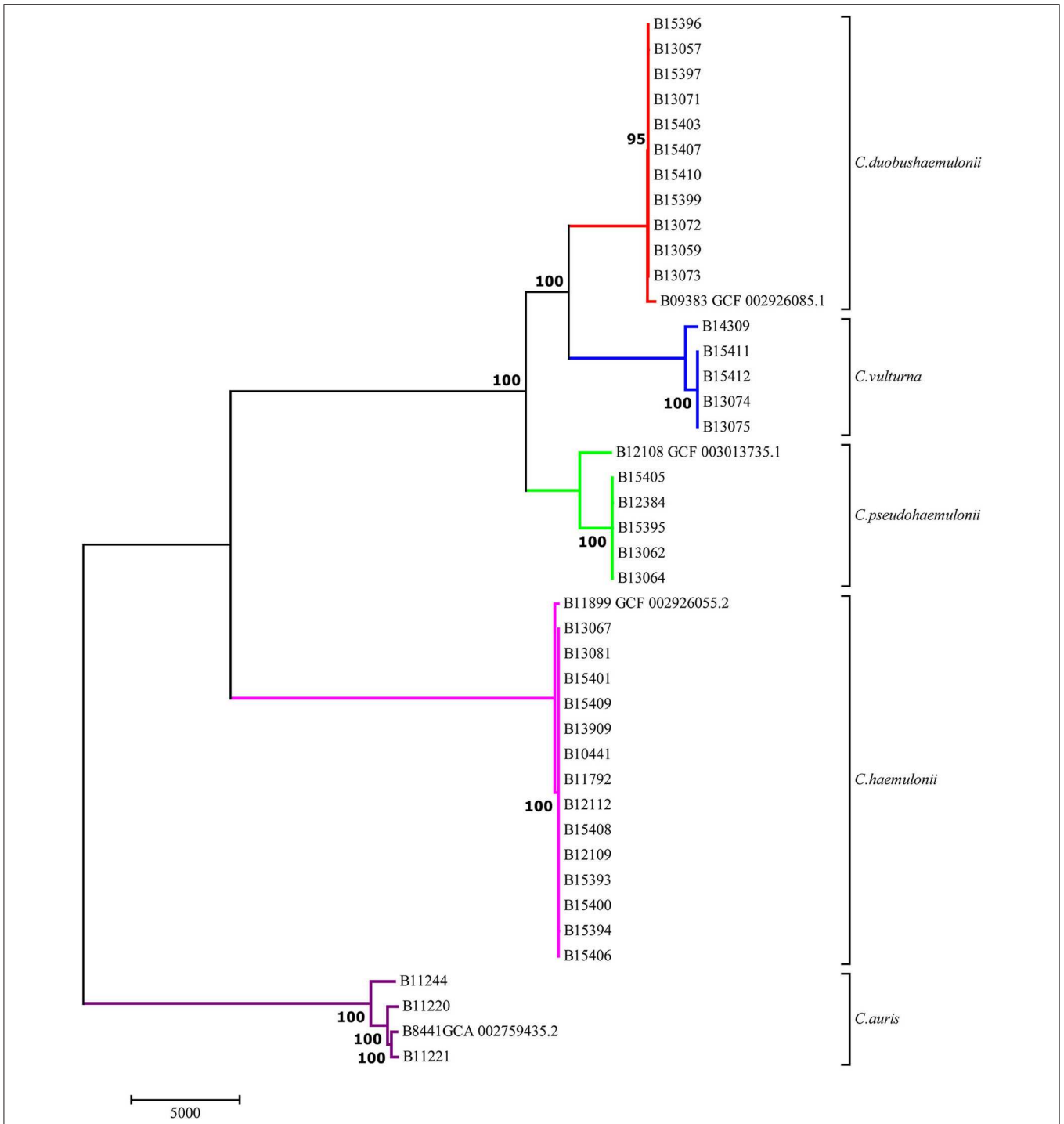

FIGURE 1 | Maximum parsimony tree illustrating the phylogenetic relationships among species from *C. haemulonii* complex constructed using 56,023 SNPs called against B8441 *C. auris* reference genome (GenBank accession PEKT00000000.2). Numbers show bootstrap support for the branches. Scale bar shows pairwise SNPs.

Antifungal Susceptibility Testing and Mutations Linked to Resistance

We observed variable levels of susceptibility to amphotericin B among 38 tested *C. haemulonii* isolates: 29 (76%) had elevated MICs from 2 μg/mL to >32 μg/mL, and the rest had MICs below 2 μg/mL (**Table 3**). Seven (18%) isolates had elevated MIC of fluconazole ranging from 32 to 256 μg/mL, and all had the Y132F mutation in *ERG11*. However, one isolate, B13067, with this mutation had MIC of fluconazole 8 μg/mL (https://microreact.org/project/Candida_haemulonii).

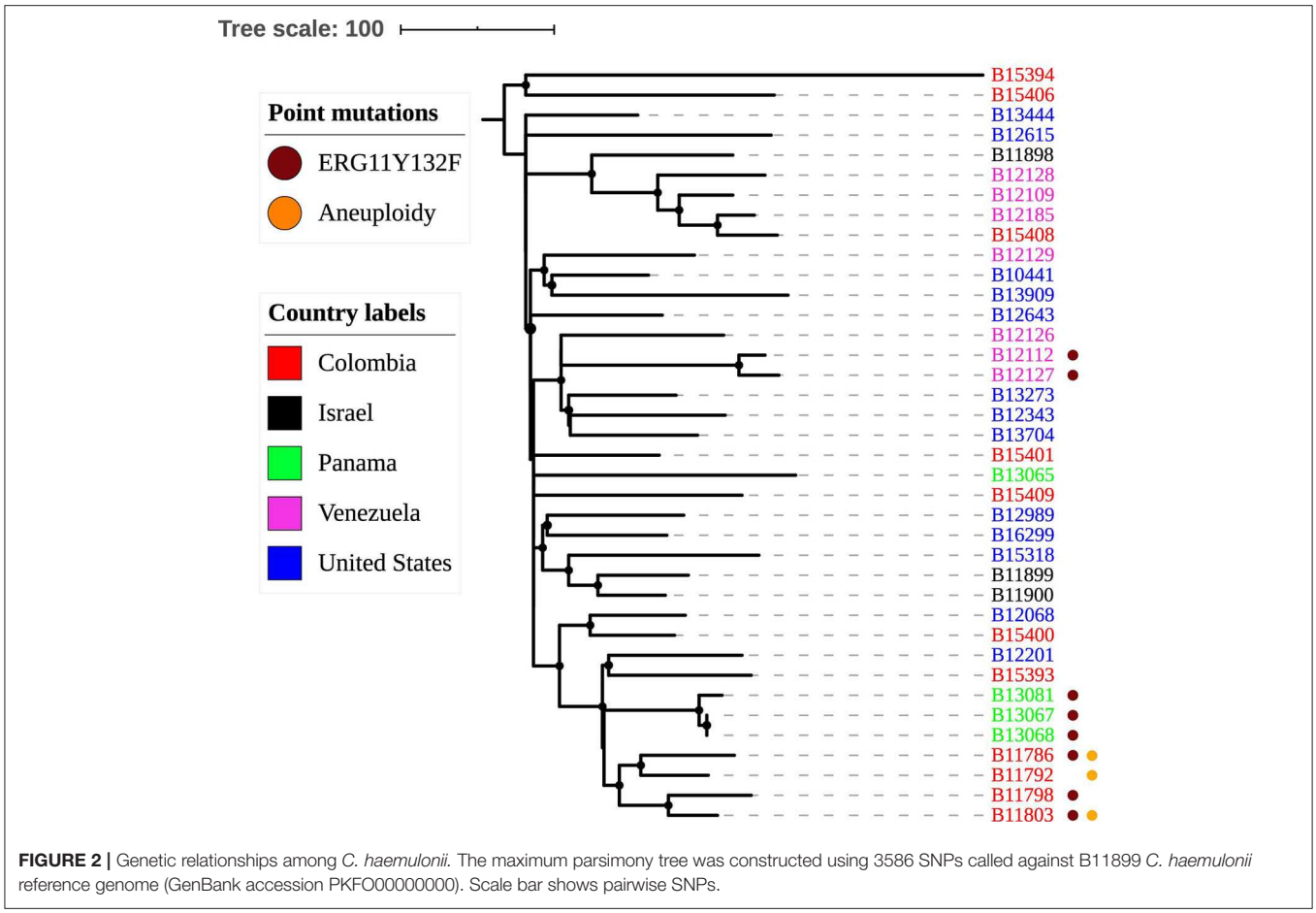

FIGURE 2 | Genetic relationships among *C. haemulonii.* The maximum parsimony tree was constructed using 3586 SNPs called against B11899 *C. haemulonii* reference genome (GenBank accession PKFO00000000). Scale bar shows pairwise SNPs.

Three *C. haemulonii* isolates, B11786, B11792, and B11803, had aneuploidy of chromosome 4 (scaffold 4) that harbors *ERG11*: B11786 and B11792 have complete duplication of chromosome 4, and B11803 has a 300-kb duplication or a region encompassing *ERG11* (**Supplementary Figure 1**). In addition to this duplication, both B11786 and B11803 had Y132F substitution, and their MIC of fluconazole was 64 μg/mL. However, the MIC of fluconazole of B11792 that had wild-type *ERG11* copy was 4 μg/mL, suggesting that the duplication alone did not increase resistance (**Table 3**).

Of the 55 *C. duobushaemulonii* isolates, 51 (93%) had highly elevated MICs of amphotericin B ranging from 12 μg/mL to more than 32 μg/mL (**Table 3**). Four isolates (7%), two from Guatemala (B13467 and B12437). and two from the United States (B12240 and B14185), had lower MICs (0.064–0.38) of amphotericin B although all four were genetically unrelated to each other (**Figure 1**). Conversely, 48 of 55 (87%) *C. duobushaemulonii* had lower MICs (≤16 μg/mL) of fluconazole, and seven (13%) had elevated MIC (≥64 μg/mL). Of those seven, five with MIC of 256 μg/mL had the Y132F mutation in the *ERG11* gene, and they also had elevated MIC of voriconazole (1–2 μg/mL) (**Table 3**). Furthermore, four of those isolates, which formed a tight cluster associated with an outbreak in Panama (**Figure 3**), also had G307A substitution, whereas B13063 had Y132H and G443D substitutions in *ERG11* and had MIC of fluconazole of 64 μg/mL (https://microreact.org/project/Candida_duobushaemulonii). All four of these mutations have been linked to resistance to fluconazole in *C. albicans* (Berkow and Lockhart, 2017).

Of the six tested *C. pseudohaemulonii* isolates, two, B12108 and B12384, had elevated MICs of amphotericin B, 12 μg/mL and >32 μg/mL, and the same two isolates had elevated MICs of fluconazole of 128 and 32 μg/mL, respectively (**Table 3**). Of those, B12108 had the Y132F substitution (Muñoz et al., 2018).

All five tested *C. vulturna* isolates had elevated MICs of amphotericin B with MICs ranging from 8 μg/mL to more than 16 μg/mL (**Table 3**). All five isolates were susceptible to fluconazole with MIC of 8 to 16 μg/mL, and no known substitutions in the *ERG11* gene were detected in these isolates (**Table 3**). All tested isolates of the four species had low MICs of echinocandins.

In addition, we examined other genes that have been implicated in azole and amphotericin B resistance in *Candida spp*. (Arendrup and Patterson, 2017); the non-synonymous substitutions identified in these genes are listed in **Supplementary Table 2**. The annotated VCF files for all isolates from this study that can be used to browse for substitutions in other genes of interest are available as https://figshare.com/projects/Genome_sequencing_of_Candida_haemulonii_species_complex/80150.

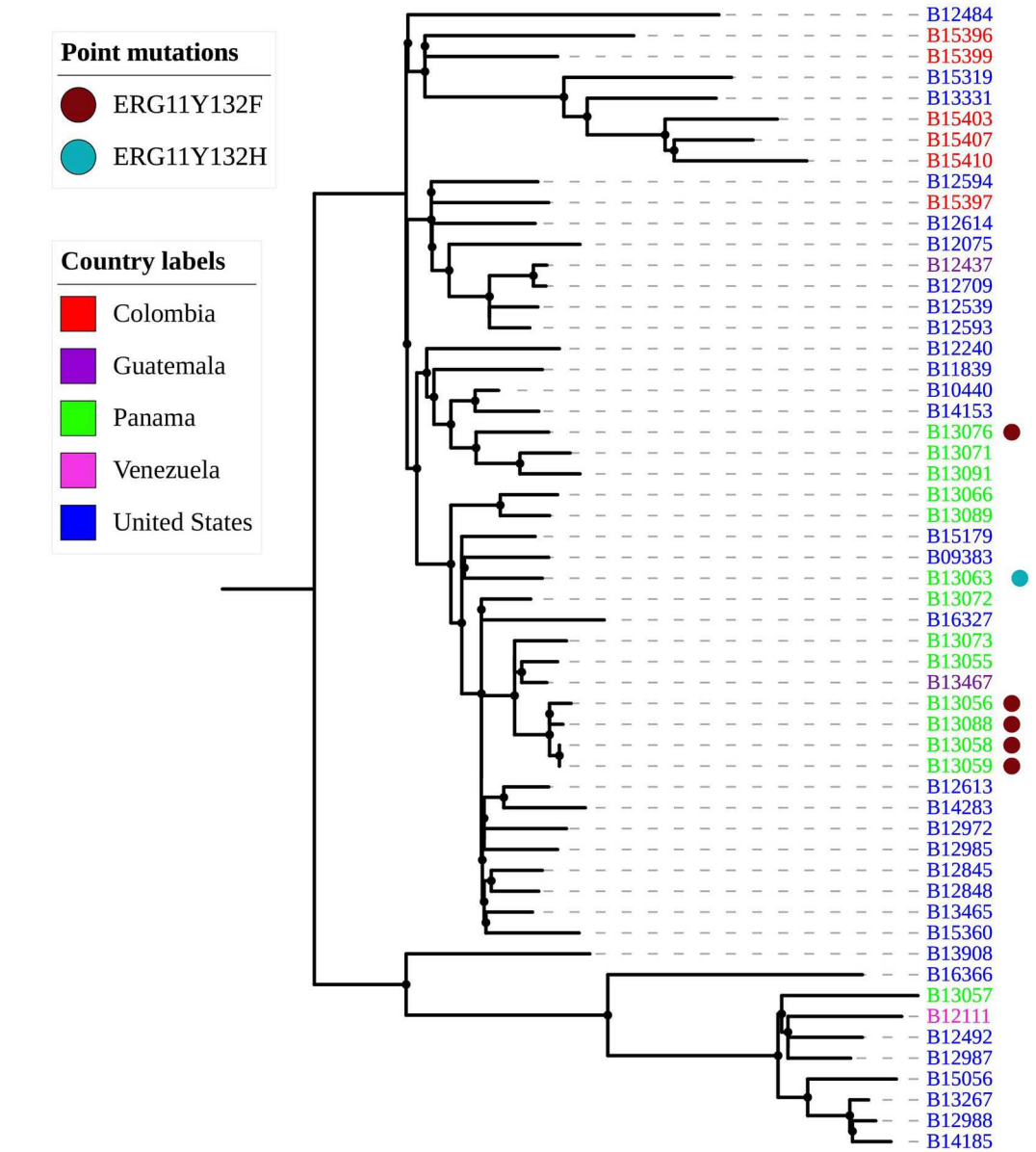

FIGURE 3 | Genetic relationships among *C. duobushaemulonii* isolates. The maximum parsimony tree was constructed using 6614 SNPs called against B09383 *C. duobushaemulonii* reference genome (GenBank accession PKFP00000000). Scale bar shows pairwise SNPs.

DISCUSSION

We present results of the population genetics and phylogenetic analyses of isolates from the *Candida haemulonii* complex that are closely related to the globally emerging pathogen, *C. auris*. Phylogenetic analysis based on WGS confirmed previously described relationships among these species (Muñoz et al., 2018; Navarro-Muñoz et al., 2019) and demonstrated that the newly described *C. vulturna* forms a distinct, well-supported clade related to *C. duobushaemulonii* and *C. pseudohaemulonii*. Here, we describe five additional clinical isolates of this new species and demonstrate that it can cause both invasive as well as non-invasive infections as isolates of this species were isolated from blood, wounds, and other body fluids. This new species was found in Panama, Colombia, and in the United States.

Isolates of *C. haemulonii* and *C. duobushaemulonii* were recovered from blood as well as from wounds and other non-invasive sites. In the United States, the vast majority of *C. haemulonii* and *C. duobushaemulonii* were from non-invasive sites, such as lower extremities or wounds, and most isolates

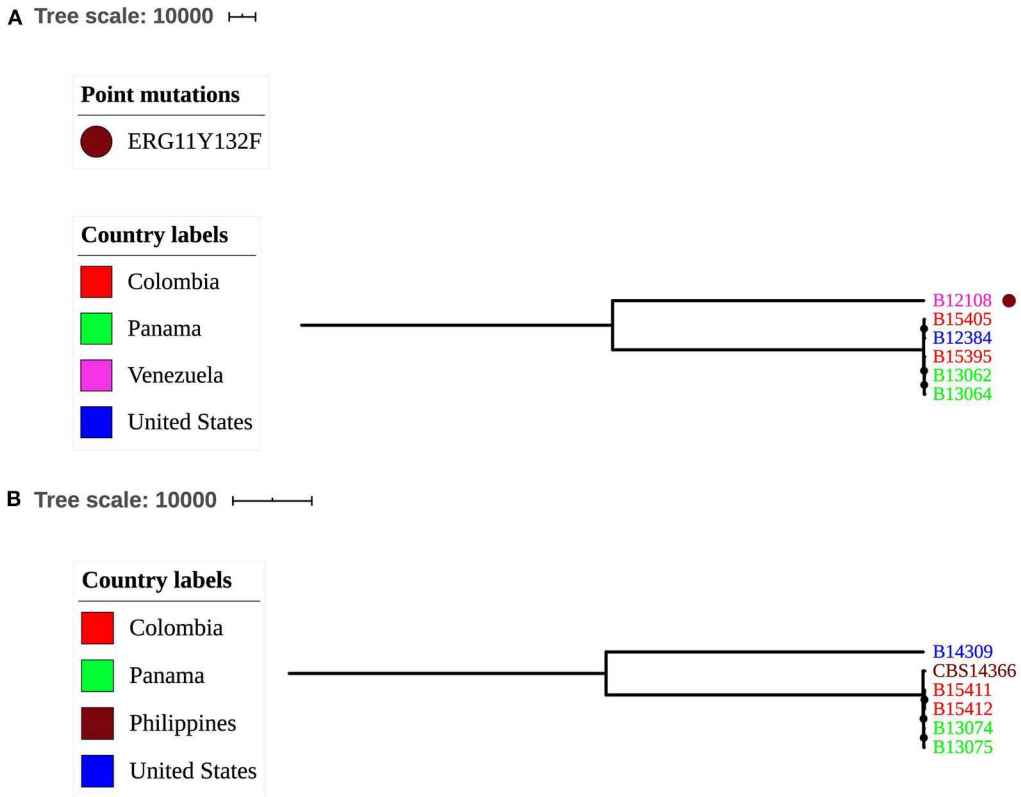

FIGURE 4 | Genetic relationships among *C. pseudohaemulonii* **(A)** and *C. vulturna* **(B)** isolates. Maximum parsimony trees were constructed using a total of 238,026 SNPs called against B12108 *C. pseudohaemulonii* reference genome (GenBank accession PKFO000000000) and 81,034 SNPs called against CBS14366 *C. vulturna* reference assembly Bio project PRJNA560499. Scale bar shows pairwise SNPs.

from Latin America were from blood. Many of the isolates from the United States were described as from foot or toe wounds, so it is possible that these species may be associated with diabetic foot infections although more epidemiological data is needed to show a definitive link. The reasons for this observed difference between the clinical presentations of the infections in the United States and Latin America are not entirely clear. One possible explanation may be that, compared to the United States, fewer *Candida* from non-invasive sites are collected and identified in Latin America; therefore, isolates from the non-invasive sites may be less likely to be reported. However, it is also possible that different infection control or clinical practices in Latin America led to more *C. haemulonii* and *C. duobushaemulonii* invasive infections. Notably, almost all azole-resistant isolates of *C. haemulonii* and *C. duobushaemulonii* were found in Latin America. Regardless of their geographic origin, all isolates of *C. pseudohaemulonii* were from blood. Whether this is truly a difference in the epidemiology among the species remains to be determined as only a few isolates of this species were available.

Population genetic analysis demonstrated that most isolates of *C. haemulonii*, *C. duobushaemulonii*, *C. pseudohaemulonii,* and *C. vulturna* were genetically distinct and do not yet show evidence of the extensive clonality that can be a sign of global emergence. However, we identified several nearly identical isolates of *C. duobushaemulonii* and *C. haemulonii* in different patients in one hospital in Panama, which reported outbreaks of *C. duobushaemulonii* and *C. auris* (Araúz et al., 2018). This finding indicates that both species are capable of transmission and causing outbreaks in healthcare settings. The reasons for the simultaneous outbreaks of *C. auris*, *C. haemulonii,* and *C. duobushaemulonii* in this hospital are unknown. Likely factors include a large patient population and poor infection control practices. It is also possible that some unique clinical practices in this facility, such as extensive use of azoles, might have contributed to multiple outbreaks. Notably, all *C. haemulonii* and *C. duobushaemulonii* from the outbreaks in this hospital were carrying *ERG11* mutations, and most had elevated MICs to fluconazole.

The overall genomic diversity (π) in the *C. haemulonii* population was relatively low and comparable with that observed in different clades of *C. auris*; no phylogeographic population substructure was observed. Although isolates of *C. haemulonii* var. *vulnera* were identified by others based on sequencing the ITS region of rDNA (Cendejas-Bueno et al., 2012), we were unable to confirm this observation with genomic data. Indeed, three isolates identified by MALDI-TOF as *C. haemulonii* var. *vulnera* were indistinguishable

TABLE 3 | Antifungal susceptibility profiles and *ERG11* point mutations.

Strain or Isolate	MIC (μg/mL)									*ERG11* point mutations
	Broth microdilution								E test	
	VOR	AND	CAS	FZ	IZ	ISA	PZ	MF	AMB	
C. haemulonii										
B10441	0.03	0.06	0.03	8	0.06	0.016	<0.008	0.016	1.5	
B11786	0.125	0.06	0.06	64	0.5	0.125	<0.008	0.03	1	Y132F
B11792	0.03	0.06	0.06	4	0.125	0.03	<0.008	0.03	16	
B11798	0.03	0.06	0.06	128	0.5	0.125	<0.008	0.06	3	Y132F
B11803	0.06	0.06	0.03	64	0.06	0.03	<0.008	0.03	0.75	Y132F
B11898	0.016	0.125	0.125	4	0.25	0.03	0.03	0.125	12	
B11899	<0.008	0.25	0.125	4	0.5	0.125	0.06	0.06	1.5	
B11900	0.03	0.06	0.03	8	0.06	0.016	<0.008	0.016	0.75	
B12068	0.06	0.125	0.125	16	0.5	0.5	0.25	0.06	4	
B12109	0.06	0.06	0.03	8	0.06	0.03	<0.008	0.03	2	
B12112	<0.008	0.03	1	256	0.5	0.25	0.016	0.03	0.75	Y132F
B12126	NG	0.03	0.06	8	0.5	0.03	0.03	0.03	0.125	
B12127	<0.008	0.125	16	256	2	1	0.5	0.016	24	Y132F
B12128	NG	0.125	0.06	2	0.25	0.016	0.016	0.125	6	
B12129	0.03	0.03	0.06	4	0.06	0.016	<0.008	0.03	1.5	
B12185	<0.008	0.125	0.06	2	0.06	0.008	0.016	0.06	2	
B12201	<0.008	0.03	0.03	4	0.5	0.03	0.03	0.06	1	
B12343	0.03	0.06	0.03	4	0.5	0.06	0.125	0.06	3	
B12615	0.03	0.06	0.125	4	0.25	0.06	0.03	0.06	0.38	
B12643	0.06	0.06	0.06	8	0.25	0.016	0.016	0.06	1.5	
B12989	0.016	0.03	0.03	2	0.016	<0.04	NG	0.016	12	
B13065	0.03	0.03	0.03	4	0.5	0.03	0.03	0.06	3	
B13067	0.06	0.06	0.03	8	0.06	0.03	0.016	0.03	32	Y132F
B13068	0.03	0.06	0.03	32	0.03	0.016	0.016	<0.008	4	Y132F
B13081	0.03	0.03	0.03	32	0.03	0.008	<0.008	0.016	1	Y132F
B13273	<0.008	0.06	0.03	2	9.25	0.008	0.016	0.03	12	
B13444	0.03	0.06	0.03	4	0.25	0.03	0.03	0.03	16	
B13704	0.03	0.03	0.03	4	0.5	0.03	0.06	0.03	12	
B13909	0.03	0.06	0.06	4	0.5	0.03	0.03	0.06	>32	
B15318	0.03	0.125	0.06	4	0.5	0.03	0.06	0.125	>32	
B15393	0.03	0.03	0.03	4	0.5	0.06	0.125	0.06	3	
B15394	0.03	0.06	0.06	4	0.25	0.03	0.016	0.06	16	
B15400	0.125	0.125	0.03	16	0.5	0.25	0.25	0.06	2	
B15401	0.03	0.25	0.125	4	0.125	0.016	0.016	0.06	3	
B15406	0.06	0.03	0.06	8	0.25	0.03	0.03	0.06	4	
B15408	0.03	0.06	0.06	2	0.125	0.016	<0.008	0.03	0.75	
B15409	0.03	0.125	0.06	4	0.125	0.03	<0.008	0.06	3	
B16299	0.03	0.06	0.03	8	0.125	0.06	0.016	0.06	1.5	
C. duobushaemulonii										
B09383	0.06	0.016	0.016	8	0.125	0.03	0.06	0.06	>32	
B10440	0.06	0.06	0.03	8	0.125	0.03	<0.008	0.06	16	
B11839	0.06	0.125	0.125	8	0.25	0.06	0.016	0.06	32	
B12075	0.03	0.06	0.125	8	0.25	0.016	0.03	0.06	12	
B12111	0.06	0.06	0.03	8	0.06	0.03	<0.008	0.03	32	
B12240	0.125	0.03	0.03	16	1	0.125	0.25	0.016	0.064	
B12437	0.03	1	0.25	2	0.25	0.016	0.03	0.25	0.25	

(Continued)

TABLE 3 | Continued

Strain or Isolate	MIC (μg/mL)									*ERG11* point mutations			
	Broth microdilution								E test				
	VOR	AND	CAS	FZ	IZ	ISA	PZ	MF	AMB				
B12484	0.5	0.25	0.06	16	1	0.25	0.25	0.06	>32				
B12492	0.125	0.25	0.125	4	0.25	0.03	0.125	0.06	>32				
B12539	0.06	0.06	0.06	4	0.03	0.03	0.125	0.125	>32				
B12593	0.06	0.125	0.06	16	0.06	0.03	0.125	0.125	>32				
B12594	0.06	0.06	0.03	4	0.25	0.03	0.06	0.06	32				
B12613	1	0.5	0.25	16	0.5	0.5	0.5	0.125	>32				
B12614	0.06	0.125	0.125	16	0.25	0.06	0.016	0.06	24				
B12709	0.06	0.5	0.125	16	0.5	0.25	0.25	0.125	>32				
B12845	0.125	0.25	0.06	8	0.5	0.125	0.125	0.125	32				
B12848	0.06	0.125	0.06	8	0.5	0.03	0.06	0.06	>32				
B12972	0.06	0.06	0.125	16	0.5	0.125	0.125	0.06	32				
B12985	0.03	0.25	0.25	4	0.06	0.03	0.016	0.03	32				
B12987	0.06	0.25	0.125	16	0.5	0.06	0.06	0.125	24				
B12988	0.06	0.25	0.06	16	0.5	0.06	0.125	0.125	32				
B13055	0.03	0.06	0.06	8	0.125	0.03	0.016	0.03	32				
B13056	2	0.25	0.06	>256	0.5	0.125	0.03	0.03	24	Y132F			G307A
B13057	0.03	0.125	0.03	8	0.125	0.03	<0.008	0.03	16				
B13058	1	0.125	0.125	256	0.25	0.06	0.03	0.03	32	Y132F			G307A
B13059	2	0.125	0.125	256	0.25	0.06	0.03	0.03	32	Y132F			G307A
B13063	8	0.125	0.06	256	2	2	0.25	0.06	24		Y132H	G443D	
B13066	0.03	0.03	0.03	8	0.06	0.016	0.016	0.016	12				
B13071	0.03	0.125	0.06	8	0.06	0.016	<0.008	0.06	>32				
B13072	0.25	1	0.25	16	0.25	0.06	0.016	0.06	>32				
B13073	0.06	0.25	0.125	16	0.5	0.06	0.06	0.06	32				
B13076	1	0.06	0.03	256	0.25	0.06	0.016	0.03	32	Y132F			
B13088	2	1	0.25	256	0.5	0.125	0.03	0.06	16	Y132F			G307A
B13089	0.06	0.03	0.03	8	0.5	0.03	0.06	0.06	24				
B13091	0.03	0.06	0.03	2	0.125	0.016	0.016	0.06	16				
B13267	0.06	0.25	0.06	8	0.25	0.03	0.03	0.06	12				
B13331	0.125	0.125	0.06	16	0.5	0.06	0.03	0.06	32				
B13465	0.06	0.03	0.06	16	0.125	0.016	0.016	0.03	24				
B13467	0.06	0.125	0.06	4	0.25	0.03	0.03	0.06	0.25				
B13908	0.06	0.25	0.06	8	0.5	0.03	0.03	0.06	32				
B14153	0.03	0.125	0.03	8	0.25	0.03	0.03	0.03	>32				
B14185	0.03	0.06	0.03	8	0.125	0.016	0.016	0.03	0.38				
B14283	0.06	0.125	0.125	16	0.125	0.03	<0.008	0.06	12				
B15056	0.06	0.25	0.125	16	0.5	0.06	0.25	0.125	>32				
B15179	0.125	0.06	0.06	8	0.5	0.06	0.06	0.06	32				
B15319	0.03	0.125	0.125	8	0.25	0.03	0.03	0.125	>32				.
B15360	0.5	2	0.5	64	2	1	0.5	0.25	32				
B15396	0.03	0.06	0.03	8	0.25	0.03	0.03	0.06	16				
B15397	0.06	0.125	0.016	8	0.5	0.03	0.06	0.06	>32				
B15399	0.06	0.5	0.125	8	0.5	0.03	0.125	0.06	>32				
B15403	0.06	0.06	0.03	8	0.25	0.06	0.03	0.125	32				
B15407	0.06	0.03	0.06	8	0.25	0.03	0.03	0.06	32				
B15410	0.016	0.25	0.25	16	0.25	0.06	0.016	0.06	32				
B16327	0.06	0.25	0.125	8	0.5	0.06	0.125	0.06	>32				
B16366	0.03	0.06	0.03	8	0.25	0.03	0.016	0.03	12				

(Continued)

TABLE 3 | Continued

Strain or Isolate	MIC (μg/mL)									*ERG11* point mutations
	Broth microdilution								E test	
	VOR	AND	CAS	FZ	IZ	ISA	PZ	MF	AMB	
C. pseudohaemulonii										
B12108	1	0.06	0.016	128	0.125	0.016	<0.008	0.03	12	Y132F
B12384	0.125	0.125	0.03	32	0.25	0.125	0.03	0.06	>32	
B13062	0.03	0.125	0.03	2	0.016	0.008	<0.008	0.03	0.125	
B13064	0.03	0.06	0.06	8	0.06	0.016	NG	0.03	0.38	
B15395	0.06	0.06	0.06	8	0.06	0.06	<0.008	0.06	0.125	
B15405	0.03	0.25	0.03	8	0.06	0.03	<0.008	0.06	0.125	
C. vulturna										
B13074	0.03	0.5	16	8	0.06	0.125	0.016	0.06	24	
B13075	0.125	0.03	0.03	16	0.5	0.03	0.125	0.03	16	
B14309	0.06	0.06	0.03	8	0.5	0.03	0.06	0.06	>32	
B15411	0.06	0.06	0.06	16	0.5	0.5	0.125	0.03	8	
B15412	0.06	0.125	0.06	8	0.25	0.125	0.03	0.03	12	

MIC, minimum inhibitory concentration; VOR, Voriconazole; AND, Anidulafungin; CAS, Caspofungin; FZ, Fluconazole; IZ, Itraconazole; ISA, Isavuconazole; PZ, Posaconazole; MF, Micafungin; AMB, Amphotericin B; NG, No growth.

from other *C. haemulonii* strains, suggesting that databases need to be updated to correctly identify all *C. haemulonii*. Whereas, both mating types have been reported in different clades of *C. auris*, all *C. haemulonii* isolates were mating type alpha. The 58-year-old B10441 (CBS 5149) isolate recovered from fish in 1962 was not notably different from other contemporaneous strains, suggesting low genetic diversity in this species.

Compared with *C. haemulonii*, more diversity was observed among *C. duobushaemulonii* isolates: Two subclades separated by more than 600 SNPs were observed. The genomic diversity (π) in *C. duobushaemulonii* was almost twice that of *C. haemulonii*, which was probably reflective of the more complex population structure. However, the genome-wide Tajima's D estimates for both species were negative and consistent with clonally expanding populations. Comparable estimates of Tajima's D were obtained for three rapidly expanding clades of *C. auris* (Chow et al., 2020). Furthermore, similarly to *C. haemulonii*, all *C. duobushaemulonii* isolates in our study were also mating type alpha.

Antifungal susceptibility testing indicated that most isolates from *C. haemulonii* species complex had highly elevated MICs of amphotericin B. Specifically, 100% of *C. vulturna*, 93% of *C. duobushaemulonii*, 76% of *C. haemulonii,* and 33% of *C. pseudohaemulonii* showed elevated MICs of at least 2 μg/mL. Elevated MIC values of fluconazole were also common but not nearly as widespread as in *C. auris*. Approximately 13% of *C. duobushaemulonii*, 18% of *C. haemulonii*, and 33% of *C. pseudohaemulonii* had MICs of fluconazole of 32 μg/mL or higher, and all isolates of *C. vulturna* were susceptible to fluconazole. All isolates of all four species had low MIC values of echinocandins.

The majority of isolates with elevated MICs of fluconazole in *C. haemulonii*, *C. duobushaemulonii,* and *C. pseudohaemulonii* contained the Y132F substitution in *ERG11*, which is associated with azole resistance in *C. albicans* and *C. auris* Clades I and IV (Berkow and Lockhart, 2017; Muñoz et al., 2018). Furthermore, additional substitutions linked to azole resistance in *C. albicans* were identified in *C. duobushaemulonii* isolates from Panama that also had Y132F/H substitutions; however, it was unclear whether these additional substitutions further affected MIC levels of azoles. No previously described drug-related mutations in the *ERG11* gene (Berkow and Lockhart, 2017) were detected in *C. vulturna* isolates with elevated MICs, suggesting a different mechanism of resistance. All *C. haemulonii* and *C. duobushaemulonii* with elevated MICs of fluconazole were found in Colombia, Venezuela, and Panama. Only a single isolate of *C. pseudohaemulonii* with a moderately high MIC of fluconazole of 32 μg/mL was isolated in the U.S. state of Georgia, and no other fluconazole-resistant isolates were found in the United States despite testing a comparable number of isolates from the United States and Latin America. In addition, all isolates with the corresponding *ERG11* mutations and chromosomal duplications that can be linked to azole resistance were found only in Latin America. Additional non-synonymous substitutions were detected in other genes implicated in antifungal resistance in *Candida* (Arendrup and Patterson, 2017); however, more research is needed to evaluate the role of these substitutions in resistance to antifungal drugs. The list of the non-synonymous substitutions and annotated VCF files is provided in our study for other investigators who might be interested in addressing these questions (https://figshare.com/projects/Genome_sequencing_of_Candida_haemulonii_species_complex/80150 and **Supplementary Table 2**).

Our results indicate that, although we are not yet observing the widespread emergence of fungi for the *C. haemulonii* species complex as human pathogens, at least two of these species can be transmitted within a healthcare facility and may cause healthcare-associated outbreaks. Outbreak isolates of both species also had elevated MICs of azoles and had corresponding *ERG11* mutations and chromosomal duplications linked to resistance. The prevalence of these mutations and duplications among *C. haemulonii* and *C. duobushaemulonii* isolates from Latin America suggests that these species may be exposed to the same evolutionary pressure from azole drugs that may have contributed to the emergence of *C. auris*. Continued surveillance to monitor azole resistance and epidemiology of these species is warranted.

DATA AVAILABILITY STATEMENT

All whole genome sequence raw reads for this study can be found in the NCBI under the following Bio Project PRJNA606185.

ETHICS STATEMENT

The studies involving human participants were reviewed and approved by CDC's IRB-Committee 2. Written informed consent for participation was not required for this study in accordance with the national legislation and the institutional requirements.

AUTHOR CONTRIBUTIONS

LG and MS generated data. LG, JM, DW, and KF performed the analysis. EB, BJ, CC, and AL supervised the study. DC, KF, RR-C, PE, MD, RB-A, and AE-B provided the materials. LG, JM, and AL wrote the manuscript. LG, SL, and AL conceived the project.

FUNDING

CC and JM were supported by the National Institute of Allergy and Infectious Diseases, National Institutes of Health, Department of Health and Human Services, under award U19AI110818 to the Broad Institute. CC was a CIFAR fellow in the Fungal Kingdom Program.

ACKNOWLEDGMENTS

We would like to acknowledge Joyce Peterson, Ngoc Le, Colleen Lysen, and Natalie Nunnally from Mycotic Diseases Branch for processing and species identification of isolates.

SUPPLEMENTARY MATERIAL

The Supplementary Material for this article can be found online at: https://www.frontiersin.org/articles/10.3389/fgene.2020.00554/full#supplementary-material

REFERENCES

Araúz, A. B., Caceres, D. H., Santiago, E., Armstrong, P., Arosemena, S., Ramos, C., et al. (2018). Isolation of *Candida auris* from 9 patients in Central America: importance of accurate diagnosis and susceptibility testing. *Mycoses* 61, 44–47. doi: 10.1111/myc.12709

Arendrup, M. C., and Patterson, T. F. (2017). Multidrug-resistant *Candida*: epidemiology, molecular mechanisms, and treatment. *J. Infect. Dis.* 216(Suppl. 3), S445–S451. doi: 10.1093/infdis/jix131

Ben-Ami, R., Berman, J., Novikov, A., Bash, E., Shachor-Meyouhas, Y., Zakin, S., et al. (2017). Multidrug-resistant *Candida haemulonii* and *C. auris, Tel Aviv, Israel. Emerg. Infect. Dis.* 23:195. doi: 10.3201/eid2302.161486

Berkow, E. L., and Lockhart, S. R. (2017). Fluconazole resistance in *Candida* species: a current perspective. *Infect. Drug Resist.* 10:237. doi: 10.2147/IDR.S118892

Cendejas-Bueno, E., Kolecka, A., Alastruey-Izquierdo, A., Theelen, B., Groenewald, M., Kostrzewa, M., et al. (2012). Reclassification of the *Candida haemulonii* complex as *Candida haemulonii* (*C. haemulonii group I), C. duobushaemulonii sp. nov. (C. haemulonii group II), and C. haemulonii var. vulnera var. nov.:* three *multiresistant human pathogenic yeasts. J. Clin. Microbiol.* 50, 3641–3651. doi: 10.1128/JCM.02248-12

Chow, N. A., Gade, L., Batra, D., Rowe, L. A., Juieng, P., Ben-Ami, R., et al. (2018a). Genome sequence of a multidrug-resistant *Candida haemulonii* isolate from a patient with chronic leg ulcers in Israel. *Genome Announc.* 6, e00176-18. doi: 10.1128/genomeA.00176-18

Chow, N. A., Gade, L., Batra, D., Rowe, L. A., Juieng, P., Loparev, V. N., et al. (2018b). Genome sequence of the amphotericin B-resistant *Candida duobushaemulonii* strain B09383. *Genome Announc.* 6:e00204-18. doi: 10.1128/genomeA.00204-18

Chow, N. A., Muñoz, J. F., Gade, L., Berkow, E. L., Welsh, R. M., Forsberg, K., et al. (2020). Tracing the evolutionary history and global expansion of *Candida auris* using population genomic analyses. *MBio* 11, e03364-19. doi: 10.1128/mBio.03364-19

Chowdhary, A., Sharma, C., Duggal, S., Agarwal, K., Prakash, A., Singh, P. K., et al. (2013). New clonal strain of *Candida auris*, Delhi, India. *Emerg. Infect. Dis.* 19, 1670–1673. doi: 10.3201/eid1910.130393

CLSI (2008). *Reference Method for Broth Dilution Antifungal Susceptibility Testing of Yeasts: Approved Standard,* 3rd Edn, M27-A3. Wayne, PA: Clinical and Laboratory Standards Institute.

Gargeya, I. B., Pruitt, W. R., Meyer, S. A., and Ahearn, D. G. (1991). *Candida haemulonii* from clinical specimens in the USA. *J. Med. Vet. Mycol.* 29, 335–338. doi: 10.1080/02681219180000511

Hou, X., Xiao, M., Chen, S. C., Wang, H., Cheng, J. W., Chen, X. X., et al. (2016). Identification and antifungal susceptibility profiles of *Candida haemulonii* species complex clinical isolates from a multicenter study in China. *J. Clin. Microbiol.* 54, 2676–2680. doi: 10.1128/JCM.01492-16

Isla, G., Taverna, C. G., Szusz, W., Vivot, W., García-Effron, G., and Davel, G. (2017). *Candida haemulonii sensu lato*: update of the Determination of Susceptibility Profile in Argentina and Literature Review. *Curr Fung Infect Rep.* 11, 203–208. doi: 10.1007/s12281-017-0300-y

Jackson, B. R., Chow, N., Forsberg, K., Litvintseva, A. P., Lockhart, S. R., Welsh, R., et al. (2019). On the origins of a species: what might explain the rise of *Candida auris*? *J Fung.* 5:58. doi: 10.3390/jof5030058

Khan, Z. U., Al-Sweih, N. A., Ahmad, S., Al-Kazemi, N., Khan, S., Joseph, L., et al. (2007). Outbreak of fungemia among neonates caused by *Candida haemulonii* resistant to amphotericin B, itraconazole, and fluconazole. *J. Clin. Microbiol.* 45, 2025–2027. doi: 10.1128/JCM.00222-07

Kumar, S., Stecher, G., Li, M., Knyaz, C., and Tamura, K. (2018). MEGA X: molecular evolutionary genetics analysis across computing platforms. *Mol. Biol. Evol.* 5, 1547–1549. doi: 10.1093/molbev/msy096

Kurtz, S., Phillippy, A., Delcher, A. L., Smoot, M., Shumway, M., Antonescu, C., et al. (2004). Versatile and open software for comparing large genomes. *Genome Biol.* 5:R12. doi: 10.1186/gb-2004-5-2-r12

Letunic, I., and Bork, P. (2019). Interactive Tree Of Life (iTOL) v4: recent updates and new developments. *Nucleic Acids Res.* 47, W256–W259. doi: 10.1093/nar/gkz239

Li, H., and Durbin, R. (2009). Fast and accurate short read alignment with Burrows–Wheeler transform. *Bioinformatics* 25, 1754–1760. doi: 10.1093/bioinformatics/btp324

Muñoz, J. F., Gade, L., Chow, N. A., Loparev, V. N., Juieng, P., Berkow, E. L., et al. (2018). Genomic insights into multidrug resistance, mating and virulence in *Candida auris* and related emerging species. *Nat. Commun.* 9, 1–3. doi: 10.1038/s41467-018-07779-6

Navarro-Muñoz, J. C., de Jong, A. W., van den Ende, B. G., Haas, P. J., Then, E. R., Tap, R. M., et al. (2019). The high-quality complete genome sequence of the opportunistic fungal pathogen *Candida vulturna* CBS 14366 T. *Mycopathologia* 84, 731–734. doi: 10.1007/s11046-019-00404-0

Ramos, L. S., Figueiredo-Carvalho, M. H., Barbedo, L. S., Ziccardi, M., Chaves, A. L., Zancopé-Oliveira, R. M., et al. (2015). *Candida haemulonii* complex: species identification and antifungal susceptibility profiles of clinical isolates from Brazil. *J. Antimicrob. Chemother.* 70, 111–115. doi: 10.1093/jac/dku321

Satoh, K., Makimura, K., Hasumi, Y., Nishiyama, Y., Uchida, K., and Yamaguchi, H. (2009). Candida auris sp. nov., a novel ascomycetous yeast isolated from the external ear canal of an inpatient in a Japanese hospital. *Microbiol Immunol.* 53, 41–44. doi: 10.1111/j.1348-0421.2008.00083.x

Sipiczki, M., and Tap, R. M. (2016). *Candida vulturna* pro tempore sp. nov., a dimorphic yeast species related to the Candida haemulonis species complex isolated from flowers and clinical sample. *Int. J. Syst. Evol. Microb.* 66, 4009–4015. doi: 10.1099/ijsem.0.001302

Van Uden, N., and Kolipinski, M. C. (1962). Torulopsis haemulonii nov. spec. a yeast from the Atlantic Ocean. *Antonie Van Leeuwenhoek* 28, 78–80. doi: 10.1007/BF02538724

Disclaimer: The use of product names in this manuscript does not imply their endorsement by the U.S. Department of Health and Human Services. The finding and conclusions in this article are those of the authors and do not necessarily represent the views of the Centers for Disease Control and Prevention.

Conflict of Interest: DW was employed by the company IHRC, Inc.

The remaining authors declare that the research was conducted in the absence of any commercial or financial relationships that could be construed as a potential conflict of interest.

frontiers in Genetics

REVIEW
published: 30 June 2020
doi: 10.3389/fgene.2020.00699

Understanding Mucormycoses in the Age of "omics"

*Alexandra Y. Soare[1,2], Tonya N. Watkins[2†] and Vincent M. Bruno[1,2]**

[1] Department of Microbiology and Immunology, University of Maryland School of Medicine, Baltimore, MD, United States,
[2] Institute of Genome Sciences, University of Maryland School of Medicine, Baltimore, MD, United States

Mucormycoses are deadly invasive infections caused by several fungal species belonging to the subphylum Mucoromycotina, order *Mucorales*. Hallmarks of disease progression include angioinvasion and tissue necrosis that aid in fungal dissemination through the blood stream, causing deeper infections and resulting in poor penetration of antifungal agents to the site of infection. In the absence of surgical removal of the infected focus, antifungal therapy alone is rarely curative. Even when surgical debridement is combined with high-dose antifungal therapy, the mortality associated with mucormycoses is >50%. The unacceptably high mortality rate, limited options for therapy and the extreme morbidity of highly disfiguring surgical therapy provide a clear mandate to understand the molecular mechanisms that govern pathogenesis with the hopes of developing alternative strategies to treat and prevent mucormycoses. In the absence of robust forward and reverse genetic systems available for this taxonomic group of fungi, unbiased next generation sequence (NGS)-based approaches have provided much needed insights into our understanding of many aspects of Mucormycoses, including genome structure, drug resistance, diagnostic development, and fungus-host interactions. Here, we will discuss the specific contributions that NGS-based approaches have made to the field and discuss open questions that can be addressed using similar approaches.

Keywords: genomics, transcriptomics, mucormycosis, RNA-seq, WGS, emerging fungal disease

OPEN ACCESS

Edited by:
Christina A. Cuomo,
Broad Institute, United States

Reviewed by:
Alexander Idnurm,
The University of Melbourne, Australia
Victoriano Garre,
University of Murcia, Spain

****Correspondence:***
Vincent M. Bruno
vbruno@som.umaryland.edu

†Present address:
Tonya N. Watkins,
Meso Scale Diagnostics, Rockville, MA, United States

Specialty section:
This article was submitted to Evolutionary and Genomic Microbiology, a section of the journal Frontiers in Genetics

Received: *26 March 2020*
Accepted: *09 June 2020*
Published: *30 June 2020*

Citation:
Soare AY, Watkins TN and Bruno VM (2020) Understanding Mucormycoses in the Age of "omics". Front. Genet. 11:699. doi: 10.3389/fgene.2020.00699

INTRODUCTION

Mucormycoses are increasingly common, life-threatening, invasive fungal infections (IFI) that are caused by various fungal species belonging to the subphylum Mucoromycotina, order *Mucorales* (Ribes et al., 2000; Spellberg et al., 2005). *Mucorales* are fast-growing, thermotolerant fungi that are ubiquitous in soil, on fruit, dust, and decaying vegetation worldwide (Rogers, 2008; Petrikkos et al., 2012). They are commonly found in homes and one study indicated that *Mucorales* species were present in 98% of samples taken from home dust (Gravesen, 1978; Quandahl and Cooper, 2018). *Mucorales* are considered opportunistic pathogens, requiring a suppressed immune system or another underlying condition to cause disease, and are the third most common cause of IFIs in immunocompromised patients (Michael et al., 2006; Rogers, 2008; Tacke et al., 2014; Millon et al., 2015). Fatal mucormycosis infections can be initiated by inhalation, ingestion, or contamination of wounds with easily aerosolized spores from the environment (Michael et al., 2006).

Mucormycoses are associated with high morbidity and mortality, >50% and approaching 100% with disseminated infection despite aggressive tissue debridement and antifungal therapy

(Puebla, 2012; Katragkou et al., 2014). Generally, mucormycoses will spread widely and cause extensive tissue damage by the time infection is diagnosed (Puebla, 2012; Katragkou et al., 2014). *Mucorales* establish infection in immunocompromised individuals with predisposing risk factors including uncontrolled diabetes resulting in hyperglycemia and ketoacidosis (DKA), chemotherapy, hematological disease, organ transplantation, elevated blood iron, deferoxamine or corticosteroid therapy, among others (Ghuman and Voelz, 2017). *Mucorales* can also cause lethal infections in a broader and more heterogeneous population than other opportunistic molds including injection drug users, patients receiving prolonged antifungal treatment lacking activity against *Mucorales* (i.e., Voriconazole), and those exposed to recent hospital construction (Michael et al., 2006; Rammaert et al., 2012; Lewis et al., 2012; Bernal-Martinez et al., 2013). Immunocompetent victims of natural disasters (earthquakes, tsunamis, tornados, etc.) and traumatic accidents such as those resulting from burns and military-related combat are also susceptible to mucormycosis (Ibrahim et al., 2012; Ibrahim and Kontoyiannis, 2013).

There are currently 27 different *Mucorales* species, across 11 genera, that have been identified as a causative agent of mucormycosis (Roden et al., 2005; Gomes et al., 2011; Jeong et al., 2019; Walther et al., 2019b). Whole genome sequences are available for 21 of the 27[1]. *Rhizopus* species are the most common cause, accounting for ∼70% of all cases and are the most common organisms isolated from patients with mucormycosis (Ribes et al., 2000; Roden et al., 2005; Spellberg et al., 2005; Ibrahim and Kontoyiannis, 2013; Gebremariam et al., 2014; Walther et al., 2019a). *Mucor* spp. and *Lichtheimia* spp. are also a significant cause of these fungal infections in Europe with each causing ∼20% of the cases (Skiada et al., 2011), while *Apophysomyces* spp. are common clinical isolates in India (Chakrabarti and Singh, 2014). In all, the number of mucormycosis incidences is increasing and is estimated to be 500 cases per year in the United States (Spellberg et al., 2005; Michael et al., 2006). A prospective surveillance study of nearly 17,000 transplant recipients performed in 23 institutions during 2001–2006 reported that mucormycosis was the third most common IFI in stem cell transplant recipients, with invasive aspergillosis (IA) and invasive candidiasis being the first and second most common, respectively (Kontoyiannis et al., 2010; Mucormycosis Statistics, 2018). The National Institute of Allergy and Infectious Disease (NIAID) now classifies mucormycosis as an emerging infectious disease (Chibucos et al., 2016; NIAID, 2018). Importantly, the true prevalence of mucormycoses is difficult to determine. Since there are no reporting requirements for fungal infections, no national surveillance in the United States, a lack of accurate diagnostic assays, and a declining rate of autopsies in high-risk populations, the true number of mucormycosis infections per year is likely to be severely underestimated (Lewis et al., 2012; Ibrahim and Kontoyiannis, 2013; Walsh et al., 2014; Mucormycosis Statistics, 2018).

[1]https://www.ncbi.nlm.nih.gov/genome

Very little is known about the molecular mechanisms that govern pathogenesis of *Mucorales*, compared to better studied fungal pathogens such as *Candida albicans*, *Cryptococcus neoformans*, and *Aspergillus fumigatus*. This knowledge gap is due, in large part, to the genetic intractability of the *Mucorales*. Furthermore, the ability to make educated guesses and form hypotheses about *Mucorales* pathogenesis based on molecular mechanisms proven in other fungal pathogens is limited by the large evolutionary distance that separates *Mucorales* from Ascomycetes (e.g., *Candida, Aspergillus*) and Basidiomycetes (e.g., *Cryptococcus*). Specifically, Mucormycetes, which include all *Mucorales*, are thought to have diverged from a common ancestor with Ascomycetes and Basidiomycetes over 800 million years ago (Galagan et al., 2005). Gene deletion strategies have been developed for *Mucor circinelloides* and RNAi-based knock-down approaches have been used to study *M. circinelloides* and *Rhizopus delemar*. These strategies have provided valuable insights into the molecular pathogenesis of mucormycoses, but their overall use has been limited to only a handful of studies (Ibrahim et al., 2010; Gebremariam et al., 2014; Liu et al., 2015; Trieu et al., 2017; Vellanki et al., 2018; Garcia et al., 2018). In the absence of robust forward and reverse genetic systems, unbiased next generation sequence (NGS)-based approaches have provided important insights and exploratory avenues into understanding, diagnosing and developing desperately needed therapies for this emerging class of infections. Here, we review the specific contributions that NGS-based approaches have made toward the overall knowledge and understanding of *Mucorales* pathogenesis (**Figure 1**) helping to lead to the development of therapies to treat this disease.

INSIGHTS INTO *Mucorales* BIOLOGY AND VIRULENCE DETERMINANTS

Genome Architecture and Structure

Sequencing of the *R. delemar* stain 99–880 genome revealed a highly repetitive genome indicative of an ancestral whole-genome duplication (WGD) event, which resulted in the replication of gene families related to cell growth, signal transduction, and cell-wall synthesis (Ma et al., 2009). Similar patterns were seen in the genomes of *M. circinelloides* and *Phycomyces blakesleeanus*, a non-pathogenic member of the *Mucorales* order known for its phototrophic growth (Corrochano et al., 2016). Both fungi showed evidence of widespread genome duplication that was concurrent with *R. delemar*, suggesting that the WGD event occurred early in the Mucoromycotina subdivision lineage. Fungi in the mucoromycotina subdivision appear to have more duplicated regions than other fungal genomes; however, evidence of a WGD event is not found in all of them. While the whole genome sequence of *Lichtheimia corymbifera* indicates a high occurrence of gene duplication and expansion, there appears to be no evidence of WGD. Rather, the duplicative nature of the *L. corymbifera* genome appears to be mediated by the high occurrence of tandem duplications (Schwartze et al., 2014). This pattern was also observed in whole genome sequencing and comparison of *Apophysomyces* species, which demonstrated

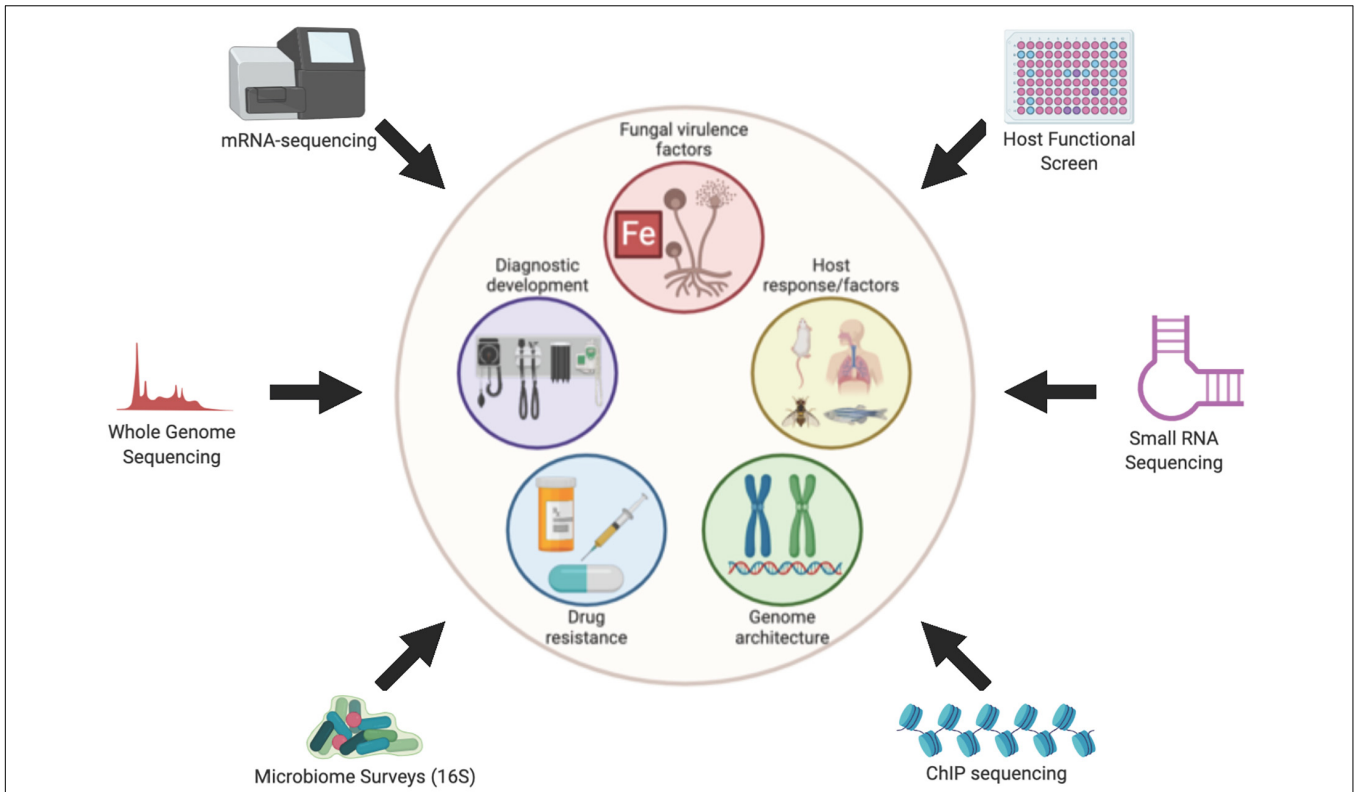

FIGURE 1 | Overview of Omics approaches used to study Mucormycoses. Figure created with BioRender.com.

extensive gene duplication and expansion across its genome but no evidence of a WGD (Prakash et al., 2017).

Other relevant features of *Mucorales* genomes have been elucidated through genome sequencing. *Rhizopus* species demonstrate remarkable variety in genome length, notably within *Rhizopus microsporus* (Gryganskyi et al., 2018). Additionally, there is wide variety in the structure of the mating type locus within *Rhizopus* genomes that vary from typical arrangements seen in Mucoralean fungi (Gryganskyi et al., 2018). Similar to *L. corymbifera* (Schwartze et al., 2014), *Apophysomyces* species had a lower number of transposable elements (TEs) in their genome when compared to other *Mucorales* species (Prakash et al., 2017). Both cases were associated with multiple copies of heterokaryon incompatibility (HET) genes and genes associated with RNA interference (RNAi) pathway (Schwartze et al., 2014; Prakash et al., 2017).

Chromatin immunoprecipitation sequencing (ChIP-seq) of *M. circinelloides* showed that it has a unique "mosaic" centromere structure in Mucoromycotina, with characteristics from point centromeres (seen in *Saccharomyces cerevisiae*) and regional centromeres (seen in *C. albicans, Candida tropicalis, Magnaporthe oryzae, Schizosaccharomyces pombe, and C. neoformans*) (Navarro-Mendoza et al., 2019).

Mucorales Growth and Metabolism

Various RNA-seq studies of *Mucorales* species have uncovered some basic principles regarding growth and metabolism. Little is known about the mechanisms behind spore germination, an important mechanism during filamentous growth as dormant spores transform to a vegetative state marked by hyphal growth. Germination and subsequent hyphal growth is responsible for the invasive nature of mucormycoses and can be initiated under multiple conditions. Sephton-Clark et al. (2018) performed a transcriptome analysis of *R. delemar* cells on a 24 h time course from dormant spores through germinating spores to full hyphal growth. Naturally, RNA from *R. delemar* spores collected at different time points after initiation of germination showed distinct transcriptional profiles (Sephton-Clark et al., 2018). Distinct gene clusters showed time-dependent expression in *R. delemar* in accordance with developmental stages of fungal growth. Most transcriptional changes occurred within the first hour of germination, followed by a period of "transcriptional consistency" during isotropic swelling. The transition to hyphal growth was marked by another shift in gene expression. Notably, hyphal growth of *R. delemar* was marked by an increase in transcripts involved in the reactive oxygen stress (ROS) response and respiration. Comparison to transcriptional data sets for *Aspergillus niger* showed similarities between the two fungi at the initiation of germination. However, there were transcriptional patterns for different metabolic processes that were uniquely regulated by *R. delemar* during isotropic and hyphal growth attributed by the authors to the duplicative nature of the *R. delemar* genome, which would require a more tightly regulated germination process (Sephton-Clark et al., 2018). This same

study also uncovered the increased expression of lipid storage and localization genes during the dormant spore stage (Sephton-Clark et al., 2018). It is likely these genes play a role in providing energy to the fungus in nutritionally deprived environment.

Other omics-based studies have demonstrated a role for lipid metabolism in *Mucorales*. In a transcriptome study comparing the transcriptome from *R. oryzae* in a mycelial morphology to a pellet-like morphology, Xu Q. et al. (2018) found that genes involved in fatty acid metabolism were amongst the differentially regulated genes. The genomes of a high-lipid and low-lipid producing *M. circinelloides* strain were sequenced and compared to elucidate potential determinants of lipid production (Tang et al., 2015). Transcriptomic analysis of *Cunninghamella echinulata* has provided some insight into mechanisms of lipid metabolism, including its ability to utilize trehalose as carbon source to produce gamma-linolenic acid (GLA) and changes in lipid metabolism according to long-term high temperature changes (Li et al., 2018, 2019).

Cases of primary cutaneous infection caused by *Myrmicaria irregularis* have increased, predominantly in China (Lu et al., 2013; Rammaert et al., 2014). Unlike most mucormycoses, *M. irregularis* infection has been characterized by chronic disease that is limited to the dermal and subcutaneous tissues. However, there is little understanding as to how *M. irregularis* adapts to the hypoxic environment of the skin. A comparison of the transcriptome of *M. irregularis* in normoxic and hypoxic atmospheres identified possible genetic determinants that allow *M. irregularis* to adapt to hypoxic conditions. Genes involved in lipid metabolism and endocytosis activation were upregulated in response to hypoxic conditions. This result was of significant interest since *M. irregularis* infections are often found in facial skin lesions where sebaceous glands are abundant (Sebum of sebaceous glands have high fatty acid concentrations). Furthermore, genes involved in carbon metabolism were downregulated, leading the authors to hypothesize that *M. irregularis* uses intracellular lipid pools rather than carbohydrates as an energy source (Xu W. et al., 2018).

The fungal cell wall plays an important role in the ability of *Mucorales* to survive in harsh conditions and its detection by the host immune system. One of the many gene families that were expanded by the WGD in *R. delemar* are genes involved in cell wall biosynthesis. The *R. delemar* genome contains nearly double the number of chitin synthases (CHS) and chitin deacetylases (CDA) encoding genes of other dikaryotic fungi (Ma et al., 2009). The expansions of the CHS- and CDA-encoding genes were also demonstrated in the genomes of 29 additional *Mucorales* species across 10 genera (Chibucos et al., 2016; Corrochano et al., 2016; Prakash et al., 2017). Genomic and transcriptomic studies have elucidated different ways in which *Mucorales* maintains and changes cell wall integrity. For example, in response to oxidative stress, *R. oryzae* upregulates genes related to chitin catabolism, most likely to reduce the chitin composition in its cell wall and reduce ROS-mediated damage (Xu Q. et al., 2018). Compared to other stages of germination, the transcriptome of *R. delemar* dormant spores show high levels of transcripts involved in chitin processes, suggesting that the turnover or degradation of the fungal cell wall may be an important process in the survival and maintenance of dormant *R. delemar* spores (Sephton-Clark et al., 2018). As expected, genes involved in cell wall biosynthesis and composition are differentially expressed as *R. delemar* undergoes germination. The identification of these genes by transcriptome analysis could allow researchers to target germination of *R. delemar* and prevent invasive mucormycosis. The genomes of *Apophysomyces* species show a unique profile of carbohydrate active enzymes (CAZymes) responsible for the generation of *Apophysomyces* cell wall polysaccharides, which may represent a novel antifungal target (Prakash et al., 2017). Difference patterns in CAZymes repertoire was also observed in the genomes of *Mucor* species that differed in lifestyle (Lebreton et al., 2020). Notably, *Mucor* species involved in cheese ripening had less CAZymes in their genome compared to more pathogenic and clinical isolates.

Steroids are a major component of fungal plasma membranes. The ergosterol biosynthesis pathway is conserved in *R. delemar* with multiple copies present for approximately half of the genes (Ma et al., 2009), However, there still remains a lot unknown about what mediates gene expression chances for steroid biosynthesis in *Mucorales*, the role of steroids in the cell wall composition, and differences within *Mucorales* species. For example, there is no significant difference in the expression of genes involves in steroid biosynthesis between *M. irregularis* strains in hypoxic versus nomoxic conditions (Xu W. et al., 2018).

Virulence and Pathogenicity

A combination of transcriptomics and comparative genomics have identified several potential novel virulence factors that can be targeted for mucormycosis therapy. Whole genome comparisons of virulent and avirulent strains of *M. circinelloides* identified nearly 800 genes that were truncated, discontiguous, or absent in the avirulent strain, suggesting that they may be candidate virulence factors (López-Fernández et al., 2018). Additionally, there are significant transcriptomic differences between virulent and avirulent strains of *M. circinelloides* undergoing germination inside macrophages. Specifically, genes involved in nutrition assimilation and metabolism were more highly expressed in the virulent strain than in the avirulent strain, which allows it to survive and germinate within a phagosome (Pérez-Arques et al., 2019). These processes appear to under the control of Aft1 and Atf2 transcription factors (Pérez-Arques et al., 2019).

Comparative genomics has allowed insight into the role of a family of spore coat proteins in host cell invasion. CotH3 has been identified as an invasin in *Mucorales* and treatment with anti-CotH3 antibodies has been shown inhibit endothelial cell invasion and protect mice from mucormycosis (Gebremariam et al., 2014). Comparing the genomes of multiple *Mucorales* strains showed that strains from species more commonly isolated from mucormycosis patients (*Mucor, Rhizopus, Rhizomucor, Cokeromyces,* and *Lichtheimia*) have 6–7 copies of the CotH-like genes (Gravesen, 1978; Michael et al., 2006) where strains isolated less frequently from infections (*Apophysomyces, Cunninghamella, Saksenae, Syncephalastrum,* and *Umbelopsis*) have 1–2 copies. In contrast, *Entomophorales* isolates, which are a taxa of fungi closely related to Mucoromycotina but

cause superficial infections, did not contain any CotH-like genes (Chibucos et al., 2016). One recent study claims that *Apophysomyces* spp. based on the examination of 3 genomes, have >15 copies of CotH-like genes (Prakash et al., 2017). The discordant estimation of CotH-like gene copy number in *Apophysomyces* spp. between the two studies (2 in Chibucos et al., 2016 versus >15 in Prakash et al., 2017) likely reflects the methods used to identify the gene family and highlights how the biological interpretation of genomic studies can be strongly biased by the analytical methods used. Additionally, correlations between CotH mRNA abundance and virulence can also be observed when comparing multiple species within a genus. When comparing the transcriptome of *Mucor* isolates that vary in lifestyles and clinical relevance, Lebreton et al. (2019) observed that the number of CotH transcripts were higher in pathogenic strains of *Mucor* compared to *Mucor* strains utilized in production.

Secreted proteases are another class of virulence factor that have been described for fungal pathogens, including *Mucorales*. Protease gene families are one of the many gene families that are expanded due to the WGD of *R. delemar*, and may account for its invasive nature (Ma et al., 2009). The genome of *L. corymbifera, Mucor* species and *Apophysomyces* species also contain a significant number of predicted secreted proteases (Schwartze et al., 2014; Prakash et al., 2017; Lebreton et al., 2020). A clinical isolate of *M*ucor *velutinosus*, which was previously not thought to be a major cause of mucormycosis, showed the presence of unique secreted aspartyl proteases which contribute to skin dissemination (Shelburne et al., 2015).

The production of secondary metabolites by fungi may account for virulence by acting as a secreted toxin. In 2013, a food-born illness outbreak occurred after a batch of Chobani yogurt was contaminated with a mold that the FDA identified as *M. circinelloides*. Whole genome analysis of the strain that caused the outbreak (named Mucho) identified multiple genes predicted to have a role in the production of secondary metabolites, indicating that production of toxins by Mucho may have been the cause of the food-borne outbreak (Lee et al., 2014). However, a comparative transcriptome analysis of different *Mucor* strains showed there was no difference in the number of transcripts involved in secondary metabolites between pathogenic and non-pathogenic strains of *Mucor*. However, it is worth noting that this study was done on *Mucor* strains grown on PDA medium and not under conditions that more closely resemble an infection (Lebreton et al., 2019).

Iron and Acquisition

Iron is a common currency required for survival for nearly all organisms. Microbes must utilize different pathways to acquire iron for growth and virulence. Commonly, microbes produce siderophores which are secreted from the organism to scavenge and bring back iron. However, sequencing of the *R. delemar* genome revealed the lack of non-ribosomal peptide synthetases (NRPs), which produce the most common siderophores used by microbes. Alternatively, the *R. delemar* genome encodes Rhizoferrin, a siderophore that collects free iron instead of serum-bound iron, and two copies of a gene encoding heme oxygenase (Ma et al., 2009). Transcriptomic analysis of *R. delemar* infected bone marrow derived macrophages (BMDM) showed an upregulation in iron acquisition genes, particularly *fet3*, a multicopper ferroxidase required for ferrous iron uptake and fungal dimorphism, and *ftr1,* a high affinity iron permease (Ibrahim et al., 2010; Andrianaki et al., 2018; Navarro-Mendoza et al., 2018). *Rhizopus* mutants with reduced *ftr1* copies showed reduced germination in BMDM phagosome following iron supplementation, demonstrating the essential role of iron acquisition for *Rhizopus* during macrophage infection (Andrianaki et al., 2018). Dormant *R. delemar* spores show an upregulation of genes involved in latter stages of iron-sulfur cluster biosynthesis compared to *R. delemar* undergoing germination. Initial phases of *R. delemar* germination are characterized by a rapid increase of iron acquisition transcripts (Sephton-Clark et al., 2018).

The genome of *L. corymbifera* contains multiple genes involved in iron acquisition, including multiple copies of the *ftr1*, which vary in levels of expression under iron limiting conditions (Schwartze et al., 2014). Transcriptomic analysis of *L. corymbifera* in iron-limiting conditions identified novel virulence factors, including potential transcription factors that act as key regulators in iron acquisition (Schwartze et al., 2014).

Similar to other *Mucorales* genomes, the *Apophysomyces* spp. lack genes encoding NRPs in their genomes and contain multiple genes involved in iron acquisition pathways, including genes in the reductive pathway and siderophores (Prakash et al., 2017). Sequencing of five different *Mucor* genomes from strains that represented different environments and lifestyles identified homologs of genes involved in different mechanisms of iron acquisition. Similar to *R. delemar*, the results suggested that *Mucor* species relied predominantly on Rhizoferrin for iron acquisition (Lebreton et al., 2020). However, the two strains associated with cheese production showed a reduced number of genes related to iron acquisition.

RNAi Silencing Pathways in *Mucorales*

RNA interference pathways are highly conserved among eukaryotes as a way of negatively regulating gene expression through small non-coding RNAs or short RNAs (sRNAs) (Billmyre et al., 2013). The canonical RNAi pathway generates double stranded RNA (dsRNA) by RNA-dependent RNA polymerases (RdRPs), which are then processed by Dicer enzymes to produce the sRNAs. In turn, these endogenous sRNAs are used to repress various target sequences (Meister and Tuschl, 2004). High throughput sequencing of small RNAs from a wild-type *M. circinelloides* strain, a strain carrying a deletion in *RdRP1*, and a strain carrying a deletion in *DCL2*, which encodes a *M. circinelloides* Dicer gene, revealed the identify of a new class of endogenous small RNAs that map to exons and regulate the expression of protein-coding genes from where they were produced (named exonic siRNAs) (Nicolas et al., 2010). The impact of these exonic siRNAs was further characterized in a follow-up study that examined the mRNA transcriptome of these mutants during different stages of vegetative growth (Nicolás et al., 2015). Deletion of genes involves in the canonical RNAi silencing machinery

resulted in significant mRNA accumulation during exponential and stationary growth phases of *M. circinelloides*. However, expression of many genes involved in processes such as growth at an acidic pH and sexual interaction were found to be unaltered in the RNAi machinery mutants, suggesting that these processes are regulated by a Dicer-independent non-canonical RNAi pathway (NCRIP) (Nicolás et al., 2015). Indeed, a NCRIP has recently been discovered in *M. circinelloides,* which relies on RdRP1 and R3B2, a novel RNase-III like protein required for cleavage activity. Transcriptomics on *rdrp1* and *r3b2* mutants demonstrated that these genes play important roles in regulating the fungal response to stressful environments, such as macrophage phagocytosis, as well as movement of TEs. These results that NCRIP play a role in controlling virulence in *M. circinelloides* (Pérez-Arques et al., 2020).

Recently, a novel role for RNAi machinery in *M. circinelloides* antifungal resistance has been elucidated through RNA sequencing on small RNAs. FK506 is an antifungal drug that interacts with the fungal FKBP12 isomerase, which inhibits protein phosphatase calcineurin, an important virulence factor in *M. circinelloides* that plays a key role in dimorphic transition. By blocking calcineurin, FK506 is able to block hyphal growth of *M. circinelloides* and restrict the fungus to yeast-phase growth (Calo et al., 2014). *M. circinelloides* can develop resistance to FK506 through Mendelian mutations in the *fkbA* gene, which encodes for FKB12. Additionally, *M. circinelloides* can exhibit a transient resistance to FK506 that is dependent on an epigenetic RNAi pathway. High throughput sequencing of small RNAs isolated from FK506-resistant epimutant strains of *M. circinelloides* revealed several sRNAs that are complementary to the *fkbA* mRNA (Calo et al., 2014). Establishment of these FK506-resistant epimutants is characterized by an abundance of these *fkbA*-targeting small RNAs to temporarily silence the expression of *fkbA* and prevent targeting by FK506 to inhibit hyphal growth.

This phenomenon was also observed in *M. circinelloides* epimutants that were resistant to 5-fluoroorotic acid (5-FOA), which is converted into a toxin by two genes, orotate phosphoribosyltransferase (*pyrF*) and orotidine-5′monophosphate decarboxylase (*pyrG*) in the uracil biosynthetic pathway (Chang et al., 2019). Sequencing of small RNAs from 5-FOA resistant mutants showed a significant increase in sense and antisense sRNAs against *pyrF* and *pyrG*, which correlated with reduced gene expression (Chang et al., 2019). The identification of transient 5-FOA resistant *M. circinelloides* epimutants, along with transient mutants against FK506, suggests that RNAi-dependent epimutation may be significant mechanism of antifungal resistance for *Mucorales*. More research is necessary to determine if this phenomenon is used by other species of *Mucorales* and how this mechanism might contribute the high rates of clinical antifungal resistance that are widely observed in *Mucorales* at large.

Extracellular Vesicles

Extracellular vesicles (EV) are produced by nearly all cells and recent research has highlighted a role of fungal-derived EVs in cell-cell communication in fungi and pathogenesis (Joffe et al., 2016). These molecules can contain a variety of molecules, including small RNAs (Peres da Silva et al., 2015). Transcriptomic analysis on EVs from two clinical strains of *R. delemar* showed an abundance of extracellular small RNAs (exRNAs) that varied in types and length (Liu et al., 2018). Prediction programs for miRNA suggested that the majority of secreted miRNA targeted host genes, specifically those related to carbohydrate metabolism, secondary metabolite biosynthesis, and the two-component system. EVs containing exRNA have emerged as potential biomarkers in fungal infection (Peres da Silva et al., 2015, 2019). Some of the small EV-derived RNAs appear to be strain-specific, demonstrating their potential use in diagnostics (Liu et al., 2018).

INSIGHTS INTO THE HOST RESPONSE AND MECHANISMS

In addition to gaining a more complete understanding of *Mucorales* biology during infection, transcriptomics has provided insight into the host response during mucormycoses as well as important host-pathogen interactions that govern the progression of disease. RNA-seq analysis of airway epithelial cells infected with *R. delemar, R. Oryzae,* or *M. circinelloides* showed a significant enrichment of genes that are known to be targets of platelet derived growth factor receptor B (PDGFRB) signaling (Mucormycosis Statistics, 2018). This pathway was of significant interest due to the angioinvasive nature of mucormycosis and the its role in host cell invasion was confirmed with the use of small molecule inhibitors of PDGFRB in an *in vitro* infection.

Transcriptome analysis of murine lungs from early-stage infection (14 h) by *R. delemar* showed a significant enrichment of genes that are known to be targets of epidermal growth factor receptor (EGFR) signaling suggesting that the EGFR pathway was activated in response to *R. delemar*. Subsequent *in vitro* and *in vivo* infection experiments demonstrated that EGFR was indeed phosphorylated (activated) upon *Mucorales* infection and governed the ability of Mucorales to invade and damage host cells. Importantly, inhibition of EGFR by gefitinib, an FDA-approved small molecule inhibitor of EGFR phosphorylation, reduced the ability of *R. delemar* to invade host cells and increased survival in a murine model of pulmonary mucormycosis (Watkins et al., 2018).

Other laboratories have utilized transcriptomics in varying animal models to further characterize the host response during mucormycosis. Chamilos et al. (2008a) used a fruit fly model to show infection-induced gene regulation in flies infected with *R. oryzae* compared to uninfected. Many of these genes that were differentially regulated have homologs in humans. Notably, *R. oryzae* infected flies showed a down-regulation of genes involved in skeletal muscle repair and tissue reconstruction and an upregulation of immune-induced and stress response genes (Chamilos et al., 2008a). Additionally, López-Muñoz et al. (2018) utilized an adult zebrafish model to characterize the host response to *M. circinelloides*. In addition to confirming previously reported links between *M. circinelloides* sporangiospore size and virulence, the authors used transcriptomics to show a

robust inflammatory response in response to *M. circinelloides*, which was characterized by upregulation of genes involved in pro-inflammatory cytokines, such as IL-1β, TNF-α, and IL-22, complement factors, peptidoglycan recognition proteins (PGRP) and iron homeostasis (López-Muñoz et al., 2018). This study also demonstrated that host genes related to lipid transport activity were significantly down-regulated during a *M. circinelloides* infection (López-Muñoz et al., 2018).

Host transcriptome analysis of *R. delemar* infected primary murine BMDMs confirmed the importance of iron acquisition for *Rhizopus,* with the expression several iron metabolism related genes differentially expressed over the course of the *Rhizopus* infection (Andrianaki et al., 2018). This expression pattern was consistent with an M2 activation program, which is in line with previous research demonstrating a role of iron metabolism in macrophage polarization (Ganz, 2012; Agoro et al., 2018). Additionally, transcriptome analysis of different mucormycosis causing species showed minor but important differences in host gene expression, such as IL-1β, CD40LG, and the PKC complex (Chibucos et al., 2016).

Another study examined the transcriptome response of a murine macrophage cell line (J774.1) following phagocytosis of *Mucorales* strains. Pérez-Arques et al. (2019) compared the macrophage responses to a virulent and an avirulent isolate of *M. circinelloides*. The virulent strain elicited specific proinflammatory and apoptotic responses while the avirulent strain did not induce a robust transcriptional response (Pérez-Arques et al., 2019). These results provide a compelling case for inflammation and macrophage apoptosis being involved in the progression of disease cause by *M. circinelloides*.

Host functional screens can also reveal important fungus-host interactions. Wang et al. (2018) screened a panel of 528 lymphoblastoid cell lines, each derived from a different individual human, for *M. circinelloides*-induced production of basic fibroblast growth factor 2 (FGF2). FGF2 is a growth factor with important roles in angiogenesis, cell survival, tissue repair, and other biological processes (Wang et al., 2018). A genome-wide association study (GWAS) identified single nucleotide polymorphisms (SNPs) that are highly associated with the ability of host cells to produce FGF2 in response to *in vitro* infection with *M. circinelloides*. The genes containing these SNPs represent candidate host factors that potentially govern the interaction between *Mucorales* and humans.

GENOME-GUIDED DIAGNOSTIC DEVELOPMENT

A major unmet clinical need in the approach to mucormycoses is the lack of a test which allows early and accurate diagnosis. There are no biomarkers identified to detect mucormycoses (Kontoyiannis and Lewis, 2011). The established fungal diagnostics assays which target ß-D-glucan and galactomannan do not detect components of the *Mucorales* cell wall (Kontoyiannis and Lewis, 2011). The pathophysiology, mode of acquisition, and underlying risk factors for mucormycoses and aspergillosis are similar, yet the therapeutic approach to treating each of these diseases is very different. Complicating matters are the observations that (a) voriconazole administration (a frontline therapy to treat aspergillosis) is considered a risk factor for developing mucormycosis and (b) exposure to voriconazole can increase the virulence of *Mucorales* species (Lamaris et al., 2009; Kontoyiannis and Lewis, 2011; Millon et al., 2015). Rapid management of disease is further hindered because there are no specific symptoms allowing differentiation between mucormycoses and infections caused by other filamentous fungi (Tacke et al., 2014). Molecular detection tools are also few and have not undergone extensive clinical validation (Kontoyiannis and Lewis, 2011). As a result, routine clinical non-culture-based molecular-based methods as a single approach for mucormycosis diagnosis is not recommended (Kontoyiannis and Lewis, 2011). Early and accurate diagnosis remains the single most important barrier for improving survival of mucormycosis patients because early identification and treatment are critical before angioinvasion and necrosis become too extensive and dissemination occurs (Chamilos et al., 2008b; Kontoyiannis and Lewis, 2011). The benefits of early diagnosis include less extensive and disfiguring surgery for the removal of necrotized tissue since antifungal therapy alone, in the absence of surgical removal of the infected focus, is rarely curative (Kontoyiannis and Lewis, 2011; Millon et al., 2015).

Biopsy and culture from sterile sites are critical to distinguish mucormycoses from more common and more antifungal-sensitive molds, such as *Aspergillus* (Spellberg et al., 2005; Kontoyiannis and Lewis, 2011). Current diagnosis of mucormycosis relies heavily on morphological identification from cultures, radiology, and histopathology (Baldin et al., 2018). Immunohistochemical reagents that detect *Mucorales* in tissue are currently available, but these methods are limited in that they do not give species-level identification (Bernal-Martinez et al., 2013). Even when hyphae are seen by histopathology, fungal cultures are only positive in 50% of cases because of the fragile nature of aseptate hyphae, which are often damaged during tissue manipulation (Kontoyiannis and Lewis, 2011). These hyphal elements often accompany tissue necrosis and fungal angioinvasion (Spellberg et al., 2005; Kontoyiannis and Lewis, 2011).

The importance of early differentiation of *Mucorales* from other mold infections has generated great interest and need in the development of non-culture- and non-histopathology-dependent diagnostic tests such as detection of specific fungal antigens or nucleic acids by PCR. Whole genome sequencing of several isolates of several mucormycosis-causing species has uncovered a pan-*Mucorales* gene family that is not present in *Aspergillus* species (Gebremariam et al., 2014; Chibucos et al., 2016; Baldin et al., 2018). To this end, Baldin et al. (2018) have demonstrated that PCR amplification of CotH genes that are universally and uniquely present in *Mucorales* represent a promising target for a sensitive, reliable, and simple method for the early detection of mucormycosis (Gebremariam et al., 2014; Chibucos et al., 2016). Using just a single primer set, the CotH genes can be PCR-amplified from plasma, urine, and BAL samples 24 h post-infection from mice infected intratracheally with *R. delemar*, *R. oryzae*, *M. circinelloides*,

L. corymbifera, and *Cunninghamella bertholletiae* as well as in urine samples of patients with proven mucormycosis (Baldin et al., 2018). Species-level identification is important because clinically relevant Mucorales (*Mucor*, *Rhizopus*, and *Lictheimia* species) show varying resistance to antifungals (Chalupova et al., 2014). Further comparative genomic studies are required to identify species- and genus-specific targets.

FUTURE DIRECTIONS

The omics studies outlined here have provided valuable insights into many aspects surrounding mucormycosis and have collectively served as an exciting proof-of-principle that these types of approaches have the potential to uncover new and interesting biology, as well as clinically actionable information. Below, we discuss some of the major unanswered questions in the field as well as some exciting aspects of *Mucorales* biology that can be addressed using unbiased, systematic, genome-wide approaches. In each of the cases below, the omics approach has the potential to serve as a significant first step and should always be combined, if technically feasible, with more focused, functional follow-up studies.

Which fungal genes are expressed during infection? This fundamental question has been very difficult to address for technical reasons. Specifically, when extracting total RNA from a host sample that has been infected with any microbe, the signal from host transcripts typically overwhelms the signal from the infecting microbe and the pathogen RNA consists of only a tiny portion (0.1% or less) of the total RNA extracted. Enrichment strategies to selectively enrich fungal transcripts from a total RNA samples harvested from infected mouse tissues have been successfully applied to murine infection models of *C. albicans* (Amorim-Vaz et al., 2015) and *A. fumigatus* (Chung et al., 2018). Application of selective enrichment techniques to study *Mucorales* gene expression of isolates from different genera in the murine models of mucormycosis is sure to unearth important virulence genes that can ultimately serve as therapeutic targets or biomarkers for diagnostics.

Does the microbiome play a role in the establishment or progression of mucormycosis? To date only two studies have performed a microbiome survey in the context of infection (Shelburne et al., 2015; Mueller et al., 2019). Mueller et al. (2019) examined the gut microbiome (both bacterial and fungal) of mice infected with *M. circinelloides* in a model of gastrointestinal (GI) mucormycosis and found a significant decrease in the abundance of the bacteria *Akkermansia muciniphila*, a microbe known to be positively correlated with good health, in the GI tract following introduction of *M. circinelloides*. Given the recent connection between the gastrointestinal microbiome and antifungal immunity in the lung (Shao et al., 2019), it is conceivable that the gut microbiome may be relevant to progression of pulmonary mucormycosis as well as gastrointestinal mucormycosis. Shelburne et al. (2015) analyzed oral and fecal microbiomes of a single leukemia patient (AML) over the course of several weeks as they progressed through chemotherapy, development of neutropenia and to subsequent invasive mucormycosis infection caused by *M. velutinosus* which occurred amid a dysbiotic microbiome with low α-diversity, dominated by staphylococci. Many more studies are required to truly establish what role, if any, the microbiome plays in the interaction between *Mucorales* and the infected host.

How do bacterial endosymbionts of Mucorales affect disease establishment and progression? Both clinical and plant pathogenic isolates of Mucorales are known to harbor bacterial endosymbionts (Ibrahim et al., 2008). Some initial experiments suggested that the bacterial endosymbionts had no effect on the virulence potential of the fungus that they live inside of Ibrahim et al. (2008) but recent work has set a precedent for a role in evasion of host innate immune cells (Itabanga et al., 2019). Specifically, *Ralstonia pickettii* promotes the ability of *R. microsporus* to survive killing by macrophages (Itabanga et al., 2019). In a transcriptome-focused companion paper, Sephton-Clark et al. (2019) examined the transcriptional response of J774.1 macrophages following phagocytosis of *R. delemar* and *R. microsporus* either with or without their bacterial endosymbionts living inside them. This study revealed that endosymbiont-cured *R. microsporus* elicited a much stronger pro-inflammatory response than did *R. microsporus* which contained the bacterial endosymbiont, consistent with increased ability of macrophages to kill *R. pickettii*-cured *R. microsporus*. These two studies provide a clear and exciting mandate for a more wide-spread analysis of the *Mucorales*-endosymbiont associations to determine how generalizable this phenomenon is to other *Mucorales*-host interactions.

Mycoviruses (fungal viruses) and their effect on fungal hosts have been well-characterized in multiple fungal species, including fungi that are pathogenic to humans (Kotta-Loizou and Coutts, 2017). Of clinical interest are mycoviruses that increase or decrease fungal virulence (hypervirulence or hypovirulent, respectively) and confer a killer phenotype. Double-stranded RNA viral elements have been found in *Mucorales* species (Vágvölgyi et al., 1993, 1998; Papp et al., 2001); however, there have been little to no published attempts to further characterize these mycoviruses or identify novel *Mucorales* infecting mycoviruses. NGS-based approaches have already been utilized to discover and characterize mycoviruses in pathogenic fungi, including *Aspergillus* (Vainio et al., 2015; Zoll et al., 2018). This approach has already shown potential in the *Mucorales* field. Whole genome sequencing and phylogenomic comparison of *Rhizopus* species showed the presence of *pol* fragments from *Caulimovirus* (plant virus) in one-third of the analyzed genomes (Gryganskyi et al., 2018). Recently, a transcriptomic analysis of *M. irregularis* demonstrated the presence of a gene for a predicted RNA polymerase domain specific to a negative strand RNA virus (Barata et al., 2019). RNA sequencing has also led to the discovery of two *Narnavirus* members in *R. microsporus* in a novel fungal-bacterial-viral holobiont system (Espino-Vazquez et al., 2020). The role of these viruses in *Rhizopus* biology are still questioned but it is clear that they play a role of in *Rhizopus* biology. Infection of the viruses alone decreased asexual reproduction by reducing the number

of *R. microsporus* sporangiospores. However, co-infection of these *Narnaviruses* with a *Mycetohabitans* bacterial symbiont speared to be required for successful sexual reproduction of *M. microsporus*.

As we continue to use -omics based approaches to characterize mucormycosis causing fungi, an emphasis should be placed on their respective mycoviruses to obtain a more complete understanding of their biology. Beyond providing novel information on potential symbioses, mycovirus therapy presents a novel therapeutic solution for IFI, especially as resistance to anti-fungal treatments are on the rise (Van De Sande et al., 2010). Success in the use of bacteriophage to treat respiratory bacterial infections suggest that parallel results could occur through the use of mycoviruses, which has been explored for *Aspergillus* therapy (van de Sande and Vonk, 2019; Takahashi-Nakaguchi et al., 2020). Further discovery and characterizations of novel mycoviruses in *Mucorales* through -omics based approaches will not only offer a more complete biology of these fungi but may identify potential use of mycovirus therapy for mucormycoses.

AUTHOR CONTRIBUTIONS

AS and VB developed the ideas, wrote, and edited the manuscript. TW wrote the manuscript. All authors contributed to the article and approved the submitted version.

FUNDING

This work was funded with federal funds from the National Institute of Allergy and Infectious Diseases (NIAID), National Institutes of Health (NIH), Department of Health and Human Services, under U19AI110820 and R01AI141360 to VB.

REFERENCES

Agoro, R., Taleb, M., Quesniaux, V. F., and Mura, C. (2018). Cell iron status influences macrophage polarization. *PLoS One* 13:e0196921. doi: 10.1371/journal.pone.0196921

Amorim-Vaz, S., Tran Vdu, T., Pradervand, S., Pagni, M., Coste, A. T., and Sanglard, D. R. N. A. (2015). Enrichment method for quantitative transcriptional analysis of pathogens in vivo applied to the fungus candida albicans. *MBio* 6:e942-15. doi: 10.1128/mBio.00942-15

Andrianaki, A. M., Kyrmizi, I., Thanopoulou, K., Baldin, C., Drakos, E., Soliman, S. S. M., et al. (2018). Iron restriction inside macrophages regulates pulmonary host defense against *Rhizopus* species. *Nat. Commun.* 9:3333. doi: 10.1038/s41467-018-05820-2

Baldin, C., Soliman, S. S. M., Jeon, H. H., Alkhazraji, S., Gebremariam, T., Gu, Y., et al. (2018). PCR-Based approach targeting mucorales-specific gene family for diagnosis of mucormycosis. *J Clin. Microbiol.* 56:e00746-18. doi: 10.1128/JCM.00746-18

Barata, R. R., Vianez-Júnior, J. L., and Nunes, M. R. (2019). Transcriptomic analysis of *Mucor* irregularis containing a negative single-stranded RNA mycovirus. *Microbiol. Resour. Announc.* 8:e503-19.

Bernal-Martinez, L., Buitrago, M. J., Castelli, M. V., Rodriguez-Tudela, J. L., and Cuenca-Estrella, M. (2013). Development of a single tube multiplex real-time PCR to detect the most clinically relevant mucormycetes species. *Clin. Microbiol. Infect.* 19, E1–E7. doi: 10.1111/j.1469-0691.2012.03976.x

Billmyre, R. B., Calo, S., Feretzaki, M., Wang, X., and Heitman, J. (2013). RNAi function, diversity, and loss in the fungal kingdom. *Chromosome Res.* 21, 561–572. doi: 10.1007/s10577-013-9388-2

Calo, S., Shertz-Wall, C., Lee, S. C., Bastidas, R. J., Nicolás, F. E., Granek, J. A., et al. (2014). Antifungal drug resistance evoked via RNAi-dependent epimutations. *Nature* 513, 555–558. doi: 10.1038/nature13575

Chakrabarti, A., and Singh, R. (2014). Mucormycosis in India: unique features. *Mycoses* 57(Suppl. 3), 85–90. doi: 10.1111/myc.12243

Chalupova, J., Raus, M., Sedlarova, M., and Sebela, M. (2014). Identification of fungal microorganisms by MALDI-TOF mass spectrometry. *Biotechnol. Adv.* 32, 230–241. doi: 10.1016/j.biotechadv.2013.11.002

Chamilos, G., Lewis, R. E., and Kontoyiannis, D. P. (2008b). Delaying amphotericin B-based frontline therapy significantly increases mortality among patients with hematologic malignancy who have zygomycosis. *Clin. Infect. Dis.* 47, 503–509. doi: 10.1086/590004

Chamilos, G., Lewis, R. E., Hu, J., Xiao, L., Zal, T., Gilliet, M., et al. (2008a). Drosophila melanogaster as a model host to dissect the immunopathogenesis of zygomycosis. *Proc. Natl. Acad. Sci.* 105, 9367–9372. doi: 10.1073/pnas.0709578105

Chang, Z., Billmyre, R. B., Lee, S. C., and Heitman, J. (2019). Broad antifungal resistance mediated by RNAi-dependent epimutation in the basal human fungal pathogen *Mucor* circinelloides. *PLoS Genet.* 15:e1007957. doi: 10.1371/journal.pgen.1007957

Chibucos, M. C., Soliman, S., Gebremariam, T., Lee, H., Daugherty, S., Orvis, J., et al. (2016). An integrated genomic and transcriptomic survey of mucormycosis-causing fungi. *Nat. Commun.* 7:12218. doi: 10.1038/ncomms12218

Chung, M., Teigen, L., Liu, H., Libro, S., Shetty, A., Kumar, N., et al. (2018). Targeted enrichment outperforms other enrichment techniques and enables more multi-species RNA-Seq analyses. *Sci. Rep.* 8:13377. doi: 10.1038/s41598-018-31420-7

Corrochano, L. M., Kuo, A., Marcet-Houben, M., Polaino, S., Salamov, A., Villalobos-Escobedo, J. M., et al. (2016). Expansion of signal transduction pathways in fungi by extensive genome duplication. *Curr. Biol.* 26, 1577–1584.

Espino-Vazquez, A. N., Bermudez-Barrientos, J. R., Cabrera-Rangel, J. F., Cordova-Lopez, G., Cardoso-Martinez, F., Martinez-Vazquez, A., et al. (2020). Narnaviruses: novel players in fungal-bacterial symbioses. *ISME J.* Online ahead of print doi: 10.1038/s41396-020-0638-y

Galagan, J. E., Henn, M. R., Ma, L. J., Cuomo, C. A., and Birren, B. (2005). Genomics of the fungal kingdom: insights into eukaryotic biology. *Genome Res.* 15, 1620–1631. doi: 10.1101/gr.3767105

Ganz, T. (2012). Macrophages and systemic iron homeostasis. *J. Innate Immun.* 4, 446–453. doi: 10.1159/000336423

Garcia, A., Vellanki, S., and Lee, S. C. (2018). Genetic tools for investigating *Mucorales* fungal pathogenesis. *Curr. Clin. Microbiol. Rep.* 5, 173–180. doi: 10.1007/s40588-018-0097-7

Gebremariam, T., Liu, M., Luo, G., Bruno, V., Phan, Q. T., Waring, A. J., et al. (2014). CotH3 mediates fungal invasion of host cells during mucormycosis. *J. Clin. Invest.* 124, 237–250. doi: 10.1172/JCI71349

Ghuman, H., and Voelz, K. (2017). Innate and adaptive immunity to *Mucorales*. *J. Fungi* 3:48 doi: 10.3390/jof3030048

Gomes, M. Z., Lewis, R. E., and Kontoyiannis, D. P. (2011). Mucormycosis caused by unusual mucormycetes, Non-Rhizopus, -*Mucor*, and -*Lichtheimia* species. *Clin. Microbiol. Rev.* 24, 411–445. doi: 10.1128/CMR.00056-10

Gravesen, S. (1978). Identification and prevalence of culturable mesophilic microfungi in house dust from 100 Danish homes. comparison between airborne and dust-bound fungi. *Allergy* 33, 268–272. doi: 10.1111/j.1398-9995.1978.tb01547.x

Gryganskyi, A. P., Golan, J., Dolatabadi, S., Mondo, S., Robb, S., Idnurm, A., et al. (2018). Phylogenetic and phylogenomic definition of *Rhizopus* species. *G3* 8, 2007–2018. doi: 10.1534/g3.118.200235

Ibrahim, A. S., and Kontoyiannis, D. P. (2013). Update on mucormycosis pathogenesis. *Curr. Opin. Infect. Dis.* 26, 508–515. doi: 10.1097/qco.0000000000000008

Ibrahim, A. S., Gebremariam, T., Lin, L., Luo, G., Husseiny, M. I., Skory, C. D., et al. (2010). The high affinity iron permease is a key virulence factor required

for Rhizopus oryzae pathogenesis. *Mol. Microbiol.* 77, 587–604. doi: 10.1111/j.1365-2958.2010.07234.x

Ibrahim, A. S., Gebremariam, T., Liu, M., Chamilos, G., Kontoyiannis, D., Mink, R., et al. (2008). Bacterial endosymbiosis is widely present among zygomycetes but does not contribute to the pathogenesis of mucormycosis. *J. Infect. Dis.* 198, 1083–1090. doi: 10.1086/591461

Ibrahim, A. S., Spellberg, B., Walsh, T. J., and Kontoyiannis, D. P. (2012). Pathogenesis of mucormycosis. *Clin. Infect. Dis.* 54(Suppl. 1), S16–S22. doi: 10.1093/cid/cir865

Itabanga, H., Sephton-Clark, P., Zhou, X., Insua, I., Probert, M., Correia, J., et al. (2019). A bacterial endosymbiont enables fungal immune evasion during fatal mucormycete infection. *bioRXiv [Preprint]* doi: 10.1101/584607

Jeong, W., Keighley, C., Wolfe, R., Lee, W. L., Slavin, M. A., Kong, D. C. M., et al. (2019). The epidemiology and clinical manifestations of mucormycosis: a systematic review and meta-analysis of case reports. *Clin. Microbiol. Infect.* 25, 26–34. doi: 10.1016/j.cmi.2018.07.011

Joffe, L. S., Nimrichter, L., Rodrigues, M. L., and Del Poeta, M. (2016). Potential roles of fungal extracellular vesicles during infection. *mSphere* 1:e99-16. doi: 10.1128/mSphere.00099-16

Katragkou, A., Walsh, T. J., and Roilides, E. (2014). Why is mucormycosis more difficult to cure than more common mycoses? *Clin. Microbiol. Infect.* 20(Suppl. 6), 74–81. doi: 10.1111/1469-0691.12466

Kontoyiannis, D. P., and Lewis, R. E. (2011). How I treat mucormycosis. *Blood* 118, 1216–1224. doi: 10.1182/blood-2011-03-316430

Kontoyiannis, D. P., Marr, K. A., Park, B. J., Alexander, B. D., Anaissie, E. J., Walsh, T. J., et al. (2010). Prospective surveillance for invasive fungal infections in hematopoietic stem cell transplant recipients, 2001-2006: overview of the transplant-associated infection surveillance network (TRANSNET) database. *Clin. Infect. Dis.* 50, 1091–1100. doi: 10.1086/651263

Kotta-Loizou, I., and Coutts, R. H. (2017). Mycoviruses in *Aspergilli*: a comprehensive review. *Front. Microbiol.* 8:1699. doi: 10.3389/fmicb.2017.01699

Lamaris, G. A., Ben-Ami, R., Lewis, R. E., Chamilos, G., Samonis, G., and Kontoyiannis, D. P. (2009). Increased virulence of Zygomycetes organisms following exposure to voriconazole: a study involving fly and murine models of zygomycosis. *J. Infect. Dis.* 199, 1399–1406. doi: 10.1086/597615

Lebreton, A., Corre, E., Jany, J.-L., Brillet-Guéguen, L., Pèrez-Arques, C., Garre, V., et al. (2020). Comparative genomics applied to *Mucor* species with different lifestyles. *BMC Genom.* 21:135. doi: 0.1186/s12864-019-6256-2

Lebreton, A., Meslet-Cladière, L., Morin-Sardin, S., Coton, E., Jany, J.-L., Barbier, G., et al. (2019). Comparative analysis of five *Mucor* species transcriptomes. *Genomics* 111, 1306–1314. doi: 10.1016/j.ygeno.2018.09.003

Lee, S. C., Billmyre, R. B., Li, A., Carson, S., Sykes, S. M., Huh, E. Y., et al. (2014). Analysis of a food-borne fungal pathogen outbreak: virulence and genome of a Mucor circinelloides isolate from yogurt. *MBio* 5:e1390-14.

Lewis, R. E., Lortholary, O., Spellberg, B., Roilides, E., Kontoyiannis, D. P., and Walsh, T. J. (2012). How does antifungal pharmacology differ for mucormycosis versus aspergillosis? *Clin. Infect. Dis.* 54(Suppl. 1), S67–S72. doi: 10.1093/cid/cir884

Li, S., Yu, H., Liu, Y., Zhang, X., and Ma, F. (2019). The lipid strategies in *Cunninghamella echinulata* for an allostatic response to temperature changes. *Proc. Biochem.* 76, 85–94. doi: 10.1016/j.procbio.2018.11.005

Li, S., Yue, Q., Zhou, S., Yan, J., Zhang, X., and Ma, F. (2018). Trehalose contributes to gamma-linolenic acid accumulation in *Cunninghamella echinulata* based on de novo transcriptomic and lipidomic analyses. *Front. Microbiol.* 9:1296. doi: 10.3389/fmicb.2018.01296

Liu, M., Bruni, G. O., Taylor, C. M., Zhang, Z., and Wang, P. (2018). Comparative genome-wide analysis of extracellular small RNAs from the mucormycosis pathogen *Rhizopus* delemar. *Sci. Rep.* 8, 1–10.

Liu, M., Lin, L., Gebremariam, T., Luo, G., Skory, C. D., French, S. W., et al. (2015). Fob1 and Fob2 proteins are virulence determinants of *Rhizopus* oryzae via facilitating iron uptake from ferrioxamine. *PLoS Pathog.* 11:e1004842. doi: 10.1371/journal.ppat.1004842

López-Fernández, L., Sanchis, M., Navarro-Rodríguez, P., Nicolás, F. E., Silva-Franco, F., Guarro, J., et al. (2018). Understanding *Mucor* circinelloides pathogenesis by comparative genomics and phenotypical studies. *Virulence* 9, 707–720. doi: 10.1080/21505594.2018.1435249

López-Muñoz, A., Nicolás, F. E., García-Moreno, D., Pérez-Oliva, A. B., Navarro-Mendoza, M. I., Hernández-Oñate, M. A., et al. (2018). An adult zebrafish model reveals that mucormycosis induces apoptosis of infected macrophages. *Sci. Rep.* 8, 1–12.

Lu, X. L., Najafzadeh, M. J., Dolatabadi, S., Ran, Y. P., Gerrits van den Ende, A. H. G., Shen, Y. N., et al. (2013). Taxonomy and epidemiology of *Mucor* irregularis, agent of chronic cutaneous mucormycosis. *Persoonia* 30, 48–56. doi: 10.3767/003158513X665539

Ma, L. J., Ibrahim, A. S., Skory, C., Grabherr, M. G., Burger, G., Butler, M., et al. (2009). Genomic analysis of the basal lineage fungus *Rhizopus* oryzae reveals a whole-genome duplication. *PLoS Genet* 5:e1000549. doi: 10.1371/journal.pgen.1000549

Meister, G., and Tuschl, T. (2004). Mechanisms of gene silencing by double-stranded RNA. *Nature* 431, 343–349. doi: 10.1038/nature02873

Michael, A., Pfaller, P. G. P., and John, R. (2006). Wingard invasive fungal pathogens: current epidemiological trends. *Clin. Infect. Dis.* 43, S3–S14.

Millon, L., Herbrecht, R., Grenouillet, F., Morio, F., Alanio, A., Letscher-Bru, V., et al. (2015). Early diagnosis and monitoring of mucormycosis by detection of circulating DNA in serum: retrospective analysis of 44 cases collected through the French surveillance network of invasive fungal infections (RESSIF). *Clin. Microbiol. Infect.* doi: 10.1016/j.cmi.2015.12.006

Mucormycosis Statistics (2018). *Mucormycosis Statistics*. Available online at: https://www.cdc.gov/fungal/diseases/mucormycosis/statistics.html (accessed March 1, 2020).

Mueller, K. D., Zhang, H., Serrano, C. R., Billmyre, R. B., Huh, E. Y., Wiemann, P., et al. (2019). Gastrointestinal microbiota alteration induced by *Mucor* circinelloides in a murine model. *J. Microbiol.* 57, 509–520. doi: 10.1007/s12275-019-8682-x

Navarro-Mendoza, M. I., Perez-Arques, C., Murcia, L., Martinez-Garcia, P., Lax, C., Sanchis, M., et al. (2018). Components of a new gene family of ferroxidases involved in virulence are functionally specialized in fungal dimorphism. *Sci. Rep.* 8:7660. doi: 10.1038/s41598-018-26051-x

Navarro-Mendoza, M. I., Pérez-Arques, C., Panchal, S., Nicolás, F. E., Mondo, S. J., Ganguly, P., et al. (2019). Early diverging fungus *Mucor* circinelloides lacks centromeric histone CENP-A and displays a mosaic of point and regional centromeres. *Curr. Biol.* 29, 3791.–3802.

NIAID (2018). *Emerging Infectious Diseases/Pathogens*. Available online at: https://www.niaid.nih.gov/research/emerging-infectious-diseases-pathogens (accessed March 1, 2020).

Nicolas, F. E., Moxon, S., de Haro, J. P., Calo, S., Grigoriev, I. V., Torres-Martínez, S., et al. (2010). Endogenous short RNAs generated by Dicer 2 and RNA-dependent RNA polymerase 1 regulate mRNAs in the basal fungus *Mucor* circinelloides. *Nucleic Acids Res.* 38, 5535–5541. doi: 10.1093/nar/gkq301

Nicolás, F. E., Vila, A., Moxon, S., Cascales, M. D., Torres-Martínez, S., Ruiz-Vázquez, R. M., et al. (2015). The RNAi machinery controls distinct responses to environmental signals in the basal fungus *Mucor* circinelloides. *BMC Genom.* 16:237. doi: 10.1186/s12864-015-1443-2

Papp, T., Nyilasi, I., Fekete, C., Ferenczy, L., and Vágvölgyi, C. (2001). Presence of double-stranded RNA and virus-like particles in *Rhizopus* isolates. *Can. J. Microbiol.* 47, 443–447. doi: 10.1139/w01-020

Peres da Silva, R., Longo, L. G. V., Cunha, J. P. C. D., Sobreira, T. J. P., Rodrigues, M. L., Faoro, H., et al. (2019). Comparison of the RNA content of extracellular vesicles derived from *Paracoccidioides brasiliensis* and *Paracoccidioides lutzii*. *Cells* 8:765. doi: 10.3390/cells8070765

Peres da Silva, R., Puccia, R., Rodrigues, M. L., Oliveira, D. L., Joffe, L. S., César, G. V., et al. (2015). Extracellular vesicle-mediated export of fungal RNA. *Sci. Rep.* 5:7763. doi: 10.1038/srep07763

Pérez-Arques, C., Navarro-Mendoza, M. I., Murcia, L., Lax, C., Martínez-García, P., Heitman, J., et al. (2019). *Mucor* circinelloides thrives inside the phagosome through an Atf-mediated germination pathway. *MBio* 10:e2765-18.

Pérez-Arques, C., Navarro-Mendoza, M. I., Murcia, L., Navarro, E., Garre, V., and Nicolas, F. (2020). A non-canonical RNAi pathway controls virulence and genome stability in *Mucorales*. *bioRxiv [Preprint]* doi: 10.1101/2020.01.14.906289

Petrikkos, G., Skiada, A., Lortholary, O., Roilides, E., Walsh, T. J., and Kontoyiannis, D. P. (2012). Epidemiology and clinical manifestations of mucormycosis. *Clin. Infect. Dis.* 54(Suppl. 1), S23–S34. doi: 10.1093/cid/cir866

Prakash, H., Rudramurthy, S. M., Gandham, P. S., Ghosh, A. K., Kumar, M. M., Badapanda, C., et al. (2017). Apophysomyces variabilis: draft genome sequence and comparison of predictive virulence determinants with other medically important *Mucorales*. *BMC Genom.* 18:736.

Puebla, L. E. J. (2012). Fungal infections in immunosuppressed patients. *Intech. Open*. 150–176.

Quandahl, R., and Cooper, J. S. (2018). *Hyperbaric, Zygomycotic Infections*. Treasure Island, FL: StatPearls Publishing LLC.

Rammaert, B., Angebault, C., Scemla, A., Fraitag, S., Lerolle, N., Lecuit, M., et al. (2014). *Mucor* irregularis-associated cutaneous mucormycosis: case report and review. *Med. Mycol. Case Rep.* 6, 62–65. doi: 10.1016/j.mmcr.2014.07.005

Rammaert, B., Lanternier, F., Zahar, J. R., Dannaoui, E., Bougnoux, M. E., Lecuit, M., et al. (2012). Healthcare-associated mucormycosis. *Clin. Infect. Dis.* 54(Suppl. 1), S44–S54. doi: 10.1093/cid/cir867

Ribes, J. A., Vanover-Sams, C. L., and Baker, D. J. (2000). Zygomycetes in human disease. *Clin. Microbiol. Rev.* 13, 236–301. doi: 10.1128/cmr.13.2.236

Roden, M. M., Zaoutis, T. E., Buchanan, W. L., Knudsen, T. A., Sarkisova, T. A., Schaufele, R. L., et al. (2005). Epidemiology and outcome of zygomycosis: a review of 929 reported cases. *Clin. Infect. Dis.* 41, 634–653. doi: 10.1086/432579

Rogers, T. R. (2008). Treatment of zygomycosis: current and new options. *J. Antimicrob. Chemother.* 61(Suppl. 1), i35–i40. doi: 10.1093/jac/dkm429

Schwartze, V. U., Winter, S., Shelest, E., Marcet-Houben, M., Horn, F., Wehner, S., et al. (2014). Gene expansion shapes genome architecture in the human pathogen Lichtheimia corymbifera: an evolutionary genomics analysis in the ancient terrestrial mucorales (*Mucoromycotina*). *PLoS Genet.* 10:e1004496. doi: 10.1371/journal.pgen.1004496

Sephton-Clark, P. C. S., Munoz, J. F., Ballou, E. R., Cuomo, C. A., and Voelz, K. (2018). Pathways of pathogenicity: transcriptional stages of germination in the fatal fungal pathogen *Rhizopus* delemar. *mSphere* 3:e00403-18 doi: 10.1128/mSphere.00403-18

Sephton-Clark, P., Munoz, J. F., Itabanga, H., Voelz, K., Cuomo, C. A., and Ballou, E. R. (2019). Host-pathogen transcriptomics of macrophages, *Mucorales* and their endosymbionts: a polymicrobial pas de trois. *bioRXiv [Preprint]* doi: 10.1101/580746

Shao, T. Y., Ang, W. X. G., Jiang, T. T., Huang, F. S., Andersen, H., Kinder, J. M., et al. (2019). Commensal candida albicans positively calibrates systemic Th17 immunological responses. *Cell Host Microbe* 25, 404–17e6. doi: 10.1016/j.chom.2019.02.004

Shelburne, S. A., Ajami, N. J., Chibucos, M. C., Beird, H. C., Tarrand, J., Galloway-Pena, J., et al. (2015). Implementation of a pan-genomic approach to investigate holobiont-infecting microbe interaction: a case report of a leukemic patient with invasive mucormycosis. *PLoS One* 10:e0139851. doi: 10.1371/journal.pone.0139851

Skiada, A., Pagano, L., Groll, A., Zimmerli, S., Dupont, B., Lagrou, K., et al. (2011). Zygomycosis in Europe: analysis of 230 cases accrued by the registry of the european confederation of medical mycology (ECMM) working group on zygomycosis between 2005 and 2007. *Clin. Microbiol. Infect.* 17, 1859–1867. doi: 10.1111/j.1469-0691.2010.03456.x

Spellberg, B., Edwards, J. Jr., and Ibrahim, A. (2005). Novel perspectives on mucormycosis: pathophysiology, presentation, and management. *Clin. Microbiol. Rev.* 18, 556–569. doi: 10.1128/cmr.18.3.556-569.2005

Tacke, D., Koehler, P., Markiefka, B., and Cornely, O. A. (2014). Our 2014 approach to mucormycosis. *Mycoses* 57, 519–524. doi: 10.1111/myc.12203

Takahashi-Nakaguchi, A., Shishido, E., Yahara, M., Urayama, S.-I., Sakai, K., Chibana, H., et al. (2020). Analysis of an intrinsic mycovirus associated with reduced virulence of the human pathogenic fungus *Aspergillus fumigatus*. *Front. Microbiol.* 10:3045. doi: 10.3389/fmicb.2019.03045

Tang, X., Zhao, L., Chen, H., Chen, Y. Q., Chen, W., Song, Y., et al. (2015). Complete genome sequence of a high lipid-producing strain of *Mucor* circinelloides WJ11 and comparative genome analysis with a low lipid-producing strain CBS 277.49. *PLoS One* 10:e0137543 doi: /10.1371/journal.pone.0137543

Trieu, T. A., Navarro-Mendoza, M. I., Perez-Arques, C., Sanchis, M., Capilla, J., Navarro-Rodriguez, P., et al. (2017). RNAi-Based functional genomics identifies new virulence determinants in mucormycosis. *PLoS Pathog* 13:e1006150. doi: 10.1371/journal.ppat.1006150

Vágvölgyi, C., Magyar, K., Papp, T., Vastag, M., Ferenczy, L., Hornok, L., et al. (1998). Detection of double-stranded RNA molecules and virus-like particles in different *Mucor* species. *Antonie van Leeuwenhoek* 73, 207–210.

Vágvölgyi, C., Varga, J., and Ferenczy, L. (1993). Detection of double-stranded RNA in *Mucor* ramannianus. *Fungal Genet. Rep.* 40:31

Vainio, E. J., Jurvansuu, J., Streng, J., Rajamäki, M.-L., Hantula, J., and Valkonen, J. P. (2015). Diagnosis and discovery of fungal viruses using deep sequencing of small RNAs. *J. Gen. Virol.* 96, 714–725. doi: 10.1099/jgv.0.000003

van de Sande, W. W., and Vonk, A. G. (2019). Mycovirus therapy for invasive pulmonary aspergillosis? *Med. Mycol.* 57(Suppl._2), S179–S188.

Van De Sande, W., Lo-Ten-Foe, J., van Belkum, A., Netea, M., Kullberg, B., and Vonk, A. (2010). Mycoviruses: future therapeutic agents of invasive fungal infections in humans? *Eur. J. Clin. Microbiol. Infect. Dis.* 29, 755–763. doi: 10.1007/s10096-010-0946-7

Vellanki, S., Navarro-Mendoza, M. I., Garcia, A., Murcia, L., Perez-Arques, C., Garre, V., et al. (2018). *Mucor* circinelloides: growth, maintenance, and genetic manipulation. *Curr. Protoc. Microbiol.* 49:e53. doi: 10.1002/cpmc.53

Walsh, T. J., Skiada, A., Cornely, O. A., Roilides, E., Ibrahim, A., Zaoutis, T., et al. (2014). Development of new strategies for early diagnosis of mucormycosis from bench to bedside. *Mycoses* 57, 2–7. doi: 10.1111/myc.12249

Walther, G., Wagner, L., and Kurzai, O. (2019a). Outbreaks of *Mucorales* and the Species Involved. *Mycopathologia* Online ahead of print doi: 10.1007/s11046-019-00403-1

Walther, G., Wagner, L., and Kurzai, O. (2019b). Updates on the taxonomy of mucorales with an emphasis on clinically important taxa. *J. Fungi* 5:106 doi: 10.3390/jof5040106

Wang, L., Pittman, K. J., Barker, J. R., Salinas, R. E., Stanaway, I. B., Williams, G. D., et al. (2018). An atlas of genetic variation linking pathogen-induced cellular traits to human disease. *Cell Host Microbe* 24, 308–23e6. doi: 10.1016/j.chom.2018.07.007

Watkins, T. N., Gebremariam, T., Swidergall, M., Shetty, A. C., Graf, K. T., Alqarihi, A., et al. (2018). Inhibition of EGFR signaling protects from mucormycosis. *MBio* 9:e1384-18.

Xu, Q., Fu, Y., Li, S., Jiang, L., Rongfeng, G., and Huang, H. (2018). Integrated transcriptomic and metabolomic analysis of *Rhizopus* oryzae with different morphologies. *Process Biochem.* 64, 74–82. doi: 10.1016/j.procbio.2017.10.001

Xu, W., Peng, J., Li, D., Tsui, C. K., Long, Z., Wang, Q., et al. (2018). Transcriptional profile of the human skin pathogenic fungus Mucor irregularis in response to low oxygen. *Med. Mycol.* 56, 631–644. doi: 10.1093/mmy/myx081

Zoll, J., Verweij, P. E., and Melchers, W. J. (2018). Discovery and characterization of novel Aspergillus fumigatus mycoviruses. *PloS one* 13:e0200511 doi: 10.1371/journal.pone.0200511

Conflict of Interest: The authors declare that the research was conducted in the absence of any commercial or financial relationships that could be construed as a potential conflict of interest.

frontiers in Genetics

ORIGINAL RESEARCH
published: 04 August 2020
doi: 10.3389/fgene.2020.00822

Genomics and Virulence of *Fonsecaea pugnacius*, Agent of Disseminated Chromoblastomycosis

Amanda Bombassaro[1], Gabriela X. Schneider[1], Flávia F. Costa[2], Aniele C. R. Leão[2], Bruna S. Soley[3], Fernanda Medeiros[4], Nickolas M. da Silva[2], Bruna J. F. S. Lima[1], Raffael J. A. Castro[5], Anamélia L. Bocca[5], Valter A. Baura[6], Eduardo Balsanelli[6], Vania C. S. Pankievicz[6], Nyvia M. C. Hrysay[7], Rosana H. Scola[7], Leandro F. Moreno[2], Conceição M. P. S. Azevedo[8], Emanuel M. Souza[6], Renata R. Gomes[1], Sybren de Hoog[1,9] and Vânia A. Vicente[1,2]**

[1] Microbiology, Parasitology and Pathology Post-graduation Program, Department of Basic Pathology, Federal University of Paraná, Curitiba, Brazil, [2] Engineering Bioprocess and Biotechnology Post-graduation Program, Department of Bioprocess Engineering and Biotechnology, Federal University of Paraná, Curitiba, Brazil, [3] Pharmacology Post-graduation Program, Department of Pharmacology, Federal University of Paraná, Curitiba, Brazil, [4] Graduation in Biology Sciences, Federal University of Paraná, Curitiba, Brazil, [5] Department of Cell Biology, University of Brasilia, Brasilia, Brazil, [6] Department of Biochemistry, Federal University of Paraná, Curitiba, Brazil, [7] Service of Neuromuscular and Demyelinating Diseases, Complex Histochemistry-Immunity Laboratory, Hospital of Clinics, Federal University of Paraná, Curitiba, Brazil, [8] Department of Medicine, Federal University of Maranhão, São Luís, Brazil, [9] Center of Expertise in Mycology of Radboud University Medical Center/Canisius Wilhelmina Hospital, Nijmegen, Netherlands

Among agents of chromoblastomycosis, *Fonsecaea pugnacius* presents a unique type of infection because of its secondary neurotropic dissemination from a chronic cutaneous case in an immunocompetent patient. Neurotropism occurs with remarkable frequency in the fungal family Herpotrichiellaceae, possibly associated with the ability of some species to metabolize aromatic hydrocarbons. In an attempt to understand this new disease pattern, were conducted genomic analysis of *Fonsecaea pugnacius* (CBS 139214) performed with *de novo* assembly, gene prediction, annotation and mitochondrial genome assembly, supplemented with animal infection models performed with *Tenebrio molitor* in *Mus musculus* lineages BALB/c and C57BL/6. The genome draft of 34.8 Mb was assembled with a total of 12,217 protein-coding genes. Several proteins, enzymes and metabolic pathways related to extremotolerance and virulence were recognized. The enzyme profiles of black fungi involved in chromoblastomycosis and brain infection were analyzed with the Carbohydrate-Active Enzymes (CAZY) and peptidases database (MEROPS). The capacity of the fungus to survive inside *Tenebrio molitor* animal model was confirmed by histopathological analysis and by presence of melanin and hyphae in host tissue. Although *F. pugnacius* was isolated from brain in a murine model following intraperitoneal infection, cytokine levels were not statistically significant, indicating a profile of an opportunistic agent. A dual ecological ability can be concluded from presence of metabolic pathways for nutrient scavenging and extremotolerance, combined with a capacity to infect human hosts.

Keywords: black fungi, cerebral infection, genome assembly, virulence, dissemination, pathology, chromoblastomycosis, neurotropism

OPEN ACCESS

Edited by:
Bridget Marie Barker, Northern Arizona University, United States

Reviewed by:
Anna Muszewska, Institute of Biochemistry and Biophysics (PAN), Poland
Aylin Döğen, Mersin University, Turkey
Macit Ilkit, Çukurova University, Turkey
Hamid Badali, The University of Texas Health Science Center at San Antonio, United States

***Correspondence:**
Sybren de Hoog
Sybren.deHoog@radboudumc.nl; s.hoog@wi.knaw.nl
Vânia A. Vicente
vaniava63@gmail.com

Specialty section:
This article was submitted to Evolutionary and Genomic Microbiology, a section of the journal Frontiers in Genetics

Received: *13 November 2019*
Accepted: *08 July 2020*
Published: *04 August 2020*

Citation:
Bombassaro A, Schneider GX, Costa FF, Leão ACR, Soley BS, Medeiros F, da Silva NM, Lima BJFS, Castro RJA, Bocca AL, Baura VA, Balsanelli E, Pankievicz VCS, Hrysay NMC, Scola RH, Moreno LF, Azevedo CMPS, Souza EM, Gomes RR, de Hoog S and Vicente VA (2020) Genomics and Virulence of Fonsecaea pugnacius, Agent of Disseminated Chromoblastomycosis. Front. Genet. 11:822. doi: 10.3389/fgene.2020.00822

INTRODUCTION

Melanized fungi that are known as 'black yeasts and relatives' and belonging to the family Herpotrichiellaceae (order Chaetothyriales) are associated with different clinical pictures such as mycetoma, phaeohyphomycosis, and chromoblastomycosis (Cañete-Gibas and Wiederhold, 2018). Chromoblastomycosis starts at the inoculation site of the etiological agent, leads to chronic acanthosis, and, triggered by the host's immune response, develops fungal structures known as muriform cells (Vicente et al., 2017). Phaeohyphomycosis can be distinguished from other infectious syndromes by tissue invasion with pigmented hyphae (Thomas et al., 2018) and is often associated with necrosis.

Significant differences in pathogenicity and virulence between the main clinical species *Cladophialophora bantiana*, *Exophiala dermatitidis, Fonsecaea pedrosoi,* and *Rhinocladiella mackenziei* on the one hand, and closely related environmental species on the other, have been reported. These species can grow at human body temperature or higher and are able to cause systemic or disseminated disease, while many others, if causing infection, remain subcutaneous (Seyedmousavi et al., 2014; Teixeira et al., 2017). Cerebral infections by black fungi are characterized by abscesses with hyphae in tissue and are therefore classified as phaeohyphomycosis. Such infections often lead to death of the patient despite combined treatment with antifungal drugs and surgery (de Azevedo et al., 2015; Arcobello and Revankar, 2020).

Infection of humans by members of Herpotrichiellaceae is enabled by their stress tolerance and adaptability in their natural, environmental niche, the human host not being a preferential habitat (Gostinčar et al., 2018). The agents are saprobes in mostly still unclarified micro-habitats, and decompose organic matter for nutrition (Vicente et al., 2017). The high adaptability and invasive potential explain the relatively high frequency in animal hosts despite a low environmental occurrence. This potential for infection appears to be polyphyletic within the family Herpotrichiellaceae, as it differs between species (Vicente et al., 2017).

Fonsecaea sibling species differ significantly in their ecology and potential of infection (Vicente et al., 2014). Some, such as *Fonsecaea pedrosoi* and *F. nubica,* are recognized etiologic agents of chromoblastomycosis in human hosts, having an ability to form muriform cell in tissue, while *F. monophora* and *F. pugnacius* may also be involved in disseminated infection with hyphal growth in the brain (de Hoog et al., 2004; Tanabe et al., 2004; Najafzadeh et al., 2009, 2011; Vicente et al., 2012; de Azevedo et al., 2015). Nine cases of primary brain infection by these species have been confirmed (Lucasse et al., 1954; Nobrega et al., 2003; Surash et al., 2005; Takei et al., 2007; Koo et al., 2010; Raparia et al., 2010; Doymaz et al., 2015; Varghese et al., 2016; Helbig et al., 2018). *Fonsecaea pugnacius* is exceptional by combining features of chromoblastomycosis and secondary neurotropic dissemination. The single strain known to date of the species presented muriform cells in subcutaneous tissue, but hyphae in the cerebrum (de Azevedo et al., 2015). This duality of local and invasive morphologies has not been observed in any other species associated with chromoblastomycosis or brain infection, suggesting that *Fonsecaea pugnacius* presents a unique pathogenic profile different from that of *Cladophialophora bantiana*, the main agent of human brain infection which presumably follows a pulmonary route (Ozgun et al., 2019).

In the present study, we sequenced the genome of the type strain of *F. pugnacius*, CBS 139214, and performed genomic analysis in order to identify the relation between black fungi and neurotropism. In addition, we compared the enzymatous gene profile of *F. pugnacius* to other previously sequenced neurotropic species, including *C. bantiana*, *E. dermatitidis* and *R. mackenziei*. To obtain more insight into virulence, we evaluated animal infection models by *F. pugnacius*, using strain CBS 139214 isolated from a cutaneous lesion of a patient with disseminated neurotropic infection.

MATERIALS AND METHODS

Genomic DNA Extraction, Sequencing and Assembly

Fonsecaea pugnacius strain CBS 139214 (type) originating from a skin lesion (de Azevedo et al., 2015) was obtained from the reference collection of Westerdijk Fungal Biodiversity Institute, Utrecht, Netherlands. The strain was grown in Sabouraud liquid medium during 7 days at 28°C for DNA extraction according to Vicente et al. (2008) using cetyltrimethylammonium bromide (CTAB) and phenol-chloroform/isoamyl alcohol and the Microbial DNA UltraClean^{TM} kit for purification. The Nextera kit (IlluminaTM) and Ion Plus Fragment Library Kit (Thermo Fisher Scientific) were used to prepare the DNA libraries for sequencing based on the producer's guidelines. FastQC[1] was used for quality control analyses of sequence reads generated. The SPAdes assembler v3.10.0 (Bankevich et al., 2012) and FGAP (Piro et al., 2014) were applied for *de novo* assembly and gap closure, respectively. The genome assembly was evaluated by BUSCO v4.0.2 using the 'chaetothyriales_odb10' dataset (Seppey et al., 2019) and the Bowtie2 program was used for assembly coverage measure (Langmead and Salzberg, 2012).

Gene Prediction, Annotation and Genomic Analysis

GeneMark-ES v4.39 (Besemer et al., 2001) was applied to predict the protein-coding genes using default parameter and RAFTS3 (Vialle et al., 2016) for automatic annotation with best hits comparison with self-score cutoff 0.5 using our internal database of sequences of *Fonsecaea* ssp. and related species from the Chaetothyriales (Vicente et al., 2017; Moreno et al., 2018). *F. pugnacius* functional characteristics were determined with GO enrichment analyses at a significance level of $\leq$0.05 according to Ashburner et al. (2000) using the InterProScan5 (Quevillon et al., 2005) to access the protein domain families. Phylogenomic trees based on orthologous clusters were obtained and generated using ORTHOFinder (Emms and Kelly, 2018). A phylogenomic tree was inferred for each and all-orthogroup trees were

[1]http://www.bioinformatics.babraham.ac.uk

resolved by the OrthoFinder duplication-loss coalescent model (Emms and Kelly, 2018) and the final tree was constructed using the STAG method, present in the OrthoFinder pipeline (Emms and Kelly, 2018). The enzymatous gene profile of *F. pugnacius* and other melanized fungi causing brain infection (*C. bantiana, E. dermatitidis, F. monophora, Verruconis gallopava*, and *R. mackenziei*) were predicted with CAZY (Cantarel et al., 2009) and MEROPS databases (Rawlings et al., 2016). In addition, numbers, classes and similarities were analyzed using an all-vs.-all similarity 40% $\geq$ search and *e*-value of 10^{-4} (Vicente et al., 2017).

Mitochondrial Genome Assembly and Annotation

The SPAdes v3.6.2 program (Bankevich et al., 2012) was used for assembly and mappingd the mitochondrial genome from the *F. pugnacius* sequencing reads previously aligned against the complete mtDNA of *Fonsecaea pedrosoi* CBS 271.37. Mitochondrial genome annotations were done based on Vicente et al. (2017) and Moreno et al. (2018) using SILA (Vialle, 2013) and the final figure was produced by the software package Circos (Krzywinski et al., 2009).

Virulence Assays in Animal Models

Tenebrio molitor Infection

A *Tenebrio molitor* larval model was used to evaluate the virulence potential based on Fornari et al. (2018) using parameters of survival and melanization after infection. Larvae were inoculated with 1×10^6 cells/mL in PBS solution above the legs and the ventral portion sterile PBS solution and SHAM without physical damage (no treatment) as negative control, using 10 larvae per group of inoculation, in triplicate. The larvae were kept in darkness at 37°C, mortality was monitored daily for 10 days and dead larvae were collected at 4, 24, 72, 168, and 240 h post infection omitting the pupae in the calculation (Scorzoni et al., 2013). Survival curves were plotted and statistical analyses were performed using the Log-rank (Mantel–Cox) test with Graph Pad Prism software and statistical differences were set at $p < 0.05$ according to Maekawa et al. (2015) and Vicente et al. (2017). Melanization was determined measuring the OD at 405 nm (Scorzoni et al., 2013; Perdoni et al., 2014).

Fungal burden and histological analysis of infected caterpillars was performed according to Fornari et al. (2018). The samples were homogenized in PBS solution with a TissueLyser (Qiagen, Hilden, Germany), inoculated on Mycosel agar at 30°C for 14 days and the number of colony forming units (CFUs) of fungal per mL of solution estimated with some colonies re-isolated and sequenced to confirm the species ID. Moreover, the caterpillar samples were embedded in Adracanth gum solution (Fornari et al., 2018), immersed in liquid nitrogen and sectioned by steel blades in a cryostat (Leica CM 1850, Wetzlar, Germany), stained with hematoxylin and eosin (HE) and observed with Axio Imager Z2 (Carl Zeiss, Jena, Germany) equipped with Metafer 4/VSlide automated capture software (Metasystems, Altlussheim, Germany).

Murine Infection

Fungal burden and cytokine production evaluation was performed using immunocompetent mice as model, according Bocca et al. (2006), Badali et al. (2011), Rodrigues et al. (2015), and Schneider et al. (2019). The animals selected were male Balb/c (6–8 weeks) and C57/BL6 mice, maintained under standard laboratory conditions with controlled temperature (23–25°C) with water and food *ad libitum*, according to recommendations of the Federal University of Paraná Ethics Committee (current approval certificate 1002).

The experiments were performed in triplicate using groups of six animals infected with *F. pugnacius* CBS 139214 and one negative control inoculated with sterile phosphate-buffered saline (PBS according to described by Fornari et al. (2018) and Schneider et al. (2019). The animals were infected intraperitoneally or intradermally (per hind footpad) with 100 μL of 1×10^6 propagules or sterile PBS and were monitored weekly and sacrificed at 7, 14, and 21 days post-infection using CO_2 anesthesia in an appropriate chamber (Fornari et al., 2018). Brain, lung, liver, kidney, spleen, footpad, and blood were aseptically collected for analysis.

For fungal burden determination, samples tissues were weighed, homogenized and diluted in PBS for culture as described by Vicente et al. (2017). Results were expressed as number of CFU ± standard error of mean (SEM) per gram of fresh tissue, counting colonies from the seventh day until the 15th day. Cytokine production was measured from homogenized tissue obtained from infected and non-infected (healthy) animals by ELISA (Vicente et al., 2017). The cytokines interleukin-1β (IL-1β), TNF-α, interleukin-6 (IL-6) and monocyte chemoattractant protein-1 (MCP-1/Ccl2) were measured with kits purchased from eBioscience and used according the manufacturer's instructions. Results were expressed as pg of cytokine ± standard error of mean (SEM) per 100 milligrams of tissue. The infected tissue samples were fixed in 10% formalin, dehydrated in alcohol, and embedded in paraffin (Fornari et al., 2018). Serial 5-μm sections were stained with hematoxylin and eosin to visualize pathogen morphology.

RESULTS AND DISCUSSION

De novo Assembly

The genome sequencing of *F. pugnacius* CBS 139214 was performed using Illumina MiSeq and Ion proton producing 5,424,908 paired-end reads and 1,853,059 mate-paired reads, respectively. The final high-quality assembly comprised 386 contigs with 34,872,293 bp and 52% of G + C content. The genome size estimated is 34.8 Mb with average coverage of 48.75X and using 97% of the reads for draft assembling. The genome completeness, checked using BUSCO, revealed that the assembly had 98.8% completeness. A total of 6188 complete BUSCO genes were found, including 6176 being single-copy BUSCOs, of the 6265 BUSCO groups searched, 12 (0.2%) were duplicated BUSCO genes, 39 (0.6%) were fragmented BUSCOs and 38 (0.6%) represented missing BUSCOs. Sequencing data were submitted to GenBank (accession number WJFF00000000). In addition,

TABLE 1 | *Fonsecaea pugnacius* genome data assembly and related species of Herpotrichiellaceae.

Species	Strains	Genome size (Mbp)	GC content (%)	Number of proteins	GenBank genome access
Fonsecaea pugnacius	CBS 139214	34.8	52	12,217	WJFF00000000
Fonsecaea pedrosoi	CBS 271.37	34.69	52.4	12,527	PRJNA233314
Fonsecaea monophora	CBS 269.37	35.23	52.2	11,984	LVKK00000000.1
Fonsecaea nubica	CBS 269.64	33.79	52.5	11,681	LVCJ00000000.1
Fonsecaea multimorphosa	CBS 102226	33.45	52.6	12,369	PRJNA233317
Fonsecaea multimorphosa	CBS 980.96	33.39	52.60	11,804	LVCI00000000.1
Fonsecaea erecta	CBS 125763	34.75	53.1	12,090	LVYI00000000.1
Cladophialophora immunda	CBS 834.96	43.03	52.8	14,033	JYBZ00000000.1
Cladophialophora bantiana	CBS 173.52	36.72	51.3	12,762	JYBT00000000.1
Cladophialophora carrionii	CBS 160.54	28.99	54.3	10,373	PRJNA185784
Cladophialophora yegresii	CBS 114405	27.90	54.0	10,118	AMGW00000000.1
Capronia epymices	CBS 606.96	28.89	53.4	10,469	GCA_000585565.1
Capronia coronata	CBS617.96	25.81	52.7	9,231	AMWN00000000.1
Exophiala dermatitidis	NIH/UT8656	26.38	51.47	9,578	GCA_000230625.1
Rhinocladiella mackenziei	CBS 650.93	32.47	50.4	11,382	JYBU00000000.1
Coniosporium apollinis	CBS 100218	28.65	52.1	9,308	AJKL00000000.1
Exophiala mesophila	CBS 40295	29.27	50.40	10,347	GCA_000836275.1
Exophiala aquamarina	CBS 119918	41.57	48.3	13,118	AMGV00000000.1

12,217 protein-coding genes and 35 tRNAs were predicted for *F. pugnacius* (**Table 1**). Expected values for *Fonsecaea* siblings were between 11,681 in *F. nubica* and 12,527 in *F. pedrosoi* (Vicente et al., 2017).

Comparing *F. pugnacius* genome size of 34.8 Mb with related species of Herpotrichiellaceae (**Table 1**), some differences were observed. The *Cladophialophora immunda* genome is nearly 8.15 Mb larger, while the *Exophiala dermatitidis* genome is 8.43 Mb smaller, being the smallest genome in the family with 26.37 Mb (Teixeira et al., 2017). Genome sizes within *Fonsecaea* were similar, i.e., between 33.39 and 35.23 Mb (Vicente et al., 2017). Judging from the phylogenomic tree (**Figure 1**), *F. pugnacius* clustered with the clinical representatives of *Fonsecaea*, in accordance with previous phylogenetic analyses of *Fonsecaea* and *Cladophialophora* based on internal transcribed spacer (ITS), partial beta-tubulin protein-coding gene (BT2) and cell division cycle 42 (CDC42) sequences performed by de Azevedo et al. (2015).

The mitochondrial genome was assembled and 3 contigs were obtained with a total of 25,098 bp and a GC% of 25.49; the largest contig was 14,011 bp. There were 44 proteins in the mtDNA, i.e., 26 hypothetical proteins and 18 with known function (**Figure 2**). The proteins encoded by mitochondrial genomes of herpotrichiellaceous species were very similar, most being proteins involved in ATP synthesis and respiratory metabolism (Vicente et al., 2017).

Protein-Coding Gene Annotation and General Characteristics

A total of 12,217 protein-coding genes were identified in *F. pugnacius*, of which 11,124 were annotated as hypothetical proteins and 1,093 proteins had inferred functions (**Supplementary Table 1**). In the GO annotation, the proteins were separated into three large groups: biological process, cellular components and molecular functions (**Figure 3** and **Supplementary Table 1**). Among proteins to which functions were attributed, various proteins were shared among the *Fonsecaea* siblings, such as proteins related to virulence in transporter families, proteins from the glyoxylate cycle, genes encoding proteins related to oxidative stress and involved in the detoxification of reactive oxygen species (ROS), cytochrome P450 monooxygenases (CYPs/P450s), heat shock proteins, proteins of melanin pathways, enzymes able to degrade aromatic carbon compounds, and others.

Carrier families of zinc, iron, manganese, and sugar have also been identified, i.e., MFS transporters and ABC transporters. In addition to basal metabolism, these carriers play a role in survival strategies. MFS is the largest family of transporters, ubiquitous to all living organisms and involved in the active excretion of antifungal drugs (Vela-Corcía et al., 2019). Reportedly, they also enhance antifungal resistance in *Candida albicans*, *Aspergillus fumigatus,* and *Cryptococcus neoformans* (Costa et al., 2014).

Sequences of proteins involved in the glyoxylate cycle were annotated: isocitrate lyase and malate synthase (**Supplementary Table 1**). The glyoxylate pathway is a metabolic strategy for the synthesis of carbohydrates from carbon compounds, such as acetate and other degradation products from ethanol, fatty acids, and poly-*b*-hydroxybutyrate (White et al., 2017). The glyoxylate cycle consists of a modification of the citric acid cycle (TCA), as it shares the same initial reactions of citrate and isocitrate generation but continues with the formation of succinate and glyoxylate (Dunn et al., 2009). This pathway has been associated with fungal virulence, since it allows energy production in environments where complex carbon compounds are poorly found (Lorenz and Fink, 2001) and has been described in infectious fungi such as *Rhinocladiella mackenziei* (Moreno et al., 2018), *Fonsecaea* siblings related to chromoblastomycosis

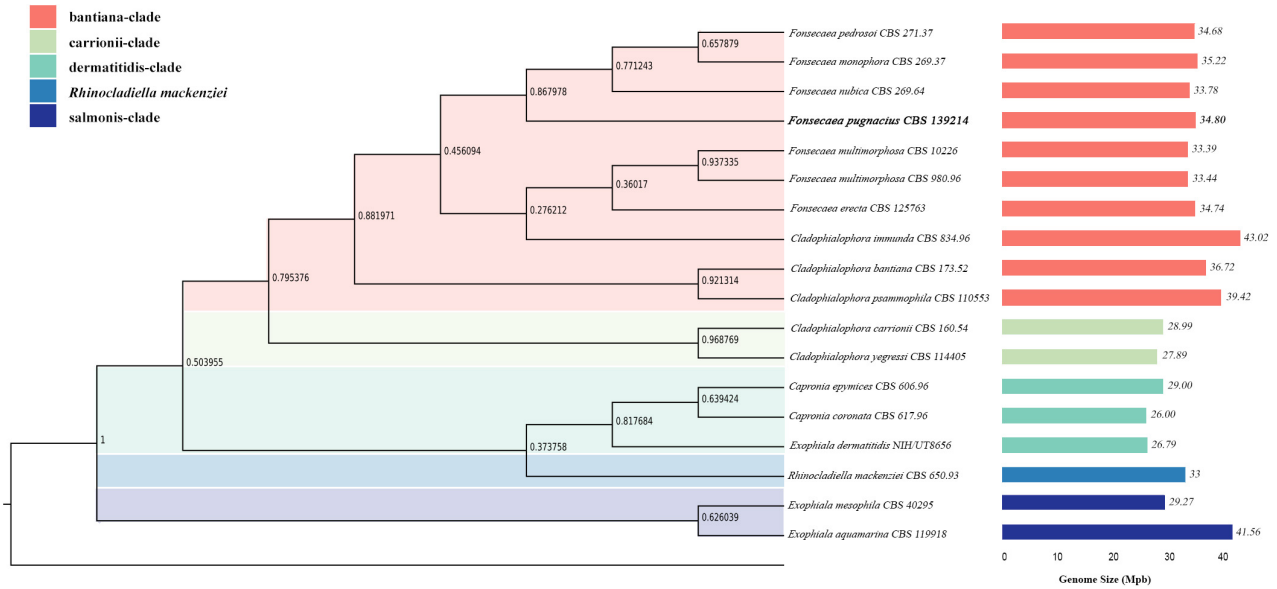

FIGURE 1 | Phylogenomic tree based on the concatenated alignment of genomes of Herpotrichiellaceae family. Species names are given between phylogenomic tree and genome size bars. The genomes size is indicated and the colors are representing the clades of Chaetothyriales summarized in colored boxes.

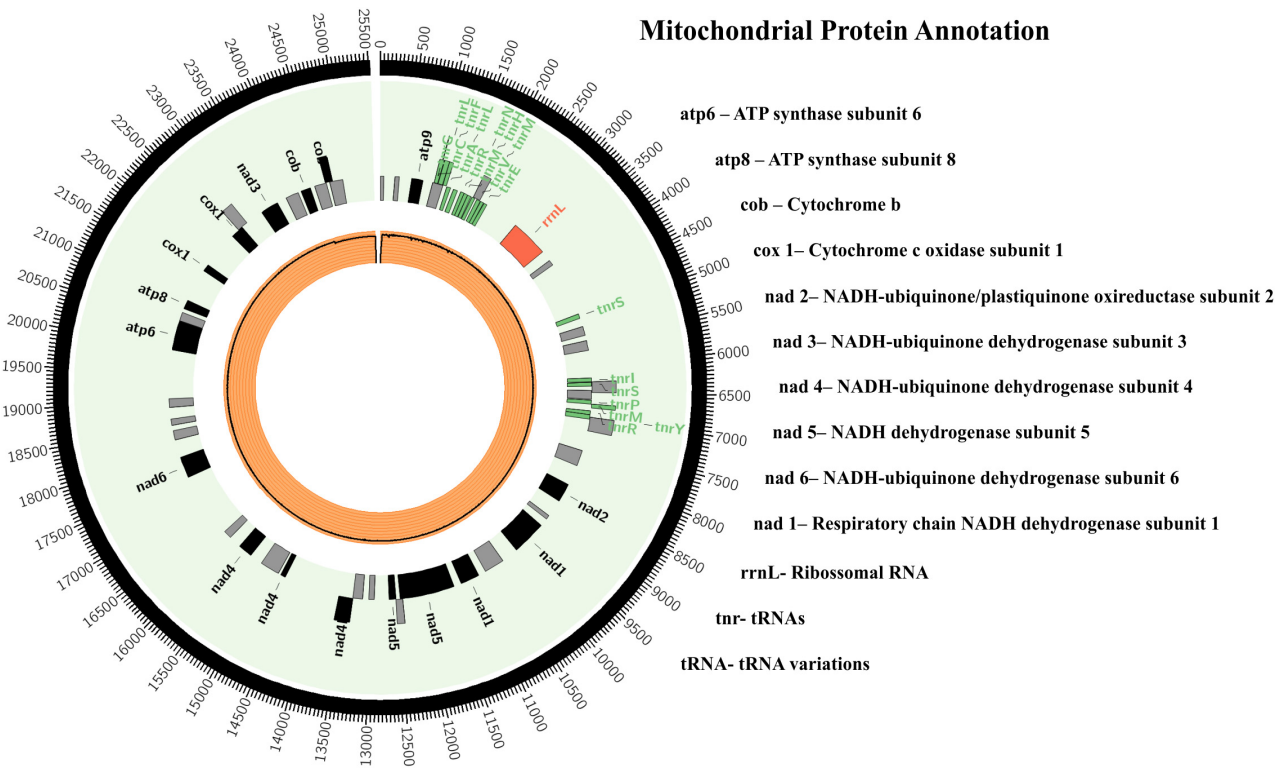

FIGURE 2 | *Fonsecaea pugnacius* CBS 139214 mtDNA. Rectangles represent annotated genes: in red the rRNAs; in green the tRNAs; in black the other genes and orange inner circle shows reads coverage.

(Vicente et al., 2017), *Beauveria bassiana* (Yang et al., 2016), *Talaromyces marneffei* (Thirach et al., 2007), and *Candida albicans* (Lorenz and Fink, 2001).

In *Paracoccidioides brasiliensis*, agent of another implantation mycosis, paracoccidioidomycosis, an increase of transcriptional levels of isocitrate lyase and malate synthase genes was reported

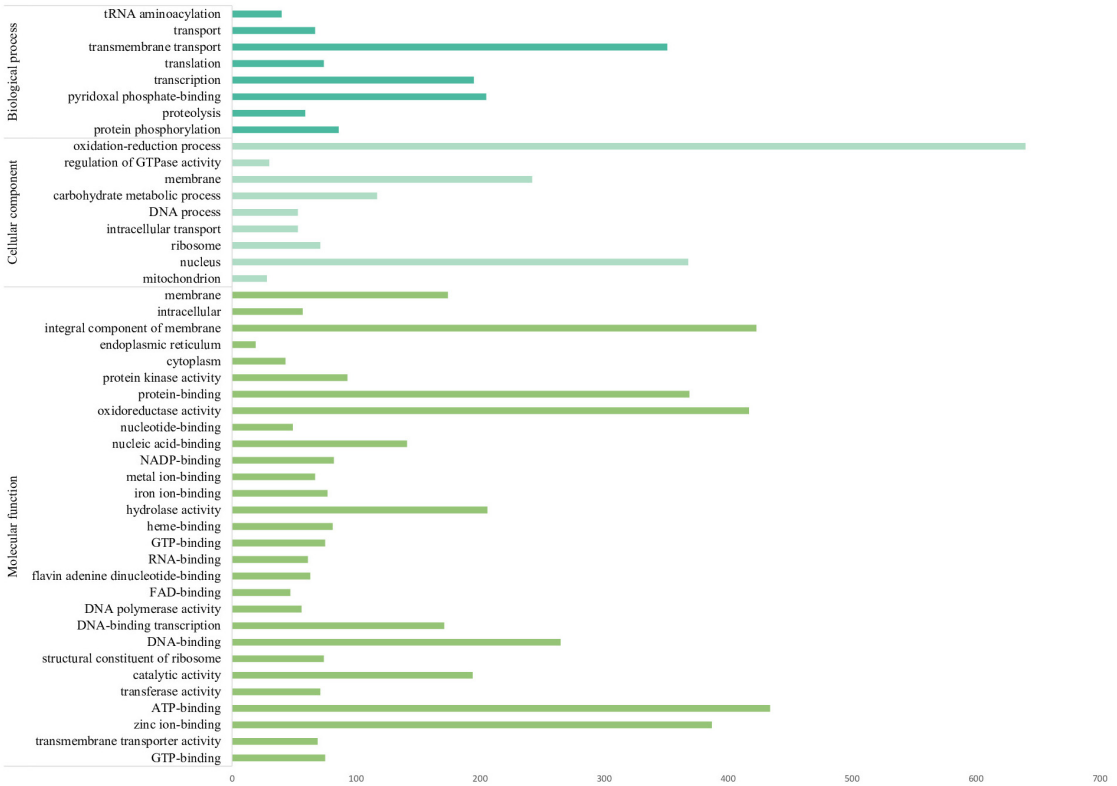

FIGURE 3 | The most numerous gene families of *Fonsecaea pugnacius* based on Gene Ontology annotation separating proteins annotated into three large groups: biological process, cellular components, and molecular functions.

in an infection model (Derengowski et al., 2008). This suggests a possible mechanism of adaptation of the fungus in response to the internal environment of the phagosome, which is poor in complex sources of carbon. The same function could be assigned to *Fonsecaea* siblings to explain fungal persistence inside macrophages, which, according to Queiroz-Telles et al. (2017), seems to be fungistatic (rather than fungicidal) against agents of chromoblastomycosis. In addition, it may be related to the ability of these fungi to survive on low carbon sources during brain infection.

Characterization of the partial genome of *F. pugnacius* revealed genes encoding proteins related to oxidative stress and involved in the detoxification of ROS, such as alternative oxidase, manganese superoxide dismutase and cytoplasmic thioredoxins. Earlier reports observed that the alternative oxidase enzyme is present in the internal mitochondrial membrane of plants and some fungi and protozoa, in an alternative route of oxidation of the electron transport chain in cellular respiration (Duvenage et al., 2018). In the fungus *Neurospora crassa*, levels of the nuclear gene transcripts *AOX1*, which encode the alternative oxidase, increase when the cytochrome C oxidase pathway is inhibited. These results indicate activation of an alternative pathway, which the organism applies to correct conditions of oxidative stress and to decrease the production of ROS in respiration when competing with electrons of the classical oxidation pathway. Some studies have revealed that *AOX1* gene expression can be stimulated under stress conditions, such as low temperature and ROS low level, *AOX1* functioning as an antioxidant (Missall et al., 2004). Some pathogens resist to oxidative stress in the hostile environment of the phagosomes by the production of antioxidant enzymes that detoxify ROS, such as alternative oxidase, catalase and superoxide dismutase (Duvenage et al., 2018). ROS is an important cellular detrimental agent associated with the activation of immune response in human cells infected with fungi causing dermatomycoses or invasive mycoses (Castro et al., 2017).

According Vicente et al. (2017), many of the CYP/P450 enzymes revealed in herpotrichiellaceous fungi are abundantly present in *Fonsecaea* siblings. Likewise, they were observed in *F. pugnacius*. Cytochrome P450 monooxygenases are heme-thiolate proteins with roles in oxidative functions, e.g., degradation of xenobiotic compounds (Jawallapersand et al., 2014). Teixeira et al. (2017) noted that some black fungi are among the species of Ascomycota with the highest numbers of CYPs, with family expansion and diversification through gene duplication which might explain opportunism. The authors noted that these enzymes are involved in the metabolism of phenolic compounds and aromatic hydrocarbons, and suggested that similar compounds present in the human brain might explain their neurotropic predilection. Studies showed that fungi belonging to the genera *Fusarium*, *Penicillium*, *Aspergillus,* and the family Herpotrichellaceae are capable of degrading

aromatic compounds (Conceição et al., 2005; Satow, 2005; Teixeira et al., 2017). Several species of black fungi have been isolated from hydrocarbon-contaminated environments (de Hoog et al., 2004). Fungi that are capable of assimilating monoaromatic hydrocarbons are enriched in the domestic environment (Sterflinger and Prillinger, 2001; Woertz et al., 2001; Prenafeta-Boldú et al., 2002). Prenafeta-Boldú et al. (2006) suggested physiological links between hydrocarbon assimilation by black fungi and certain patterns of brain infection. The brain contains small molecules that resemble alkylbenzene, phenylalanine metabolic products and lignin biodegradation intermediates, having structural similarity to neurotransmitters such as dopamine, which is catabolized in the brain (Fernstrom and Fernstrom, 2007). Tyrosine, used for the biosynthesis of the neurotransmitters dopamine, noradrenaline and adrenaline, has phenylalanine as precursor and it is involved in the formation of melanin and neuromelanin, dark pigments synthesized from L-dopamine for brain protection (Teixeira et al., 2017; Moreno et al., 2018).

Heat shock proteins are considered virulence factors because of their roles in thermotolerance and as molecular chaperones and are found in all prokaryotes and eukaryotes. They are classified based on approximate molecular weight (Tiwari et al., 2015). In *F. pugnacius,* the following families were identified: Hsp7, Hsp60, Hsp70, Hsp80, and Hsp90. Factors triggering the synthesis of heat shock proteins are oxidative or nutritional stress, UV radiation and exposure to chemical substances, indicating a protective role and aiding in cellular adaptation (Pockley, 2001).

Melanins confer resistance to heat, cold, enzymatic action and organic solvents, function as antioxidants and increase antifungal resistance (Nosanchuk and Casadevall, 2003). Main production route in *Fonsecaea* is the DHN pathway from acetate (acetyl-CoA) derived from glucose metabolism (Cunha et al., 2005; Casadevall and Eisenman, 2012). Melanin is a recognized virulence factor in several black and white pathogenic and opportunistic fungi, such as *Candida albicans, Cryptococcus neoformans*, *Aspergillus fumigatus*, *Exophiala dermatitidis*, *Paracoccidioides brasiliensis*, *Histoplasma capsulatum,* and *Sporothrix schenckii* (Jacobson, 2000; Langfelder et al., 2003; Morris-Jones et al., 2003; Nosanchuk and Casadevall, 2003). Homologous proteins were identified in the herpotrichiellaceous black fungi *Exophiala dermatitidis* (Youngchim et al., 2004). In *F. pugnacius,* melanin-associated proteins related to DHN and DOPA pathways were observed (**Supplementary Table 1**), as reported previously in *F. monophora* (Liu et al., 2019), such as tyrosinase, homogentisate dioxygenase and scytalone. Histopathological studies of organs such as brain, lung, liver and spleen in animal models did not clarify how the melanin production pathways are blocked in albino mutants of *E. dermatitidis* (Sudhadham et al., 2008), but the ability to block the oxidative burst increases significantly the pathogenic potential of *E. dermatitidis*, since the host is unable to eliminate this fungus (Kumar et al., 2019).

Virulence in Animal Models

The chromoblastomycosis agent *F. pugnacius* was described causing a secondary disseminated infection in an apparently immunocompetent patient. Among all agents of chromoblastomycosis, this is a unique type of infection, starting with a chronic skin disease and finally evolving to cerebritis. de Azevedo et al. (2015) reported that *F. pugnacius* was able to produce muriform cells in skin, but hyphae were present in the brain. Dissemination from skin to brain apparently led to conversion to another type of invasive morphology which has not been observed in agents of chromoblastomycosis. In *F. monophora*, which has also been reported from brain infection, the infection route was probably by inhalation, as no skin involvement was observed in any of the patients. Brain infection with a subcutaneous origin has thus far only been observed in *F. pugnacius* (de Azevedo et al., 2015).

Tenebrio molitor larvae were infected with inoculum concentrations of 5×10^6 cells/mL and observed for 10 days. The larvae infected with *F. pugnacius* exhibited higher mortality rates than control groups, PBS and SHAM (**Figure 4A**). *Fonsecaea pugnacius* presented a lower mortality rate than *F. monophora*, *F. erecta,* and *F. pedrosoi,* as reported by Fornari et al. (2018). This indicates that *F. pugnacius* infection presents a slower development compared to *Fonsecaea* siblings involved in chromoblastomycosis, as well as to environmental saprobes. The fungal burden inside the larvae was assessed and presented significant numbers of CFUs, despite the low mortality rates caused by *F. pugnacius*: CFU values were initially countless and decreased along 72, 164, and 240 h post-infection (**Figure 4B**).

Melanization of the larvae is an intracellular defense response and an effective barrier to infection. After 24 h, the larvae infected with *F. pugnacius* presented a dark pigmentation, caused by melanization in the hemolymph, which was observed during the entire 10-day period of analysis by visual observation and spectrophotometry (**Figure 4C**). Similar results were obtained by Fornari et al. (2018) in *Fonsecaea* siblings, showing maximum melanization with 24 h post infection. The capacity of the fungus to survive inside the larvae was confirmed by histopathology, revealing melanized hyphae in tissue that had developed within 4–72 h (**Figure 4D**).

Virulence tests using murine models Balb/c and C57/BL6 were conducted using two infection pathways: intradermal (per hind footpad) and intraperitoneal. In view of determination of fungal burden, *F. pugnacius* was recovered from kidney, lung and liver after 7 days of incubation, indicating a certain preference of the fungus for these organs. After 14 days of intraperitoneal inoculation, *F. pugnacius* was recovered from the brain. At 21 days after infection, a muriform cell was observed in histopathology of the footpad (**Figure 4E**). The animal host infected intraperitoneally presented 1×10^2 and 1×10^4 CFU/mL in blood and organs (lung, kidney and spleen) after 7 and 14 days, respectively. The animals infected intradermally presented 2×10^6 CFU/g in the plantar cushion. The clinical aspects of these animals were evaluated, but no lesions, tissue necrosis or morphological alterations of internal organs were observed, except for plantar cushion swellings with (sub)cutaneous lesions (**Figure 4F**). Vicente et al. (2017) obtained similar results with Balb/c mice infected with *F. pedrosoi* by intradermal inoculation.

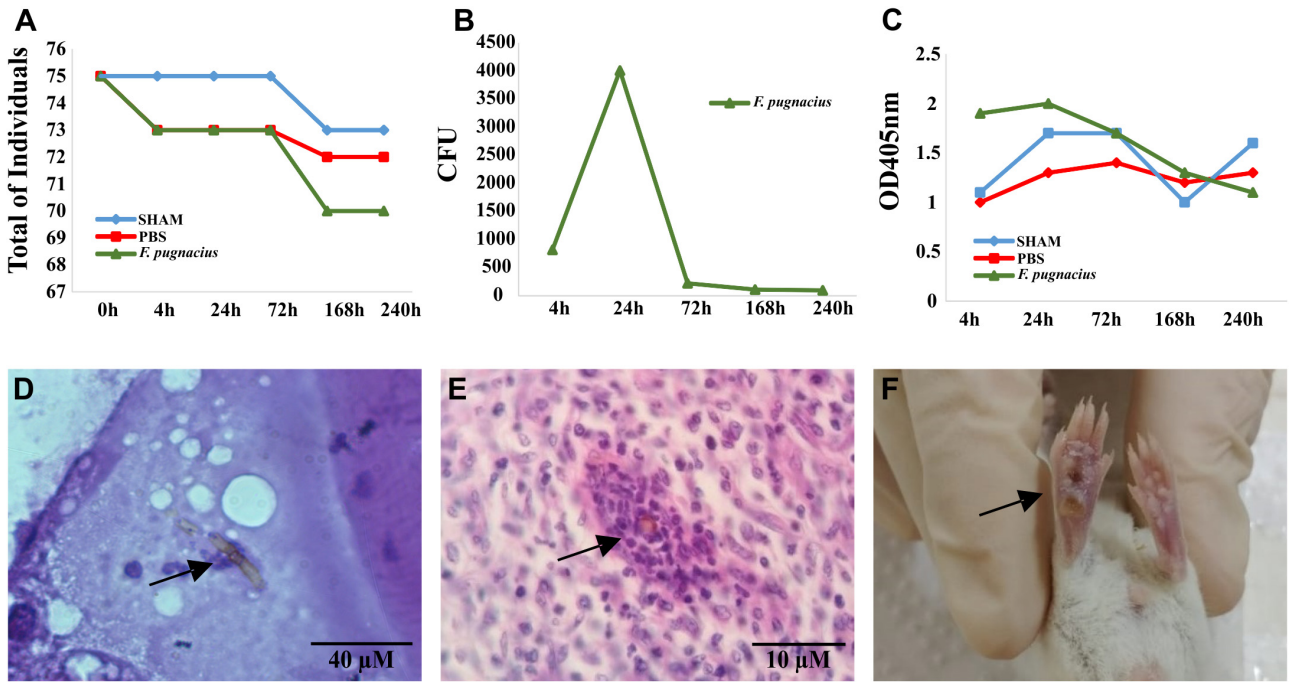

FIGURE 4 | Virulence test of *Fonsecaea pugnacius* using animal models: *Tenebrio molitor* and Balb/c (*Mus musculus*). **(A)** Mortality of the *Tenebrio molitor* larvaes at intervals of 4, 24, 72, 168, and 240 h post-infection. **(B)** Fungal burden of *Tenebrio molitor* larvae tissues at intervals of 4, 24, 72, 168, and 240 h post-infection. **(C)** Melanization of *Tenebrio molitor* hemolymph demonstrated by measuring the OD405 nm at 4, 24, 72, 168, and 240 h post-infection. **(D)** Presence of melanized hyphae in *Tenebrio molitor* larvae tissue 72 h post-infection. **(E)** Histopathology of footpad Balb/c tissue with presence of muriform cell after 21 days of intradermal infection. **(F)** Necrotic lesion in footpad of Balb/c mice after 7 days of intradermal inoculation.

Immunological assays revealed insignificant levels of IL-2, INF-γ, TNF-α, IL-6 and IL-10, compared to what was described for other chromoblastomycosis agents including *F. pedrosoi* (Dong et al., 2018) and *F. monophora* (Jiang et al., 2018). The low immune response could be associated with a low virulent ability of *F. pugnacius*. Although the fungus carries several genes with roles in pathogenicity and ability to survive in murine tissue, the immune system may not recognize their protein products, judging from absence of a cytokine response.

Potential Virulence Related to Enzymatous Genes

The observed brain infection might have been enhanced by the fungus ability to metabolize monoaromatic substrates as carbon source. Among these compounds, vanillic acid, phenyl acid, L-tyrosine, L-dopa, L-phenylanine, dopamine, sphingosine, and others are present in mammalian brain (Prenafeta-Boldú et al., 2006). Subsequently, we verified whether an enzymatic apparatus competent to degrade these compounds is present in the *F. pugnacius* genome, i.e., with carboxylases, reductases, aldolases, and kinases. The enzymatous gene profile was established with CAZymes and MEROPS databases. Carbohydrate-active enzyme analysis resulted in 476 genes encoding putative CAZymes, comprising 93 auxiliary activities (AA), 5 carbohydrate binding modules (CBM), 145 carbohydrate esterases (CE), 121 glycoside hydrolases (GH), 112 glycosyl transferases (GT), and zero polysaccharide lyases (PL). For MEROPS, 21 aspartic peptidases (A) were annotated, 59 cysteine peptidases (C), 14 trypsin peptidases (I), 133 metallo-peptidases (M), zero glutamic peptidases (G), zero asparagines peptidases (N), zero mixed peptidases (P), 189 serine peptidases (S) and 21 threonine peptidases (T) (**Figure 5**).

We performed a comparative analysis of *F. pugnacius* with closely related neurotropic species: *Cladophialophora bantiana*, *Exophiala dermatitidis*, *Fonsecaea monophora*, *Rhinocladiella mackenziei*, and *Verruconis gallopava* (**Figure 5** and **Supplementary Table 2**), which have been reported as agents of cutaneous and deep infection in skin, lungs, lymphatic system, kidneys, spleen, liver and thyroid glands (Cardeau-Desangles et al., 2013; de Azevedo et al., 2015; Geltner et al., 2015; Jennings et al., 2017; Mukhopadhyay et al., 2017; Stokes et al., 2017; Grewal et al., 2018; Sideris and Ge, 2018; Klasinc et al., 2019; Miossec et al., 2019; Wang et al., 2019; Alabdely and Alzahrani, 2020). The CAZy database is an exceptional reporter of fungal lifestyles degrading complex polysaccharides (Cantarel et al., 2009; Vicente et al., 2017). The GH class contains the majority of catalytic enzymes to degrade lignocelluloses (Cantarel et al., 2009) and seems to be expanded in species associated with disseminated infection (**Figure 5**). Through this analysis (**Supplementary Table 3**), we observed a high number of GH enzymes in all genomes analyzed, except for GH32 which was present in low numbers (*C. bantiana*: 3; *F. pugnacius*: 2; *E. dermatitidis*, *F. monophora*,

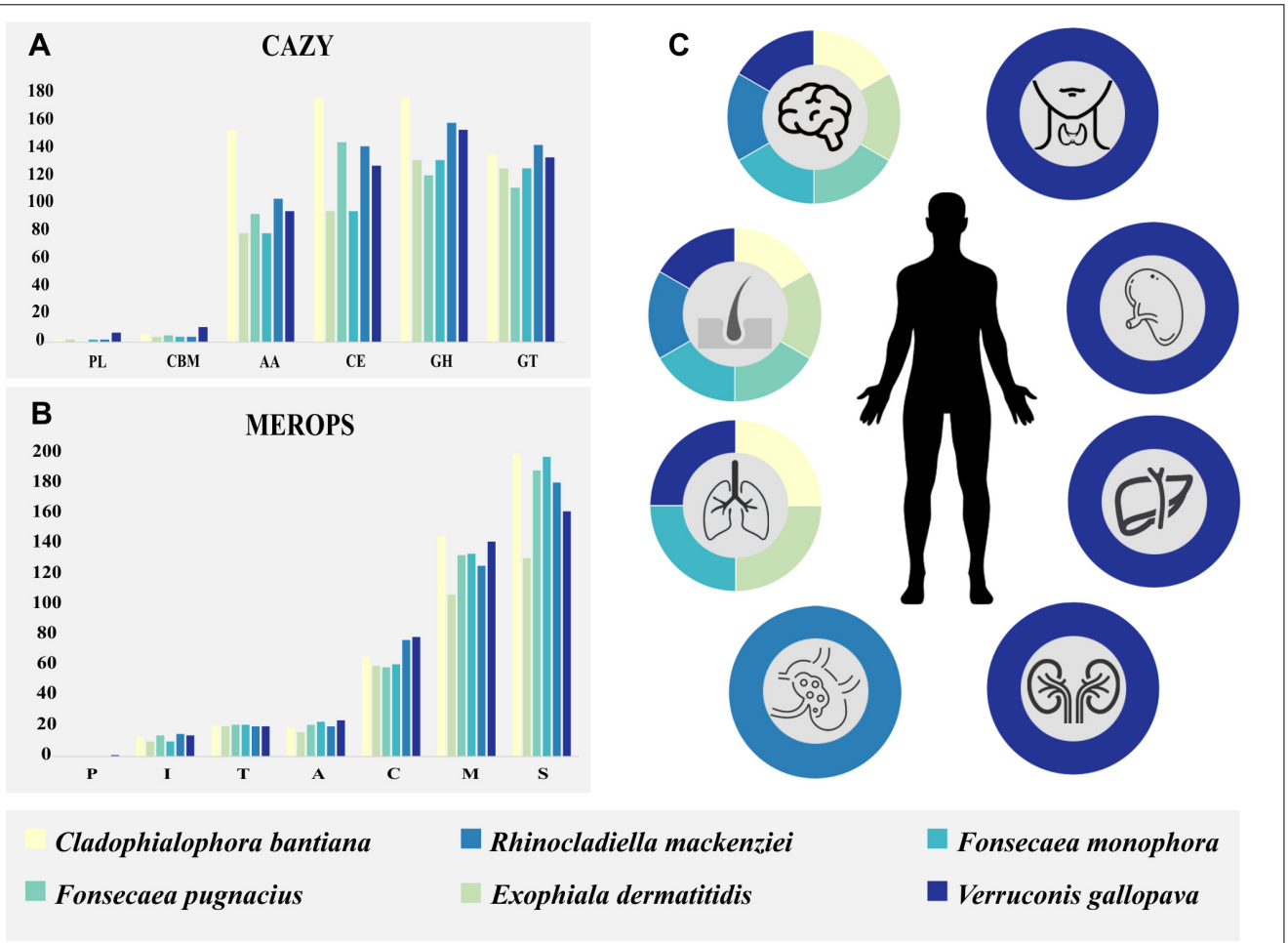

FIGURE 5 | Species enzymatous gene profiles and epidemiology of human host pathogenicity are summarized in colored boxes. *Cladophialophora bantiana*: beige; *Exophiala dermatitidis*: light green; *Fonsecaea pugnacius*: medium green; *Fonsecaea monophora*: light blue; *Rhinocladiella mackenziei*: medium blue; *Verruconis gallopava*: dark blue. **(A)** Carbohydrate-active enzyme (CAZY) annotation separated by classes. **(B)** MEROPS annotation separated by classes. **(C)** The species of black fungi related to subcutaneous and cerebral human infection and others affected organs: lungs, lymphatic system, kidneys, spleen, liver, and thyroid gland.

V. gallopava: 1, *R. mackenziei*: 0). The CAZyme family GH32 are enzymes associated with energy storage and seem to provide energy for survival in extreme environments (Oren, 2011). Additionally, the GH18 family, observed in the species under study, are chitinases. β-1,3-Glucanases are able to degrade chitin that is normally present in animal exoskeletons. Likewise, 29 GH families involved in the degradation of plant biomass (Li et al., 2011) were observed in the strains evaluated, explaining the dual ability of these fungi to invade plant and animal tissues.

The high number glycosyltransferases (GTs) can also be linked to neurotropism, since these enzymes are responsible for the biosynthesis of glycoside (Cantarel et al., 2009). Some fungi are able to convert phenolic compounds into their corresponding glycosides (Tronina et al., 2013) and this ability may be derived from xenobiotic metabolism (Yang et al., 2014). The vertebrate brain contains a wide variety of gangliosides that are localized in specific cell types, such as on the surface of plasmatic membranes (Stanley, 2016). Gangliosides contain a fatty acid and a sphingosine base and are involved in neural functions such as memory formation, synaptic transmission, regeneration (Zitman et al., 2010). In cases of cerebral infection, the first symptoms described are locomotor difficulties and severe headache (Koo et al., 2010; de Azevedo et al., 2015). The GT41 family was the most numerous in our annotation, it is related to the metabolism of serine-threonine as indicated and involved in the process of subcutaneous infection (Vicente et al., 2017). Also, the GT2 family was abundant; proteins that act as chitin synthases (Breton et al., 2006) are numerous in many fungi (Lee et al., 2018; Stone et al., 2018).

The AA CAZyme family is composed of lignolytic enzymes and are commonly found in plant pathogens. Similar to the GH and CMB families, they have a role in breaking down plant cell-wall polysaccharides (Lowe et al., 2015). The CBM family is composed of lectins and sugar transporters, while GH are glycosyltransferases such as lignocelluloses or chitinases (Yang et al., 2014). However, the GH class was more numerous in the species related to disseminated and cerebral infection (**Figure 5**).

The lectins from yeasts and fungi have been associated with early stages of human infection (Varrot et al., 2013), whereas in bacteria they seem to be involved in recognition of host glycans (Imberty and Varrot, 2008).

Polysaccharide lyases are enzymes able to cleave polysaccharide chains. This group presents many fold types (or classes), indicating that PLs are polyphyletic (Lombard et al., 2010). Many fungi that do not have enzymes from the PL CE and GH families are saprobes, as these classes have enzymes related to cell wall degradation in plants (Zhao et al., 2013). This enzymatous gene profile suggested a dual ecological ability of these agents, in line with their extremotolerance and adaptability to variable environmental niches, which is a prerequisite for their opportunistic profiles.

Peptidases play key roles in penetration of microorganisms into host tissue and are involved in pathogen-host interactions (Ohm et al., 2012). Herpotrichiellaceous agents produce a variety of extracellular peptidases for the degradation of environmental substrates, indicating a poorly specialized nutritional strategy (Sriranganadane et al., 2010; Vicente et al., 2017). The MEROPS S (serine) and M (metallo) peptidase families were the highest in number in the analyzed species causing brain infection. These two groups have been reported to be significantly enriched in transcriptome analyses of *E. dermatitidis* during infection (Poyntner et al., 2018). Among the Serine families, classes S33 and S9 were more numerous (**Supplementary Table 3**), both involved in prolyl metabolism. Class S33 is a prolyl aminopeptidase family, which is not essential for growth but may confer a selective advantage allowing the organism to use proline-rich substrates (Iqbal et al., 2018). Teixeira et al. (2017) observed an expansion of the protein-degrading peptidase enzyme family M38 (isoaspartyl dipeptidases) in the bantiana-clade, the most numerous of metallo-peptidases family in the analyzed strains. This family is unusual in that the majority of characterized proteins are not peptidases but are associated with β-aspartic dipeptidase acting in the release of iso-aspartate residues from peptides (Palmeira et al., 2018).

Differences between closely related taxa are expected in ecology-related genes. The enzymatic repertoire of these fungi shows their ability to degrade a wide variety of substrates (**Figure 5**). This may suggest generalist and opportunistic ecology comparable to *Aspergillus* spp. permitting transfer from the environment to the animal host (Vicente et al., 2017), rather than pathogenicity where focused adaptation (Moran et al., 2011). In addition, we analyzed genes codifying proteins related to degradation aromatic carbons pathway (Teixeira et al., 2017; Moreno et al., 2018) and the strains studied present a range of genes encoding homologous proteins (**Table 2**). The virulence of these strains is partially explained by general factors like the presence of melanin in the cell wall, thermotolerance and the ability to assimilate of monoaromatic hydrocarbons (Moreno et al., 2018). Furthermore, CYPs are involved in the degradation of aromatic hydrocarbons and xenobiotic metabolism, developing functions in the fungal pathogenicity and in the detoxification of exogenous compounds (Moreno et al., 2018).

The family Herpotrichiellaceae contains numerous black fungi that present tolerance to various types of stress, showing great adaptability to extreme environmental conditions, presumably resulting from genomic information. Genomic studies of

TABLE 2 | Proteins related to degradation aromatic carbons pathway in *Fonsecaea pugnacius* and homologs in black fungi related to subcutaneous and brain infection.

	A	B	C	D	E	F
Fonsecaea pugnacius	gi| 628298155		gi| 915117215	gi| 915113179 gi| 915117218	gi| 915082939	gi| 915113183 gi| 915117846 gi| 915047106 gi| 915117212 gi| 915114200
Cladophialophora bantiana		XP_016622135.1	XP_016621839.1 XP_016624089.1 XP_016620669.1	XP_0166207751 XP_0166218381	XP_016619449.1	XP_016625963.1 XP_016624090.1 XP_016621840.1
Exophiala dermatitidis		HMPREF1120_09097	HMPREF1120_02976 HMPREF1120_03465 HMPREF1120_03826	HMPREF1120_ 03827	HMPREF1120_03438	HMPREF1120_ 03825
Fonsecaea monophora	AYO21_00136 AYO21_09571	AYO21_05363 AYO21_04106	AYO21_12165	AYO21_04852 AYO21_01974	AYO21_00578	AYO21_07675 AYO21_04851
Verruconis gallopava	PV09_08030		PV09_06763	PV09_04037 PV09_05381 PV09_02442		PV09_02443 PV09_02062
Rhinocladiella mackenziei		Z518_08486	Z518_05387	Z518_05995 Z518_05388 Z518_06895 Z518_09726	Z518_00072	Z518_02618 Z518_04953 Z518_04319 Z518_05993 Z518_05386 Z518_09725

*(A) Benzyl alcohol dehydrogenase, **(B)** β-carboxy-cis, cis-muconate lactonizing enzyme, **(C)** phenylacetate 2-hydroxylase, **(D)** homogentisate 1,2-dioxygenase, **(E)** maleylacetoacetate isomerase, **(F)** fumarylacetoacetase.*

F. pugnacius showed the wide variety of genes involved in extreme tolerance and enzymes associated to occurrence of virulence factors. The survival capacity of fungi in animal models was confirmed by histopathological analysis and the presence of melanin in the host tissue. We have shown that *F. pugnacius* can colonize the brain and cause subcutaneous lesions with the formation of muriform cells in the murine model. An ecological capacity can be concluded from the presence of metabolic pathways for extremetolerance combined with the ability to infect human hosts. However, complementary molecular studies must be carried out in order to strengthen the connections between ecology and clinical profiles.

Gostinčar et al. (2018) found a link between (poly-)extremotolerance and opportunism, the ability to metabolize monoaromatic hydrocarbons improving human or animal disease. The order Chaetothyriales comprises opportunists, in which tolerance to various types of stress is associated with adaptability, presumably resulting in a large potential for habitat changes. The infection is as a side effect of the fungus adaptation to the human host, demonstrating that is not a favorable habitat, nor relevant to their evolutionary process. This defines opportunism against pathogenicity, where the infection is advantageous for the fitness of the species. Most organisms considered opportunistic are unable to transmit from host to host, so specific adaptations will be lost with the cure of the infection, explaining the lack of complex virulence characteristics. Therefore, opportunistic infections can be considered an evolutionary dead end, which is unlikely to lead to true pathogenicity (Gostinčar et al., 2018).

DATA AVAILABILITY STATEMENT

The datasets generated for this study can be found in the GenBank/accession number: WJFF00000000/ waiting to publish for to be public date.

ETHICS STATEMENT

All animal experiments in this study were approved by the Federal University of Paraná Ethics Committee (approval certificate 1002) and performed according to the Committee's recommendations.

AUTHOR CONTRIBUTIONS

AB, VV, RG, and SH contributed to the conception and design of the study. FC, AL, LM, and NS organized the database. AB, GS, BS, FM, BL, RC, VB, EB, VP, and NH performed the analysis. AB wrote the first draft of the manuscript. GS wrote sections of the manuscript. All the authors contributed to the manuscript revision, read and approved the submitted version.

FUNDING

This work was supported by the Brazilian Federal Agency for Support and Evaluation of Graduate: Education Coordination for the Improvement of Higher Education Personnel—CAPES (PVE project grant number 0592012), the PRINT (www.capes.gov.br), and the National Council for Scientific and Technological Development (http://cnpq.br/), Brazil; and by The National Institute of Science and Technology of Biological Nitrogen Fixation/CNPq/MCT (grant number 573828/2008-3). VV received fellowships from the National Council for Scientific and Technological Development (CNPq), Brasilia, Brazil.

SUPPLEMENTARY MATERIAL

The Supplementary Material for this article can be found online at: https://www.frontiersin.org/articles/10.3389/fgene.2020.00822/full#supplementary-material

REFERENCES

Alabdely, M. H., and Alzahrani, H. A. (2020). Inferior vena cava filter eroding the aorta. *J. Appl. Hematol.* 11:37. doi: 10.4103/joah.joah_71_19

Arcobello, J. T., and Revankar, S. G. (2020). Phaeohyphomycosis. *Semin. Respir. Crit. Care Med.* 41, 131–140. doi: 10.1055/s-0039-3400957

Ashburner, M., Ball, C. A., Blake, J. A., Botstein, D., Butler, H., Cherry, J. M., et al. (2000). Gene Ontology: tool for the unification of biology. *Nat. Genet.* 25, 25–29. doi: 10.1038/75556

Badali, H., Prenafeta-Boldu, F. X., Guarro, J., Klaassen, C. H., Meis, J. F., and de Hoog, G. S. (2011). *Cladophialophora psammophila*, a novel species of Chaetothyriales with a potential use in the bioremediation of volatile aromatic hydrocarbons. *Fungal Biol.* 115, 1019–1029. doi: 10.1016/j.funbio.2011.04.005

Bankevich, A., Nurk, S., Antipov, D., Gurevich, A. A., Dvorkin, M., Kulikov, A. S., et al. (2012). SPAdes: a new genome assembly algorithm and its applications to single-cell sequencing. *J. Comput. Biol.* 19, 455–477. doi: 10.1089/cmb.2012.0021

Besemer, J., Lomsadze, A., and Borodovsky, M. (2001). GeneMarkS: a self-training method for prediction of gene starts in microbial genomes. Implications for finding sequence motifs in regulatory regions. *Nucleic Acids Res.* 29, 2607–2618. doi: 10.1093/nar/29.12.2607

Bocca, A. L., Brito, P. P. M. S., Figueiredo, F., and Tosta, C. E. (2006). Inhibition of nitric oxide production by macrophages in chromoblastomycosis: a role for *Fonsecaea pedrosoi* melanin. *Mycopathologia* 161, 195–203. doi: 10.1007/s11046-005-0228-6

Breton, C., Šnajdrová, L., Jeanneau, C., Koča, J., and Imberty, A. (2006). Struc- tures and mechanisms of glycosyltransferases. *Glycobiology* 16, 29R–37R.

Cañete-Gibas, C. F., and Wiederhold, N. P. (2018). The black yeasts: an update on species identification and diagnosis. *Curr. Fungal Infect. Rep.* 12, 59–65. doi: 10.1007/s12281-018-0314-0

Cantarel, B. L., Coutinho, P. M., Rancurel, C., Bernard, T., Lombard, V., and Henrissat, B. (2009). The Carbohydrate-Active EnZymes database (CAZy): an expert resource for glycogenomics. *Nucleic Acids Res.* 37, 233–238. doi: 10.1093/nar/gkn663

Cardeau-Desangles, I., Fabre, A., Cointault, O., Guitard, J., Esposito, L., Iriart, X., et al. (2013). Disseminated *Ochroconis gallopava* infection in a heart transplant patient. *Transplant Infect. Dis.* 15, E115–E118. doi: 10.1111/tid.12084

Casadevall, A., and Eisenman, E. C. (2012). "Synthesis and assembly of fungal melanin," in *Applied Microbiology and Biotechnology*, Vol. 93, ed. A. Steinbüchel (New York, NY: Springer Press), 931–940. doi: 10.1007/s00253-011-3777-2

Castro, R. J. A., Siqueira, M. I, Jerônimo, M. S., Basso, A. M. M., Veloso, P. H. Jr., Magalhães, K. G., et al. (2017). The major chromoblastomycosis etiologic

agent *Fonsecaea pedrosoi* activates the NLRP3 inflammasome. *Front. Immunol.* 8:1572. doi: 10.3389/fimmu.2017.01572

Conceição, D. M., Angelis, D. A., Bidoia, E. D., and Angelis, D. F. (2005). Fungos filamentosos isolados do rio Atibaia, SP, e refinarias de petróleo biodegradadores de compostos fenólicos. *Rev. Inst. Biol.* 72, 99–106.

Costa, C., Dias, P. J., Sá-Correia, I., and Teixeira, M. C. (2014). MFS multidrug transporters in pathogenic fungi: do they have real clinical impact? *Front. Physiol.* 5:197. doi: 10.3389/fphys.2014.00197

Cunha, M. M., Franzen, A. J., Alviano, D. S., Zanardi, E., Alviano, C. S., Souza, W., et al. (2005). Inhibition of melanin synthesis pathway by tricyclazole increases susceptibility of *Fonsecaea pedrosoi* against mouse macrophages. *Microsc. Res. Tech.* 68, 377–384. doi: 10.002/jemt.20260

de Azevedo, C. M. P. S., Gomes, R. R., Vicente, V. A., Santos, D. W. C. L., Marques, S. G., do Nascimento, M. M. F., et al. (2015). *Fonsecaea pugnacius*, a novel agente of disseminated chromoblastomycosis. *J. Clin. Microbiol.* 53, 2674–2685. doi: 10.1128/JCM.00637-15

de Hoog, G. S., Attili-Angelis, D., Vicente, V. A., Van Den Ende, A. H., and Queiroz-Telles, F. (2004). Molecular ecology and pathogenic potential of *Fonsecaea* species. *Med. Mycol.* 42, 405–416. doi: 10.1080/13693780410001661464

Derengowski, L. S., Tavares, A. H., Silva, S., Procópio, L. S., Felipe, M. S., and Silva-Pereira, I. (2008). Upregulation of glyoxylate cycle genes upon *Paracoccidioides brasiliensis* internalization by murine macrophages and *in vitro* nutritional stress condition. *Med. Mycol.* 46, 125–134. doi: 10.1080/13693780701670509

Dong, B., Tong, Z., Li, R., Chen, S. C. A., Liu, W., Liu, W., et al. (2018). Transformation of *Fonsecaea pedrosoi* into sclerotic cells links to the refractoriness of experimental chromoblastomycosis in BALB/c mice via a mechanism involving a chitin-induced impairment of IFN-γ production. *PLoS Negl. Trop. Dis.* 12:e0006237. doi: 10.1371/journal.pntd.0006237

Doymaz, M. Z., Seyithanoglu, M. F., Hakyemez, I., Gultepe, B. S., Cevik, S., and Aslan, T. (2015). A case of cerebral phaeohyphomycosis caused by *Fonsecaea monophora*, a neurotropic dematiaceous fungus, and a review of the literature. *Mycoses* 58, 187–192. doi: 10.1111/myc.12290

Dunn, M. F., Ramirez-Trujillo, J. A., and Hernández-Lucas, I. (2009). Major roles of isocitrate lyase and malate synthase in bacterial and fungal pathogenesis. *Microbiology* 155, 3166–3175. doi: 10.1099/mic.0.030858-0

Duvenage, L., Walker, L. A., Bojarczuk, A., Johnston, A. S., MacCallum, D. M., Munro, C. A., et al. (2018). Alternative oxidase induction protects *Candida albicans* from respiratory stress and promotes hyphal growth. *bioRxiv* [Preprint]. doi: 10.1101/405670

Emms, D. M., and Kelly, S. (2018). OrthoFinder2: Fast and accurate phylogenomic orthology analysis from gene sequences. *bioRxiv* [Preprint]. doi: 10.1101/466201

Fernstrom, J., and Fernstrom, M. (2007). Tyrosine, phenylalanine, and catecholamine synthesis and function in the brain. *J. Nutr.* 137, 1539–1548. doi: 10.1093/jn/137.6.1539S

Fornari, G., Gomes, R. R., Degenhardt-Goldbach, J., Dos Santos, S. S., De Almeida, S. R., Dos Santos, G. D., et al. (2018). A model for trans-kingdom pathogenicity in *Fonsecaea* agents of human chromoblastomycosis. *Front. Microbiol.* 9:2211. doi: 10.3389/fmicb.2018.02211

Geltner, C., Sorschag, S., Willinger, B., Jaritz, T., Saric, Z., and Lass-Florl, C. (2015). Necrotizing mycosis due to *Verruconis gallopava* in an immunocompetent patient. *Infection* 43, 743–746. doi: 10.1007/s15010-015-0757-y

Gostinčar, C., Zajc, J., Lenassi, M., Plemenitas, A., de Hoog, G. S., Al-Hatmi, A. M. S., et al. (2018). Fungi between extremotolerance and opportunistic pathogenicity on humans. *Fungal Divers.* 93, 195–213. doi: 10.1007/s13225-018-0414-8

Grewal, H. K., Kumar, P. N., Shah, N., and Timpone, J. G. (2018). *Verruconis Gallopava:* recurrent infection in a renal transplant recipient. *Infect. Dis. Clin. Pract.* 26, e12–e15. doi: 10.1097/IPC.0000000000000569

Helbig, S., Thuermer, A., Dengl, M., Krukowski, P., and de With, K. (2018). Cerebral abscess by Fonsecaea monophora —The first case reported in Germany. *Open Forum Infect. Dis.* 5:ofy129. doi: 10.1093/ofid/ofy129.2018

Imberty, A., and Varrot, A. (2008). Microbial recognition of human cell surface glycoconjugates. *Curr. Opin. Struct. Biol.* 18, 567–576. doi: 10.1016/j.sbi.2008.08.001

Iqbal, M., Dubey, M., Gudmundssn, M., Viketoft, M., Jesen, D. F., Karlsson, M., et al. (2018). Comparative evolutionary histories of fungal proteases reveal gene gains in the mycoparasitic and nematode-parasitic fungus *Clonostachys rósea*. *BMC Evol. Biol.* 18:171. doi: 10.1186/s12862-018-1291-1

Jacobson, E. S. (2000). Pathogenic roles for fungal melanins. *Clin. Microbiol. Rev.* 13, 708–717. doi: 10.1128/CMR.13.4.708-717.2000

Jawallapersand, P., Mashele, S. S., Kovačič, L., Stojan, J., Komel, R., Pakala, S. B., et al. (2014). Cytochrome P450 Monooxygenase CYP53 Family in fungi: comparative structural and evolutionary analysis and its role as a common alternative anti-fungal drug target. *PLoS One* 9:107209. doi: 10.1371/journal.pone.0107209

Jennings, Z., Kable, K., Halliday, C. L., Nankivell, B. J., Kok, J., Wong, G., et al. (2017). *Verruconis gallopava* cardiac and endovascular infection with dissemination after renal transplantation: case report and lessons learned. *Med. Mycol. Case Rep.* 15, 5–8. doi: 10.1016/j.mmcr.2016.12.006

Jiang, M., Cai, W., Zhang, J., Xie, T., Xi, L., Li, X., et al. (2018). Melanization of a meristematic mutant of *Fonsecaea monophora* increase the pathogenesis in a BALB/c mice infection model. *Med. Mycol.* 56, 979–986. doi: 10.1093/mmy/myx148

Klasinc, R., Riesenhuber, M., Bacher, A., and Willinger, B. (2019). Invasive fungal infection caused by *Exophiala dermatitidis* in a patient after lung transplantation: case report and literature Review. *Mycopathologia* 184, 107–113. doi: 10.1007/s11046-018-0275-4

Koo, S., Klompas, M., and Marty, F. M. (2010). *Fonsecaea monophora* cerebral phaeohyphomycosis: case report of successful surgical excision and voriconazole treatment and review. *Med. Mycol.* 48, 769–774. doi: 10.3109/13693780903471081

Krzywinski, M., Schein, J., Birol, I., Connors, J., Gascoyne, R., Horsman, D., et al. (2009). Circos: an information aesthetic for comparative genomics. *Genome Res.* 19, 1639–1645. doi: 10.1101/gr.092759.109

Kumar, D., Anjum, N., Kumar, A., and Das, S. (2019). Role of Melanin production in fungal pathogenesis. *Int. J. Sci. Res.* 8, 20–22.

Langfelder, K., Streibel, M., Jahn, B., Haase, G. E., and Brakhage, A. A. (2003). Biosynthesis of fungal melanins and their importance for human pathogenic fungi. *Fungal Genet. Biol.* 38, 143–158. doi: 10.1016/S1087-1845(02)00526-1

Langmead, B., and Salzberg, S. L. (2012). Fast gapped-read alignment with bowtie 2. *Nat. Methods* 9, 357–359. doi: 10.1038/nmeth.1923

Lee, C.-S., Kong, W.-S., and Park, Y.-J. (2018). Genome Sequencing and Genome-Wide Identification of Carbohydrate-Active Enzymes (CAZymes) in the White Rot Fungus *Flammulina fennae*. *Biotechnol. Lett.* 46, 300–312. doi: 10.4014/mbl.1808.08012

Li, D. C., Li, A. N., and Papageorgiou, A. C. (2011). Cellulases from thermophilic fungi: recent insights and biotechnological potential. *Enzyme Res.* 2011:308730. doi: 10.4061/2011/308730

Liu, Y., Huang, X., Liu, H., Xi, L., and Cooper, C. R. (2019). Increased virulence of albino mutant of *Fonsecaea monophora* in *Galleria mellonella*. *Med. Mycol.* 57, 1018–1023. doi: 10.1093/mmy/myz007

Lombard, V., Bernard, T., Rancurel, C., Brumer, H., Coutinho, P. M., and Henrissat, B. (2010). A hierarchical classification of polysaccharide lyases for glycogenomics. *Biochem. J.* 432, 437–444. doi: 10.1042/BJ20101185

Lorenz, M., and Fink, G. R. (2001). The glyoxylate cycle is required for fungal virulence. *Nature* 412, 83–86. doi: 10.1038/35083594

Lowe, R. G. T., McCorkelle, O., Bleackley, M., Collins, C., Faou, P., Mathivanan, S., et al. (2015). Extracellular peptidases of the cereal pathogen *Fusarium graminearum*. *Front. Plant Sci.* 6:962. doi: 10.3389/fpls.2015.00962

Lucasse, C., Chardome, J., and Magis, P. (1954). Cerebral mycosis from *Cladosporium tricho.ides in a native of the Belgian Congo*. *Ann. Soc. Belge Med. Trop.* 34, 475–478.

Maekawa, L. E., Rossoni, R. D., Barbosa, J. O., Jorge, A. O. C., Junqueira, J. C., and Valera, M. C. (2015). Different extracts of Zingiber officinale decrease Enterococcus faecalis infection in Galleria mellonella. *Braz. Dent. J.* 26, 105–109. doi: 10.1590/0103-6440201300199

Miossec, C., Jacob, S., Peipoch, L., Brard, M., Jolivet, E., Hochedez, P., et al. (2019). Cerebral phaeohyphomycosis due to *Cladophialophora bantiana* in a French Guianese child. *J. Mycol. Méd.* 30:100918. doi: 10.1016/j.mycmed.2019.100918

Missall, T. A., Lodge, J. K., and Mcewen, J. E. (2004). Mechanisms of resistance to oxidative and nitrosative stress: implications for fungal survival in mammalian hosts. *Eukaryot. Cell* 3, 835–846. doi: 10.1128/ec.3.4.835-846.2004

Moran, G. P., Coleman, D. C., and Sullivan, D. J. (2011). Comparative genomics and the evolution of pathogenicity in human pathogenic fungi. *Eukaryot. Cell* 10, 34–42. doi: 10.1128/EC.00242-10

Moreno, L. F., Ahmed, A. A. O., Brankovics, B., Cuomo, C. A., Menken, S. B. J., Taj-Aldeen, S. J., et al. (2018). Genomic understanding of an infectious brain disease from the desert. *G3* 8, 909–922. doi: 10.1534/g3.117.300421

Morris-Jones, R., Youngchim, S., Gomez, B. L., Aisen, P., Hay, R. J., Nosanchuk, J. D., et al. (2003). Synthesis of melanin-like pigments by *Sporothrix schenckii in vitro* and during mammalian infection. *Infect. Immun.* 71, 4026–4033. doi: 10.1128/iai.71.7.4026-4033.2003

Mukhopadhyay, S. L., Mahadevan, A., Bahubali, V. H., Dawn Bharath, R., Prabhuraj, A. R., Maji, S., et al. (2017). A rare case of multiple brain abscess and probably disseminated phaeohyphomycosis due to *Cladophialophora bantiana* in an immunosuppressed individual from India. *J. Mycol. Méd.* 27, 391–395. doi: 10.1016/j.mycmed.2017.04.002

Najafzadeh, M. J., Gueidan, C., Badali, H., van den Ende, A. H. G., Xi, L., and de Hoog, G. S. (2009). Genetic diversity and species delimitation in the opportunistic genus *Fonsecaea*. *Med. Mycol.* 47, 17–25. doi: 10.1080/13693780802527178

Najafzadeh, M. J., Vicente, V. A., Sun, J., Meis, J. F., and de Hoog, G. S. (2011). *Fonsecaea multimorphosa* sp. nov., a new species of Chaetothyriales isolated from a feline cerebral abscess. Fungal Biol. 115, 1066–1076. doi: 10.1016/j.funbio.2011.06.007

Nobrega, J. P. S., Rosemberg, S., Adami, A. M., Heins-Vaccari, E. M., Lacaz, C. S., and Brito, T. (2003). Feohifomicose cerebral ("cromoblastomicose") por *Fonsecaea pedrosoi*: primeiro caso demonstrado por cultura do fungo no Brasil. *Rev. Inst. Med. Trop. S. Paulo* 45, 217–220. doi: 10.1590/S0036-46652003000400008

Nosanchuk, J. D., and Casadevall, A. (2003). The contribution of melanin to microbial pathogenesis. *Cell. Microbiol.* 5, 203–223. doi: 10.1046/j.1462-5814.2003.00268.x

Ohm, R. A., Feau, N., Henrissat, B., Schoch, C. L., Horwitz, B. A., Barry, K. W., et al. (2012). Diverse lifestyles and strategies of plant pathogenesis encoded in the genomes of eighteen Dothideomycetes fungi. *PLoS Pathog.* 8:e1003037. doi: 10.1371/journal.ppat.1003037

Oren, A. (2011). Thermodynamic limits to microbial life at high salt concentrations. *Environ. Microbiol.* 13, 1908–1923. doi: 10.1111/j.1462-2920.2010.02365.x

Ozgun, H. D., Jacobs, D. L., and Toms, S. A. (2019). "Cladophialophora bantiana," in *Fungal Infections of the Central Nervous System*, eds M. Turgut, S. Challa, and A. Akhaddar (Cham: Springer).

Palmeira, V. F., Goulart, F. R. V., Granato, M. Q., Alviano, D. S., Alviano, C. S., Kneipp, L. F., et al. (2018). *Fonsecaea pedrosoi* sclerotic cells: secretion of aspartic-type peptidase and susceptibility to peptidase inhibitors. *Front. Microbiol.* 9:1383. doi: 10.3389/fmicb.2018.01383

Perdoni, F., Falleni, M., Tosi, D., Cirasola, D., Romagnoli, S., Braidotti, P., et al. (2014). A histological procedure to study fungal infection in the wax moth *Galleria mellonella*. *Eur. J. Histochem.* 58:2428. doi: 10.4081/ejh.2014.2428

Piro, V. C., Faoro, H., Weiss, V. A., Steffens, M. B. R., Pedrosa, F. O., Souza, E. M., et al. (2014). FGAP: an automated gap closing tool. *BMC Res. Notes* 7:371. doi: 10.1186/1756-0500-7-371

Pockley, A. G. (2001). Heat shock proteins in health and disease: therapeutic targets or therapeutic agents? *Expert Rev. Mol. Med.* 3, 1–21. doi: 10.1017/S1462399401003556

Poyntner, C., Mirastschijski, U., Sterflinger, K., and Tafer, H. (2018). Transcriptome study of an *Exophiala dermatitidis* PKS1 mutant on an ex vivo skin model: Is melanin important for infection? *Front. Microbiol.* 9:1457. doi: 10.3389/fmicb.2018.01457

Prenafeta-Boldú, F. X., Summerbell, R., and Sybren De Hoog, G. (2006). Fungi growing on aromatic hydrocarbons: biotechnology's unexpected encounter with biohazard? *FEMS Microbiol. Rev.* 30, 109–130. doi: 10.1111/j.1574-6976.2005.00007.x

Prenafeta-Boldú, F. X., Vervoort, J. J. M., Grotenhuis, T., and van Froenestijn, J. W. (2002). Substrate interactions during the biodegradation of benzene, toluene, ethylbenzene, and xylene (BTEX) hydrocarbons by the fungus *Cladophialophora* sp. strain T1. *Appl. Environ. Microbiol.* 68, 2660–2665. doi: 10.1128/AEM.68.6.2660-2665.2002

Queiroz-Telles, F., De Hoog, S., Santos, D. W. C. L., Salgado, C. G., Vicente, V. A., Bonifaz, A., et al. (2017). Chromoblastomycosis. *Clin. Microbiol. Rev.* 30, 233–276. doi: 10.1128/CMR.00032-16

Quevillon, E., Silventoinen, V., Pillai, S., Harte, N., Mulder, N., Apweiler, R., et al. (2005). InterProScan: protein domains identifier. *Nucleic Acids Res.* 33, 116–120. doi: 10.1093/nar/gki442

Raparia, K., Powell, S. Z., Cernoch, P., and Takei, H. (2010). Cerebral mycosis: 7-year retrospective series in a tertiary center. *Neuropathology* 30, 218–223. doi: 10.1111/j.1440-1789.2009.01067.x

Rawlings, N. D., Barrett, A. J., and Finn, R. (2016). Twenty years of the MEROPS database of proteolytic enzymes, their substrates and inhibitors. *Nucleic Acids Res.* 44, 343–350. doi: 10.1093/nar/gkv1118

Rodrigues, A. M., de Hoog, G. S., and Camargo, Z. P. (2015). Molecular diagnosis of pathogenic *Sporothrix* Species. *PLoS Negl. Trop. Dis.* 9:e0004190. doi: 10.1371/journal.pntd.0004190

Satow, M. M. (2005). *"Screening" de Fungos Degradadores de Hidrocarbonetos Complexos*. Master's dissertation, Universidade Estadual Paulista, Rio Claro.

Schneider, G. X., Gomes, R. R., Bombassaro, A., Zamarchi, K., Voidaleski, M. F., Costa, F. F., et al. (2019). New molecular markers distinguishing fonsecaea agents of chromoblastomycosis. *Mycopathologia* 184, 493–504. doi: 10.1007/s11046-019-00359-2

Scorzoni, L., de Lucas, M. P., Mesa-Arango, A. C., Fusco-Almeida, A. M., Lozano, E., Cuenca-Estrella, M., et al. (2013). Antifungal efficacy during Candida krusei infection in non-conventional models correlates with the yeast *in vitro* susceptibility profile. *PLoS One* 8:e60047. doi: 10.1371/journal.pone.0060047

Seppey, M., Manni, M., and Zdobnov, E. M. (2019). BUSCO: assessing genome assembly and annotation completeness. *Methods Mol. Biol.* 1962, 227–245. doi: 10.1007/978-1-4939-9173-0_14

Seyedmousavi, S., Netea, M. G., Mouton, J. W., Melchers, W. J., Verweij, P. E., and de Hoog, G. S. (2014). Black yeasts and their filamentous relatives: principles of pathogenesis and host defense. *Clin. Microbiol. Rev.* 27, 527–542. doi: 10.1128/CMR.00093-13

Sideris, E., and Ge, L. (2018). Chromoblastomycosis in immunosuppressed petients. *Med. J. Aust.* 209:295. doi: 10.5694/mja18.00350

Sriranganadane, D., Waridel, P., Salamin, K., Reichard, U., Grouzmann, E., Neuhaus, J., et al. (2010). *Aspergillus* protein degradation pathways with different secreted protease sets at neutral and acidic pH. *J. Proteome Res.* 9, 3511–3519. doi: 10.1021/pr901202z

Stanley, P. (2016). What have we learned from glycosyltransferase knockouts in mice? *J. Mol. Biol.* 428, 3166–3182. doi: 10.1016/j.jmb.2016.03.025

Sterflinger, K., and Prillinger, H. J. (2001). Molecular taxonomy and biodiversity of rock fungal communities in an urban environment (Vienna, Austria). *Antonie Van Leeuwenhoek* 80, 275–286. doi: 10.1023/A:1013060308809

Stokes, W., Fuller, J., Meier-Stephenson, V., Remington, L., and Meatherall, B. L. (2017). Case report of cerebral phaeohyphomycosis caused by *Fonsecaea monophora*. *Off. J. Assoc. Med. Microbiol. Infect. Dis. Canada* 2, 86–92. doi: 10.3138/jammi.2.1.013

Stone, B. A., Jacobs, A. K., Hrmova, M., Burton, R. A., and Fincher, G. B. (2018). Biosynthesis of plant cell wall and related polysaccharides by enzymes of the GT2 and GT48 families. *Annu. Plant Rev.* 41, 109–165. doi: 10.1002/9781119312994.apr0434

Sudhadham, M., Prakitsin, S., Sivichai, S., Chaiyarat, R., Dorrestein, G. M., Menken, S. B. J., et al. (2008). The neurotropic black yeast *Exophiala dermatitidis* has a possible origin in the tropical rain forest. *Stud. Micol.* 61, 145–155. doi: 10.3114/sim.2008.61.15

Surash, S., Tyagi, A., Hoog, G. S., Zeng, J. S., Barton, R. C., and Hobson, R. P. (2005). Cerebral phaeohyphomycosis caused by *Fonsecaea monophora*. *Med. Mycol.* 43, 465–472. doi: 10.1080/13693780500220373

Takei, H., Goodman, J. C., and Powell, S. Z. (2007). Cerebral phaeohyphomycosis caused by *Cladophialophora bantiana* and *Fonsecaea monophora*: report of three cases. *Clin. Neuropathol.* 26, 21–27. doi: 10.5414/NPP26021

Tanabe, H., Kawasaki, M., Mochizuki, T., and Ishizaki, H. (2004). Species identification and strain typing of *Fonsecaea pedrosoi* using ribosomal RNA gene internal transcribed spacer regions. *Nippon Ishinkin Gakkai Zasshi* 45, 105–112. doi: 10.3314/jjmm.45.105

Teixeira, M. M., Moreno, L. F., Stielow, B. J., Muszewska, A., Hainaut, M., Gonzaga, L., et al. (2017). Exploring the genomic diversity of black yeasts and relatives

(Chaetothyriales, Ascomycota). *Stud. Mycol.* 86, 1–28. doi: 10.1016/j.simyco.2017.01.001

Thirach, S., Cooper, C. R. J., Vanittanakom, P., and Vanittanakom, N. (2007). The copper, zinc superoxide dismutase gene of *Penicillium marneffei*: cloning, characterization, and differential expression during phase transition and macrophage infection. *Med. Mycol.* 45, 409–417. doi: 10.1080/13693780701381271

Thomas, E., Bertolotti, A., Barreau, A., Klisnick, J., Tournebize, P., Borgherini, G., et al. (2018). From phaeohyphomycosis to disseminated chromoblastomycosis: a retrospective study of infections caused by dematiaceous fungi. *Med. Malad. Infect.* 48, 278–285. doi: 10.1016/j.medmal.2017.09.011

Tiwari, S., Thakur, R., and Shankar, J. (2015). Role of heat-shock proteins in cellular function and in the biology of fungi. *Biotechnol. Res. Int.* 2015:132635. doi: 10.1155/2015/132635

Tronina, T., Bartmanska, A., Milczarek, M., Wietrzyk, J., Poplonski, J., Roj, E., et al. (2013). Antioxidant and antiproliferative activity of glycosides obtained by biotransformation of xanthohumol. *Bioorg. Med. Chem. Lett.* 23, 1957–1960. doi: 10.1016/j.bmcl.2013.02.031

Varghese, P., Jalal, M. J. A., Ahmad, S., Khan, Z., Johny, M., Mahadevan, P., et al. (2016). Cerebral phaeohyphomycosis caused by *Fonsecaea monophora*: first report from India. *Int. J. Surg. Med.* 2, 44–49. doi: 10.5455/ijsm.neurosurgery01

Varrot, A., Basheer, A. M., and Imberty, A. (2013). Fungal lectins: structure, function and potential applications. *Curr. Opin. Struct. Biol.* 23, 678–685. doi: 10.1016/j.sbi.2013.07.007

Vela-Corcía, D., Aditya Srivastava, D., Dafa-Berger, A., Rotem, N., and Barda, O. (2019). MFS transporter from *Botrytis cinerea* provides tolerance to glucosinolate-breakdown products and is required for pathogenicity. *Nat. Commun.* 10:2886. doi: 10.1038/s41467-019-10860-3

Vialle, R. A. (2013). *SILA - Um Sistema para Anotação Automática de Genomas Utilizando Técnicas Independentes de Alinhamento*. Master's dissertation, Universidade Federal do Paraná, Curitiba.

Vialle, R. A., Pedrosa, F. O., Weiss, V. A., Guizelini, D., Tibaes, J. H., Marchaukoski, J. N., et al. (2016). RAFTS3: rapid alignment-free tool for sequences similarity search. *bioRxiv*. [Preprint]. doi: 10.1101/055269

Vicente, V. A., Attili-Angelis, D., Pie, M. R., Queiroz-Telles, F., Cruz, L. M., Najafzadeh, M. J., et al. (2008). Environmental isolation of black yeast-like fungi involved in human infection. *Stud. Mycol.* 61, 137–144. doi: 10.3114/sim.2008.61.14

Vicente, V. A., Najafzadeh, M. J., Sun, J., Gomes, R. R., Robl, D., Marques, S. G., et al. (2014). Environmental siblings of black agents of human chromoblastomycosis. *Fungal Divers.* 62, 1–17. doi: 10.1007/s13225-013-0246-5

Vicente, V. A., Orélis-Ribeiro, R., Najafzadeh, M. J., Sun, J., Guerra, R. S., Miesch, S., et al. (2012). Black yeast-like fungi associated with lethargic Crab disease (LCD) in the mangrove-land crab, *Ucides cordatus* (Ocypodidae). *Vet. Microbiol.* 158, 109–122. doi: 10.1016/j.vetmic.2012.01.031

Vicente, V. A., Weiss, V. A., Bombassaro, A., Moreno, L. F., Costa, F. F., Raittz, R. T., et al. (2017). Comparative genomics of sibling species of *Fonsecaea* associated with human chromoblastomycosis. *Front. Microbiol.* 8:1924. doi: 10.3389/fmicb.2017.01924

Wang, C., Xing, H., Jiang, X., Zeng, J., Liu, Z., Chen, J., et al. (2019). Cerebral phaeohyphomycosis caused by *Exophiala dermatitidis* in a Chinese CARD9-Deficient Patient: a case report and literature review. *Front. Neurol.* 10:938. doi: 10.3389/fneur.2019.00938

White, C., Laird, D. W., and Hughes, L. H. (2017). From carbon waste to carbon product: converting oxalate to polyhydroxybutyrate using a mixed microbial culture. *J. Environ. Chem. Eng.* 5, 2362–2365. doi: 10.1016/j.jece.2017.04.040

Woertz, J. R., Kinney, K. A., McIntosh, N. D. P., and Szaniszlo, P. J. (2001). Removal of toluene in a vapor phase bioreactor containing a strain of the dimorphic black yeast *Exophiala lecaniicorni*. *Biotechnol. Bioeng.* 75, 550–558. doi: 10.1002/bit.10066

Yang, L., Wang, Z., Lei, H., Chen, R., Wang, X., Peng, Y., et al. (2014). Neuroprotective glucosides of magnolol and honokiol from microbial-specific glycosylation. *Tetrahedron* 70, 8244–8251. doi: 10.1016/j.tet.2014.09.033

Yang, Y. T., Lee, S. T., Nai, Y. S., Kim, S., and Kim, J. S. (2016). Up-regulation of carbon metabolism-related glyoxylate cycle and toxin production in *Beauveria bassiana* JEF-007 during infection of bean bug, *Riptortus pedestris* (Hemiptera: Alydidae). *Fungal Biol.* 120, 1236–1248. doi: 10.1016/j.funbio.2016.07.008

Youngchim, S., Morris-Jones, R., Hay, R. J., and Hamilton, A. J. (2004). Production of melanin by *Aspergillus fumigates*. *J. Med. Microbiol.* 53, 175–181. doi: 10.1099/jmm.0.05421-0

Zhao, Z., Liu, H., Wang, C., and Xu, J. (2013). Correction: comparative analysis of fungal genomes reveals different plant cell wall degrading capacity in fungi. *BMC Genomics* 14:274. doi: 10.1186/1471-2164-15-6

Zitman, F. M., Todorov, B., Furukawa, K., Willison, H. J., and Plomp, J. J. (2010). Total ganglioside ablation at mouse motor nerve terminals alters neurotransmitter release level. *Synapse* 64, 335–338. doi: 10.1002/syn.20747

Conflict of Interest: The authors declare that the research was conducted in the absence of any commercial or financial relationships that could be construed as a potential conflict of interest.

The reviewer AM declared a past co-authorship with one of the authors SH to the handling editor.

frontiers in Microbiology

ORIGINAL RESEARCH
published: 04 August 2020
doi: 10.3389/fmicb.2020.01751

Updates and Comparative Analysis of the Mitochondrial Genomes of *Paracoccidioides* spp. Using Oxford Nanopore MinION Sequencing

*Elizabeth Misas[1,2†], Oscar M. Gómez[1,3†], Vanessa Botero[1], José F. Muñoz[1,4], Marcus M. Teixeira[5], Juan E. Gallo[1,3], Oliver K. Clay[6] and Juan G. McEwen[1,7]**

[1] Cellular and Molecular Biology Unit, Corporación para Investigaciones Biológicas, Medellín, Colombia, [2] Colombia Wisconsin One Health Consortium, Universidad Nacional de Colombia, Medellín, Colombia, [3] Genoma CES, Universidad CES, Medellín, Colombia, [4] Broad Institute of MIT and Harvard, Cambridge, MA, United States, [5] Faculty of Medicine, University of Brasília, Brasília, Brazil, [6] Translational Microbiology and Emerging Diseases (MICROS), School of Medicine and Health Sciences, Universidad del Rosario, Bogotá, Colombia, [7] School of Medicine, Universidad de Antioquia, Medellín, Colombia

OPEN ACCESS

Edited by:
Ludmila Chistoserdova, University of Washington, United States

Reviewed by:
Fernando Gustavo Alvarez-Valin, Universidad de la República, Uruguay
Alexandre Melo Bailao, Universidade Federal de Goiás, Brazil

***Correspondence:**
Juan G. McEwen
mcewen@une.net.co

[†] *These authors have contributed equally to this work*

Specialty section:
This article was submitted to Evolutionary and Genomic Microbiology, a section of the journal Frontiers in Microbiology

Received: *31 January 2020*
Accepted: *06 July 2020*
Published: *04 August 2020*

Citation:
Misas E, Gómez OM, Botero V, Muñoz JF, Teixeira MM, Gallo JE, Clay OK and McEwen JG (2020) Updates and Comparative Analysis of the Mitochondrial Genomes of Paracoccidioides spp. Using Oxford Nanopore MinION Sequencing. Front. Microbiol. 11:1751. doi: 10.3389/fmicb.2020.01751

The mitochondrial genome of the *Paracoccidioides brasiliensis* reference isolate Pb18 was first sequenced and described by Cardoso et al. (2007), as a circular genome with a size of 71.3 kb and containing 14 protein coding genes, 25 tRNAs, and the large and small subunits of ribosomal RNA. Later in 2011, Desjardins et al. (2011) obtained partial assemblies of mitochondrial genomes of *P. lutzii* (Pb01), *P. americana* (Pb03), and *P. brasiliensis sensu stricto* (Pb18), although with a size of only 43.1 kb for Pb18. Sequencing errors or other limitations resulting from earlier technologies, and the advantages of NGS (short and long reads), prompted us to improve and update the mtDNA sequences and annotations of two *Paracoccidioides* species. Using Oxford Nanopore and Illumina read sequencing, we generated high-quality complete *de novo* mitochondrial genome assemblies and annotations for *P. brasiliensis* (Pb18) and *P. americana* (Pb03). Both assemblies were characterized by an unusually long spacer or intron region (>50 kb) between exons 2 and 3 of the nad5 gene, which was moderately conserved between Pb03 and Pb18 but not similar to other reported sequences, except for an unassigned contig in the 2011 assembly of Pb03. The reliability of the insert missing from previous mtDNA genome assemblies was confirmed by inspection of the individual Nanopore read sequences containing nad5 coding DNA, and experimentally by PCR for Pb18. We propose that the insert may aid replication initiation and may be excised to produce a smaller structural variant. The updated mtDNA genomes should enable more accurate SNP and other comparative or evolutionary analyses and primer/probe designs. A comparative analysis of the mtDNA from 32 isolates of *Paracoccidioides* spp., using the SNPs of the aligned mitochondrial genomes, showed groupings within the *brasiliensis* species complex that were largely consistent with previous findings from only five mitochondrial loci.

Keywords: mitochondria, genome, *Paracoccidioides*, Oxford Nanopore, NGS

INTRODUCTION

Paracoccidioides spp. is a thermal dimorphic fungus, pathogenic for humans, which at temperatures below 24°C grows as mycelium in the environment and at a temperature of 37°C grows as yeast in a mammalian host or *in vitro*. *Paracoccidioides* spp. is the causative agent of paracoccidioidomycosis (PCM), a systemic mycosis that affects the population of Latin America (Brummer et al., 1993).

In the genus *Paracoccidioides*, five species have been described, *P. lutzii, P. brasiliensis* (S1), *P. americana* (PS2), *P. restrepiensis* (PS3), and *P. venezuelensis* (PS4). The last four constitute the *brasiliensis* species complex. Each of the *Paracoccidioides* species can be identified using molecular and morphological criteria (Turissini et al., 2017), but the grouping of the species within the *brasiliensis* complex has not been entirely consistent across nuclear and mitochondrial studies.

Mitochondrial genome assemblies from whole genome sequencing projects are currently available as draft sequences for three strains of the genus *Paracoccidioides*, two isolates of the *brasiliensis* species complex, *P. brasiliensis* (Pb18) and *P. americana* (Pb03), and one representative isolate of the species *P. lutzii* (Pb01) (Desjardins et al., 2011). For isolate Pb18, there is also available an independent, earlier assembly and annotation by Cardoso et al. (2007) (GenBank: AY955840). Unlike the draft sequences mentioned previously, which are partial, the annotated assembly Pb18 AY955840 covers almost all of the mitochondrial gene content and was used in this work as a reference.

In the work of Cardoso et al. (2007) the mitochondrial genome was obtained by physical separation of the mitochondria followed by Sanger sequencing; said genome was described as a circular molecule of 71.3 kb with 14 sequences of protein coding genes. By contrast, in the work of Desjardins et al. (2011) the nuclear and partial mitochondrial genomes of three strains of *Paracoccidioides* spp. (Pb18, Pb03, and Pb01) were sequenced together using Sanger technology. These genomes were assembled with Arachne and the mitochondrial scaffolds were identified and separated *in silico*. For the Pb18 isolate, four supercontigs with a total size of only 43.12 kb were reported, that is, covering only 60.4% of the mitochondrial genome reported by Cardoso et al. (2007).

In the present work, we re-sequenced the DNA with Oxford Nanopore and Illumina to obtain improved whole mitochondrial genome sequences and annotations for strains Pb18 and Pb03. We used the SPAdes program, which implements a *de novo* hybrid assembly strategy that combines both types of sequencing.

In addition to long and short read sequencing of the two reference isolates Pb18 and Pb03, we also used Illumina technology to sequence four isolates of *P. lutzii* and 28 isolates of the *brasiliensis* species complex from four countries, Brazil, Colombia, Argentina, and Venezuela, thus covering a large part of the geographic distribution of *Paracoccidioides* spp. (Muñoz et al., 2016).

The reads of all of these isolates were included in the present work to identify the polymorphisms present in the mitochondrial genome of *Paracoccidioides* and to determine, using the new data, the grouping of the isolates from the *brasiliensis* species complex that are indicated by the mitochondrial sequences.

MATERIALS AND METHODS

Sampling, DNA Extraction, and WGS

Thirty-four isolates of the *Paracoccidioides* genus of different geographic origins were included in this study, namely, 20 isolates from Brazil, 6 isolates from Colombia, 3 isolates from Argentina, and 5 isolates from Venezuela (Muñoz et al., 2016).

The selected isolates were distributed in the phylogenetic species as follows: 15 from *P. brasiliensis* (11 from S1a and 4 from S1b), 7 isolates from *P. restrepiensis* (PS3), 4 from *P. americana* (PS2), 4 from *P. venezuelensis* (PS4), and 4 from *P. lutzii* (**Supplementary Table S1**). PbT1F1, T15N1, PbCAB, Pb337, and PbT10B1 were isolated from armadillo, Pb300 was isolated from the soil, Pb262 was isolated from dog food, and the others were clinical isolates from patients with PCM (**Supplementary Table S1**).

The DNA was extracted using the phenol-chloroform method (Diez et al., 1999) with some modifications. Before the treatment with organic solvents, the biomass was macerated with liquid nitrogen. Library preparation and sequencing was carried out in three sequencing centers (University of California at Berkeley, University of Illinois Urbana–Champaign, Broad Institute) following the protocols proposed by Illumina in the guide "Preparing Samples for Sequencing Genomic DNA[1]."

All isolates were sequenced using Illumina HiSeq2500 platforms. In addition, the Pb18 and Pb03 isolates, representing the reference strains for *P. brasiliensis* and *P. americana*, respectively, were sequenced using Oxford Nanopore technology R9.5 flowcells at the University of Illinois Urbana–Champaign.

Assembly and Annotation of the Mitochondrial Genomes of *P. brasiliensis* (Pb18) and *P. americana* (Pb03) Using Oxford Nanopore Reads

Two *de novo* assembly programs, SPAdes v-3.10 (Bankevich et al., 2012) and Canu v-1.5 (Koren et al., 2017), were used to obtain complete genome assemblies (nuclear and mitochondrial scaffolds) for the isolates Pb18 and Pb03. The Oxford Nanopore reads were assembled using Canu v-1.5, whereas SPAdes v-3.10 allowed the construction of a hybrid assembly in a single run including both the Illumina and Oxford Nanopore reads (**Supplementary Table S2**).

Subsequently, the contigs corresponding to the mitochondrial sequences were identified and extracted from each assembly. After comparing them with the available draft genome sequences, the mitochondrial contig assembled by SPAdes v-3.10, i.e., incorporating the contiguity information from the Oxford Nanopore long reads, was selected for each of the two isolates. The Canu v-1.5 contigs served to confirm that each of the two assemblies obtained via SPAdes v-3.10 represented a complete mtDNA genome because the repeated sequences at the ends of the selected mitochondrial contig, identified using MUMmer v-3.23, could be joined to circularize the sequence, which then had the same extent as the corresponding SPAdes assembly. Finally,

[1]https://support.illumina.com/sequencing/sequencing_kits/genomic_dna_sample_prep_kit.html

the sequence was used as a reference to map the Illumina reads with BWA v-0.6.1 (Li and Durbin, 2009).

In the mitochondrial contigs of both Pb03 and Pb18, a region was observed that had been absent in the previously available assemblies. This "insert" was consistently found both in assemblies obtained by SPAdes v-3.10 and in those obtained by Canu v-1.5. We used BLAST-ncbi, EMBOSS isochore for GC plots, and remapping of the reads to characterize this insert.

The annotation of the mitochondrial assemblies for Pb03 and Pb18 was performed via homology based on tBLASTn (Boratyn et al., 2013), using as a basis the previously curated annotation of Cardoso et al. (2007) for the mitochondrial genome of Pb18 (E. Misas, M.Sc. thesis) except in the case of its apparently incomplete gene *nad5*, where we used an annotation of *Neurospora crassa* (KC683708.1) as reference. tRNA coordinates were predicted using tRNAScan-SE[2] (Chan and Lowe, 2019). As a check, we then used MFannot[3] (Lang et al., 2007) to automatically draft-annotate all genes except *nad5* (which was split by the boundaries of the linear sequence), and manually compared and clarified any inconsistencies.

Analyses of SNPs Identified in the Whole Mitochondrial Genomes of the *Paracoccidioides* Genus

For the 33 isolates of the genus *Paracoccidioides*, the reference assembly program BWA v-0.5.9 was run with default parameters, using as reference the obtained mitochondrial genome sequence of Pb18 assembled by SPAdes v-3.10.

From the resulting BWA alignments, the Pilon v-1.6 program was run with the "-variant" parameter, which generated a report of SNPs for each of the 33 isolates in the *.vcf (Variant Call Format) format.

To build a phylogenetic tree with the information of the mitochondrial SNPs, the variable positions in Fasta format were recovered from the.vcf files generated by Pilon v-1.6 using a Perl script. To consider a position as a variable, we required that it should have a minimum coverage of 4 reads and be variable in at least one of the 32 isolates. The resulting sequences were aligned with the ClustalW v-2.1 program, and maximum-likelihood phylogenies were constructed using IQ-Tree v-1.4.4 program (Nguyen et al., 2015) using the TVM nucleotide substitution model and bootstrap analysis based on 1000 replicates.

RESULTS

WGS and Assembly of the Mitochondrial Genomes of *P. brasiliensis* (Pb18) and *P. americana* (Pb03)

For Pb18, we obtained 36,126 long reads with an average size of 2.6 kb, and for Pb03 we obtained 71,528 long reads with an average size of 3.1 kb, using MinION. The Illumina HiSeq2500 paired-end short read sequencing produced 46.8 million pairs of reads with a length of 101 bp for the Pb18 strain, and 62 million 101 bp read pairs for the Pb03 strain. The quality of the short reads was evaluated using FastQC v0.11.2 (Brown et al., 2017) and for the Oxford Nanopore long reads of the Pb18 strain, length histograms of the total reads and of the reads mapped to the mitochondrial genome were constructed.

Although generally large differences were observed in the *de novo* assemblies obtained with Canu v-1.5 and SPAdes v-3.10, the recovered mitochondrial contig sequences obtained using the two programs were very similar.

The SPAdes v-3.10 assembler allowed the construction of a single contig corresponding to the whole mitochondrial genome of the strains Pb18 and Pb03, although in both cases the contig was longer than expected on the basis of previous assemblies. In both mitochondrial sequences, a region, or "insert," was identified that had been absent in all previously reported mitochondrial genome sequences. This "insert" region, defined as the segment that could not be matched to the previous reference genome of Pb18 or Pb03, respectively, had a length of 47 kb in Pb18 and 38 kb in Pb03 (**Figure 1**), and a lower percentage of GC than the rest of the contig (**Figure 2**). The insert sequence of Pb03 is highly similar (> 80% identity) to that of Pb18 throughout its length, and these inserts appear to contain no genes, except for a part of *nad5* exon 2 that had been truncated in the Pb18 reference assembly of Cardoso et al. (2007).

The presence of the insert region was then experimentally confirmed by PCR amplification of two regions near the boundaries of the insert in the Pb18 species of *Paracoccidioides* (**Supplementary Material**). The two amplicon sequences, both of which amplified successfully in Pb18, were then found by BLASTn to be present also in the new assembly of Pb03, but the Pb18 primers for one of the amplicons did not match precisely in Pb03, and indeed only one of the two amplicons was experimentally observed in that species (**Supplementary Material**).

A second check that the insert was not just an assembly artifact was done by searching the Oxford Nanopore long reads of Pb03 for individual long reads that contained coding DNA from exons 2 or 3 of nad5, and then inspecting the sequence-level alignment of the six longest reads with high-quality tBLASTn matches to *nad5* obtained on the exon 2 end (total alignment length 5423 nt). The contiguous long sequence reads all corresponded to the full genome assembly for Pb03 we report here. Furthermore, this observation suggests that in the sample we sequenced, no appreciable structural heteroplasmy (e.g., a structural variant corresponding to the assembly, plus another more compact alternative variant) was present; this observation does not, however, exclude that such heteroplasmy may be present in other conditions *in vivo*.

Annotation

In the mitochondrial genome assembly of the Pb18 strain, the 14 protein coding genes were identified, in the following order: NAD dehydrogenase subunit 2 (*nad2*), apocytochrome b (*cob*), NAD dehydrogenase subunits 3 (*nad3*), 1 (*nad1*), and 4 (*nad4*), ATP synthase subunits 8 (*atp8*) and 6 (*atp6*), NAD dehydrogenase subunit 6 (*nad6*), cytochromoxidase subunit 3 (*cox3*), ribosomal

[2]http://lowelab.ucsc.edu/tRNAscan-SE/

[3]https://megasun.bch.umontreal.ca/RNAweasel/

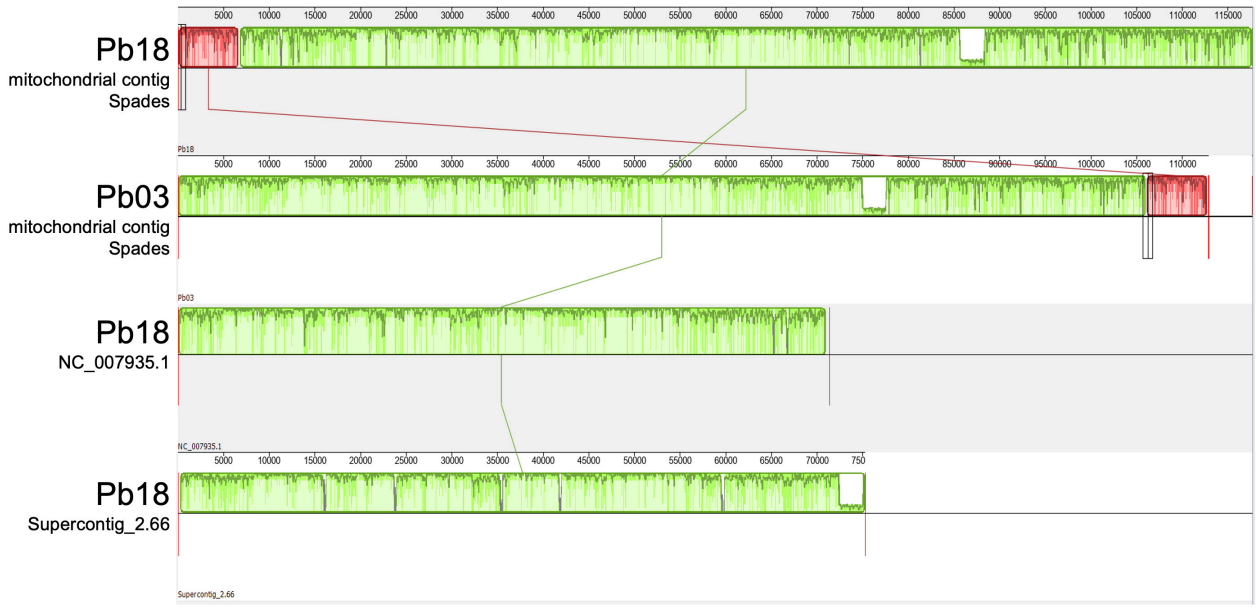

FIGURE 1 | Mauve alignment of present and previous Pb18 and Pb03 assemblies. The top two tracks present the mitochondrial contigs assembled by the SPAdes v-3.10 program in this study, for the Pb18 and Pb03 strains. The bottom two tracks represent the previously available mitochondrial genome draft assemblies for Pb18 (NC_007935.1) reported by Cardoso et al. (2007) and for Pb03 (Supercontig_2.66) reported by Desjardins et al. (2011). Green and red boxes represent Locally Collinear Blocks (LCBs), i.e., conserved segments that appear to be internally free from genome rearrangements. The order of the LCBs is given by the original coordinates of the sequences specified by the assembly program and the coordinates in the previously reported sequences when they are presented as a linear sequence. The plot inside the boxes represents the local quality of the alignment.

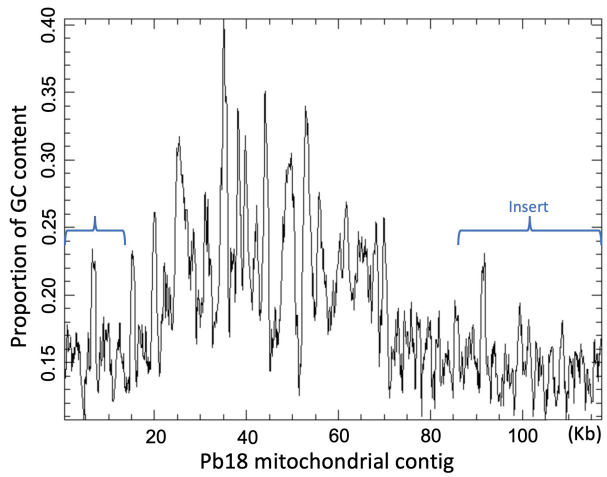

FIGURE 2 | GC plot of the mitochondrial contig of Pb18 assembled by SPAdes v-3.10. The brackets mark the region that is absent in the sequence previously reported by Cardoso et al. (2007).

protein rms5 (*rms5*), cytochromoxidase subunit 1 (*cox1*), ATP synthase subunit 9 (*atp9*), cytochromoxidase subunit 2 (*cox2*), and NAD dehydrogenase subunits 4l (*nad4l*) and 5 (*nad5*) (**Figure 3**).

Some of these genes contain introns, e.g., in the sequence of the cob gene, two introns were identified, and one of them was recognized as containing a part of *cob-il*, which spans the sequence of *cob* exon 2 and intron 2. The *nad1* gene has one intron. In the *nad5* gene, three exons were identified. Finally, in the sequence of the *cox1* gene, eight exons were identified, and the intron located between exons 1 and 2 was annotated as *cox1-il*. The two subunits of ribosomal RNA were identified by BLASTn and 25 tRNAs.

In the annotation of the assembly of the mitochondrial genome of Pb03, the genes conserve the same order. Also, an additional protein with function laglidadg endonuclease was identified between exons 2 and 3 of the *cox1* gene.

Analyses of SNPs Identified in the Whole Mitochondrial Genome of the *Paracoccidioides* Genus

Read data were aligned by BWA v-0.5.9 using as reference the region 14517-85557 of the mitochondrial contig of the isolate Pb18 from Brazil we had obtained via Oxford Nanopore sequencing after excluding the insert region. Because the sequence of the insert is highly AT rich, we decided to exclude it to avoid bias in the process of calling SNPs coming from low-quality mapping of short reads. Single-nucleotide polymorphism (SNP) variants were identified using Pilon v-1.6. The mean coverage of the mapped reads for the 32 isolates was 4165×. The isolates PbED01 and Pb1578 were excluded from the phylogenetic analysis because they presented very low coverage, 12× and 19×, respectively (**Supplementary Table S1**).

For the phylogenetic reconstruction, 1294 variable positions were used. At least one strain in each of these positions had

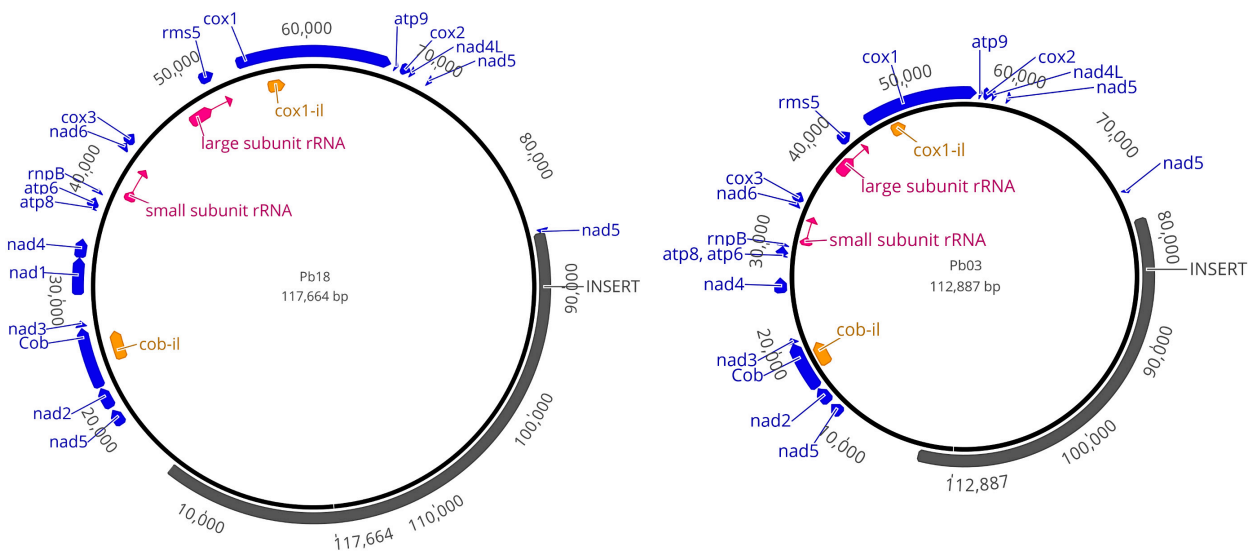

FIGURE 3 | (A,B) Physical map of the mitochondrial genomes of *P. brasiliensis* (Pb18 and Pb03). Protein coding genes are shown in blue, rRNAs are shown in pink, and ORFs in introns are shown in orange. The regions that were absent in the sequences previously reported are annotated as "insert" and allow comparison with previous studies but do not represent a biological feature of the sequence.

a variant and the minimum coverage was four reads. In the phylogenetic tree, seven clusters are observed, of which four correspond to the described phylogenetic species. The cluster that corresponds to the species *P. lutzii* is the one that presents the greatest number of changes with respect to the rest, and in particular the isolates of Pb01 and PbEE have accumulated many differences in their mitochondrial genomes (**Figure 4**).

The phylogenetic tree for the *brasiliensis* species complex succeeds in grouping the seven isolates of the species *P. restrepiensis* (PS3), which all grouped in the same cluster. Another cluster corresponds to *P. americana*, where the four isolates of this species were grouped together. The *P. americana* species shows a greater number of changes than other species in the *brasiliensis* species complex.

The isolates corresponding to *P. brasiliensis* (S1a and S1b) are separated into three distinct groups (**Figure 4**). The isolates PbCazon, PbBLO, Pb113, and Pb18 form a single clade suggesting monophyly. These four isolates also clustered in a previous analysis of whole nuclear genome SNPs by Muñoz et al. (2016), where the cluster was named S1b. Indeed, that study of nuclear genomes showed two internal groups of S1, i.e., S1b and a clade formed by other S1 isolates, called S1a.

DISCUSSION

Updated and Annotated Mitochondrial Genome Sequences for Pb18 and Pb03

The mitochondrial genomes of some fungi can be surprisingly difficult to assemble *de novo*, despite their small size, which is generally less than 100 kb (Muñoz et al., 2014). The fungal mitochondrial genome may contain a high number of repeated regions, which may hinder the process of *de novo* assembly, as we have discussed previously (Muñoz et al., 2014; Misas et al., 2016). At the (≤17 bp) oligonucleotide level, *Paracoccidioides* has one of the most pronounced repeat abundances of the fungal genera we compared in Misas et al. (2016), where the abundant repeats are furthermore dominated by those consisting only of A and T. The difficulty of assembling fungal mitochondrial genomes is not limited to the use of NGS sequencing. With previous sequencing technologies, problems were reported in earlier attempts to obtain mitochondrial assemblies of high quality for the model yeast *S. cerevisiae* (Foury et al., 1998). The difficulty for *Paracoccidioides* is apparently reflected in the large gaps present in the partial mitochondrial assemblies that were available for all three strains, Pb18, Pb03, and Pb01, and that were obtained as part of a whole genome project using Sanger sequencing (Desjardins et al., 2011), where for example a region containing a low-complexity, pyrimidine-rich segment (between *nad3* and *nad1*) that is present in the previous sequence of Pb18 (Cardoso et al., 2007) and in our new assemblies seems to have been particularly hard to bridge.

We achieved the assembly of the complete mitochondrial genome in a single contig, using a strategy that involves long and short read sequencing. Recently, the assembly of the mtDNA genome of *S. cerevisiae* S288C using Oxford Nanopore sequencing for *de novo* assembly and Illumina/Pilon for fine tuning was reported (Istace et al., 2017), and we also followed a methodology that integrates information from both long and short reads.

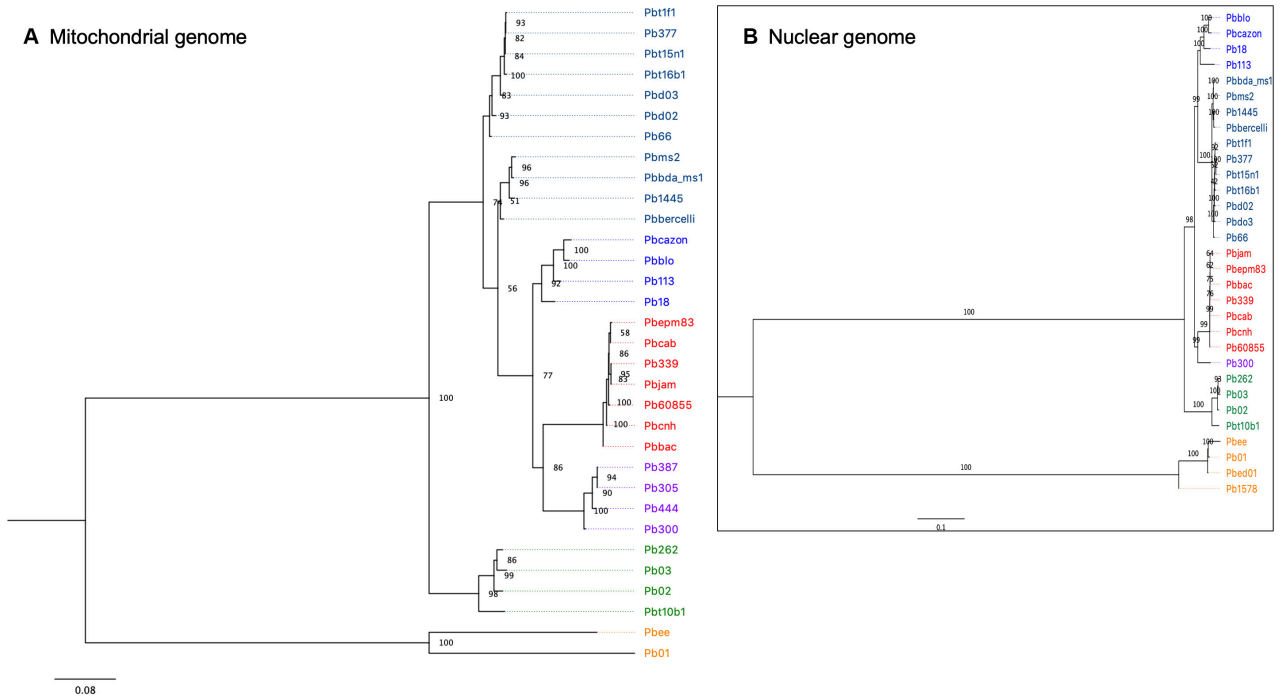

FIGURE 4 | (A) Maximum-likelihood phylogeny (with model TMV) obtained using IQ-tree v.1.4.4. The final data set included a total of 1294 nucleotide sites for 32 isolates of the *Paracoccidioides* genus. Bootstrap values calculated using 1000 reiterations are shown. **(B)** Maximum-likelihood phylogeny constructed with RAxML, using 614,570 nuclear SNPs.

The Long Second Intron or Spacer of the *nad5* Gene

An unexpected finding in both of our *de novo* mitochondrial genome assemblies, those of *Paracoccidioides* strains Pb18 (*brasiliensis* complex) and Pb03 (*P. americana*), was a large insertion of largely repetitive sequences without any encoded gene product, located between the second and third exon of the gene for nad5. So far, the longest sequenced fungal intron located at this position in the coding sequence of *nad5*, corresponding to position 217 in the nad5 protein sequence of *Neurospora crassa* (Zubaer et al., 2019), appears to have been 5513 bp, in the mitochondrial genome of *Endoconidiophora resinifera* [Helotiales; (Zubaer et al., 2018)]. By contrast, the introns or spacers at the corresponding position in both Pb18 and Pb03 are an order of magnitude longer, namely 51,431 bp for Pb18 and 49,922 bp for Pb03.

The intron or intragenic, inter-exon spacer of about 50 kb we observe, exhibiting moderate sequence similarity along the entire spacer between Pb03 and Pb18, appears at first sight to be unlike other *nad5* introns (Zubaer et al., 2019), and indeed only its first few kilobases are recognized as (group IB) intronic DNA by RNAweasel (Lang et al., 2007). Despite various searches of the long intron, we could not unambiguously identify any known elements such as ORFs (using NCBI ORFfinder) with similarity to known proteins, repetitive elements (e.g., Censor reported matches of very AT-rich segments to elements such as Gypsy-1B_CaPs-I and Gypsy-2_PaPs-I but with mismatches at almost all of the few G's and C's), or G-quadruplexes as suggested by the visible clusters of G's (regions reported by QGRS Mapper or imgqfinder appeared to be chance matches to criteria in some of the many purine-only tracts of the intron). However, already *nad5* can present surprises (in addition to its absence together with other complex I genes in some species, including but not limited to the Saccharomycetaceae; Freel et al., 2015), such as an intron of length 4411 bp at the same position, that harbors a classic protein-coding gene, *cox3*, in the fungus *Flammulina velutipes* (Basidiomycota/Agaricales; Zubaer et al., 2019). More generally, other surprises or spontaneous genome transconformations are not uncommon in intergenic DNA of fungal mitochondrial genomes and in some intronic DNA (Bernardi, 2005, p. 21–48).

In this wider context of large expanses of intergenic or non-coding fungal mtDNA, the region between exons 2 and 3 of our Pb18 and Pb03 assemblies appears to follow a classic pattern of long, extremely GC-poor segments (where the complexity reduces almost to that of a two-letter alphabet, A and T) alternating with much shorter, GC-richer clusters. Such a scenario leads, in some species including *Saccharomyces cerevisiae*, to a landscape of secondary structures (in some cases temperature dependent; Bernardi, 2005, p. 42), where copies (repeats) of certain oligonucleotides can occur at high frequencies and also open the possibility of out-of-register recombination between similar sequence motifs, leading to occasional excision of circularizable subsequences or subgenomes. In the case of *S. cerevisiae*, some pronounced

structural features of such landscapes correspond to the mtDNA genome's origins of replication (*ori*'s). We refer to Zubaer et al. (2019) for illustrations of the rich secondary structures that can be expected for some introns of *nad5*, to Bernardi (2005) for a review of secondary structures in yeasts and other fungi and some of the functional correlates that have been observed for them, and to Misas et al. (2016) for a comparative analysis of oligonucleotide repeat distributions in 11 fungal species with sequenced mitochondrial genomes and a discussion of the phenomenon of heteroplasmy in mitochondrial genomes of fungi. In this last study, *Paracoccidioides* (Pb18, already in the reduced genome of Cardoso et al., 2007) stood out as being one of the most highly repetitive species, yet, among those species, it was characterized by an almost complete preponderance of repeated oligonucleotides (17-mers) that contain no C's or G's. This observation suggests not only that the complete assembly of the mtDNA genomes of *Paracoccidioides* spp. is likely to be particularly difficult (as it indeed appears to have been in the past) but also, by the same token, that this genus may be more prone to exhibit structural variants as a result of likely ectopic recombination between very similar, recurring segments and subsequent deletions or excisions of circularizable subsequences.

It might seem unwise to speculate further, in imagining what a possible advantage could be of retaining (at least in one structural variant) the unusually long intron or spacer of *nad5*. This long intron appears to have been present in the mtDNA of both isolates, Pb18 and Pb03, that we sequenced. There could obviously be a disadvantage (as mentioned in a different context by Stearns (1992, p. 201), although possibly with a low energetic expense) in having to replicate, maintain, and/or transcribe long regions of mtDNA (in this case, about 50 kb) that are of no use for the organism. The parallels in *S. cerevisiae*, however, suggest that there might be a benefit in ensuring efficient replication and that, if this is facilitated by structures that the long *nad5* intron can form and that could differ in stability between different temperatures, it could possibly offset maintenance/replication costs. Such a hypothesis could, finally, be considered in the context of the thermal dimorphism of *Paracoccidioides* and other dimorphic Onygenales genera: the organism's need to function efficiently at two quite different temperature ranges (around 25°C as a saprophyte and around 37°C as a dedicated parasitic yeast), but with only one mtDNA genome sequence at its disposal, would suggest that there might be an advantage in endowing the mtDNA genome with an option to switch between at least two structural variants. However, in the samples we sequenced, none of our experimental observations and *in silico* evidence supported any particular, precise model (DNA sequence) for a likely, more compact variant of the mtDNA genome that does not possess a large *nad5* intron.

From a more general perspective, excessive repetition within a mtDNA genome sequence can result in unfavorable DNA deletion, atypical origins of replication, and chromosomal instability, among other hazards. The permanence of repeats in a mitochondrial genome despite such risks may suggest that some of them could have been favored by selection and may have a structural or functional significance that is still unknown (Misas et al., 2016).

Mitochondrial Genome Sequences of Onygenales Fungi

In addition to the assemblies of mitochondrial genomes of *Paracoccidioides* spp., there are also available draft assemblies of mitochondrial genomes of other thermally dimorphic fungi within the Onygenales order, such as *Histoplasma capsulatum* (e.g., NCBI accession no. ABBS02000356) and *Blastomyces dermatitidis* (e.g., NCBI accession no. ACBT01000592).

Despite the available information, no comparative studies of the mitochondrial genomes of dimorphic fungi have been conducted. In Onygenales fungi, studies of the comparative genomics at the nuclear level have contributed to an understanding of the different mechanisms of host–pathogen interaction and have facilitated the identification of possible candidate genes for virulence factors (Neafsey et al., 2010; Desjardins et al., 2011; Sharpton, 2014). It is known that in *Paracoccidioides* and other dimorphic fungi, mitochondrial functions play a very important role in the transition from the mycelial to the yeast phase, which is an indispensable step for colonization of the host (Maresca et al., 1981; Medoff et al., 1987; Martins et al., 2008). Studies of mitochondrial genomes can lead to a better understanding of biodiversity and pathophysiology, and of how mitochondrial functions can affect the pathogenicity of this group of dimorphic fungi.

For comparative analyses, the assemblies or annotations of the previously available mitochondrial genomes have unfortunately often been of insufficient quality or have represented only sparsely sampled fungal species. Future analyses of dimorphic fungi should benefit from identification and correction of existing sequence errors or gaps in the available mitochondrial genome assemblies, and from the sequencing and assembly of additional species or strains. In addition to their utility for comparative genomics studies, the new assemblies and annotations of *Paracoccidioides* reported here should be useful as a reliable source for experimental studies, e.g., for investigating how mitochondrial function affects the virulence of *Paracoccidioides* spp.

For such reasons, the availability of optimized mitochondrial sequences such as those reported here responds to a real need of the scientific community. Our updating of the mitochondrial genome assemblies and annotations of the reference strains *P. brasiliensis* Pb18 and *P. americana* Pb03 complements the previously published updating of the corresponding nuclear assemblies for the same strains (Muñoz et al., 2014). The corrected sequences of *Paracoccidioides* spp. are the first genomes of the family Ajellomycetaceae to be revised and optimized in this way, with the aim of providing improved reference sequences for dimorphic fungi.

Implications for Phylogenetic Analyses

The phylogenetic analysis we have presented was based on the variable positions that were identified in the sequences of the

mitochondrial genomes for the 32 isolates of *Paracoccidioides* spp. Although the sizes of the mitochondrial genomes are very much smaller than those of the corresponding nuclear genomes, and thus also have a smaller number of variable sites, those sites have a high confidence because particularly high coverage values were obtained as a result of the depth of sequencing achieved with Illumina. The high coverage is probably largely attributable to the presence of multiple mitochondria per cell, which increases the representation of the mitochondrial genome in the sequencing results.

The genus *Paracoccidioides* includes the species *P. lutzii* and the *brasiliensis* species complex. This main division of the genus *Paracoccidioides* is supported by both nuclear and mitochondrial markers (Matute et al., 2006; Salgado-Salazar et al., 2010; Turissini et al., 2017). However, some lack of convergence has been observed for the grouping of the four species belonging to the *brasiliensis* complex, more specifically between phylogenies recovered from nuclear markers and previous phylogenies based on mitochondrial markers.

Using nuclear sequences, Matute et al. (2006) initially identified three phylogenetic species or lineages within the complex, S1, PS2, and PS3, and the increase of available sequences of *P. brasiliensis* allowed the identification of another group within this species as PS4 (Theodoro et al., 2008; Teixeira et al., 2014), which corresponds to clinical isolates from Venezuela. By contrast, using mitochondrial DNA sequences from five genes, Salgado-Salazar et al. (2010) reported three monophyletic groups, PS2, PS3, and CS1, which corresponds to PS4, but the group S1 (Matute et al., 2006; Turissini et al., 2017) was not recovered and the isolates corresponding to this group were broadly distributed across the tree.

More recently, Turissini et al. (2017) analyzed 12 previously reported loci (five mitochondrial and seven nuclear protein coding genes), together with 10 nuclear non-coding loci and 10 microsatellite loci they sequenced, and proposed that the mito-nuclear incongruence in the *brasiliensis* species complex is the result of interspecific hybridization and mitochondrial introgression. In that report, it was proposed, based on the data then available, that there have been at least three independent mitochondrial gene exchange events between *Paracoccidioides* species (PS3 and S1, PS2 and PS4, and possibly S1 and PS2/PS4). Indeed, the authors found that mitochondrial genes have a less than expected genetic divergence and reported that mitochondrial variation was also more similar between samples from the same geographical region than between samples of the same species, but different regions.

In our phylogenetic reconstruction based on whole mitochondrial SNP analysis of the 32 isolates of the genus *Paracoccidioides* spp., the two isolates of the species *P. lutzii* separate from the others as expected.

Our findings from whole-genome mitochondrial data of the isolates used in Muñoz et al. (2016) confirm an apparent splitting or dispersal of the nuclear genome-based S1 clade of Matute et al. (2006) that was reported when sequences from five loci in the same isolates' mitochondrial genomes were used instead of nuclear sequences (Salgado-Salazar et al., 2010; Turissini et al., 2017). Although a recent population genomic analysis has characterized a deep subdivision of the *P. brasiliensis* species S1 into two lineages (S1a and S1b) that are distinctly prevalent along eastern Brazil and southern South America, for the isolates we analyzed here we observe three main groups: the S1a group observed by Muñoz et al. (2016) is, in our data, split further into two different clusters (**Figure 4**). Another finding is that isolates of *P. brasiliensis* S1b, which were denominated as mitochondrial type B21 of S1 in the study by Turissini et al. (2017), appear as the ancestral clade of the *brasiliensis* species complex. Future analyses using nuclear genomes, for example, pooling the isolates we analyzed here with those used in Turissini et al. (2017) and/or other isolates, should help resolve the question of monophyly or paraphyly of S1.

Another feature that has characterized phylogenies constructed from the previously obtained mitochondrial sequences of five loci (Salgado-Salazar et al., 2010; Turissini et al., 2017) was a sister group relationship between PS2 and PS4, which was inconsistent with the isolates' nuclear phylogenies. In the whole-genome mitochondrial groupings that we find for our set of isolates, PS2 and PS4 do not appear as sister groups (**Figure 4**). In our reconstruction of relationships in the *brasiliensis* species complex, the taxon *P. venezuelensis* (PS4) tends to group with *P. restrepiensis* (PS3), which would be compatible with both of the nuclear arrangements (Muñoz et al., 2016; Turissini et al., 2017), and confirmation of this finding could reduce the observed nuclear-mitochondrial discrepancies.

CONCLUSION

This work presents the update of assemblies and annotations of the mitochondrial genomes of the reference strains *P. brasiliensis* Pb18 and *P. americana* Pb03, complementing the update of the nuclear genomes reported by Muñoz et al. (2014). They are the first mitochondrial sequences of a genus in the Ajellomycetaceae family to be carefully checked and annotated and could therefore be useful as a reference. The phylogenetic reconstruction using the SNPs of the whole mitochondrial genome supports the species differentiation previously described.

DATA AVAILABILITY STATEMENT

The datasets generated for this study can be found in the NCBI under accession numbers PRJNA322632, SAMN05171520, SRX8563352/SRR12032017, SRX8563354/SRR12032015, SAMN05171542, SRX8563353/SRR12032016, and SRX8563355/SRR12032014.

AUTHOR CONTRIBUTIONS

EM, JGM, and OC conceptualized and designed the study. EM and OG assembled, annotated, and analyzed the data of *Paracoccidioides* mitochondrial genomes. EM, OC, OG, VB, MT, JFM, and JGM wrote the manuscript. EM and VB designed and performed the experiments. All authors contributed to the article and approved the submitted version.

FUNDING

This research was supported by the "Departamento Administrativo de Ciencia, Tecnología e Innovación" (COLCIENCIAS), Colombia via the Grant 221365842971, and via a student scholarship to EM (COLCIENCIAS National Doctorate Program, call 647). Support was also received by the University of Antioquia via the grant "Sostenibilidad" 2017/2018.

ACKNOWLEDGMENTS

We thank Angela Lopez for her support in the experimental verification.

SUPPLEMENTARY MATERIAL

The Supplementary Material for this article can be found online at: https://www.frontiersin.org/articles/10.3389/fmicb.2020.01751/full#supplementary-material

FIGURE S1 | Mitochondrial genome assembly showing in yellow the insert, i.e., the region absent in the mitochondrial genome Pb18 assembled by Cardoso et al. (2007), in dark green the forward primers and in light green the reverse primer for the two amplicons in flanking regions.

FIGURE S2 | PCR amplicons on a 1.2% agarose gel electrophoresis A. for Mito1 primers and B. for Mito2 primers.

TABLE S1 | Primer sequences used to determine presence/absence of the insert.

TABLE S2 | Summary characteristics of the de novo assemblies obtained using Canu v-1.5 and SPAdes v-3.10.

REFERENCES

Bankevich, A., Nurk, S., Antipov, D., Gurevich, A. A., Dvorkin, M., Kulikov, A. S., et al. (2012). SPAdes: a new genome assembly algorithm and its applications to single-cell sequencing. *J. Comput. Biol.* 19, 455–477. doi: 10.1089/cmb.2012.0021

Bernardi, G. (2005). *Structural and Evolutionary Genomics: Natural Selection and Genome Evolution*. Amsterdam: Elsevier.

Boratyn, G. M., Camacho, C., Cooper, P. S., Coulouris, G., Fong, A., Ma, N., et al. (2013). BLAST: a more efficient report with usability improvements. *Nucleic Acids Res.* 41, W29–W33. doi: 10.1093/nar/gkt282

Brown, J., Pirrung, M., and McCue, L. A. (2017). FQC Dashboard: integrates FastQC results into a web-based, interactive, and extensible FASTQ quality control tool. *Bioinformatics* 33, 3137–3139. doi: 10.1093/bioinformatics/btx373

Brummer, E., Castaneda, E., and Restrepo, A. (1993). Paracoccidioidomycosis: an update. *Clin. Microbiol. Rev.* 6, 89–117. doi: 10.1128/cmr.6.2.89

Cardoso, M. A., Tambor, J. H., and Nobrega, F. G. (2007). The mitochondrial genome from the thermal dimorphic fungus *Paracoccidioides brasiliensis*. *Yeast* 24, 607–616. doi: 10.1002/yea.1500

Chan, P. P., and Lowe, T. M. (2019). tRNAscan-SE: searching for tRNA genes in genomic sequences. *Methods Mol. Biol.* 1962, 1–14. doi: 10.1007/978-1-4939-9173-0_1

Desjardins, C. A., Champion, M. D., Holder, J. W., Muszewska, A., Goldberg, J., Bailao, A. M., et al. (2011). Comparative genomic analysis of human fungal pathogens causing paracoccidioidomycosis. *PLoS Genet.* 7:e1002345. doi: 10.1371/journal.pgen.1002345

Diez, S., Garcia, E. A., Pino, P. A., Botero, S., Corredor, G. G., Peralta, L. A., et al. (1999). PCR with *Paracoccidioides brasiliensis* specific primers: potential use in ecological studies. *Rev. Inst. Med. Trop. Sao Paulo* 41, 351–358. doi: 10.1590/s0036-46651999000600004

Foury, F., Roganti, T., Lecrenier, N., and Purnelle, B. (1998). The complete sequence of the mitochondrial genome of *Saccharomyces cerevisiae*. *FEBS Lett.* 440, 325–331. doi: 10.1016/s0014-5793(98)01467-7

Freel, K. C., Friedrich, A., and Schacherer, J. (2015). Mitochondrial genome evolution in yeasts: an all-encompassing view. *FEMS Yeast Res.* 15:fov023. doi: 10.1093/femsyr/fov023

Istace, B., Friedrich, A., d'Agata, L., Faye, S., Payen, E., Beluche, O., et al. (2017). de novo assembly and population genomic survey of natural yeast isolates with the Oxford Nanopore MinION sequencer. *Gigascience* 6, 1–13. doi: 10.1093/gigascience/giw018

Koren, S., Walenz, B. P., Berlin, K., Miller, J. R., Bergman, N. H., and Phillippy, A. M. (2017). Canu: scalable and accurate long-read assembly via adaptive k-mer weighting and repeat separation. *Genome Res.* 27, 722–736. doi: 10.1101/gr.215087.116

Lang, B. F., Laforest, M. J., and Burger, G. (2007). Mitochondrial introns: a critical view. *Trends Genet.* 23, 119–125. doi: 10.1016/j.tig.2007.01.006

Li, H., and Durbin, R. (2009). Fast and accurate short read alignment with Burrows-Wheeler transform. *Bioinformatics* 25, 1754–1760. doi: 10.1093/bioinformatics/btp324

Maresca, B., Lambowitz, A. M., Kumar, V. B., Grant, G. A., Kobayashi, G. S., and Medoff, G. (1981). Role of cysteine in regulating morphogenesis and mitochondrial activity in the dimorphic fungus *Histoplasma capsulatum*. *Proc Natl Acad Sci U.S.A.* 78, 4596–4600. doi: 10.1073/pnas.78.7.4596

Martins, V. P., Soriani, F. M., Magnani, T., Tudella, V. G., Goldman, G. H., Curti, C., et al. (2008). Mitochondrial function in the yeast form of the pathogenic fungus *Paracoccidioides brasiliensis*. *J. Bioenerg. Biomembr.* 40, 297–305. doi: 10.1007/s10863-008-9163-9

Matute, D. R., McEwen, J. G., Puccia, R., Montes, B. A., San-Blas, G., Bagagli, E., et al. (2006). Cryptic speciation and recombination in the fungus *Paracoccidioides brasiliensis* as revealed by gene genealogies. *Mol. Biol. Evol.* 23, 65–73. doi: 10.1093/molbev/msj008

Medoff, G., Painter, A., and Kobayashi, G. S. (1987). Mycelial- to yeast-phase transitions of the dimorphic fungi *Blastomyces dermatitidis* and *Paracoccidioides brasiliensis*. *J. Bacteriol.* 169, 4055–4060. doi: 10.1128/jb.169.9.4055-4060.1987

Misas, E., Muñoz, J. F., Gallo, J. E., McEwen, J. G., and Clay, O. K. (2016). From NGS assembly challenges to instability of fungal mitochondrial genomes: a case study in genome complexity. *Comput. Biol. Chem.* 61, 258–269. doi: 10.1016/j.compbiolchem.2016.02.016

Muñoz, J. F., Farrer, R. A., Desjardins, C. A., Gallo, J. E., Sykes, S., Sakthikumar, S., et al. (2016). Genome diversity, recombination, and virulence across the major lineages of *Paracoccidioides*. *mSphere* 1:e00213-16. doi: 10.1128/mSphere.00213-16

Muñoz, J. F., Gallo, J. E., Misas, E., Priest, M., Imamovic, A., Young, S., et al. (2014). Genome update of the dimorphic human pathogenic fungi causing paracoccidioidomycosis. *PLoS Negl. Trop. Dis.* 8:e3348. doi: 10.1371/journal.pntd.0003348

Neafsey, D. E., Barker, B. M., Sharpton, T. J., Stajich, J. E., Park, D. J., Whiston, E., et al. (2010). Population genomic sequencing of *Coccidioides* fungi reveals recent hybridization and transposon control. *Genome Res.* 20, 938–946. doi: 10.1101/gr.103911.109

Nguyen, L. T., Schmidt, H. A., von Haeseler, A., and Minh, B. Q. (2015). IQ-TREE: a fast and effective stochastic algorithm for estimating maximum-likelihood phylogenies. *Mol. Biol. Evol.* 32, 268–274. doi: 10.1093/molbev/msu300

Salgado-Salazar, C., Jones, L. R., Restrepo, A., and McEwen, J. G. (2010). The human fungal pathogen *Paracoccidioides brasiliensis* (Onygenales: Ajellomycetaceae) is a complex of two species: phylogenetic evidence from fice mitocondial markers. *Cladistics* 26, 613–624. doi: 10.1111/j.1096-0031.2010.00307.x

Sharpton, T. J. (2014). An introduction to the analysis of shotgun metagenomic data. *Front. Plant Sci.* 5:209. doi: 10.3389/fpls.2014.00209

Stearns, S. S. (1992). *The Evolution of Life Histories*. Oxford: Oxford University Press.

Teixeira, M. M., Theodoro, R. C., Nino-Vega, G., Bagagli, E., and Felipe, M. S. (2014). *Paracoccidioides* species complex: ecology, phylogeny, sexual reproduction, and virulence. *PLoS Pathog.* 10:e1004397. doi: 10.1371/journal.ppat.1004397

Theodoro, R. C., Bagagli, E., and Oliveira, C. (2008). Phylogenetic analysis of PRP8 intein in *Paracoccidioides brasiliensis* species complex. *Fungal Genet. Biol.* 45, 1284–1291. doi: 10.1016/j.fgb.2008.07.003

Turissini, D. A., Gomez, O. M., Teixeira, M. M., McEwen, J. G., and Matute, D. R. (2017). Species boundaries in the human pathogen *Paracoccidioides*. *Fungal Genet. Biol.* 106, 9–25. doi: 10.1016/j.fgb.2017.05.007

Zubaer, A., Wai, A., and Hausner, G. (2018). The mitochondrial genome of Endoconidiophora resinifera is intron rich. *Sci. Rep.* 8:17591. doi: 10.1038/s41598-018-35926-y

Zubaer, A., Wai, A., and Hausner, G. (2019). The fungal mitochondrial Nad5 pan-genic intron landscape. *Mitochondrial DNA A DNA Mapp. Seq. Anal.* 30, 835–842. doi: 10.1080/24701394.2019.1687691

Conflict of Interest: The authors declare that the research was conducted in the absence of any commercial or financial relationships that could be construed as a potential conflict of interest.

frontiers in Genetics

ORIGINAL RESEARCH
published: 25 September 2020
doi: 10.3389/fgene.2020.530915

Functional Characterization of a Novel Oxidative Stress Protection Protein in the Pathogenic Yeast *Candida glabrata*

Jane Usher[1,2], Yogesh Chaudhari[2,3], Victoria Attah[2], Hsueh-lui Ho[2] and Ken Haynes[2†]*

[1] Medical Research Council Centre for Medical Mycology, University of Exeter, Exeter, United Kingdom, [2] School of Biosciences, University of Exeter, Exeter, United Kingdom, [3] Hawkesbury Institute for the Environment, Western Sydney University, Penrith, NSW, Australia

OPEN ACCESS

Edited by:
Christina A. Cuomo, Broad Institute, United States

Reviewed by:
Sascha Brunke, Leibniz Institute for Natural Product Research and Infection Biology, Germany
Miguel Teixeira, Universidade NOVA de Lisboa, Portugal
Katy Kao, San Jose State University, United States

***Correspondence:**
Jane Usher
j.usher@exeter.ac.uk

† Deceased

Specialty section:
This article was submitted to Evolutionary and Genomic Microbiology, a section of the journal Frontiers in Genetics

Received: *30 January 2020*
Accepted: *27 August 2020*
Published: *25 September 2020*

Citation:
Usher J, Chaudhari Y, Attah V, Ho H-l and Haynes K (2020) Functional Characterization of a Novel Oxidative Stress Protection Protein in the Pathogenic Yeast Candida glabrata. Front. Genet. 11:530915. doi: 10.3389/fgene.2020.530915

Candida species are important pathogens of humans and the fourth most commonly isolated pathogen from nosocomial blood stream infections. Although Candida albicans is the principle causative agent of invasive candidosis, the incidence of *Candida glabrata* infections has rapidly grown. The reason for this increase is not fully understood, but it is clear that the species has a higher innate tolerance to commonly administered azole antifungals, in addition to being highly tolerant to stresses especially oxidative stress. Taking the approach that using the model organism, *Saccharomyces cerevisiae*, with its intrinsic sensitivity to oxidative stress, we hypothesized that by expressing mediators of stress resistance from C. glabrata in *S. cerevisiae*, it would result in induced resistance. To test this we transformed, en-masse, the *C. glabrata* ORFeome library into *S. cerevisiae*. This resulted in 1,500 stress resistant colonies and the recovered plasmids of 118 ORFs. Sequencing of these plasmids revealed a total of 16 different C. glabrata ORFs. The recovery of genes encoding known stress protectant proteins such as GPD1, GPD2 and TRX3 was predicted and validated the integrity of the screen. Through this screen we identified a C. glabrata unique ORF that confers oxidative stress resistance. We set to characterise this gene herein, examining expression in oxidative stress sensitive strains, comet assays to measure DNA damage and synthetic genetic array analysis to identify genetic interaction maps in the presence and absence of oxidative stress.

Keywords: *Candida glabrata*, oxidative stress, SGA, human fungal pathogens, comet assay (Single cell gel electrophoresis)

INTRODUCTION

Biological systems function in constantly changing complex environments, where they are subject to wide ranging perturbations. Their ability to adapt to these perturbations is essential for all life and understanding the mechanisms that underpin these adaptations are of fundamental biological interest. Although, *Candida albicans* is the principle causative agent of invasive candidosis, the incidence of *Candida glabrata* infection has grown rapidly over the last 20 years, and it is now responsible for approximately 25% of cases (Hajjeh et al., 2004). The reason for this increasing

incidence of *C. glabrata* infection is not fully understood. The molecular mechanisms underpinning the response to stress is relatively well characterized in a number of model and pathogenic species (Gellon et al., 2001; Lackner et al., 2012; Boiteux and Jinks-Robertson, 2013; Miramón et al., 2013; Storr et al., 2013), but remains relatively unexplored in *C. glabrata*.

When engulfed by phagocytic cells pathogenic fungi are submitted to combinations of stress that cause oxidative damage, which if not repaired can result in cell death (Fang, 2004). *C. glabrata* is highly resistant to oxidative stress conditions, having evolved capabilities to cope with such stress (Nikolaou et al., 2009; Roetzer et al., 2011). *C. glabrata* can persist for long periods as a human commensal, and live cells can be isolated weeks after infection (Brieland et al., 2001; Jacobsen et al., 2010), clearly demonstrating that *C. glabrata* can adapt to the stresses encountered within the host. Indeed, *C. glabrata* has been shown to survive and multiply inside murine phagocytic cells (Kaur et al., 2007; Roetzer et al., 2008; Seider et al., 2011). When engulfed by phagocytes, *C. glabrata* cells are exposed to reactive oxygen species (ROS) plus cationic fluxes activated by intracellular ion currents (Fang, 2004). The mechanistic basis of *C. glabrata* stress resistance is not understood but genes encoding functions in cell wall biosynthesis, nutrient acquisition, metal (calcium and iron) ion homeostasis and stress response have been implicated by functional genomics (Seider et al., 2014). Previous studies have demonstrated that the *C. glabrata* response to *in vitro* exerted oxidative stress is very similar to that observed upon phagocyte engulfment, both at the level of gene expression (Kaur et al., 2007; Fukuda et al., 2013), where the up-regulation of genes encoding functions related to stress adaptation and nutrient recycling overlap substantially, and in growth kinetics (Kaloriti et al., 2012) where in both environments, approximately 20% of *C. glabrata* cells survive initial contact with a substantial delay occurring prior to growth re-commencing. These data sets demonstrate that *in vitro* oxidative stress is a realistic model of host-induced stress and the ability to survive oxidative stress is an important virulence determinant for pathogens. Understanding this network, and the role that selected components play in stress resistance, is essential to the long-term development of small molecule inhibitors.

Oxidative stress is generated by normal cellular metabolism or produced via exogenous chemicals (such as hydrogen peroxide) and can induce several types of DNA damage including DNA base damage and the formation of apurinic/apyrimidinic (AP) sites, which are thought to be processed primarily through the base excision repair (BER) pathway (Eide et al., 1996; Swanson et al., 1999). In the BER pathway, a damaged base is removed by a specific N-glycosylase (Ntg1 and Ntg2), (Alseth et al., 1999; Meadows et al., 2003; Griffiths et al., 2009), and the resulting AP site is cleaved by an AP endonuclease. Following the processing of the 5′ terminus by deoxyribose phosphodiesterase, DNA polymerase fills in the gap and DNA ligase seals the ends together (**Supplementary Figure 1**). The other main DNA repair pathway is the nucleotide excision repair (NER) pathway, which generally removes bulky DNA lesions and is also implicated in the repair of oxidative stress damage (Huang et al., 1994; Boiteux and Jinks-Robertson, 2013). The damaged DNA bases are removed by introducing nicks 5′ and 3′ to the DNA damage. The 3′ incision is produced by *RAD2* and the 5′ incision by the *RAD1-RAD10* complex (Habraken et al., 1993). Once the oligonucleotide including the damaged DNA is removed, DNA polymerase fills in the gap and DNA ligase joins the ends (**Supplementary Figure 1**). Recombination is involved in the repair of single or double stranded breaks. Cells deficient in the Rad52 epistasis group of proteins are highly sensitive to the killing effects of agents that produce strand breaks (Mortensen et al., 1996; Pâques and Haber, 1999; Symington, 2002). Recombination rates are known to increase upon exposure to hydrogen peroxide, playing a role for recombination in response to oxidative induced DNA damage. There is an overlap between the different DNA repair mechanisms and DNA damage tolerance pathways in the processing of oxidative DNA damage (Giglia-Mari et al., 2011).

In the model yeast *Saccharomyces cerevisiae,* the removal of oxidative stress induced damage is thought to be conducted primarily through the base excision pathway (Farrugia and Balzan, 2012). The main genes involved are *NTG1* and *NTG2*, N-glycosylase-associated apurinic/apyrimidinic lyases that recognize a wide variety of damaged pyrimidines and *APN1*, a major AP endonuclease in yeast, with the majority of AP sites *in vivo* processed via this pathway (Ramotar et al., 1991; Ildiko et al., 2000; Ishchenko et al., 2005). In general, the majority of yeast cells lacking these three genes are hyper-recombinogenic and exhibit a mutator phenotype but are not sensitive to all oxidative stress chemicals. However, the additional disruption of *RAD52* confers a high degree of sensitivity to oxidative stress damage by eliminating the nucleotide excision repair pathway.

In this study, we transformed *S. cerevisiae* cells, which are exquisitely sensitive to oxidative stress, with a *C. glabrata* genomic library and isolated oxidative stress resistant clones and identified the genes that encoded mediators of oxidative stress resistance. We have identified a novel *C. glabrata* protein, CAGL0G06710g, designated *ORI1* (Oxidative stress Resistance Increased) for this work, (**Table 1**) which can confer oxidative stress resistance in *S. cerevisiae*. *ORI1* is a *C. glabrata* specific protein, which has no homology to proteins encoded in any other sequenced genome. We hypothesized that this gene plays a role in oxidative stress resistance in *C. glabrata* via comet assays and genetically interacts with genes playing a role in the base excision via SGA screens in the presence and absence of oxidative stress (H_2O_2) and nucleotide excision DNA damage repair pathways.

MATERIALS AND METHODS

Screening of *Candida glabrata* ORFeome

The *C. glabrata* ORFeome (Ho and Huvet, unpublished), was generated using the Gateway cloning system, whereby pENTRY plasmids were generated for each ORF in the *C. glabrata* genome and shuttled to destination vectors of interest using the LR clonase protocol, for this work the destination plasmid used was pAG423GPD-ccdB, a constitutive promoter with HIS3 selection (Ho and Haynes, 2015). The *C. glabrata* ORFeome was pooled and transformed *en mass* into *S. cerevisiae* strain BY4741, using the lithium acetate method (Gietz and Schiestl, 2007).

TABLE 1 | *Candida* glabrata genes identified in ORFeome screen.

C. glabrata ORF	*S. cerevisiae* ORF	Identity	Number of hits
CAGL0G06710g	**N/A**	**99%**	**34**
CAGL0E06094g	**N/A**	**99%**	**9**
CAGL0H04059g	**N/A**	**99%**	**2**
CAGL0A00649g	**N/A**	**100%**	**2**
CAGL0H05181g	VPS28	99%	7
CAGL0E00583g	TRX3	93%	2
CAGL0G03531g	SPR6	99%	8
CAGL0G01848g	SNT309	100%	2
CAGL0J11220g	RPS3	98%	2
CAGL0F02673g	RPB7	98%	3
CAGL0J09482g	RMI1	98%	3
CAGL0L09042g	HAT1	68%	2
CAGL0C05137g	GPD2	75%	2
CAGL0K01683g	GPD1	73%	4
CAGL0D03630g	CET1	99%	2
CAGL0I07975g	BRX1	82%	8

Following the transformation of the C. glabrata ORFeome into S. cerevisiae, a number of colonies were identified as being resistant to oxidative stress when screened on hydrogen peroxide. The plasmids were recovered and sequenced to identify the ORFs conferring increased levels of oxidative stress resistance. 16 ORFs were identified, 4 of which are unique to C. glabrata (highlighted in bold).

Transformants were recovered from selective media plates containing 5 mM hydrogen peroxide, a concentration known to inhibit growth in *S. cerevisiae*. The individual colonies were isolated and grown on fresh media containing 5 mM hydrogen peroxide to remove any break through colonies. Using the QIAprep Spin miniprep kit (Qiagen), the plasmid DNA was recovered and sent for sequencing to identify the *C. glabrata* ORFs conferring stress tolerance.

Generation of *Candida glabrata* Deletion and Over Expression Strains

The *KanMX* cassette was amplified from plasmid pFA6-kanMX4 with complementary up and down stream sequences for *ORI1*, (**Supplementary Table 1** for primers used), using the following conditions for a 50 μl reaction; 1× Taq buffer, 0.2 μM dNTPs, 0.5 μM of each primer, 1 μl Taq-polymerase and plasmid DNA; 93°C for 3 min, with 30 cycles of 93°C for 30 s, 50°C for 30 s, 72°C for 2 min with 10 min at 72°C. The fragments were gel-purified in 0.7% agarose gels and the final deletion construct purified via ethanol precipitation.

Transformations

Candida glabrata CAGL0G06710g was cloned into the pDONR221 entry vector using GATEWAY cloning techniques and were shuttled into pAG423GPD-ccdB destination vector (Addgene) using the LR clonase reaction. Destination vectors were transformed into *C. glabrata* via electroporation (Istel et al., 2015) and *S. cerevisiae* cells via the LiAc transformation method (Gietz and Schiestl, 2007). The correct transformants were selected for growth on SC-HIS media. Three independent transformants of each strain were collected.

Comet Assays

Aliquots of 10^6cells/ml *C. glabrata* and *S. cerevisiae* cells were collected by centrifugation and mixed with 1.5% low melting point agarose (w/v) in S buffer containing 2 mg/ml zymolyase (20T), 80 μl of this mixture was spread over a slide coated in 0.5% normal melting point agarose (w/v) and covered with a coverslip and incubated for 20 min at 30°C for cell wall enzymatic degradation, following which the cover slips were removed. All remaining steps were performed at 4°C. The slides were incubated in lysis solution (30 mM NaOK, 1M NaCl, 0.05% lauryl sarcosine (w/v), 50 mM EDTA, 10 mM Tris–HCl, pH10) for 20 min in order to lyse spheroplasts. The slides were then washed three times for 20 min each in electrophoresis buffer (30 mM NaOH, 10 mM Tris–HCl, pH10) to remove the lysis solution. The slides were then electrophoresis in the same buffer for 10 min at 0.7V/cm. After electrophoresis, the slides were incubated in neutralization buffer (10 mM Tris–HCl, pH7.4) for 10 min, followed by 10 min in 76 and 96% ethanol, respectively. The slides were then stained with ethidium bromide (10 μg/ml) and visualized using a Leica microsystem DM fluorescence microscope. Each condition was repeated in triplicate with 20 representative images of each slide acquired. The images were analyzed using Comet Score software.

SGA Screens

Synthetic Genetic Array (SGA) screens were performed in triplicate with double spotting within each triplicate. The *S. cerevisiae* deletion mutant library was arrayed using a Singer RoToR HDA (Singer Instruments). For the genome-wide synthetic lethal SGA screens (SL-SGA) the MATα query strain Y7092[1] was transformed with the *C. glabrata* gene of interest, *ORI1*. The resulting query strain was mated with the *S. cerevisiae* MATa deletion mutant array library and SGA methodology was used (Hin et al., 2001; Measday et al., 2005). For the screens in the presence of stress, the last plate of the screen (double mutant plates) was then spotted onto media containing oxidative stress (2 mM H_2O_2) and incubated for 24 h at 30°C. To identify deletion mutants that showed growth defects due to the expression of the *C. glabrata* genes, all screens were performed in triplicate. Growth was scored for three main criteria, slow growth (SS), lethality (SL or suppression S, improved growth) after 24 h on the final DMA plates. For verification, any potential genetic interactions had to be identified in a minimum of two out of the three replicated in any screen.

Dotty Plates

Dot assays were performed by spotting 5 μl of 10-fold serial dilutions (OD600 = 0.1, 0.01, 0.001, 0.0001) onto specified media, and sealed plates were incubated at 30°C for 24 h. All dot assay experiments were repeated in triplicate using three different isolates of each strain.

[1]http://sites.utoronto.ca/boonelab/sga_technology/

RESULTS

Identification of *C. glabrata* ORFs Mediating Oxidative Stress Resistance by Genetic Complementation

Saccharomyces cerevisiae is exquisitely sensitive to oxidative stress. We hypothesized that expression of effectors of *C. glabrata* stress resistance in *S. cerevisiae* would lead to increased oxidative stress resistance. We transformed, *en-bloc*, our recently constructed *C. glabrata* partial ORFeome (∼3,000 genes) into *S. cerevisiae* strain BY4741 and screened the transformants on media containing the oxidative stress agent, hydrogen peroxide (5 mM). From this we identified 1,500 stress resistant colonies, which were then individually regrown on hydrogen peroxide containing media to remove break-out colonies. The plasmids were recovered from each of these and their *C. glabrata* ORFS identified by sequencing. A total of 16 *C. glabrata* ORFs were isolated (**Table 1**). Recovery of genes encoding known stress protectant proteins e.g., *GPD1, GPD2*, and *TRX3* (Albertyn et al., 1994; Trotter and Grant, 2005; Tkach et al., 2012) were predicted and validated the integrity of the screen. In addition, we identified a number of genes encoding proteins with general roles in transcription/translation, epigenetic modification and endosomal sorting e.g., *BRX1, CET1, HAT1, RPB7*, *SNT309*, and *VPS28* whose over-expression are likely to have pleiotropic effects and hence deciphering a specific role in stress resistance would be extremely difficult.

Finally, we isolated four *C. glabrata* specific ORFs, encoding proteins of unknown function, *CAGL0G06710g, CAGL0E06094g, CAGL0H04059g*, and *CAGL0A00649g* (**Table 1**). We have taken ORF *CAGL0G6710g* forward for further investigation and for the purpose of this work refer to it as *ORI1* (Oxidative Stress Resistance Increased). It was isolated in 34/85 of the stress resistant mutants.

Confirmation of the Role of *ORI*1 in Stress Resistance

To confirm that the expression of *ORI1* conferred oxidative stress protection in *C. glabrata*, following its identification in the *S. cerevisiae* screen, we generated an *ORI1* deletion strain and over-expression strain in *C. glabrata* wild-type strain CBS138. This also confirmed that the gene is not essential for viability. The strains were then screened on oxidative (2 mM hydrogen peroxide), osmotic (1.5 M sodium chloride) and combinatorial stress plates [oxidative (H_2O_2) and osmotic (NaCl)] (**Figure 1**). The *C. glabrata*Δ*ori1* mutants are sensitive to combinatorial stress, whereas the *ORI1* over-expressing strains had an increased combinatorial stress tolerance but most striking was the increased tolerance to oxidative stress. This demonstrated a potential role for *ORI1* in mediating *C. glabrata* stress resistance.

Following from the spot assay, we utilized Comet assays as an uncomplicated and sensitive method to detect DNA damage at the level of individual cells. The term "comet" refers to the pattern of DNA migration through the electrophoresis gel after exposure to a DNA damaging agent, in this study, hydrogen peroxide. The intensity of the comet tail relative to the head reflects the number of DNA strand breaks. The basis for this is that loops containing a break lose their supercoiling and become free to extend toward the anode during electrophoresis. We examined *C. glabrata* and *S. cerevisiae* wild-type strains and ones over-expressing *ORI1* (**Figure 2**). As can be clearly seen the over-expression on *ORI1* offers protection from the DNA damage induced by the oxidative stressor H_2O_2 at a range of different concentrations when compared to the level of damage experienced by the wild-type cells due to the shortened tail lengths observed. This effect was most pronounced in the *S. cerevisiae* cells overexpressing *ORI1*. This may be due to the fact that *S. cerevisiae* is sensitive to oxidative stress. Control cells (i.e., no exposure to hydrogen peroxide) were also observed to display comet-like features, this is likely due to initial DNA damage present, replication forks or damage induced by the handling of cells during preparation of comets. The use of this methodology is interesting, as the combination of yeast cells, either pathogenic or non-pathogenic and the comet assay is an extremely accessible technique for genotoxicity testing.

Synthetic Genetic Interaction Maps for Ori1 Differ in the Presence of Oxidative Stress

Synthetic Genetic Array screens enable the construction of double mutants on a genome wide scale and as such this trend for large scale genetic screens reveal a wealth of genetic interaction information on biological systems. Therefore we performed unbiased SGA screens on *ORI1* in the *S. cerevisiae* background in order to determine what genes it genetically interacts in both the presence and absence of oxidative stress (2 mM hydrogen peroxide). Interactions were identified by slow growth (synthetic sick) or death [synthetic lethality (SL)]. These genetic interactions arise from mechanistically distinct genetic origins, as the interactions are occurring between members of the same pathway. Using the principle that an increased amount of an exogenously expressed substrate may cause a fitness defect in a mutant background, this methodology has proven successful in identification of downstream targets as well as targets of specific proteolytic pathways (Costanzo et al., 2010). Therefore using this methodology can identify genetic interactions previously unknown especially when exogenous genes from yeast with no high throughput screening systems can be expressed in a model system such as *S. cerevisiae*. A SL or synthetic sick genetic interaction is defined as the combination of two genes, each individually viable, that cause a fitness defect not predicted from the multiplicative effect of combining the single mutations (either deletions or over-expression). Classically, this type of genetic interaction is that the cell cannot tolerate the disruption of a shared function of the two genes, implying that the encoded proteins work in parallel to one another. Conversely, SL genetic interaction profiles can predict genes that function in the same pathway or protein complex.

In an attempt to identify the genetic interactors of *ORI1* in *C. glabrata*, we performed genome-wide SGA screens. In brief the *S. cerevisiae* query strain containing *C. glabrata ORI1* was mated to the yeast deletion mutant arrays and the SDL

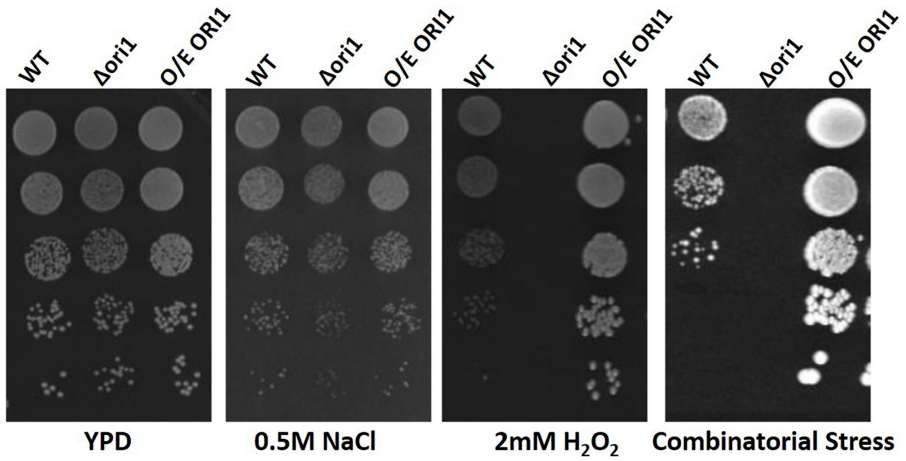

FIGURE 1 | Spot plate assay of *ORI1* on stress media. *C. glabrata* wild-type, *Ori1* (CAGL0G06710g) deletion and overexpression strains. Strains were serially diluted and 5 μl spots were placed onto minimal media containing either oxidative stress (2 mM H_2O_2), Osmotic stress (0.5 M NaCl) and combinatorial stress (2 mM H_2O_2 and 0.5 M NaCl). The plates were then incubated for 24 h at 37°C. Each spot assay was performed in triplicate.

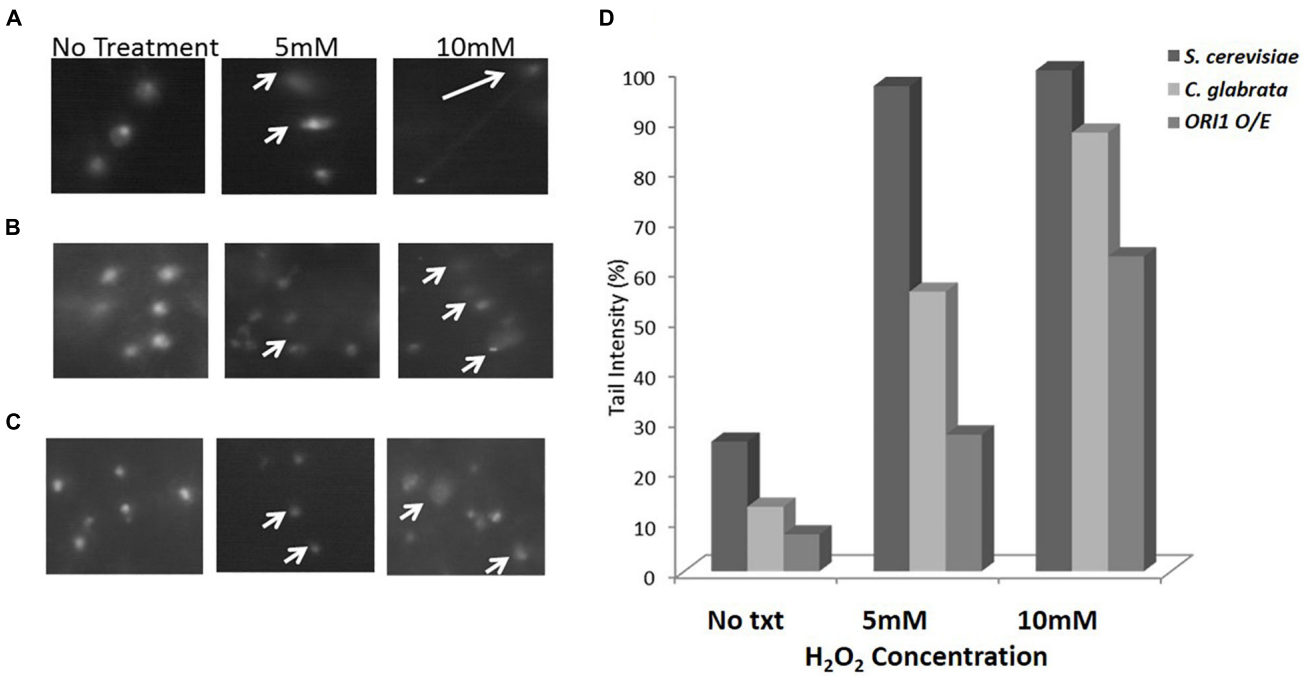

FIGURE 2 | Comet assay on *C. glabrata* and *S. cerevisiae* wild-type and *ORI1* overexpressing strains. Comet assays were performed on **(A)** *S. cerevisiae* wild-type cells, **(B)** *C. glabrata* wild-type cells, and **(C)** *S. cerevisiae* cells overexpressing *ORI1* in the presence of no stress (No Txt in figure), 5 mM H_2O_2 and 10 mM H_2O_2. DNA damage was measured in 100 comets for each strain time for each condition and analysis with Comet Assay V4.0. **(D)** The DNA damage is represented as a mean ratio of tail length to head intensity allowing for positional variations in intensity. 100 comets were scored per experiment for each concentration.

methodology was used to incorporate the plasmid into the deletion mutants. Growth of the deletion mutants containing the plasmids was scored for sickness or lethality. We identified 14 synthetic lethal interactions (**Supplementary Table 2**) including *alo1* (*ALO1* is a mitochondrial membrane protein that catalyses the last reaction in biosynthesis of the antioxidant D-ascorbate). This allowed us to hypothesize that *ORI1* may play a role in protection from oxidative damage. In addition to *ALO1*, there were also genetic interactions with genes that play a specific role in the DNA damage and repair pathways namely *CRT10, NTG1, RAD52*, and *ECM11* (**Supplementary Table 2**), these genes identified in both the screens in the absence and presence

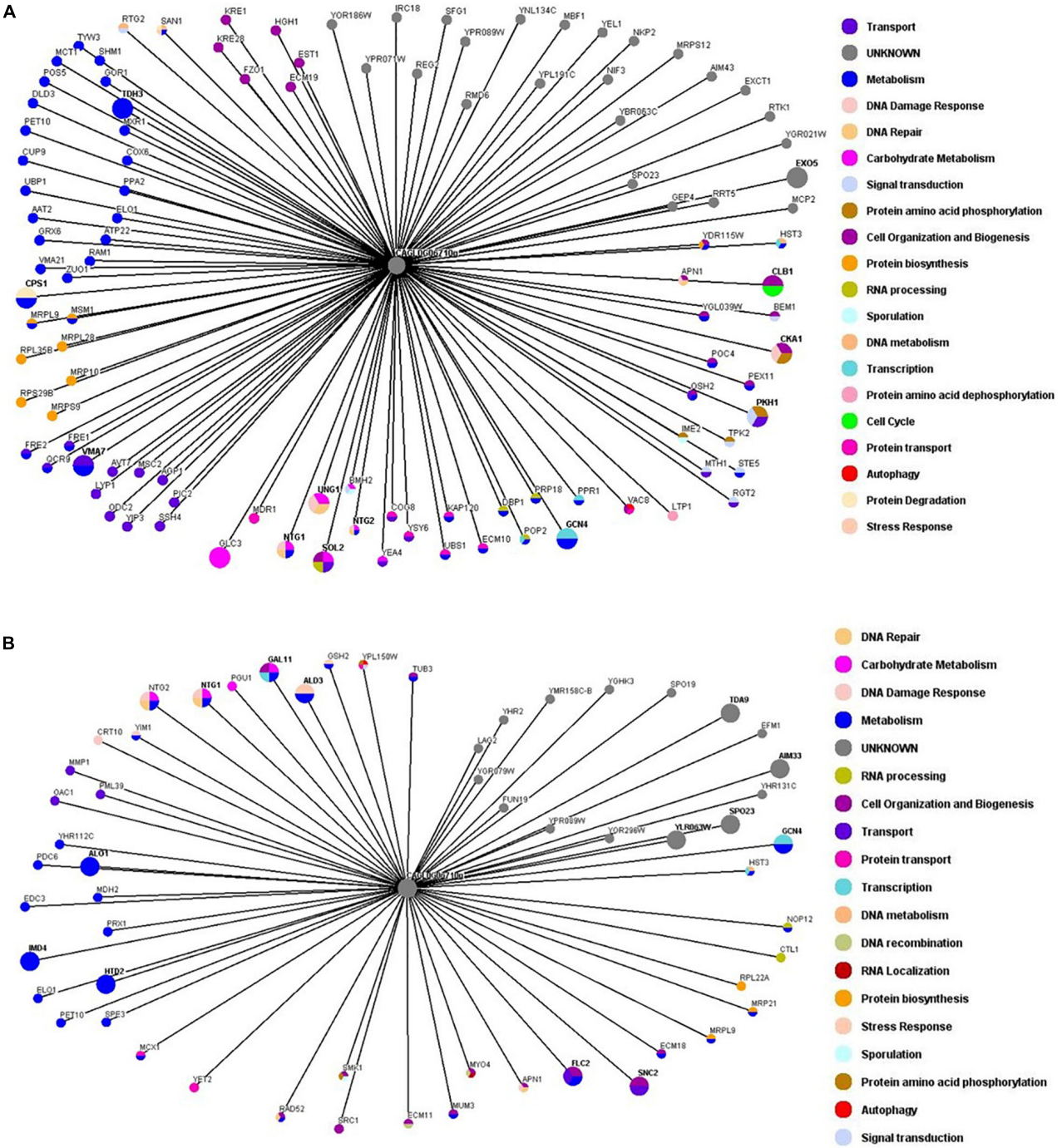

FIGURE 3 | Genetic interaction network maps of *ORI1* in the presence or absence of oxidative stress. Genome wide synthetic interaction SGA screens were performed using the query strain that was transformed with *ORI1* (CAGL0G06710g) from *C. glabrata*. Genes are represented by nodes that are color-codes according to the *S. cerevisiae* database (SGD) cellular roles (www.yeastgenome.org). The interactions are represented by edges. All screens were performed in triplicate with double spotting on each plate. Deletion mutants that displayed a synthetic sick or synthetic lethal interaction are detailed in **Supplementary Table 1**. **(A)** Genetic interaction map of *ORI1* in the absence of stress. **(B)** Genetic interaction map of *ORI1* in the presence of oxidative stress (2 mM H_2O_2). It can be seen that the presence of oxidative stress affects the genes that *ORI1* genetically interacts with.

of oxidative stress. The SGA screens also highlight the different genetic interactors involved in the presence of oxidative stress (**Figure 3** and **Supplementary Table 3**). The synthetic lethal interactions (**Supplementary Table 3**) remained the same under both conditions indicating that the cells may be primed to encounter a stress.

Interaction With DNA Damage Repair Pathways

Following the identification of the genetic interactions with genes that play a key role in the BER and NER pathways (**Supplementary Figure 1**), we obtained the deletion strains from the lab of Prof Jinks-Robertson (Swanson et al., 1999) in the *S. cerevisiae* background, where the main elements of each pathway were deleted. Using these backgrounds we were able to transform *ORI1* to determine if the overexpression of this gene can compensate for the removal of these pathways (**Figure 4A**). As can be observed in media with no treatment (i.e., no hydrogen peroxide added), many of the mutants already exhibit a growth defect, due to the loss of different components of the DNA repair pathways which in turn was exacerbated upon exposure to hydrogen peroxide (**Figures 4B,C**). However, upon the addition of *ORI1,* into the different deletion strains we can observe some recovery of the sickness phenotype notably in the quadruple deletion strain, Δ*ntg1*Δ*ntg2*Δ*apn1*Δ*rad1,* on minimal media and media with increasing amounts of hydrogen peroxide as an agent of inducing oxidative stress damage. There is no improvement in the fitness of triple knockout, Δ*ntg1*Δ*ntg2*Δ*apn1,* upon the introduction of *ORI1* indicating that the exogenous gene may be hindering the other DNA damage pathways compensating for the partial lack of *ntg1, ntg2 and apn1*. The mutant background with the most significant improvement upon exposure to hydrogen peroxide when transformed with *ORI1,* was the quadruplicate knockout, Δ*ntg1*Δ*ntg2*Δ*apn1*Δ*rad1*, which is generally highly sensitive to oxidative stress and has had the nucleotide excision repair pathway deleted.

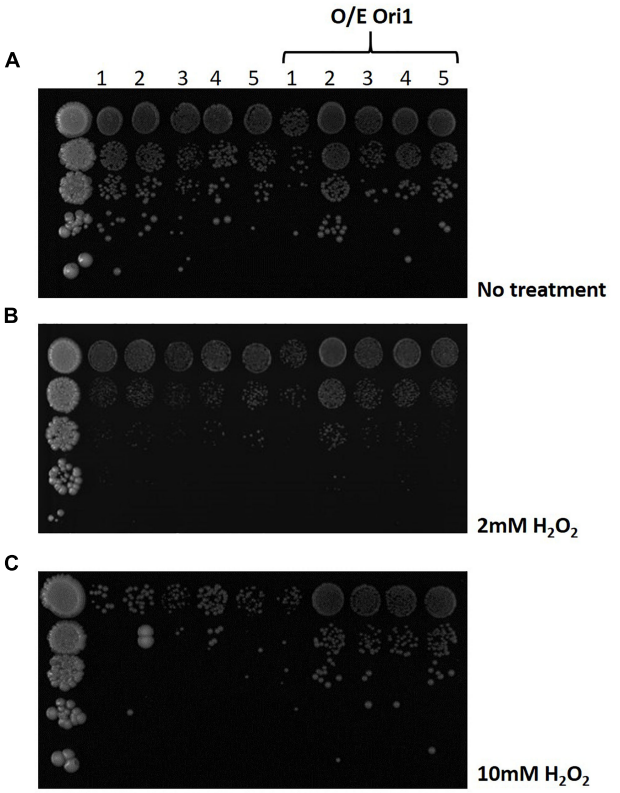

FIGURE 4 | Screening of DNA pathway deletion mutants overexpressing *ORI1* on oxidative stress media. A series of *S. cerevisiae* knock-out strains for different elements of the DNA damage repair pathways were screened on media with **(A)** no stress, **(B)** 2 mM H_2O_2 and **(C)** 10 mM H_2O_2. The different deletion mutants were 1: Δntg1 ntg2 apn1 (BER pathway); 2: Δ*ntg1 ntg2 apn1 rad1* (NER pathway), 3: Δ*ntg1 ntg2 apn1 rad52* (Recombination pathway); 4: Δ*ntg1 ntg2 rad1* and 5: Δ*ntg1 ntg2 apn1 rev3* (BER pathway). Plates were spotted with 10 fold serial dilutions of cells and incubated at 30°C for 24 h. Wild-type cells were used as a control.

DISCUSSION

The natural environments for *C. glabrata* and *S. cerevisiae* are significantly different. *C. glabrata* is a commensal of mucosal surfaces where it encounters phagocytic cells from the immune system and competition from other microbes for nutrients. These environments have selected for evolution of its high resistance to numerous stress conditions such as drug exposure, temperature shifts, osmotic and oxidative stresses. *C. glabrata* has evolved the capabilities to cope with oxidative stress and can proliferate inside phagocytes when engulfed, currently the mechanism to suppress reactive oxygen species production by phagocytes is unknown. The strong resistance to oxidative stress in *C. glabrata* is believed to be mediated through the functions of a catalase (CgCta1), two superoxide dismutases (CgSod1 and CgSod2) as well as the glutathione and thioredoxin detoxification systems (Cuéllar-Cruz et al., 2008). Our current knowledge of the oxidative stress response (OSR) in *C. glabrata* has increased significantly in the last decade with the characterization of the core elements as mentioned above in addition to key transcription factors Yap1, Skn7 and the general stress response regulators Msn2 and Msn4 and the newly identified Ada2 (Yu et al., 2018). However, this current understanding of the OSR in *C. glabrata* is far from comprehensive with additional genetic components and molecular mechanisms that remain to be explored.

Knowing that *S. cerevisiae* is intrinsically sensitive to oxidative stress (Farrugia and Balzan, 2012), we utilized this trait as a model to identify oxidative stress resistant genes in *C. glabrata.* Due to their relative closeness, the need for codon optimization was nullified, allowing for the transformation of the *C. glabrata* ORFeome *en masse* into the *S. cerevisiae* background. The identification of the four novel *C. glabrata* isolates that have no sequence or synteny homology to any *S. cerevisiae* genes, highlighted potential ORFs that are conferring these increased levels of oxidative stress resistance to this human fungal pathogen. We confirmed the phenotype of one *C. glabrata* specific ORF on *CAGL0G06710g (ORI1)* as it resulted in the strongest phenotype on increasing levels of oxidative stress exposure. Following the comet assays which showed that the expression of *ORI1* in *S. cerevisiae* were offering a level of protection to DNA damage, this lead us to hypothesize that these *C. glabrata* specific genes may also play a role in DNA damage/repair pathways. DNA damage repair pathways in yeast have been extensively

studied (Boiteux and Jinks-Robertson, 2013), however, this does not explain the resistance to DNA damaging agents from oxidative stress in the human fungal pathogen *C. glabrata*. Our unbiased *ORFeome* screen, which resulted in the identification of *C. glabrata* specific genes may add to this fungal pathogens story. These genes are unique to the genome of *C. glabrata,* potentially having evolved as the fungi carved out its niche as a pathogen.

Utilizing the SGA methodology to systematically screen the yeast deletion mutant array we sought to identify genetic interactions of *ORI1*. While phenotypic analysis of mutants can provide an important tool to define gene function, the effect of gene under- and over-expression when assessed globally demonstrates high levels of genetic redundancy in the yeast genome. This redundancy has resulted in the powerful approach of SGA screens to study gene function by identifying genetic relationships between genes. This is based on the knowledge that combinations of endogenous and exogenous genes that reduce cell fitness can pinpoint a shared function. With the aid of SGA screening we were able to show that *ORI1* genetically interacts with the main genes involved in DNA repair (*NTG1, NTG2 and APN1; p*-value 7.99E-05, see **Supplementary Table 3**) in both the presence and absence of oxidative stress. In the presence of stress, (i.e., oxidative stress), we observed an overrepresentation of genes playing a role in base-excision repair (*p*-value 0.0002993), oxidation-reduction processing (*p*-value 0.001902).

To gain insight into the role of *ORI1* in DNA damage repair in response to oxidative stress exposure, we obtained a series of deletion mutants with specific pathways deleted in the *S. cerevisiae* background (**Supplementary Figure 1** and **Figure 4**). The removal of oxidative stress damage from yeast DNA is believed to be primarily through the base excision repair pathway. In general, cells lacking Ntg1, Ntg2, and Apn1 are not shown to be sensitive to hydrogen peroxide but upon the additional disruption of *RAD52* there is an increased sensitivity to such oxidative stress elements. These mutants were previously determined to have a growth defects, therefore through the addition of *ORI1,* we were able to circumvent this defect in the presence of oxidative stress. We observed that the quadruplicate deletion strain Δ*ntg1*Δ*ntg2*Δ*apn1*Δ*rad1* had increased resistance to increasing hydrogen peroxide upon the addition of *ORI1*. This quadruplicate deletion strain is defective in the nucleotide excision repair pathway and base excision repair pathway, and is therefore sensitive to hydrogen peroxide. With both of these pathways defective, the DNA damage tolerance pathways (recombination and translesion synthesis) must deal with exposure to oxidative stress and the resulting DNA damage. This also suggests that BER and NER are competing pathways in *C. glabrata.*

Currently, we are GFP-tagging *ORI1* to determine where it localizes to in the cell in the presence and absence of oxidative stress and if this can be correlated to its genetic interactions with *NTG1, NTG2, APN1* and *RAD52.* In addition, with the GFP-tagged strains we are building the protein interaction networks in the presence of oxidative stress in both *C. glabrata* and *S. cerevisiae.* Notwithstanding, the specific role Ori1 plays in oxidative stress resistance, it is essential for this resistance and therefore has potential as a therapeutic target being further investigated.

DATA AVAILABILITY STATEMENT

All datasets generated for this study are included in the article/**Supplementary Material**.

AUTHOR CONTRIBUTIONS

H-lH and YC performed the initial screen to identify *C. glabrata* isolates. YC and JU performed comet assays. JU, YC, and VA performed SGA screens. JU, H-lH, and KH initial concept. JU, YC, VA, and H-lH data analysis. JU wrote the manuscript. All authors contributed to the article and approved the submitted version.

FUNDING

This work was funded by grants to KH BB/F00513X/1 and BB/F005210/2 from the BBSRC. JU is based at the MRC CMM at the University of Exeter (MR/N006364/2).

ACKNOWLEDGMENTS

We thank Prof. Sue Jink-Robertson and her group for sharing strains used in this work. We thank the Candida Research Community for their continued support to continue with this research following the death of KH.

SUPPLEMENTARY MATERIAL

The Supplementary Material for this article can be found online at: https://www.frontiersin.org/articles/10.3389/fgene.2020.530915/full#supplementary-material

Supplementary Figure 1 | Schematic of DNA repair pathways. The "X" represents DNA damage as either a base that is recognize and removed by with the base excision repair pathway (BER) or the nucleotide excision repair pathway (NER). In recombination pathway the polymerase is blocked thus blocking replication and allowing for recombination to occur. (Modified from Swanson et al., 1999).

Supplementary Table 1 | Primers used in this work for the generation of *ORI1* deletion strains and ORF amplification for plasmid construction.

Supplementary Table 2 | Analysis of SGA screen with *ORI1 (*CAGL0G06710g*)* as the gene of interest.

Supplementary Table 3 | Analysis of the SGA screenings with *ORI1 (*CAGL0G06710g) in the presence and absence of oxidative stress in the form of hydrogen peroxide.

REFERENCES

Albertyn, J., Hohmann, S., Thevelein, J. M., and Prior, B. A. (1994). GPD1, which encodes glycerol-3-phosphate dehydrogenase, is essential for growth under osmotic stress in saccharomyces cerevisiae, and its expression is regulated by the high-osmolarity glycerol response pathway. *Mol. Cell. Biol.* 14, 4135–4144. doi: 10.1128/mcb.14.6.4135

Alseth, I., Eide, L., Pirovano, M., Rognes, T., Seeberg, E., and Bjørås, M. (1999). The *Saccharomyces cerevisiae* homologues of endonuclease III from *Escherichia Coli*, Ntg1 and Ntg2, are both required for efficient repair of spontaneous and induced oxidative DNA damage in yeast. *Mol. Cell. Biol.* 19, 3779–3787. doi: 10.1128/mcb.19.5.3779

Boiteux, S., and Sue Jinks-Robertson, S. (2013). DNA repair mechanisms and the bypass of DNA damage in *Saccharomyces cerevisiae*. *Genetics* 193, 1025–1064. doi: 10.1534/genetics.112.145219

Brieland, J., Essig, D., Jackson, C., Doyle, F., Loebenberg, D., Menzel, F., et al. (2001). Comparison of pathogenesis and host immune responses to *Candida glabrata* and *Candida albicans* in systemically infected immunocompetent mice. *Infect. Immun.* 69, 5046–5055. doi: 10.1128/IAI.69.8.5046

Costanzo, M., Baryshnikova, A., Bellay, J., Kim, Y., Spear, E. D., Sevier, C. S., et al. (2010). The genetic landscape of a cell. *Science* 327, 425–431. doi: 10.1126/science.1180823

Cuéllar-Cruz, M., Briones-Martin-del-Campo, M., and Cañas-Villamar, I. (2008). High resistance to oxidative stress in the fungal pathogen *Candida glabrata* is mediated by a single catalase, Cta1p, and is controlled by the transcription factors Yap1p, Skn7p, Msn2p, and Msn4p. *Eukaryot. Cell* 7, 814–825. doi: 10.1128/EC.00011-08

Eide, L., Bjørås, M., Pirovano, M., Alseth, I., Berdal, K. G., and Seeberg, E. (1996). Base excision of oxidative purine and pyrimidine DNA damage in *Saccharomyces cerevisiae* by a DNA glycosylase with sequence similarity to endonuclease III from *Escherichia Coli*. *Proc. Natl. Acad. Sci. U.S.A.* 93, 10735–10740. doi: 10.1073/pnas.93.20.10735

Fang, F. C. (2004). Antimicrobial reactive oxygen and nitrogen species: concepts and controversies. *Nat. Rev. Microbiol.* 2, 820–832. doi: 10.1038/nrmicro1004

Farrugia, G., and Balzan, R. (2012). Oxidative stress and programmed cell death in yeast. *Front. Oncol.* 2:64. doi: 10.3389/fonc.2012.00064

Fukuda, Y., Tsai, H. F., Myers, T. G., and Bennett, J. E. (2013). Transcriptional profiling of *Candida glabrata* during phagocytosis by neutrophils and in the infected mouse spleen. *Infect. Immun.* 81, 1325–1333. doi: 10.1128/IAI.00851-12

Gellon, L., Barbey, R., Auffret Van der Kemp, P., Thomas, D., and Boiteux, S. (2001). Synergism between base excision repair, mediated by the DNA glycosylases Ntg1 and Ntg2, and nucleotide excision repair in the removal of oxidatively damaged DNA bases in *Saccharomyces cerevisiae*. *Mol. Genet. Genomics* 265, 1087–1096. doi: 10.1007/s004380100507

Gietz, R. D., and Schiestl, R. H. (2007). High-efficiency yeast transformation using the LiAc/SS carrier DNA/PEG method. *Nat. Protoc.* 2, 31–34. doi: 10.1038/nprot.2007.13

Giglia-Mari, G., Zotter, A., and Vermeulen, W. (2011). DNA damage response. *Cold Spring Harb. Perspect. Biol.* 3, 1–19. doi: 10.1101/cshperspect.a000745

Griffiths, L. M., Swartzlander, D., Meadows, K. L., Wilkinson, K. D., Corbett, A. H., and Doetsch, P. W. (2009). Dynamic compartmentalization of base excision repair proteins in response to nuclear and mitochondrial oxidative stress. *Mol. Cell. Biol.* 29, 794–807. doi: 10.1128/mcb.01357-1358

Habraken, Y., Sung, P., Prakash, L., and Prakash, S. (1993). Yeast excision repair gene RAD2 encodes a single-stranded DNA endonuclease. *Nat. Lett.* 30, 365–368.

Hajjeh, R. A., Sofair, A. N., Harrison, L. H., Lyon, G. M., Arthington-skaggs, B. A., Mirza, S. A., et al. (2004). Incidence of bloodstream infections due to candida species and in vitro susceptibilities of isolates collected from 1998 to 2000 in a population-based active surveillance program. *J. Clin. Microbiol.* 42, 1519–1527. doi: 10.1128/JCM.42.4.1519

Hin, A., Tong, Y., Evangelista, M., Parsons, A. B., Xu, H., Bader, G. B., et al. (2001). Systematic genetic analysis with ordered arrays of yeast deletion mutants. *Science* 294, 2364–2369.

Ho, H.-l., and Haynes, K. (2015). *Candida glabrata*: new tools and technologies-expanding the toolkit. *FEMS Yeast Res.* 15:fov066. doi: 10.1093/femsyr/fov066

Huang, J. C., Hsu, D. S., Kazantsev, A., and Sancar, A. (1994). Substrate spectrum of human excinuclease: repair of abasic sites, methylated bases, mismatches, and bulky adducts. *Proc. Natl. Acad. Sci. U.S.A.* 91, 12213–12217. doi: 10.1073/pnas.91.25.12213

Ildiko, U., Haracska, L., Johnson, R. E., Prakash, S., and Prakash, L. (2000). Apurinic endonuclease activity of yeast Apn2 protein. *J. Biol. Chem.* 275, 22427–22434. doi: 10.1074/jbc.M002845200

Ishchenko, A. A., Yang, X., Ramotar, D., and Saparbaev, M. (2005). The 3′->5′ exonuclease of Apn1 provides an alternative pathway to repair 7,8-Dihydro-8-oxodeoxyguanosine in *Saccharomyces cerevisiae*. *Mol. Cell. Biol.* 25, 6380–6390. doi: 10.1128/mcb.25.15.6380-6390.2005

Istel, F., Schwarzmuller, T., Tscherner, M., and Kuchler, K. (2015). Genetic transformation of *Candida glabrata* by electroporation. *Bio Protoc.* 5:e1528. doi: 10.21769/bioprotoc.1528

Jacobsen, I. D., Brunke, S., Seider, K., Schwarzmüller, T., Firon, A., D'Enfért, C., et al. (2010). *Candida glabrata* persistence in mice does not depend on host immunosuppression and is unaffected by fungal amino acid auxotrophy. *Infect. Immun.* 78, 1066–1077. doi: 10.1128/IAI.01244-1249

Kaloriti, D., Tillmann, A., Cook, E., Jacobsen, M., You, T., Lenardon, M., et al. (2012). Combinatorial stresses kill pathogenic candida species. *Med. Mycol.* 50, 699–709. doi: 10.3109/13693786.2012.672770

Kaur, R., Ma, B., and Cormack, B. P. (2007). A family of glycosylphosphatidylinositol-linked aspartyl proteases is required for virulence of *Candida glabrata*. *Proc. Natl. Acad. Sci. U.S.A.* 104, 7628–7633. doi: 10.1073/pnas.0611195104

Lackner, D. H., Schmidt, M. W., Wu, S., Wolf, D., and Bähler, J. (2012). Regulation of transcriptome, translation, and proteome in response to environmental stress in fission yeast. *Genome Biol.* 13:R25. doi: 10.1186/gb-2012-13-4-r25

Meadows, K. L., Song, B., and Doetsch, P. W. (2003). Characterization of AP lyase activities of *Saccharomyces cerevisiae* Ntg1p and Ntg2p: implications for biological function. *Nucleic Acids Res.* 31, 5560–5567. doi: 10.1093/nar/gkg749

Measday, V., Baetz, K., Guzzo, J., Yuen, K., Kwok, T., Sheikh, B., et al. (2005). Systematic yeast synthetic lethal and synthetic dosage lethal screens identify genes required for chromosome segregation. *Proc. Natl. Acad. Sci. U.S.A.* 102, 13956–13961. doi: 10.1073/pnas.0503504102

Miramón, P., Kasper, L., and Hube, B. (2013). Thriving within the host: *Candida* Spp. interactions with phagocytic cells. *Med. Microbiol. Immunol.* 202, 183–195. doi: 10.1007/s00430-013-0288-z

Mortensen, U. H., Bendixen, C., Sunjevaric, I., and Rothstein, R. (1996). DNA strand annealing is promoted by the yeast RaD52 protein. *Proc. Natl. Acad. Sci. U.S.A.* 93, 10729–10734. doi: 10.1073/pnas.93.20.10729

Nikolaou, E., Agrafioti, I., Stumpf, M., Quinn, J., Stansfield, I., and Brown A. J. (2009). Phylogenetic diversity of stress signalling pathways in fungi. *BMC Evol. Biol.* 9:44. doi: 10.1186/1471-2148-9-44

Pâques, F., and Haber, J. E. (1999). Multiple pathways of recombination induced by double-strand breaks in *Saccharomyces cerevisiae*. *Microbiol. Mol. Biol. Rev.* 63, 349–404.

Ramotar, D., Popoff, S. C., Gralla, E. B., and Demple, B. (1991). Cellular role of yeast apn1 apurinic endonuclease/3′-diesterase: repair of oxidative and alkylation DNA damage and control of spontaneous mutation. *Mol. Cell. Biol.* 11, 4537–4544. doi: 10.1128/mcb.11.9.4537

Roetzer, A., Gregori, C., Jennings, A. M., Quintin, J., Ferrandon, D., Butler, G., et al. (2008). *Candida glabrata* environmental stress response involves *Saccharomyces cerevisiae* Msn2/4 orthologous transcription factors. *Mol. Microbiol.* 69, 603–620. doi: 10.1111/j.1365-2958.2008.06301.x

Roetzer, A., Klopf, E., Gratz, N., Marcet-Houben, M., Hiller, E., Rupp, S., et al. (2011). Regulation of *candida glabrata* oxidative stress resistance is adapted to host environment. *FEBS Lett.* 585, 319–327. doi: 10.1016/j.febslet.2010.12.006

Seider, K., Brunke, S., Schild, L., Jablonowski, N., Wilson, D., Majer, O., et al. (2011). The facultative intracellular pathogen *Candida glabrata* subverts macrophage cytokine production and phagolysosome maturation. *J. Immunol.* 187, 3072–3086. doi: 10.4049/jimmunol.1003730

Seider, K., Gerwien, F., Kasper, L., Allert, S., Brunke, S., Jablonowski, N., et al. (2014). Immune evasion, stress resistance, and efficient nutrient acquisition

are crucial for intracellular survival of *Candida glabrata* within macrophages. *Eukaryot. Cell* 13, 170–183. doi: 10.1128/EC.00262-13

Storr, S. J., Woolston, C. M., Zhang, Y., and Martin, S. G. (2013). Redox environment, free radical, and oxidative DNA damage. *Antioxid. Redox Signal.* 18, 2399–2408. doi: 10.1089/ars.2012.4920

Swanson, R. L., Morey, N. J., Doetsch, P. W., and Jinks-Robertson, S. (1999). Overlapping specificities of base excision repair, nucleotide excision repair, recombination, and translesion synthesis pathways for DNA base damage in *saccharomyces cerevisiae*. *Mol. Cell Biol.* 19, 2929–2935. doi: 10.1128/mcb.19.4.2929

Symington, L. S. (2002). Role of RAD52 epistasis Group genes in homoogous recombinaiton and double-strand break repair. *Microbiol. Mol. Biol. Rev.* 66, 630–670. doi: 10.1128/MMBR.66.4.630

Tkach, J. M., Yimit, A., Lee, A. Y., Riffle, M., Costanzo, M., Jaschob, D., et al. (2012). Dissecting DNA damage response pathways by analysing protein localization and abundance changes during DNA replication stress. *Nat. Cell Biol.* 14, 966–976. doi: 10.1038/ncb2549

Trotter, E. W., and Grant, G. W. (2005). Overlapping roles of the cytoplasmic and mitochondrial redox regulatory systems in the yeast. *Eukaryot. Cell* 4, 392–400. doi: 10.1128/EC.4.2.392

Yu, S. J., Chang, Y. L., and Chen, Y. L. (2018). Deletion of ADA2 increases antifungal drug susceptibility and virulence in *Candida glabrata*. *Antimicrob. Agents Chemother.* 62:e01924-17. doi: 10.1128/AAC.01924-17

Conflict of Interest: The authors declare that the research was conducted in the absence of any commercial or financial relationships that could be construed as a potential conflict of interest.

frontiers in Cellular and Infection Microbiology

ORIGINAL RESEARCH
published: 02 December 2020
doi: 10.3389/fcimb.2020.571147

Robust, Comprehensive Molecular, and Phenotypical Characterisation of Atypical *Candida albicans* Clinical Isolates From Bogotá, Colombia

Giovanni Rodríguez-Leguizamón[1,2], *Andrés Ceballos-Garzón*[3], *Carlos F. Suárez*[2,4], *Manuel A. Patarroyo*[2,5] *and Claudia M. Parra-Giraldo*[3]*

[1] Hospital Universitario Mayor Méderi-Universidad del Rosario, Bogotá, Colombia, [2] School of Medicine and Health Sciences, Universidad del Rosario, Bogotá, Colombia, [3] Unidad de Proteómica y Micosis Humanas, Grupo de Enfermedades Infecciosas, Departamento de Microbiología, Facultad de Ciencias, Pontificia Universidad Javeriana, Bogotá, Colombia, [4] Biomathematics Department, Fundación Instituto de Inmunología de Colombia (FIDIC), Bogotá, Colombia, [5] Molecular Biology and Immunology Department, Fundación Instituto de Inmunología de Colombia (FIDIC), Bogotá, Colombia

OPEN ACCESS

Edited by:
Nelesh P. Govender,
National Institute of Communicable Diseases (NICD), South Africa

Reviewed by:
Vishukumar Aimanianda,
Institut Pasteur, France
Daniel Alford Powell,
University of Arizona, United States

***Correspondence:**
Claudia M. Parra-Giraldo
claudia.parra@javeriana.edu.co

Specialty section:
This article was submitted to Fungal Pathogenesis, a section of the journal Frontiers in Cellular and Infection Microbiology

Received: 10 June 2020
Accepted: 03 November 2020
Published: 02 December 2020

Citation:
Rodríguez-Leguizamón G, Ceballos-Garzón A, Suárez CF, Patarroyo MA and Parra-Giraldo CM (2020) Robust, Comprehensive Molecular, and Phenotypical Characterisation of Atypical Candida albicans Clinical Isolates From Bogotá, Colombia. Front. Cell. Infect. Microbiol. 10:571147. doi: 10.3389/fcimb.2020.571147

Candida albicans is commensal in human microbiota and is known to be the commonest opportunistic pathogen, having variable clinical outcomes that can lead to up to 60% mortality. Such wide clinical behaviour can be attributed to its phenotypical plasticity and high genetic diversity. This study characterised 10 Colombian clinical isolates which had already been identified as *C. albicans* by molecular tests; however, previous bioinformatics analysis of protein mass spectra and phenotypical characteristics has shown that this group of isolates has atypical behaviour, sharing characteristics of both *C. africana* and *C. albicans*. This study was aimed at evaluating atypical isolates' pathogenic capability in the *Galleria mellonella* model; susceptibility profiles were determined and MLST was used for molecular characterisation. Cluster analysis, enabling unbiased bootstrap to classify the isolates and establish their cluster membership and e-BURST, was used for establishing clonal complexes (CC). Both approaches involved using representative MLST data from the 18 traditional *C. albicans* clades, as well as *C. albicans*-associated and minor species. Ten atypical isolates were distributed as follows: 6/10 (B71, B41, B60, R6, R41, and R282) were grouped into a statistically well-supported atypical cluster (AC) and constituted a differentiated CC 6; 2/10 of the isolates were clearly grouped in clade 1 and were concurrent in CC 4 (B80, B44). Another 2/10 atypical isolates were grouped in clade 10 and concurred in CC 7 (R425, R111); most atypical isolates were related to geographically distant isolates and some represented new ST. Isolates B41 and R41 in the AC had greater virulence. Isolate B44 was fluconazole-resistant and was grouped in clade 1. The atypical nature of the isolates studied here was demonstrated by the contrast between phenotypical traits (*C. africana*-like), molecular markers (*C. albicans*-like), virulence, and antifungal resistance, highlighting the widely described genetic plasticity for this genus. Our results showed that the atypical isolates forming well-differentiated groups belonged to *C. albicans*. Our findings could

contribute towards developing molecular epidemiology approaches for managing hospital-acquired infection.

Keywords: *Candida albicans*, *Candida africana*, atypical isolates, pathogenicity, antifungal susceptibility, multilocus (MLST) genotypes

INTRODUCTION

Candida albicans has been recognised as a member of healthy humans' fungal microbiome (Zhang et al., 2017); however, it has been described that this opportunist fungi's proliferation in suitable conditions can have a serious impact on its host's health (this has led to it being defined recently as a pathobiont) (Sam et al., 2017). The range of pathologies associated with *C. albicans* proliferation includes localised oral and urogenital infections as well as cases of invasive fungal disease (IFD), having mortality percentages which can reach 60% (Mayer et al., 2013; Kadosh, 2019).

Concomitant diseases leading to the weakening of the immune system in intra-hospital (Costa-de-oliveira and Rodrigues, 2020) and immunosuppression populations favours the occurrence of clinical pictures associated with *C. albicans*, demonstrating the important role of a host's immune state (Znaidi, 2020). However, this microorganism's phenotypical plasticity has been identified during the last few years as the aspect contributing most to its successful proliferation, mainly regarding the expression of virulence factors, since this could provide it with the flexibility to survive in a target host's hostile conditions and make it tolerant to treatment schemes (Basmaciyan et al., 2019).

C. albicans detection and monitoring strategies have been based on descriptions of clinical isolates' phenotypical and microbiological characteristics, taking the species' ability to grow at 42°C, shorter germ tube formation, inability to produce chlamydospores and assimilate trehalose and/or amino-sugars as indicators (Tietz et al., 1995).

Such assays have contributed towards clarifying the epidemiological panorama in some regions worldwide (Borman et al., 2013; Chowdhary et al., 2017); however, disagreement amongst regarding these assays' results and the strains' clinical impact have revealed the need for introducing more robust assays/tests for describing the isolates. This is why proteomics and molecular profile-based tests have recently gained importance for more precisely detecting *C. albicans* infection events (Chowdhary et al., 2017).

Our research group adopted a strategy in 2007 for describing the local epidemiology of *C. albicans* and that of related *Candida* species; this study classified 101 clinical *Candida* isolates obtained from 10 tertiary care hospitals in Bogotá, Colombia, using microbiological tests. MALDI-TOF-MS confirmed 31 of them as *C. albicans* (Rodríguez-Leguizamón et al., 2015b). Such screening revealed the importance of the intra-hospital spread of *C. albicans* in Colombia and led to describing circulating strains' antifungal susceptibility profiles (Rodríguez-Leguizamón et al., 2015a).

Incongruity has been identified between traditional assays and proteomic and molecular strategies (using individual genes) (Alonso-vargas et al., 2008), demonstrating atypical clinical isolates in Spain (*C. dubliniensis*) (Albaina et al., 2015) and Colombia (*C. albicans*) (Rodríguez-Leguizamón et al., 2015b). This identified a set of isolates having phenotypical characteristics typical of *C. africana*, identified as *C. albicans/africana* by MALDI-TOF MS. However, molecular tests (D1/D2 rRNA and HWP1) and direct analysis of MALDI-TOF spectra showed that these atypical isolates were related to *C. albicans* (Rodríguez-Leguizamón et al., 2015b).

This required *C. albicans* typing strategies having greater discrimination power, such as the multilocus sequence typing (MLST)-based strategy which is extremely useful for identifying the types of sequences circulating in different regions of the world (Scordino et al., 2018). It currently has an easy access, debugged database, involving low complexity analysis (Pérez-Losada et al., 2013). A proposal regarding population structure for *C. albicans* based on 18 main clades agreed with epidemiological characteristics, such as the infection's anatomical location, geographical distribution, and susceptibility to antifungal drugs (Bougnoux et al., 2004; McManus and Coleman, 2014); however, such associations are not absolute and have become even more diversified with an increase in the isolates making up the baseline.

Considering the incongruities regarding assay results when using the set of Colombian atypical *C. albicans* isolates and completing their phenotypical characterisation involved pathogenicity assays concerning antifungal susceptibility profiles in the *Galleria mellonella* model. MLST was used for determining diploid sequence types (DSTs) for these atypical isolates; this led to obtaining information for hierarchical cluster analysis and defining related DST groups (using the BURST algorithm) for describing these isolates' relationships with representative strains from the 18 clades traditionally accepted for *C. albicans* and from other *C. albicans*-related species (*C. africana* and *C. dubliniensis*).

METHODS

Ethics Statement

Both the Universidad del Rosario and Hospital San Ignacio ethics' committees (i.e. its associated institution) approved this study.

Strains and Isolates

Ten atypical clinical isolates have already been reported by our group. These strains were collected from third-level hospitals in

Abbreviations: AC, atypical cluster; AMB, amphotericin B; CAIP, *C. albicans* informative position; CAS, caspofungin; CC, clone complex; DST, diploid sequence type; FLU, fluconazole; IFD, invasive fungal disease; MALDI-TOF-MS, matrix-assisted laser desorption/ionization time-of-flight mass spectrometry; MIC, minimal inhibitory concentration; MLST, multilocus sequence typing; PBS, phosphate-buffered saline; RPMI, Roswell Park Memorial Institute; TIP, total informative position; UPGMA, unweighted pair group method with arithmetic mean.

Bogotá, Colombia, and then characterised by phenotypic and MALDI-TOF MS using the Bruker Daltonics protocol (Rodríguez-Leguizamón et al., 2015b).

DNA Extraction and Molecular Characterisation

The genomic DNA (gDNA) used in this study was extracted from a pellet of isolates grown on Sabouraud agar (in previously described incubation conditions), using an UltraClean Microbial DNA isolation kit (Mo Bio Laboratories, Solana), following the manufacturer's instructions. The DNA used for the isolates' molecular characterisation involved two procedures: amplifying the HWP1 gene (for discriminating between species) (Romeo and Criseo, 2008; Hazirolan et al., 2017) and amplifying and sequencing the seven housekeeping genes in the *C. albicans*-standardised MLST scheme (Bougnoux et al., 2003). Both approaches involved adding 50 ng DNA to a 25 µl volume for the PCR reaction, using a Kapa HiFi PCR kit (KAPA Biosystems). These genes were amplified using 5 min cycles at 94°C for primary denaturing, followed by 35 cycles at 94°C (30s), 55°C (60 s), and 72°C (60 s), with a final 5 min extension step at 72°C. The amplicons were visualised by electrophoresis on 1.5% agarose gels, stained with SYBR Safe DNA Gel Stain (Invitrogen). The sequenced products had already been purified using a Wizard SV Gel and PCR Clean-Up System (Promega) and both strands were subsequently sequenced by the dideoxy terminal method (Sanger sequencing) by Macrogen (Korea).

Cluster Analysis Using MLST Data

Together with the atypical Colombian isolates (10 isolates), a representative set of MLST data available for *C. albicans* (clades 1 to 18, 82 isolates), two for *C. africana* isolates and one for *C. dubliniensis* was analysed (95 isolates in total) (**Table 1**). Clustal Omega was used for aligning the gene sequences (Sievers et al., 2011) which were then encoded using four binary digits for each IUPAC nucleic acid notation symbol and all identical positions were removed from the resulting binary matrix. Cluster analysis was performed for each marker and all were concatenated using Euclidean metrics and the unweighted pair group method with arithmetic mean (UPGMA). Unbiased bootstrap values were used to support the trees (10,000 replicas) using the pvclust package in R 3.4.3 (Suzuki and Shimodaira, 2006; Dean and Nielsen, 2007). A cluster having a ≥95 bootstrap value was considered supported (**Figure 1**).

Each isolate's membership in a particular cluster was evaluated by separately analysing its clustering pattern for each gene. Membership was defined in terms of clade differentiation and neighbourhood. For example, a membership of 1 occurred if an isolate was in a clearly differentiated clade; a membership of 0.5 was assigned for each clade if it occurred in a group where two clades concurred, and so on. An isolate's stability regarding MLST (7 genes: *AAT1a, ACC1, ADP1, MPIb, SYA1, VPS13*, and *ZWF1b*) was computed as the percentage at which a given isolate was observed in a clade (100% if it always occurred in a specific clade, or 14% if an isolate belonging to a clade occurred in one gene out of the 7 analysed here).

BURST Analysis

The allele profiles from the set of data used for phylogenetic analysis (**Table 1**) were analysed for identifying closely related, delimited and mutually exclusive groups, defined as clone complexes (CC); the eBURST V3 package (http://eburst.mlst.net/) was used for this (Feil et al., 2004), considering triple-locus variation (TLV) as cut-off for delimiting groups. The goeBURST algorithm was used for creating minimum spanning trees providing information about evolutionary patterns in conditions comparable to those for most natural microbial populations (Francisco et al., 2009). STs having six or more different alleles were defined as singletons.

Killing Assays in *G. mellonella*

Killing assays were performed in *G. mellonella*, as previously described (Cotter et al., 2000; Fuchs et al., 2010b; Fuchs et al., 2010a). Briefly, final (sixth) instar larvae weighing approximately 300 mg were used. Suspensions of individual *Candida* isolates which had been grown on Sabouraud agar for 24 h at 37°C were harvested by gently scraping colony surfaces with sterile plastic loops, washed twice in sterile phosphate-buffered saline (PBS), counted in haemocytometers and adjusted to 10^7 cells/ml in sterile PBS. Individual larvae were inoculated with 10^5 yeast (10 µl final inoculum volume) in the left rear proleg using a 0.5 ml BD syringe. At least ten larvae were inoculated per isolate per experiment (experiments involved using three independent isolates from each *Candida* test species). The larvae were monitored for 10 days and survival outcome was determined; larvae were considered dead when no response was observed following touch. Larval control groups received 10 µl sterile PBS in the same manner. Inoculated larvae were incubated at 37°C and scored for viability at 24 h intervals.

Antifungal Susceptibility

Yeast isolates were tested for *in vitro* susceptibility by the agar diffusion method using Etest reagent strips for echinocandin (caspofungin - CAS), triazole (fluconazole - FLU), and polyene (amphotericin B - AMB), according to the manufacturer's instructions (bioMérieux SA). Roswell Park Memorial Institute (RPMI) agar supplemented with 2% glucose was used as test medium for the assays. The 106 cell/ml yeast suspensions were spread uniformly on RPMI agar plates with sterile swabs and allowed to dry for 15 min. MIC readings for all agents were made following 24 h incubation at 35°C. MIC values were determined at the point of inhibition growth ellipse intersection with E-test strip. The MIC was read as the drug concentration that leads to complete inhibition 100% for amphotericin B and 80% inhibition for azoles and echinocandins. The MICs for *C. parapsilosis* ATCC 22019 and *C. krusei* ATCC 6258 quality control strains all came within reference ranges (data not shown).

Statistical Analysis

All experiments involved using three independent biological replicates; GraphPad Prism 7.0. was used for creating survival curves following the Kaplan-Meier method. Yeast isolate cumulative survival was estimated, along with the mean ± standard deviations, medians and quartiles; overall and between-pair survival distributions were compared by Log Rank (Mantel-Cox) test with multiple Bonferroni comparison adjustment, using $\{\propto^* = 1\text{-}(1\text{-}\propto)\ \hat{}\ [1/(\#\text{comparisons})]\}$ significance level. Asymptotic likelihood ratio and Cox proportional hazards tests were used for comparing all isolates' mortality rates after 10 days (a regression

TABLE 1 | The isolates analysed here, including origin, source, country, ST numbers, and CC.

								ST Numbers								
Code	Isolate	Specie	Clade/Cluster	Country	Year	Host	Source	AAT1a	ACC1	ADP1	MPIb	SYA1	VPS13	ZWF1b	DST (MLST)	CC
C. dubliniensis CD36	CD36	*C. dubliniensis*	*C. dubliniensis*	*Ireland*	*1988*	*Human*	oral swab	1	1	1	4	5	1	1	6	--
CO_AC_B41	B41	*C. albicans*	Atypical cluster	Colombia	2014	Human	Bronchoalveolar lavage	74	26	5	3	2	53	12	3267	6
CO_AC_B60	B60	*C. albicans*	Atypical cluster	Colombia	2014	Human	Bronchoalveolar lavage	13	26	5	3	93	53	12	1097	6
CO_AC_B77	B77	*C. albicans*	Atypical cluster	Colombia	2014	Human	Bronchoalveolar lavage	13	26	5	3	8	53	12	3268	6
CO_AC_R282	R282	*C. albicans*	Atypical cluster	Colombia	2007	Human	urine	13	26	5	3	156	53	12	3265	6
CO_AC_R41	R41	*C. albicans*	Atypical cluster	Colombia	2007	Human	blood	13	26	5	3	93	53	12	1097	6
CO_AC_R6	R6	*C. albicans*	Atypical cluster	Colombia	2007	Human	urine	13	26	5	3	218	53	12	3263	6
CA_01_AM2003_0046	AM2003_0046	*C. albicans*	Clade 1	UK	2003	Human	vaginal swab	2	5	5	2	2	6	5	69	4
CA_01_BougnCP01	BougnCP01	*C. albicans*	Clade 1	France		Human	faeces	2	5	5	2	2	21	5	37	4
CA_01_SC5314	SC5314	*C. albicans*	Clade 1	USA				2	3	5	9	2	24	5	52	4
CO_01_B44	B44	*C. albicans*	Clade 1	Colombia	2014	Human	vaginal swab	2	3	90	9	2	6	5	1867	4
CO_01_B80	B80	*C. albicans*	Clade 1	Colombia	2014	Human	urine	5	5	5	2	2	24	5	197	4
CA_02_85_007	85_007	*C. albicans*	Clade 2	UK	1985	Human	wound	4	7	17	4	15	26	20	41	Singleton
CA_02_AM2003_0053	AM2003_0053	*C. albicans*	Clade 2	UK	2003	Human	vaginal swab	4	2	4	4	34	4	4	174	9
CA_02_ATCC10231	ATCC10231	*C. albicans*	Clade 2	Unknown				4	7	4	4	4	4	4	119	9
CA_02_FC13	FC13	*C. albicans*	Clade 2	USA	1991	Human	other	4	23	14	4	4	4	4	153	9
CA_02_T30	T30	*C. albicans*	Clade 2	Canada		Human	oral swab	36	4	4	4	4	4	4	216	9
CA_03_81_174	81_174	*C. albicans*	Clade 3	USA	1981	Human	urine	13	7	27	24	7	49	15	138	12
CA_03_BougnCP11	BougnCP11	*C. albicans*	Clade 3	France		Human	wound	13	7	14	6	7	22	15	22	12
CA_03_C82	C82	*C. albicans*	Clade 3	Switzerland	1993	Human	oral swab	13	10	20	15	19	32	24	51	Singleton
CA_03_J990102	J990102	*C. albicans*	Clade 3	Belgium	1999	Human	vaginal swab	13	11	15	6	16	29	15	45	Singleton
CA_03_T65	T65	*C. albicans*	Clade 3	Canada		Human	oral swab	13	7	10	6	7	66	15	222	12
CA_04_b30972_4	b30972_4	*C. albicans*	Clade 4	UK	2003	Human	oral swab	8	3	8	4	7	10	60	247	247
CA_04_IHEM16731	IHEM16731	*C. albicans*	Clade 4	Rwanda		Human	CSF	11	26	6	4	34	60	8	167	Singleton
CA_04_J990683	J990683	*C. albicans*	Clade 4	Belgium	1999	Human	vaginal swab	8	14	8	4	35	10	8	128	13
CA_04_L343	L343	*C. albicans*	Clade 4	UK	1985	Human	oral swab	8	16	6	4	7	42	32	80	Singleton
CA_04_RV4688	RV4688	*C. albicans*	Clade 4	Congo		Human	other	8	14	8	4	7	10	35	87	13
CA_05_81_078	81_078	*C. albicans*	Clade 5	UK	1981	Human	vaginal swab	13	3	6	2	7	56	15	147	15
CA_05_AM2003_0084	AM2003_0084	*C. albicans*	Clade 5	UK		Human	blood	13	7	6	2	7	20	29	286	15
CA_05_AM2004_0006	AM2004_0006	*C. albicans*	Clade 5	France	2004	Human	oral swab	49	3	6	35	64	20	3	347	14
CA_05_AM2004_0007	AM2004_0007	*C. albicans*	Clade 5	France	2004	Human	oral swab	49	12	6	35	51	20	74	348	14
CA_05_AM2004_0008	AM2004_0008	*C. albicans*	Clade 5	France	2004	Human	oral swab	49	12	6	35	64	20	75	349	14
CA_06_AM2004_0022	AM2004_0022	*C. albicans*	Clade 6	UK	2004	Human	oral swab	21	26	14	18	47	65	61	321	3
CA_06_b30071_4	b30071_4	*C. albicans*	Clade 6	UK	2003	Human	oral swab	21	8	14	32	47	65	61	250	3
CA_06_IHEM20462	IHEM20462	*C. albicans*	Clade 6	Belgium		Human	oral swab	21	3	14	18	47	65	61	290	3
CA_06_IHEM20488	IHEM20488	*C. albicans*	Clade 6	UK		Human	oral swab	4	26	14	9	47	86	61	301	3
CA_06_T50	T50	*C. albicans*	Clade 6	Canada		Human	oral swab	21	26	14	18	47	65	55	221	3
CA_07_73_024	73_024	*C. albicans*	Clade 7	UK	1973	Human	vaginal swab	6	3	29	2	38	46	12	145	1
CA_07_b31331_6	b31331_6	*C. albicans*	Clade 7	UK	2003	Human	blood	3	3	37	2	38	73	12	252	1
CA_07_HUN122	HUN122	*C. albicans*	Clade 7	UK	1987	Human	other	6	3	21	4	30	46	12	101	1
CA_07_L1123	L1123	*C. albicans*	Clade 7	Saudi Arabia	1986			6	3	28	12	38	46	12	143	1
CA_07_T125	T125	*C. albicans*	Clade 7	Canada		Human	oral swab	13	3	37	2	38	72	12	238	1
CA_08_AM2003_0059	AM2003_0059	*C. albicans*	Clade 8	UK	2003	Human	vaginal swab	25	7	6	3	6	45	47	179	2
CA_08_b30956_5	b30956_5	*C. albicans*	Clade 8	China	2001	Human	blood	55	14	4	3	6	45	15	365	2
CA_08_HUN93	HUN93	*C. albicans*	Clade 8	UK	1987	Human	blood	27	7	4	3	6	45	15	98	2
CA_08_IHEM17983	IHEM17983	*C. albicans*	Clade 8	Peru		Human	CSF	24	7	6	3	6	27	37	298	2
CA_08_YsU123	YsU123	*C. albicans*	Clade 8	Malaysia	1995	Human	urine	25	7	6	3	6	27	37	90	2
CA_09_81_191	81_191	*C. albicans*	Clade 9	USA	1981	Human	oral swab	23	3	22	3	3	40	13	72	8
CA_09_BougnCP06	BougnCP06	*C. albicans*	Clade 9	France		Human	faeces	3	3	3	3	3	3	3	3	8
CA_09_IHEM20440	IHEM20440	*C. albicans*	Clade 9	Belgium		Human	oral swab	30	3	46	3	67	99	80	359	Singleton
CA_09_J981326	J981326	*C. albicans*	Clade 9	USA	1998	Human	vaginal swab	22	3	3	3	3	39	13	71	8
CA_09_OTG10	OTG10	*C. albicans*	Clade 9	New Zealand	1991	Human	rectal swab	30	3	3	3	3	48	3	109	8
CA_10_Bougn17	Bougn17	*C. albicans*	Clade 10	France		Human	blood	4	7	13	7	13	19	14	19	7
CA_10_Bougn27	Bougn27	*C. albicans*	Clade 10	France		Human	blood	4	7	16	11	13	19	14	35	7
CO_10_R111	R111	*C. albicans*	Clade 10	Colombia	2007	Human	urine	74	7	16	7	13	19	52	3264	7
CO_10_R425	R425	*C. albicans*	Clade 10	Colombia	2007	Human	urine	13	7	16	2	13	19	52	3266	7
CA_11_564	SC590831	*C. albicans*	Clade 11	UK	2005	Human	blood	30	12	53	4	6	30	4	564	18
CA_11_588	CL4748	*C. albicans*	Clade 11	Venezuela		Human	blood	37	7	21	1	56	11	15	588	19
CA_11_754	AM2005/0370	*C. albicans*	Clade 11	Hungary		Human	blood	7	3	21	5	6	4	126	754	Singleton
CA_11_891	DPC28	*C. albicans*	Clade 11	Belgium	2000	Human	oral swab	88	12	69	1	6	30	4	891	18
CA_11_1370	M49	*C. albicans*	Clade 11	Morocco	2008	Human	vaginal swab	60	28	21	1	7	11	15	1370	19
CA_12_217	T36	*C. albicans*	Clade 12	Canada		Human	oral swab	13	13	15	19	2	37	22	217	Singleton
CA_12_264	S02	*C. albicans*	Clade 12	Italy	2000	Human	oral swab	4	17	21	19	53	32	22	264	10
CA_12_292	IHEM17135	*C. albicans*	Clade 12	Rwanda		Human	oral swab	4	17	6	19	27	83	22	292	10
CA_12_859	AS-1	*C. albicans*	Clade 12	UK	2006	Human	oral swab	21	8	21	19	27	152	22	859	10
CA_12_IHEM20415	IHEM20415	*C. albicans*	Clade 12	Germany		Human	oral swab	4	17	21	19	27	83	22	299	10
C. africana AM2003	AM2003	*C. africana*	Clade 13	Chile		Human	blood	33	7	32	26	2	61	48	182	17
C. africana MYA2669	MYA2669	*C. africana*	Clade 13	Germany		Human	other	33	7	32	26	2	61	48	182	17
CA_13_182	AM2003/0025	*C. albicans*	Clade 13	UK	2003	Human	vaginal swab	33	7	32	26	2	61	48	182	17
CA_13_782	JIMS500002	*C. albicans*	Clade 13	Japan		Human	vaginal swab	33	7	32	43	2	61	48	782	17
CA_14_670	P01	*C. albicans*	Clade 14	Taiwan		Human	urine	6	3	21	50	27	3	13	670	1
CA_14_711	P04	*C. albicans*	Clade 14	Taiwan		Human	urine	6	3	21	6	27	109	112	711	1
CA_14_1793	C1138	*C. albicans*	Clade 14	South Korea	2002	Human	catheter	3	3	21	50	27	45	13	1793	1
CA_14_1968	ZB002	*C. albicans*	Clade 14	China	2008	Human	oral swab	13	3	10	4	53	3	162	1968	Singleton
CA_14_1969	ZB013	*C. albicans*	Clade 14	China	2008	Human	oral swab	6	3	21	4	27	109	13	1969	1
CA_15_172	AM2003/0045	*C. albicans*	Clade 15	UK	2003	Human	vaginal swab	13	3	4	6	34	20	18	172	16
CA_15_191	AM2003/0065	*C. albicans*	Clade 15	UK	2003	Human	vaginal swab	13	28	5	6	34	37	15	191	Singleton
CA_15_643	AM2005/0485	*C. albicans*	Clade 15	Ecuador		Human	blood	77	14	6	6	4	20	15	643	Singleton
CA_15_759	AM2005/0360	*C. albicans*	Clade 15	South Africa		Human	blood	13	3	4	4	34	20	18	759	16
CA_15_928	CCHHCRM4	*C. albicans*	Clade 15	France	2001	Human	blood	24	3	6	4	31	20	15	928	Singleton
CA_16_357	IHEM17984	*C. albicans*	Clade 16	Belgium		Dolphin		54	3	10	36	66	98	79	357	Singleton
CA_16_452	HK03M120736	*C. albicans*	Clade 16	China	2003	Human	blood	53	3	10	36	83	113	10	452	11
CA_16_669	AM2005/0411	*C. albicans*	Clade 16	Argentina		Human	blood	54	31	10	36	83	113	111	669	11
CA_16_676	P09	*C. albicans*	Clade 16	Taiwan		Human	sputum	53	31	10	4	83	113	121	676	11
CA_16_1397	M61	*C. albicans*	Clade 16	Morocco	2008	Human	vaginal swab	54	31	10	36	83	113	197	1397	11
CA_17_305	IHEM17128	*C. albicans*	Clade 17	Rwanda				47	14	21	2	59	80	69	305	Singleton
CA_17_687	P18-2	*C. albicans*	Clade 17	Taiwan		Human	urine	10	46	21	28	67	141	108	687	Singleton
CA_17_827	JIMS187105	*C. albicans*	Clade 17	Japan		Human	blood	59	55	35	62	44	30	6	827	Singleton
CA_17_896	DPC35	*C. albicans*	Clade 17	Belgium	2000	Human	oral swab	47	14	52	28	18	4	6	896	Singleton
CA_17_2013	NICU_6725	*C. albicans*	Clade 17	South Korea		Human	urine	47	26	103	35	162	200	8	2013	Singleton
CA_18_463	HK01M100350	*C. albicans*	Clade 18	China	2001	Human	blood	5	32	21	19	7	55	5	463	5
CA_18_822	JIMS160530	*C. albicans*	Clade 18	Japan		Human	blood	8	32	64	34	7	55	5	822	5
CA_18_1599	C5800	*C. albicans*	Clade 18	South Korea				5	32	21	34	7	74	25	1599	5
CA_18_1792	C950	*C. albicans*	Clade 18	South Korea	2001	Human	blood	5	32	21	34	7	74	12	1792	5
CA_18_2004	NICU_4805	*C. albicans*	Clade 18	South Korea				5	3	21	127	7	55	5	2004	5

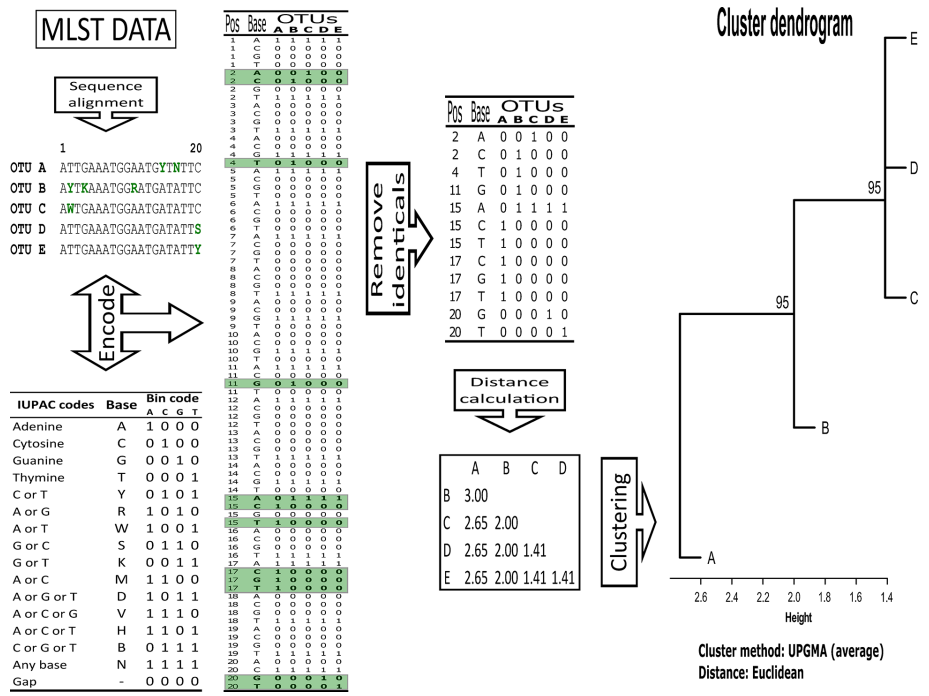

FIGURE 1 | Overview of the methodological pipeline for MLST data cluster analysis.

model was used for comparing proportional hazard ratios). Schoenfeld's residue-based test had been used for checking the proportional hazards (PH) assumption. Statistical tests were evaluated at a 5% significance level of (with Bonferroni adjustment p <0.00465), using the statistical package SPSS 27.

RESULTS

Cluster Analysis

The proposed pipeline (**Figure 1**) enabled constructing dendrograms in which Colombian isolates were assigned to the reported clades. MLST analysis (using the seven concatenated genes) differentiated all 18 C. *albicans* clades (**Figure 2**) and found 16/18 clades in well-supported clusters (clades 5 and 12 were nearly supported, having higher than 90% bootstrap values).

C. albicans clades were divided into two large groups; the first contained seven clades (11, 12, 14–18) and the second 10 (clades 1–10). Clade 13, having two *C. africana* and two *C. albicans* isolates, appeared as a basal branch, followed by *C. dubliniensis* isolate as outgroup. Colombian atypical isolates were grouped into clades 1 (2 isolates) and 10 (2 isolates). A well-supported and differentiated cluster could also be observed (named atypical cluster - AC: six isolates) which was associated with clade 1 (**Figure 2**).

Candida albicans Isolates Had Multiple Clade Memberships, Depending on the Locus Being Considered

Separate analysis of each gene for studying isolate membership of the different clades showed that relationships between clades varied significantly (**Table 2** and **Supplementary Figures** and **Tables A to G**). The total amount of informative positions (TIP) and the amount of informative positions just for *C. albicans* sequences (CAIP) were reduced by analysing each locus separately. The informative positions defining *C. albicans* clade classification varied between 36 (for SYA1) and 13 (ACC1). Given the reduction in the amount of informative positions considered, it was to be expected that differentiation support and capacity for the clusters decayed notably (Satta et al., 2000).

It has been observed that single-gene analysis has revealed incompatible association patterns (Rokas et al., 2003). However, it was observed here that clusters supported in MLST formed by sequences tending to be preferentially associated, regardless of the gene being considered and those having less than 95% support, contained isolates having associations with multiple clades (**Table 2**).

Consolidated isolate membership (**Table 2**) showed that they had a fuzzy assignment, having associations unnoticed in MLST cluster analysis. This fuzziness was observed for all clusters and separate membership analysis for each locus (**Supplementary Tables A to G**) showed that no clade consisted of perfectly differentiated isolates for all loci analysed in *C. albicans*, indicating that all groups could have shared alleles amongst different loci. Although classifications based on individual genes may have been incompatible with gene concatenation classification, combining the informational positions of all loci considered in the total analysis led to classification supported by well-differentiated clusters. AC isolates had strong stability in AC clusters, alternating their membership, mainly with clade 1 (and

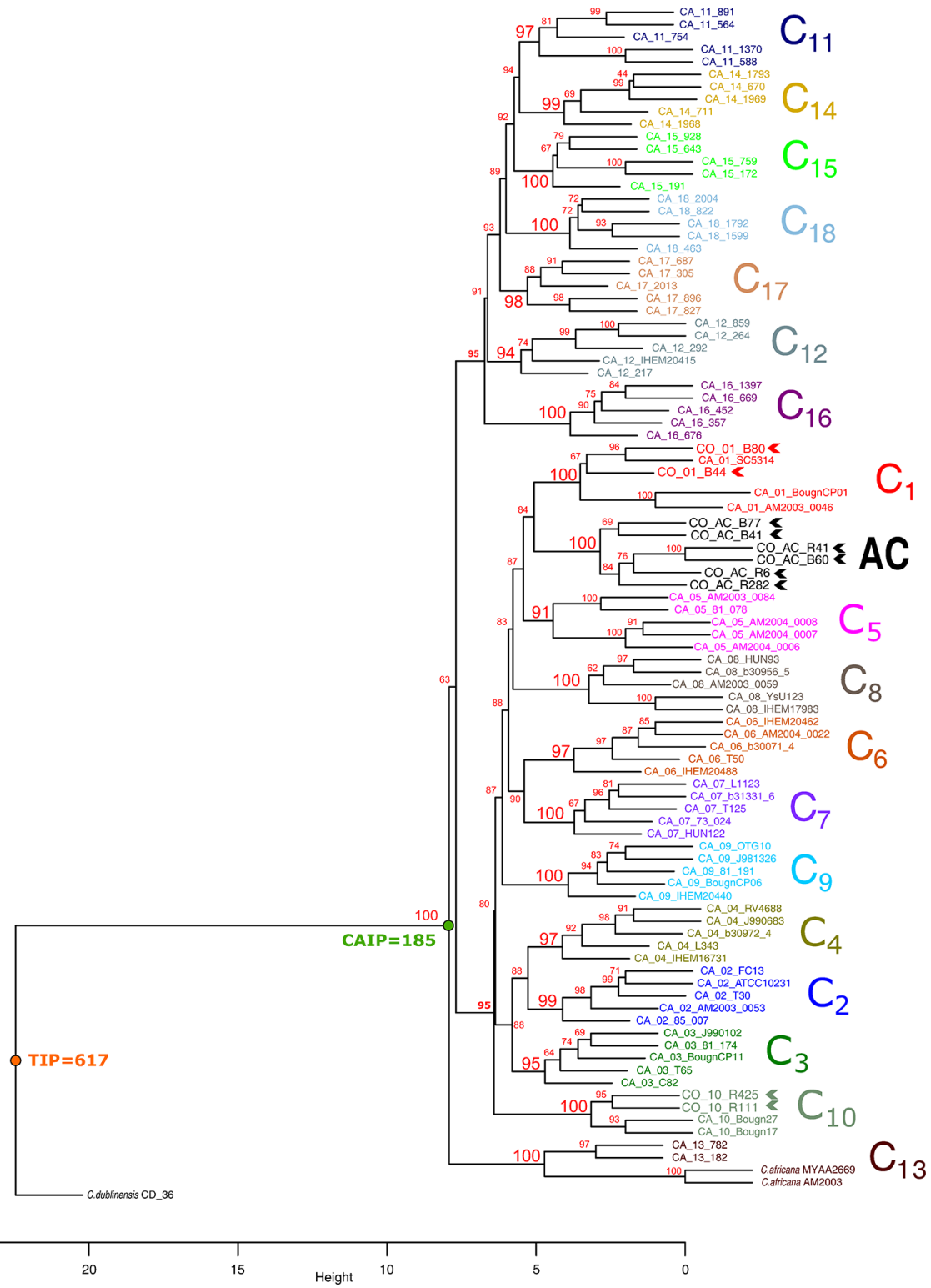

FIGURE 2 | Cluster analysis of MLST data, using the UPGMA method. Each clade is shown in a different colour. Colombian isolates are indicated in bold and chevrons. Bootstrap values above 95% were considered significant. Large numbers in red denote support for each clade. TIP: total informative positions, CAIP: *C. albicans* informative positions.

TABLE 2 | Isolates' clade membership.

	CD	AC	C1	C2	C3	C4	C5	C6	C7	C8	C9	C10	C11	C12	AF/13	C14	C15	C16	C17	C18
C. dubliniensis CD36	100	0	0	0	0	0	0	0	0	0	0	0	0	0	0	0	0	0	0	0
CO_AC_B41	0	29	21	0	2	0	2	0	7	5	5	0	0	0	7	0	2	2	17	0
CO_AC_B60	0	46	14	0	6	0	2	4	7	5	5	0	0	0	0	0	6	2	2	0
CO_AC_B77	0	32	21	0	6	0	2	4	7	5	5	0	0	0	7	0	6	2	2	0
CO_AC_R282	0	46	14	0	6	0	2	4	7	5	5	0	0	0	0	0	6	2	2	0
CO_AC_R41	0	46	14	0	6	0	2	4	7	5	5	0	0	0	0	0	6	2	2	0
CO_AC_R6	0	46	14	0	6	0	2	4	7	5	5	0	0	0	0	0	6	2	2	0
CA_01_AM2003_0046	0	14	46	3	0	0	4	0	4	0	0	6	3	0	7	0	0	0	4	10
CA_01_BougnCP01	0	14	46	3	0	0	4	0	4	0	0	6	3	0	7	0	0	0	4	10
CA_01_SC5314	0	12	24	3	0	5	0	2	2	10	7	3	5	0	7	7	2	0	0	10
CO_01_B44	0	6	32	4	1	1	1	3	3	6	8	4	6	1	7	3	3	1	1	11
CO_01_B80	0	19	31	3	0	5	0	0	0	10	5	3	3	0	7	5	0	0	0	10
CA_02_85_007	0	0	17	41	0	4	0	0	0	4	0	11	6	4	4	4	0	0	4	3
CA_02_AM2003_0053	0	0	3	30	0	4	0	0	0	14	0	7	10	19	4	4	0	0	0	6
CA_02_ATCC10231	0	0	3	44	0	4	0	0	0	4	0	11	10	4	7	4	0	0	4	6
CA_02_FC13	0	0	3	30	0	4	0	17	2	0	2	7	12	4	4	6	2	0	0	6
CA_02_T30	0	0	3	44	0	4	0	0	0	0	0	7	10	19	4	4	0	0	0	6
CA_03_81_174	0	6	0	0	21	5	10	4	7	4	3	11	0	0	4	3	16	2	6	0
CA_03_BougnCP11	0	6	0	0	21	5	10	18	0	4	3	4	0	0	4	3	16	2	6	0
CA_03_C82	0	6	0	0	35	10	15	4	0	5	3	0	0	0	0	3	16	2	2	0
CA_03_J990102	0	6	0	0	35	5	10	4	7	0	3	7	0	0	0	3	16	2	2	0
CA_03_T65	0	4	0	4	18	5	8	4	0	4	17	4	4	0	7	3	14	0	4	4
CA_04_b30972_4	0	0	0	4	5	36	10	2	2	13	2	0	6	4	0	11	2	4	0	0
CA_04_IHEM16731	0	7	7	4	5	21	10	0	0	13	0	0	4	4	0	8	0	4	14	0
CA_04_J990683	0	0	0	4	0	31	5	0	0	31	0	4	4	4	4	8	0	4	4	0
CA_04_L343	0	0	0	4	5	36	10	0	0	17	0	4	4	4	4	8	0	4	4	0
CA_04_RV4688	0	0	0	4	5	36	10	0	0	17	0	4	4	4	4	8	0	4	4	0
CA_05_81_078	0	4	0	0	11	10	16	11	11	5	10	4	2	0	0	5	9	0	4	0
CA_05_AM2003_0084	0	6	0	0	14	10	18	4	4	10	3	8	0	0	5	3	9	2	6	0
CA_05_AM2004_0006	0	2	0	0	10	10	25	2	6	5	5	4	10	0	0	5	8	2	6	0
CA_05_AM2004_0007	0	2	0	0	10	10	25	2	6	5	5	4	10	0	0	5	8	2	6	0
CA_05_AM2004_0008	0	2	0	0	10	10	25	2	6	5	5	4	10	0	0	5	8	2	6	0
CA_06_AM2004_0022	0	11	7	0	4	0	0	51	12	0	5	0	0	0	0	0	4	0	0	7
CA_06_b30071_4	0	4	0	0	4	0	0	51	12	0	5	0	0	14	0	0	4	0	0	7
CA_06_IHEM20462	0	4	0	0	4	0	0	54	14	0	7	0	2	0	0	2	6	0	0	7
CA_06_IHEM20488	0	12	7	6	0	0	0	40	12	5	10	4	0	4	0	0	0	0	0	0
CA_06_T50	0	11	7	0	4	0	0	37	12	0	5	0	0	0	14	0	4	0	0	7
CA_07_73_024	0	7	0	0	0	0	4	14	32	0	21	4	2	0	0	10	2	0	4	0
CA_07_b31331_6	0	7	0	0	0	0	4	14	39	0	7	11	2	0	0	10	2	0	4	0
CA_07_HUN122	0	7	0	4	0	4	0	14	36	0	7	7	6	0	0	13	2	0	0	0
CA_07_L1123	0	7	0	0	0	0	4	14	39	0	7	11	2	0	0	10	2	0	4	0
CA_07_T125	0	11	0	0	4	5	4	13	27	5	2	11	2	0	0	7	6	0	4	0
CA_08_AM2003_0059	0	5	0	0	0	13	5	0	0	44	5	5	0	4	12	5	0	4	0	0
CA_08_b30956_5	0	5	0	14	3	5	3	0	0	36	8	5	0	0	12	8	3	0	0	0
CA_08_HUN93	0	5	0	14	3	5	3	0	0	29	8	5	0	0	5	8	3	14	0	0
CA_08_IHEM17983	0	5	14	0	0	8	5	0	0	32	5	5	0	4	5	0	0	18	0	0
CA_08_YsU123	0	5	14	0	0	8	5	0	0	39	5	5	0	4	12	0	0	4	0	0
CA_09_81_191	0	5	7	0	3	0	3	7	7	5	43	0	2	0	0	5	5	0	0	7
CA_09_BougnCP06	0	5	0	0	3	5	3	2	10	10	39	0	2	0	0	17	5	0	0	0
CA_09_IHEM20440	0	5	7	0	3	0	10	7	7	5	29	0	10	0	7	5	5	0	0	0
CA_09_J981326	0	5	7	0	3	0	3	7	7	5	43	0	2	0	0	5	5	0	0	7
CA_09_OTG10	0	5	0	0	3	0	10	7	7	5	43	0	10	0	0	5	5	0	0	0
CA_10_Bougn17	0	0	3	9	0	0	4	0	11	4	0	50	3	4	4	0	0	0	7	3
CA_10_Bougn27	0	0	3	9	0	0	4	0	11	4	0	50	3	4	4	0	0	0	7	3
CO_10_R111	0	0	3	3	0	0	4	0	11	4	0	46	3	0	4	0	0	0	21	3
CO_10_R425	0	4	3	3	4	0	4	4	11	4	0	46	3	0	4	0	4	0	7	3
CA_11_564	0	2	3	6	2	4	9	2	2	0	2	3	20	6	0	10	8	16	2	3
CA_11_588	0	0	0	7	3	4	10	0	0	5	3	5	18	4	8	10	3	7	0	14
CA_11_754	0	1	4	11	1	4	1	3	3	1	3	4	20	8	4	14	7	1	1	11
CA_11_891	0	2	3	6	2	4	9	2	2	0	2	3	23	9	0	13	8	2	2	6
CA_11_1370	0	0	0	7	17	4	10	0	0	0	3	0	18	4	4	10	3	7	0	14
CA_12_217	0	6	1	1	6	4	3	4	1	4	1	1	4	24	1	4	6	6	17	4
CA_12_264	0	2	0	6	2	4	2	0	0	4	0	4	7	46	0	7	6	6	2	4
CA_12_292	0	0	0	6	0	4	0	5	5	4	5	4	4	40	0	4	18	4	0	0
CA_12_859	0	6	0	0	6	4	2	4	0	4	0	0	7	41	0	7	9	6	2	4
CA_12_IHEM20415	0	0	0	6	0	4	0	12	19	4	5	11	0	36	0	0	0	4	0	0
C. africana AM2003	0	0	7	4	0	0	0	0	0	11	0	4	4	0	64	0	0	0	4	4
C. africana MYA2669	0	0	7	4	0	0	0	0	0	11	0	4	4	0	64	0	0	0	4	4
CA_13_182	0	0	0	4	0	0	0	0	0	11	0	4	4	0	57	0	0	0	18	4
CA_13_782	0	0	0	4	0	0	0	0	0	11	0	4	4	0	57	0	0	0	18	4
CA_14_670	0	0	0	4	3	8	3	2	10	5	5	0	13	7	0	28	9	0	0	4
CA_14_711	0	0	0	0	7	8	0	2	10	8	2	0	10	11	0	21	13	4	0	4
CA_14_1793	0	0	0	4	3	8	3	2	10	5	5	0	13	7	0	28	9	0	0	4
CA_14_1968	0	4	3	6	4	8	0	6	2	5	2	3	12	4	0	16	10	14	0	3
CA_14_1969	0	0	0	4	3	8	3	2	10	5	5	0	13	7	0	28	9	0	0	4
CA_15_172	0	6	0	0	13	4	2	6	2	4	2	0	6	9	0	6	33	6	2	0
CA_15_191	0	6	0	0	30	0	5	4	0	0	3	0	4	6	0	6	33	2	2	0
CA_15_643	0	2	0	0	12	0	5	0	0	4	3	4	0	2	4	3	26	23	6	7
CA_15_759	0	6	0	4	6	7	2	6	2	4	2	0	10	9	0	10	26	6	2	0
CA_15_928	0	2	0	4	5	4	5	2	2	0	5	0	10	6	0	12	25	16	2	0
CA_16_357	0	2	0	0	2	4	2	2	2	4	2	0	2	6	0	2	4	56	2	7
CA_16_452	0	2	0	0	2	0	2	2	2	0	2	0	2	2	14	2	4	52	2	7
CA_16_669	0	2	0	0	2	4	2	0	0	4	0	0	0	6	0	0	2	70	2	7
CA_16_676	0	3	1	4	3	4	3	1	1	1	1	1	4	3	1	4	3	53	3	8
CA_16_1397	0	2	0	0	2	4	2	0	0	4	0	0	0	6	0	0	2	70	2	7
CA_17_305	0	2	0	0	5	0	8	0	4	4	3	7	4	6	4	6	5	2	38	4
CA_17_687	0	2	0	0	2	0	6	0	4	4	0	7	4	6	18	4	2	16	23	4
CA_17_827	0	2	0	0	2	0	6	14	4	4	0	7	0	2	4	0	2	2	52	0
CA_17_896	0	0	0	4	0	0	4	14	4	4	0	7	4	0	7	0	0	0	50	4
CA_17_2013	0	9	7	0	2	4	6	0	4	4	0	4	4	9	0	4	2	6	34	4
CA_18_463	0	0	10	6	0	0	0	0	0	0	0	3	10	18	4	4	0	7	0	39
CA_18_822	0	0	3	6	0	14	0	7	0	0	0	3	10	4	4	4	0	7	0	39
CA_18_1599	0	0	10	6	0	0	0	7	0	0	0	3	10	4	4	4	0	7	0	46
CA_18_1792	0	7	7	4	0	0	0	7	7	0	0	0	7	4	4	4	0	7	0	43
CA_18_2004	0	0	10	6	0	0	4	2	6	0	2	6	12	4	4	6	2	7	4	24

An isolate's consolidated membership is shown as a percentage. Large numbers denote predominant membership.

vice versa). The clustering pattern could be explained as a combined effect of random sorting of alleles, recombination events, and genetic drift (Satta et al., 2000; Rokas et al., 2003).

Atypical isolates in clade 1 had high membership in this clade, as did atypical isolates in clade 10 (**Table 2**). The SYA1 marker showed atypical isolates B41, B77 (AC cluster) and B44 and B80 (clade 1) association with *C. africana* (**Supplementary Figure** and **Table E**). The ACC1 marker had an association with atypical isolates R111 and R425 (clade 10) and *C. africana* (**Supplementary Figure** and **Table B**).

Identifying Clone Complexes

Nineteen clone complexes (CC) and 18 singletons were identified after using the goeBURST algorithm regarding allele profiles for the only 91 DSTs in the data set analysed here. CC1 included more DSTs formed by members of clades 7 and 14. It was found that most clades formed independent CC, confirming this strategy's usefulness for describing the relationships between related DSTs. It was ascertained that atypical Colombian isolates were located in CC 4 (B44, B80), 7 (R11, R425), and 6 (R6, R282, B60, B77, R41, B41), the first two from clades 1 and 10 and the third from the isolates in the AC (**Figure 3** and **Table 1**).

Killing Assays in *G. mellonella*

C. albicans (SC5314), *C. africana* (CAAF1), and atypical isolates' pathogenicity was compared in a systemic infection model (i.e. the *G. mellonella* insect larvae model). The 10^5 CFU per larva concentration had significant differences in some strains evaluated. *C. albicans* R41 and B41 were the most virulent strains, both being members of the AC; conversely, larval killing by *C. africana* isolates was significantly slower than that observed with *C. albicans* in larvae, having statistically significant results (**Figure 4A**). All the strains had similar pathogenicity to the *C. albicans* SC5314 refence strain, lacking statistical significance ($p > 0.05$). Nevertheless, the R41, R11, R282, R435, B41, B44, and B80 strains had statistical differences regarding pathogenicity profiles compared to the *C. africana* CAAF1 reference strain; regarding pathogenicity, it was evident that *C. africana* could not kill the larvae on the days evaluated here, demonstrating this species' inability compared to that of *C. albicans* (**Figure 4B**). Concerning pathogenicity by clade, AC clade R41 and B41 strains were the only strains having statistically significant differences regarding the other *C. albicans* strains. The differences concerned members of the same clade (AC) and one member of the C10 Clade. Concerning the AC clade, 3/6 strains had differences from CAAF1. As for clade C1, both members (2/2) only had statistical differences regarding CAAF1. The C10 clade had 1/2 members having differences regarding the CAAF1, R41, and B41 strains (**Figure 4B**).

Antifungal Susceptibility

The susceptibility results showed that all the reference strains were susceptible to the antifungal drugs tested here, highlighting the susceptibility tests' inability to differentiate between species (*C. albicans, C. africana*) in ATCC yeasts. The results for the ten atypical strains were grouped into three clades (AC, 1 and 10). Reference strains' susceptibility results were homogeneous, having no evidence of species differentiation or clade association. All of them were susceptible to CAS and AMB; none had resistance or dose-dependent susceptibility. Atypical *Candida* had a slightly increased FLU MIC and the B44 strain (clade 1) was resistant (**Table 3**).

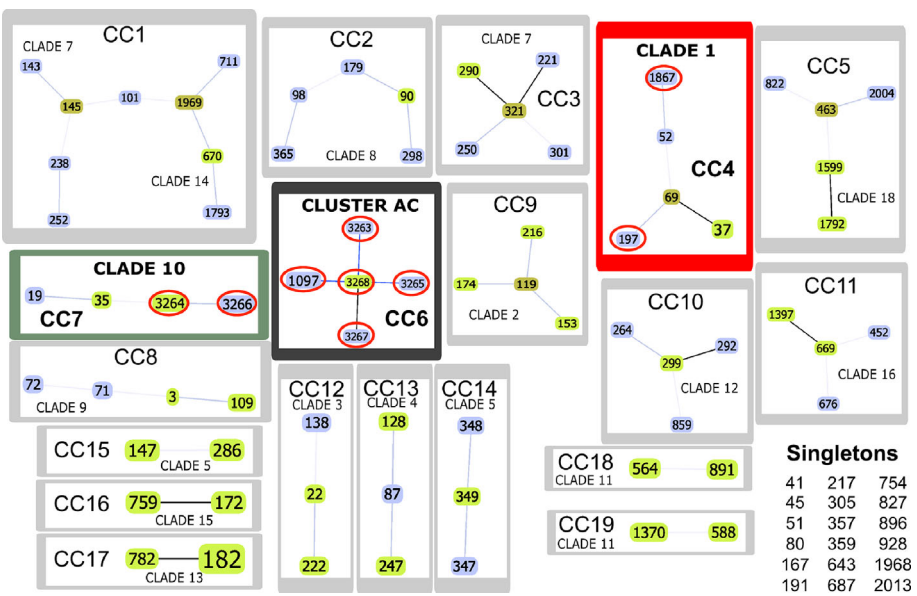

FIGURE 3 | goeBURST analysis. The Colombian atypical isolates (red line ovals) were found in CC4 (framed in red), CC6 (black frame) and CC7 (green frame). Link colours: black links drawn without recourse to tiebreak rules; blue links drawn using tiebreak rule 1 (amount of single locus variations (SLV)); grey links drawn regarding triple locus variation (TLV) (lighter grey). Sequence type (ST) node colours: light green - founder group; dark green - founder sub-group; light blue - common node.

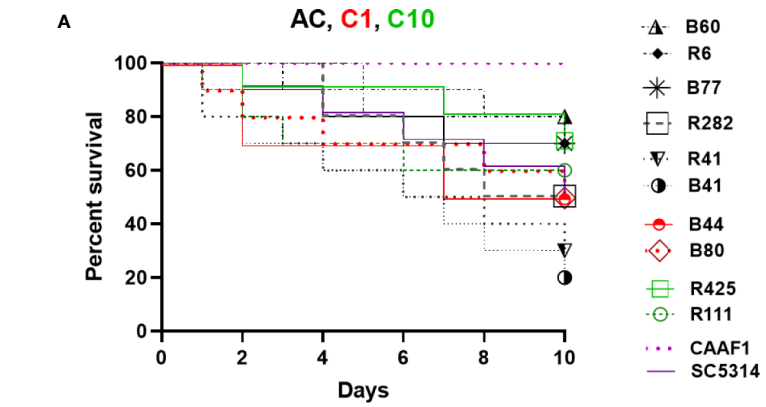

B

		AC						C1		C10		REF	
		R41	B41	R6	B77	R282	B60	B80	B44	R425	R111	SC5314	CAAF1
REF	SC5314	NS	NS	NS	NS	NS	NS	NS	NS	NS	NS	ND	**0,001**
	CAAF1	**0,000**	**0,000**	NS	NS	**0,000**	NS	**0,000**	**0,000**	**0,002**	NS	**0,001**	ND
AC	R41	ND	NS	**0,000**	NS	NS	NS	NS	NS	**0,001**	NS	NS	**0,000**
	B41		ND	**0,000**	NS	NS	NS	NS	NS	**0,000**	NS	NS	**0,000**
	R6			ND	NS	NS	NS	NS	NS	NS	NS	NS	NS
	B77				ND	NS	NS	NS	NS	NS	NS	NS	NS
	R282					ND	NS	NS	NS	NS	NS	NS	**0,000**
	B60						ND	NS	NS	NS	NS	NS	NS
C1	B80							ND	NS	NS	NS	NS	**0,000**
	B44								ND	NS	NS	NS	**0,000**
C10	R425									ND	NS	NS	NS
	R111										ND	NS	NS

FIGURE 4 | Pathogenicity in a *G. mellonella* infection model. **(A)** A Kaplan–Meier plot of *G. mellonella* survival after injection with 10^5 CFU/larvae at 37°C. The data is expressed as survival percentage. No larval killing was observed in control larvae injected with an equivalent volume of PBS (data not shown). **(B)** log-rank (Mantel-Cox) statistical comparison of each survival curve. Data is representative of three independent experiments. Atypical clade shown in black, clade 1 red and clade 10 green.

TABLE 3 | Atypical *C. albicans* antifungal activity.

	ID	Clade	Minimum inhibitory concentration (μg/ml)		
			Fluconazole 24 h	Amphotericin 24 h	Caspofungin 24 h
Reference strains	*C. africana* (CAAF1)	13	0.19	0.025	0.016
	C. africana (MYA2669)	13	0.025	<0.002	0.002
	C. albicans (ATCC90028)	N/A	0.5	<0.002	0.032
	C. albicans (SC5314)	1	1.5	0.75	0.016
Atypical isolates	R6	AC	1	<0.002	<0.002
	B41	AC	1	0.016	<0.002
	B77	AC	2	0.032	0.08
	R282	AC	1	0.064	0.094
	R41	AC	0.038	0.016	<0.002
	B60	AC	2	<0.02	0.19
	B80	1	1.5	0.032	<0.002
	B44	1	>256*	0.004	0.032
	R425	10	2	0.032	0.12
	R111	10	1.5	0.016	<0.002

**Resistance.*

DISCUSSION

Finding genetic markers for devising an approach involving patterns enabling transcending *C. albicans* epidemiology and predicting treatment protocols for this mycosis is one of the challenges in understanding its dynamics as a pathogen (Alanio et al., 2017). This work thus involved the molecular study of ten isolates having atypical phenotypical characteristics (Rodríguez-Leguizamón et al., 2015b). The study's main objective was to determine how they were grouped regarding other isolates reported in the MLST database; an algorithm was thus designed for evaluating the robustness of the clades described to date, finding

the groupings described in clades 1 and 10 as well as a well-differentiated cluster which was named AC.

Classification analysis of atypical isolates concerning the isolates characteristic of the 18 clades described for *C. albicans* showed that most atypical isolates (six of them: **B41, B60, B77, R282, R41, and R6**) concurred in a well-supported cluster (AC) (**Figure 2**) and also constituted CC6 (**Table 1**, **Figure 3**). These isolates had common ST for markers ACC1, ADP1, MPI, VPS13, and ZWF1b markers (**Table 1**), concurring in cluster analysis as a whole and regarding individual genes (**Table 2**, **Supplementary Figure/Tables A to G**). Isolate source did not seem to be a defining item, even though three of the isolates had urinary tract as source and two bronco-alveolar lavage (**Table 1**). DST 1097 (characterised by the five ST shared for this group) was observed in KW2558/11 (Kuwait, 2011. Source: blood), LH1-225 (USA, 2008), and XA14 isolates (China, 2007. S: oral swab) reported in the PubMLST database (Jolley et al., 2018). DST 590 was observed in KW106/13 (Kuwait, 2013, S: blood), KW150/13 (Kuwait, 2013. S: blood) and CL4752 isolates (Venezuela. S: blood), sharing four ST with the AC (ACC1, ADP1, VPS13 and ZWF1b) and the AAT1a marker, which had ST 13 that was common for 5/6 isolates in this group. The exception was B41 (**Table 1**), being the closest geographical reference for these Colombian isolates. ST diversity for the SYA1 marker in the atypical Colombian isolates was greater than that observed for its equivalent in isolates reported to date (**Table 1**), meaning that 4/6 AC isolates had unique DST.

Isolates B44 and B80 were associated with clade 1, having significant support and high co-occurrence (**Figure 2**, **Table 2**). The AC and clade 1 were related and their isolates were co-grouped in cluster analysis for individual markers (**Supplementary Figures A to G**). Isolate source was not a common defining characteristic and only 2 markers shared common ST (SYA1 and ZWF1b). The isolates analysed from clade 1 formed CC4 (**Table 1**, **Figure 3**). Isolate B44 had DST 1867 which was similar to thirty-five isolates previously reported in PubMLST (https://pubmlst.org/); all of them had exclusive geographical origin in China and vaginal swab as source, the same source as isolate B44. Isolate B80 had DST 197, similar to isolates AM2003/0073 (UK, 2003. S: blood) and BK04417 (Germany, 2008. S: blood).

The remaining atypical isolates, R111 and R425, were associated with isolates from clade 10 in a supported cluster, showing that all the members had high co-occurrence (**Figure 2**, **Table 2**, **Supplementary Figures** and **Tables A–G**) and formed CC7 (**Figure 3**). The group was defined by having three ST markers in common (ACC1, SYA1, VPS13) and both atypical samples had been isolated from urinary tracts (**Table 1**). The two atypical isolates in clade 10 differed regarding *AAT1a* and *MPIb* ST. R111 had the only DST 3264, sharing six markers with DST 1363 (except for ZWF1b from ST 14), comprising six isolates already reported in PubMLST: M15 and M16 (Morocco, 2008. S: vaginal swab), KW575/12, KW78/12, and KW98/12 (Kuwait, 2012. S: blood), and TW-CDC514 (Taiwan, 2000). R425 had the only DST 3266, differing regarding markers with DST 1362 (AAT1a = ST4, ZWF1b = ST14), being similar to isolate M14 (Morocco, 2008. S: vaginal swab).

Great similarity between both approaches was found when comparing e-BURST and cluster analysis. The amount of clonal complexes (CC) was very close to the amount of clusters (19 and 18, respectively), differences concerning the fusion of clades 7 and clade 14 in CC1, the separation of clades 5 and 11 (into CC15 - CC14 and CC18 and CC19, respectively) and 18 strains assigned as singletons (**Table 1** and **Figure 3**). Both analyses revealed the same association pattern for atypical isolates, identifying three well-defined classes.

Our group has described that atypical isolates share phenotypical features with *C. africana* even though analysis with molecular markers has identified these isolates as *C. albicans* (Rodríguez-Leguizamón et al., 2015b). Our results from analysing MLST data have shown that these isolates could be classified as *C. albicans*. A relationship between the atypical isolates and *C. africana* was only found concerning isolates B41 and B77 from the AC and isolates B44 and B80 from clade 1 with the SYA1 marker and isolates R111 and R425 from clade 10 with the ACC1 marker; this was not sufficient for classifying these atypical isolates as *C. africana*.

Atypical isolates' pathogenic capability regarding *C. africana* in the *G. mellonella* model was different. *C. africana* did not cause larval mortality; interestingly, isolates R41 and B41 belonging to the AC and CC6 had greater virulence, demonstrating variability regarding their performance (**Figure 4**). It has been reported that *C. africana* cannot survive in the haemolymph along with high *G. mellonella* antimicrobial peptide (AMP) concentrations. Virulence factors have been extensively studied in *C. albicans* and include adhesins (ALS), enzymes (e.g. SAPS, PLA, PLB, PLC) and, notably, the ability to alternate between hyphal and budding yeast forms. No proteomics approach to date has deciphered the particularities concerning *C. albicans* and *C. africana*. It has been proposed that hyphal formation plays a crucial role in binding to host cell surface, tissue invasion, biofilm formation, and immune evasion. Alterations associated with delayed hyphal formation (possibly associated with different *HWP1* gene size), the absence of chlamydospores and the loss of enzyme battery could have reduced an ability to tolerate environmental stress, resulting in reduced *Galleria* larval virulence, as reduced *C. dubliniensis* virulence compared to that for *C. albicans* has been attributed to lower filamentation rates (Borman et al., 2013). *C. africana* was avirulent in the present study, as has been described in other studies regarding this species. It was observed that many isolates had a pathogenicity profile similar to that observed in the C. albicans SC5314 reference strain, despite having an atypical phenotype.

Atypical isolates conserved their pathogenic capability and had different fluconazole MIC values and resistance cut-off points were identified regarding the B44 strain (**Table 3**). Such results highlighted these yeasts' great plasticity and ratified the difficulty involved in determining patterns in *Candida*. The study's results enabled completing details regarding these isolates' preliminary characterisation, selective pressure complexity, host supply and microenvironment diversity in hospital conditions. They also highlighted the need for the

detailed phenotypical and functional characterisation of the atypical isolates studied here.

CONCLUSION

The proposed classification analysis for the atypical isolates characterised here identified isolates belonging to *C. albicans*, in spite of having phenotypical characteristics coinciding with those for *C. africana*. Most were new DSTs (6/10); all were related to DST reported for regions geographically remote from Colombia, underlining circulating strains' global dispersion or, less probably, MLST variants convergence between isolates from Colombia, northern Africa, North America, Europe and Asia. The AC's distinctive characters suggested its relevance as a new clade for *C. albicans*. The AC has been consistently differentiated from the clades reported to date by MLST characterisation, trehalose metabolism and an inability to form chlamydospores, unlike typical *C. albicans* (Rodríguez-Leguizamón et al., 2015b).

This study concluded that most atypical isolates belonged to *C. albicans* species and represented new DSTs, or came within DSTs reported in distant geographical regions. The isolates were clearly differentiated from *C. africana* regarding individual markers and concatenation, except for isolates having ST 2 in the *SYA1* gene (B41, B77, B44 and B80) and ST 7 in the *ACC1* gene (R111 and R425) shared by isolates from clade 13 to which *C. africana* belongs (**Table 1**, **Supplementary Figures A to G**).

The proposed classification methodology enabled hierarchical clustering using unbiased Bootstrap as statistical support for MLST characterisation together and separately, clearly recovering established clades (Bougnoux et al., 2004; McManus and Coleman, 2014). It offered an image coinciding with *C. albicans*' complex population structure where classification patterns highlighted the dynamic nature of this pathobiont's populations. The *C. albicans* population's genetic structure is extremely heterogeneous and great variation could be observed here regarding the descriptions available in the pertinent medical literature, consistently grouping clinical isolates sharing complex hospital environments.

The phenotypical patterns described in our group's studies have been close to the descriptions in the literature about phenotypical plasticity really affecting features such as the virulence seen in both strains from the AC in the *G. mellonella* model and another strain from clade 1 that had fluconazole resistance. This type of finding highlights the need for more studies in this field as a response to the challenge of difficult-to-diagnose and manage hospital-acquired infections.

DATA AVAILABILITY STATEMENT

The raw data supporting the conclusions of this article will be made available by the authors, without undue reservation.

ETHICS STATEMENT

The studies involving human participants were reviewed and approved by the Universidad del Rosario's ethics committee and the Hospital San Ignacio's ethics committee.

AUTHOR CONTRIBUTIONS

GR-L: conceived the study, participated in its design, participated in acquiring MLST data and analysed it. AC-G: performed killing assays in *G. mellonella* and susceptibility tests. CS: designed, carried out and discussed the cluster and membership analysis of MLST. MP: coordinated acquiring MLST data, participated in its design and critically reviewed the manuscript. CP-G: coordinated the study and participated in its design. All authors contributed to the article and approved the submitted version.

FUNDING

This study was funded by the Fundación Instituto de Inmunología de Colombia (FIDIC), the Universidad del Rosario and Universidad Javeriana, Ponticia Universidad Javeriana ID006878 Call 777/2017 MinCiencias. Hospital Universitario Mayor ID 24668.

ACKNOWLEDGMENTS

We would like to thank Jason Garry for thoroughly revising the text, Milciades Ibanez Pinilla for statistical support and Marina Muñoz and Juan David Ramírez for fruitful discussion regarding the results. We would like to thank the Universidad Javeriana and the Colombian Science, Technology and Innovation Department (COLCIENCIAS) for sponsoring AC's PhD training in Colombia.

SUPPLEMENTARY MATERIAL

The Supplementary Material for this article can be found online at: https://www.frontiersin.org/articles/10.3389/fcimb.2020.571147/full#supplementary-material

SUPPLEMENTARY FIGURE 1 | (A–G) Cluster analysis of separated MLST markers using the UPGMA method. Each clade is shown in a different colour. Colombian isolates are indicated in bold and chevrons. Bootstrap values above 95% were considered significant. Large numbers in red denote support for each clade. TIP, total informative positions; CAIP, *C. albicans* informative positions.

SUPPLEMENTARY TABLE 1 | (A–G) Isolates' clade membership for each MLST marker. An isolate's membership is shown as a percentage. Values close to 1 denote predominant membership.

REFERENCES

Alanio, A., Desnos-Ollivier, M., Garcia-Hermoso, D., and Bretagne, S. (2017). Investigating clinical issues by genotyping of medically important fungi: Why and how? *Clin. Microbiol. Rev.* 30, 671–707. doi: 10.1128/CMR.00043-16

Albaina, O., Sahand, I. H., Brusca, M.II, Sullivan, D. J., De Larrinoa, I. F., and Moragues, M. D. (2015). Identification and characterization of nine atypical Candida dubliniensis clinical isolates. *J. Med. Microbiol.* 64, 147–156. doi: 10.1099/jmm.0.078832-0

Alonso-vargas, R., Elorduy, L., Eraso, E., Francisco cano, J., Guarro, J., Pontón, J., et al. (2008). Isolation of Candida africana, probable atypical strains of Candida albicans, from a patient with vaginitis. *Med. Mycol.* 46, 167–170. doi: 10.1080/13693780701633101

Basmaciyan, L., Bon, F., Paradis, T., Lapaquette, P., and Dalle, F. (2019). Candida Albicans Interactions With The Host: Crossing The Intestinal Epithelial Barrier. *Tissue Barriers* 7, 1–31. doi: 10.1080/21688370.2019.1612661

Borman, A. M., Szekely, A., Linton, C. J., Palmer, M. D., Brown, P., and Johnson, E. M. (2013). Epidemiology, antifungal susceptibility, and pathogenicity of Candida africana isolates from the United Kingdom. *J. Clin. Microbiol.* 51, 967–972. doi: 10.1128/JCM.02816-12

Bougnoux, M. E., Tavanti, A., Bouchier, C., Gow, N. A. R., Magnier, A., Davidson, A. D., et al. (2003). Collaborative Consensus for Optimized Multilocus Sequence Typing of Candida albicans. *J. Clin. Microbiol.* 41, 5265–5266. doi: 10.1128/JCM.41.11.5265-5266.2003

Bougnoux, M. E., Aanensen, D. M., Morand, S., Théraud, M., Spratt, B. G., and D'Enfert, C. (2004). Multilocus sequence typing of Candida albicans: Strategies, data exchange and applications. *Infect. Genet. Evol.* 4, 243–252. doi: 10.1016/j.meegid.2004.06.002

Chowdhary, A., Hagen, F., Sharma, C., Al-Hatmi, A. M. S., Giuffrè, L., Giosa, D., et al. (2017). Whole Genome-Based Amplified Fragment Length Polymorphism Analysis Reveals Genetic Diversity in Candida africana. *Front. Microbiol.* 8:556. doi: 10.3389/fmicb.2017.00556

Costa-de-oliveira, S., and Rodrigues, A. G. (2020). Candida albicans antifungal resistance and tolerance in bloodstream infections: The triad yeast-host-antifungal. *Microorganisms* 8, 154. doi: 10.3390/microorganisms8020154

Cotter, G., Doyle, S., and Kavanagh, K. (2000). Development of an insect model for the *in vivo* pathogenicity testing of yeasts. *FEMS Immunol. Med. Microbiol.* 27, 163–169. doi: 10.1111/j.1574-695X.2000.tb01427.x

Dean, C. B., and Nielsen, J. D. (2007). Generalized linear mixed models: A review and some extensions. *Lifetime Data Anal.* 13, 497–512. doi: 10.1007/s10985-007-9065-x

Feil, E. J., Li, B. C., Aanensen, D. M., Hanage, W. P., and Spratt, B. G. (2004). eBURST: Inferring Patterns of Evolutionary Descent among Clusters of Related Bacterial Genotypes from Multilocus Sequence Typing Data. *J. Bacteriol.* 186 (5), 1518–1530. doi: 10.1128/JB.186.5.1518-1530.2004

Francisco, A. P., Bugalho, M., Ramirez, M., and Carriço, J. A. (2009). Global optimal eBURST analysis of multilocus typing data using a graphic matroid approach. *BMC Bioinf.* 10:152. doi: 10.1186/1471-2105-10-152

Fuchs, B. B., Eby, J., Nobile, C. J., El Khoury, J. B., Mitchell, A. P., and Mylonakis, E. (2010a). Role of filamentation in Galleria mellonella killing by Candida albicans. *Microbes Infect.* 12, 488–496. doi: 10.1016/j.micinf.2010.03.001

Fuchs, B. B., O'Brien, E., El Khoury, J. B., and Mylonakis, E. (2010b). Methods for using *Galleria mellonella* as a model host to study fungal pathogenesis. *Virulence* 1, 475–482. doi: 10.4161/viru.1.6.12985

Hazirolan, G., Altun, H. U., Gumral, R., Gursoy, N. C., Otlu, B., and Sancak, B. (2017). Prevalence of Candida africana and Candida dubliniensis, in vulvovaginal candidiasis: First Turkish Candida africana isolates from vulvovaginal candidiasis. *J. Mycol. Med.* 27, 376–381. doi: 10.1016/j.mycmed.2017.04.106

Jolley, K. A., Bray, J. E., and Maiden, M. C. J. (2018). Open-access bacterial population genomics: BIGSdb software, the PubMLST.org website and their applications [version 1; referees: 2 approved]. *Wellcome Open Res.* 3, 124. doi: 10.12688/wellcomeopenres.14826.1

Kadosh, D. (2019). Regulatory mechanisms controlling morphology and pathogenesis in Candida albicans. *Curr. Opin. Microbiol.* 52, 27–34. doi: 10.1016/j.mib.2019.04.005

Mayer, F. L., Wilson, D., and Hube, B. (2013). Candida albicans pathogenicity mechanisms. *Virulence* 4, 119–128. doi: 10.4161/viru.22913

McManus, B. A., and Coleman, D. C. (2014). Molecular epidemiology, phylogeny and evolution of Candida albicans. *Infect. Genet. Evol.* 21, 166–178. doi: 10.1016/j.meegid.2013.11.008

Pérez-Losada, M., Cabezas, P., Castro-Nallar, E., and Crandall, K. A. (2013). Pathogen typing in the genomics era: MLST and the future of molecular epidemiology. *Infect. Genet. Evol.* 16, 38–53. doi: 10.1016/j.meegid.2013.01.009

Rodríguez-Leguizamón, G., Fiori, A., Lagrou, K., Gaona, M. A., Ibáñez, M., Patarroyo, M. A., et al. (2015a). New echinocandin susceptibility patterns for nosocomial Candida albicans in Bogotá, Colombia, in ten tertiary care centres: an observational study. *BMC Infect. Dis.* 15, 108. doi: 10.1186/s12879-015-0840-0

Rodríguez-Leguizamón, G., Fiori, A., López, L. F., Gómez, B. L., Parra-Giraldo, C. M., Gómez-López, A., et al. (2015b). Characterising atypical Candida albicans clinical isolates from six third-level hospitals in Bogotá, Colombia. *BMC Microbiol.* 15, 199. doi: 10.1186/s12866-015-0535-0

Rokas, A., Williams, B. L., King, N., and Carroll, S. B. (2003). Genome-scale approaches to resolving incongruence in molecular phylogenies. *Nature* 425, 798–804. doi: 10.1038/nature02053

Romeo, O., and Criseo, G. (2008). First molecular method for discriminating between Candida africana, Candida albicans, and Candida dubliniensis by using hwp1 gene. *Diagn Microbiol. Infect. Dis.* 62, 230–233. doi: 10.1016/j.diagmicrobio.2008.05.014

Sam, Q., Chang, M., and Chai, L. (2017). The Fungal Mycobiome and Its Interaction with Gut Bacteria in the Host. *Int. J. Mol. Sci.* 18:330. doi: 10.3390/ijms18020330

Satta, Y., Klein, J., and Takahata, N. (2000). DNA archives and our nearest relative: the trichotomy problem revisited. *Mol. Phylogenet. Evol.* 14, 259–275. doi: 10.1006/mpev.2000.0704

Scordino, F., Giuffrè, L., Barberi, G., Merlo, F. M., Orlando, M. G., Giosa, D., et al. (2018). Multilocus sequence typing reveals a new cluster of closely related Candida tropicalis genotypes in Italian patients with neurological disorders. *Front. Microbiol.* 9:679. doi: 10.3389/fmicb.2018.00679

Sievers, F., Wilm, A., Dineen, D., Gibson, T. J., Karplus, K., Li, W., et al. (2011). Fast, scalable generation of high-quality protein multiple sequence alignments using Clustal Omega. *Mol. Syst. Biol.* 7, 539. doi: 10.1038/msb.2011.75

Suzuki, R., and Shimodaira, H. (2006). Pvclust: an R package for assessing the uncertainty in hierarchical clustering. *Bioinformatics* 22, 1540–1542. doi: 10.1093/bioinformatics/btl117

Tietz, H. J., Kussner, A., Thanos, M., De Andrade, M. P., Presber, W., and Schonian, G. (1995). Phenotypic and genotypic characterization of unusual vaginal isolates of Candida albicans from Africa. *J. Clin. Microbiol.* 33, 2462–2465. doi: 10.1128/jcm.33.9.2462-2465.1995

Zhang, I., Pletcher, S. D., Goldberg, A. N., Barker, B. M., and Cope, E. K. (2017). Fungal Microbiota in Chronic Airway Inflammatory Disease and Emerging Relationships with the Host Immune Response. *Front. Microbiol.* 8:2477. doi: 10.3389/fmicb.2017.02477

Znaidi, S. (2020). mSphere of Influence: Decoding Transcriptional Regulatory Networks To Illuminate the Mechanisms of Microbial Pathogenicity. *mSphere* 5, 00917–19. doi: 10.1128/msphere.00917-19

Conflict of Interest: The authors declare that the research was conducted in the absence of any commercial or financial relationships that could be construed as a potential conflict of interest.

Advantages of publishing in Frontiers

OPEN ACCESS
Articles are free to read for greatest visibility and readership

FAST PUBLICATION
Around 90 days from submission to decision

HIGH QUALITY PEER-REVIEW
Rigorous, collaborative, and constructive peer-review

TRANSPARENT PEER-REVIEW
Editors and reviewers acknowledged by name on published articles

Frontiers
Avenue du Tribunal-Fédéral 34
1005 Lausanne | Switzerland

Visit us: www.frontiersin.org
Contact us: frontiersin.org/about/contact

REPRODUCIBILITY OF RESEARCH
Support open data and methods to enhance research reproducibility

DIGITAL PUBLISHING
Articles designed for optimal readership across devices

FOLLOW US
@frontiersin

IMPACT METRICS
Advanced article metrics track visibility across digital media

EXTENSIVE PROMOTION
Marketing and promotion of impactful research

LOOP RESEARCH NETWORK
Our network increases your article's readership